UNIVERSIDADE FEDERAL DO PARÁ
CENTRO DE GEOCIÊNCIAS
PROGRAMA DE PÓS-GRADUAÇÃO EM GEOLOGIA E GEOQUÍMICA

TESE DE DOUTORADO

EVOLUÇÃO GEOLÓGICA DA PORÇÃO CENTRO-SUL DO ESCUDO DAS GUIANAS COM BASE NO ESTUDO GEOQUÍMICO, GEOCRONOLÓGICO E ISOTÓPICO DOS GRANITÓIDES PALEOPROTEROZÓICOS DO SUDESTE DE RORAIMA, BRASIL

Tese apresentada por:

MARCELO ESTEVES ALMEIDA

BELÉM
2006

Dados Internacionais de Catalogação-na-Publicação(CIP)
Biblioteca Geól. Rdº Montenegro G. de Montalvão

Almeida, Marcelo Esteves

A447 e Evolução geológica da porção centro-sul do Escudo das Guianas com base no estudo geoquímico, geocronológico e isotópico dos granitóides Paleoproterozóicos do Sudeste de Roraima, Brasil. / Marcelo Esteves Almeida; orientador, Moacir José Buenano Macambira. – 2006

227 f. : il.

Tese (Doutorado em Geoquímica e Petrologia) – Universidade Federal do Pará, Centro de Geociências, Curso de Pós-Graduação em Geologia e Geoquímica, Belém, 2006.

1.Geocronologia. 2.Geoquímica. 3.Isótopos radiogênicos. 4.Petrologia. 5.Evolução crustal. 6.Paleoproterozóico. 7.Escudo das Guianas.8. Sudeste de Roraima I.Universidade Federal do Pará. II.Macambira, Moacir José Buenano, orient. III. Título.

CDD 20º ed.:558114

Universidade Federal do Pará
Centro de Geociências
Programa de Pós-Graduação em Geologia e Geoquímica

EVOLUÇÃO GEOLÓGICA DA PORÇÃO CENTRO-SUL DO ESCUDO DAS GUIANAS COM BASE NO ESTUDO GEOQUÍMICO, GEOCRONOLÓGICO E ISOTÓPICO DOS GRANITÓIDES PALEOPROTEROZÓICOS DO SUDESTE DE RORAIMA, BRASIL

TESE APRESENTADA POR

MARCELO ESTEVES ALMEIDA

Como requisito parcial à obtenção do Grau de Doutor em Ciências na Área de GEOQUÍMICA E PETROLOGIA.

Data de Aprovação: **17/11/2006**
Co-orientador: Franck Poitrasson (LMTG-CNRS,TOULOUSE, FRANÇA)

Comitê de Tese

MOACIR JOSÉ BUENANO MACAMBIRA (Orientador)

CLAUDIO DE MORISSON VALERIANO

SÉRGIO DE CASTRO VALENTE

CANDIDO AUGUSTO VELOSO MOURA

CLAUDIO NERY LARAMÃO

Universidade Federal do Pará
Curso de Pós-Graduação
Geologia e Geoquímica
TESE APROVADA
COM DISTINÇÃO
Belém

Belém

SUMÁRIO

- Aos meus queridos pais (João e Glória)
e avós (Rufina *in memoriam e* Guida)
- Aos meus amores Adriana e Maria Júlia

AGRADECIMENTOS

Apesar da redação de uma tese de doutorado ser um produto de responsabilidade e "*stress"* de natureza individual, sem o apoio contínuo e incondicional da família e a contribuição e a dedicação coletiva dos amigos, certamente este trabalho não chegaria a bom termo. A todos eles registro minha mais profunda gratidão.

Minha gratidão ao professor Dr. Moacir Macambira, meu orientador, que tive a oportunidade e a alegria de conhecer desde a minha primeira visita de trabalho ao Pará-Iso (há mais de 10 anos atrás). Desde essa época pude descobrir o grande profissional e a pessoa extremamente generosa que é, justificando a admiração de todos os seus colegas e alunos. Sua experiência de vida e profissional (muitas das vezes transmitidas on-line ou por e-mail!) foram determinantes ao longo da construção desta tese de doutorado. A sua disponibilidade irrestrita, sua forma crítica, inteligente e criativa de arguir as idéias apresentadas deram norte a este trabalho, facilitando o alcance de seus objetivos. Ao "Moa Mac Ambira", e a seu clã (Cristina, Aline e Amanda), meus sinceros agradecimentos.

Aos professores Drs. Jean-Michel Lafon, Cândido Augusto Veloso Moura e Thomas Scheller, que com sua dedicação e paixão pela geologia isotópica conseguiram colocar a UFPA e o Pará-Iso num nível de reconhecida competência tanto no cenário nacional quanto internacional. O meu profundo agradecimento pelo aprendizado durante esse período de tese. Ao prof. Dr. Cândido Augusto Veloso Moura vale ainda o agradecimento pela gentileza de ter aceitado fazer parte da banca de tese.

Ao professor Dr. Claúdio Nery Lamarão (UFPA), o meu muito obrigado pelo aceite em compor esta banca de doutorado, pois certamente seu conhecimento petrológico acerca dos granitóides em geral e particularmente aqueles do sudoeste do Pará, trará enormes ganhos na interpretação petrognenética e evolutiva dos granitóides do sudeste de Roraima. Gostaria também de agradecer ao professor Dr e comendador Roberto Dall´Agnol (UFPA) pelas observações e reflexões sobre a granitogênese do Escudo das Guianas. Sua visão sobre a geologia dos granitos muito no ajudou a compreendê-los na sua essência.

Ao professor Dr. Sérgio de Castro Valente da Universidade Federal Rural do Rio de Janeiro, o mais talentoso professor e pesquisador que tive a oportunidade de conhecer durante minha vida acadêmica e figura humana das mais queridas, a minha profunda gratidão. O prof. Sérgio tem sido de uma disponibilidade irrestrita sempre que procurado para tratar de assuntos

relacionados à petrologia e a geoquímica elementar e isotópica. Um mestre de verdade. Nossos agradecimentos também pela sua participação nesta banca de doutorado, o que certamente enriquecerá nosso trabalho.

Ao Professor Dr. Cláudio de Morisson Valeriano da Universidade do Estado do Rio de Janeiro, geólogo de grande competência e paixão pelos estudos tectônicos, tem nos acompanhado desde os tempos de mestrado na UFRJ, onde pude constatar como suas sugestões e observações podem enriquecer uma tese. Manifesto aqui minha gratidão pelo aceite em compor novamente uma banca, agora neste novo desafio.

À secretaria do CPGG (Gladys, Nilza, Profs Gorayeb, Cândido e José Augusto) pelo apoio constante, aos colegas e estagiários bolsistas do Pará-Iso (Rose Brabo, Rosi Rocha, Elma, Roberta Florêncio, Roberta, Krymsky, Valter Avelar, Marco Antonio, Pablo Rolando, Pablo Monteiro, Keila, César, etc.) e a todos os colegas da turma de doutorado (Alex, Davis, Marivaldo) pelo ambiente amigo e fraterno durante todo o curso, amizades que certamente se perpetuarão. Le même je peux dire aux collègues du LMTG (*Laboratoire des Mécanismes et Transferts em Gèologie*), surtout à Franck Poitrasson et à Remi Freydier, qu´ont fait me sentir comme chez-moi pendant mon séjour de chercheur-invité dans l´Université Pierre Sabatier (Toulouse III).

Ao bibliotecário Hélio Martins da biblioteca Raimundo Montalvão (CG-UFPA), pelo trabalho paciente e meticuloso de revisão das normas bibliográficas desta tese.

Ao professor e jornalista Cláudio Pedro de Alcântara pela sua obstinação e paciência na árdua tarefa de ensinar a língua francesa a alunos com tanta dificuldade de aprendizagem (nos quais certamente eu me incluo).

A população dos municípios de Rorainópolis, São Luiz do Anauá, São João da Baliza, Caroebe, Caracaraí, incluindo todas as comunidades pertencentes aos assentamentos de terra do INCRA do SE de Roraima, o meu muito obrigado pela receptividade e colaboração durante os trabalhos de campo.

Ao superintendente (Daniel Nava) e aos companheiros de trabalho da CPRM-Serviço Geológico do Brasil (Manaus) pelo incentivo, discussão dos dados e apoio constantes, incluindo a infra-estrutura de preparação de amostras (João Almeida e sua equipe), editoração e geoprocessamento (Amaro Luiz Ferreira, Aldenir Justino, Miguel Hollanda e Teresa Dias) e laboratório petrográfico (René Luzardo), além dos motoristas Valdir e Luiz Rodrigues. Agradeço

ainda aos diretores passados (Luiz Augusto Bizzi) e presentes (Agamenon Dantas, Fernando Pereira de Carvalho e Manoel Barretto) que acreditaram e facilitaram, no que foi possível, a realização desta tese.

A CPRM-Serviço Geológico do Brasil em conjunto com a UFPA (Pará-Iso), FINEP (Projeto CT Mineral 01/2001 "Geocronologia Aplicada ao modelamento metalogenético da Plataforma Amazônica"-2002-2004), Capes (Proc. BEX 1041/05-3), além do PRONEX/UFPA/CNPq/FADESP (662103/1998-0) e da Université Paul Sabatier e CNRS (LMTG), constituíram as fontes de financiamento desta pesquisa.

As mulheres da minha vida, Adriana e Maria Júlia (nascida durante a elaboração da tese), pelo amor, encorajamento e compreensão, que tanto me ajudaram nessa caminhada. Posso me considerar um sujeito de (muita) sorte. Sorte sim, pois tive a felicidade de escolher a profissão certa e de encontrar a companheira perfeita tão cedo, numa fase da vida em que o nível de maturidade não costuma ajudar muito nestas escolhas. Logo depois, Maria Júlia chegou e deu logo um novo (e mais amplo) sentido às nossas vidas. Só Deus sabe (e ele foi decisivo) o quanto foi difícil passar algumas temporadas longe de casa por conta dos trabalhos da tese.

A toda minha família, em especial aos meus doces pais João e Glória, ao meu querido irmão Sérgio, minha cunhada-irmã Selma, aos meus sobrinhos Pedro e João e aos meus maravilhosos sogros Adelino e Zilda, meus eternos agradecimentos. Vocês são simplesmente fundamentais na minha vida, responsáveis diretos pela minha saúde afetiva.

Aqueles não lembrados ou não citados me perdoem a injustiça do esquecimento**.**

CERTEZA

De tudo ficaram 3 coisas:
A certeza de que estamos sempre começando
A certeza de que precisamos continuar
A certeza de que seremos interrompidos antes de terminar

Portanto devemos:
Fazer da interrupção um novo caminho
Da queda, um passo de dança
Do medo, uma escada
Do sonho, uma ponte
Da procura, um encontro

Fernando Pessoa

RESUMO

Este estudo focaliza a região centro-sul do Escudo das Guianas (sudeste de Roraima, Brasil), área caracterizada essencialmente por dois domínios tectono-estratigráficos denominados Guiana Central (DGC) e Uatumã-Anauá (DUA) e considerada limite entre províncias geocronológicas (Ventuari-Tapajós ou Tapajós-Parima, Amazônia Central e Maroni-Itacaiúnas ou Transamazônica). O objetivo principal deste trabalho é o estudo geoquímico, isotópico e geocronológico dos granitóides desta região, buscando ao mesmo tempo subsidiar a análise petrológica e litoestratigráfica local e contribuir com as propostas e modelos evolutivos regionais.

O DGC é apenas localmente abordado na sua porção limítrofe com o DUA, tendo sido apresentados novos dados geológicos das rochas ortognáissicas e duas idades de zircão (evaporação de Pb) de biotita granodiorito milonítico (1,89 Ga) e de hastingsita-biotita granito foliado (1,72 Ga). Essas idades contrastam com as idades obtidas para os protólitos de outras áreas do DGC (1,96-1,93 Ga), sugerindo a existência de cenários litoestratigráficos distintos dentro do mesmo domínio.

Mapeamento geológico regional, petrografia, geoquímica, e geocronologia por evaporação de Pb e U-Pb ID-TIMS em zircão efetuadas nas rochas do DUA apontam para a existência de um amplo magmatismo granítico paleoproterozóico cálcio-alcalino. Estes granitóides estão distribuídos em diversas associações magmáticas com diferentes intervalos de idade – entre 1,97 e 1,89 Ga - estruturas e afinidades geoquímicas, individualizados em dois sub-domínios no DUA, denominados de norte e sul.

No setor norte dominam granitos tipo S (Serra Dourada) e tipo-I cálcio-alcalino com alto-K (Martins Pereira) mais antigos (1,97-1,96 Ga), ambos intrusivos em *inliers* do embasamento composto por associação do tipo TTG e sucessões meta-vulcanossedimentares de médio a alto grau (>2,03 Ga). No setor sul, o Granito Igarapé Azul (1,89 Ga) é caracterizado por conter enclaves ricos em biotita, além de xenólitos do Granito Martins Pereira e de paragnaisses do Grupo Cauarane. Este granitóide é caracterizado por seu quimismo cálcio-alcalino de alto-K, restrito a termos monzograníticos ricos em SiO_2. O Granito Caroebe (1,90-1,89 Ga) também apresenta quimismo cálcio-alcalino de alto-K, mas possui composição mais expandida e ocorre associado a rochas vulcânicas co-genéticas (1,89 Ga, vulcânicas Jatapu) e a charnoquitóides (1,89 Ga, p.ex. Enderbito Santa Maria). As características petrográficas similares, aliadas à idade obtida em amostra do Granito Água Branca em sua área-tipo (1,90 Ga) permitem incluí-los numa

mesma suíte (Suíte Água Branca). O setor sul é caracterizado apenas por discretas e localizadas zonas de cisalhamento dúctil-rúpteis destrais com direção NE-SW.

Duas gerações de granitos tipo-A (Moderna, 1,81 Ga; Mapuera. 1,87 Ga) cortam o DUA, embora sejam mais freqüentes no setor sul. Foram identificados três tipos diferentes de metalotectos nesta região: a) mineralização de ouro hospedada em granitóides Martins Pereira-Serra Dourada (setor norte), b) columbita-tantalita aluvionar assentada em região dominada por granitóides Igarapé Azul (setor sul), e c) ametista associada a pegmatitos hospedados em granitos do tipo Moderna.

Os dados isotópicos dos sistemas do Nd (rocha total) e do Pb (feldspato) sugerem que todos os granitóides do DUA analisados são produtos de fontes crustais mais antigas, sejam elas de natureza mais siálica (de idade sideriana-arqueana) e/ou juvenil (de idade transamazônica), afastando a possibilidade de participação direta de magmas mantélicos na sua geração. Embora o mecanismo de subducção possa ter sido dominante no estágio inicial da evolução do setor norte do DUA, o magmatismo pós-colisional do setor sul teve significante participação na adição de material crustal. É possível que após o fechamento do oceano do sistema de arco Anauá (2,03 Ga) e após a orogenia colisional (1,97-1,94 Ga?), líquidos basálticos tenham sido aprisionados na base da crosta (mecanismo de *underplating*). Estes líquidos basálticos puderam então interagir com a crosta inferior, fundi-la e gerar, subsequentemente em ambiente pós-colisional, imenso volume de granitos e vulcânicas observados entre 1,90 e 1,87 Ga.

Quadro similar é identificado no domínio Tapajós (DT), sugerindo que ambos domínios (DUA e DT) fazem parte de uma mesma província (Ventuari-Tapajós ou Tapajós-Parima). Apesar dessas semelhanças, o estágio colisional parece não ter sido tão efetivo no DT, como atestam os escassos indícios de granitos tipo-S e de rochas de alto grau metamórfico.

ABSTRACT

This study focuses the granitoids of center-southern portion of Guyana Shield, southeastern Roraima, Brazil. The region is characterized by two tectono-stratigraphic domains, named as Central Guyana (GCD) and Uatumã-Anauá (UAD) and located probably in the limits of geochronological provinces (e.g. Ventuari-Tapajós or Tapajós-Parima, Central Amazonian and Maroni-Itacaiúnas or Transamazon). The aim this doctoral thesis is to provide new petrological and lithostratigraphical constraints on the granitoid rocks and contribute to a better understanding of the origin and geodynamic evolution of Guyana Shield.

The GCD is only locally studied near to the UAD boundary, and new geological data and two single zircon Pb-evaporation ages in mylonitic biotite granodiorite (1.89 Ga) and foliated hastingsite-biotite granite (1.72 Ga) are presented. These ages of the protholiths contrast with the lithostratigraphic picture in the other areas of CGD (1.96-1.93 Ga).

Regional mapping, petrography, geochemistry and zircon geochronology carried out in the UAD have showed widespread Paleoproterozoic calc-alkaline granitic magmatism. These granitoid rocks are distributed into several magmatic associations with different Paleoproterozoic (1.97-1.89 Ga) ages, structural and geochemical affinities. Detailed mapping, petrographic and geochronological studies have distinguished two main subdomains in the UAD. In the northern UAD, the high-K calc-alkaline Martins Pereira (1.97 Ga) and Serra Dourada S-type granites (1.96 Ga) are affected by NE-SW and E-W ductile dextral shear-zones, showing coexistence of magmatic and deformational fabrics related to heterogeneous deformation. Inliers of basement (2.03 Ga) crop out northeast of this area, and are formed by metavolcano-sedimentary sequence (Cauarane Group) and TTG-like calc-alkaline association (Anauá Complex). Xenoliths of metadiorites (Anauá Complex) and paragneisses (Cauarane Group) reinforce the intrusive character of Martins Pereira Granite. On the other hand, xenoliths of Martins Pereira and biotite-bearing enclaves are founded in the younger, undeformed, and SiO_2-rich Igarapé Azul Granite (1.89 Ga). This last and the high-K calc-alkaline Caroebe Granite (1.90-1.89 Ga, Água Branca Suite), including coeval volcanic rocks (1.89 Ga, Jatapu volcanics) and charnockitoids (1.89 Ga, e.g. Santa Maria Enderbite), crop out in the southern UAD. This subdomain is characterized only by local and slight NE-SW ductile-brittle dextral shear zones. A-type granites such as Moderna (ca. 1.81 Ga) and Mapuera (ca. 1.87 Ga) granites, cross cut both areas of UAD. The geological mapping also identified three main types of metalotects in this region. Gold mineralization is

observed in Martins Pereira-Serra Dourada granitoids (northern UAD); alluvial columbite-tantalite is related to Igarapé Azul granitoids (southern UAD); and amethyst is associated to pegmatites from Moderna A-type granites.

The Nd-Pb isotope data suggest that all granitoids of UAD were generated by reworking of older and previous crustal sources (sialic Rhyacian-Archean and/or juvenile Transamazonian origin) and mantle input is not problably a viable model. Although the dominant process may be subduction in the early stage of NUAD evolution, post-colisional magmatism may be a significant process in the production of new continental crust in the southern UAD. It is possible that, following oceanic closure in the Anauá arc system (2.03 Ga) and subsequent collisional orogeny (1.97-1.94 Ga?), underplated mantle melts (basalt liquids) were trapped below pre-existing lower crustal rocks of various compositions (*e.g.* granulites, metatonalites, amphibolites). The basalt liquids and subsequently melted lower crust could produced the immense volumes of granite (and volcanics) observed at 1.90-1.87 Ga. This geological picture is similar to the Tapajós Domain (TD) in the southern Amazonian Craton and suggest that both belong to the same province (Ventuari-Tapajós or Tapajós-Parima). Nevertheless, the scarcity of S-type granites and high-grade metamorphic rocks show that the collisional stage was not so evident in TD.

1 - INTRODUÇÃO

A região sudeste do Estado de Roraima constitui o foco desta pesquisa, cuja área selecionada perfaz um total de aproximadamente 3500 km^2 (**Fig. 01**). Embora esteja delimitada por coordenadas fixas, a área selecionada foi algumas vezes ao longo do estudo reduzida ou ampliada em função do objeto geológico a ser analisado. Esta área está localizada na porção centro-sul do Escudo das Guianas (**Fig. 01**, Gibbs & Barron, 1993) e abriga uma extensa floresta tropical. Parte dela possui um acesso relativamente fácil para os padrões amazônicos, sendo comuns as estradas não pavimentadas, que servem de ligação entre os diversos assentamentos rurais patrocinados pelo INCRA. Partindo-se da cidade de Manaus (AM) pode-se acessá-la através da rodovia federal (Manaus-Boa Vista: BR-174), que corta a área investigada na direção aproximada N-S. Os principais povoados da região são Vila Nova Colina, Rorainópolis, Martins Pereira, Vila Novo Paraíso, Vila Moderna, São Luis do Anauá, Serra Dourada, São João da Baliza, Caroebe e Entre Rios e constituíram importante suporte de apoio logístico.

O foco principal deste trabalho é o estudo geoquímico, isotópico e geocronológico dos granitóides do sudeste de Roraima, e tem como objetivo subsidiar a análise petrológica e litoestratigráfica, buscando contribuir assim com as propostas e modelos evolutivos regionais. Entretanto, apesar de ter atingido localmente nível de detalhamento (1:50.000), normalmente difícil de ser alcançado em estudos amazônicos em função da acessibilidade, do elevado grau de intemperismo e da escassez de afloramentos, o mapa geológico resultante engloba no geral informações na escala 1:250.000. Ou seja, longe de querer ter a pretensão de ser um trabalho de detalhe, a síntese apresentada aqui tem conotação essencialmente regional. Regiões montanhosas (parte noroeste, divisa com a Guiana), sem acessibilidade por estradas ou legalmente demarcadas, como áreas indígenas ou de proteção ambiental (partes leste e sudeste, divisa com o Pará), tiveram sua investigação restrita aos sensores remotos (JERS, Geocover, SRTM, Landsat 7, MDT e aerogeofísica).

Esta tese de doutorado é composta por cinco artigos submetidos (ou em vias de submissão) a revistas com corpo editoral, além desta parte introdutória, e dos capítulos referentes ao ferramental metodológico e as conclusões gerais. Uma listagem das referências bibliográficas utilizadas nestes capítulos é disponibilizada no final do volume, enquanto as referências bibliográficas relativas aos artigos acompanham os mesmos.

Do ponto de vista geológico, alguns trabalhos pioneiros levados a cabo em Roraima (*e.g.* Paiva 1929) foram decisivos para delinear os primeiros traços da geologia da região. Outros estudos pontuais retomados, sobretudo na primeira metade da década de 70, também constituem importantes fontes de consulta históricas (Arantes & Mandeta, 1970; Ramgrab & Damião, 1970; Ramgrab *et al.*, 1972; Braun, 1973; Bomfim *et al.*, 1974; Muniz & Dall´Agnol, 1974). Mas, somente a partir da década de 70, é que os levantamentos geológicos sistemáticos, baseados numa cartografia de natureza regional, foram iniciados no Estado de Roraima e também na porção nordeste do Estado do Amazonas. Estes foram conduzidos principalmente pelo convênio DNPM/CPRM (Santos *et al.*, 1974) e pelo projeto RADAMBRASIL (Montalvão *et al.*, 1975), culminando assim com o estabelecimento das primeiras grandes unidades geológicas.

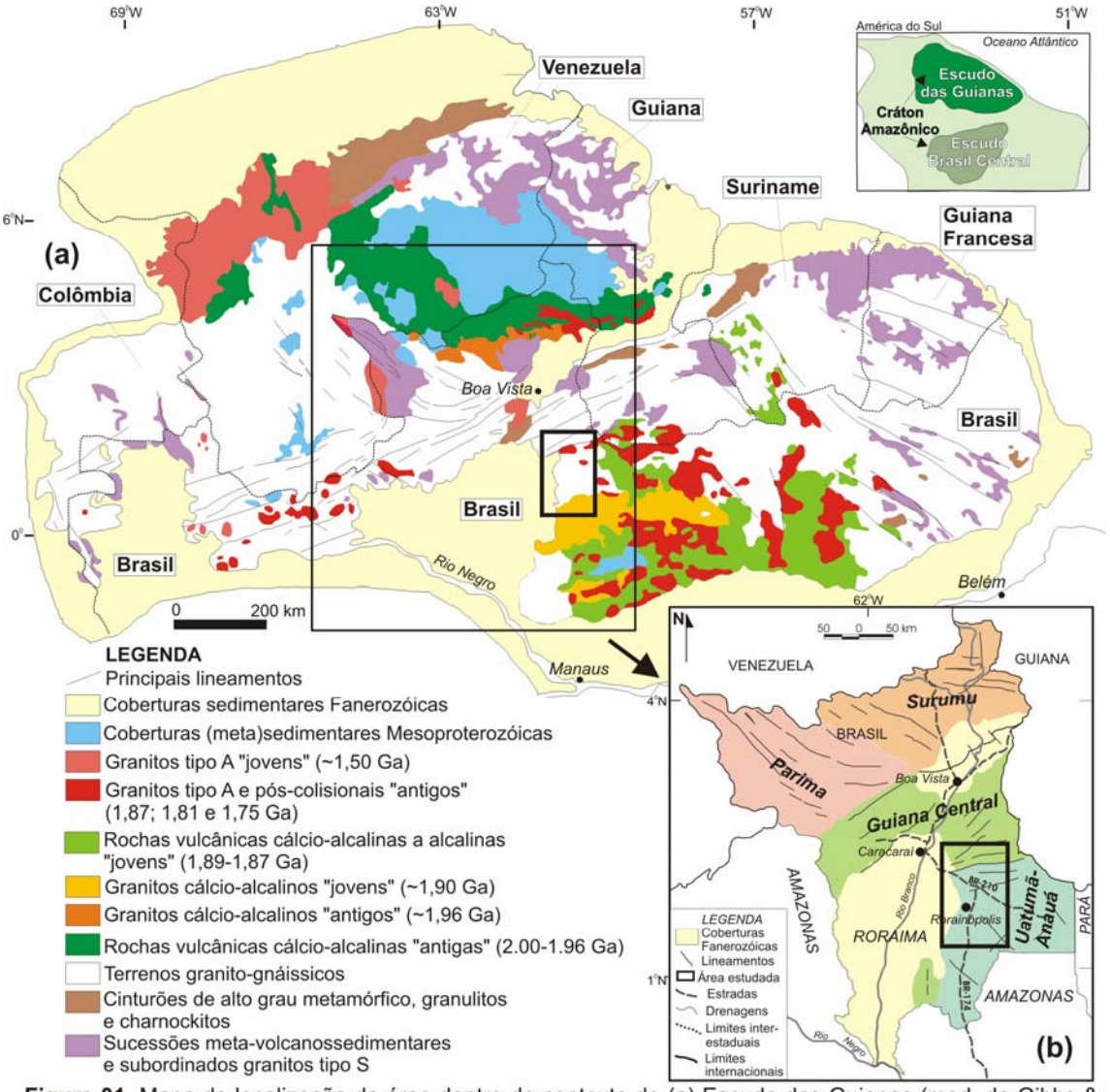

Figura 01. Mapa de localização da área dentro do contexto do (a) Escudo das Guianas (mod. de Gibbs & Barron, 1993) e dos (b) domínios tectono-estratigráficos de Roraima (Reis & Fraga, 2000; Reis *et al.*, 2003; mod. por CPRM, 2006).

Além dos trabalhos citados, diversos outros foram executados entre as décadas de 70 e 90 (Araújo Neto & Moreira, 1976; Melo *et al.*, 1978; Veiga Jr. *et al.*, 1979; Pinheiro *et al.*, 1981; Costi *et al.*, 1984). Mais recentemente grandes avanços no conhecimento geológico puderam ser sentidos através dos resultados de alguns projetos de mapeamento geológico executados na escala 1:500.000 (CPRM, 1999, 2000a) e alguns trabalhos de síntese e organização de dados nas escalas 1:2.500.000 e 1:1.000.000 (CPRM, 2003, 2004). Entretanto, em todo este conjunto bibliográfico nota-se uma grande carência (até mesmo ausência) de dados laboratoriais, principalmente aqueles de natureza geocronológica e isotópica. A maior parte deste escasso acervo de dados, relacionada especificamente ao sudeste de Roraima e nordeste do Amazonas, foi produzida e publicada apenas nos últimos dez anos (Sato & Tassinari, 1997; Almeida *et al.*, 1997, Santos *et al.*, 1997; Costi *et al.*, 2000; Macambira *et al.*, 2002; CPRM 2003; Valério, 2006), constituindo ainda um conjunto de informações limitado e de caráter pontual.

Estes trabalhos, sem exceção, sempre identificaram nesta porção do Escudo das Guianas grandes áreas de exposição granítica, sejam elas preservadas ou não por evento(s) deformacional(is) posteriores. A individualização dessas grandes massas continentais graníticas *senso lato* e o avanço do conhecimento cartográfico e geológico dos últimos anos, tornou possível também a sua separação em grandes domínios (Reis *et al.,* 2003) tectono-estrátigraficos e localmente sua subdivisão em "subdomínios" (Almeida *et al.,* 2002). Dois destes domínios ocorrem no sudeste de Roraima, sendo denominados de Guiana Central e Uatumã-Anauá.

O Domínio Guiana Central abrange apenas uma pequena parte da área estudada (porção nor-noroeste). O primeiro artigo aborda exatamente os litótipos graníticos e gnáissicos ortoderivados do Domínio Guiana Central junto ao limite com o Domínio Uatumã-Anauá. Além do contexto geológico local, são apresentadas duas idades pelo método Pb-Pb de evaporação de zircão em biotita granodiorito milonítico (1,89 Ga) e em hastingsita-biotita sienogranito com fluxo magmático (1,72 Ga), as quais contrastam com aquelas encontradas por outros autores no restante do domínio (1,96-1,93 Ga, Gaudette *et al.* 1996; Fraga, 2002; CPRM, 2003). Foliação NE-SW e mergulho subvertical associada a zonas de cisalhamento dúctil são as feições estruturais dominantes neste setor.

O restante do escopo da tese privilegia os granitóides do Domínio Uatumã-Anauá, os quais têm suas características de campo e petrográficas descritas num segundo artigo. Além do mapeamento faciológico dos corpos graníticos, neste artigo foi abordada também a relação entre

a granitogênese e as principais ocorrências minerais catalogadas na região. Este artigo reforça ainda a separação do Domínio Uatumã-Anauá em dois subdomínios distintos (norte e sul), ambos marcados por magmatismos com evolução petrológica e história tectono-estrutural distintas.

Estas diferenças foram reforçadas posteriormente pelo conjunto de dados geoquímico e geocronológico, este último utilizando-se os métodos de evaporação de Pb e U-Pb ID-TIMS em zircão. O terceiro artigo aborda exclusivamente o setor (ou subdomínio) norte do Domínio Uatumã-Anauá, onde dominam granitóides do tipo-S (Serra Dourada) e do tipo-I cálcio-alcalino com alto-K (Martins Pereira) mais antigos (1,97-1,96 Ga), ambos intrusivos em *inliers* do embasamento composto por associação do tipo TTG e sucessões meta-vulcanossedimentares de médio a alto grau (>2,03 Ga).

No quarto artigo, o mesmo procedimento foi adotado para tratar os granitóides do setor (ou subdomínio) sul. O panorama apresentado pelos dados geoquímicos e geocronológicos demonstrou amplo predomínio de uma granitogênese tipo-I cálcio-alcalina de alto-K mais jovem (1,90-1,89 Ga), representado pelos granitos Igarapé Azul e Caroebe, que, ao contrário do observado no setor norte, apresenta vulcanismo co-genético associado (1,89 Ga, vulcânica Jatapu). Charnoquito (1,89 Ga) e granitos tipo A (1,87 Ga) também têm seus resultados geocronológicos em zircão discutidos.

O quinto e último artigo apresenta um estudo isotópico baseado nos sistemas do Nd (rocha total) e do Pb (em feldspatos) que abrange os granitóides dos dois subdomínios. Os resultados reforçam uma origem eminentemente crustal, cujas fontes devem ser siálicas (de idade Sideriana-Arqueana) e/ou juvenis (de idade Rhiaciana-Transamazônica), com pouca ou nenhuma contribuição direta de magmas mantélicos. Estes dados isotópicos, associados às características de campo, petrográficas, geoquímicas e geocronológicas, permitem sugerir um modelo evolutivo baseado em 3 estágios distintos.

O primeiro estágio diz respeito à formação de um orógeno acrescionário relacionado ao sistema de arco Anauá (2,03 Ga), os quais devem estar associados a bacias do tipo retro-arco (?). Num segundo e subsequente estágio, a fase acrescionária dá lugar a um orógeno colisional, causando espessamento crustal, aumento da temperatura e geração por fusão parcial dos granitóides Martins Pereira e Serra Dourada (1,97-1,96 Ga). Este estágio colisional pode ter evoluído ao longo do tempo, tendo sido responsável por alçar tectonicamente as rochas granulíticas a níveis crustais mais rasos e pela geração de parte das rochs do Domínio Guiana

Central (1,94-1,93 Ga?). O último estágio diz respeito aos granitóides do setor sul do DUA. A ausência de eventos tectono-deformacionais, de remanescentes de crosta oceânica ou de coberturas meta-vulcanossedimentares relacionadas a ambiente de arco, sugere que o setor sul não deve ter evoluído a partir de um sistema acrescionário via subducção clássica (tipo-B). É possível que após o fechamento do oceano do sistema de arco Anauá (2,03 Ga) e após a orogenia colisional (1,97-1,94 Ga?), líquidos basálticos através do mecanismo de *underplating* tenham sido trapeados na base da crosta, fundindo esta última e gerando em seguida um grande volume magmas graníticos pós-colisionais do tipo I e do tipo A entre 1,90 e 1,87 Ga.

Ao final deste volume, em anexo, pode ser consultado o mapa geológico e de estações geológicas na escala 1:250.000, contendo ainda perfis esquemáticos que buscam traduzir o arranjo estrutural e a inter-relação entre as grandes unidades litoestratigráficas paleoproterozóicas.

2 - PROBLEMÁTICA GEOLÓGICA

Alguns aspectos da problemática geológica regional do ponto de vista litoestrátigrafico, estrutural, petrológico e evolutivo serão listados abaixo, tendo como foco os domínios tectono-estratigráficos (Guiana Central e Uatumã-Anauá) estudados e suas respectivas associações graníticas e gnáissicas.

2.1 - DOMÍNIO GUIANA CENTRAL (DGC)

- O DGC é composto por um terreno essencialmente granito-gnáissico afetado por ampla deformação regional, caracterizada por extensos lineamentos e uma ampla variação de protólitos, estilos de deformação e graus metamórficos. Esta variação, associada a escassez de dados, confere ao DGC um elevado grau de complexidade geológica.
- As rochas ortoderivadas, na sua maioria agrupadas na Suíte Metamórfica Rio Urubu (atual Complexo), atestam a existência de litótipos com significativa variedade textural (metagranitóides, milonitos e gnaisses) e importantes particularidades composicionais. Dados geoquímicos apontam protólitos com assinaturas distintas (*e.g.*. tipo A e tipo I) e com idades de cristalização variada (1,96 a 1,92 Ga; Gaudette *et al.*, 1996; Fraga, 2002; CPRM, 2003), tornando necessária uma investigação mais aprofundada na tentativa de identificar áreas ou domínios onde há predomínio espacial de cada tipo particular.
- Dentro deste intervalo de idade são descritas rochas charnoquíticas sin-cinemáticas (Suíte Serra da Prata) e granulíticas (Granulito Barauana). Ambas apresentam idades similares, apesar da escassez de dados não garantir uma perfeita correlação. No caso do Granulito Barauana (1,94 Ga), além do resultado geocronológico ser determinado a partir de zircões ígneos (idade do evento anatético?), o intrincado padrão estrutural indica deformação polifásica e a migmatização associada contrasta com o quadro apresentado pelos charnoquitos da Suíte Serra Prata (1,94-1,93 Ga; Fraga, 2002). A dificuldade de posicionamento deste evento metamórfico granulítico no tempo e o desconhecimento da sua evolução P-T-t trazem sérios prejuízos para entendimento da litoestratigrafia regional e dificulta a elaboração de um modelo evolutivo mais adequado para o DGC.
- O termos paraderivados encontra-se agrupados no Grupo Cauarane e na Suíte Metamórfica Murupu, localmente contendo tipos migmatíticos e bolsões leucograníticos (p.ex. região do Taiano) e granitos tipo S associados (p.ex. Granito Curuxuim). Apenas uma idade de

cristalização para esse magmatismo foi obtida (1,97 Ga, CPRM, 2003), sendo insuficiente para caracterizar um evento granítico tipo S em escala regional.

- A existência de granulitos e rochas paraderivadas de alto grau associadas com granitogênese tipo S, sugerem um modelo evolutivo colisional para o DGC (p.ex. Cordani & Brito Neves, 1982; Hasui *et al.*, 1984; Gibbs & Barron, 1993; Fraga & Reis, 1996; Costa & Hasui; 1997, CPRM, 1999; Santos *et al.*, 2000, 2006a,b). Esse provável orógeno colisional seria resultado de sucessivos eventos deformacionais que contribuiriam para o espessamento crustal, caso a evolução PT obedeça um sentido anti-horário (p.ex. Ellis, 1987; Brown & Dallmeyer, 1996; Brown, 2001). Entretanto, se desconhece quais massas continentais teriam colidido e em qual contexto geodinâmico.
- A complexidade geológico-estrutural do DGC demanda uma análise na sua proximidade com o DUA, delimitada pelo sistema de falhas do Ita. Seria este limite apenas um limite estrutural ou este limite separa realmente associações petrotectônicas distintas? Em termos composicionais e geocronológicos estes domínios poderiam ser correlacionados?

2.2 - DOMÍNIO UATUMÃ-ANAUÁ (DUA)

- O DUA é caracterizado por um amplo predomínio de granitóides em geral pouco deformados, variando de tipos foliados a norte até tipos isótropos a sul. Entretanto seu quadro litoestratigráfico está reduzido a um conjunto muito limitado de suítes graníticas (Suítes Igarapé Azul e Água Branca), cujas idades e petrogênese apresentam-se pouco esclarecidas.
- Apenas o setor norte é provido de algum resultado geocronológico, tendo apontado intervalo de idade entre 1,97 e 1,96 Ga para os granitóides (*e.g.* Almeida *et al.*, 1997; CPRM, 2003), intervalo este atribuido anteriormente às suítes Igarapé Azul (Faria *et al.*, 1999) e Água Branca (Araújo Neto & Moreira, 1976; Veiga Jr. *et al.*, 1979, Oliveira *et al.*, 1996), respectivamente. Posteriormente, este conjunto de granitóides passou a ser agrupado no Granito Martins Pereira (Almeida *et al.*, 2002) e a continuidade dos estudos geocronológicos apontou idades de cristalização menores (1,90-1,89 Ga) para granitos relacionados ao magmatismo Igarapé Azul e Água Branca no setor sul do DUA.
- Entretanto, a gênese destes granitóides permanece em discussão. De acordo com alguns autores (Oliveira *et al.*, 1996), a suíte Água Branca no DUA foi caracterizada como cálcio-

alcalina e tem como processo petrogenético dominante a cristalização fracionada (p.ex. plagioclásio e hornblenda). Processos alternativos como *magma mixing* e fusão parcial também foram recentemente postulados (Almeida & Macambira, 2003). Portanto, algumas questões permanecem: a) Qual seria o processo petrogenético (ou seria mais de um?) dominante na formação dos granitóides interpretados como Água Branca? b) Sua origem e fonte(s) seriam semelhantes aos dos demais granitóides gerados no mesmo intervalo de tempo?

- Parte da suíte Água Branca definida por Oliveira *et al.* (1996) com características químicas peraluminosas foi desmembrada dando origem à Suíte Igarapé Azul (Faria *et al.,* 1999). Além desses tipos peraluminosos à biotita, granitóides à muscovita, cordierita e silimanita aflorantes no setor norte do DUA foram adicionados a esta suíte. Entretanto, Sardinha (1999) através de análise petrográfica e de susceptibilidade magnética nos tipos peraluminosos da Suíte Igarapé Azul, não identificaram características compatíveis com granitos tipo S, sugerindo uma possível origem híbrida (fontes sedimentares e ígneas) para explicar sua geração. Posteriormente, Almeida *et al.* (2002) incluem os granitos tipo S *senso stricto* (à cordierita) sob a denominação Granito Serra Dourada, retirando-os da suíte Igarapé Azul. Estes granitos estão localizados na parte norte do DUA em associação com seqüências meta-volcanosedimentares do Grupo Cauarane, distantes cerca de 80 km da área-tipo dos granitóides Igarapé Azul. Mesmo tendo sido desmembrado, por apresentar localização e feições de campo e petrográficas distintas, teria o Granito Igarapé Azul gênese independente ou seria esta compatível com a dos demais granitóides da Suíte Água Branca?
- Além dos granitos de natureza cálcio-alcalina, o DUA (em especial o setor sul) apresenta abundantes intrusões de granitóides tipo A correlacionados ao magmatismo Madeira-Água Boa (~1,81 Ga) e Abonari-Mapuera (~1,87 Ga) (CPRM, 2003). Entretanto estas correlações são definidas na maioria das vezes apenas por critérios petrográficos (p.ex. presença ou não de hastingsita), carecendo maciçamente de dados geoquímicos e geocronológicos, devendo esta correlação regional (embora possível) ser avaliada com cautela;
- Além disso, o vulcanismo da região do rio Jatapu (andesitos e dacitos dominantes e quimismo cálcio-alcalino) está espacial (CPRM, 2000a) e temporalmente (Macambira *et al.*, 2002) associado à granitogênese do setor sul do DUA. Estas vulcânicas são tradicionalmente vinculadas ao magmatismo Mapuera nessa região e, portanto, foram

englobadas no Grupo Iricoumé numa tentativa de correlação com o vulcanismo aflorante no nordeste do Amazonas e distante cerca de 150 km (CPRM, 2000a). Entretanto, os dados preliminares existentes apontam uma maior possibilidade de vinculação do vulcanismo Jatapu com os granitóides Água Branca, abrindo espaço para o questionamento a respeito da existência de diferentes tipos vulcânicos, penecontemporâneos, vinculados a magmatimos distintos ("aluminoso ou alcalino tipo A" e "cálcio-alcalino tipo I"). Situação semelhante é descrita também no Grupo Iriri na região do Tapajós (*e.g.* CPRM, 2000b).

- A carência de dados que auxiliem no entendimento da cronologia dos eventos graníticos, além da sua petrogênese, tem complicado bastante a elaboração de modelos evolutivos para o DUA, gerando quase sempre controvérsia e debates acerca do tema. Um modelo evolutivo acrescionário baseado na existência de arcos magmáticos amalgamados sucessivamente a um núcleo estável arqueano tem sido o preferido da maioria dos autores (p.ex. Tassinari & Macambira, 1999, 2004; Santos *et al.,* 2006a,b). Proposta alternativa (*underplating*) é utilizada na região do Tapajós para explicar a geração dos granitóides mais jovens, inclusive aqueles de filiação cálcio-alcalina, considerados pós-colisionais (1,90-1,87 Ga; Lamarão *et al.*, 2002; Vasquez *et al.*, 2002).
- Tais dificuldades repercutem também fortemente na definição das rochas hospedeiras e metalotectos das mineralizações descritas na região, como por exemplo, as de ouro (garimpo Anauá) e ametista (Vila Moderna) primários e as de columbita-tantalita (bacia do Igarapé Azul) aluvionar (CPRM, 2000a).

Na visão dos modelos existentes, e de acordo com os diferentes limites entre Províncias propostos, a área em questão (DGC e DUA) pode estar englobada por duas (K´Mudku Shear Belt e Tapajós-Parima) ou três (Maroni-Itacaiúnas, Ventuari-Tapajós e Amazônia Central) províncias geocronológicas, demonstrando a sua real importância no contexto dos modelos evolutivos vigentes neste segmento do Escudo das Guianas. Apesar da inegável necessidade e aplicabilidade destes modelos, os mesmos têm como base um limitado acervo de dados geocronológicos e isotópicos (em que pesem o aporte recente de dados), devendo ser analisados, sobretudo do ponto de vista local, com prudência.

3 - MÉTODOS UTILIZADOS

A obtenção de dados desta pesquisa foi dividida basicamente em três fases principais: a) levantamento e revisão do acervo geológico existente, b) trabalhos de campo e c) laboratoriais. Estas fases, além dos recursos metodológicos empregados, são descritas a seguir.

3.1 - LEVANTAMENTO E REVISÃO DO ACERVO GEOLÓGICO PRÉ-EXISTENTE

Um conjunto significativo de dados e informações pré-existentes foi levantado e analisado, a maioria deles provenientes de instituições como o Serviço Geológico do Brasil e de algumas universidades que atuam na região. Entre as atividades desenvolvidas destacam-se:

a) Análise e atualização de bancos de dados de afloramento, petrografia, geoquímica e geocronologia existentes e sua comparação com os dados gerados nesta pesquisa;
b) Consulta e compilação de mapas geológicos pré-existentes, auxiliando na confecção do mapa geológico da área em questão;
c) Consulta a banco de amostras de rochas e de lâminas petrográficas, implicando na reanálise e reavaliação das unidades litoestratigráficas pré-estabelecidas;
d) Revisão da literatura geológica do tema específico (petrologia, geoquímica, geocronologia e evolução crustal) e da geologia regional, continuamente atualizada ao longo do período de execução da pesquisa.

3.2 - TRABALHOS DE CAMPO E CARTOGRAFIA GEOLÓGICA

Foram realizados mais de 2000 km de caminhamentos geológicos, sendo 180 km deles em vias fluviais, culminando com a análise e descrição de **352** afloramentos. Estes perfis geológicos permitiram, ao mesmo tempo, a individualização das grandes unidades litoestratigráficas (informações na escala 1:250.000) e o mapeamento faciológico dos granitóides Igarapé Azul, Caroebe e Martins Pereira (informações na escala 1:100.000), além da coleta sistemática de amostras de rocha (**447** amostras no total) e seleção posterior para estudos laboratoriais subseqüentes.

Este mapeamento geológico regional integrado teve o apoio cartográfico de sensores remotos como imagens (fundidas ou não) de radar (SRTM - Shuttle Radar Topography Mission; JERS - Japanese Earth Resources Satellite), de satélite (landsat TM7 - Thematic Mapper; Geocover) e aerogeofísicas (derivada 1ª., sinal analítico, contagem total e ternário U-Th-K). O

resultado final deste trabalho pode ser consultado nos anexos 1 (mapa de amostragem) e 2 (mapa geológico).

O acervo de dados materializados pelos mapas matriciais e vetoriais, assim como todo o conjunto de afloramentos e amostras de rocha coletadas encontram-se georrefrenciados e armazenados em plataforma SIG (ArcView 3.2a).

3.3 - TRABALHOS LABORATORIAIS

3.3.1 - Análise Petrográfica e Geoquímica Multielementar

A análise petrográfica detalhada de **234** seções delgadas (p.ex. classificação textural e composicional, descrição mineralógica, ordem aproximada de cristalização, caracterização de paragêneses minerais), integrada com as informações de campo, constituindo subsídio básico para a seleção de elenco de rochas representativo visando obtenção de análises químicas e geocronológicas.

Após avaliação petrográfica, os litótipos selecionados (**28** amostras) foram submetidos a análise química multielementar (rocha total) envolvendo método de espectrometria de massa por ICP (*Inductively Coupled Plasma*) para determinação de elementos maiores, perda ao fogo, e mais 42 elementos traços, incluindo elementos terras raras (ACMELAB, Vancouver, Canadá).

A preparação das amostras individuais seguiu o procedimento inicial de fragmentação *in situ* (no campo). No laboratório de preparação de amostras da CPRM (Manaus) estes fragmentos foram britados (britador de mandíbula), quarteados e pulverizados (moinho de porcelana) visando a obtenção de uma granulometria da ordem de 200 mesh.

3.3.2 - Análise Isotópica (Isótopos Radiogênicos)

As análises geocronológicas e isotópicas foram realizadas no laboratório da UFPA (Pará-Iso), utilizando-se dois espectrômetros (Finnigan MAT262 e VG Isomass 54). A preparação química das amostras também foi efetuada nas dependências do Pará-Iso, assim como parte da preparação dos minerais a serem analisados (CPRM e UFPA). A seguir serão listados os métodos empregados durante a fase analítica.

3.3.2.1 - Evaporação de Pb em monocristais de zircão

O método de evaporação Pb em monocristais de zircão em rotina no Pará-Iso (UFPA) segue o mesmo princípio do método desenvolvido por Kober (1986; 1987), utilizando-se um

espectrômetro de massa de ionização termal (Finningan MAT262). Segundo esses autores, admite-se que a estrutura cristalina do zircão resista o suficiente para preservar as informações isotópicas da época de sua cristalização até o presente.

Os concentrados contendo os cristais de zircão para análise foram obtidos após processo prévio de britagem, moagem e pulverização das amostras de rocha, e subseqüente peneiramento nas frações de 60, 80 mesh (rochas plutônicas) e 100 mesh (rochas vulcânicas). Na fase final de preparação os minerais passam por uma separação magnética (imã de mão e separador magnético isodinâ,ico Frantz) e por densidade (líquidos densos). Após o processo de preparação, procedeu-se a triagem manual dos cristais de zircão através do uso de lupa binocular. Os cristais selecionados têm ainda sua imagem capturada mediante equipamento fotográfico acoplado a microscópio petrográfico, visando assim uma melhor avaliação das condições físicas dos grãos. No total foram analisadas **16** amostras de rochas por este método.

O método de evaporação de Pb utiliza um duplo filamento de rênio, sendo um deles utilizado para o processo de evaporação, e o outro para a ionização. Os cristais escolhidos são depositados individualmente nos filamentos de evaporação, introduzidos no espectrômetro de massa e, então, gradativamente aquecidos em diferentes etapas de evaporação. Com o aumento da temperatura o Pb presente no retículo cristalino do mineral é liberado (ou evaporado), ficando retido no filamento de ionização (desligado durante a etapa de evaporação). As temperaturas de evaporação utilizadas são normalmente de 1450˚C, 1500˚C e 1550˚C (ou mais, como por exemplo, 1600˚C), mas pode se flexível e variável de acordo com as características dos zircões analisados, podendo ser efetuada até que se esgote todo o Pb do cristal.

Numa etapa seguinte, desliga-se o filamento de evaporação e inicia-se o aquecimento do filamento de ionização, em geral a temperaturas entre 950ºC e 1150ºC, dependendo do comportamento de cada amostra. Em seguida, as intensidades dos diferentes isótopos são medidas com um contador de íons na seqüência de massa 206, 207, 208, 206, 207 e 204, gerando um bloco com 8 razões $^{207}Pb/^{206}Pb$ em cinco varreduras, em um máximo de cinco blocos por etapa de evaporação. Para cada etapa de evaporação é obtida uma idade a partir da média das razões $^{207}Pb/^{206}Pb$. A idade de uma amostra é então calculada a partir da média das razões $^{207}Pb/^{206}Pb$ obtidas, em geral, nas etapas de maior temperatura de evaporação de cada grão analisado. Nesse cálculo, são utilizadas apenas idades similares, sendo descartados as etapas ou

grãos com idades inferiores (p.ex. perda de Pb após a cristalização, Vanderhaeghe *et al*., 1998) ou superiores (p.ex. zircão herdado proveniente de rochas mais antigas).

As razões $^{207}Pb/^{206}Pb$ são corrigidas por um fator de discriminação de massa de 0,12 ± 0,03% por u.m.a. (unidade de massa atômica), determinado a partir de análises repetidas do padrão de Pb NBS-982. Correções do Pb comum foram feitas através do modelo de evolução do Pb na Terra em dois estágios (Stacey & Kramers, 1975). As médias ponderadas e erros associados às determinações são calculados de acordo com Gaudette *et al*. (1998). Estimativas da razão Th/U inicial modelo foram feitas usando os valores atuais (medidos) corrigido do Pb comum da razão $^{208}Pb/^{206}Pb$ (Klotzli, 1999; Bartlett *et al*., 1998): $Th = [(^{208}Pb/^{206}Pb)/(\lambda Th * T)-1] + (^{208}Pb/^{206}Pb)$; $U = [(^{208}Pb/^{206}Pb)/(\lambda U * T)-1] + (^{208}Pb/^{206}Pb)$; $\lambda Th = 4.94750 * 10^{-12}$; $\lambda U = 1.55125 * 10^{-11}$.

A idade dos cristais de zircão é calculada a partir das duas equações de desintegração dos isótopos, ^{235}U em ^{207}Pb e ^{238}U em ^{206}Pb: (a) $^{207}Pb = {}^{235}U*(e^{\lambda 235*t} -1)$; (b) $^{206}Pb = {}^{238}U*(e^{\lambda 238*t} -1)$. Onde, λ - constante de desintegração; t – tempo decorrido entre o fechamento do sistema U-Pb e a geração dos isótopos filhos intermediários; $\lambda_{235} = 1,55125*10^{-10}$ e $\lambda_{238} = 9,8485*10^{-10}$ (Steiger & Jäger 1977). A partir dessas equações fundamentais obtém-se a razão $^{207}Pb/^{206}Pb$ em função da idade: (c) $^{207}Pb/^{206}Pb = 1/137,88*[(e^{\lambda 235*t} -1)/(e^{\lambda 238*t} -1)]$. Com base na equação (c), após a correção do Pb comum (^{204}Pb) e independente da determinação do U, é possível determinar a idade do mineral em questão (idade "aparente"). Em um diagrama de Concórdia, por exemplo, a idade obtida corresponde a uma determinada inclinação da discórdia, traçada entre o ponto na Concórdia e a origem dos eixos (vide item U-Pb em zircão por diluição isotópica).

No entanto, apesar da impossibilidade de avaliar se tal ponto é discordante ou concordante - uma vez que qualquer ponto de natureza experimental localizado na discórdia, definida pela equação, fornece a mesma idade "aparente" - a repetitividade dos resultados mostra estatisticamente que o método de evaporação de Pb em monocristais de zircão fornece idades próximas, senão similares à idade de cristalização da rocha obtidas por outros métodos (p.ex. Macambira & Scheller, 1994; Söderlund, 1996; Gaudette *et al.*, 1998).

Em suma o método de evaporação de Pb em monocristais de zircão possui, entre outras vantagens, a capacidade de fornecer resultados rápidos, de baixo custo e de boa qualidade analítica, pois não há necessidade de tratamento químico prévio dos cristais. Além disso, os valores absolutos mostram-se, em determinadas situações geológicas, similares ao obtidos em

outras metodologias, inclusive aquelas de alta resolução, conforme atestam, por exemplo, os resultados deste trabalho.

3.3.2.2 - U-Pb em zircão por diluição isotópica (ID-TIMS ou *Isotope Dilution–Thermal Ionization Mass Spectrometry*)

Duas amostras foram analisadas no Pará-Iso (espectrômetro de massa Finnigan MAT 262), utilizando-se o método U-Pb em zircão por diluição isotópica modificado por Krymsky (2002) a partir de Krogh (1973) e Parrish (1987). Os grãos de zircão após triagem inicial foram previamente pesados e submetidos à abrasão por 30 a 40 minutos sob pressão de 1,2 a 1,8 psi. Posteriormente foram lavados no ultra-som com metanol e uma mistura de HCl + HNO_3. Em seguida, as amostras foram dissolvidas em micro-cápsulas de teflon utilizando-se HF + HNO_3 e HCl em duas etapas distintas. Em cada etapa as micro-cápsulas foram colocadas em uma bomba de Parr e aquecidas em forno a temperatura a 245°C por cerca de 12 horas. Foi utilizado um traçador misto ^{235}U-^{205}Pb (10 μL) visando determinar as concentrações de urânio e chumbo.

O branco total medido foi de <30 pg para o chumbo e de <1 pg para o urânio e a repetição das análises no padrão NBS-982 forneceram as seguintes razões médias: $^{204}Pb/^{206}Pb$ = 0,0272145; $^{207}Pb/^{206}Pb$ = 0,467041; $^{208}Pb/^{206}Pb$ = 0,9998292. O fracionamento de massa para o Pb foi estabelecido em 0,12 u.m.a. e 0,18 u.m.a. para o UO_2, enquanto os cálculos foram efetuados através dos programas PbDat (Ludwig, 1993) e Isoplot (Ludwig, 2001).

3.3.2.3 - Sm-Nd em Rocha Total

Foram analisadas **22** amostras de rocha pelo método Sm-Nd em rocha total. O processo de preparação das amostras seguiu o mesmo procedimento adotado para a realização das análises geoquímicas multielementares, gerando alíquotas com cerca de 200 mesh. Os procedimentos listados a seguir seguem a rotina desenvolvida por Oliveira (2002).

A abertura química dessas amostras (aproximadamente 100 mg) foi alcançada utilizando-se sequencialmente os ácidos HNO_3, HF e HCl. Na solução resultante, o Sm e o Nd foram separados em duas etapas distintas através de cromatografia de troca iônica. A primeira etapa consistiu na separação dos ETR (Elementos Terras Raras) dos demais elementos, sendo a troca iônica realizada em colunas de teflon contendo resina Dowex 50Wx8. Nesta etapa são adicionados de modo sequencial HCl e HNO_3 em diferentes concentrações.

Na segunda etapa de separação cromatográfica, Sm e Nd são separados dos demais ETR através da combinação HNO_3 + metanol. A troca iônica é realizada em resina Dowex AG1x4 eluída com HNO_3-metanol, igualmente colocada em colunas de teflon. No processo analítico foi utilizado traçador misto ^{150}Nd-^{149}Sm, de modo a identificar as razões isotópicas e o conteúdo de Sm e Nd. Durante a análise espectrométrica (Finnigan modelo MAT 262) na etapa de evaporação o Sm e o Nd são depositados em filamentos de tântalo, enquanto que a ionização é feita com filamentos de rênio.

Os dados de Nd foram normalizados para a razão $^{146}Nd/^{144}Nd$ de 0,7219. Durante o período de análises, razões $^{143}Nd/^{144}Nd$ médias de 0,5118339 ± 9 e 0,5126335 ± 5 foram obtidas respectivamente para os padrões La Jolla e BCR-01 e as concentrações de Sm (6,56 ppm) e Nd (28,58 ppm) para este também foram obtidas. Os brancos totais medidos foram de 0,160 ng para o Sm e 0,587 ng para o Nd.

3.3.2.4 - Pb-Pb em feldspato

As amostras de feldspato analisadas foram obtidas, sobretudo de tipo porfiríticos, tendo sido inicialmente fragmentadas no próprio afloramento e posteriormente pulverizadas em laboratório em frações granulométrica entre 1 e 2 mm. Foram selecionadas alíquotas com 30 a 50 mg de um total de 14 amostras. O método Pb-Pb feldspato por lixiviação sequencial utilizado foi modificado de Ludwig & Silver (1977) e Housh & Bowring (1991).

Inicialmente os fragmentos de feldspato foram lavados com HCl e HNO_3 e em seguida lixiviados em várias etapas (de 3 a 8 etapas) com HF e HBr. A separação do Pb do restante dos outros elementos foi feita através da adição sequencial monitorada de HBr e HCl em colunas de teflon contendo resina Dowex AG1x8 (200-400 mesh). O Pb separado obtido foi depositado em filamento de rênio com uma combinação de 1µL de sílica gel + H_3PO_4 e a composição isotópica das amostras foi medida no espectrômetro de massa VG ISOMASS 54E com monocoletor.

Foram considerados para o estudo isotópico os resultados das etapas de lixiviação com menor interferência de Pb estranho (em geral as últimas), e que conseqüentemente refletem o Pb inicial da rocha no tempo de sua formação. Os brancos totais medidos variaram de 0,27 a 1,40 ng e o tratamento dos dados e construção dos diagramas foi feito utilizando-se o programa Isoplot (Ludwig, 2001).

4 - ARTIGOS CIENTÍFICOS

Os resultados obtidos ao longo desta pesquisa encontram-se materializados nos artigos submetidos (ou em fase de submissão) aos periódicos especializados. Estes serão apresentados a seguir, iniciando pelos litótipos do domínio Guiana Central, próximos ao limite com o Domínio Uatumã-Anauá, passando pelos resultados geológicos, petrográficos, geoquímicos e geocronológicos obtidos nos granitóides deste último domínio, culminando com a assinatura isotópica dos sistemas do Nd e Pb da crosta no sudeste de Roraima e elaboração de modelo de evolução geológica.

Vale lembrar que os artigos submetidos, ou em vias de submissão, disponíveis neste volume representam o momento atual do conhecimento geológico, podendo ser objeto de reavaliação e modificação até o momento final de sua publicação.

4.1 - New geological and single-zircon Pb-evaporation data from the Central Guyana Domain, southeastern Roraima, Brazil: Tectonic implications for the central region of the Guyana Shield

Marcelo E. Almeida[1,2*], Moacir J.B. Macambira[2], Sérgio de C. Valente[2]

[1]CPRM – Geological Survey of Brazil, Av. André Araújo 2160, Aleixo, CEP 69060-001, Manaus, Amazonas, Brazil

[2] Isotope Geology Laboratory, Center of Geosciences, Federal University of Pará, Rua Augusto Corrêa s/n, Guamá, CEP 66075-110, Belém, Pará, Brazil

[3] Geosciences Department, Federal University Rural of Rio de Janeiro, Km 7 – BR-465, Seropédica, CEP 23890-000, Rio de Janeiro, Brazil

* Corresponding author; ph.: +55-92-2126-0357, fax: +55-92-2126-0319, e-mail adress: marcelo_almeida@ma.cprm.gov.br

ARTIGO SUBMETIDO AO CORPO EDITORIAL DA REVISTA

"*JOURNAL OF SOUTH-AMERICAN EARTH SCIENCES*"

Words: summary (73), resumo (173), abstract (159), body text (6455, including references), figure captions (316) and table caption (138). Total: 1 table and 9 figures.

RESUMO
Hornblenda e biotita (meta) granitóides, milonitos, leucognaisses e granulitos, com estruturas preferencialmente NE-SW e E-W, ocorrem no Domínio Güiana Central (DGC), próximo do limite com o Domínio Uatumã-Anauá (DUA), região central do Escudo das Güianas, sudeste de Roraima (Brasil). Os resultados fornecidos pelo método evaporação de Pb (zircão) apontam idades de 1.724 ± 14 Ma e 1.889 ± 4 Ma, respectivamente, para hornblenda-biotita monzogranito foliado (granito sincinemático) e granodiorito milonítico (Suíte Água Branca?). Desta forma, sugere-se, além dos eventos tectônicos marcados pelo intervalo de 1,94-1,93 Ga (pós-Transamazônico) e 1,35-0,98 Ga (K´Mudku), a existência de outro evento tectônico em torno de 1,72 Ga (Evento Itã), provavelmente relacionado, nesta região, à evolução do Supercontinente Columbia. Além disso, os dados sugerem que o Sistema de Falhas do Itã pode ter sido gerado ou reativado pós-1,89 Ga e os protólitos ortoderivados estudados nesta porção do DGC não se mostraram correlacionáveis àqueles de áreas vizinhas (cujas idades variam de 1,96 a 1,93 Ga), indicando a necessidade de revisão das propostas litoestratigráficas e dos limites entre os domínios conhecidos.
Palavras-chave: Guiana Central, Roraima, Escudo das Guianas, Geologia, Geocronologia

ABSTRACT
Metagranitoid rocks, mylonites, leucogneisses and granulites occur in the Central Guyana Domain (CGD) near the Uatumã-Anauá Domain (UAD) boundary, southeastern Roraima (Brazil). These rocks are oriented along NE-SW and E-W trends and dip to NW and N, respectively. Single-zircon Pb evaporation results yielded 1724 ± 14 Ma and 1889 ± 3 Ma for a syn-kynematic foliated hornblende-biotite monzogranite and a granodioritic mylonite, respectively. These results point to a new tectonic event (Itã Event) in the area in addition to the 1.94-1.93 Ga (late- to post-Transamazonian) and the 1.35-0.98 Ga (K´Mudku) thermal tectonic events. This new event may be related, at least locally, with the evolution of the Columbia Supercontinent. In addition, the Itã Fault System is younger than 1.89 Ga (granodioritic mylonite age), contrasting with the Barauana high grade lineament and 1.94 Ga polydeformed rocks, pointing to the needs of a major revision of lithostratigraphic column currently proposed for the CGD as well as the CGD and UAD boundary.
Keywords: Central Guyana, Roraima, Guyana Shield, Geology, Geochronology

INTRODUCTION

The Central Guyana Domain (Reis and Fraga, 2000a, Reis *et al.,* 2003) or K´Mudku Shear Belt (Santos *et al.,* 2000, 2006a,b) has been considered as the most important structural feature in central-western Guyana Shield (**Fig. 1**). This major NE-SW-trending tectonic domain extends over northernmost Brazil and large areas within Guyana and Surinam. This domain has been interpreted as a collisional orogen (Hasui *et al.*, 1984; Gibbs and Barron, 1993), although no relicts of oceanic crust have been recorded. Nevertheless, some orthogneisses (calc-alkaline crustal sources) that occur within this domain display typical subduction-related geochemical signatures. According to CPRM (1999), this calc-alkaline signature is not directly associated with mantle partial melting processes during the subduction-related, pre-collisional setting but may reflect an origin associated with an ensialic mobile belt (Cordani and Brito Neves, 1982). As such, CPRM (1999) suggested that the Central Guyana Domain was generated during an event in late- to post-Transamazonian times (2.26-2.01 Ga; Santos *et al.*, 2003a) previous to an oblique

movement along the limits of two colliding lithospheric plates (*ie.* intrancontinental orogenic belt). Further tectonic events, such as the K´Mudku (Guyana) or the Nickerie (Surinam) ones, would have erased the records of igneous and metamorphic processes that took place within the present northern and southern limits of the Central Guyana Domain.

This paper presents geological data for granulites, orthogneisses, mylonites and (meta)granitoid rocks and new zircon Pb geochronological data for mylonites and granitoid rocks from the Central Guyana Domain in southeastern Roraima (Brazil). The aim of this study is to put constraints in the southern limits of this domain as well as in chronology of the major igneous, metamorphic and tectonic events that took place in the central portion of the Guyana Shield.

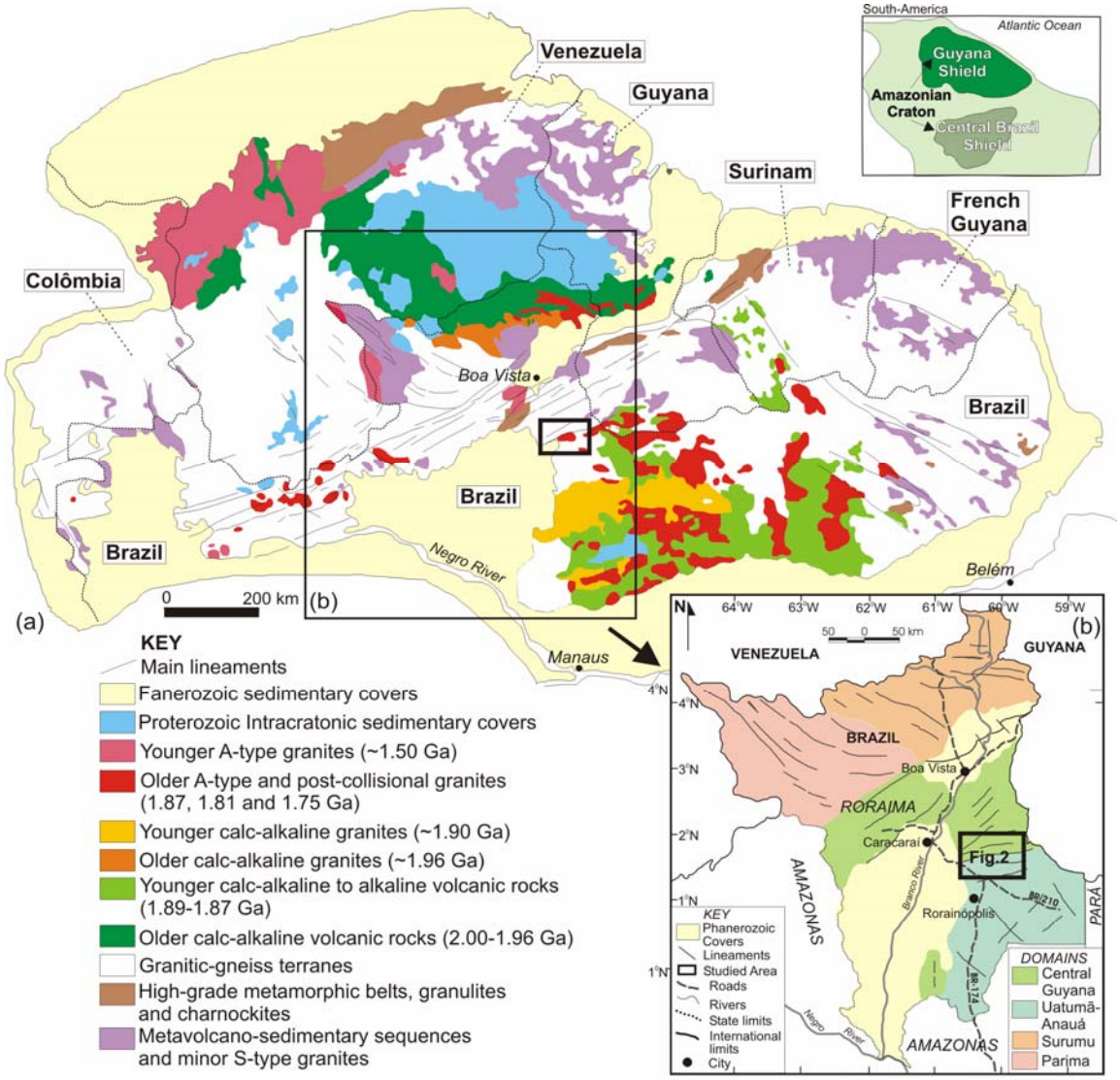

Fig. 1. Geological sketch map of the Guyana Shield (modified from Gibbs and Barron, 1993) and the location of the study area showing southeastern Roraima. The lithostructural domains of Roraima after Reis and Fraga (2000a), Reis *et al.* (2003) and CPRM (2006) are also shown.

GEOLOGY OF SOUTHEASTERN RORAIMA

Two main lithostructural domains can be depicted within southern Roraima state in Brazil: the Central Guyana and Uatumã-Anauá (**Fig. 1**, Reis *et al.,* 2003; CPRM, 2006). These two domains correspond, respectively, to the K`Mudku Shear Belt and the Tapajós-Parima Belt (Santos *et al.*, 2000, 2006a,b). According to CPRM (1999), the Central Guyana Domain (CGD) is essentially a shear belt composed of orthogneisses, metagranitoid rocks and minor granulites with a strong NE-SW and E-W foliation (**Fig. 2**) dipping steeply to NW. Although the age and the evolution of this shear-belt still remain uncertain, Fraga and Reis (1996) reinforced that its main tectonic feature can be related to oblique thrust structures associated with a NW to SE main stress component. The most common rocks that crop out in southern CGD are orthogneisses, mylonites, metagranitoid rocks and subordinated lenses of granulites and leucogneisses (the Rio Urubu Metamorphic Suite; CPRM, 1999) associated with low- and medium- (Cauarane Group, CPRM, 1999) to high-grade (Murupu Suite, Luzardo and Reis, 2001) metavolcanosedimentary sequences and S-type granites (Curuxuim Granite, CPRM, 1999).

The Uatumã-Anauá Domain (UAD) is characterized by E-W to NE-SW-trending lineaments and a metamorphic basement (**Fig. 2**) comprising TTG-like metagranitoid rocks and orthogneisses, with metamafic to metaultramafic enclaves (Anauá Complex) that have been associated with an island arc environment (Faria *et al.*, 2002). Metavolcano-sedimentary rocks (Cauarane and Murupu related rocks) have also been associated with the basement rocks within this area (CPRM, 2000).

The TTG and the supracrustal basement sequences were intruded by S-type (the Serra Dourada Granite) and I-type calc-alkaline (Martins Pereira) granites (**Fig. 2**). Altogether, they comprise the 1.96 to 2.03 Ga Martins Pereira-Anauá granitic terrain (Almeida *et al.,* 2002) or the Northern Uatumã-Anauá Domain (NUAD, Almeida and Macambira, 2006 in press) taken as the "deformed" portion of the UAD.

Younger, unmetamorphosed and undeformed sequences are represented by the Caroebe (Água Branca Suite, **Fig. 2**) and Igarapé Azul calc-alkaline granitoid rocks. These granitoid rocks were associated with the Iricoumé volcanic rocks (Macambira *et al.,* 2002; Reis *et al.,* 2000) and subordinate charnockitoid plutons (Almeida *et al.*, 2002), and altogether comprise the "undeformed" Igarapé Azul-Água Branca granitic terrain (Almeida *et al.,* 2002) located on the Southern Uatumã-Anauá Domain (SUAD, Almeida and Macambira, 2006 in press). Several A-

type granite plutons (**Fig. 2**) are represented by the Moderna and Madeira (1.81 Ga), and Mapuera and Abonari (1.87 Ga) granites that occur within the SUAD as well as the NUAD.

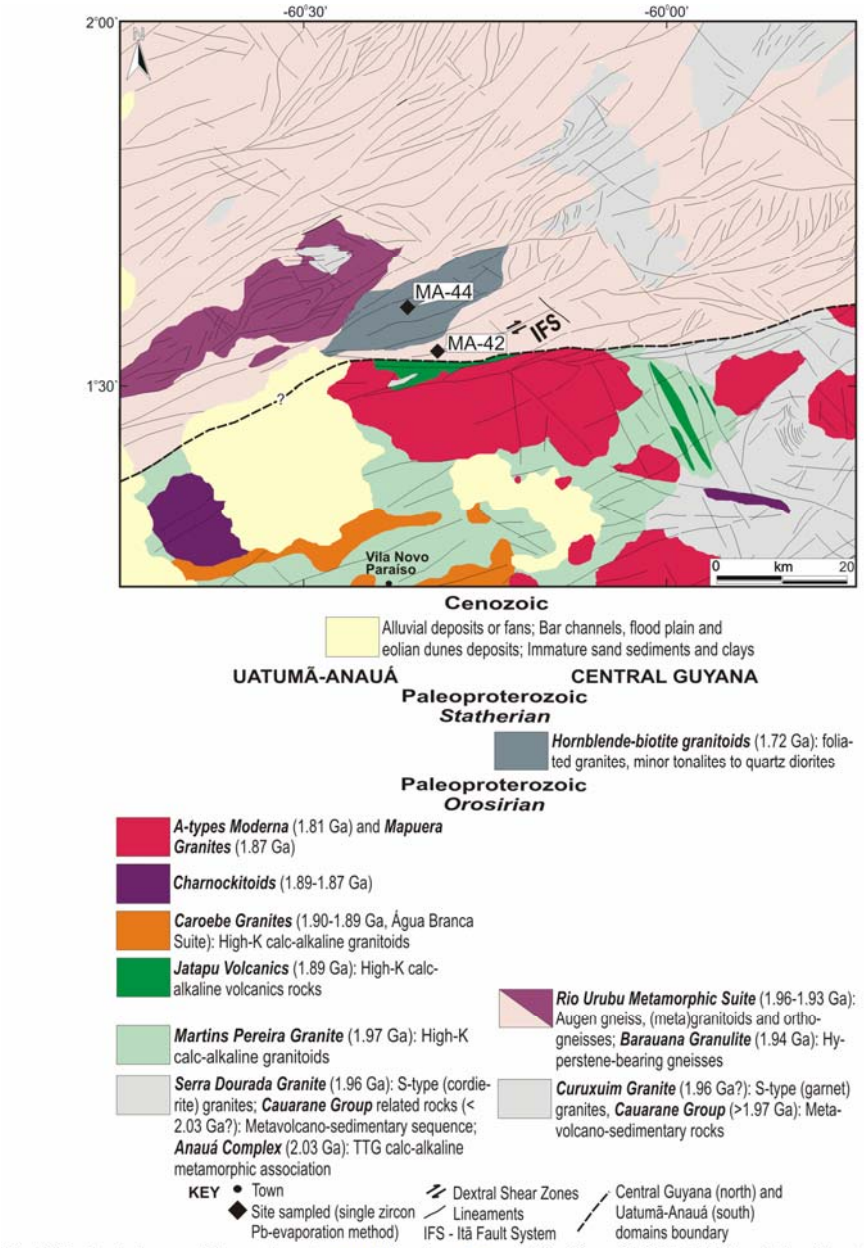

Fig. 2. Geological map of the southeasternmost Roraima state modified from CPRM (2000) and Almeida *et al.* (2002).

THE CENTRAL GUYANA DOMAIN (CGD) IN SOUTHEASTERN RORAIMA

Metagranitoid, high-grade metamorphic rocks and other metamorphic and granitoid rocks found within the CGD nearby the UAD were grouped into the Rio Urubu Metamorphic Suite (CPRM, 1999, 2000; Reis and Fraga, 2000b). The hypersthene-bearing gneisses (Barauana granulite), leucogneisses (Igarapé Khalil leucogneiss), epidote-rich biotite mylonites (Itã mylonite) and hornblende-biotite gneisses to foliated granitoid rocks of this suite were mapped

along the southern limit of the CGD as part of the present work and will be described in the following sections.

The Barauana granulite

In the Guyana Shield (**Fig. 1**; Gibbs and Barron, 1993), high-grade metamorphic domains have been reported in the Imataca Complex (Venezuela), Kanuku (Guyana) and Bakhuis Mountains and the Coeroeni area (Surinam), as well as in eastern Amapá and central-southern Roraima (Brazil). Among these terrains, the Barauana Mountain represents a major granulite-facies domain (CPRM, 2000) in southern Roraima (**Fig. 2**).

The Barauana Mountain is constituted of banded, polydeformed, locally migmatized hypersthene-bearing gneisses with charnockite and enderbite composition. The migmatites show stromatic, agmatic and schollen structures and anathectic mobilizates **(Fig. 3)**. Thin section analyses have shown that igneous textures have not been preserved in these rocks. The gneisses show grano-lepidoblastic textures and a mineral assemblage composed of plagioclase, alkali feldspar, hypersthene, quartz and brownish red biotite, as well as opaque minerals (mainly magnetite), apatite and zircon **(Fig. 4a-b)**.

Fig. 3. Outcrop of banded charnockitic gneiss (Barauana Granulite) with enderbitic enclaves as lenses (MA-207 outcrop).

On a regional scale, the NE-SW foliation (N60^{o}E/80^{o}NW to N35^{o}E/90^{o}) dips steeply to NW and is generally parallel to the Central Guyana Domain regional trend. Similar trends are observed in the Kanuku Mountains, in Guyana (McConnel, 1962; Gibbs and Barron, 1993), as well as in the Bakhuis and Coeroeni Mountains, in Surinam (Bosma *et al.,* 1983; De Roever *et al.,* 2003).

Rims of zircon crystals in the Barauana granulite (anatexite sample) were interpreted as having a late metamorphic origin (1818 Ma, U-Pb SHRIMP), while the cores (1942 +7/-8 Ma, U-

Pb SHRIMP) have been related to an anatectic event (igneous zircons) under granulitic conditions (CPRM, 2002, 2003).

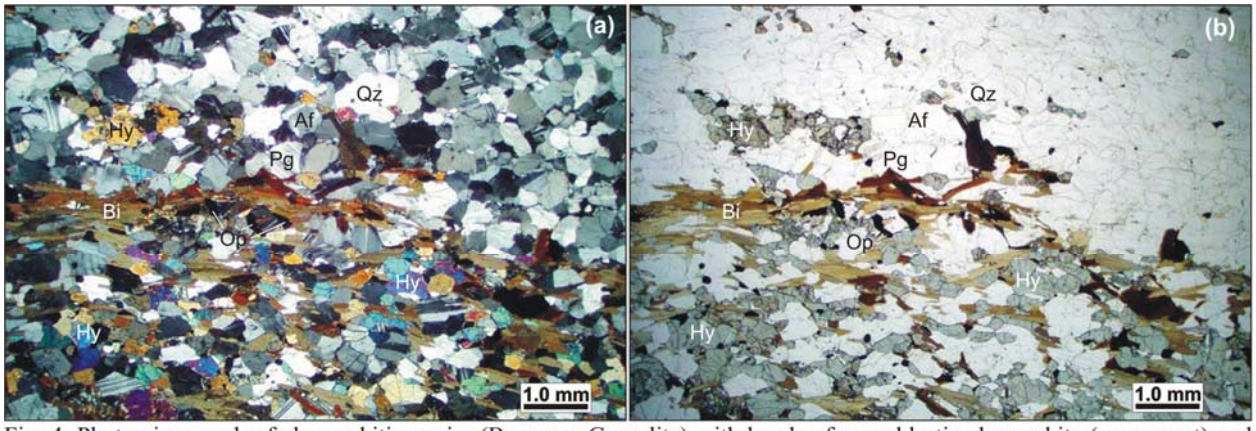

Fig. 4. Photomicrograph of charnockitic gneiss (Barauana Granulite) with bands of granoblastic charnockite (uppermost) and granolepidoblastic enderbite (lowermost). (a) Cross-polarized light and (b) plane-polarized light (1.25x). Af. Alkali feldspar; Bi. Biotite; Hy. Hypersthene; Op. Opaque minerals; Pg. Plagioclase; Qz. Quartz.

Syn-kynematic charnockites within the Central Guyana Domain (the Serra da Prata Suite, as reviewed by Fraga, 2002) yielded ages between 1934 Ma and 1943 Ma (single-zircon Pb evaporation). These ages are in general agreement with those of the Barauana granulite and all these data suggest an important granulite-facies metamorphism and a pyroxene-bearing rocks generation (anhydrous) event. Nevertheless, despite their (Barauana and Serra da Prata) similar ages, a coeval origin is yet debatable. Those ages are also younger than the Amapá (2.06-2.05 Ga; Lafon *et al.,* 2001; Avelar *et al.,* 2003) and Bakhuis (2.07–2.05 Ga and ~2.15 Ga inherited component; De Roever *et al.,* 2003) ultra high-temperature (UHT) granulites, revealing an elapsed time (140 to 110 m.y.) related to diachronous high-grade metamorphic episodes in the Guyana Shield **(Fig. 1)**.

The Itã mylonite and the Igarapé Khalil orthogneiss

The Itã mylonite crops out near the RR-170 road, within the Itã Fault System, located on the boundary of the CGD and the UAD (**Fig. 2**). According to CPRM (2000), older mylonites are observed to the north, in the Lua Mountains (Vila Vilhena region), associated with fine grained biotite gneisses. The Itã mylonite is a medium- to fine-grained augen gneiss with granodioritic to monzogranitic compositions and abundant ovoid feldspar porphyroclasts (**Fig. 5**). These rocks display a N75^{o}E to N70^{o}E S-C foliation (dextral sense), steep NW dipping, showing mineral lineation (quartz ribbons and locally stretched feldspar) with medium-angle rake (N80^{o}W/60^{o}).

Fig. 5. Granodioritic to monzogranitic biotite mylonite showing a conspicuous mylonitic foliation with ENE-WSW trend and NW steep dip (MA-42 outcrop).

The mineral assemblage is mainly composed of alkali feldspar, plagioclase and biotite (and associated epidote). Epidote, quartz and feldspars are very fine-grained, recrystallized and, locally, quartz and feldspar display a granoblastic texture (**Fig. 6a-b**). Other accessory minerals are sphene, allanite, opaque minerals (mainly magnetite), apatite and zircon. Secondary minerals are chlorite and subordinate sphene. Relict igneous textures are scarcely observed in these rocks.

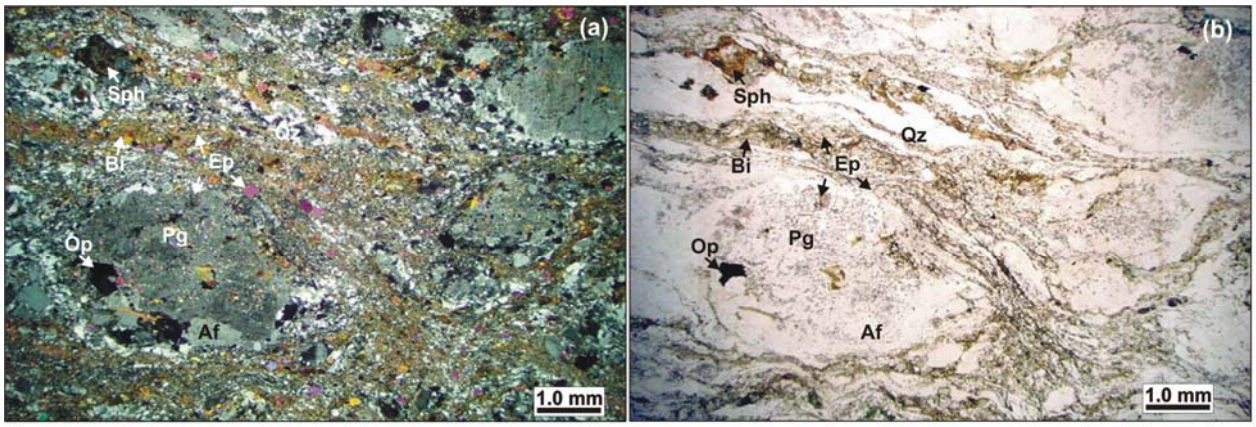

Fig. 6. Photomicrograph of porphyritic granodiorite with mylonitic texture and conspicous foliation as well as a local fine-grained matrix and feldspar relicts. (a) Cross-polarized light and (b) plane-polarized light (1.25x). Af. Alkali feldspar; Bi. Biotite; Ep. Epidote; Op. Opaque minerals; Pg. Plagioclase; Qz. Quartz; Sph. Sphene.

The Igarapé Khalil orthogneiss crops out along the BR-174 highway being leucocratic, equigranular, fine-grained and granolepidoblastic to locally protomilonitic textures with subvertical N80^{o}E to N50^{o}E foliation. The mineral assemblage is composed essentially of quartz, microcline and plagioclase. Biotite and muscovite occur subordinately in this rock (~3 vol. %). Accessory minerals are represented by allanite, primary epidote, zircon, apatite and opaque minerals. Epidote, chlorite and sericite occur as secondary minerals.

The amphibole-biotite foliated granitoid rocks

Biotite-amphibole gneisses and (meta)granitoid rocks are commonly found between the Barauana Mountain and the Itã Fault System, along RR-170 road (**Fig. 2**). They comprise an ENE-WSW trending, lens-shaped body with slightly higher radiometric features than ohers orthogneisses in the CGD (CPRM, 1984). These rocks display a steeply NW dipping, N70^{o}E to N75^{o}E conspicous foliation (**Fig. 7**) and a S-C fabric as a result of emplacement under amphibolite-facies conditions and a dextral transpressive regime.

Fig. 7. Foliated hornblende-biotite granite ("streaky gneiss") showing strong foliation and mineral lineation by magma flow (MA-44 outcrop).

These rocks are grey in color and equigranular alghouth some display a few porphyry surrounded by a fine-grained groundmass. They have monzogranitic to syenogranitic and rarely granodioritic to quartz dioritic compositions. Biotite and amphibole (hastingsite) are the main mafic minerals and sphene, allanite, epidote, opaque minerals, apatite and zircon constitute the main accessory phases. These rocks display a mineral lineation defined by the preferred orientation of amphibole and feldspars (mainly plagioclase), as well as a foliation given by the subparallel orientation of biotite flakes.

With the exception of these structures, these granitoids seem to be strain-free or low strained rocks, suggesting deformation in the presence of a melt phase (*ie.* syn-kynematic emplacement). There is no evidence for dynamic and/or stactic conspicuous recrystallization and the igneous mineralogy and textures are well preserved (**Fig. 8a-b**). Only a few quartz grains show local grain reduction (dynamic recrystallization) and ondulatory extinction. On the other hand, CPRM (1999, 2000) have pointed out to highly deformed (solid state) rocks of similar compositions in the Barauana River and Lua Mountain, suggesting that the granite had been at least partially crystallized at the time of deformation. According to CPRM (1999), these rocks

(Barauana River and Lua Mountain) can be correlated with the Kusad and Corentyne (augen) gneisses in southern Guyana.

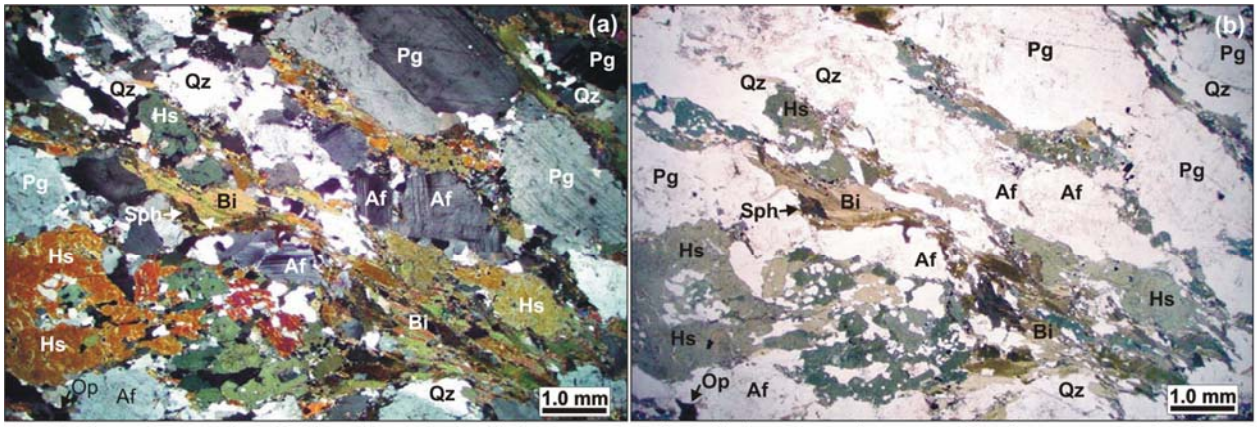

Fig. 8. Photomicrograph of foliated hornblende-biotite monzogranite with low dynamic recrystallization texture and relicts of igneous texture. (a) Cross-polarized light and (b) plane-polarized light (1.25x). Af. Alkali feldspar; Bi. Biotite; Hs. Hastingsite; Op. Opaque minerals; Pg. Plagioclase; Qz. Quartz; Sph. Sphene.

In general, the petrographic and field features described for foliated amphibole-biotite granitoid rocks suggest that they were at least partially molten by the time of their emplacement in an active tectonic zone. According to Brown and Solari (1999), sheet-like, concordant to subconcordant granites can be related with magma transport along planar conduits through an AFZ (apparent flattening zone). These authors also state that the S > L fabrics observed in these granites record the apparent flattening-to-plane strain, mainly in the case of "straight" belts.

SINGLE-ZIRCON Pb-EVAPORATION GEOCHRONOLOGY

Analytical procedures

Two to twenty kg of each rock sample were crushed (milled to 60-80 mesh), sieved, washed and dried out for at least 12 hours. Heavy mineral fractions were obtained by water-mechanical and dense liquid concentrations, and processed under a hand magnet and a Frantz Isodynamic Separator. As much as possible, only alteration-free zircon grains were selected for analysis (zircon descriptions are presented below). In order to remove impurities, the zircon concentrates were washed with HNO_3 at 100^o C (10 minutes), taken to an ultrasound cube (5 minutes) and finally washed under twice-distilled H_2O. After drying, the concentrates were observed under the petrographic microscope and the zircon grains were selected by hand-picking.

Selected grains were then tied in Re-filaments and charged into a Finnigan MAT262 mass spectrometer for isotope analysis. The $^{207}Pb/^{206}Pb$ ratios were corrected for a mass discrimination factor of 0.12% ± 0.03 $a.m.u^{-1}$, determined by repeated measurements of the NBS-982 Pb-standard. The $^{207}Pb/^{206}Pb$ ratio was measured during three evaporation steps at temperatures of

1450°C, 1500°C, and 1550°C. The average $^{207}Pb/^{206}Pb$ ratio obtained in the highest evaporation temperature was taken for age calculations. The data were acquired using the ion-counting system of the instrument. The Pb signal was measured by peak hopping in the 206, 207, 208, 206, 207, 204 mass order along 10 mass scans, defining one block of data with 18 $^{207}Pb/^{206}Pb$ ratios. Outliers were eliminated using the Dixon's test. The $^{207}Pb/^{206}Pb$ ratio average of each step was determined on the basis of five blocks, or until the intensity beam was sufficiently strong for a reliable analysis. The ages were calculated with 2 sigma error and common Pb correction from values derived from the Stacey and Kramers (1975) model in the blocks in which the $^{204}Pb/^{206}Pb$ ratios were lower than 0.0004. The statistic levels are express by the USD or Unified Standard Deviation (square root of MSWD – Mean Standard Weigth Deviation). The data were processed using the DOS-based *Zircon* shareware (Scheller, 1998).

Samples, results and interpretation

Two fresh rock samples representing the Itã granodioritic mylonite (MA-42: 1° 32`50``N; 60° 19` 48``W) and the foliated biotite-amphibole monzogranite (MA-44: 1° 36´ 35´´N; 60° 21´ 36´´W) were collected and analyzed by the single-zircon Pb evaporation method.

Six zircon crystals from sample MA-42 (porphyritic granodioritic mylonite) were analyzed, but only three (crystals #2, #4 and #5) gave results that led to age calculations. The zircon grains were non-magnetic, euhedral, pale yellow to brown, transparent to translucent crystals showing few inclusions and fractures. The crystals showed preserved faces, were 220-360 μm in length and bear a length:width ratio of around 3:1 to 2:1.

The analyzed crystals yielded a mean age of 1889 ± 4 Ma (**Fig. 9a, Table 1**) and the $^{207}Pb/^{206}Pb$ individual ages obtained at higher temperature steps were rather uniform, showing values between 1889 ± 4 Ma (grain #2) and 1892 ± 2 Ma (grain #5). Thus, the 1889 ± 4 Ma was interpreted as the crystallization age and the time of emplacement of the igneous protholith of the MA-42 mylonite. The data obtained at the lower temperature steps were eliminated from the calculation of the mean age for being less consistent, yielding younger ages (1828 ± 10 Ma to 1879 ± 8 Ma) and higher $^{204}Pb/^{206}Pb$ ratios. The Th/U ratios ranged uniformily from 0.51 to 0.58 (**Table 1**), similarly to the other magmatic rocks.

The mean age (1889 ± 4 Ma) is, at least, 20 Ma to 75 Ma younger than that of other igneous protholiths from ortogneisses and mylonites commonly related to the Rio Urubu Metamorphic Suite in the CGD, such as the Vilhena mylonite (1950 ± 9 Ma; magmatism age and 1879 ± 4 Ma;

metamorphism age) according to U-Pb zircon SHRIMP analysis (CPRM, 2002, 2003). Locally, younger mylonites were described to the south, in the Alalaú and Jauaperi rivers (CPRM, 2000), yielding 1869 ± 9 Ma by the U-Pb zircon SHRIMP method (Santos *et al.*, 2002; CPRM, 2003). On the other hand, igneous ages of around 1.89 Ga to 1.90 Ga were only observed nearby the Igarapé Dias (CPRM, 2003) and Caroebe granitoid rocks (Água Branca Suite), both in the southeast of Roraima. Thus, despite the difficulties concerning the protholith identification, the 1.89 Ga age in association with the mineral assemblage (*e.g.* biotite, epidote and calcic zoned plagioclase), as well as granodioritic to monzogranitic compositions, suggest that the igneous protholith of the Itã mylonite is a granitoid rock related with the Caroebe (Água Branca Suite) magmatism.

Twenty zircon crystals collected from sample MA-44 (foliated hornblende-bearing granite) were analysed, but only five crystals (crystals #6, #8, #12, #14 and #18) gave results that led to age calculations (**Fig. 9b, Table 1**). The zircon grains were euhedral crystals with 180-370 μm in length and length:width ratio of around 2:1. They showed slightly rounded vertices and slightly irregular faces. The grains were pale yellow, transparent to translucent, with several inclusions and fractures, being also weakly magnetic.

The analyzed crystals yielded a mean age of 1724 ± 14 Ma (**Fig. 9b**), but the $^{207}Pb/^{206}Pb$ individual ages obtained under the 1450°C to 1500°C evaporation steps were not homogeneous, giving high errors, and values between 1707 ± 16 Ma (grain #8) and 1755 ± 10 Ma (grain #12). Thus, this mean age is interpreted as a minimum crystallization age of the analyzed crystals. Grain #3 gave the oldest age (1827 ± 23 Ma) and has been taken as an inherited crystal. This age is similar to those obtained for the Moderna Granite (Santos *et al.,* 1997). The Th/U ratios ranged from 0.36 to 0.50 (**Table 1**), resembling those found in magmatic systems.

The mean minimum crystallization age of 1.72 Ga is at least 200 Ma younger than those of the other orthogneisses and metagranitoid rocks correlated to the Rio Urubu Metamorphic Suite, in the CGD (Gaudette *et al.,* 1996; Fraga, 2002). These foliated granitoid rocks yielded Nd model age (T_{DM}) of 2.07 Ga and $\varepsilon_{Nd(i)}$ = -0.91 (T_{cryst} 1724 Ma), suggesting probably juvenile (depleted) crustal protholiths with late-Transamazonian ages and no appreciable mantle contribution.

Ar-Ar ages on a muscovite crystal from sheared granitoid rocks within the UAD, close to the boundary with GCD, yielded values between 1656 ± 4 Ma and 1710 ± 4 Ma (CPRM, 2002), recording an important cooling event (near 350°C Ar-Ar blocking temperature; Hodges, 1991) in

southeastern Roraima. These Ar-Ar ages are in good agreement with the foliated amphibole-biotite granite age (1724 ± 14 Ma).

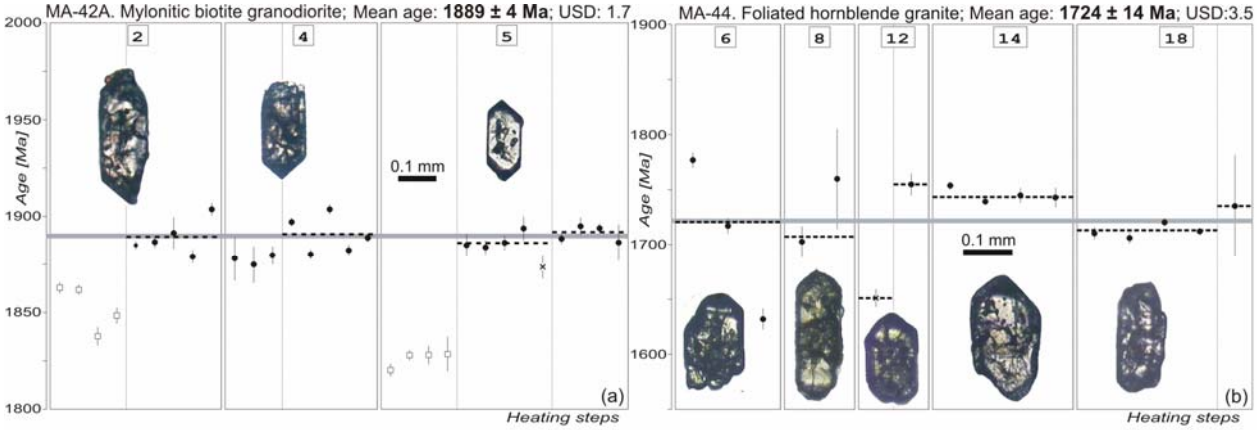

Fig. 9. Single zircon Pb-evaporation age diagram of (a) mylonitic biotite granodiorite and (b) foliated hornblende-biotite monzogranite. Filled circle - accepted blocks for age calculation. Square - blocks not used due to their higher or lower values of the $^{207}Pb/^{206}Pb$ ratio in relation to the mean. X - rejected blocks due to show $^{204}Pb/^{206}Pb > 0.0004$. Crystal numbers are indicated (see table 1).

TECTONIC SETTING OF THE CENTRAL GUYANA DOMAIN IN SOUTHEASTERN RORAIMA: A DISCUSSION ON THE COLLISIONAL MODEL

The CGD has been taken as a major collisional orogen by many authors in the past years (*e.g.* Cordani and Brito Neves, 1982; Hasui *et al.,* 1984; Gibbs and Barron, 1993; Fraga and Reis, 1996; Costa and Hasui, 1997; CPRM, 1999; Santos *et al.,* 2000, 2006a,b). In general, granulite terranes in collisional orogens follow a clockwise PT path (*e.g.* Ellis, 1987; Brown and Dallmeyer, 1996; Brown, 2001) and their exposure has been attributed to isostatic rebound as a result of crustal thickening during one or more tectonic events (Ellis, 1987).

Nevertheless, many granulite terranes seem to have been too hot to have formed during continental collision and may represent thickened hot orogens associated with underplating processes within other tectonic settings (Collins, 2002a). For instance, granite generation in the Paleozoic Lachlan Folded Beld and Circum Pacific regions was assisted by heat advected from the mantle during protracted regional extension under low- to medium-P granulite facies (Collins, 2002b). These recent studies have pointed out that some granulites are unlikely to be related with collisional tectonics. Furthermore, collisional orogens develop when an ocean closes between continental blocks. However, many orogenic systems have not experienced collision, being called accretionary (*e.g.* Coney, 1992), with the Lachlan orogen as an excellent example.

Even in classic collisional orogens, such as the European Alps and Himalayas, coeval granites and granulites are rare. On the contrary, broad zones of anomalously high heat flow occur in extensional and accretionary orogens, leading to widespread silicic magmatism, as in the

Basin and Range Province, the Taupo volcanic zone, the Circum-Pacific orogens and some Precambrian terranes (*e.g.* Central Australia, Collins, 2002a). These orogens are characterized by voluminous granitic batholiths associated with repeated extensive-compressive events and are underlain by granulites. The latter are only scarcely exposed (*e.g.* Ducea, 2001) because crustal thickening rarely occurs. Even so, granulite xenoliths found in modern basalts in those orogens point out to the existence of a granulite basement (*e.g.* Chen *et al.*, 1998). All these data suggest that granulites would have been more commonly associated with accretionary orogens than collisional ones. Nevertheless other authors have argued that the association of granulite terranes with repeated tectonic events has only local application, as in the case of the Lachlan orogen, since it does not apply to other UHT and HP granulite terrains undoubtly related to collisional tectonics as in the case of the Variscan, Brasília and Grenville orogens (Brown, 2003).

CRUSTAL AMALGAMATION PROCESSES IN GLOBAL-SCALE: THE SUPERCONTINENT THEORY AND ITS APPLICATION IN THE CENTRAL GUYANA DOMAIN

The Amazonian Craton evolution has been closely associated with those of the Laurentia and Baltic cratons in the northern hemisphere (*e.g.* Rogers, 1996). Lateral magmatic arc accretion seems to have taken place in those cratons in Statherian times (Paleoproterozoic: 1.80-1.60 Ga) as well as taphrogenic events within the pre-Statherian domains (*e.g.* Atlantica) onto the Columbia supercontinent (Rogers and Santosh, 2002; Brito Neves and Almeida, 2003). These Statherian events are well-recorded in the Yavapai (1.75-1.68 Ga; *e.g.* Duebendorfer *et al.*, 2001) and Cheyenne (1.78-1.75 Ga; *e.g.* Sims and Stein, 2003) orogens within Laurentia as well as in the Rio Negro (1.82-1.52 Ga) and Rondonian-Juruena (1.82-1.54 Ga) provinces within the Amazonian Craton (Santos *et al.*, 2000, 2006a).

In the central portion of Guyana Shield in southern Roraima (**Fig. 1**), granitic magmatism is unknown at Statherian times but could be represented by the syn-kynematic biotite-amphibole granite emplaced around 1.72 Ga. In the western region of the Guyana Shield (Rio Negro Province), Statherian rocks are represented by arc-related meta-quartz diorites with ~1.70 Ga (Tassinari *et al.*, 1996, zircon U-Pb ID TIMS;), ~1.75 Ga A-type granites (Almeida *et al.*, 2006, single-zircon Pb evaporation) and ~1.79 Ga basement rocks (CPRM, 2003, zircon U-Pb SHRIMP). In the Central Brazil Shield, the Rondonian-Juruena (1.82-1.54 Ga) province has also

tonalities, granites and coeval volcanic rocks with 1.79-1.75 Ga, all formed in an arc-related tectonic setting (Alto Jauru orogen, Pinho *et al.*, 1997; Geraldes *et al.*, 2001).

This apparent scarcity of Statherian magmatism in Roraima contrasts with that of Laurentia and Baltic cratons. For instance, in Laurentia zircon geochronology studies (U-Pb SHRIMP and ID TIMS) gave ages of 1721 ± 15 Ma for the Boulder Creek Batholith (Premo and Fanning, 2000) as well as 1737 ± 4.3 Ma, 1719 ± 1.2 Ma and 1721 ± 2.4 Ma for the Big Wash, Diana and Chloride granites, respectively (Duebendorfer *et al.,* 2001). Similarly, ~1.70 Ga syntectonic plutons (Wet Mountains; Siddoway *et al.,* 2000) and muscovite and biotite Ar-Ar plateau ages (~1.74-1.70 Ga) obtained for samples from the western Trans-Hudson Orogeny (Heizler *et al.,* 2000) closely resemble those in southeastern Roraima obtained for foliated hornblende-biotite granites (1.72 Ga, this paper) and muscovite in shear zones (1.71-1.66 Ga, CPRM, 2002). These data suggest the involvement of the southeastern Roraima lithosphere in the Columbia supercontinent evolution at least on a local scale.

Accretionary and collisional orogens have also affected the Amazonian, Laurentia and Baltica cratons in late Mesoproterozoic times. Geochronological Rb-Sr and K-Ar data (Pinson *et al.,* 1962; Barron, 1966; Priem *et al.,* 1971; Amaral, 1974; Lima *et al.,* 1974; Basei and Teixeira, 1975; Tassinari, 1996) showed that the K'Mudku Event (Barron, 1966) took place within the 1.35-0.98 Ga range as confirmed by recent Rb-Sr and Ar-Ar geochronology (Fraga, 2002; Santos *et al.*, 2003b). As such, the K'Mudku Event in Roraima can be interpreted as a far-field, intracratonic effect of the continental collision (Grenvilian-Sunsas belt) within the southwestern and northwestern Amazonian Craton. This event can also be related with the Rodinia supercontinent amalgamation, according to Brito Neves (1999).

In summary, the data presented in this section strongly suggest that the central portion of the Guyana Shield (northern Amazonian Craton) in southeastern Roraima has played a role in repeated episodes of supercontinental amalgamation as follows: the Atlantica (1.94-1.93 Ga, late-collisional stage?), Columbia (1.72-1.66 Ga, accretionary stage?) and Rodinia (1.35-0.98 Ga, collisional stage) supercontinents. According Fraga (2002), the older (~1.94 Ga) and younger (~1.20 Ga) tectonic events are related to higher (> 450^{o} C) and lower (< 300^{o} C) temperatures, respectively. CPRM (1999) suggest also an intermediate tectonic event in age (not dated), named as Macuxi event, this last one probably related to the 1.72-1.66 Ga interval age (this paper).

DISCUSSION AND CONCLUSIONS

The gneissic and granitic rocks of the Central Guyana Domain in the studied area have been distinctly affected by varied tectono-metamorphic processes. These rocks comprise at least three of metaigneous types: 1) high-grade polydeformed granulitic rocks, with local retrograde low- to medium-grade metamorphism (Barauana granulite), 2) leucogneisses and mylonitic rocks affected by a single deformation phase under medium- to high-grade metamorphism (the Itã Mylonite), and 3) low-grade metamorphic metagranitoids rocks and hornblende-biotite granites with flow foliation and relict igneous fabric (foliated hornblende-biotite granite).

These rocks were originally taken as part of the Rio Urubu Metamorphic Suite (CPRM, 1999) but the ages obtained for the Itã mylonite (1.89 Ga) and the foliated hornblende-biotite granites (1.72 Ga) are respectively 40-70 m.y and 200-240 m.y. younger than those obtained for the magmatic protoliths found elsewhere within the Rio Urubu Metamorphic Suite (1.93 to 1.96 Ga). In addition, these rocks show post-1.89 Ga deformation episodes. The new geochronological data presented in this paper indicate that the proposed lithostratigraphy for the CGD has to be reviewed, including its boundary with the Uatumã-Anauá Domain.

The 1.72 Ga, syn-kynematic granitic magmatism (foliated hornblende-biotite granitoid rocks) in the Central Guyana Domain as well as the Ar-Ar ages (~1.70 Ga, CPRM 2002) suggest that a tectonic event intermediate in age to the late- to post-Transamazonian (~1.94 Ga, Fraga, 2002) and K´Mudku (~1.20 Ga, Fraga, 2002) events took place in the studied area. On a preliminary basis, we suggest this to be named as the Itã Event, althought it may be related with the Macuxi event as seen elsewhere (CPRM, 1999).

The K'Mudku Event has been detected in the area by means of several Rb-Sr (*e.g.* Amaral, 1974; Santos *et al.,* 2000; Fraga, 2002), K-Ar (*e.g.* Amaral, 1974) and a few Ar-Ar (Santos *et al.*, 2003b) ages. These ages are normally related with low to medium temperatures shear zones, locally associated with pseudotachyllites (CPRM, 1999).

The 1.89 Ga Itã granodioritic mylonite is similar in composition with the Caroebe granitoids (Água Branca Suite), located in the Uatumã-Anauá Domain. The mylonite is probably the result of greenschist to epidote-amphibolite metamorphism of the Caroebe granite within wide shear zones. Thus, the E-W Itã Fault System post-dates these 1.89 Ga granitoids (K´Mudku or Itã related events?), and the location of the Central Guyana Domain boundaries also need to be reviewed. This boundary probably would be displaced to the north and placed along the older NE-SW Barauana lineament trends, but detailed mapping and new geophysical airbone data are still needed to test for this hypothesis.

In conclusion, the data presented in this paper indicate that the structural pattern observed in the Central Guyana Domain in southeastern Roraima can be related with a main 1.94-1.93 Ga tectonic event affected by decoupled younger events (reactivation processes), namely the Itã (1.72-1.66 Ga) and the K'Mudku (1.35-0.98 Ga) events. This implies that the studied area has been subjected to major, recurrent tectonics in the the Central Guyana Domain, possibly related with continental-scale processess in the central portion of the Guyana Shield.

Acknowledgements

Special thanks to E. Klein (CPRM-Geological Survey of Brazil), P. A. Rolando and M. A. Galarza (Pará-Iso/UFPA) for help during Pb analytical procedures, and N. J. Reis (CPRM-Geological Survey of Brazil) and Claúdio de M. Valeriano (Rio de Janeiro State University) for relevant discussions. The authors are also grateful to CPRM-Geological Survey of Brazil, FINEP (CT-Mineral 01/2001 Project) and the Isotope Geology Laboratory of UFPA (Federal University of Pará) for support during the field and laboratorial work. Thanks also to R.A. Fuck (University of Brasília), C. Cingolani (La Plata University) and M.Remus (Federal University of Rio Grande do Sul) for the critical analysis of the manuscript.

References

Almeida, M.E., Macambira, M.J.B. 2006. Geology and petrography of Paleoproterozoic granitoids from Uatumã-Anauá Domain, central region of Guyana Shield, southeastern Roraima, Brazil. Revista Brasileira de Geociências, in press.

Almeida, M.E, Macambira, M.J.B., Faria, M.S.G. de. 2002. A Granitogênese Paleoproterozóica do Sul de Roraima. *In*: SBG, Cong. Bras. Geol., 41, João Pessoa, Anais..., pp. 434. (in Portuguese)

Almeida, M.E, Reis, N.J., Macambira, M.J.B. 2006. Evolução geológica do oeste do Escudo das Guianas com base em novos dados Sm-Nd e evaporação de Pb de zircão. *In*: SBG, Cong. Bras. Geol., 43, Aracaju, Anais..., pp. 30. (in Portuguese)

Amaral, G. 1974. Geologia Pré-Cambriana da região Amazônica. Tese de livre docência, Instituto de Geociências, Universidade de São Paulo, São Paulo. 212 pp. (abstract in English).

Avelar, V.G., Lafon, J.M., Delor, C., Guerrot, C., Lahondère, D. 2003. Archean crustal remnants in the easternmost part of the Guyana Shield: Pb-Pb and Sm-Nd geochronological evidence for Mesoarchean versus Neoarchean signatures. *Géologie de la France*, 2-3-4, 83-99.

Barron, C.N. 1966. Notes on the Stratigraphy of Guyana. In: Guyana Geol. Conf., 7, Paramaribo, *Proceed*., 6, 1-28.

Basei, M.A.S., Teixeira, W. 1975. Geocronologia do Território de Roraima. In: Conf. Geol. Interguianas, 10, Belém, *Anais*, 453-473. (in Portuguese)

Bosma, W., Kroonenberg, S.B., Maas, K., De Roever, E.W.F. 1983. Igneous and Metamorphic Complexes of the Guyana Shield in Suriname. *Geol. Mijnbouw*, 62, 241-254p.

Brito Neves, B.B. 1999. América do Sul: quatro fusões, quatro fissões e o processo acrescionário andino. *Rev. Bras. Geoc.*, 29, 379-392. (abstract in English).

Brito Neves, B.B., Almeida, F.F.M. 2003. A Evolução dos Cratons Amazônico e São Francisco comparada com o dos seus homólogos do hemisfério norte – 25 anos depois. In: SBG-Núcleo Norte, Simp. Geol. Amaz., 8, Manaus. CD-ROM. (in Portuguese).

Brown, M., 2001. From microscope to mountain belt: 150 years of petrology and its contribution to understanding geodynamics, particularly the tectonics of orogens: *Journal of Geodynamics*, 32, 115–164.

Brown, M. 2003. Hot orogens, tectonic switching, and creation of continental crust: Comment and reply. *Geology*, 31 (6), 9.

Brown, M., Dallmeyer, R.D. 1996. Rapid Variscan exhumation and role of magma in core complex formation: Southern Brittany metamorphic belt, France: Journal of Metamorphic *Geology*, 14, 361–379.

Brown, M, Solari, G.S. 1999. The mechanism of ascent and emplacement of granite magma during transpression: a syntectonic granite paradigm. *Tectonophysics*, 312 (1), 1-33.

Chen, Y.D., O'Reilly, S.Y., Griffin, W.L., Krogh, T.E. 1998. Combined U-Pb dating and Sm-Nd studies on lower crustal and mantle xenoliths from the Delegate basaltic pipes, southeastern Australia. *Contrib. Miner. Petrol.*, 130, 154–161.

Collins, W.J., 2002a. Nature of extensional accretionary orogens. *Tectonics*, 21 (4), 6-1.

Collins, W.J., 2002b. Hot orogens, tectonic switching, and creation of continental crust. *Geology*, 30, 535–538.

Coney, P.J., 1992. The Lachlan belt of eastern Australia and circum-Pacific tectonic evolution: *Tectonophysics*, 214, 1–25.

Cordani, U.G., Brito Neves, B.B. 1982. The Geologic Evolution of South America during the Archean and Early Proterozoic. *Rev. Bras. Geoc.*,12 (1-3), 78-88.

CPRM. 1984. Projeto Aerogeofísico Rio Branco. Convênio CPRM/DNPM, Rio de Janeiro, volumes I e II. (in Portuguese).

CPRM. 1999. Programa Levantamentos Geológicos Básicos do Brasil. *Roraima Central, Folhas NA.20-X-B e NA.20-X-D (integrais), NA.20-X-A, NA.20-X-C, NA.21-V-A e NA.21-V-C (parciais)*. Escala 1:500.000. Estado de Roraima. Manaus, CPRM, 166 p. CD-ROM. (abstract in English)

CPRM. 2000. Programa Levantamentos Geológicos Básicos do Brasil. *Caracaraí, Folhas NA.20-Z-B e NA.20-Z-D (integrais), NA.20-Z-A, NA.21-Y-A, NA.20-Z-C e NA.21-Y-C (parciais)*. Escala 1:500.000. Estado de Roraima. Manaus, CPRM, 157 p. CD-ROM. (abstract in English).

CPRM. 2002. Workshop de campo: Manaus (AM)-Pacaraima (RR) Transect. GIS Brasil Program. CPRM, Manaus, Internal Report. (in Portuguese)

CPRM. 2003. Programa Levantamentos Geológicos Básicos do Brasil. *Geologia, Tectônica e Recursos Minerais do Brasil: sistema de informações geográficas - SIG*. Rio de Janeiro: CPRM, 2003. Mapas Escala 1:2.500.000. 4 CDs ROM. (abstract in English)

CPRM. 2006. Programa Integração, Atualização e Difusão de Dados da Geologia do Brasil: Subprograma Mapas Geológicos Estaduais. *Geologia e Recursos Minerais do Estado do Amazonas*. Manaus, CPRM/CIAMA-AM, 2006. Mapa Escala 1:1.000.000. Texto explicativo, 148p. CD ROM. (abstract in English)

Costa, J.B., Hasui,Y. 1997. Evolução Geológica da Amazônia, in Costa, M.L., and Angelica, R.S. (eds), Contribuições à Geologia da Amazônia. FINEP, Sociedade Brasileira de Geologia, Núcleo Norte, Belém, Brazil, 1, pp. 15-90. (abstract in English)

De Roever, E.W.F., Lafon, J-M., Delor, C., Cocherie, A., Rossi, P., Guerrot, C., Potrel, A. 2003. The Bakhuis ultrahigh-temperature granulite belt (Surinam): I. petrological and geochronological evidence for a counterclockwise P-T path at 2.07-2.05 Ga. *Géologie de la France*, 2-3-4, 175-205.

Ducea, M. 2001. The California arc: Thick granitic batholiths, eclogitic residues, lithospheric-scale thrusting and magmatic flare-ups: *GSA Today,* 11 (11), 4–10.

Duebendorfer, E.M., Chamberlain, K.R., Jones, C.S. 2001. Paleoproterozoic tectonic history of the Cerbat Mountains, northwestern Arizona: Implications for crustal assembly in the southwestern United States. *Geol. Soc. Amer. Bull.*, 113 (5), 575–590.

Ellis, D.J. 1987. Origin and evolution of granulites in normal and thickened crusts: *Geology*, 15 : 167–170.

Faria, M.S.G. de, Santos, J.O.S. dos, Luzardo, R., Hartmann, L.A., McNaughton, N.J. 2002. The oldest island arc of Roraima State, Brazil – 2.03 Ga: zircon SHRIMP U-Pb geochronology of Anauá Complex. *In*: SBG, Congr. Bras. Geol., 41, *Anais*..., pp. 306.

Fraga, L.M.B. 2002. A Associação Anortosito–Mangerito–Granito Rapakivi (AMG) do Cinturão Güiana Central, Roraima e Suas Encaixantes Paleoproterozóicas: Evolução Estrutural, Geocronologia e Petrologia. Doctoral thesis, CPGG/CG, Universidade Federal do Pará, Belém. 386 pp. (abstract in English)

Fraga, L.M.B., Reis, N.J. 1996. A Reativação do Cinturão de Cisalhamento Guiana Central durante o Episódio K'Mudku. In: SBG, Congr. Bras. Geol., 39, Salvador, BA, *Anais*, v. 1, pp. 424-426. (in Portuguese)

Gaudette, H. E., Olszewski, W.J. Jr., Santos, J.O.S. 1996. Geochronology of Precambrian rocks from the northern part of Guiana Shield, State of Roraima, Brazil. *Journ. South Am. Earth Sci.*, 9, 183-195.

Geraldes, M.C., Van Schmus, W.R., Condie, K.C., Bell, S., Teixeira, W., Babinski, M. 2001. Proterozoic Geologic Evolution of the SW Part of the Amazonian Craton in Mato Grosso State, Brazil. *Precamb. Res.*, 111, 91–128.

Gibbs, A.K., Barron, C.N. 1993. *The geology of the Guyana Shield*. Oxford University Press, Oxford, N. York, 245 p.

Hasui, Y., Haralyi., N.L.E., Schobbenhaus Fº, C. 1984. Elementos geofísicos e geológicos da região amazônica: subsídios para o modelo geotectônico. *In*: SBG-núcleo Norte, Symposium Amazonico, 2, Manaus. *Anais*... v. 1, pp. 129-148. (in Portuguese)

Heizler, M.T., Kelley, S., Condie, K., Perilli, S., Bickford, M.E., Wortman, G.L., Lewry, J., Syme, R., Bailes, A., Corkery, T., Zwanzig, H. 2000. The thermal history of the Trans-Hudson Orogen, Canada. GeoCanada 2000, Calgary, AB, Program with abstracts CD-ROM.

Hodges, K.V. 1991. Pressure-temperature-time paths. *Annu. Rev. Earth Planet. Sci.* 19 : 207-236.

Klötzli, U.S. 1999. Th/U zonation in zircon derived from evaporation analysis: a model and its implications. *Chem. Geol.* **158**, 25-333.

Lafon, J.-M., Delor, C., Barbosa, O.S. 2001. Granulitos tardi-Transamazônicos (2,06 Ga) na região norte do Estado do Amapá: o charnockito de Calçoene. In: SBG-Núcleo Norte, Simp. Geol. Amaz., 7, Belém, pp. 39-42. CD-ROM (in Portuguese)

Lima, M.I.C. de, Montalvão, R.M.G. de, Issler, R.S., Oliveira, A. da S., Basei, M.A.S., Araújo, J.V.F., Silva, G.G. da. 1974. Geologia da Folha NA/NB.22 - Macapá. In: BRASIL, DNPM. Projeto RADAMBRASIL, Rio de Janeiro, (Levantamento de Recursos Naturais, 6). (in Portuguese)

Luzardo, R., Reis, N.J. 2001. O Grupo Cauarane (Estado Roraima): uma breve revisão litoestratigráfica. In: SBG-Núcleo Norte, Simp. Geol. Amaz., 7, Belém. CD-ROM. (in Portuguese)

Macambira, M.J.B., Almeida, M.E., Santos, L.S. 2002. Idade de Zircão das Vulcânicas Iricoumé do Sudeste de Roraima: contribuição para a redefinição do Supergrupo Uatumã. *In*: SBG, Simpósio Sobre Vulcanismo e Ambientes Associados, 2, *Anais*..., pp. 22. (in Portuguese)

McConnel, R.B. 1962. Provisional geological map of British Guyana: 1:1.000.000. Geological Survey of British Guyana, Georgetown, Guyana.

Pinho, F.E.C., Fyfe, W.S., Pinho, M.A.S.B. 1997. Early Proterozoic evolution of the Alto Jauru greenstone belt, southern Amazonian craton, Brazil. *Int. Geol. Rev.* 39, 220–229.

Pinson, W.H., Hurley, P.M., Mencher, E., Fairbain, H.W. 1962. K-Ar and Rb-Sr ages of biotites from Colombia, South America. *Geol. Soc. Amer. Bull*., 73, 907-910.

Premo, W.R., Fanning, C.M. 2000. SHRIMP U-Pb zircon ages for Big Creek gneiss, Wyoming and Boulder Creek batholith, Colorado: Implications for timing of Paleoproterozoic accretion of the northern Colorado province: *Rocky Mountain Geology*, 35, 31–50.

Priem, H.N.A., Boelrijk, N.A.I.M., Hebeda, E.H., Verdurmen, E.A.Th., Verschure, R.H. 1971. Isotopic ages of the Trans-Amazonian acidic magmatism and the Nickerie Metamorphic Episode in the Precambrian Basement of Suriname, South America. *Geol. Soc. Amer. Bull.*, 82, 1667-1680.

Reis, N.J., Faria, M.S.G. de, Fraga, L.M.B., Haddad, R.C. 2000. Orosirian calc-alkaline volcanism from eastern portion of Roraima State – Amazon Craton. *Rev. Bras. Geoc.,* 30 (3), 380-383.

Reis, N.J., Fraga, L.M.B. 2000a. Geological and tectonic framework of Roraima State, Guyana Shield – An overview. *In*: Int. Geol. Congr., 31, Rio de Janeiro, *Expanded Abstract*. CD-ROM

Reis N.J., Fraga, L.M.B. 2000b. The Kanuku Concept Review in That Portion of Central Guiana Domain, Guiana Shield. *In*: Int. Geol. Congr., 31, Rio de Janeiro, *Expanded Abstract*. CD-ROM

Reis, N.J., Fraga, L.M., Faria, M.S.G. de, Almeida M.E. 2003. Geologia do Estado de Roraima. *Géologie de la France*, 2-3, 71-84. (abstract in English)

Rogers, J.J.W. 1996. A history of continents in the past three billions years. *Journ. Geology*, 104, 91-107.

Rogers, J.J.W., Santosh, M. 2002. Configuration of Columbia, a Mesoproterozoic supercontinent. *Gond. Res.* 5, 5–22.

Santos, J.O.S. dos, Faria, M.S.G. de, Hartmann, L.A., McNaughton, N.J. 2002. Significant presence of the Tapajós-Parima Orogenic Belt in the Roraima region, Amazon Craton based on SHRIMP U-Pb zircon geochronology. In: SBG, Cong. Bras. Geol., 51, João Pessoa, *Anais...* pp. 336.

Santos, J.O.S. dos, Faria, M.S.G. de, Riker, S.R.L., Souza, M.M. de, Hartmann, L.A., Almeida, M.E., McNaughton, N.J., Fletcher, I.R. 2006b. A faixa colisional K'Mudku (idade Grenvilliana) no norte do Cráton Amazonas: reflexo intracontinental do Orógeno Sunsás na margem ocidental do cráton. In: SBG, Simp. Geol. Amaz., 9, Belém, CD-ROM.

Santos, J.O.S dos, Hartmann, L.A., Bossi, J., McNaughton, N.J., Fletcher, I.R. 2003a. Duration of the Trans-Amazon Cycle and its correlation within South America based on U–Pb SHRIMP geochronology of the La Plata Craton, Uruguay. *Intern. Geol. Rev.*, 45 (1), 27–48.

Santos, J.O.S. dos, Hartmann, L.A., Faria, M.S.G. de, Riker, S.R.L., Souza, M.M. de, Almeida, M.E., McNaughton, N.J. 2006a. A Compartimentação do Cráton Amazonas em Províncias: Avanços ocorridos no período 2000-2006. In: SBG-Núcleo Norte, Simp. Geol. Amaz., 9, Belém, CD-ROM. (in Portuguese)

Santos, J.O.S. dos, Hartmann, L.A., Gaudette, H.E., Groves, D.I., McNaughton, N.J., Fletcher, I.R. 2000. A new understanding of the provinces of the Amazon Craton based on integration of field mapping and U-Pb and Sm-Nd geochronology. *Gond. Res.* 3 (4), 453-488.

Santos, J.O.S. dos, Potter, P.E., Reis, N.J., Hartmann, L.A, Fletcher, I.R., McNaughton, N.J. 2003b. Age, source and Regional Stratigraphy of the Roraima Supergroup and Roraima-like Sequences in Northern South America, based on U-Pb Geochronology. *Geol. Soc. Amer. Bull.* 115 (3), 331-348.

Santos, J.O.S. dos, Silva, L.C., Faria, M.S.G. de, Macambira, M.J.B. 1997. Pb-Pb single crystal, evaporation isotopic study on the post-tectonic, sub-alkalic, A-type Moderna granite, Mapuera intrusive suite, State of Roraima, northern Brazil. *In*: SBG, Symposium of Granites and Associated Mineralizations, 2. Extended Abstract and Program., Brazil, pp. 273-275.

Scheller, T. 1998. *Zircon*. DOS Shareware, UFPA, Pará-Iso.

Siddoway, C., Givot, R.M., Bodle, C.D., Heizler, M.T. 2000. Dynamic setting for Proterozoic plutonism: information from host rock fabrics, central and northern Wet Mountains, Colorado. Special issue: Proterozoic Magmatism of the Rocky Mountain Region, Carol Frost (ed.), *Rocky Mountain Geology*, 35 (1), 91-111.

Sims, P.K., Stein, H.J. 2003. Tectonic evolution of the Proterozoic Colorado province, Southern Rocky Mountains. *Rocky Mountain Geology*, 38 (2), 183-204.

Stacey, J.S., Kramers, J.D. 1975. Approximation of terrestrial lead isotope evolution by a two-stage model. *Earth Plan. Sci. Letters,* 26, 207-221.

Tassinari, C.C.G. 1996. O Mapa Geocronológico do Cráton Amazônico no Brasil: revisão dos dados isotópicos. Tese de Livre docência, Instituto de Geociências da Universidade de São Paulo. 139p. (in Portuguese).

Tassinari, C.C.G., Cordani, U.G., Nutman, A.P., Van Schmus, W.R., Bettencourt, J.S., Taylor, P.N. 1996. Geochronological systematics on Basement Rocks from the Rio Negro-Juruena Province (Amazonian Craton) and Tectonic Implications. *Intern. Geol. Rev*., 38, 161-175.

Table 1. Single-zircon Pb-evaporation isotopic data for mylonitic biotite granodiorite (MA-042) and foliated hornblende-biotite monzogranite (MA-044) samples.

sample / zircon number	Temp. (^{0}C)	ratios	$^{204}Pb/^{206}Pb$	2σ	$^{208}Pb/^{206}Pb$	2σ	$^{207}Pb/^{206}Pb$	2σ	$(^{207}Pb/^{206}Pb)_{(c)}$	2σ	age	2 σ	Th/U
Mylonitic biotite granodiorite													
MA42/01	*1450	0/8	0.000116	26	0.18932	213	0.11578	63	0.11578	72	1868	11	0.54
MA42/02	*1450	0/28	0.000112	23	0.17927	74	0.11535	25	0.11354	64	1857	10	0.51
	1500	36/36	0.000014	2	0.19437	71	0.11565	47	0.11559	50	1888	8	0.55
MA42/03	#1450	0/32	0.000651	41	0.20128	60	0.12094	23	0.11176	63	1828	10	0.58
MA42/04	1450	18/18	0.000154	12	0.19439	168	0.11663	38	0.11490	50	1879	8	0.55
	1500	32/32	0.000016	9	0.20432	107	0.11578	49	0.11567	54	1891	8	0.58
MA42/05	*1450	0/20	0.000359	12	0.14187	189	0.11625	20	0.11159	26	1826	4	0.44
	1500	38/38	0.000063	9	0.17983	160	0.11622	28	0.11528	33	1885	5	0.51
	1550	26/26	0.000077	5	0.17843	63	0.11684	22	0.11575	22	1892	3	0.51
MA42/06	*1450	0/36	0.000157	26	0.18369	195	0.11334	39	0.11171	71	1828	12	0.57
	*1500	0/8	0.000073	16	0.19334	296	0.11483	41	0.11385	47	1862	7	0.60
		150 (282)							**mean age**		**1890**	**4**	**USD 1.7**
Foliated hornblende-biotite monzogranite													
MA44/03	*1450	0/16	0.000494	89	0.07691	73	0.10150	194	0.09526	110	1533	22	0.22
	*1500	0/16	0.000086	2	0.17460	132	0.11172	139	0.11167	141	1827	23	0.50
MA44/05	*1450	0/8	0.000000	0	0.15711	169	0.10363	53	0.10363	53	1690	9	0.45
MA44/06	1450	22/22	0.000079	26	0.16616	3523	0.10633	370	0.10534	222	1721	77	0.48
MA44/07	#1450	0/8	0.000521	44	0.15396	118	0.11148	41	0.10437	73	1703	13	0.44
MA44/08	1500	14/14	0.000363	106	0.11318	224	0.10925	65	0.10459	179	1707	32	0.33
MA44/11	*1450	0/28	0.000375	3	0.13889	105	0.10778	30	0.10258	45	1672	8	0.40
MA44/12	#1450	0/8	0.001250	58	0.19704	106	0.11860	35	0.10153	88	1652	16	0.57
	1500	8/8	0.000136	34	0.17190	192	0.10918	108	0.10733	118	1755	20	0.50
MA44/14	1450	26/26	0.000391	6	0.16686	70	0.11208	16	0.10666	26	1743	9	0.48
MA44/16	*1450	0/14	0.000314	6	0.15654	249	0.10736	16	0.10736	16	1684	6	0.45
MA44/17	*1450	0/28	0.000305	2	0.13550	37	0.10395	36	0.10395	28	1617	5	0.39
MA44/18	1450	26/26	0.000277	21	0.13612	113	0.10872	37	0.10492	29	1713	5	0.39
	1500	8/8	0.0000092	12	0.12460	670	0.10618	268	0.10618	268	1735	46	0.36
		104 (230)							**mean age**		**1724**	**14**	**USD 3.5**

Notes: The total blocks analyzed are shown in brackets in the *number of blocks* column, but only the first figure (out of bracket) was used for age calculation. Values in italic were not included in the age calculation of the grain (# - step not used due to scatter greater than two standard deviations from the average age; * - step manually discarded due to higher or lower values of the $^{207}Pb/^{206}Pb$ ratio in relation to the mean). $(_c)$ ratios corrected for initial common Pb. Th/U ratios were calculated as such: $Th = [(^{208}Pb/^{206}Pb)/(\lambda Th * T)-1] + (^{208}Pb/^{206}Pb)$; $U = [(^{208}Pb/^{206}Pb)/(\lambda U * T)-1] + (^{208}Pb/^{206}Pb)$; $\lambda Th = 4.94750 * 10^{-12}$; $\lambda U = 1.55125 * 10^{-11}$ (in Klotzli, 1999).

4.2 - Geology and petrography of Paleoproterozoic granitoid rocks from Uatumã-Anauá Domain, central region of Guyana Shield, southeastern Roraima, Brazil

Marcelo Esteves Almeida[1,2*], Moacir José Buenano Macambira[2]

[1]CPRM – Geological Survey of Brazil, Av. André Araújo 2160, Aleixo, CEP 69060-001, Manaus, Amazonas, Brazil

[2]Isotope Geology Laboratory, Center of Geosciences, Federal University of Pará, Rua Augusto Corrêa s/n, Guamá, CEP 66075-110, Belém, Pará, Brazil

* Corresponding author; ph.: +55-92-2126-0357, fax: +55-92-2126-0319, e-mail adress: marcelo_almeida@ma.cprm.gov.br

ARTIGO SUBMETIDO AO CORPO EDITORIAL DA

"REVISTA BRASILEIRA DE GEOCIÊNCIAS"

Words: summary (81), resumo (240), abstract (191), body text (8367), table (249) and figure (743) captions. Total: 3 tables and 11 figures

RESUMO
Mapeamentos geológicos na escala regional identificaram no Domínio Uatumã-Anauá (DUA), sudeste do Estado de Roraima (Brasil), porção central do Escudo das Güianas, um amplo domínio de granitóides cálcio-alcalinos a alcalinos, além de subordinados granitos peraluminosos de natureza crustal. Estes granitóides estão distribuídos em diferentes associações magmáticas com idades, estilos de deformação e afinidades químicas distintos. Neste trabalho, mapeamento geológico de maior detalhe, apoiado por estudo petrográfico, propiciou a distinção de algumas dessas associações que ocorrem em duas áreas distintas (norte e sul). Os granitóides deformados do setor norte do DUA (1,97-1,96 Ga) são representados pelos granitos Martins Pereira (do tipo I, cálcio-alcalino) e Serra Dourada (do tipo S), e em geral estão associados a amplas zonas de cisalhamento dúctil destrais de direção NE-SW a E-W. Ainda no setor norte do DUA, remanescentes do embasamento (2,03 Ga) são representados por sucessão metavulcanossedimentar (Grupo Cauarane) e associação granítica do tipo TTG (Complexo Anauá). Os granitóides do setor sul do DUA (1,90-1,89 Ga), que incluem os granitos lgarapé Azul e Caroebe da suíte Água Branca (tipo I, cálcio-alcalino), são isotrópicos e estão afetados apenas localmente por zonas de cisalhamento NE-SW. Dois eventos graníticos tipo-A intrusivos ocorrem no DUA: granitóides Moderna (~1,81 Ga) e Mapuera-Abonari (~1,87 Ga). Ocorrências primárias de ouro estão hospedadas nos granitóides Martins Pereira (setor norte), ocorrências aluvionares de Nb-Ta são encontradas no granito Igarapé Azul (setor sul), enquanto que pegmatitos com ametista estão presentes em corpos relacionados ao granito Moderna.
Palavras-chaves: Granitóides, Petrografia, Roraima, Escudos das Guianas, Paleoproterozóico

ABSTRACT
Regional mapping carried out in the Uatumã-Anauá Domain (UAD), Guyana Shield, southeastern Roraima (Brazil), has showed widespread calc-alkaline granitic to alkaline magmatism and local peraluminous granites. These granitoids are distributed into several magmatic associations with different Paleoproterozoic (1.97-1.89 Ga) ages, structural and geochemical affinities. In this paper, detailed mapping and petrographic studies have distinguished two main subdomains in UAD. In the northern UAD, the Martins Pereira I-type, calc-alkaline granitoids and Serra Dourada S-type granite (1.97-1.96 Ga) are deformed and affected by NE-SW and E-W shear zones. Basement inliers (2.03 Ga) crop out to the northeastern part of this area, and are formed by rocks from metavolcano-sedimentary sequence (Cauarane Group) and TTG-like calc-alkaline association (Anauá Complex). Younger and undeformed (with local discrete NE-SW shear zones) Igarapé Azul and Caroebe granites (I-type, calc-alkaline Água Branca suite) crop out in the southern UAD. A-type granites such as Moderna (1.81 Ga) and Mapuera (1.87 Ga) plutons, cross cut both areas of UAD. Gold mineralization is observed in the Martins Pereira granitoids (northern UAD), alluvial columbite-tantalite is related to the Igarapé Azul granitoids (southern UAD), and amethyst is associated to pegmatites of the Moderna A-type granites.
Keywords: Granitoids, Petrography, Roraima, Guyana Shield, Paleoproterozoic

INTRODUCTION

Calc-alkaline I-type granitoids, including aluminous to alkaline A-type granites, charnockitic rocks and minor S-type granites (CPRM 1999, 2000) are widespread in the central portion of the Guyana Shield, southeastern Roraima State, Brazil **(Fig. 1)**. The polycyclic geological setting in the area presents strong differences between low- and high-grade terranes; the tectonic regime is complex as there is overprinting of events whereas the relationship between granitogenesis and the major Transamazonian orogeny is not well established. This uncertain geological picture is mainly resulted from scarce geological mapping.

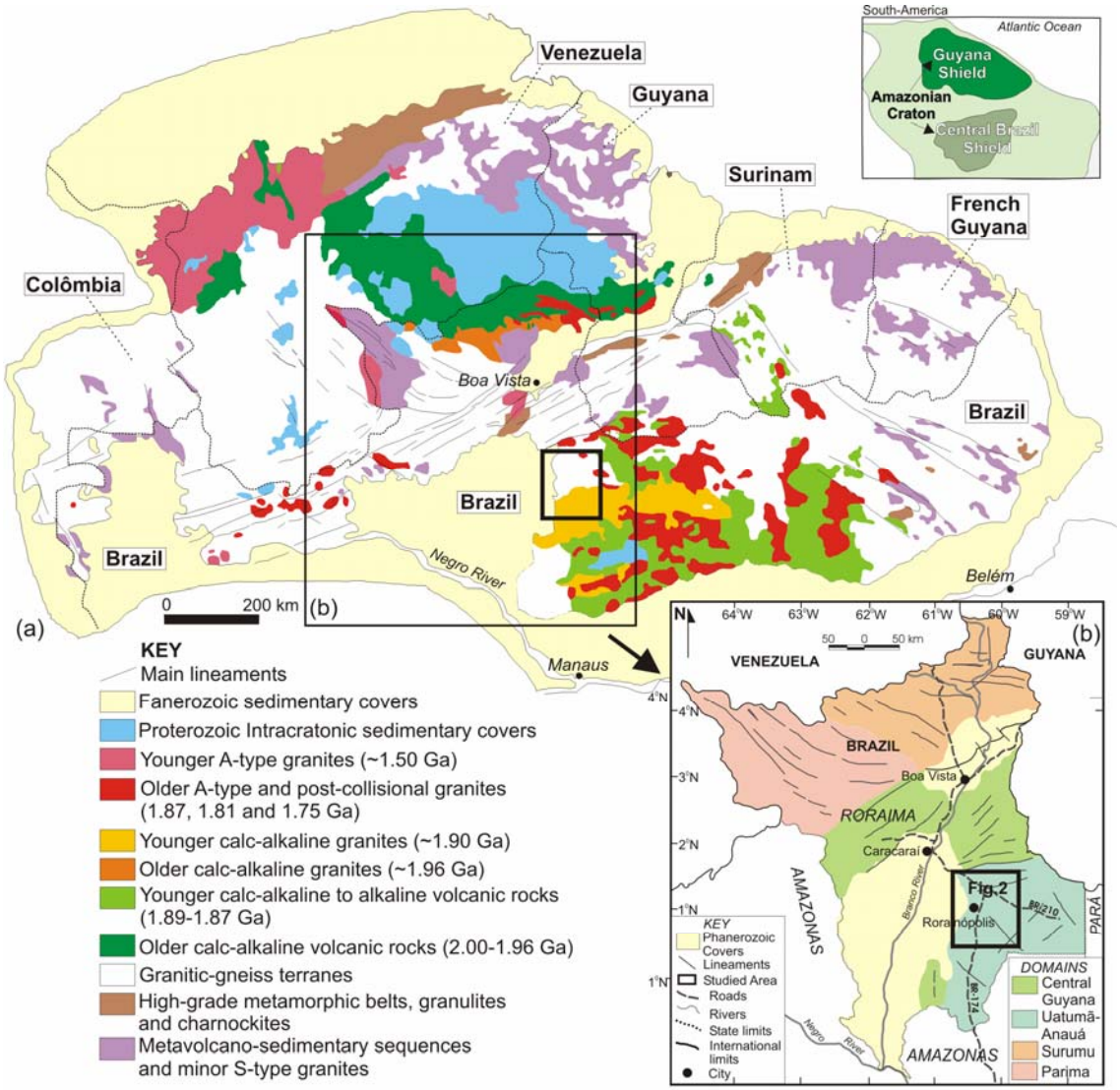

Fig. 1. Geological sketch map of (a) Guyana Shield (after Gibbs and Barron 1993) and location of the studied area showing the (b) southeast of Roraima and boundaries, including the lithostructural domains (after Reis and Fraga 2000, Reis *et al.* 2003 modified by CPRM 2006). For studied area details see fig. 2.

Nevertheless, recent regional geological mapping supported by lithostructural and geochronology **(Fig. 1**; CPRM 2006, modified from Reis *et al.* 2003) outlined different lithological associations in Roraima State related with four domains is proposed:

→ The Surumu domain (north-northeastern Roraima) exhibits WNW-ESE and E-W structural trends. In this domain calc-alkaline granites and volcanic rocks (1.98-1.95 Ga) show local deformation at greenschist-facies. Cratonic sedimentary sequences (1.87-1.78 Ga) partly cover the volcanic rocks. Late to post-Transamazonian supracrustal rocks (2.03-1.97 Ga?) are exposed only in the southwestern part of this domain.

→ The Parima domain (west-northwestern Roraima) includes extensive late to post-Transamazonian granite–greenstone terranes and has predominantly NW-SE to E-W foliation.

Granitic plutons and volcanic rocks, similar to those exposed in the Surumu domain, are subordinated. Batholiths and stocks of rapakivi granite (1.55 Ga) as well as sedimentary covers are also present.

→ The Central Guyana domain (central Roraima) shows NE-SW structural trends, and amphibolite-facies gneiss predominates over granulite-facies rocks (1.96-1.93 Ga). A typical Mesoproterozoic Anorthosite-Mangerite-Granite association (1.56-1.53 Ga) intrudes the older units.

→ The Uatumã-Anauá domain (southeastern Roraima, northeastern Amazonas and northwestern Pará) comprises widespread granite magmatism (2.03-1.81 Ga) and supracrustal rocks with NW-SE (and NE-SW) foliations and deformed at greenschist to amphibolite-facies conditions.

The studied area encompasses mainly calc-alkaline granitoids intrusive in the Uatumã-Anauá domain (UAD), such as Martins Pereira (Almeida *et al.* 2002), Igarapé Azul (Faria *et al.* 1999, Almeida *et al.* 2002) and Caroebe granites. Locally, they host ore mineral like gold and columbite-tantalite.

In this paper, we summarize field and petrographic studies and propose a new geological map based on the groups of granitoid rocks and related mineralizations, for the northwestern part of the UAD, providing new insights about the tectonic significance of the granitoids in southeastern Roraima.

GEOLOGICAL SETTING

The Uatumã-Anauá domain (UAD, CPRM 2006 modified from Reis and Fraga 2000, Reis *et al.* 2003), also named as northern Tapajós-Parima belt (Uaimiri domain, Santos *et al.* 2000) or northern Ventuari-Tapajós province (Tassinari and Macambira 1999), is characterized by metamorphic basement and intrusive granitoids **(Fig. 2)**.

According to Faria *et al.* (2002), in the northern Uatumã-Anauá domain (NUAD) the basement rocks comprise an island arc setting (Anauá arc) formed by TTG-like metagranitoids and orthogneiss with metamafic to metaultramafic enclaves (Anauá Complex), and inliers of metavolcano-sedimentary rocks (Cauarane Group). The basement rocks occur in the northern part of the studied area **(Fig. 2)**, and is intruded by S-type (Serra Dourada) and I-type calc-alkaline (Martins Pereira) granites, which correspond to the 2.03 to 1.96 Ga Martins Pereira-Anauá granitic terrane (Almeida *et al.* 2002).

In the southern part of the Uatumã-Anauá domain (SUAD**, Fig. 2**), the Caroebe and Igarapé Azul calc-alkaline granitoids are ~70 M.y. younger than Martins Pereira and Serra Dourada granites, and do not show regional deformation and metamorphic features (*e.g.* CPRM 2000, Almeida *et al.* 2002). The Caroebe granitoids are coeval to volcanic rocks (Macambira *et al.* 2002) and both have similar geochemical characteristic (Reis *et al.* 2000). Locally, charnockitic (Igarapé Tamandaré) and enderbitic (Santa Maria) plutons may occur. The SUAD comprises the Igarapé Azul-Água Branca granitic terrane proposed by Almeida *et al.* (2002).

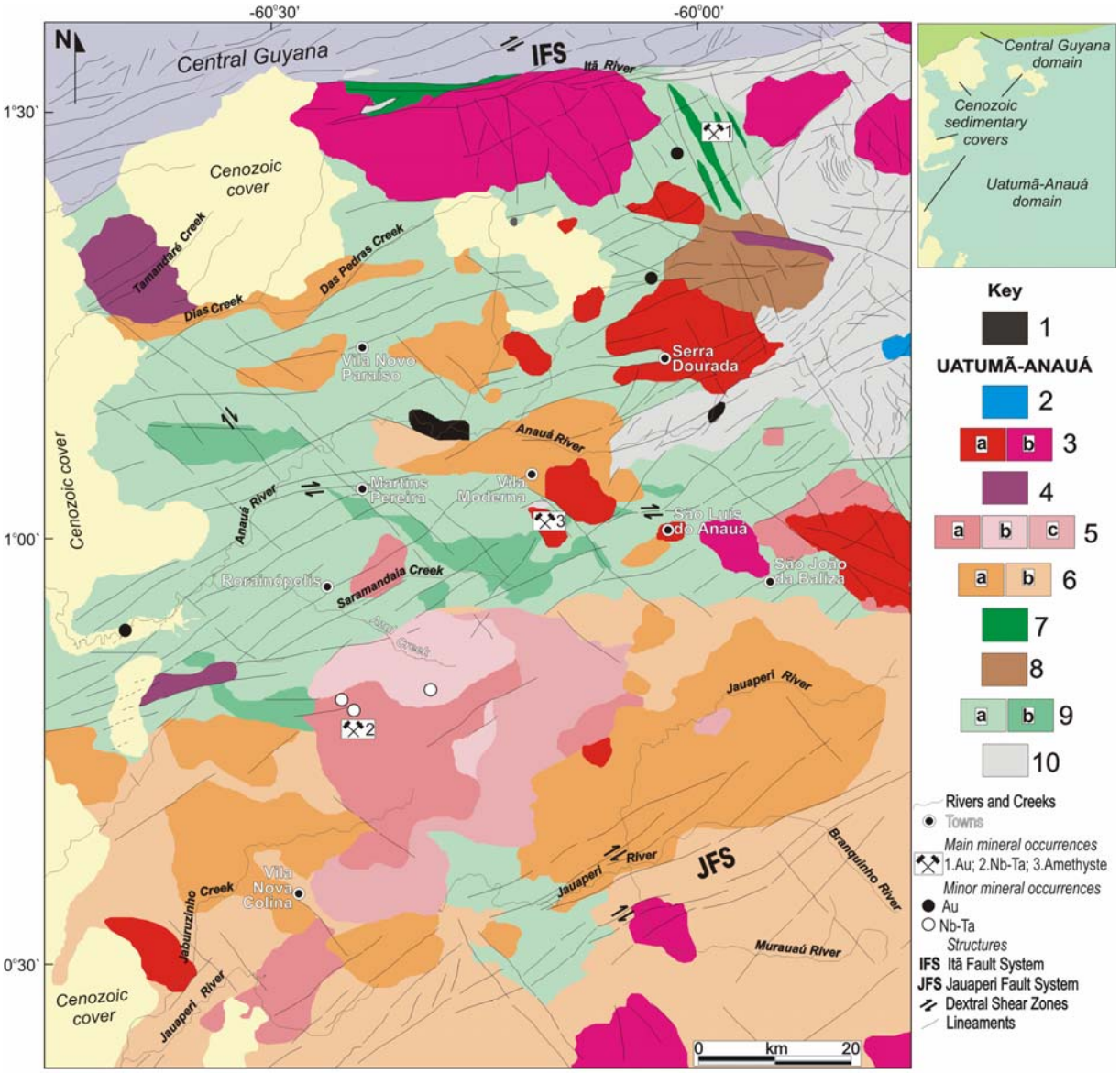

Fig. 2. Geological sketch map of southeastern Roraima (modified from Almeida *et al.* 2002 and CPRM 2000). 1. Undiscriminated plutonic mafic rocks, 2. A-type granites: a) Moderna (1.81 Ga), b) Mapuera (1.87 Ga); 3. Santa Maria enderbite, Tamandaré charnockite and undiscriminated charnockitoids; 4. Igarapé Azul granites (1.89 Ga): a) Vila Catarina, b) Estrela Guia, and c) Saramandaia facies; 5. Caroebe granites (1.90-1.89 Ga): a) Jaburuzinho, b) Alto Alegre facies; 6. Calc-alkaline volcanic rocks (1.89 Ga); 7. S-type (cordierite) Serra Dourada granite (1.96 Ga), 8. High-K calc-alkaline Martins Pereira granitoids (1.97 Ga): a) normal to b) high U, Th, K contents, 9. Metavolcano-sedimentary sequence (Cauarane Group related: <2.03 Ga?) and TTG calc-alkaline association (Anauá Complex: 2.03 Ga).

Several A-type granitic bodies, such as the Moderna (~1.81 Ga, Santos *et al.* 1997), which is correlated to Madeira intrusive suite (CPRM 2006) with 1.82-1.79 Ga ages (*e.g.* Costi *et al.* 2000), and the Mapuera and Abonari granites (~1.87 Ga, *e.g.* CPRM 2003), are widespread in the UAD (**Fig. 2**) and cross cut the rocks described above. They are considered as related to a "post-orogenic to anorogenic" setting. All interval ages presented above have been determined mainly by single-zircon Pb evaporation, U-Pb ID TIMS and SHRIMP methods.

GEOLOGY AND PETROGRAPHY RESULTS

In this section will be describing the results of the mapping and the petrographical aspects of the main granitic associations of the UAD, which was subdivided into northern and southern areas.

Northern area

BASEMENT ROCKS: TTG-LIKE ANAUÁ COMPLEX AND CAUARANE GROUP RELATED ROCKS

The Anauá Complex (CPRM 2000) crops out along Anauá and Novo rivers, and is mostly composed of 2.03 Ga metagranitoids and metadiorites, chemically comparable to calc-alkaline rocks of TTG terranes, enclosing mafic and ultramafic enclaves (Faria *et al.* 2003). The Anauá Complex rocks show two main deformational phases: a) $D_{1,}$ dominant with N63^{o}E/34^{o}NW foliation, and b) $D_{2,}$ represented by a mylonitic foliation.

The Cauarane Group rocks are associated with the Anauá Complex and represent an important metavolcano-sedimentary of low- to high-grade metamorphism, locally in anatexis. Faria *et al.* (2002) suggest that these supracrustal rocks are a back-arc basin sequence, related to Anauá island arc, developed in the first accretionary orogenic event of the Tapajós-Parima cycle (Santos *et al.* 2000). According to CPRM (2000) this metavolcano-sedimentary sequence is correlated to the Kwitaro Group, located in south Guyana (Berrangé 1972).

The Cauarane Group comprises mica schists, quartzites, paragneisses, metacherts, phyllites and amphibolites with at least two deformational phases (CPRM 2000): a) S_n main foliation (N56^{o}E/87^{o}SE) and b) S_{n+1} foliation (N45^{o}E/70^{o}NW). According to CPRM (2000), the paragneisses are geochemically similar to immature clastic sedimentary rocks (graywackes and arkoses); the amphibolitic rocks have high TiO_2 contents and MORB-REE pattern.

Detrital zircon crystals from one Cauarane schist yielded two different age populations: i) 2229 ± 8 Ma (U-Pb ID-TIMS, CPRM 2003 modified from Gaudette *et al.* 1996) and ii) 2074 ± 15 Ma and 2038 ± 17 Ma (U-Pb SHRIMP, CPRM 2003), this last one interpreted as the maximum age of the sedimentation. This data suggests basement sources related mainly to the Transamazonian terrains, including probably rocks from the Anauá arc.

S-TYPE SERRA DOURADA GRANITE

The S-type granitoids of southeastern Roraima were initially described by Faria *et al.* (1999). These authors have been included all granitoids with S-type tipology in the Igarapé Azul granite unit. However, Almeida *et al.* (2002) and Almeida and Macambira (2003), based on geochemical features and more detailed geological mapping in the type area, subdivided the Igarapé Azul granite into three different granitic types: Serra Dourada granite ("truly" S-type), Martins Pereira granite (older and deformed I-type high-K calc-alkaline) and the Igarapé Azul granite (younger and undeformed I-type high-K calc-alkaline).

The S-type Serra Dourada granite has approximately 170 km^2, crops out near the homonymous small town, and is intrusive in rocks from the Anauá Complex and Cauarane Group (**Fig. 2**). These granitoids show monzogranitic and minor syenogranitic and granodioritic compositions, with diagnostic aluminous minerals, equigranular texture and coarse to medium grained (**Fig 3a, Table 1**). The mineral assemblage is composed of alkali feldspar (16-39 %), quartz (18-31 %), plagioclase (19-39 %), biotite (1-21 %), muscovite (2-6 %), minor cordierite, monazite, xenotime, opaque minerals, apatite, zircon and sillimanite, and secondary minerals are epidote, titanite, chlorite and leucoxene (**Table 1**). Minor evidences of dynamic recrystallization and planar fabric are also present.

Quartz shows commonly embayement contacts. The slight red-brown biotite is intergrown with muscovite or occurs as subhedral isolated crystals showing several metamict mineral inclusions. Muscovite rarely occurs as large separate crystals. Cordierite appears as crystals around 2 mm long with sillimanite inclusions, partly to totally altered (pinitization and sericitization) and commonly having a rectangular tabular habit. Ilmenite and magnetite are also observed. Monazite and xenotime show pale yellow color to colorless and wide orange pleochroic haloes in the host mineral.

The existence of associated supracrustal rocks and aluminous paragenesis suggests that the Serra Dourada granite is derived from a metasedimentary source, involving anatexis in low

(cordierite crystallization) to moderate H_2O-activity (minor magnetite and biotite crystallization), and low to medium pressure (cordierite) conditions (White 1992). Other S-type granite was dated in Central Guiana domain by zircon U-Pb SHRIMP (CPRM 2003) that yielded ages of 1968 ± 3.5 Ma (crystallization age) and 2.05 to 2.07 Ga (late-Transamazonian inheritance).

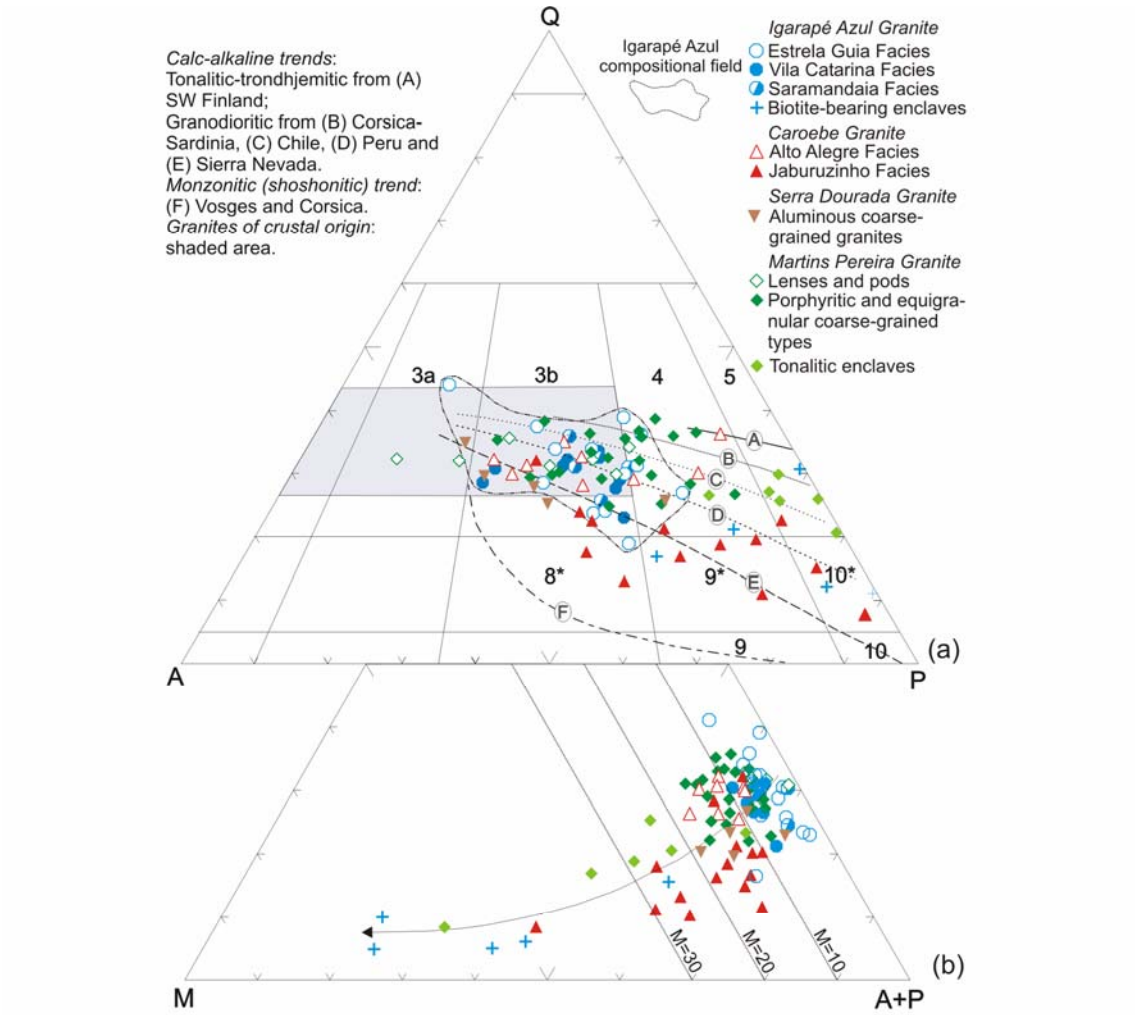

Fig. 3. QAP (a) and QM(A+P) (b) diagrams (Streckeisen, 1976) for samples from Martins Pereira, Serra Dourada, Caroebe and Igarapé Azul granitoids (including enclaves). For modal contents see the tables 1, 2 and 3. Q. Quartz, A. Alkalifeldspar, P. Plagioclase, M. Mafic minerals. The average trends of some plutonic suites was taken of Lameyre & Bowden (1982) and Lameyre and Bonin (1991). Fields: 3a. syenogranite; 3b. monzogranite; 4. granodiorite; 5. tonalite; 9. Monzodiorite/monzogabbro; 10. diorite/gabbro; 8*. quartz monzonite; 9*. quartz monzodiorite/quartz monzogabbro; 10*. quartz diorite/quartz gabbro.

MARTINS PEREIRA GRANITOIDS

The Martins Pereira granitoids (up to 3780 km^2 in area) occur southward of the Itã system fault and its main outcrops have been recorded around the Martins Pereira (type-area), Rorainópolis and São Luís do Anauá towns (**Fig. 2**). This batholith is composed of medium-grained porphyrytic gray granodiorites to monzogranites and locally by fine to medium-grained dark gray tonalites showing a calc-alkaline granodioritic trend (Chile related; Lameyre and

Bowden 1982, Lameyre and Bonin 1991) in the QAP diagram (**Fig 3a, Table 1**). Small intrusive blobs and lenses of leucogranites are also associated with the batholith.

Granodiorites and monzogranites

In general, the granodiorites and monzogranites are slightly blueish gray and have conspicuous porphyrytic (locally equigranular) texture with feldspar megacrysts (**Fig. 4a and 4b**), medium to coarse-grained groundmass and 10% to 18% of mafic minerals (**Fig 3b, Table 1**). Foliation with local banding and subparalel (N75°E/80°SE) mylonitic foliation are common in these granitoids **(Fig. 5a)**. In spite of heterogeneous solid-state deformation, only locally quartz shows in thin section high dynamic recrystallization features **(Fig. 5b)**. Exceptionally, in ductile narrow mylonitic zones, feldspars and quartz show granoblastic texture and corel-and-mantle structure, which suggests metamorphic temperature over ca. 400°–500°C (*e.g.* Passchier and Trouw 1996). The mineral assemblage of these rocks is composed by alkali feldspar (10-37 %), quartz (21-35 %), plagioclase (23-53 %), biotite (4-12 %), muscovite (0.1-4 %) and minor epidote, opaque minerals, titanite, allanite, apatite, zircon and rare tourmaline (**Table 1**).

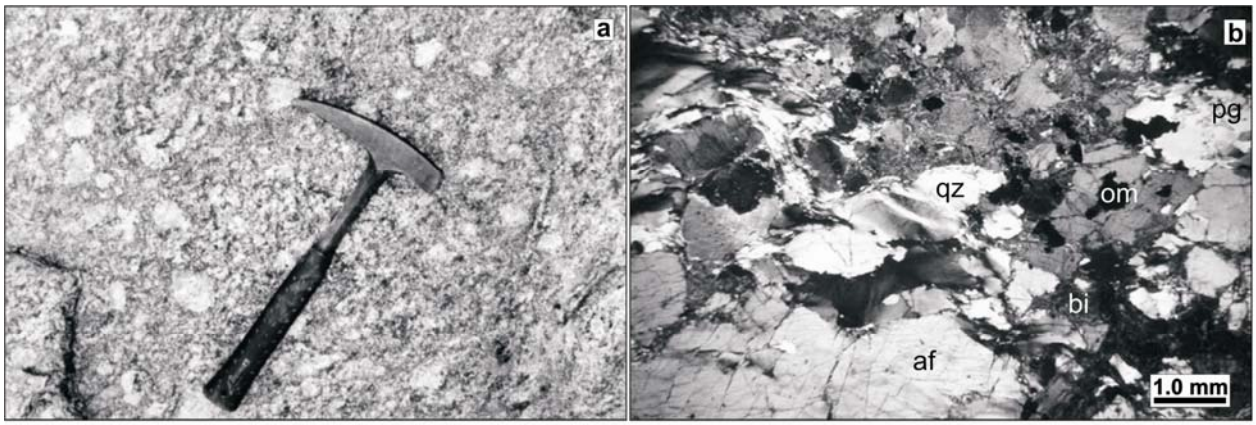

Fig. 04. Features of Martins Pereira Granite: a) Isotropic porphyrytic biotite monzogranite (outcrop MA-218), showing ovoid alkalifeldspar megacrystals (< 80 mm in diameter). b) Photomicrography of slightly orientated biotite, dynamically recrystallized quartz and fractured alkalifeldspar (Cross-polarized light, 1.25x). Obs: af. alkalifeldspar, pg. plagioclase, qz. quartz, biotite, om. opaque mineral.

Feldspar megacrysts (mainly alkali feldspar) have ovoid and tabular shapes **(Fig. 4a)**, ranging in size from 2 to 8 cm and presenting white to slightly pink colors. They are enclosed by weakly to highly deformed and foliated groundmass. These megacrysts are parallel to the foliation, including also types in which the groundmass does not have strong anisotropic fabric (magma flow?). Plagioclase is weakly zoned and locally shows obliterated multiple twining. Highly altered calcic cores are uncommon. Anhedral to subhedral quartz shows ondulatory extinction or partially recrystalized grains. Drop-like quartz inclusions are common in the alkali feldspar megacrysts. Subhedral biotite has brown-greenish to straw-yellow colors, medium grain

size and is associated with epidote, opaque minerals, allanite, titanite and rarely with tourmaline prysmatic crystals. Biotite crystals are frequently oriented, overcoat in highly deformed types. In this case, the biotite cleavages are filled with iron-titanium oxides, locally wick and folded kink forming bands. Biotite also occurs partially replaced by muscovite and chlorite. Muscovite occurs as irregular grains, mostly associated with biotite. Prismatic or irregular muscovite crystals also replace plagioclase and alkali feldspar megacrysts.

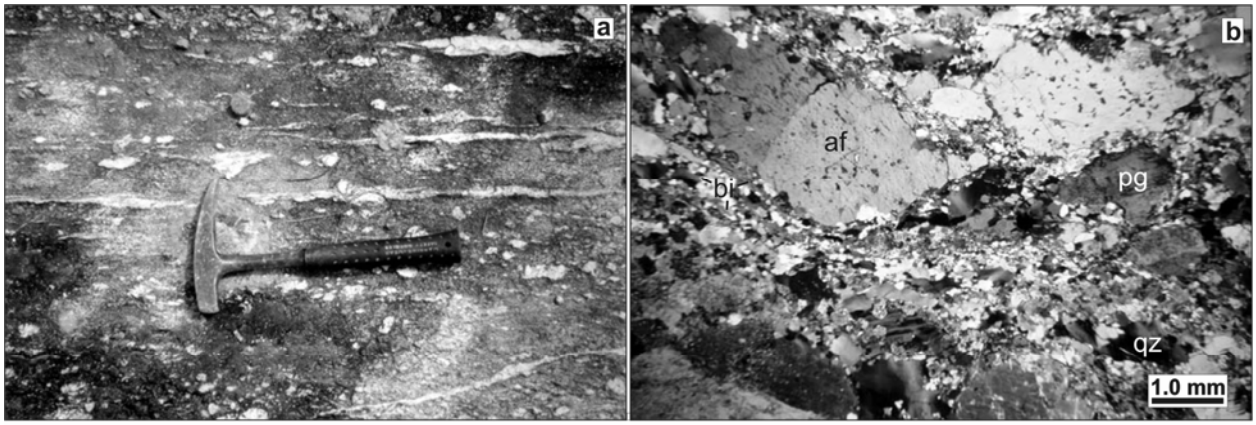

Fig. 5. Deformational features of the Martins Pereira granitoids: a) Biotite monzogranite (porphyrytic facies) showing mylonitic foliation (N75°E/90° to N82°E/90°), rounded megacrysts with pressure shadows and locally quartz ribbons in dextral shear zone (outcrop MA-61). b) Photomicrography showing protomylonitic texture. Note the local groundmass grain reduction by dynamic recrystallization, oriented mafic minerals and rounded alkali feldspar megacrysts (cross-polarized light, 1.25x). Obs: af. alkali feldspar, pg. plagioclase, qz. quartz, bi. biotite.

Blobs and lenses of leucogranites

Leucogranites show granodioritic to syenogranitic compositions, equigranular and medium to coarse grained texture. They are very restricted and crops out as blobs, veins and lenses with few centimeters (rarely 5 meters) thick, subconcordant to the foliation of Martins Pereira host rock. The contacts between leucogranites and foliated granitoid hosts are lobate to irregular, occasionally diffuse, and progressively change to regular and concordant style **(Fig 6)**. These leucogranites are more commom near to the Igarapé Azul contacts.

The rocks are characterized by a grayish white color, generally with sugar-like and isotropic fabric, locally showing dynamic recrystallization and cataclastic features. The mineral assemblage is composed by alkali feldspar (21-55 %), quartz (27-33 %), plagioclase (8-42 %), biotite (1-5 %), muscovite (0.1-3 %), and minor epidote, opaque minerals, titanite, allanite, apatite and zircon **(Table 1)**.

Alkali feldspar is medium to coarse grained, subhedral to anhedral, and tabular, showing locally microperthites and ondulatory extinction. It encloses plagioclase, quartz and muscovite. Sericitization and fractures are also present. Plagioclase shows slight compositional zoning,

locally marked by cores with secondary alteration (epidote, carbonate and sericite). It is tabular, subhedral, locally embayed with alkali feldspar grains and shows slight ondulatory extinction. Quartz has ondulatory extinction, is partially recrystallized, subhedral to anhedral and fine to medium-grained with abundant embayement features. Biotite has moderate pleocroism, straw yellow color, slightly ondulatory extinction, medium to fine-grain size. It is partially to totally transformed into muscovite. Muscovite occasionally occurs as isolated crystals with ondulatory extinction and associated with biotite and plagioclase. Tourmaline and igneous garnet are uncommon.

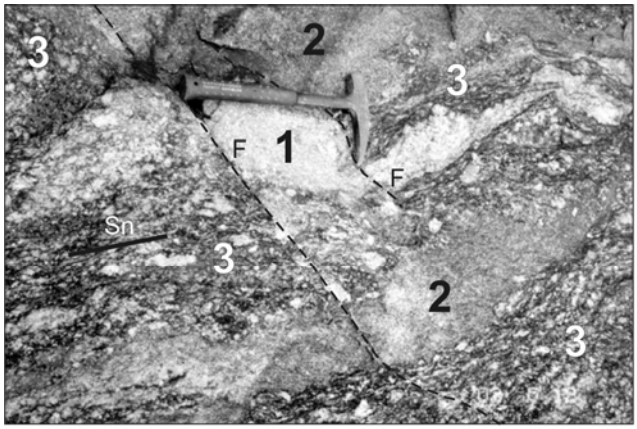

Fig. 06. Outcrop (MA-07) of the Martins Pereira granitoids showing blobs and lenses of leucogranite (1) and monzogranite (2) in porphyrytic biotite granodiorite (3) with N80°W/18°NE strike foliation locally disrupted by NS normal faults (F).

Enclaves

Tonalitic (and minor granodioritic) rocks in the Martins Pereira granitoids may occur as oblate and ellipsoidal enclaves concordant with the foliation of the host rock **(Fig. 7a)**. Furthermore, these enclaves have an internal structure visible at naked eye, emphasized by biotite crystals, systematically parallel to the foliation of the host rock. These elongate biotite-bearing tonalitic enclaves, and the leucogranitic blobs and lenses are concordant to subconcordant to the structures of the host rocks, generating local banding.

The tonalitic enclaves are foliated and characterized by equigranular, medium to fine grained **(Fig. 7b)** with local slightly ondulatory extinction in quartz and feldspar crystals, although recrystallization and mineral stretching is not observed. They show high mafic mineral contents **(Fig. 3b, Table 1)**, such as epidote (0.1-13 %), titanite (1-4 %) and biotite (3-42 %), the last one partially replaced by muscovite (1-6 %) and chlorite (0.1-14 %). Other accessory minerals are allanite, apatite, magnetite and zircon.

Other enclaves observed as xenoliths of amphibolites, hornblende-rich metaigneous rocks of the Anauá Complex and paragneisses of the Cauarane Group, but they are rare. Amphibolitic and metaigneous enclaves with dioritic to quartz-monzodioritic compositions are quite angular with slightly rounded vertices, greenish and isotropic to foliated. They are locally disrupted by tonalitic veins network, but both (amphibolitic and tonalitic types) are enclosed by Martins Pereira granitoids. These xenoliths are equigranular, medium to coarse grained and have high mafic contents (45 %). Plagioclase (40 %) and quartz (10 %) show ondulatory extinction and local dynamic recrystallization features. The accessory minerals are mainly opaque minerals (3 %), epidote (1 %) and apatite. Paragneissic xenoliths with cm-scale, angular shape and fine to medium-grained are very rare. They have an internal structure marked by micaceous bands and metasedimentary relicts.

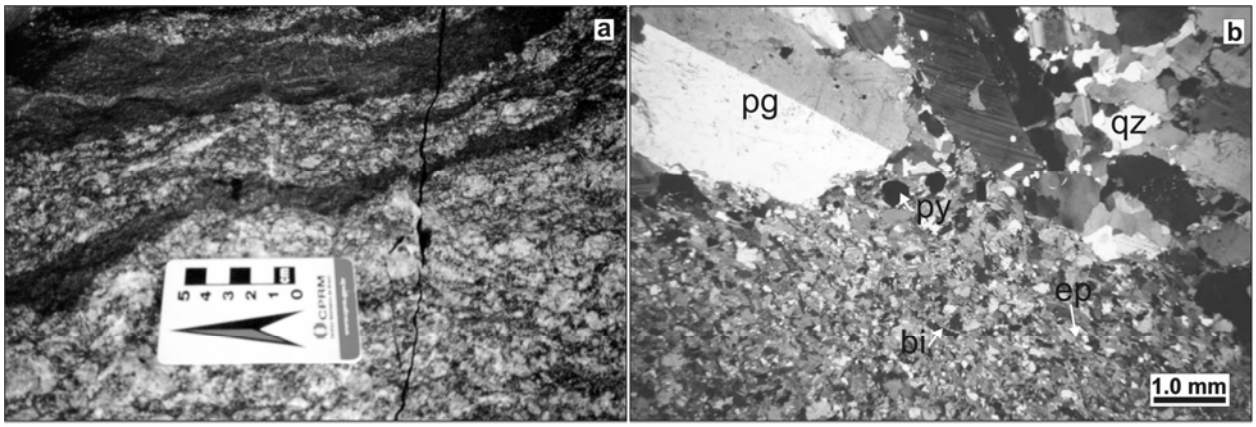

Fig. 07. Features of the Martins Pereira granitoids: a) Deformed biotite granodiorite (porphyrytic facies) showing lenses of mafic tonalitic gneiss (outcrop MA-07). b) Photomicrography showing porphyrytic granodiorite host (uppermost) and biotite-bearing tonalite enclave (lowermost) contact (cross-polarized light, 1.25x). Obs: pg. plagioclase, qz. quartz, bi. biotite, ep. epidote, py. pyrite.

Southern area

CAROEBE GRANITOIDS

Calc-alkaline granitic bodies in southern Roraima (Costi *et al.* 1984, Oliveira *et al.* 1996, CPRM 2000, Almeida *et al.* 2002) has been associated to the Água Branca suite (Araújo Neto and Moreira 1976, Veiga *et al.* 1979, Jorge-João *et al.* 1985). The main granitic body of Água Branca suite in this region, named as Caroebe granite, is located south of Rorainópolis, São Luiz do Anauá, São João da Baliza and Caroebe towns in the region of the Jauaperi and Anauá river basins.

The Caroebe granite has about 65000 km^2 (CPRM 2003) and extends to northwestern Pará and northeastern Amazonas states. Only the northwestern part (near to 4000 km^2) of this pluton has been studied up to now. This granitic batholith was emplaced along EW to ENE-WNW

structures, parallel to Martins Pereira (meta)granitoids regional foliation, which is observed in other minor and similar granitic bodies of the region **(Fig. 2)**. Neogene sediments recover the western side of the Caroebe granite. In the eastern and north sides it is in contact with coeval volcanic rocks (Reis and Fraga 1996; Reis *et al.* 2000, Macambira *et al.* 2002) and is intrusive into Martins Pereira (meta)granitoids.

The Caroebe granite is characterized by extended compositional granitic association and calc-alkaline granodioritic series such as the Peru and Sierra Nevada trends (Lameyre and Bowden 1982, Lameyre and Bonin 1991, **Fig. 3a)**. They are subdivided into two main petrographic facies: Alto Alegre and Jaburuzinho (**Fig. 2)**.

Jaburuzinho facies

The Jaburuzinho facies consists of hornblende-bearing granitoids, such as granodiorites, monzogranites and tonalites, with minor diorites, quartz monzodiorites and quartz diorites **(Fig. 3a, Table 2)**. The main outcrops are located in Anauá (Jaburuzinho creek) and Jauaperi river basins. They show homogeneous, equigranular to porphyrytic textures (10% to 15% megacrysts), are medium to coarse grained and show gray color. The tabular alkali feldspar megacrysts show white to slightly pinkish color, and 15 to 25 mm in length, locally up to 50 mm (ratio 1:3), and ENE-WSW orientation, suggesting magma flow process.

These granitoids have also abundant mafic clots and rounded circular autholiths **(Fig. 8a)**, including variable mafic mineral contents (12%-65%, **Fig. 3b**). The mafic clots are sometimes interlinked and slightly oriented, without solid-state deformation evidence, which points out also to magma flow structure. On the other hand, granitoids submitted to solid-state deformation are very rare, related with a strong ENE-WSW shear zone (Jauaperi fault system), that affects the Jauaperi and Branquinho rivers. The mineral assemblage **(Table 2)** is formed by plagioclase (23-54 %), quartz (4-30 %), alkali feldspar (2-35 %), biotite (6-20 %), hornblende (0.3-37 %), opaque minerals (mainly magnetite: 0.7-4 %), titanite (0.2-5 %), epidote, apatite, zircon and allanite. Muscovite and relicts of clinopyroxene are uncommon.

Plagioclase crystals are subhedral to euhedral, tabular, medium to coarse grained and shows strong to normal oscillatory zoning **(Fig. 8b)**, which is well marked by saussuritization in the An-rich zones. Polysynthetic twinning is very common and eventually also occurs combined with carlsbad twinning. Desequilibrum features are locally present in partially corroded (irregular and embayment) rims. Subtle linear flow, parallel to that the mafic minerals (ENE-WSW to NE-SW),

is also observed. Plagioclase enclosed by alkali feldspar megacrysts is subhedral, fine grained and shows subtle normal compositional zoning.

Two quartz textural types are observed: a) interstitial, anhedral, medium grained, and b) subhedral, fine to medium grained with slight ondulatory extinction. Under solid-sate deformation (local mylonitic zones), the quartz shows variable recrystallization stages. Normally, it shows fine grained subgrains outlining preserved ones, but granoblastic texture is also observed. Quartz ribbons are rare.

Microperthitic alkali feldspar megacrysts **(Fig. 8b)** are anhedral (locally interstitial), tabular and show several inclusions (plagioclase, drop-like quartz, biotite, apatite, opaque minerals). Likewise plagioclase megacrysts, they show an ENE-WSW flow foliation. Tartan twinning, occasionally combined with carlsbad twinning, is very common. Microfractures and myrmequite are scarce. Alkali feldspar is not very abundant in groundmass and shows subhedral, tabular (1:1 to 1:2), weak tartan twinning and rare inclusions. In the deformed types, these megacrysts are contourned by oriented mafic minerals and, in general, show core-and-mantle structure and microfractures (normally filled by quartz).

Biotite is straw yellow to greenish yellow, subhedral to euhedral, and shows strong to moderate pleocroism. It normally occurs in mafic clots associated with hornblende, titanite, epidote, opaque minerals and apatite **(Fig. 8b)**. Apatite, zircon and primary epidote inclusions are very common. Biotite crystals occasionally are oriented, due to either by magma flow (most common) or to solid-state flow, both with similar direction (ENE-WSW). Muscovite is uncommon and partially replaces biotite.

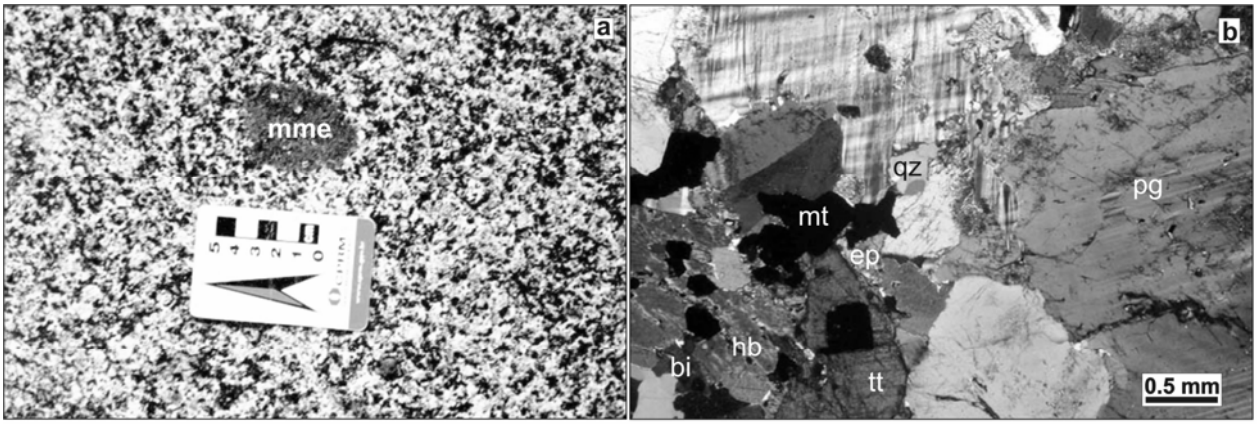

Fig. 08. Features of the Jaburuzinho facies from the Caroebe granite (outcrop MA-33): a) Hornblende-bearing tonalite showing rounded mafic clots and mafic microgranular enclave (mme); b) Photomicrography of mafic clots (bi. biotite, hb. hornblende, mt. magnetite, tt. titanite and ep. epidote) and coarse-grained feldspars and quartz fine-medium grained (af. alkali feldspar, pg. plagioclase, qz. quartz, my. myrmekite) in quartz-monzodiorite (cross-polarized light, 2.5x).

Hornblende is subhedral to euhedral, straw yellow, dark olive green to dark green and shows strong to moderate pleocroism. Few inclusions are observed, such as apatite, opaque minerals and minor titanite. Preserved clinopyroxene cores are very rare. Biotite and hornblende appear as rounded aggregates. Titanite is the most important accessory mineral in the Jaburuzinho facies. It occurs as euhedral to subhedral crystals, medium to coarse grained **(Fig. 8b)**, and generally perfect losangle shape, associated to biotite, hornblende, opaque minerals and epidote in mafic clots. It also occurs as euhedral fine grained crystals, included in biotite, and anhedral grains bordering opaque minerals.

Alto Alegre facies

The Alto Alegre facies is mainly composed of biotite monzogranites (around 80%) with subordinated granodiorites**,** syenogranites and tonalites **(Fig. 3a; Table 2).** These granitoids are generally isotropic, equigranular, medium- to coarse-grained, and eventually porphyrytic. The tabular alkali feldspar megacrysts are white to grayish and pale pinkish, showing 1 to 4 cm in length (ratio 3:1), 5 to 30% (locally 50%) in volume and ENE-WSW orientation (magma flow). Similarly to the Jaburuzinho facies, the Alto Alegre facies shows some portions with anisotropic texture. Two anisotropic features are observed and may include remnants of the Jaburuzinho facies: a) oriented tabular megacrysts and lenticular mafic enclaves that indicate magma flow (predominate), and b) solid-state deformed minerals, including moderate recrystallization and mineral stretching. Both structures have ENE-WSW to NE-SW strikes, parallel to the regional trends.

The Alto Alegre granitoids enclose hornblende-bearing microgranular enclaves (dioritic to granodioritic in composition) mainly near Jaburuzinho facies boundaries. These enclaves have 5 cm to 20 m in length and are elliptical, slightly rounded **(Fig. 9a)** and elongate **(Fig. 9g)**, locally with irregular and wispy terminations **(Fig. 9c)**.

Felsic coarse-grained monzogranite enclaves are also enclosed by the Alto Alegre granitoids. These enclaves are equigranular, pale gray, circular, rounded **(Figs. 9a, b and c),** irregular, elongate or angular **(Figs. 9d, f and, h),** showing linear orientation **(Figs. 9b and f)**. These three magmatic phases (Alto Alegre granitoids, hornblende-bearing enclaves related to Jaburuzinho facies and felsic coarse-grained monzogranite enclaves) show a complex physical interaction **(Fig. 9h)**, but chemical effects are also possible (Almeida and Macambira 2003).

The angular and rounded forms observed in the felsic monzogranite enclaves suggest different stages of assimilation. The contacts are sharp and chilled margins are not recorded. On the other hand, the hornblende-bearing enclaves show lobate to crenulate (flame-like) contacts with host monzogranite to granodiorite **(Fig. 9c)**, locally with "dropped" megacrysts, which suggests that the amount of liquid was high at the time of emplacement. In detail, the boundaries of these enclaves reproduce the overall contacts with the host granitoid (mimetization or ghost structures), suggesting a probable incomplete mingling process. Furthermore, the abundance of elongate to rounded enclaves and net veining in the mafic enclaves by the host granitoid, both suggest according to Vernon *et al.* (1988) mingling and/or mixing of magmas at the site of emplacement.

In this sense, only one outcrop of the Alto Alegre facies record field features of magma mixing. The possible mixing magma conduit has nearly 2 m of length and shows strong to extreme elongate enclaves **(Fig. 9g and h)** in which the distortion has been accomplished by magmatic flow without solid state deformation, as evidenced by strong orientation of the minerals, coupled with lack of microstructural evidence of intergranular plastic strain (Vernon *et al.* 1988).

The Alto Alegre granitoids show mineral assemblage **(Table 2)** composed of plagioclase (23-46 %), quartz (19-31 %), alkali feldspar (15-38 %), biotite (5-12 %), minor titanite, opaque minerals, epidote, apatite, allanite and zircon. In some samples muscovite also replaces biotite. The mafic mineral content is quite variable **(Fig. 3b)** and has biotite as the main mafic mineral.

Plagioclase is tabular, subhedral to euhedral, medium to coarse grained, locally as megacrysts showing combined polysynthetic and Carlsbad twinning. These crystals exhibit normal (mainly) to oscillatory compositional zoning, which stands out optically by secondary alteration (saussuritization) in the An-rich portions. Some megacrysts are irregular and show embayed rims in contact with alkali feldspar grains. Quartz is heterogranular, anhedral, and sometimes occurs as monocrystalline aggregates. Inclusions of drop-like quartz are also very common in the alkali feldspar megacrysts. Locally, it shows ondulatory extinction and dynamic (fine grained subgrains) to static recrystallization (granoblastic texture) effects in the solid-state deformed types.

Alkali feldspar shows two main generations. The first type is characterized by fine grained crystals with euhedral to subhedral shapes and tartan twinning in the groundmass. The second generation is marked by anhedral perthitic and poikilitic megacrysts encompassing several

inclusions (biotite, drop-like quartz, plagioclase and first generation alkali feldspar). In the solid-state deformed types, the alkali feldspar megacrysts are contoured by biotite trails, showing core-and-mantle structure and eventually granoblastic texture, suggesting upper greenschist to amphibolite-facies conditions.

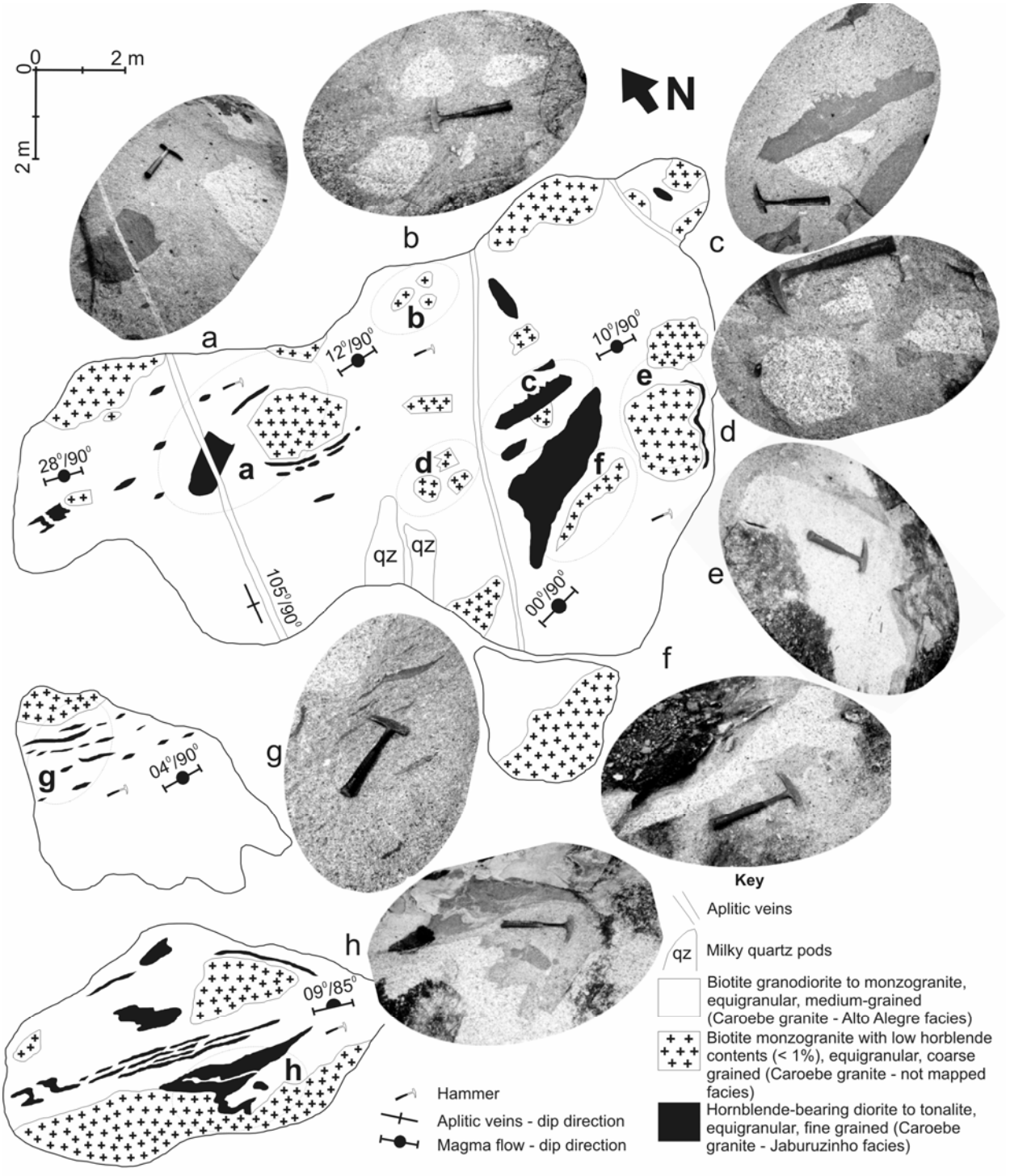

Fig. 09. Mingling-mixing features in the Alto Alegre facies (Caroebe granite, outcrop MA-53). See text for details.

Biotite is subhedral, medium grained, moderately pleocroic, and straw yellow to yellow greenish. Normally, it forms crystal aggregates and has apatite, epidote, allanite, zircon and opaque mineral inclusions, generally occurring as circular or irregular mafic clots. Locally, it is slightly to strongly oriented; some crystals are partially altered into muscovite. Titanite is medium to fine grained, euhedral, showing diamond shape or anhedral grains bordering opaque minerals.

Alkali feldspar shows two main generations. The first type is characterized by fine grained crystals with euhedral to subhedral shapes and tartan twinning in the groundmass. The second generation is marked by anhedral perthitic and poikilitic megacrysts encompassing several inclusions (biotite, drop-like quartz, plagioclase and first generation alkali feldspar). In the solid-state deformed types, the alkali feldspar megacrysts are contoured by biotite trails, showing core-and-mantle structure and eventually granoblastic texture, suggesting upper greenschist to amphibolite-facies conditions.

Biotite is subhedral, medium grained, moderately pleocroic, and straw yellow to yellow greenish. Normally, it forms crystal aggregates and has apatite, epidote, allanite, zircon and opaque mineral inclusions, generally occurring as circular or irregular mafic clots. Locally, it is slightly to strongly oriented; some crystals are partially altered into muscovite. Titanite is medium to fine grained, euhedral, showing diamond shape or anhedral grains bordering opaque minerals.

IGARAPÉ AZUL GRANITE

Based on petrographic (*e.g.* muscovite presence) and chemical (peraluminous character) parameters, Faria *et al.* (1999) individualized a portion of the Água Branca suite as a new granitic body that they called Igarapé Azul granite, initially interpreted as an S-type granite. The Igarapé Azul granite was revisited by Almeida *et al.* (2002) who noted that S-type granitoids in southeast Roraima are restricted to the Serra Dourada region and not in the Igarapé Azul type-area.

In the type-area the Igarapé Azul granite is characterized only by (muscovite)-biotite leucomonzogranites and monzogranites to rare syenogranites and granodiorites, generally with low mafic contents (**Fig. 3b**), showing a compositional field in the QAP diagram similar to granites of crustal origin (*e.g.* Lameyre and Bowden 1982, Lameyre and Bonin 1991, **Fig. 3a, Table 3**), but no aluminous diagnostic minerals are described. The main granitic body has 1120 km^2 and shows also an important textural asymmetric zoning with three main granitic facies: Vila

Catarina, Saramandaia and Cinco Estrelas **(Fig. 2)**. Other minor correlated granitic bodies have around 30 km^2 to 125 km^2. Thus, all granitic bodies with these same characteristics must be grouped in the Igarapé Azul Intrusive Suite (this paper).

Common petrographic features

Despite local textural variations, all facies of the batholith have similar composition (mainly monzogranite and minor granodiorite to syenogranite) and mineral assemblages, including accessory (epidote, allanite, opaque minerals, zircon and apatite) and secondary minerals (epidote, chlorite and muscovite).

Subhedral and tabular plagioclase are medium to fine-grained, show polyssinthetic twinning and normal zoning. Locally, its nucleus is partially altered to epidote and minor sericite and chlorite. Euhedral megacrysts are rare and eventually show oscillatory zoning, biotite inclusion and preferred orientation. Anhedral crystals with embayment are also observed and sometimes they show obliterated zoning and twinning. Quartz is fine to coarse-grained, anhedral, sometimes interstitial, locally fractured with ondulatory extinction and partially recrystallized (subgrains).

Alkali feldspar is partially altered to sericite and muscovite, and occurs as two different types: a) subhedral to anhedral, fine to coarse grained (3-8 mm long), tabular crystals showing tartan twinning, rarely combined with carlsbad twinning; b) tabular, anhedral and microperthitic megacrysts (25-40 mm long), locally with embayed rims and drop-like quartz, very altered plagioclase, biotite and locally opaque minerals and epidote inclusions. Myrmekite intergrowth is also common.

Subhedral biotite is fine to coarse grained, moderate to strongly pleocroic and straw yellow to brown greenish. Biotite with red brownish color is very uncommon. Eventually it occurs as mafic clots associated to epidote and/or allanite, opaque mineral, zircon and apatite. In general, it is slightly oriented and some crystals are partially or totally replaced by muscovite and/or chlorite.

Epidote is the main accessory mineral in the Igarapé Azul granite. The crystals are fine to medium grain size, subhedral to euhedral shapes, pale yellow to pale green and locally zoned, showing cores of allanite. Anhedral crystals are commonly observed as inclusions in plagioclase. Metamitic allanite shows pale brown to orangish brown colors. Twinned crystals are uncommon. Sulfides and oxides are subhedral to euhedral, fined to medium-grained and show hexagonal and square habits, normally associated with biotite. Rarely they show anhedral and interstitial forms.

These petrographic characteristics in commom represent transitional features among nucleus and margins facies of the Igarapé Azul pluton. This granite shows textural differences only (*e.g.* feldspar megacrysts modal volume and groundmass grain-size), suggesting local P_{H2O} variations.

Vila Catarina facies

The Vila Catarina facies has nearly 340 km^2 and occurs in the center-western portion of the Igarapé Azul granite, showing several Nb-Ta alluvial mineral occurrences, including abundant aplitic to pegmatitic dikes. It has also similar structural trend (NE-SW) to that observed in Cinco Estrelas facies described below.

The Vila Catarina granitoids are characterized by mainly monzogranites and restrict syenogranite **(Fig. 3a)** pale gray to pale pink, showing equigranular to slightly porphyrytic (<5% alkali feldspar megacrysts), medium to coarse-grained texture and variable mafic mineral content (always <10%). In thin section, the groundmass is granular, anhedral and, locally, encompasses alkali feldspar megacrysts (1.5 to 2.0 cm long) and mafic clots. The mineral assemblage **(Table 3)** is composed of plagioclase (24-45 %), quartz (21-38 %), alkali feldspar (20-41 %), biotite (0.6-8 %), locally transformed into muscovite (0.2-2 %), and opaque minerals, epidote, allanite, zircon and apatite. The most important secondary minerals are epidote, chlorite and titanite.

Saramandaia facies

The Saramandaia facies has nearly 735 km^2 in area and occurs in the northern portion of the batholith. This granitoid is cross-cut by dykes and blobs of the Cinco Estrelas and Vila Catarina facies. In the Saramandaia facies, the granitoids have porphyrytic texture showing alkali feldspar megacrysts (5% to 20%) with heterogeneous size (<1 to 5 cm long) and spatial distribution **(Figs. 10a,b)**, similar to those of the Vila Catarina facies. These megacrysts are microperthitic, tabular, euhedral, white to slightly pinkish and eventually are oriented due to magma flow. They are enveloped by homogeneous and medium grained groundmass of monzogranitic to granodioritic composition.

The megacryst direction is locally outlined by ellipsoidal biotite-bearing enclaves, following ENE-WSW to NE-SW-trends. Similar trends are observed in the megacryst direction of the Caroebe granitoids that are also subparallel to the regional foliation strikes observed in the

host Martins Pereira granitoid. However, the low amount of megacrysts makes this flow to be almost imperceptible.

In this facies, monzogranites are dominant; granodiorites are subordinated **(Fig. 3a)** as well as leucogranites. The mineral assemblage **(Table 3)** is composed by plagioclase (26-44 %), quartz (24.3-33.0 %), alkali feldspar (23.3-28.6 %), biotite (0.4-5.7 %), muscovite (0.2-1.0 %), opaque minerals, primary epidote, allanite, and minor zircon and apatite. Epidote, chlorite and, exceptionally titanite, are the main secondary minerals in the Saramandaia facies.

Cinco Estrelas facies

The Cinco Estrelas facies has 445 km^2, located at the easternmost portion of the Igarapé Azul batholith, showing granitoids with very low mafic contents, and equigranular, homogeneous and fine to medium-grained texture **(Figs. 10c,d)**. These granitoids are also whitish gray, monzogranitic in composition with subordinated syenogranite, granodiorite and quartz monzonite (**Fig. 3a**). They are emplaced according to a NE-SW structural direction and locally also occur as blobs and dikes subconcordant with magma flow direction, as observed in the porphyrytic types of the Saramandaia facies.

The Cinco Estrelas facies mineral assemblage **(Table 3)** is composed by plagioclase (11-52 %), quartz (16-38 %), alkali feldspar (18-36 %), biotite (1-5 %), totally or partially transformed into muscovite (0.1-5 %), and opaque minerals, allanite, primary epidote, zircon and apatite. The most important secondary minerals are epidote, chlorite and leucoxene.

Enclaves

The enclaves found in the Igarapé Azul granitoids are dominantly biotite-rich (**Table 3**) with fine to coarse-grained muscovite crystals. These enclaves show sharp and irregular **(Fig. 10c)** to elliptical **(Fig. 10b)** shapes, locally with gneissic texture. Several enclaves have also elongated shapes and biotite trails and schlieren only. In general, these enclaves are parallel to the magma flow defined by alkali feldspar megacrysts in the host granitoids **(Fig. 10b)**. The contact enclaves-host granitoid is normally sharp, however, sometimes it shows transitional and gradational features.

The biotite-bearing enclaves show quartz dioritic, tonalitic and quartz monzodioritic compositions **(Fig. 3a, Table 3)**, equigranular fine to coarse grained texture, and black to gray colors. They also show foliation defined by biotite and muscovite **(Fig. 11)**, but it is not always

observed at naked eye. Its mineral assemblage is composed by biotite (27.6-57.7 %), plagioclase (12.5-40.0 %), muscovite (2.0-10.0 %), quartz (4.4-12.9 %), alkali feldspar (0.1-12.9 %), epidote (0.4-4.7 %) and opaque minerals (1.0-6.7 %). Other minerals are rare, such as titanite, apatite, zircon and allanite. Secondary epidote and sericite are common.

Fig. 10. Igarapé Azul granite outcrops: a) Slightly porphyrytic biotite monzogranite (Saramandaia facies) showing tabular alkali feldspar megacrysts with approximately N60°E strike magma flow (outcrop MA-322); b) Tabular alkali feldspar megacrysts in leucogranodiorite (Saramandaia facies) turning around elliptical tonalite gneiss enclave (outcrop MA-213); c) Irregular biotite-rich diorite gneiss enclave showing fine grained equigranular texture surrounded by biotite leucomonzogranite (Cinco Estrelas facies). Note that the host granite fill the enclave foliation planes (outcrop MA-147); d) Porphyrytic biotite granodiorite enclave (Martins Pereira granite) enclosed by the Igarapé Azul granite (Cinco Estrelas facies). The enclave is rotated and biotite trails are observed in its extremities (outcrop MA-99). e) Rounded paragneiss enclave showing strong compositional layering and local growing of biotite and muscovite. f) Rounded and circular mafic microgranular enclave with porphyrytic texture (outcrop MA-322).

Subhedral biotite is fine to coarse grained, brown greenish to straw yellow, locally reddish brown, and moderately pleocroic. Inclusions such as zircon, apatite, epidote, and occasionally allanite, are common. Muscovite is also subhedral, fine to medium-grained and aligned at the same direction of biotite. Large individual crystals are intergrowth or replacing biotite. Plagioclase shows two crystal generations: a) coarse grained (eventually megacrysts), subhedral to anhedral (embayed contacts are very common), slight ondulatory extinction, normal zoning (rarely oscillatory) with calcic zones steeply replaced by epidote, carbonate and minor sericite; b) fine to medium grained, subhedral to euhedral, tabular, clear polyssinthetic twinning and rarely replaced by secondary minerals. Fine to medium-grained subhedral quartz has ondulatory extinction and locally shows dynamic recrystallization features. Subhedral to anhedral alkali feldspar is very uncommon. Subhedral epidote and allanite occurs as inclusion in biotite and plagioclase crystals. Opaque minerals occur as euhedral and tabular crystals and titanite is rare, eplacing calcic portions of plagioclase cores, and biotite cleavages. Locally, titanite occurs as subhedral, fine to medium-grained and isolate crystals.

Other enclaves are subordinated within the Igarapé Azul granite. Xenoliths similar to the Martins Pereira granitoids **(Fig. 10d)** and Cauarane paragneiss with preserved banding **(Fig. 10e)** are rotated, rounded and partially modified, with local "migmatitic" features, suggesting local assimilation by the host rock. Mafic (porphyrytic) microgranular enclaves **(Fig 10f)** are observed only locally.

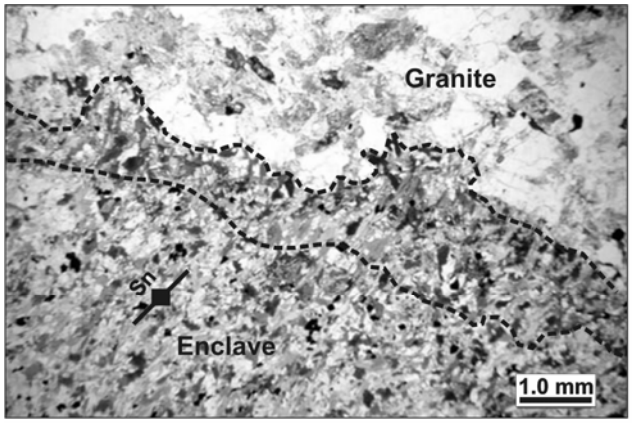

Fig. 11. Photomicrography showing granite-enclave contact. Dashed lines show the growing and high concentration of biotite crystals from the biotite-bearing gneissic enclave (quartz dioritic) close to the contact with isotropic leucomonzogranite (Igarapé Azul Granite, Cinco Estrelas facies). This biotite grain size increasing is probably due to static recrystallization related to the high thermal gradient among host-enclave. The enclave foliation (Sn) is also showed. Parallel-polarized light (1.25x).

A-type granites

In general, the A-type granites in the southern Roraima and northern Amazonas states cross-cut the basement rocks during two main magmatic events (Costi *et al.* 2000, CPRM 2000, 2003): Abonari-Mapuera (1.88-1.86 Ga) and Moderna-Madeira (1.82-1.79 Ga) granitic episodes. The interval ages are determined mainly by single-zircon Pb evaporation and zircon U-Pb SHRIMP methods.

MAPUERA GRANITE AND COEVAL GRANITOIDS

The Mapuera A-type granites (CPRM 2000, 2003) and coeval granitoids occur at the south and southeast of the studied area **(Fig. 2)**, in the Jauaperi and Murauaú rivers, showing biotite only as the mafic mineral. Three main granitic bodies were observed. The first one has 46 km^2 and occurs near to the São João da Baliza and São Luís do Anauá towns at the Jauaperi river basin. It shows monzogranitic to syenogranitic composition, porphyrytic texture (locally with ovoid megacrysts) and coarse to medium grain size. The second granitic body has 49 km^2 and occurs along the Murauaú River, being composed of monzogranites with equigranular to slightly porphyrytic texture, and medium grain size. Locally in the northern portion it is steeply deformed by NE-SW dextral shear zones. The Serra do Itã granite (520 km^2 in area) has E-W trend emplaced near the Itã fault zone and in the headwaters of the Anauá, Dias and Pedras rivers.

The mineral assemblage is represented by microperthitic alkali feldspar, plagioclase (eventually bordered by alkali feldspar), quartz and biotite, this last one in association with accessory minerals such as titanite, zircon, apatite, opaque minerals and rarelly allanite, fluorite and garnet. Locally quartz and feldspars show ondulatory extinction and dynamic recrystallization. Granophyric texture and myrmekite are also commom. Secondary minerals are sericite (and muscovite), chlorite, epidote and clay-minerals.

MODERNA GRANITE AND COEVAL GRANITOIDS

The Moderna (Santos *et al.* 1997) and coeval granitoids **(Fig. 2)** are dominantly monzogranite to syenogranite, rarely alkali feldspar granite in composition, showing pale pink to pale gray colors, equigranular to slightly porphyrytic texture, coarse grain size and amphibole (hastingsite) and biotite mafic clots. Paragneissic xenoliths of the Cauarane Group and pegmatitic and amethyst-bearing quartz veins are also observed.

At least, four granitic bodies related to the Moderna-Madeira granitic episode, all structurally-controled by NW-SE trends, were mapped by aerogeophysical airbone and radar

images: 1) the type-area of the Moderna granite occurs near the Moderna town, and has two main plutonic bodies of 51 km^2 and 15 km^2 controlled by a NW-SE structure; 2) Serra da Tentativa granite has 58 km^2 and crops out in the Jaburuzinho river; 3) Igarapé do Banho granite shows 210 km, cross-cuted by E-W dextral shear zones; and 4) northern Caroebe granite has 330 km^2 and is also structurally controlled by an NW-SE trend.

The mineral assemblage shows microperthitic alkali feldspar, albite, plagioclase (oligoclase), quartz, biotite and amphibole (intersticial hastingsite with local clinopyroxene relics). The accessory minerals are opaque minerals, apatite, zircon, allanite, titanite (intregrown with amphibole) and fluorite (as individual crystals or filling microfractures mainly in the biotite). Secondary minerals are represented by clay-minerals, sericite and epidote.

MINERAL OCCURRENCES

Until few years ago, all mineral occurrences in the southern Roraima were associated to the "Água Branca" suite and "Igarapé Azul" granite (CPRM 2000). However, the results of geological mapping and petrographic study in this work demonstrated that amethyst, columbite-tantalite and gold occurrences are related with three different granitic types.

In the northern area (NUAD), the highly deformed, showing quartz-vein related to shear zones, and hydrothermallized (muscovitization and tourmalinization) host rocks of the Anauá small gold mine (Faria *et al.* 1996) overprint the igneous features. In other two sites, there has been detected Au in alluvial sediments overlying Martins Pereira granitoids basement. Despite the difficulty of recognizing the primary rocks, the host of mineralization shows composition, texture and age (1972 ± 7 Ma, zircon U-Pb SHRIMP, CPRM 2003) similar to the I-type Martins Pereira granitoids. Furthermore, relationship among gold occurrences and S-type granites (*e.g.* Serra Dourada granite) is uncommom (*e.g.* Neiva 2000).

In the SUAD, several columbite-tantalite occurrences in alluvial sediments have been described (CPRM 2000); all of them are located in the Igarapé Azul granite region. The main Nb-Ta occurrences are related to the central Vila Catarina facies, which is characterized by pegmatites and alluvial fans with conglomeratic levels (0.5 m in average) showing angular and subrounded fragments of columbite-tantalite were ranging from 80 mm to 0.2 mm in length. Also in this area, the amethyst crystals occur in regular veins, pegmatites or in stockwork structures, hosted by the A-type Moderna granitoids. According to CPRM (2000) this amethyst mineralization probably has an epithermal origin.

SUMMARY AND CONCLUDING REMARKS

Geological mapping and petrographic studies of granitoids in the north and south areas of the Uatumã-Anauá domain provide new insights in the geologic framework of the central portion of Guyana Shield **(Fig. 1)**, including mineralization occurrence relationship, and implications for the tectonic evolution.

The Martins Pereira and Serra Dourada granites in NUAD are characterized by penetrative deformation and dextral shear zones associated with NE-SW to E-W-trendings, and both are associated with metavolcano-sedimentary covers and older basement inliers (Anauá Complex and Cauarane Group). The S-type Serra Dourada granite suggests, at least locally, a widespread anatexis of dominant sedimentary sources in this region.

In the Martins Pereira granitoids, the petrographic similarities point out that the granitoid host-rocks (monzogranites and granodiorites) and the biotite-bearing enclaves (tonalites) are cogenetic. The origin of leucogranitic blobs is not well understood, but two explanations can be envisaged: a) highly fractionated types from Martins Pereira calc-alkaline association, or b) new granitic magmas from small-scale remelting of Martins Pereira granitoids (local anatexis).

The tectonic evolution is yet debatable, but the relationship of the NUAD granitoids with the Anauá Arc (Faria *et al.* 2002) is possible, due mainly the geographic aspects and features of ntrusion. The I-type calc-alkaline and S-type granites chemistry and ages suggest that they could be related to the final stages, or after, of the Anauá Arc (2.03 Ga) development. The ~60 Ma elapsed time among Anauá arc formation and the emplacement of the Martins Pereira-Serra Dourada granitoids point out a late(?)-collisional event at 1.97-1.96 Ga in the southeastern Roraima.

On the other hand, the SUAD area is characterized by only undeformed calc-alkaline Caroebe and Igarapé Azul granites (Água Branca suite) and local coeval volcanic rocks, but no arc-related metavolcano-sedimentary rocks and low-K calc-alkaline granitoids are recorded. A petrogenetic evolution following fractional crystallization process was suggested by Oliveira *et al.* (1996) for the Água Branca suite, however, at least locally, other petrogenetic processes can be involved in the genesis of the Caroebe granite (*e.g.* partial melting, magma mixing or assimilation fractional crystallization).

The magma mixing hypothesis for the Alto Alegre facies of the Caroebe granite is based on field observations, where two end-members, represented by felsic monzogranite and hornblende

diorite-tonalite, produced an intermediate homogeneous granodioritic member (hybrid magma). However, some authors (*e.g.* Chappell and McCulloch 1990, Chappell 1996) argue that this petrogenetic process is related only to the small-scale granite generation and do not support large bodies generation due to the large viscosity contrast between two magmas of contrasting compositions that inhibit the mixing. According to them, magma mixing is limited in most granitoid evolution. Magma mixing is an important petrogenetic model for granitoids generation, but only mixing events could be recorded in the pluton, generating local hybrid rocks.

Other authors believe that large granitic batholiths are produced mainly by magma mixing process, such as the Itaporanga batholith in northeastern Brazil (Mariano and Sial 1990) and H-type granitoids in Spain (Castro *et al.* 1990, 1991). They are based on the geochemical and experimental constraints mainly observed in volcanic rocks (*e.g.* Turner and Campbell 1986, Gourgaud *et al.* 1989) and their application to plutonic rocks (*e.g.* Blake and Koyaguchi 1991). According to Blake and Koyaguchi (1991), if hybrid volcanic magmas are produced in the magma chambers (that are the precursors of plutonic rocks) then, the plutonic analogues of these same chambers should contain hybrid facies. However, likewise the volcanic types, areas of hybrid rock within pluton could record mixing events related to the intermittent generations of batch melts. Thus, a geochemical study in the Caroebe granite is necessary for a better evaluation of the petrogenetic model.

The Igarapé Azul granite also shows calc-alkaline affinity (Almeida and Macambira 2003), but it is almost restrict to felsic monzogranites types, which are characterized by homogeneous texture. These granitoids show similar compositional field of the crustal granite origin and petrographic features to felsic granites occurring as lenses and blobs in the Martins Pereira granite (*e.g.* monzogranitic composition, textural homogeneity, low modal content of mafic minerals, biotite and late muscovite as the varietal minerals, and epidote and opaque minerals as the main accessory minerals).

The magmatic flow and shape of granitic bodies with NE-SW to E-W-trends observed in the Igarapé Azul and Caroebe granites suggest that the emplacement was probably structurally-controlled by older lineaments, such as observed in the Martins Pereira granitoids.

The two generations of A-type granites which are widespread in UAD, are related to a post-orogenic (1.87 Ga) to anorogenic (1.81 Ga) setting respectively, and mark the tectonic stability period in the southeastern Roraima. The emplacement of these A-types granites has E-W and NW-SE-trending structural-control, filling mainly brittle structures.

Finally, the relationship between mineralization and the granitoid hosts in the UAD, as a whole, opens new metaloctec perspectives, emphasizing the mineral potential of this region for gold (Martins Pereira granitoids), columbite-tantalite (mainly in the central facies of Igarapé Azul granite) and amethyste (Moderna granite, pegmatite).

Acknowledgements

Special thanks to M.S.G. de Faria (MJ-DPF-Manaus), N. J. Reis, S. S. Pinheiro and R. Luzardo (Geological Survey of Brazil) for discussions. The authors are grateful also to the Geological Survey of Brazil (CPRM) and Federal University of Pará (UFPA) for the support to this research. Thanks also to the three anonymous referees for suggestions to the manuscript.

References

Almeida M.E. & Macambira M.J.B. 2003. Aspectos geológicos e litoquímicos dos granitóides cálcio-alcalinos Paleoproterozóicos do sudeste de Roraima. *In*: SBGq, Cong. Brasil. Geoq., 9, Anais, p. 775-778.

Almeida M.E., Macambira M.J.B., Faria M.S.G. de. 2002. A Granitogênese Paleoproterozóica do Sul de Roraima. *In*: SBG, Cong. Bras. Geol., 41, Anais, p 434.

Araújo Neto H. & Moreira H.L. 1976. *Projeto Estanho do Abonari*. Manaus, Convênio DNPM/CPRM, Relatório Final. 2v .

Berrangé J.P. 1972. The Tectonic/Geological Map of Southern Guyana. *In*: Ministerio de Minas e Hidrocarburos, Conferencia Geológica Inter-Guayanas, 9, *Boletin de Geología, Publicacion Especial* **6** : 161-174.

Blake S. & Koyaguchi T. 1991. Insights on the magma mixing model from volcanic rocks. *In*: J. Didier and B. Barbarin (eds) Enclaves and granite petrology, Elsevier, p.403-413.

Castro A., de la Rosa J.D., Stephens W.E. 1990. Magma mixing in the subvolcanic environment. Petrology of the Gerena interaction zone near Seville, Spain. *Contrib. Mineral. Petrol.,* **105**: 9-26.

Castro A., Moreno-Ventas I., de la Rosa J.D. 1991. H-type (Hybrid) granitoids: A proposed revision of the granite-type classification and nomenclature. *Earth Science Rev.,* 31: 237-253.

Chappell B.W. 1996. Magma mixing and the production of compositional variation within granite suites: evidence from the granites of southeastern Australia. *Journ. Petrol.,* **37** : 449-470.

Chappell B.W. & McCulloch M.T. 1990. Possible mixed source rocks in the Bega Batholith: constraints provided by combined chemical and isotopic studies. *Abst. Geol. Soc. Australia,* **27**: 17.

Costi H.T., Dall'Agnol R., Moura, C.A.V. 2000. Geology and Pb-Pb geochronology of Paleoproterozoic volcanic and granitic rocks of the Pitinga Province, Amazonian craton, northern Brazil. *Intern. Geol. Rev.,* **42**: 832-849.

Costi H.T., Santiago A.F., Pinheiro S.S. 1984. *Projeto Uatumã–Jatapu*. Manaus, CPRM, Relatório Final. 133p.

CPRM. 1999. Programa Levantamentos Geológicos Básicos do Brasil. *Roraima Central, Folhas NA.20-X-B e NA.20-X-D (integrais), NA.20-X-A, NA.20-X-C, NA.21-V-A e NA.21-V-C (parciais)*. Escala 1:500.000. Estado de Roraima. Manaus, CPRM, 166 p. CD-ROM.

CPRM. 2000. Programa Levantamentos Geológicos Básicos do Brasil. *Caracaraí, Folhas NA.20-Z-B e NA.20-Z-D (integrais), NA.20-Z-A, NA.21-Y-A, NA.20-Z-C e NA.21-Y-C (parciais)*. Escala 1:500.000. Estado de Roraima. Manaus, CPRM, 157 p. CD-ROM. (abstract in english)

CPRM. 2003. Programa Levantamentos Geológicos Básicos do Brasil. *Geologia, Tectônica e Recursos Minerais do Brasil: sistema de informações geográficas - SIG*. Rio de Janeiro : CPRM, 2003. Mapas Escala 1:2.500.000. 4 CDs ROM.

CPRM. 2006. Programa Integração, Atualização e Difusão de Dados da Geologia do Brasil: Subprograma Mapas Geológicos Estaduais. *Geologia e Recursos Minerais do Estado do Amazonas*. Manaus, CPRM/CIAMA-AM, 2006. Escala 1:1.000.000. Texto explicativo, 148p. CD ROM.

Faria M.S.G. de, Almeida M.E., Santos J.O.S. dos, Chemale Jr. F. 2003. Evolução Geológica da Região do Alto Rio Anauá - Roraima. *In*: SBG, *Simp. Geol. Amaz.*, 8, Anais, CD-ROM.

Faria M.S.G.de, Luzardo R., Pinheiro S. da S. 1999. Litoquímica e petrogênese do Granito Igarapé Azul. *In*: SBG, Simp. Geol. Amaz., 6, Anais, p. 577-580.

Faria M.S.G. de, Oliveira M.J.R., Luzardo R, Pinheiro S. da S. 1996. Garimpo do Anauá, Sudeste do Estado de Roraima: dados preliminares sobre ocorrência aurífera associada à zona de cisalhamento. *In*: SBG, Cong. Bras. Geol., 39, Anais, v. 3 p. 316-319.

Faria M.S.G. de, Santos J.O.S.dos, Luzardo R., Hartmann L.A., McNaughton N.J. 2002. The oldest island arc of Roraima State, Brazil – 2.03 Ga: zircon SHRIMP U-Pb geochronology of Anauá Complex. *In*: SBG, Congr. Brasil. Geol., 41, Anais, p. 306.

Gaudette H.E., Olszewski W.J. Jr., Santos J.O.S. dos. 1996. Geochronology of Precambriam rocks from the northern part of Guiana Shield, State of Roraima, Brazil. *Journ. South Am. Earth Sci.*, **9**: 183-195.

Gibbs A.K., Barron C.N. 1993. *The geology of the Guyana Shield*. Oxford University Press, Oxford, N. York, 245 p.

Gourgaud A, Fichaut M, Joron J -L 1989. Magmatology of Mt. Pelee (Martinique, F.W.I.). I: Magma mixing and triggering of the 1902 and 1929 Pelean nuees ardentes. *J. Volc. Geotherm. Res.*, **38**: 143-169.

Jorge-João X.S., Santos C.A., Provost A. 1985. Magmatismo adamelítico Água Branca (Folha Rio Ma puera, NW do Estado do Pará). *In*: SBG, Simp. Geol. Amaz., 2, Anais, v.2, p. 93-109.

Lameyre J. & Bowden P., 1982. Plutonic rock type series: discrimination of various granitoids series and related rocks. *J. Volc. Geotherm. Res.*, 14, 169-186.

Lameyre J. & Bonin B., 1991. Granites in the main plutonic series. In: J. Didier and B. Barbarin (eds.), *Enclaves and Granite Petrology*. Development in Petrology, 13, 3-17.

Macambira M.J.B., Almeida M.E., Santos L.S. 2002. Idade de Zircão das Vulcânicas Iricoumé do Sudeste de Roraima: contribuição para a redefinição do Supergrupo Uatumã. *In*: SBG, Simpósio Sobre Vulcanismo e Ambientes Associados, 2, Anais, p. 22 .

Mariano G. & Sial A.N. 1990. Coexistence and Mixing of Magmas in the Late Precambrian Itaporanga Batholith, State of Paraiba, Northeastern Brazil. *Rev. Bras. Geoc.*, **20** (1-4): 101-110.

Neiva A.M.R. 2000. Comparison between Portuguese granites associated with Sn-W mineralizations and with Au mineralization. *In*: SBG, Intern. Geol. Cong., 31 Abstr. Vol. CD-ROM.

Oliveira M.J.R., Almeida M.E., Luzardo R., Faria M.S.G. de. 1996. Litogeoquímica da Suíte Intrusiva Água Branca - SE de Roraima. *In*: SBG, Congr. Bras. Geol., 39, Anais, v.2, p. 213-216 .

Passchier C.W. & Trouw R.A.J. 1996. *Microtectonics*. Springer Verlag, London, 326p.

Reis N.J. & Fraga L.M.B. 2000. Geological and tectonic framework of Roraima State, Guyana Shield – An overview. *In*: SBG, Intern. Geol. Cong., 31, Abstr. Vol., Gen. Simp. 9. CD-ROM.

Reis N.R. & Fraga L.M.B. 1996. Vulcanismo Surumu - Estado de Roraima: Caracterização de seu comportamento químico à luz de novos dados. *In*: SBG, Congr. Bras. Geol., 39, Anais..., v. 2, p. 88- 90 .

Reis N.J., Fraga L.M., Faria M.S.G. de, Almeida M.E. 2003. Geologia do Estado de Roraima. *Géologie de la France*, **2-3**: 71-84.

Reis N.R., Faria M.S.G. de, Fraga L.M.B., Haddad R.C. 2000. Orosirian calc-alkaline volcanism from eastern portion of Roraima State – Amazon Craton. *Rev. Bras. Geoc.* **30** (3): 380-383.

Santos, J.O.S. dos, Hartmann, L.A., Gaudette, H.E., Groves, D.I., McNaughton, N.J., Fletcher, I.R. 2000. A new understanding of the provinces of the Amazon Craton based on integration of field mapping and U-Pb and Sm-Nd geochronology. *Gond. Res.* **3** (4) : 453-488.

Santos J.O.S. dos, Silva L.C., Faria M.S.G. de, Macambira, M.J.B. 1997. Pb-Pb single crystal, evaporation isotopic study on the post-tectonic, sub-alkalic, A-type Moderna granite, Mapuera intrusive suite, State of Roraima, northern Brazil. *In*: SBG, Symposium of Granites and Associated Mineralizations, 2, Extended Abstract, p.273-275.

Sardinha A.S. 1999. *Petrografia do Granito Igarapé Azul, Sudeste do Estado de Roraima*. Trabalho de Conclusão de Curso, Centro de Geociências, Universidade Federal do Pará, 32p.

Streckeisen A.C. 1976. To each plutonic rock its proper name. *Earth Sci. Rev.*, **12**: 1-33.

Tassinari, C.C.G. & Macambira M.J.B. 1999. Geochronological Provinces of the Amazonian Craton. *Episodes,* **22** (3): 174-182.

Turner J.S. & Campbell I.H., 1986. Convection and mixing in agma chambers. *Earth Sci. Rev.*, **23**: 255-52.

Veiga Jr. J.P., Nunes A.C.B., Souza E.C. de, Santos J.O.S. dos, Amaral J.E., Pessoa M.R., Souza S.A. de S. 1979. *Projeto Sulfetos do Uatumã*. Manaus, DNPM/CPRM, Relatório Final, 6 v.

Vernon R.H., Etheridge M.A., Wall V.J. 1988. Shape and microstructure of microgranitoid enclaves: indicators of magma mingling and flow. *Lithos* 22: 1-11.

White A.J.R. 1992. *Granite Handbook: description, genesis and some associated ore deposits*. Short course, SBG, São Paulo. 49p.

Table 1. Modal mineral contents of samples from Martins Pereira and Serra Dourada granitoids and associated rocks.

samples	classification	facies	qz	af	pg	bi	ms	tt	al	ep	zi	ap	om	cd	gr	si	tu	mz-xt	cl	lx	ss	my	ph	cb	ref.
MF-151	syenogranite	A	31.0	39.0	19.0	5.0	3.0	-	-	tr	tr	tr	1.0	2.0	-	tr	-	tr	tr	-	tr	-	-	-	2
MF-156	monzogranite	A	24.0	35.5	20.6	7.8	5.0	-	-	-	0.2	tr	1.8	2.8	-	0.4	-	0.5	0.2	-	1.2	-	-	-	3
MF-157	monzogranite	A	21.0	29.0	27.0	13.0	5.0	-	-	tr	1.0	1.0	2.0	1.0	-	-	-	tr	tr	tr	tr	-	-	-	2
MF-155	granodiorite	A	19.1	15.8	39.3	20.8	1.7	-	-	-	0.3	tr	1.3	0.3	-	-	-	tr	0.0	-	0.7	0.7	-	-	3
MF-154	monzogranite	A	18.4	29.8	28.8	0.9	6.4	1.2	0.0	12.0	tr	tr	0.3	-	-	-	-	-	2.1	-	-	-	-	-	3
MJ-013B	granodiorite	B	35.3	14.8	41.0	6.1	0.1	0.6	-	1.6	0.1	0.1	0.2	-	-	-	-	-	0.1	-	-	-	-	-	1
MF-011B	monzogranite	B	34.5	28.4	27.1	6.1	3.1	0.1	0.1	0.1	0.1	0.1	0.2	-	-	-	-	-	0.1	-	-	-	-	-	1
MJ-055B	meta-granodiorite	B	32.8	10.6	46.3	7.2	1.0	0.3	-	0.4	0.1	0.2	0.7	-	-	-	-	-	0.1	-	0.3	-	-	-	1
MJ-024B2	monzogranite gneiss	B	32.7	36.6	23.3	4.3	1.4	0.1	-	-	0.1	0.1	0.8	-	-	-	-	-	0.1	0.2	0.3	-	-	-	1
RL-137B	granodiorite	B	32.3	20.0	38.6	6.0	1.1	0.1	-	0.9	0.1	0.1	0.3	-	-	-	-	-	-	-	0.5	-	-	-	1
MF-007B	meta-granodiorite	B	32.2	17.1	38.3	8.3	2.2	0.1	0.1	0.5	0.1	0.1	0.6	-	-	-	-	-	0.1	0.1	0.2	-	-	-	1
MA-007A	meta-monzogranite	B	31.4	22.8	32.2	9.7	0.8	0.5	0.2	0.7	0.1	0.3	1.3	-	-	-	-	-		-	-	-	-	-	3
MJ-213A	monzogranite	B	31.0	28.0	29.0	5.0	2.0	-	1.0	0.1	1.0	1.0	1.0	-	-	-	-	-	0.4	-	0.5	-	-	-	2
PT-006A	monzogranite	B	31.0	28.0	29.0	5.0	2.0	1.0	-	0.1	1.0	1.0	1.0	-	-	-	-	-	0.4	-	0.5	-	-	-	2
MA-045	meta-granodiorite	B	30.2	13.1	35.9	11.4	1.0	1.0	1.0	1.7	0.0	1.0	1.7	-	-	-	-	-	0.0	-	0.7	0.3	1.0	-	3
MF-011A	granodiorite	B	30.0	16.4	37.4	12.0	2.1	0.1	-	1.1	0.1	0.3	0.3	-	-	-	-	-	0.2	-	-	-	-	-	1
MJ-055A	meta-monzogranite	B	29.7	23.7	38.2	5.5	1.2	0.2	-	0.5	0.1	0.1	0.6	-	-	-	-	-	0.1	-	0.1	-	-	-	1
RL-016	meta-granodiorite	B	28.6	19.4	41.2	8.8	-	0.4	-	0.2	0.1	0.1	0.8	-	-	-	-	-	-	-	0.4	-	-	-	1
PT-007	monzogranite	B	28.4	31.6	34.0	4.6	0.1	0.1	0.1	0.1	0.1	0.1	0.8	-	-	-	-	-	-	-	-	-	-	-	1
MF-132A	meta-monzogranite	B	28.0	26.0	26.0	10.0	5.0	1.0	-	0.3	0.2	1.0	1.0	-	-	-	-	-	0.5	-	1.0	-	-	-	2
RL-013(2)	monzogranite	B	27.3	26.5	39.7	4.3	0.3	0.2	0.1	0.4	0.1	0.1	1.0	-	-	-	-	-	-	-	-	-	-	-	1
RL-046	granodiorite	B	27.0	12.0	42.0	10.0	4.0	-	-	0.1	1.0	0.3	3.0	-	-	-	-	-	0.3	-	0.3	-	-	-	2
MA-061A	monzogranite	B	26.9	22.6	24.7	10.1	1.3	0.6	0.0	3.4	0.2	0.6	0.9	-	-	-	-	-	-	-	7.1	1.1	0.4	-	3
RL-050	granodiorite	B	26.5	22.0	43.0	5.0	1.0	-	-	0.2	-	1.0	0.3	-	-	-	-	-	0.5	-	0.5	-	-	-	2
MF-010A	meta-granodiorite	B	26.1	18.8	43.2	5.0	4.4	0.1	0.1	1.2	0.1	0.1	0.7	-	-	-	-	-	0.1	0.1	-	-	-	-	1
MA-172A	monzogranite	B	25.2	32.6	22.7	9.9	0.4	1.1	0.4	0.4	0.4	1.4	1.1	-	-	-	-	-	0.4	-	4.3	-	-	-	3
PT-010	granodiorite	B	25.0	22.0	42.0	6.0	3.0	-	-	0.1	-	0.8	0.9	-	-	-	-	-	0.1	-	0.1	-	-	-	2
MJ-013A	granodiorite	B	24.7	14.6	48.1	7.8	0.1	0.9	0.1	3.3	0.1	0.1	0.1	-	-	-	-	-	0.1	-	-	-	-	-	1
MA-119	monzogranite	B	24.1	27.6	23.9	12.1	-	2.0	-	2.9	0.3	tr	0.9	-	-	-	-	-	0.5		4.6	1.1	-	-	3
NR-018	meta-monzogranite	B	22.7	27.1	41.9	5.9	0.2	0.3	0.1	0.4	0.1	0.2	0.7	-	-	-	-	-	-	-	0.4	-	-	-	1
RL-139	granodiorite	B	22.6	9.7	52.5	10.7	-	2.3	-	0.4	0.1	0.3	0.9	-	-	-	-	-	0.1	-	0.4	-	-	-	1
MA-261B	meta-granodiorite	B	20.5	23.4	40.2	9.2	-	1.6	-	1.1	0.2	0.4	1.1	-	-	-	0.7	-	-	-	0.4	1.1	-	-	3
MJ-013C	leucogranodiorite	C	32.5	21.1	41.7	3.0	0.3	0.1	0.1	0.7	0.1	0.1	0.2	-	-	-	-	-	0.1	-	-	-	-	-	1
MF-011C2	leucomonzogranite	C	31.4	27.4	38.7	1.2	0.1	0.1	-	0.3	0.1	0.1	0.1	-	-	-	-	-	0.2	-	0.3	-	-	-	1
MA-246C2	leucosyenogranite	C	30.8	54.6	8.4	tr	0.3	-	-	1.0	0.1	tr	tr	-	-	-	-	-	-	-	4.4	-	-	0.5	3
MA-46B	monzogranite	C	30.2	34.3	20.9	4.9	3.2	-	-	0.2	tr	tr	1.4	-	tr	-	-	-	0.2	-	4.3	0.4	-	-	3
RL-138	leucomonzogranite	C	30.2	33.4	33.3	1.3	0.1	0.1	0.1	0.8	0.1	0.1	0.5	-	-	-	-	-	-	-	-	-	-	-	1
MA-007B	leucosyenogranite	C	29.8	43.1	20.1	1.9	2.8	0.2	0.6	0.6	0.1	0.1	0.6	-	-	-	-	-	0.1	-	-	-	-	-	3
MF-012	monzogranite	C	27.1	23.5	40.1	4.4	1.8	0.4	-	1.4	0.1	0.2	0.6	-	-	-	-	-	0.1	-	0.3	-	-	-	1
MA-246C1	tonalite gneiss	D	21.6	2.7	26.4	3.4	5.8	3.8	0.3	5.5	0.3	0.3	1.7	-	-	-	-	-	14.0	-	13.7	-	-	0.3	3

Table1 (*Continued*)

samples	classification	facies	qz	af	pg	bi	ms	tt	al	ep	zi	ap	om	cd	gr	si	tu	mz-xt	cl	lx	ss	my	ph	cb	ref.
MA-176B	meta-granodiorite	D	20.5	15.1	42.8	8.8	1.6	tr	tr	3.1	0.3	tr	0.5	-	-	-	-	-	0.3		5.4	1.6	-	-	3
MF-073B2	tonalite	D	20.0	5.0	50.0	15.0	1.0	1.0	-	2.0	-	2.0	3.0	-	-	-	-	-	1.0	-	-	-	-	-	2
RL-040B	tonalite gneiss	D	18.0	4.0	48.0	20.0	1.0	-	-	2.0	-	2.0	3.0	-	-	-	-	-	1.0	-	1.0	-	-	-	2
MA-009B	tonalite gneiss	D	17.0	-	48.0	29.9	-	1.0	-	0.1	0.1	0.5	3.4	-	-	-	-	-	-	-	-	-	-	-	3
MA-007C	tonalite gneiss	D	8.5	-	32.1	42.4	-	2.2	0.8	12.5	0.2	0.4	0.8	-	-	-	tr	-	0.1	-	-	-	-		3

Modal analysis from (1) Sardinha (1999), (2) CPRM (2000) and (3) this paper. Serra Dourada Granite: A. aluminous coarse-grained granites. Martins Pereira granitoids: B. porphyrytic and equigranular coarse grained, C. blobs and lenses, D. biotite-bearing enclaves. Abbreviations: qz. quartz, af. alkali feldspar, pg. plagioclase, bi. biotite, ms. muscovite, tt. titanite, al. allanite, ep epidote, zi. zircon, ap. apatite, om. opaque minerals, cd. cordierite, gr. garnet, si. sillimanite, tu. tourmaline, mz-xt. monazite and/or xenotime, cl. chlorite, lx. leucoxene, ss. saussurite, cb carbonate, ph. prehnite, tr. trace, ref. references.

Table 2. Modal mineral contents of samples from Caroebe granite.

samples	classification	facies	qz	af	pg	bi	amp	ms	tt	al	ep	zi	ap	om	cl	cpx	ss	my	ph	Ref
MA-276	granodiorite	A	31.2	7.8	45.6	7.5	-	0.3	1.5	0.6	0.9	0.3	0.3	0.9	0.3	-	2.7	-	-	3
MA 130A	monzogranite	A	30.0	27.0	34.3	7.0	-	-	0.6	0.1	0.2	0.1	0.1	0.5	0.1	-	-	-	-	3
MA 124A	monzogranite	A	29.5	38.0	23.3	8.0	-	-	0.2	0.1	0.1	0.1	0.1	0.5	0.1	-	-	-	-	3
MA-150	granodiorite	A	26.1	12.2	44.8	6.5	-	0.3	1.6	0.0	2.2	0.3	0.0	1.6	0.5		3.0	0.5	0.3	3
MA 120	monzogranite	A	26.0	35.0	25.5	12.0	-	-	0.5	0.1	0.3	0.1	0.1	0.3	0.1	-	-	-	-	3
MA 123	monzogranite	A	25.0	28.0	35.7	10.0	-	0.1	-	-	0.2	0.1	0.1	0.7	0.1	-	-	-	-	3
MJ 061C	monzogranite	A	25.0	30.0	25.0	5.0	-	2.0	3.0	-	3.0	-	1.0	3.0	3.0	-	-	-	-	2
MA 053A	granodiorite	A	23.6	20.3	38.9	9.9	-	0.8	0.4	0.3	1.7	-	-	1.1	-	-	1.9	1.1	-	3
MA-144A	granodiorite	A	19.2	20.0	43.7	7.0	-	-	1.2	0.4	1.9	0.4	0.2	1.2	-	-	4.5	0.3	-	3
MA 104	monzogranite	B	30.0	34.5	23.0	6.0	5.0	-	0.1	-	0.1	0.1	0.1	1.0	0.1	-	-	-	-	3
MA 112	monzogranite	B	26.0	28.4	26.0	11.0	7.0	-	0.2	0.1	0.1	0.1	0.1	1.0	-	-	-	-	-	3
RL 006	monzogranite	B	20.6	29.2	36.2	11.8	0.6	-	0.4	-	0.1	0.1	0.2	0.7	-	0.1	-	-	-	1
HM-181*	monzogranite	-	19.1	27.4	34.1	8.4	2.7	-	0.3	-	2.1	0.5	0.2	1.0	-	-	3.3	0.5	-	3
MA 053C	tonalite	B	16.3	4.9	42.7	19.9	7.0	0.4	0.8	0.1	1.5	0.1	0.1	1.2	0.1	-	4.7	0.2	-	3
MA 121	quartz monzodiorite	B	15.8	14.5	54.0	9.7	2.3	0.1	1.1	0.1	0.8	0.2	0.2	1.1	0.1	-	-	-	-	3
MA 103	granodiorite	B	15.0	12.0	43.0	10.0	12.0	-	0.6	-	0.6	0.1	0.1	1.7	0.1	4.8	-	-	-	3
MA-187	quartz monzodiorite	B	14.9	9.5	48.9	11.2	3.4	0.0	3.2	0.0	1.7	0.0	0.3	2.3	0.6	-	3.2	0.9	-	3
MA 053B	quartz monzonite	B	14.2	30.4	38.3	12.1	0.3	0.3	0.4	-	0.6	0.1	0.2	1.9	0.2	-	0.6	0.4	-	3
MF 068A	quartz monzodiorite	B	10.0	14.0	35.0	10.0	8.0	2.0	2.0	-	2.0	-	3.0	4.0	2.0	7.0	1.0	-	-	2
MJ 061B	quartz monzonite	B	9.0	23.0	37.0	6.0	16.0	1.0	2.0	-	1.0	-	2.0	1.0	2.0	-	-	-	-	2
MA-178B	quartz monzodiorite	B	7.2	9.3	42.5	14.7	9.3	-	1.8	-	4.8	0.7	0.9	3.6	-	-	3.8	1.4	-	3
MF 073C	quartz diorite	B	5.0	2.0	26.0	14.0	37.0	2.0	5.0	-	2.0	-	2.0	4.0	1.0	-	-	-	-	2
MA-144B	quartz diorite	B	4.1	1.9	44.2	18.0	13.5	-	4.4	-	3.3	0.6	0.6	3.0	-	-	6.6	-	-	3

Modal analysis from (1) Sardinha (1999), (2) CPRM (2000) and (3) this paper. A. Alto Alegre and B. Jaburuzinho facies. Abbreviations: qz. quartz, af. alkali feldspar, pg. plagioclase, bi. biotite, amp. amphibole, ms. muscovite, tt. titanite, al. allanite, ep. epidote, zi. zircon, ap. apatite, om. opaque minerals, cpx. clinopyroxene, cl. chlorite, ss. saussurite, my. myrmequite, ph. prehnite, tr. trace, ref. references. *Água Branca granite (type-area).

Table 3. Modal mineral contents of Igarapé Azul granite and their enclaves.

samples	classification	facies	qz	af	pg	bi	ms	tt	al	ep	zi	ap	om	cl	lx	ss	my	Ref
MA 088	syenogranite	A	38.0	36.4	11.3	4.5	4.6	0.2	1.0	1.1	0.1	-	0.7	0.6	-	1.5	-	3
MJ 018	leucomonzogranite	A	35.3	31.1	27.9	3.0	1.4	0.1	0.1	0.3	0.1	0.1	0.5	0.1	-	-	-	1
RL 010	leucogranodiorite	A	33.7	18.2	41.5	4.0	0.1	0.2	0.1	0.4	0.1	0.1	1.0	0.1	-	0.5	-	1
NR 013	leucomonzogranite	A	32.2	30.8	32.1	2.2	-	0.1	0.1	0.6	0.1	0.1	1.4	0.2	0.2	-	-	1
RL 007B	leucomonzogranite	A	32.0	26.1	36.6	3.6	-	0.1	0.1	0.4	0.1	0.1	0.9	0.1	0.1	0.3	-	1
MF 014	leucogranodiorite	A	30.0	21.6	44.5	2.3	0.9	-	-	0.1	0.1	-	0.1	0.3	0.1	-	-	1
RL 009B	leucomonzogranite	A	28.5	24.0	43.1	2.8	-	0.1	-	0.4	0.1	0.1	0.5	0.1	0.2	0.5	-	1
MF 006C	leucogranodiorite	A	25.6	17.7	52.0	3.5	0.2	0.2	0.1	0.1	0.1	0.1	0.4	0.3	-	-	-	1
MA 147A	monzogranite	A	24.6	31.8	24.2	1.3	1.9	0.1	0.1	4.6	0.1	0.1	1.0	3.4	-	6.1	0.7	3
MF 006B	leucomonzogranite	A	23.0	31.3	42.7	1.4	-	0.1	-	0.1	0.1	0.1	0.7	0.6	-	-	-	1
MA 079	quartz monzonite	A	16.0	25.0	33.7	9.5	2.4	0.3	-	1.5	-	-	1.0	0.2	-	9.5	0.9	3
RL 011	monzogranite	B	33.0	27.0	32.0	5.7	0.6	0.3	0.1	0.4	0.1	0.1	0.6	0.1	-	-	-	1
MJ 014	monzogranite	B	30.6	25.2	37.3	4.8	0.6	0.1	0.1	0.4	0.1	0.1	0.7	-	-	-	-	1
MJ 017B	leucogranodiorite	B	30.2	23.3	44.1	0.4	0.2	0.1	-	0.7	0.1	0.1	0.4	0.4	-	-	-	1
MA 186A	monzogranite	B	29.0	27.9	26.4	4.6	1.0	-	-	1.1	-	-	0.9	0.2	-	7.9	1.0	3
MA 201A	monzogranite	B	25.8	25.1	31.6	3.9	0.3	-	-	1.5	0.1	0.2	0.3	0.2	-	10.5	0.5	3
MJ 017A	leucomonzogranite	B	24.3	28.6	41.5	3.6	0.2	0.1	0.1	0.2	0.1	0.1	0.5	0.8	-	-	-	1
MF 006A	leucogranodiorite	C	38.1	20.1	39.6	1.4	tr	-	-	0.1	0.1	0.1	0.3	0.1	0.1	-	-	1
MA 002	leucomonzogranite	C	30.5	29.1	33.0	2.5	0.4	0.2	0.2	0.6	0.1	-	0.8	0.3	-	1.2	1.1	3
RL 008	monzogranite	C	30.3	24.0	35.9	7.9	0.5	0.1	-	0.6	0.1	0.1	0.5	-	-	-	-	1
RL 009A	monzogranite	C	29.2	30.5	33.7	4.5	0.2	0.1	0.1	0.5	0.1	0.1	0.7	0.1	0.1	0.1	-	1
MF 010B	monzogranite	C	27.5	37.7	24.3	7.2	1.6	0.1	-	0.4	0.1	0.2	0.6	0.3	-	-	-	1
MJ 012	monzogranite	C	26.4	23.7	41.0	6.9	0.5	0.2	0.1	0.4	0.1	0.1	0.3	-	-	0.3	-	1
MJ 015B	monzogranite	C	25.8	40.5	24.0	6.0	1.5	0.1	-	0.3	0.1	0.1	0.4	0.2	-	1.0	-	1
MA 102A	leucomonzogranite	C	22.9	28.7	36.8	0.6	0.7	0.1	0.3	1.0	0.1	-	1.1	0.2	-	6.4	1.1	3
MF 079	monzogranite	C	21.2	26.1	44.7	6.2	tr	0.1	0.4	0.1	0.1	0.1	1.0	-	-	-	-	1
MA-085B	granodiorite	D	12.9	8.8	34.1	27.6	-	0.6	-	1.2	0.6	1.2	4.7	1.2	-	5.9	1.2	3
MA 186B	tonalite	D	9.0	0.1	20.0	55.0	10.0	-	-	4.7	0.1	0.1	1.0	-	-	-	-	3
MA 213B	quartz monzodiorite	D	6.0	3.0	40.0	46.0	2.0	-	-	tr	tr	0.1	2.9	-	-	-	-	3
MA 147B	quartz diorite	D	5.0	0.1	39.0	49.7	2.0	0.1	0.1	1.1	0.1	0.1	2.7	-	-	-	-	3
MA 201B	quartz diorite	D	4.4	7.0	12.5	57.7	6.3	0.2	-	0.4	0.7	1.5	6.7	0.4	-	2.1	0.1	3

Modal analysis from (1) Sardinha (1999) and (3) this paper. A. Cinco Estrelas, B. Saramandaia, C. Vila Catarina, D. biotite-bearing enclave. Abbreviations: qz. quartz, af. alkali feldspar, pg. plagioclase, bi. biotite, ms. muscovite, tt. titanite, al. allanite, ep. epidote, zi. zircon, ap. apatite, om. opaque minerals, cl. chlorite, lx. leucoxene, ss. saussurite, my. myrmequite, tr. trace, ref. references.

4.3 - Geochemistry and Zircon Geochronology of I-type High-K Calc-alkaline and S-Type granitoid rocks from Southeastern Roraima, Brazil: Orosirian Collisional Magmatism (1.98-1.96 Ga) in central Guyana Shield

Marcelo E. Almeida[1,2*], Moacir J.B. Macambira[2], Elma C. Oliveira[2]

[1]CPRM – Geological Survey of Brazil, Av. André Araújo 2160, Aleixo, CEP 69060-001, Manaus, Amazonas, Brazil

[2] Isotope Geology Laboratory, Center of Geosciences, Federal University of Pará, CP. 8608, CEP 66075-110, Belém, Pará, Brazil

* Corresponding author; ph.: +55-92-2126-0357, fax: +55-92-2126-0319, e-mail address: marcelo_almeida@ma.cprm.gov.br

ARTIGO SUBMETIDO AO CORPO EDITORIAL DA REVISTA "*PRECAMBRIAN RESEARCH*"

Words: summary (76), abstract (169), body text (10915), table (446) and figure (933) captions.

Total: 6 tables and 12 figures

ABSTRACT
The understanding of the geological evolution of the Uatumã-Anauá Domain in southeastern Roraima, central region of Guyana Shield, is of major significance in the study of the Amazonian craton. This region lies between some Paleoproterozoic geological-geochronological provinces: Tapajós-Parima or Ventuari-Tapajos (dominant), Maroni-Itacaiúnas or Transamazon (northwest) and Central Amazonian or Central Amazon (southeast and east). Geological mapping of the northern area of Uatumã-Anauá Domain, integrated with whole rock geochemistry data and previous and new Pb-evaporation and U-Pb zircon geochronology, point out for a plutonic collisional magmatic event (1975-1968 Ma) represented by I-type high-K calc-alkaline (Martins Pereira) and S-type (Serra Dourada) granitoid rocks. This magmatism was probably generated from crustal sources by partial melting during amalgamation of TTG-like Anauá magmatic arc (2028 Ma) with Transamazonian (2.2-2.0 Ga) and Central Amazonian (older than 2.3 Ga) terranes. Local cumulatic leucogranites fills planar structures of the Martins Pereira granites. These leucogranites show younger ages (1909 Ma) and several inherited zircons (2354 Ma; 2134 Ma; 1997 Ma and 1959 Ma), suggesting origin from crustal sources.
Keywords: Paleoproterozoic, Granitoids, Guyana Shield, Zircon geochronology, Geochemistry

INTRODUCTION

The Guyana Shield, with a surface area of nearly 1.5 million km^2, represents the northernmost section of the Amazonian craton. This shield was predominately formed during protracted periods of intense granitic magmatism, bracketed between 2.1 and 1.9 Ga **(Fig. 1a-b;** *e.g.* Tassinari and Macambira, 1999, 2004; Santos *et al.*, 2000, 2006). Despite representing an intricate component of the Amazonian craton, the Guyana Shield has seen only limited attention among the scientific community. Geological maps of the region are scarce (*e.g.* CPRM, 1999, 2000a; Delor *et al.,* 2003), and only few petrographical, geochemical and geophysical studies are available. Comparison between previous studies from the Guyana Shield has been hampered by a lack of dependable age determinations, implying large errors (± 50-100 Ma), which preclude any attempt to establish a fine chronology of the magmatic and metamorphic events.

The study area is concentrates on the central part of the Guyana Shield, in southeastern Roraima State (Brazil). Recent zircon geochronology data demonstrate that igneous rocks cropping out in this region (c. 4970 km^2, Fig. 2) show ages of 2.03 Ga (Faria *et al.*, 2002) and 1.97-1.96 Ga (Almeida *et al.*, 1997, CPRM, 2003), similar to the Tapajós Domain in Central Brazil Shield (Santos *et al.*, 2000, Lamarão *et al.*, 2002). However, the characteristics and significance of these events and ages are not fully understood (CPRM, 2000a; Almeida and Macambira, 2003). An example of this can be seen in the 2.03-1.96 Ga magmatic event which, unlike the 1.90 Ga calc-alkaline magmatism, is uncommon in other regions of the world. In addition the Tapajós Domain in Central Brazil Shield (southern Amazonian craton) and parts of the São Francisco Craton, Paleoproterozoic tectonic and magmatic activity between c. 2.0 and 1.9 Ga is recorded in Western Australia (Gascoigne Complex, Dalgaringa Supersuite, 2005-1970 Ma,

Sheppard *et al.* 2004) and southern Australia (Gawler Craton, Miltalie Gneiss, ca. 2000 Ma, Daly *et al.* 1998). The Taltson Magmatic Zone of northern Canada (McDonough *et al.*, 1993) and Kora-Karelian orogen of northern Baltic Shield (Daly *et al.,* 2001) also show 2.0-1.9 Ga magmatic events.

The aim of this paper is to provide new geochemical and geochronological constraints on the Martins Pereira and Serra Dourada granitoid rocks (Almeida *et al.,* 2002). It is hoped that such studies will contribute to a better understanding of the lithostratigraphy, origin and geodynamic evolution of the northern part of the Uatumã-Anauá Domain, in the central portion of the Guyana Shield (**Fig. 1**). These data will be integrated with previous geochemical and geochronological data for other magmatic associations, mainly calc-alkaline granitoids older than 1.90 Ga. Particular focus will be placed on comparative geochemical and geochronology data from previous studies in the same region and from the southern part of the Amazonian craton.

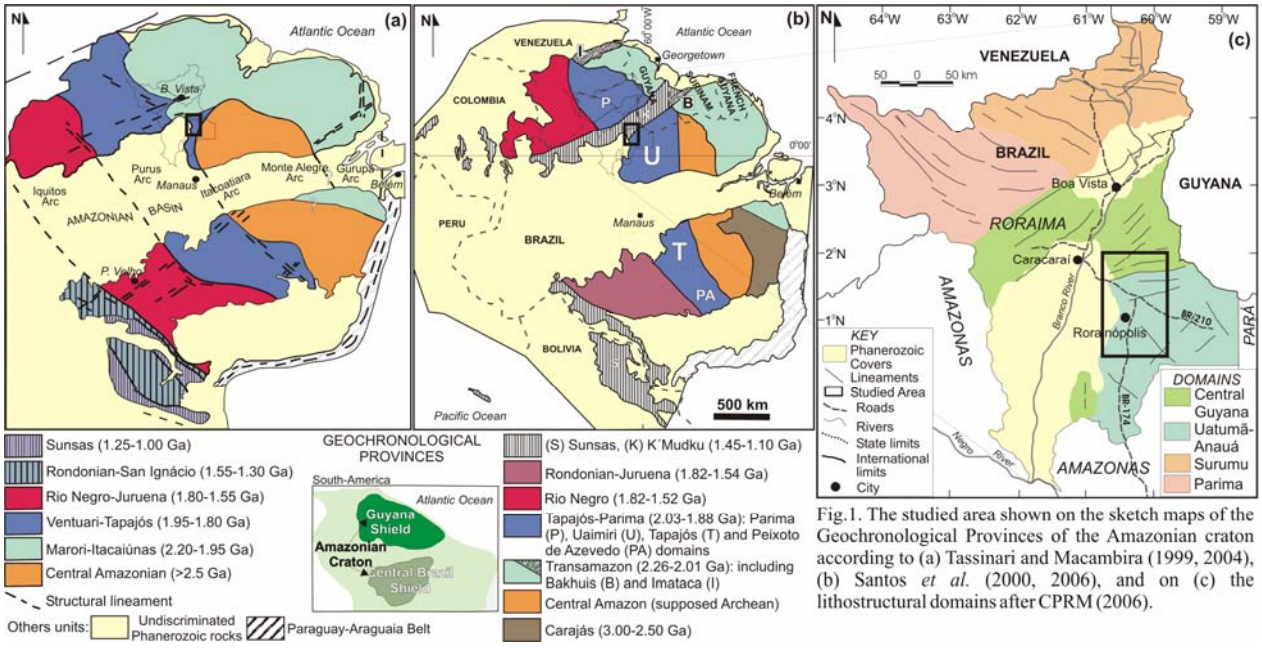

Fig.1. The studied area shown on the sketch maps of the Geochronological Provinces of the Amazonian craton according to (a) Tassinari and Macambira (1999, 2004), (b) Santos *et al.* (2000, 2006), and on (c) the lithostructural domains after CPRM (2006).

GEOLOGICAL SETTING

Regional geological maps (CPRM 2000a, Almeida *et al.*, 2002) and zircon geochronological data (Almeida *et al.,* 1997, Santos *et al.,* 1997, Macambira *et al.,* 2002, CPRM, 2003) have shown that Paleoproterozoic granitoid and volcanic rocks (1.97 to 1.81 Ga) are widespread in southeastern Roraima. These intrusive and extrusive rocks are emplaced within poorly exposed basement rocks that have maximum ages of around 2.03 Ga (Faria *et al.,* 2002).

According to recent evolutionary models proposed for the Amazonian craton, the study area can be divided into several provinces. According to the work of Tassinari and Macambira (1999, 2004), the study area is largely enclosed in the Ventuari-Tapajós and Central Amazonian provinces, with a subordinate northeastern section falling within the Maroni-Itacaiúnas province. Santos *et al.* (2000, 2006) argue that all provinces were collectively affected by the K´Mudku Shear Belt in this same region **(Fig. 1 a-b)**. These conclude that Paleoproterozoic orogenic belts or magmatic arcs (*e.g.,* Ventuari-Tapajós or Tapajós-Parima, and Maroni-Itacaiúnas or Transamazon provinces) were accreted to the Archean craton with time and/or represent a set of rocks produced from melting of Archean crust (Fig. **1a-b**; Cordani *et al.,* 1979, Teixeira *et al.,* 1989, Tassinari 1996, Tassinari and Macambira, 1999, 2004; Santos *et al.,* 2000, 2004, 2006).

The Tapajós-Parima (or Ventuari-Tapajós) Province is a Paleoproterozoic orogenic belt trends north-northwest and includes geological units which range from ~2.10 to 1.87 Ga in age (Santos *et al.,* 2000, 2006; Tassinari and Macambira 1999, 2004). This province was subdivided into four domains by Santos *et al.* (2000): Parima and Uaimiri, to the north, Peixoto Azevedo and Tapajós, to the south. Southeastern Roraima belongs to the Uaimiri Domain. The Central Amazonian Province of the study area **(Fig. 1a-b)** displays granitoid and volcanic rocks (1.88 to 1.70 Ga) lacking regional metamorphism and compressional folding (Santos *et al.,* 2000, Tassinari and Macambira 1999), and its basement is exposed scarcely. The age for this basement has been estimated via Nd-model ages at around 2.3-2.5 Ga (Tassinari and Macambira, 1999, 2004). According to these authors, the recorded Archean rocks in the Amazonian craton are only exposed in Imataca (Venezuela), Carajás and southern Amapá-northwestern Pará (Brazil).

The Maroni-Itacaiúnas (or Transamazon) Province is also an orogenic belt with Rhyacian ages (2.25 to 2.00 Ga, **Fig. 1a-b**) and is correlated to the Birimian belt in West Africa (Tassinari and Macambira, 1999, 2004; Santos *et al.,* 2000; Delor *et al.,* 2003). The K´Mudku Shear Belt is characterized by low grade mylonitic zones with ca. 1.20 Ga ages, and cross-cuts the Rio Negro, Tapajós-Parima and Transamazon provinces (Santos *et al.,* 2000).

Taking into account lithological associations and geochronological data, Reis *et al.* (2003) and CPRM (2006) divided Roraima into four major domains – Surumu, Parima, Central Guyana and Uatumã-Anauá **(Fig. 1c).** Each of these domains contains a wide range of rock types and stratigraphic units. Southeastern Roraima is composed of the Central Guyana and Uatumã-Anauá lithostructural domains, that correspond to the K`Mudku Shear Belt and Uaimiri Domain, respectively (northern Tapajós-Parima Province) proposed by Santos *et al.* (2000).

The Central Guyana Domain (CGD) consists primarily of granulites, orthogneiss, mylonites and metagranitoids (Rio Urubu Metamorphic Suite) associated with low to high metamorphic grade metavolcanosedimentary covers (Cauarane Group) and S-type granite (Curuxuim Granite). The lineaments trend is strongly NE-SW **(Figs. 1c and 2)**. The Uatumã-Anauá Domain (UAD) is characterized by E-W to NE-SW lineaments and the northern part of the domain (NUAD) shows an older metamorphic basement **(Figs. 1 and 2)** formed in a presumed island arc environment (Faria *et al.*, 2002). This basement is composed of TTG-like metagranitoids to orthogneisses (Anauá Complex), enclosing meta-mafic to meta-ultramafic xenoliths, and is associated with some inliers of metavolcano-sedimentary rocks (Cauarane-like). The basement rocks are intruded by S-type (Serra Dourada Granite) and high-K, I-type calc-alkaline (Martins Pereira) granite plutons of c. 1.98-1.96 Ga (see zircon geochronology section).

In the southern area of the Uatumã-Anauá domain (SUAD), intrusive younger granites (with no regional deformation and metamorphism) are very common. The most prominent magmatism is related to the calc-alkaline Caroebe and Igarapé Azul granitoids (Água Branca Suite) with coeval Iricoumé volcanic rocks. Locally igneous charnockitic (Igarapé Tamandaré) and enderbitic (Santa Maria) plutons were also recorded. Several A-type granite bodies are widespread in the Uatumã-Anauá Domain **(Fig. 2)** represented by Moderna-Água Boa (1.81 Ga) and Mapuera-Abonari (1.87 Ga) granites.

ANALYTICAL PROCEDURES

Whole-rock Geochemistry Analysis

Whole-rock chemical analyses of 11 samples (milled under 200 mesh) were done at the Acme Analytical Laboratories Ltd, Vancouver, British Columbia, Canada. The analytical package includes inductively coupled plasma-atomic emission spectrometer (ICP-AES) analyses after LiO_2 fusion for all major oxides (SiO_2, TiO_2, Al_2O_3, MnO, MgO, CaO, K_2O, Na_2O, P_2O_5) and LOI. Total iron concentration is expressed as Fe_2O_3. The trace elements were analyzed by inductively coupled plasma-mass spectrometer (ICP-MS), with rare-earth and incompatible elements determined from a $LiBO_2$ fusion and precious and base metals determined from an aqua regia digestion. Additional 16 analyses were compiled (and partially reinterpreted) from CPRM (2000a). These last whole-rock chemical analyses were done at the Geosol Laboratories S.A., Belo Horizonte, Minas Gerais, Brazil.

Zircon Isotope Analysis

For isotope analysis, the zircon crystals were obtained from samples with 2 to 20 kg. After crushing (milled to 60-80 mesh) and sieving, heavy mineral fractions were obtained by water-

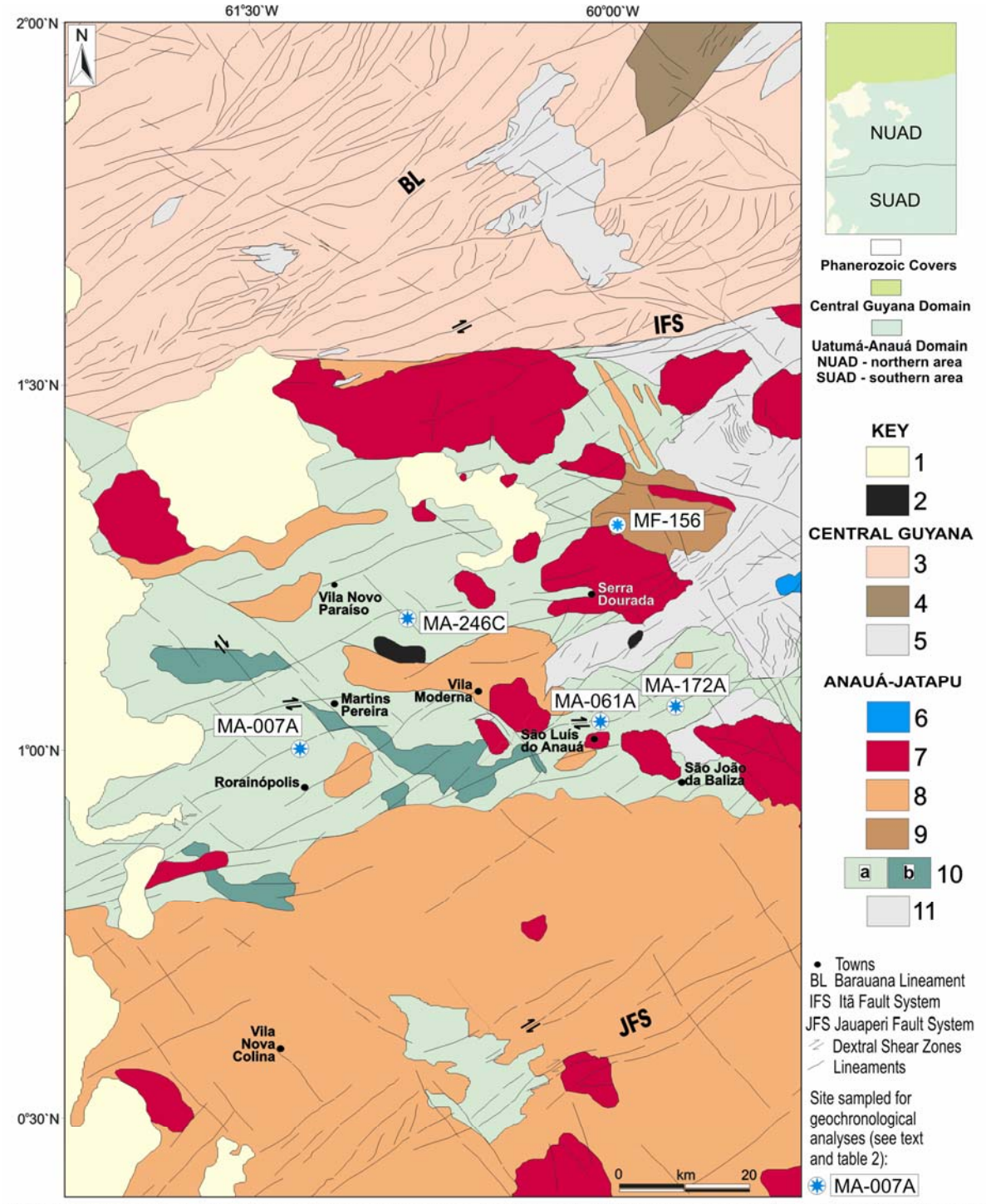

Fig.2. Simplified geological map of southeastern Roraima (mod. Almeida *et al.,* 2002; CPRM, 2000a, 2005). 1. Cenozoic sedimentary covers; 2. Undiscrimined plutonic mafic rocks; 3. Foliated granitoids (1.72 Ga), mylonites (1.89 Ga), granulites, augen gneisses, metagranitoids and orthogneisses (1.96-1.93 Ga, Rio Urubu Complex); 4. S-type Curuxuim (garnet) Granite (1.97 Ga?); 5. Metavolcano-sedimentary sequence (Cauarane Group); 6. Proterozoic sedimentary cover (Urupi Formation); 7. a) A-type Moderna (1.81 Ga), Mapuera granites (1.87 Ga) and minor charnockitoids (1.89 Ga); 8. Igarapé Azul-Caroebe granites and scarce volcanic rocks (1.90-1.89 Ga); 9. S-type Serra Dourada (cordierite) Granite (1.96 Ga); 10. High-K calc-alkaline Martins Pereira Granite: (a) normal to (b) high U, Th, K contents (1.97 Ga); 11. Metavolcano-sedimentary sequence (Cauarane Group?) and TTG calc-alkaline Anauá Complex (2.03 Ga).

-mechanical and dense liquid concentrations, and processed under hand magnet and Frantz Isodynamic Separator. In order to remove impurities, zircon concentrates were washed with

HNO_3 at 100^0 C (10 minutes), submitted to ultrasound cube (5 minutes) and finally washed with bidistilled H_2O. The less magnetic zircon concentrates (from five magnetic fractions) were preferred for hand-picking. Whenever possible only zircon grains free of alteration, metamictization features, inclusions and fractures were selected for analysis (see zircon descriptions below). All selected grains for analysis were photomicrographed via a conventional optical microscope.

Single-zircon dating by Pb-evaporation and U-Pb isotopic dilution in thermal ionization mass spectrometry (ID-TIMS) methods was performed at the Isotope Geology Laboratory (Pará-Iso), Federal University of Pará (UFPA), Brazil. The U decay constants are those recommended by Steiger and Jäger (1977), and errors are given at the 95% confidence level. Ages of 5 samples were obtained by the Pb-evaporation technique established by Kober (1986, 1987), and only one sample was analyzed by U-Pb ID-TIMS. All isotope analyses were carried out on a Finnigan MAT 262 mass spectrometer in dynamic mode, using the ion counting detector.

In the Pb-evaporation method on a single zircon, the selected grains were tied in Re-"evaporation"-filament and introduced in the mass spectrometer. The Pb was normally extracted from the crystals by heating in three evaporation steps at temperatures of 1450°, 1500° and 1550°C. The evaporated Pb was loaded on an "ionization" filament, which is heated for the isotope analyses. In this technique, the data were dynamically acquired, using the ion counting system of the instrument. Pb signal was measured by peak hopping in the 206, 207, 208, 206, 207, 204 mass order along 10 scans, defining one block of data with 18 $^{207}Pb/^{206}Pb$ ratios. The $^{207}Pb/^{206}Pb$ ratio average of each step was based on five blocks or less, till the intensity beam was sufficiently high for a reliable analysis. Usually, the average $^{207}Pb/^{206}Pb$ ratio obtained in the highest temperature step was taken for age calculation, but the other steps are also considered. Outliers were eliminated using Dixon's test. The $^{207}Pb/^{206}Pb$ ratios were corrected for a mass discrimination factor of 0.12% ± 0.03 $a.m.u^{-1}$, and results with $^{204}Pb/^{206}Pb$ ratios higher than 0.0004 were, in general, discarded. The ages were calculated with 2 sigma error and common Pb correction was done using age values derived from the two-stage model of Stacey and Kramers (1975). The obtained data were processed in software *Zircon* program (Scheller, 1998), DOS system version.

The Pb-evaporation on a single zircon method yields apparent $^{207}Pb/^{206}Pb$ ages and the degree of concordance of the analytical points is not possible to assess. Furthermore, zircon grains exhibiting a complex history often yield mixed ages with no geological meaning

(Dougherty-Page and Bartlett, 1999). With these uncertainties in mind, the age obtained for a single grain is considered as a minimum age. This being the case, as has been proposed in several studies (Kober, 1986; Andsell and Kyser, 1991; Macambira and Scheller, 1994; Söderlund, 1996), if a set of magmatic grains from the same sample yields similar ages, it is possible to suggest that such similarities indicate the time of the magmatic crystallization or episodic Pb loss.

The U-Pb ID-TIMS procedures undertaken in the Pará-Iso Laboratory followed those presented by Krymsky (2002). All zircon fractions selected for analysis were previously air abraded with pyrite crystals (20 mg and 0.1-0.5 mm diameter) in 1.2-1.8 p.s.i. pressure for 30-40 minutes. After abrasion the zircon grains were washed with HNO_3 and HCl (100^0 C, 30 minutes) and H_2O-Millipore (3 times). The grains were then washed with metanol, weighed, spiked with ^{235}U-^{205}Pb tracer and dissolved with a mixture of HF and HCl in PTFE Teflon® bombs. Uranium and lead were separated with anion-exchange resin (Dowex® 1x8 200-400 mesh) in HCl medium in 50-70 µL columns. Uranium and Lead were loaded with Si-gel and H_3PO_4 (1N) onto the same out-gassed Re-filament and analyzed at 1400^0-1600^0 C. For zircon analyses, blanks are <30 pg Pb and <1 pg U. The obtained data were processed in ISOPLOT/Excel program version 2 (Ludwig, 1999). The $^{208}Pb/^{206}Pb$ ratios were corrected for common Pb, using also the Stacey and Kramers (1975) model. The quality statistics is express for USD or Unified Standard Deviation (square root of MSWD value – Mean Standard Weigth Deviation).

The Pb-evaporation on a single zircon method yields apparent $^{207}Pb/^{206}Pb$ ages and the degree of concordance of the analytical points is not possible to assess. Furthermore, zircons exhibiting a complex history, often furnish mixed ages with no geological meaning (Dougherty-Page and Bartlett, 1999). With these uncertainties in mind, the age obtained for a single grain is considered as a minimum age. This being the case, as has been proposed in several studies (Kober, 1986; Andsell and Kyser, 1991; Macambira and Scheller, 1994; Söderlund, 1996), if a set of magmatic grains from the same sample yields similar ages, it is possible to suggest that such similarities indicate the time of the magmatic crystallization.

The U-Pb ID-TIMS (Pará-Iso Laboratory) procedure followed those presented by Krymsky (2002). All zircon fractions selected for analysis were previously air abraded with pyrite crystals (20 mg and 0.1-0.5 mm diameter) in 1.2-1.8 p.s.i. pressure for 30-40 minutes. After abrasion the zircon grains were washed with HNO_3 and HCl (100^0 C, 30 minutes) and H_2O-Millipore (3 times). The grains were then washed with metanol, weighed, spiked with ^{235}U-^{205}Pb tracer and dissolved with a mixture of HF and HCl in PTFE Teflon® bombs. Uranium and lead were

separated with anion-exchange resin (Dowex® 1x8 200-400 mesh) in HCl medium in 50-70 μL columns. Uranium and Lead were loaded with Si-gel and H_3PO_4 (1N) onto the same out-gassed Re-filament and analyzed at 1400^0-1600^0 C. For zircon analyses, blanks are <30 pg Pb and <1 pg U. The obtained data were processed in ISOPLOT/Excel program version 2 (Ludwig, 1999). The common Pb interference was corrected using also the Stacey and Kramers (1975) model.

WHOLE-ROCK GEOCHEMICAL RESULTS

Major and Minor Oxides, and Trace Elements Geochemistry

Analytical results of representative samples from Martins Pereira, Serra Dourada and Anauá granitoid rocks of the Northern Uatumã-Anauá Domain, including leucogranite blobs and lenses, are presented in **Table 1** and plotted in diagrams in **Figs. 3** to **7**. Serra Dourada and Anauá results are extracted form CPRM (2000a). Creporizão (CPRM, 2000b) and Old São Jorge (Lamarão *et al.,* 2002) granitoid rocks data from Tapajós region are also plotted in some diagrams for comparison with Martins Pereira granitoid rocks.

The Martins Pereira Granite consists of a compositionally wide series of rocks with SiO_2 contents between 49.3 and 74.6 wt. % **(Table 1)**. The associated leucogranite blobs and lenses have high SiO_2 contents (72.9 to 73.9 wt. %), but in the Harker diagrams show no correlation with the Martins Pereira Granite. For instance, leucogranites with the same SiO_2 contents as Martins Pereira granitoid rocks, have low Na_2O **(Fig. 3g)**, MnO **(Fig. 3d)**, Fe_2O_3+FeO **(Fig. 3c)** and very high K_2O **(Fig. 4a)** values.

Rock samples from Martins Pereira Granite are also characterized by linear trends in the all Harker diagrams **(Fig. 3a-h)**. In these diagrams, excluding Na_2O *vs.* SiO_2, the statistic parameters show negative linear correlations with regression agreement between 99% and 99.9%. Linear trends can result from several petrogenetic processes, such as contamination, mixing, crystal fractionation with no crystallizing phases change and partial melting (*e.g.* Cox *et al.,* 1987, Wilson, 1991). The lack of significant compositional gaps in Harker diagrams for Martins Pereira samples suggests that the main petrogenetic process is related likely to partial melting or crystal fractionation with no change in the mineral assemblage being fractionated. However this last one requires a great volume of mafic parental magma, not detected in the region. The same is true for fractional crystallization process with change in the crystallizing mineral phases (e.g. hornblende out and biotite in), but in this case the result are usually curvelinear Harker-plot trends (*e.g.* Cox *et al.,* 1987, Wilson, 1991) that are not observed for Martins Pereira samples.

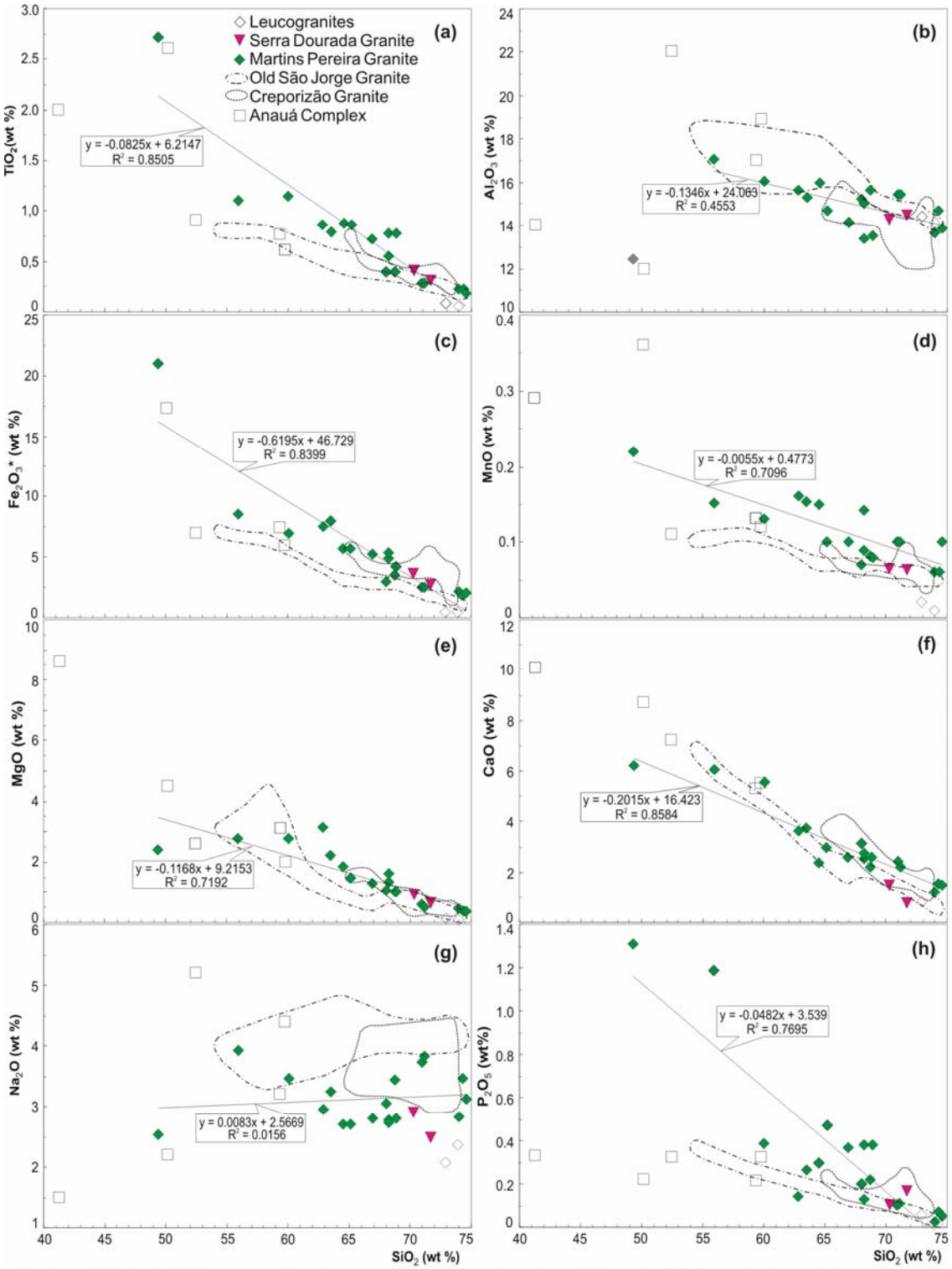

Fig. 3. (a-h) Selected Harker variation diagrams for leucogranites, Anauá Complex, Martins Pereira and Serra Dourada granites. For references see table 1. Fields representing Creporizão (CPRM, 2000b) and Old São Jorge granites (Lamarão *et al.*, 2002) of the Tapajós Domain are plotted for comparison. For the linear regression are used only the Martins Pereira samples.

In contrast to the Martins Pereira samples, the Anauá Complex and related rocks show lower SiO_2 contents ranging from 41.3% to 59.8% **(Table 1),** and dispersion in the Harker diagrams (*e.g.* TiO_2, MnO, Al_2O_3, Na_2O and Fe_2O_{3t}). When compared to the Martins Pereira

granitoid rocks, the Anauá samples are characterized by lower K_2O and P_2O_5 contents (**Fig. 4a, 3h),** while having higher Na_2O and MgO **(Fig. 3e-g)** contents. The Serra Dourada Granite shows remarkable low Na_2O **(Fig. 3g)** and K_2O contents **(Table 1)**.

Compared to the Martins Pereira granitoid rocks, the 1.99-1.96 Ga Old São Jorge and Creporizão granites from the Tapajós Domain have lower TiO_2 **(Fig. 3a)**, MnO **(Fig. 3d)** and P_2O_5 **(Fig. 3h),** and higher Na_2O **(Fig. 3g)** contents. The corresponding Harker diagrams demonstrate that the Creporizão granites have a shorter range and higher contents of SiO_2 (65.2 % to 73.4%, **table 1**), as well as lower MnO **(Fig. 3d)**, Al_2O_3 **(Fig. 3b)** and K_2O **(Fig. 4a)** contents.

In the log [CaO/(Na_2O+K_2O)] *vs.* SiO_2 diagram **(Fig. 4b)**, all the studied granitoid rocks (excluding Serra Dourada Granite) indicate calc-alkaline affinity, with the samples plotting in the normal calc-alkaline andesitic field. Only the Old São Jorge Granite shows exclusive transitional character between normal and mature arc series. Most of the granitoid samples also plot in the high-K field (K_2O *vs.* SiO_2 diagram, **Fig. 4a**), however, the Martins Pereira and Old São Jorge granites have a transitional high-K to slightly shoshonitic character. It is also apparent from the K_2O vs SiO_2 diagram that samples from the Creporizão Granite display a transitional high-K to locally medium-K trend, whereas Anauá types are medium-K to slightly low-K. The leucogranites show high K contents (>7%) and a highly fractionated character.

The Martins Pereira and Creporizão granite compositions are transitional between metaluminous to peraluminous, while the Old São Jorge granite is metaluminous to slightly peraluminous **(Fig. 5a)**. Almost all these granites show A/NK molar ratios < 2. Only the Anauá Complex rocks (A/NK molar > 2) and the lenses of leucogranite are metaluminous and peraluminous. The Serra Dourada Granite is broadly peraluminous, plotting in the S-type granite compositions. This granite body shows A/CNK molar ratios of 1.1 and 1.3, while some samples of the Martins Pereira Granite also show locally high A/CNK values. In the Na_2O *vs.* K_2O diagram, the Martins Pereira granitoid rocks plot on the I-type field, but several samples also plot near to the S-type field boundary **(Fig. 5b)** showing, as well as the Serra Dourada Granite samples, the lowest Na_2O/K_2O ratios.

In the Rb *vs.* (Y+Nb) tectonic discriminator diagrams **(Fig. 5c)**, the Martins Pereira granite samples show transitional VAG (granites to granodiorites) to WPG (biotite-rich tonalites) trends. Anauá rock-types generally plot in the VAG field, with correspondingly low Rb contents. The Creporizão and Old São Jorge granites samples dominantly plot in the VAG field, falling near to

the WPG boundary. Thus, excluding Anauá rocks, most of the analyzed samples fall in the postcollisional field of Pearce (1996), which suggests an increasing in arc maturity (Brown *et al.,* 1984, see **Fig. 4a**) or the beginning of the transition from calc-alkaline to alkaline magmatic series in orogenic to post-orogenic tectonic settings (Bonin, 1990; Barbarin, 1999).

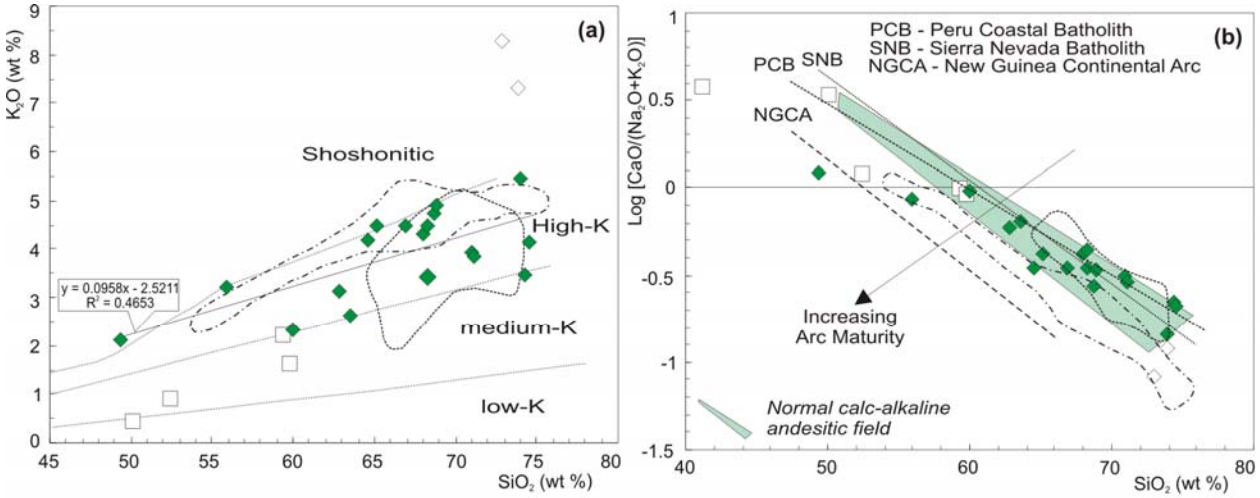

Fig.4. Geochemical diagrams showing results from Martins Pereira Granite, leucogranites and Anauá Complex rocks (for references see table 1). Fields representing Creporizão (CPRM, 2000b) and Old São Jorge granites (Lamarão *et al.*, 2002) are plotted for comparison: (a) K_2O *vs.* SiO_2 contents displaying the shoshonite, high-K, medium-K and low-K fields (from Peccerilo and Taylor, 1976; mod. by Rickwood, 1989). For the linear regression are used only the Martins Pereira Granite samples. (b) log[CaO/(Na_2O+K_2O)] *vs.* SiO_2 contents (from Brown *et al.,* 1984). Symbols as in Fig. 3.

In the (K_2O + Na_2O)/CaO *vs.* (Zr + Nb + Ce + Y) diagram **(Fig. 5d)**, the calc-alkaline Martins Pereira, Creporizão and Old São Jorge granites plot on the unfractionated S- and I-type granites to transitional A-type fields. Concerning the Martins Pereira granitoid rocks, the higher Zr, Y and Ce contents are probably related to the presence of accessory minerals such as epidote, allanite and zircon, mainly in biotite-rich tonalite types. However, their metaluminous to peraluminous nature **(Fig. 5a)** and VAG character **(Fig. 5c)** point to I-type granite affinity. Samples from Anauá Complex plot in the unfractionated S- and I-type granites field with low (K_2O + Na_2O)/CaO ratios. Only the blobs of leucogranites and few Creporizão Granite samples plot on the fractionated felsic granites field **(Fig. 5d)**.

In the primordial mantle-normalized spidergrams, the Martins Pereira Granite **(Fig. 6a)** exhibits depleted trace element patterns for some HFSE such as Ta, Nb, P, and Ti, and does not show significant LILE depletion (*e.g.* Sr and Ba), as observed for alkali-calcic granitoid rocks of more mature arcs (Brown *et al.,* 1984). This pattern is somewhat similar to those of the calc-alkaline granitoid rocks from normal arcs (cf. Brown *et al.,* 1984), though some samples of the Martins Pereira Granite show strong Ti and P depletion, like the average of mature arc granitoid

rocks. This geochemical behavior suggests that Martins Pereira Granite belongs to transitional granitic magmatism, from normal to mature continental arcs (see also **Fig. 4a**).

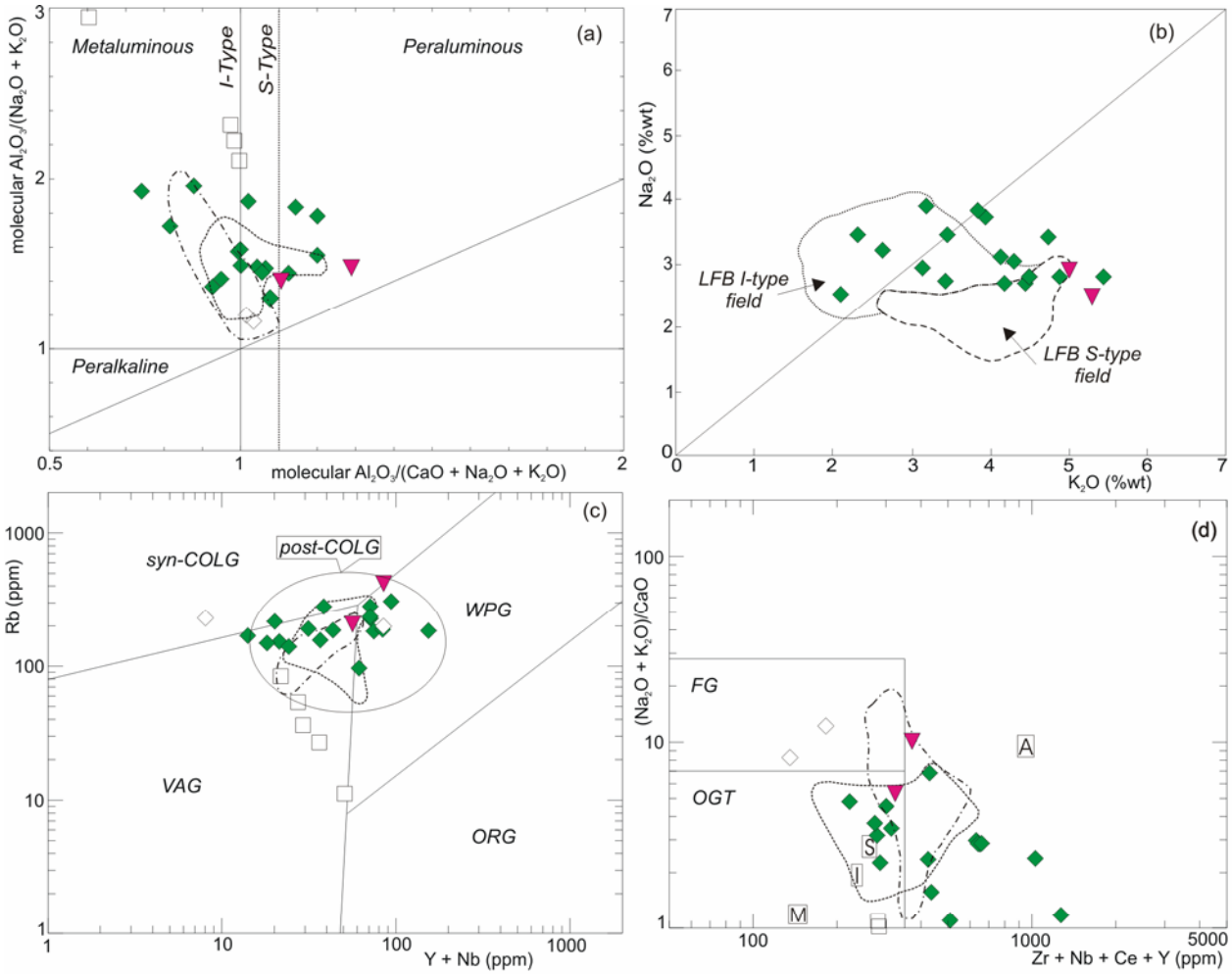

Fig.5. Martins Pereira and Serra Dourada granites, leucogranites and Anauá Complex samples plotted in the diagrams (for references see table 1): (a) Molecular $Al_2O_3/(Na_2O+K_2O)$ *vs.* molecular $Al_2O_3/(CaO+Na_2O+K_2O)$ (Maniar and Piccoli, 1989; mod. Shand, 1927) and (b) Na_2O vs. K_2O plots showing S-type and I-type granites compositional data from Lachlan Folded Belt (LFB); (c) Rb *vs.* (Y+Nb) and (d) $(K_2O+Na_2O)/CaO$ *vs.* (Zr+Nb+Ce+Y). Fields representing Creporizão (CPRM, 2000b) and Old São Jorge granites (Lamarão *et al.*, 2002) are plotted for comparison. In (c), VAG (Volcanic Arc Granites), ORG (Ocean Ridge Granites), syn-COLG (Syn-collisional Granites) and WPG (Within-Plate Granites) fields are from Pearce *et al.* (1984) and post-COLG (post-collisional granites) from Pearce (1996); In (d), OGT (Orogenic granite types: unfractioned I- and S-type granites) and FG (Fractionated felsic I- and S-type granites) fields are taken from Whalen *et al.* (1987). Compositional average of A-, M-, I-, S- and I-type are also represented. Symbols as in Fig. 3.

The Anauá spidergram pattern **(Fig. 6b)** displays coherent Rb, Ba and K contents with primitive arcs (Brown *et al.,* 1984), however, U, Ta, Zr, Sm, Ti and Y are enriched in relation to the primitive arc pattern. All other elements (Th, Nb, La, Ce, Sr, and P) in the Anauá rocks show primitive to mature arcs transitional values. The spidergram pattern of the blobs and lenses of leucogranite **(Fig. 6c)** displays the higher Nb, Ta, La, Ce and Hf fractionated values and steeply negative P and Ti anomalies. The leucogranites also show moderate to high Rb, Ba, Th and K contents in relation to chondrite values. The Serra Dourada Granite **(Fig. 6d)** has Rb, Ba, Sr, P

and Ti (locally Rb, Nb and P) patterns remarkably similar to the normal S-type average and La, Ce and Y display more enriched contents than normal S-type granites (*e.g.* Chappell and White 1992).

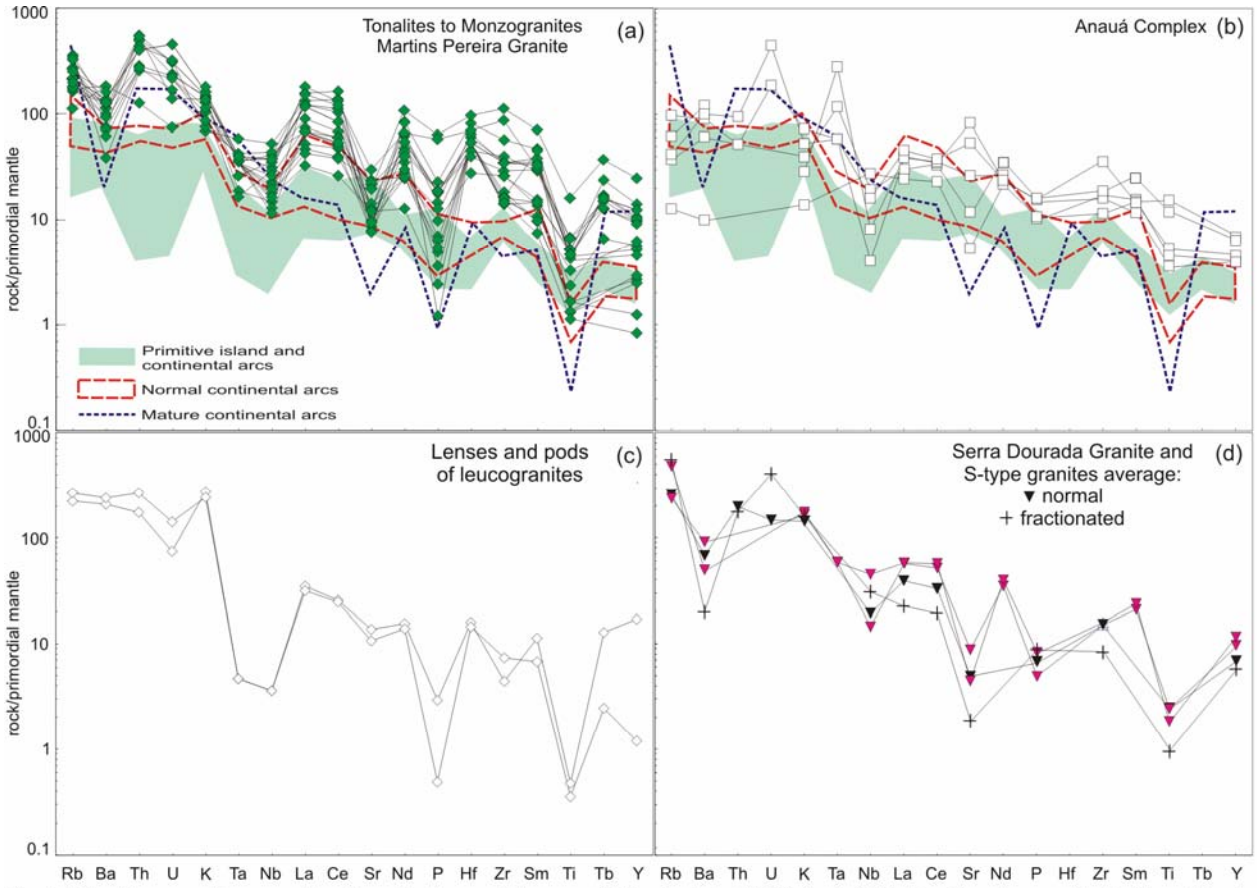

Fig.6. Primitive mantle-normalized multi-element diagrams (Wood *et al.,* 1979) for (a) Martins Pereira granitoids (tonalites to monzogranites); (b) Anauá Complex; (c) Blobs and lenses of leucogranites, and (d) Serra Dourada Granite. Data from granitoids of primitive, normal and mature arcs (Brown *et al.,* 1984) are also plotted for comparison. Symbols as in Fig. 3.

Rare Earth Element (REE) Geochemistry

The total REE contents of the studied granitoid rocks are relatively similar **(Table 1)**, except in the Anauá Complex (138 to 148 ppm) and leucogranites (100 to 153 ppm) samples. Martins Pereira (97 to 624 ppm) and Creporizão granites (104 to 541 ppm) show some REE enriched samples, contrasting with Old São Jorge Granite which displays moderate to low REE contents (52 to 244 ppm).

The REE chondrite-normalized pattern of the Martins Pereira Granite **(Fig. 7a)** is enriched in the LREE (*e.g.* La with 80x to 400x the chondrite values), but the LREE fractionation [$(La/Sm)_n$ ratios range from 3.4 to 6.7, exceptionally 8.0] is similar to the Creporizão and Old São Jorge granites **(Fig 7b)**. By contrast, the Anauá Complex **(Fig 6c)** shows lower LREE contents

(*e.g.* La with 50x to 100x the chondrite values) and low $(La/Sm)_n$ ratios (1.9 to 4.6). The Anauá REE pattern is probably controlled by hornblende and allanite-epidote fractionation.

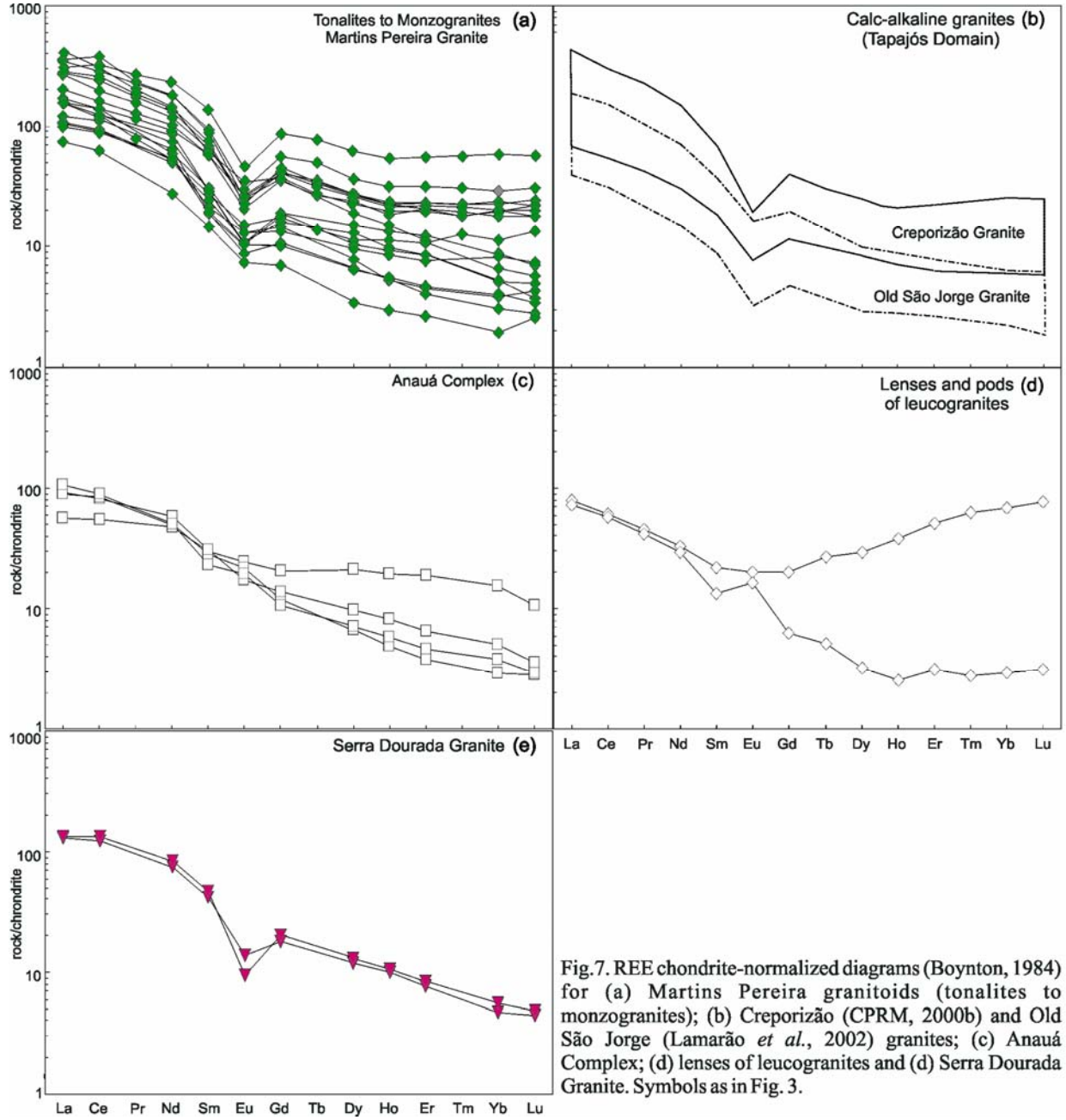

Fig.7. REE chondrite-normalized diagrams (Boynton, 1984) for (a) Martins Pereira granitoids (tonalites to monzogranites); (b) Creporizão (CPRM, 2000b) and Old São Jorge (Lamarão *et al.*, 2002) granites; (c) Anauá Complex; (d) lenses of leucogranites and (d) Serra Dourada Granite. Symbols as in Fig. 3.

The Martins Pereira Granite shows variable HREE contents (*e.g.* Yb and Lu ranging 3x to 60x the chondrite values) and the degree of HREE fractionation $[(Gd/Yb)_n]$ is similar to the Creporizão, Old São Jorge and Anauá granites (1.1 to 4.5). In the more HREE enriched granites, the HREE patterns are normally flat. The wide HREE range in the Martins Pereira types is probably associated to the variable residual zircon retention during partial melting and different Zr saturation level of magma (Watson and Harrison 1983). The same is observed in the

leucogranite samples, though these samples have atypical REE patterns, including positive to weak negative Eu anomaly, which point out for cumulatic plagioclase occurrence **(Fig 7d)**. These REE patterns may be also related to high hydrothermal activity in the final stages of crystallization or chemical heterogeneities related to source(s). The Old São Jorge **(Fig 7b)** and Anauá **(Fig 7c)** granitoid rocks exhibit the most HREE depleted patterns.

The Anauá types show discrete negative to positive Eu anomaly, with Eu_n/Eu^* ratios ranging from 0.8 to 1.2 **(Table 1; Fig. 7c)**, suggesting occurrence of cumulate plagioclase and/or hornblende fractionation. Overall, the REE and Eu anomaly patterns **(Table 1; Fig. 7a, b)** are similar among Martins Pereira (Eu_n/Eu^* = 0.4-0.7), Creporizão (Eu_n/Eu^* = 0.3-0.8) and Old São Jorge (Eu_n/Eu^* = 0.4-1.0) granites. In the case of Martins Pereira, the moderate to discrete negative Eu anomaly probably demonstrates variable residual plagioclase retention in the restite.

The Serra Dourada S-type granite **(Table 1; Fig. 7e)** shows moderate total REE content (205 to 223 ppm) and negative Eu anomaly (Eu_n/Eu^*= 0.5-0.3). The LREE fractionation [$(La/Sm)_n$ = 3.2-2.8] and HREE fractionation [$(Gd/Yb)_n$ = 3.6-3.8] are moderate to high.

MARTINS PEREIRA AND SERRA DOURADA GRANITES: PETROGENETIC CONSIDERATIONS

The Martins Pereira Granite is one of the most prominent examples of Orosirian high-K calc-alkaline plutonism in southern Roraima, outcropping in the Northern Uatumã-Anauá Domain. The geological literature (*e.g.* Roberts and Clemens, 1993; Barbarin, 1999) shows that high-K calc-alkaline granitoid rocks are very common in orogenic belts since Proterozoic times, corresponding to 35%-40% of all post-Archean metaluminous granitoid rocks found around the world. The two main tectonic environments envisaged for high-K magma generation are (Roberts and Clemens, 1993): a) continental arc (Cordilleran- or Andean-type), and b) post-collisional (Caledonian-type) settings.

In general, the tectonic setting discrimination diagrams (*e.g.* Pearce *et al.*, 1984) diagnose the settings in which the protoliths were formed better than the environment where the magma was generated (*e.g.* Barbarin, 1999). This implies that these diagrams could denote geochemical (and isotopic) characteristics of the sources (inheritance), irrespective of the residual mineral components. In the hornblende-free Martins Pereira high-K calc-alkaline granitoid rocks, for instance, linear and continuous trends in Harker diagrams and absence of coeval and large mafic batholith, suggest that the rocks were generated by partial melting processes. However, the

sources are not yet fully understood, despite a number of geochemical features (*e.g.* K, U, Th, Rb and REE enrichment) pointing towards the importance of crustal rocks in the magma source.

Experimental data on the potential sources for high-K calc-alkaline granitoid rocks have suggested several possibilities of crustal sources (*e.g.* Roberts and Clemens, 1993). These partial melting hypotheses yield compositional differences among magmas produced by partial melting of common crustal rocks, such as amphibolites, tonalitic gneisses, metagreywackes and metapelites under variable melting conditions (*e.g.* Patiño-Douce, 1996, 1999). This compositional variation can be visualized in terms of major oxides ratios **(Fig. 8a-c)** or molar oxide ratios **(Fig. 8d)**. It can be seen in these plots that partial melts derived from mafic to intermediate source rocks have lower $Al_2O_3/(FeO+MgO+TiO_2)$, $(Na_2O+K_2O)/(FeO+MgO+TiO_2)$ and molar $Al_2O_3/(MgO+FeO_{tot})$ ratios relative to those originated from metapelites and metagreywackes **(Fig 8a-d)**.

The Martins Pereira Granite samples generally plot in the amphibolite and metabasalt-metatonalite fields **(Fig 8a-d)**, showing low $Al_2O_3/(FeO+MgO+TiO_2)$, $(Na_2O+K_2O)/(FeO+MgO+TiO_2)$ and molar $Al_2O_3/(MgO+FeO_{tot})$ ratios, but exhibit relatively high $CaO/(FeO+MgO+TiO_2)$. This feature, associated with relatively high Mg# values (32.5-45.3), precludes a derivation from felsic pelite and/or metagreywacke for Martins Pereira Granite, particularly the low-SiO_2 samples (<70%). Most SiO_2-rich samples (>65%), however, have lower Mg# values (24.7-30.7), higher $Al_2O_3/(FeO+MgO+TiO_2)$ and $(Na_2O+K_2O)/(FeO+MgO+TiO_2)$ ratios, and lower $Al_2O_3+FeO+MgO+TiO_2$ (15-18%) and $Na_2O+K_2O+FeO+MgO+TiO_2$ (8-10%) contents. These Martins Pereira SiO_2-rich samples, as well as the Serra Dourada Granite samples, also show low $CaO+FeO+MgO+TiO_2$ contents (2-4%) and plot in the metagreywacke field **(Fig 8a-d)**, suggesting metasedimentary source contribution (at least locally) in the Martins Pereira magma genesis. The most suitable metasedimentary source rocks available in the Northern Uatumã-Anauá Domain are related to the Cauarane Group.

By combining the above mentioned geochemical features with petrographic and other geochemical parameters, the Serra Dourada Granite is considered as dominantly derived from a metagreywacke source by partial melting. In contrast to the Serra Dourada Granite, the Martins Pereira granitic magma could be linked with the partial melting of metatonalite or amphibolite sources, and further input of metagreywacke sources, either by partial melting or contamination-assimilation processes. A similar hybrid origin was proposed by Sardinha (1999) for the 1.89 Ga Igarapé Azul Granite (Almeida *et al.*, 2002). Similarly, an origin for high-K, calc-alkaline I-type

granitoid rocks by partial melting of metagreywacke-sources was also proposed by Barker *et al.* (1992), Altherr *et al.* (2000) and Thuy Nguyen *et al.* (2004), in Alaska, Germany and Vietnam, respectively.

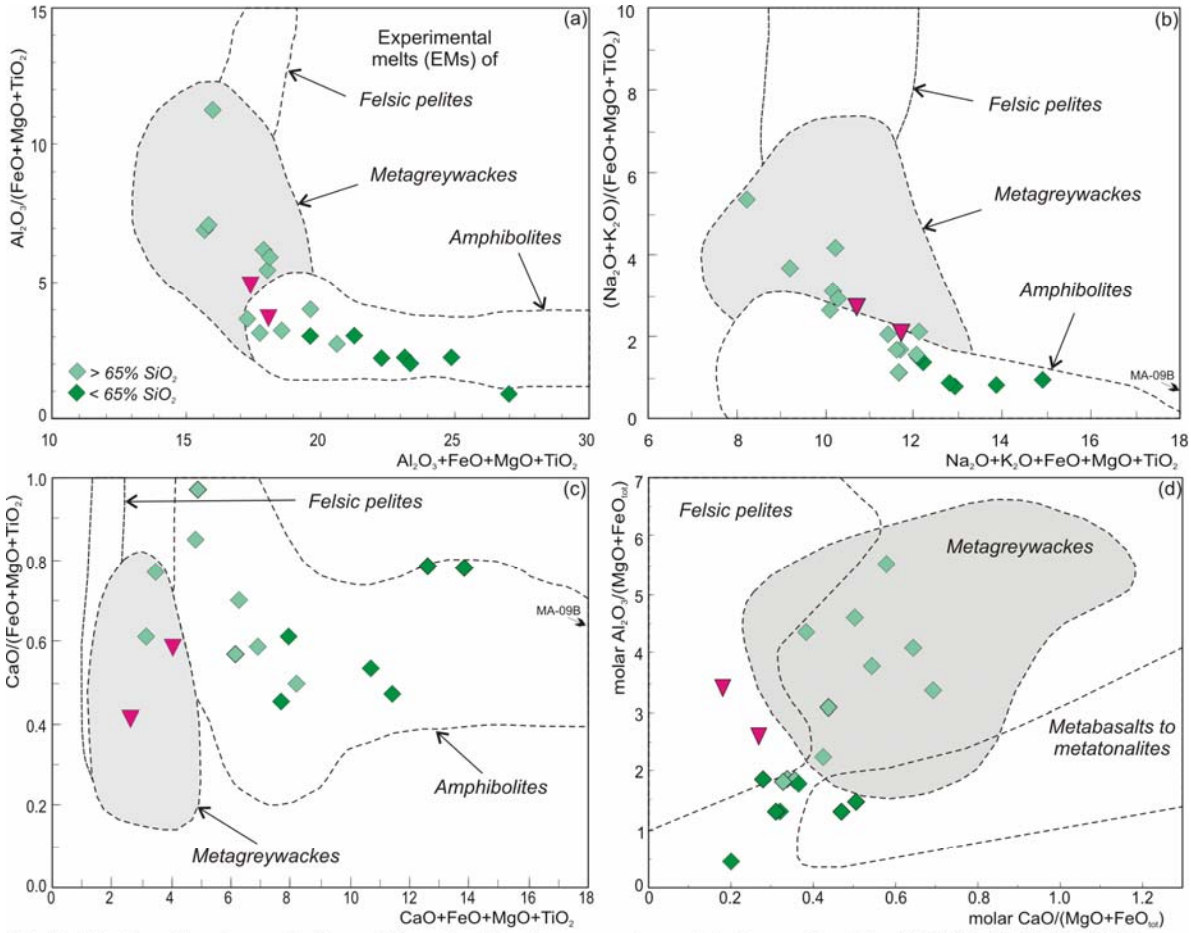

Fig.8. Martins Pereira and Serra Dourada Granites samples plotted on the (a) $Al_2O_3/(FeO+MgO+TiO_2)$ *vs.* $Al_2O_3+FeO+MgO+TiO_2$, (b) $(Na_2O+K_2O)/(FeO+MgO+TiO_2)$ *vs.* $Na_2O+K_2O+FeO+MgO+TiO_2$, (c) $CaO/(FeO+MgO+TiO_2)$ *vs.* $CaO+FeO+MgO+TiO_2$ and (d) molar $Al_2O_3/(MgO+FeO_{tot})$ *vs.* molar $CaO/(MgO+FeO_{tot})$ diagrams. Outlined fields denote compositions of partial melts obtained in experimental studies by dehydration melting of felsic pelites, metagreywackes, amphibolites-metabasalts and metatonalites sources (Wolf and Wyllie, 1994; Patiño-Douce, 1999; Patiño-Douce and Beard, 1996, Thompson, 1996, and references therein). Symbols as in fig. 03. See text for discussion.

ZIRCON GEOCHRONOLOGY

Five fresh granitic rocks of Northern Uatumã-Anauá Domain were sampled and analyzed by Pb-evaporation and U-Pb ID-TIMS methods **(Table 2)**. Three samples from Martins Pereira Granite and one from leucogranite lenses were analyzed by zircon Pb-evaporation, whereas the same sample from Serra Dourada Granite was analyzed by both methods.

Martins Pereira Granite (MA-172A, 061A and 007A samples)

In the general sense, hornblende-free Martins Pereira (meta)granitoid rocks are composed of porphyritic coarse- to medium-grained granodiorites, monzogranites and rare fine- to medium-grained (epidote)-biotite-rich tonalites (calc-alkaline granodioritic trend in QAP diagram), locally associated with small lenses and blobs of leucogranites. Three samples from the Martins Pereira Granite were analyzed by the single-zircon Pb evaporation method **(Table 2)**: cataclastic porphyritic monzogranite (MA-172A), mylonitic granodiorite (MA-61A) and porphyritic metamonzogranite (MA-007A).

The sample of cataclastic coarse-grained monzogranite (MA-172A) shows translucent crystals with local opaque portions, pale brown to pale yellow colours, prismatic (length/width ratios between 2.9:1 to 1.8:1) and 90-400 μm in length, exhibiting well-defined faces and vertices. Mineral inclusions (such as apatite and Fe-Ti oxides) and fractures are common. A total of 6 crystals were analyzed yielding a mean age of 1975 ± 6 Ma (USD: 2.9) from 162 isotopic ratios **(Table 3, Fig. 9a)**. Individual ages of these analyses vary from 1988 Ma to 1962 Ma.

The MA-61A mylonitic biotite granodiorite was sampled along an ENE-WSW mylonitic zone to the north of São Luiz do Anauá. Two different zircon populations were described in this sample: a) prismatic (length/width ratios between 2.4:1 and 1.6:1), translucent and brown to pale brown crystals showing fractures and rounded vertices; b) prismatic (length/width ratios between 3.8:1 and 2:1), transparent, pale yellow crystals showing few fractures and vertices, and well-defined faces. Both zircon populations showed scarce mineral inclusions, crystals with 140-360 μm in length and local irregular internal zoning, this last observation suggesting igneous overgrowth and/or older inherited cores. The mean age of analyses of 8 crystals (264 isotopic ratios) from both populations by the Pb-evaporation method yielded 1973 ± 2 Ma (USD: 2.1) **(Table 3, Fig. 9b)**, exhibiting individual ages varying from 1978 Ma to 1962 Ma. Anomalous ages were observed in crystals # 4 (2042 ± 20 Ma, 1450^0C and 1500^0C step-heatings) and # 9 (1994 ± 4 Ma, 1500^0C step-heating), which could represent inherited components.

The sample of the porphyritic metamonzogranite facies (MA-007A) selected for dating is locally foliated and banded. The zircon crystals are pale brown, transparent to translucent, prismatic and bypiramidal, with 190-450 μm in length (3.5:1 to 2.2:1 length/width ratios). They show fractures, sometimes radial-like, well-defined faces and rounded vertices. Inclusions are very rare in these zircon samples. A total of 4 crystals were analyzed, yielding individual ages varying from 1973 Ma to 1967 Ma, and a mean age of 1971 ± 2 Ma age **(Table 3, Fig. 9c).** The

25 blocks and 180 isotopic ratios show a very homogeneous pattern, yielding a well-defined mean age (USD: 1.1).

The results obtained from Martins Pereira Granite show a small interval age (1980-1968 Ma) and local 1.99 Ga and 2.04 Ga inheritances, these last probably related to the Anauá Complex. Other granitoid rocks from Martins Pereira Granite area, and equivocally related to Água Branca Suite and Igarapé Azul Granite, were dated by Almeida *et al.* (1997) and CPRM (2003) yielding 1960 ± 21 Ma and 1972 ± 8 Ma, respectively **(Table 5)**. These ages are in agreement with the results obtained in this paper **(see Fig. 9a-c)** and mark an important magmatic event in southeastern Roraima, here named as Rorainópolis event. In general sense, these results are uniform, homogeneous and establish a 1.98-1.96 Ga age range, despite the observed heterogeneous textures (*e.g.* igneous, mylonitic and cataclastic), different geographical site sampling, and different applied methodologies **(Tables 2 and 5, Fig. 2)**.

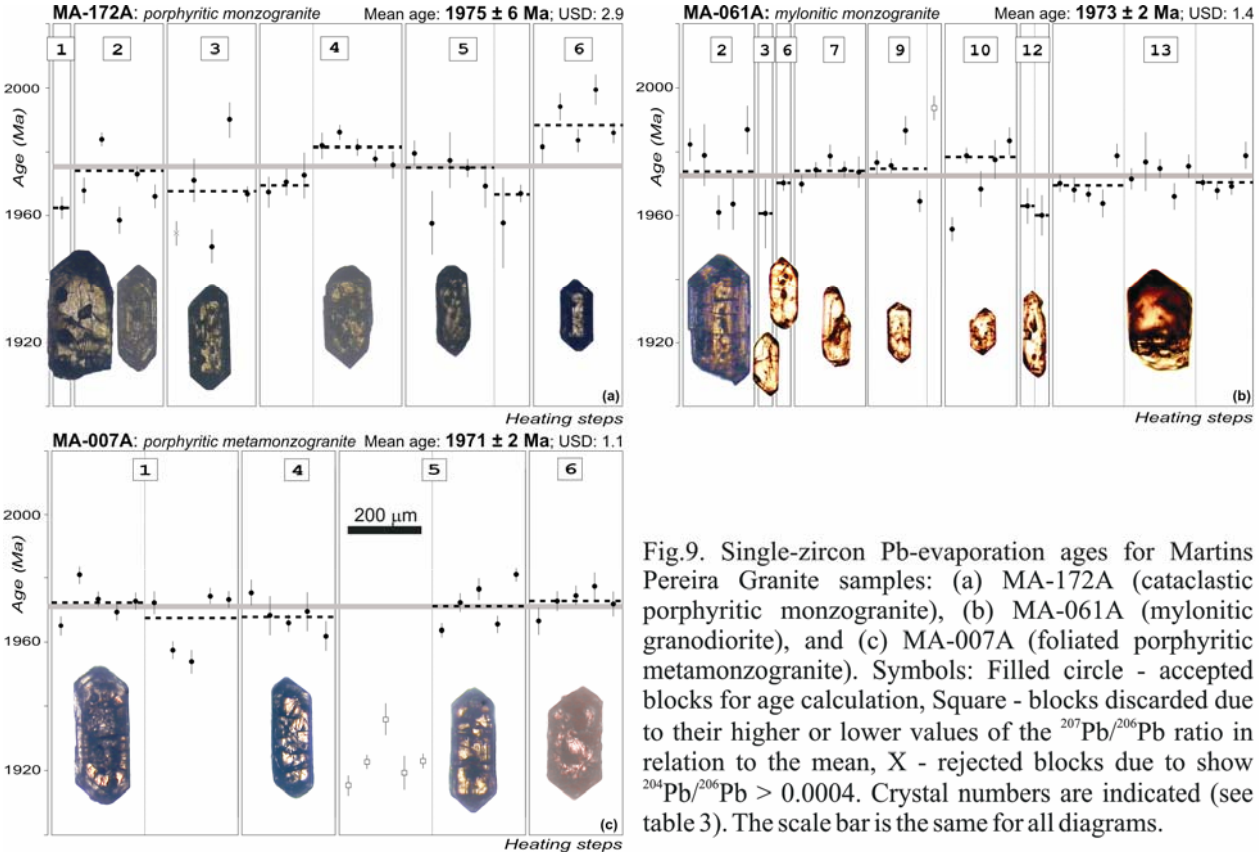

Fig.9. Single-zircon Pb-evaporation ages for Martins Pereira Granite samples: (a) MA-172A (cataclastic porphyritic monzogranite), (b) MA-061A (mylonitic granodiorite), and (c) MA-007A (foliated porphyritic metamonzogranite). Symbols: Filled circle - accepted blocks for age calculation, Square - blocks discarded due to their higher or lower values of the $^{207}Pb/^{206}Pb$ ratio in relation to the mean, X - rejected blocks due to show $^{204}Pb/^{206}Pb > 0.0004$. Crystal numbers are indicated (see table 3). The scale bar is the same for all diagrams.

Serra Dourada Granite (MF-156 samples)

The S-type granitoid rocks in southeastern Roraima were initially described by Faria *et al.* (1999) and incorporated into the Igarapé Azul Granite. However, Almeida *et al.* (2002)

subdivided the Igarapé Azul Granite into three different types: Serra Dourada Granite (true S-type), Martins Pereira Granite (I-type high-K calc-alkaline) and the proper Igarapé Azul Granite (I-type felsic high-K calc-alkaline).

A monzogranite sample of Serra Dourada Granite (MF-156) with biotite, muscovite and cordierite **(Table 2)**, including monazite, xenotime, sillimanite and tourmaline as accessory minerals, was analyzed by single-zircon Pb-evaporation method. This sample shows two zircon populations with different features, however these differences are not reflected in the age results. The first group is scarce and shows rounded vertices, irregular faces (corrosion?), light yellow colour, 310-500 μm in length (length/width ratios between 2.3:1 to 1.5:1), translucent to transparent opacity, and is generally free of inclusions. The second type of zircon shows slightly rounded crystals, is light brown to brown, 170-340 μm in length (length/width ratios between 3.1:1 to 1.5:1), transparent and locally with few inclusions and fractures. This second type of zircon is characterized by well-developed {211} pyramid, similar to zircon crystallized from peraluminous melt (Pupin, 1980).

In the Pb-evaporation method, the zircon fractions yielded two different age patterns, irrespective of the few analyzed grains and isotopic ratios obtained **(Table 3)**. The lower age (1948 ± 11 Ma) was obtained from two blocks from two crystals. The higher age (2138 ± 3 Ma) was obtained from nine blocks of isotopic ratios from two zircon crystals **(Fig. 10a)**, and is interpreted as an age of inherited origin.

U-Pb ID-TIMS was carried out on the same sample with the aim of interpreting the ages obtained by the Pb-evaporation method. The regression of four experimental points yields a discordia line which indicates an upper intercept at 1962 ± 2 Ma (**Table 4, Fig. 10b**), interpreted as the crystallization age of the analyzed crystals and, similarly, that of the Serra Dourada Granite. This age is very close to the age yielded with the Pb-evaporation method for the same sample which, taking into account the errors, almost overlap one another.

The geological similarities between Serra Dourada (Uatumã-Anauá Domain) and Taiano (Central Guyana Domain) S-type granites are also pointed out by our U-Pb and Pb-evaporation zircon ages. The Taiano anathetic leucogranite yields 1969 ± 3.5 Ma (zircon U-Pb SHRIMP, CPRM, 2003) and the minimum crystallization age yielded by single-zircon Pb-evaporation (1948 ± 11 Ma) and U-Pb ID-TIMS (1962 +2/-6 Ma) methods for the Serra Dourada type are quite similar **(Table 5)**, confirming an important anathetic process in central-southern Roraima

occurred 1.98-1.96 Ga. Other S-type granitoid rocks in Roraima, such as Curuxuim and Amajari granites (CPRM, 1999), could be related also to this same event, however they are not dated yet.

The inherited ages in both S-type granites also show ages ranging from 2138 ± 3 Ma (Serra Dourada Granite) to 2047 ± 7 Ma and 2072 ± 3 Ma (Taiano Granite), probably related to sedimentary contribution. This hypothesis is partially confirmed by Transamazonian detrital zircon crystals detected in the metavolcanosedimentary rocks from the Cauarane Group **(Table 6)**, from which two paragneiss samples were dated by U-Pb ID-TIMS (2223 ± 19 Ma, Gaudette *et al.,* 1996) and U-Pb SHRIMP (2038 ± 17 Ma and 2093 ± 62 Ma, CPRM, 2003) methods.

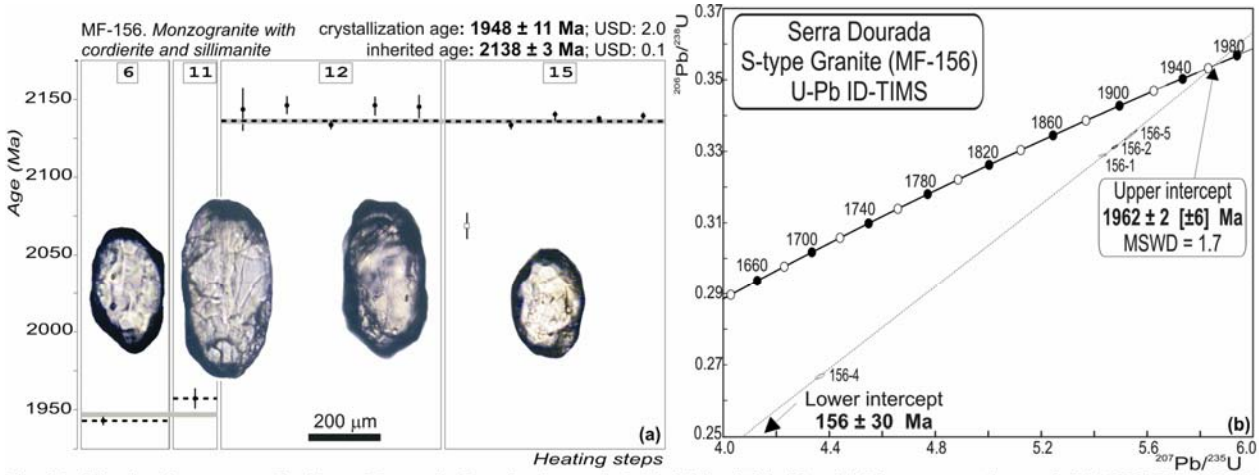

Fig.10. Single-zircon ages for Serra Dourada Granite (sample MF-156) yielded by (a) Pb-evaporation and (b) U-Pb ID-TIMS (concordia diagram) methods. Crystal numbers are indicated (see tables 3 and 4). Symbols: Filled circle - accepted blocks for age calculation; Square - blocks discarded due to too low value of the $^{207}Pb/^{206}Pb$ ratio in relation to the average.

Leucogranite (MA-246C2 sample)

Leucosyenogranite lens sample (MA-246C2) associated with Martins Pereira (meta)granitoid rocks showed a complex set of results. All zircons were analysed based on 2 sigma = 0.0006, because 2 sigma = 0.0004 yielded ages with higher USD values and errors, although the results are not so different. For instance, the younger zircon population yielded by 2 sigma 0.0006 and 0.0004, 1909 ± 6 Ma (USD = 4.1) and 1909 ± 7 Ma (USD = 4.7), respectively. Five groups of zircon occur in this sample, in decreasing age order **(Table 5, Fig. 11a-b)**:

Group I is represented by only one pale brown, transparent to translucent zircon grain with 265 μm in length (length/width ratio 1.9:1), showing regular internal zoning, well-defined faces and dark inclusions in the core. It yielded an age of 2354 ± 6 Ma (crystal #1).

Group II exhibits pale yellow and transparent grains (locally translucent to opaque) being 250-330 μm in length (length/width ratios between 3.2:1 and 2.5:1). Cracks are common, but

inclusions are rare. This group comprises 3 zircon crystals with individual ages varying from 2148 Ma to 2126 Ma, and yielded a mean age of 2134 ± 15 Ma (crystals #10, 14, and 16).

Group III encompasses colorless to pale yellow crystals which are 166-180 μm in length (length/width ratios around 2.7:1), with crystals locally exhibiting internal zoning and cracks in the core. This group yielded 1997 ± 8 Ma as a mean age (crystals #17 and 21).

In general, zircon crystals of group IV are characterized by brown to pale brown and translucent grains with well-defined faces (locally broken) and 210-260 μm in length (length/width ratios around 2.6:1). This group consists of 4 crystals with individual ages varying from 1968 Ma to 1952 Ma, and yielded a mean age of 1959 ± 5 Ma (crystals #7, 9, 13, and 23).

Zircon crystals of group V are 164-330 μm in length (length/width ratios between 3.1:1 and 1.8:1), are pale yellow to pale brown in colour, transparent, and show local cracks and inclusions. This group displays a mean age of 1909 ± 6 Ma from 5 crystals (#5, 6, 8, 18, and 19), with individual ages varying from 1933 Ma to 1892 Ma. This lowest age (group V) is interpreted as the crystallization age, whereas the higher ages (groups I, II, III and IV) probably represent inherited zircon of different origins. However, this crystallization age may have, at least locally, grains with younger border (igneous) and older cores (inherited), suggesting partial contribution of isotopic content from different events (e.g. crystals #5 and 6). Another interpretation is related to the high Pb loss of the 1.90 Ga zircon populations. In this last situation, the 1.96 Ga age (Group IV) could be the crystallization age.

Despite the wide variety of zircon populations from sample MA246C2, including grains with internal complexity or zoning ("mixing age") or partial resetting, the results obtained by the single-zircon Pb-evaporation method allow for the following interpretation:

a) The 1909 ± 6 Ma (group V) is interpreted as the minimum crystallization age of leucosyenogranite. Other ages, around 1.89 to 1.90 Ga, which are related to Igarapé Azul and Água Branca granitoid rocks (*e.g.* CPRM, 2003, Almeida *et al.,* 2002) are described in this region, mainly in the southern Uatumã-Anauá Domain. These leucogranitic lenses also show some petrographic similarities with Igarapé Azul granitoid rocks and were both probably generated in the same magmatic event;

b) The 1997 ± 8 Ma (group III) and 1959 ± 5 Ma (group IV) ages probably correspond to inherited components from the Surumu volcanics and Martins Pereira granitoid rocks (or Urubu orthogneisses?), respectively; however the former are not exposed in the Uatumã-Anauá Domain and correlated igneous rocks are not found there.

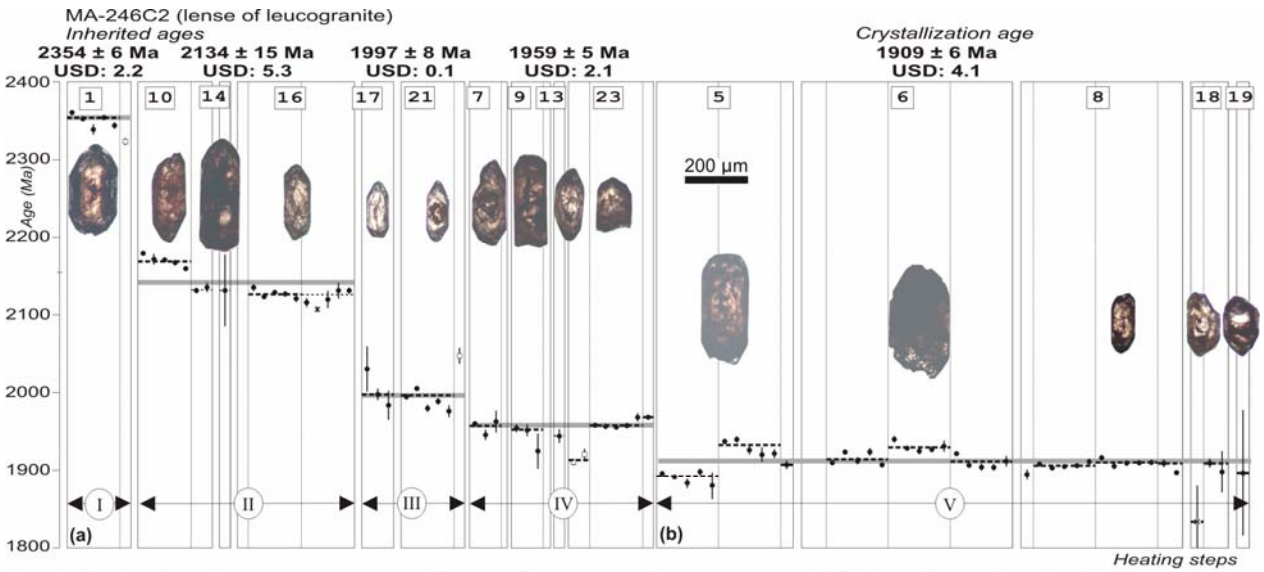

Fig.11. Single-zircon Pb-evaporation ages of lenses of leucogranite in association with Martins Pereira Granite. (a) Inherited ages: I - Pre-Transamazonian (Siderian); II Transamazonian; III - Anauá Complex (?); IV - Martins Pereira granite, and (b) V - Minimum crystallization age (Igarapé Azul and Caroebe magmatic event?). Symbols: Filled circle - accepted blocks for age calculation; Square - blocks discarded due their higher or lower values of the $^{207}Pb/^{206}Pb$ ratio in relation to the mean; X - rejected blocks due to $^{204}Pb/^{206}Pb > 0.0006$. Crystal numbers are indicated (see table 3). The scale bar is the same for all diagrams.

c) The 2354 ± 6 Ma (Siderian, group I) and 2134 ± 15 Ma (Sthaterian, group II) ages suggest local inheritance from older crust (not outcropping), respectively related to the pre-Transamazonian and Transamazonian magmatic events. Transamazonian rocks with 2.26-2.01 Ga (Santos *et al.,* 2003a) have been described ~600 km northeast from the sampled site, in the Maroni-Itacaiúnas or Transamazon Province (**Fig. 1**). Transamazonian rocks mainly occur in Brazil (Amapá State; Avelar *et al.,* 2001, Rosa Costa *et al.,* 2003), French Guyana (Vanderhaerghe *et al.,* 1998, Delor *et al.,* 2003), São Luis Craton (Klein and Moura, 2001) and (its extension) in the West Africa craton (Boher *et al.,* 1992, Milési *et al.,* 1992, Gasquet *et al.,* 2003). In the last case, they are related to Birimian (2185-2150 Ma) and Bandamian (2115-2100 Ma) events.

In West Africa, pre-Birimian ages (Burkinian, according to Lemoine *et al.,* 1990) are described by Gasquet *et al.* (2003) in Dabakala (Ivory Coast). The 2312 ± 17 Ma age has seen two interpretations by the previously mentioned authors. The first interpretation considers this age representing an Archean inheritance (and not Siderian) based on the complex model of lead loss in the analyzed zircon crystals. The second interpretation holds that this age is related to the ca. 2.3 Ga pre-Birimian crust. According to these authors, the second hypothesis is more consistent due to the systematically well-defined age patterns around 2.2-2.3 Ga (without

evidence of older Archean ages). This second hypothesis gains additional support from the fact that these rocks are not spatially close to the Archean core.

The Siderian age in Uatumã-Anauá Domain (Tapajós-Parima Province) is the first zircon data reported in any section of the central-western Guyana Shield and suggests probably contamination-assimilation of older country rocks with pre-Transamazonian and post-Archean ages, not exposed in surface. The proximity with Central Amazonian Province (older than 2.3 Ga) is uncertain, because provincial boundaries are not precise. Although Siderian-Neoarchean Nd model ages are describe (Faria *et al.*, 2002; Costa, 2005) in the central Guyana Shield, this province remains poorly investigated, while U-Pb and Pb-Pb geochronological data are scarce, showing ages systematically lower than 2.3 Ga.

Other Siderian ages have been found in the Amazonian Craton, but not in the Guyana Shield. Additionally, the Siderian age (2354 Ma) in Uatumã-Anauá is lower than the Siderian inheritance (2380-2483 Ma) obtained by Santos *et al.* (2001) in Cuiú-Cuiú rocks from the Tapajós Domain (Brazil Central Shield). Other Siderian ages are reported in the Transamazonian terrane (2.20 to 1.99 Ga, Vasquez *et al.,* 2003) of Bacajá domain (to north-northwest of Carajás Province) where zircon dating from Vasquez *et al.* (2003), Santos *et al.* (in Faraco *et al.,* 2003), and Macambira *et al.* (2004) yielded 2.44-2.30 Ga, 2.47-2.31 Ga, and 2.36 Ga, respectively.

Thus, the several zircon inherited populations observed in the leucogranite analysed preliminarily suggest multisource origin for these rocks, including metasedimentary ones.

TAPAJÓS AND UATUMÃ-ANAUÁ DOMAINS: CHRONOSTRATIGRAPHY AND GEOLOGICAL IMPLICATIONS FOR THE TAPAJÓS-PARIMA (OR VENTUARI-TAPAJÓS) PROVINCE

Previous and new geochronological data have shown several similarities among granitoid rocks from the Northern Uatumã-Anauá Domain and Tapajós Domain (orogenic subdomain, CPRM, 2000b) (T**ables 5 and 6**). The Orosirian primitive arc inliers, for example, are represented by the Anauá (Northern Uatumã-Anauá Domain) and Cuiu-Cuiu (Tapajós) TTG-like complexes and are the oldest rocks outcropping in these regions.

In Northern Uatumã-Anauá Domain, the Anauá Tonalite is 2028 ± 9 Ma old **(Table 5, Fig. 12)**, but does not have inheritance evidence and shows $\varepsilon Nd_{2.03\ Ga}$ of –0.20. This is interpreted as being of juvenile origin (Faria *et al.,* 2002), although only one sample had been analyzed. The Cuiú-Cuiú Complex of the Tapajós Domain shows an age range of 2033-2005 Ma and the older

types are coeval to the Anauá granitoid rocks from the Northern Uatumã-Anauá Domain **(Table 5, Fig. 12)**. In contrast to Anauá types, the Cuiú-Cuiú Complex yields several inherited zircon components **(Table 6, Fig 12)**, in which, the main inheritance is from Transamazonian (2040-2100 Ma), with minor Siderian to Archean records (2380-2483 Ma).

The well-defined interval age of Martins Pereira Granite (1980-1969 Ma) in the Northern Uatumã-Anauá Domain is also very similar to that shown by the Creporizão Suite (1980-1951 Ma) from the Tapajós Domain (**Table 5, Fig. 12**, CPRM, 2000b, Santos *et al.,* 2000, 2001). Similarly, the Old São Jorge Granite (Lamarão *et al.,* 2002) of the Tapajós Domain is c. 10 Ma older than the Creporizão Suite, but both high-K calc-alkaline granites are related to the Creporizão Orogeny (1.98-1.96 Ga), according to Santos *et al.* (2004). The Pedra Pintada granitoid rocks (Fraga *et al.,* 1996) in the Surumu Domain (Orocaima event, Reis *et al.,* 2000) are also coeval (1958 Ma, CPRM, 2003) to the calc-alkaline Martins Pereira Granite.

In Northern Uatumã-Anauá Domain, lenses of leucosyenogranite are ~70 m.y. younger than the Martins Pereira host-rock and show crystallization age (1906 ± 4 Ma) similar to those of the Igarapé Azul-Caroebe granitoid rocks (Água Branca magmatism: 1906-1885 Ma) described in the Southern Uatumã-Anauá Domain. Some similar inherited ages are also observed in both granitic types, such as Martins Pereira granitoid rocks and Transamazonian inheritances (table 6), whereas Siderian inheritance is restrict to the leucogranites. The same 1.90-1.88 Ga age interval corresponds also to the Tropas and Parauari magmatism, in the Tapajós Domain (**Table 5,** *e.g*. Santos et al., 2000; CPRM, 2000b)

In contrast with Roraima region - where S-type granites (e.g. Serra Dourada, Curuxuim and Amajari), granulites (e.g. Barauana) and charnockites are relatively common - these rock types are scarce in the Tapajós Domain. They are locally described as small garnet leucogranite bodies (not mapped on the 1:250.000 scale) associated with Cuiú-Cuiú metagranitoid rocks (Almeida *et al.,* 2001) and have not been dated previously. The scarcity of S-type granites and granulite metamorphism suggests that the collisional processes were less intense in the Tapajós domain.

CONCLUSIONS

Geological, geochronological and geochemical data available for granitoid rocks from southeastern Roraima (Brazil) suggest Paleoproterozoic evolution in at least two stages: the Anauá orogeny is related to 2.03 Ga TTG granitoid rocks (*accretionary phase* generating the Anauá granitoid rocks and Cauarane metavolcanosedimentary cover), followed by crustal

thickening and anatexis around 1.97-1.96 Ga (*collisional phase* generating Martins Pereira and Serra Dourada granitoid rocks). A juvenile origin is envisaged for Anauá but scarce Nd isotopic data do not make this hypothesis conclusive. The Northern Uatumã-Anauá crust, characterized by Orosirian granitoid rocks, is mainly thought to have been generated by reworking of older Transamazonian and minor Siderian crust, according to inherited zircon records.

The folowing magmatic events can be listed for the Northern Uatumã-Anauá Domain:

A) 2.03 Ga - crystallization of Anauá Tonalite within the TTG association, representing a primitive arc (?) in southeastern Roraima with related back arc basins;

B) 1.98-1.96 Ga - Martins Pereira high-K calc-alkaline granitoid rocks and Serra Dourada S-type granite showing similar crystallization ages. These granitoid rocks are probably related to crustal thickening and anatexis in the latest (or after) stage of Anauá arc evolution;

C) ca. 1.90 Ga - meter to centimeter scale leucogranite blobs and lenses (low degree of partial melting?). It is thought that these blobs in-filled older, planar structures in the Martins Pereira granitoid rocks. A regional-scale magmatic event (1.90-1.89 Ga) is mentioned in the southern Uatumã-Anauá Domain, and is believed to be related to the Igarapé Azul and Água Branca granitoid rocks and coeval volcanism (Almeida *et al.*, 2002; Almeida and Macambira, 2003).

Furthermore, possibly two main periods are also recorded in inherited zircon:

A) Siderian (2.35 Ga) - only one zircon crystal with this age was detected in the lenses of leucogranite, but it represents the first indication of Siderian crust (host-rock or material source) in the central Guyana Shield. Alternatively, this Siderian age could be the result of an isotopic mixing between "Transamazonian" and "Archean" components of the same zircon or partial resetting of an older grain. On the other hand, similar ages are also recorded in West Africa craton (2312 Ma, Gasquet *et al.,* 2003), Bacajá (2359 ± 3 Ma, Macambira *et al.,* 2004) and Tapajós domains (2483-2380 Ma, Santos *et al.,* 2001) in Amazonian craton.

B) Rhyacian (2.14-2.13 Ga, Transamazonian) - this age interval is yielded by the oldest zircon crystals from the Serra Dourada S-type granite (two crystals) and group II from the lenses of leucogranite (three crystals). Similar inheritance (2163-2100 Ma) was observed in Surumu, Central Guyana and Tapajós domains (CPRM, 2003, Santos *et al.,* 2001, 2003b).

Neoarchean inheritance is not recorded in the Northern Uatumã-Anauá Domain, but is recorded locally in other domains of Tapajós-Parima Province, such as Tapajós (2852-2591 Ma, Lamarão *et al.,* 2002) and Parima (2872-2781 Ma, Santos *et al.,* 2003c).

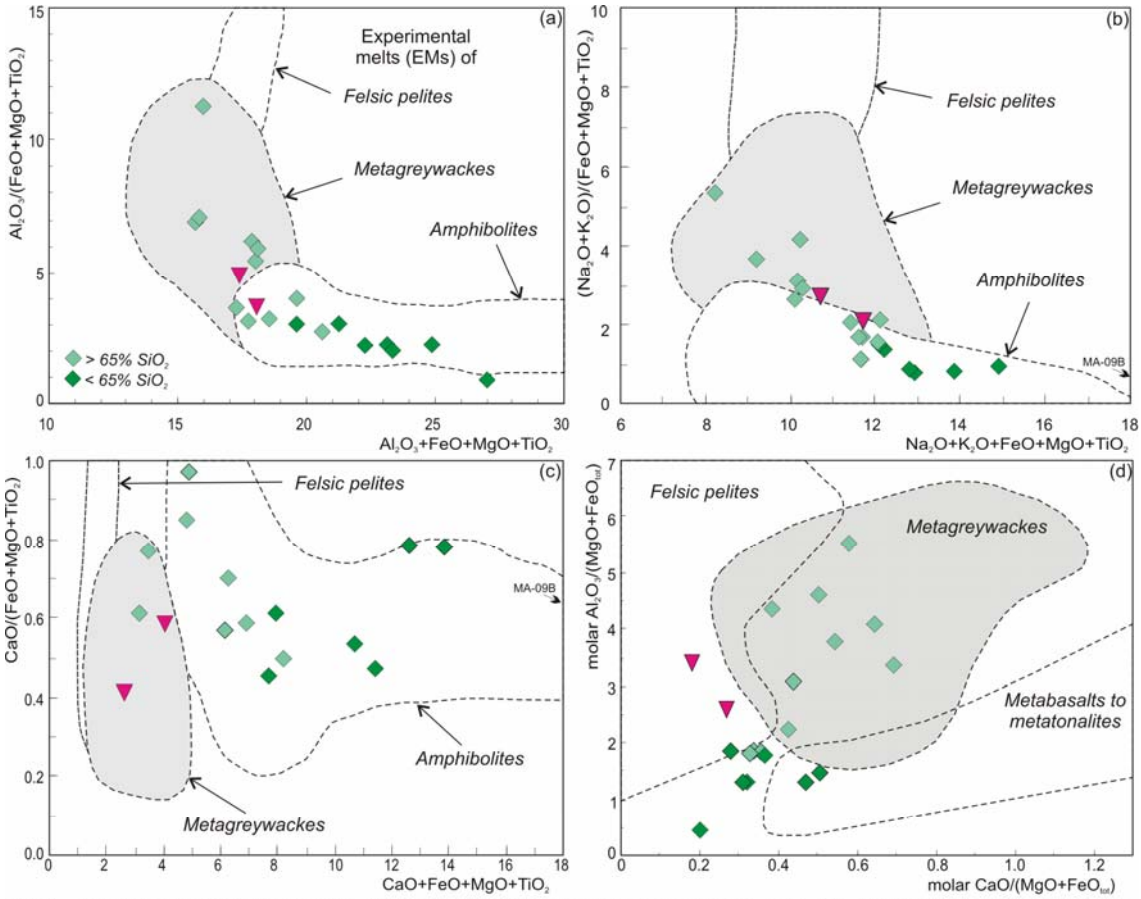

Fig.8. Martins Pereira and Serra Dourada Granites samples plotted on the (a) $Al_2O_3/(FeO+MgO+TiO_2)$ *vs.* $Al_2O_3+FeO+MgO+TiO_2$, (b) $(Na_2O+K_2O)/(FeO+MgO+TiO_2)$ *vs.* $Na_2O+K_2O+FeO+MgO+TiO_2$, (c) $CaO/(FeO+MgO+TiO_2)$ *vs.* $CaO+FeO+MgO+TiO_2$ and (d) molar $Al_2O_3/(MgO+FeO_{tot})$ *vs.* molar $CaO/(MgO+FeO_{tot})$ diagrams. Outlined fields denote compositions of partial melts obtained in experimental studies by dehydration melting of felsic pelites, metagreywackes, amphibolites-metabasalts and metatonalites sources (Wolf and Wyllie, 1994; Patiño-Douce, 1999; Patiño-Douce and Beard, 1996, Thompson, 1996, and references therein). Symbols as in fig. 03. See text for discussion.

Previous studies have recognized three geochronological provinces in southeastern Roraima, but new geological, geochronological and geochemical data presented here shows that this region is very similar to the Tapajós Domain (Santos *et al.,* 2004) and reinforce the Ventuari-Tapajós or Parima-Tapajós provinces prolongation in southeastern Roraima, taking into account that rocks older than 2.03 Ga are not exposed in the studied region. However, the Central Amazonian and Maroni-Itacaiúnas provinces seem to be important crustal sources for the rocks of the Northern Uatumã-Anauá Domain, suggesting partial or total crustal recycling.

In summary, the I-type high-K calc-alkaline Martins Pereira (meta)granitoid rocks and S-type Serra Dourada granites were generated in the Northern Uatumã-Anauá Domain (Ventuari-Tapajós or Tapajós-Parima provinces), probably during amalgamation of TTG-like Anauá magmatic arc (2028 Ma) with Transamazon (2.2-2.0 Ga) and Central Amazonian (older than 2.3 Ga) terranes.

Some authors argue that most collision orogenic systems have a prior accretion history (*e.g.* Van Staal *et al.,* 1998), so it is easy to confuse the accretion and collision histories in ancient examples, such as the Ventuari-Tapajós or Tapajós-Parima provinces. This makes it difficult to rebuild the histoy of the Anauá orogeny and the hypothesis presented in this paper is only a suggestion of the tectonic evolution of the central portion of the Guyana Shield.

Acknowledgements

Special thanks to the colleagues of CPRM (Geological Survey of Brazil) for discussions and Nicholas Tailby (Australian National University) for the English review. The authors are also grateful to CPRM-Geological Survey of Brazil for the research grants and FINEP (CT-Mineral 01/2001 Project) and Isotope Geology Laboratory of Federal University of Pará for support of laboratorial work. Thanks also to the two anonymous referees for suggestions to the manuscript.

References

Almeida, M.E., Macambira, M.J.B. 2003. Aspectos geológicos e litoquímicos dos granitóides cálcio-alcalinos paleoproterozóicos do sudeste de Roraima. In: SBGq, Cong. Brasil. Geoq., 9, Anais, p. 775-778 (in Portuguese).

Almeida, M.E., Macambira, M.J.B. Geology and petrography of Paleoproterozoic granitoids from Uatumã-Anauá Domain, central region of Guyana Shield, southeastern Roraima, Brazil. *Revista Brasileira de Geociências*, in press.

Almeida, M.E., Fraga, L.M.B., Macambira, M.J.B. 1997. New geochronological data of calc-alkaline granitoids of Roraima State, Brazil. In: IG/USP, South-American Symposium on Isotope Geology, 1, Abstract, p.34-37.

Almeida, M.E., Brito, M.F.L., Ferreira, A.L., Monteiro, M.A.S. 2001. Evolução tectono-estrutural da região do médio-alto curso do rio Tapajós. In: N.J. Reis and M.A.S. Monteiro (Orgs), Contribuições à Geologia da Amazônia, 2, , Belém, SBG, p.57-112. (in Portuguese).

Almeida, M.E., Macambira, M.J.B., Faria, M.S.G. de. 2002. A Granitogênese Paleoproterozóica do Sul de Roraima. In: SBG, Congresso Brasileiro de Geologia, 41, Anais, p 434 (in Portuguese).

Altherr, R., Holl, A., Hegner, E., Langer, C., Kreuzer, H. 2000. High-potassium, calc-alkaline I-type plutonism in the European Variscides: northern Vosges (France) and northern Schwarzwald (Germany). *Lithos* 50, 51–73.

Andsell, K.M., Kyser, T.K. 1991. Plutonism, deformation and metamorphism in the Proterozoic Flin Flon greenstone belt, Canada: Limits on timing provided by single-zircon Pb-evaporation technique. *Geology*, **19**, p. 518-521.

Avelar, V.G. de, Lafon, J.-M., Delor, C. 2001. Geocronologia Pb-Pb em zircão e Sm-Nd em rocha total da porção centro-norte do Amapá. Implicações para a evolução geodinâmica do Escudo das Guianas. *In*: SBG, Simpósio de Geologia da Amazônia, 7, Belém, Resumos Expandidos (CD-ROM) (in Portuguese).

Barbarin, B. 1999. A review of the relationships between granitoid types, their origins and their geodynamic environments. *Lithos* 46, 605–626.

Barker, F., Farmer, G.L., Ayuso, R.A., Plafker, G., Lull, J.S. 1992. The 50 Ma granodiorites of the eastern Gulf of Alaska: melting in an accretionary prism in the forearc. *J. Geophys. Res.* 97, 6757–6778.

Boher, M., Abouchami, W., Michard, A., Albarède, F., Arndt, N. 1992. Crustal growth in West Africa at 2.1 Ga. *Journal of Geophysical Research* **97**, 345–369.

Bonin, B. 1990. From orogenic to anorogenic settings: evolution of granitoid suites after a major orogenesis. *Geol. J.* 25, 261–270.

Boynton, W.V. 1984. Cosmochemistry of the rare earth elements: meteorite studies. In: Henderson, P. (ed), Rare earth element geochemistry, Elsevier Publ. p. 63-114.

Brown, G.C., Thorpe, R.S., Webb, P.C. 1984. The geochemical characteristics of granitoids in contrasting arcs and comments on magma sources. *Journal of Geological Society of London* **141**, 413-426.

Chappell, B.W., White, A.J.R. 1992. I- and S-type granites in the Lachlan Fold Belt. *Transactions of Royal Society of Edinburg*: Earth Sciences **83,** 1-26.

Cordani, U.G., Tassinari, C.C.G., Teixeira, W., Basei, M.A.S., Kawashita, K. 1979. Evolução tectônica da Amazônia com base nos dados geocronológicos. In: Congresso Geológico Chileno, 2, 1979, Arica, Anais, v.4, p.177-148 (in Portuguese).

Costa, J.A.V., Costa, J.B.S., Macambira, M.J.B. 2001. Grupo Surumu e Suíte Intrusiva Saracura, RR - Novas Idades Pb-Pb em Zircão e Interpretação Tectônica. In: SBG, Simpósio de Geologia da Amazônia, 7, Belém, Pará, Resumos Expandidos, CD-ROM. p. 16- 19 (in Portuguese).

Costa, S. dos S. 2005. Análise integrada dos dados geofísicos, geológicos e de sensoriamento remoto do Cinturão Guiana Central e áreas adjacentes do estado de Roraima. Doctoral thesis, Unicamp, São Paulo. 157 p. Unpublished. (abstract in english)

Cox, K.G.; Bell, J.D., Pankhurst, R.J. 1987. The interpretation of igneous rocks. George Allen and Unwin ltd., 5th ed., London. 450p.

CPRM. 1999. Programa Levantamentos Geológicos Básicos do Brasil. *Roraima Central*, *Folhas NA.20-X-B e NA.20-X-D (integrais), NA.20-X-A, NA.20-X-C, NA.21-V-A e NA.21-V-C (parciais)*. Escala 1:500.000. Estado de Roraima. Manaus, CPRM. 166 p. [CD-ROM]. (in Portuguese)

CPRM. 2000a. Programa Levantamentos Geológicos Básicos do Brasil. *Caracaraí, Folhas NA.20-Z-B e NA.20-Z-D (integrais), NA.20-Z-A, NA.21-Y-A, NA.20-Z-C e NA.21-Y-C (parciais)*. Escala 1:500.000. Estado de Roraima. Manaus, CPRM, 157 p. CD-ROM. (abstract in English)

CPRM. 2000b. Programa Levantamentos Geológicos Básicos do Brasil. Projeto Especial Província Mineral do Tapajós. Geologia e Recursos Minerais. *Vila Riozinho*, *Folha SB.21-Z-A*. Escala 1:250.000. Estado do Pará. Nota Explicativa. CPRM/Serviço Geológico do Brasil [CD-ROM] (in Portuguese).

CPRM. 2003. Programa Levantamentos Geológicos Básicos do Brasil. *Geologia, Tectônica e Recursos Minerais do Brasil: sistema de informações geográficas - SIG*. Rio de Janeiro : CPRM, 2003. Mapas Escala 1:2.500.000. 4 CDs ROM. (abstract in English)

CPRM. 2005. Programa Levantamentos Geológicos Básicos do Brasil. *Mapa Geológico do Brasil.* Escala 1:1000.000. 41 mapas Brasília, MME. Edição 2004. CD-ROM. (in Portuguese)

CPRM. 2006. Programa Integração, Atualização e Difusão de Dados da Geologia do Brasil: Subprograma Mapas Geológicos Estaduais. *Geologia e Recursos Minerais do Estado do Amazonas.* Manaus, CPRM/CIAMA-AM, 2006. Escala 1:1.000.000. Texto explicativo, 148p. CD ROM. (in Portuguese)

Daly, S.J., Fanning, C.M., Fairclough, M.C., 1998. Tectonic evolution and exploration potential of the Gawler Craton, South Australia. *AGSO J. Aust. Geol. Geophys*. 17, 145–168.

Daly, J.S., Balagansky, V.V., Timmerman, M.J., Whitehouse, M.J., de Jong, K., Guise, P., Bogdanova, S., Gorbatschev, R., Bridgewater, D., 2001. Ion microprobe U–Pb zircon geochronology and isotopic evidence for a trans-crustal suture in the Lapland–Kola Orogen, northern Fennoscandian Shield. *Precamb. Res* 105,289–314.

Delor, C., Lahondère, D., Egal, E., Lafon, J.-M., Cocherie, A., Guerrot, C., Rossi, P., Truffert, C., Théveniaut, H., Phillips, D., Avelar, V.G. de. 2003. Transamazonian crustal growth and reworking as revealed by the 1:500,000-scale geological map of French Guiana (2nd edition). *Géologie de la France* **2-3-4,** 5-57.

Dougherty-Page, J.S., Bartlett, J. M. 1999. New analytical procedures to increase the resolution of zircon geochronology by the evaporation technique. *Chem. Geol.* **153**, 227-240.

Faraco, M.T.L., Vale, A.G., Santos, J.O.S. dos, Luzardo, R., Ferreira, A.L., Oliveira, M.A., Marinho, P.A.C. 2003. Levantamento geológico na região a norte do Bloco Carajás: Notícias preliminares. In: SBG, Simpósio de Geologia da Amazônia, 8, Manaus, AM, Anais (CD-ROM) (in Portuguese).

Faria, M.S.G. de, Luzardo, R., Pinheiro, S.S. 1999. Litoquímica e petrogênese do Granito Igarapé Azul. In: SBG, Simpósio de Geologia da Amazônia, 6, Anais, p. 577-580 (in Portuguese).

Faria, M.S.G. de, Santos, J.O.S. dos, Luzardo, R., Hartmann, L.A., McNaughton, N.J. 2002. The oldest island arc of Roraima State, Brazil – 2.03 Ga: zircon SHRIMP U-Pb geochronology of Anauá Complex. *In*: SBG, Congresso Brasileiro de Geologia, 41, Anais, p. 306.

Fraga, L.M.B. 2002. A Associação Anortosito–Mangerito–Granito Rapakivi (AMG) do Cinturão Guiana Central, Roraima e Suas Encaixantes Paleoproterozóicas: Evolução Estrutural, Geocronologia e Petrologia. CPGG, UFPA, Tese de Doutorado. 386p (inédito) (in Portuguese).

Fraga, L.M.B., Reis, N.J., Araújo, R.V., Haddad, R.C. 1996. Suíte Intrusiva Pedra Pintada - Um Registro do Magmatismo Pós-colisional no Estado de Roraima. In: SBG, Simpósio de Geologia da Amazônia, 5, Belém, PA. Anais, 76-78 (in Portuguese).

Fraga, L.M.B., Almeida, M.E., Macambira, J.B. 1997. First lead-lead zircon ages of charnockitic rocks from Central Guiana Belt (CGB) in the state of Roraima, Brazil. In: South-American Symposium on Isotope Geology, Campos do Jordão, Resumo, p. 115-117.

Fraga, L.M.B., Macambira, M.J.B., Dall'Agnol, R., Costa, J.B.S. 2003. The age of the charnockitic rocks of the Serra da Prata Intrusive Suite, Central Guyana Belt, Guyana Shield. In: *SBG*, Simpósio de Geologia da Amazônia, 8, Manaus, AM, Anais. (CD-ROM).

Gasquet, D., Barbey, P., Adoua, M., Paquette, J.L. 2003. Structure, Sr–Nd isotope geochemistry and zircon U–Pb geochronology of the granitoids of the Dabakala area (Cote d'Ivoire): evidence for a 2.3 Ga crustal growth event in the Palaeoproterozoic of West Africa? *Precamb. Res.* **127**, 329–354.

Gaudette, H.E., Olszewski, W.J. Jr., Santos, J.O.S. dos. 1996. Geochronology of Precambriam rocks from the northern part of Guiana Shield, State of Roraima, Brazil. *Journal of South-American Earth Sciences* **9**, 183-195.

Klein, E.L., Moura, C.A.V. 2001. Age constrains on the granitoids and metavolcanic rocks of the São Luís Craton and Gurupi Belt, Northern Brazil: Implications for lithostratigraphy and geological evolution. *Intern. Geol. Rev.* **43**, 237-253.

Klötzli, U.S. 1999. Th/U zonation in zircon derived from evaporation analysis: a model and its implications. *Chem. Geol.* **158**, 25-333.

Kober, B. 1986. Whole grain evaporation for $^{207}Pb/^{206}Pb$ age investigations on single zircons using a double filament source. *Contrib. Mineral. Petrol.* **93**, 82-490.

Kober, B. 1987. Single-grain evaporation combined with Pb+ emitter bedding for $^{207}Pb/^{206}Pb$ investigations using thermal ion mass spectrometry, and implications for zirconology. *Contrib. Mineral. Petrol*. **96**, 63-71.

Krymsky, R. 2002. Metodologia de análise de U-Pb em mono zircão com traçador ^{235}U-^{205}Pb. Universidade Federal do Pará, Laboratório de Geologia Isotópica. 7p. (in Portuguese).

Lamarão, C.N., Dall'Agnol, R., Lafon, J.-M., Lima, E.F., 2002. Geology, geochemistry and Pb–Pb zircon geochronology of the Paleoproterozoic magmatism of Vila Riozinho, Tapajós gold province, Amazonian craton, Brazil. *Precamb. Res.* 119 (1-4), 189–223.

Lemoine, S., Tempier, P., Bassot, J.-P., Caen-Vachette, M., Vialette, Y., Toure, S., Wenmenga, U., 1990. The Burkinian, an orogenic cycle, precursor of the Eburnean. *Geol. Journal* **25**, 171–188.

Ludwig, K.R. 1999. Using ISOPLOT/Ex, version 2: a geochronological toolkit for Microsoft Excel. Berkeley Geochronological Center Special Publication Ia, 47 pp.

Macambira, M.J.B., Scheller, T. 1994. Estudo comparativo entre métodos geocronológicos aplicados em zircões: o caso do Granodiorito Rio Maria. In: Simpósio de Geologia da Amazônia., 4, Belém, 1994. Bol. Res. Exp., Belém/SBG. p. 343-346 (in Portuguese).

Macambira, M.J.B., Almeida, M.E., Santos, L.S. 2002. Idade de Zircão das Vulcânicas Iricoumé do Sudeste de Roraima: contribuição para a redefinição do Supergrupo Uatumã. In: SBG, Simpósio Sobre Vulcanismo Ambientes Associados, 2, Anais, p.22 (in Portuguese).

Macambira, M.J.B.; Silva, D.C.C.; Vasquez, M.L.; Barros, C.E.M. 2004. Investigação do limite Arqueano-Paleoproterozóico ao norte da Província de Carajás, Amazônia Oriental. In: Congresso Brasileiro de Geologia, 42, Araxá. Anais. CD-ROM.

Maniar, P.D., Piccoli, P.M. 1989. Tectonic discrimination of granitoids. *Geol. Soc. Am. Bull.* **101**, 635-643.

McDonough, M.R., Grover, T.W., McNicoll, V.J., Lindsay, D.D. 1993. Preliminary geology of the southern Taltson magmatic zone, Canadian Shield, northeastern Alberta. *Geol. Surv. Can. Pap.* 93-1C, 221–231.

Milési, J.P., Ledru, P., Feybesse, J.L., Dommanget, A., Marcoux, E. 1992. Early Proterozoic ore deposits and tectonics of the Birimian orogenic belt, West Africa. *Precamb. Res.* **58**, 305–344.

Patiño-Douce, A.E. 1996. Effects of pressure and H_2O content on the composition of primary crustal melts. *Trans. R. Soc. Edinburgh: Earth Sci.* 87, 11–21.

Patiño-Douce, A.E. 1999. What do experiments tell us about the relative contributions of crust and mantle to the origin of granitic magmas? In: Castro, A., Fernandez, C., Vigneressese, J.L. (Eds.), Understanding Granites: Integrating New and Classical Techniques, 168. *Geol. Soc. London*, Special Publication 168, pp. 55–75.

Patiño-Douce, A.E., Beard, J.S. 1996. Effects of P, fO_2 and Mg/Fe ratio on dehydration melting of model metagreywackes. *J. Petrol.* **37**, 999–1024.

Pearce, J.A. 1996. Sources and settings of granitic rocks. *Episodes* **19**, 120-125

Pearce, J.A., Harris, N.B., Tindle, A.G. 1984. Trace element discrimination diagrams for the tectonic interpretation of granitic rocks. *J. Petrol.* 25, 956–983.

Peccerillo, A., Taylor, S.R. 1976. Geochemistry of Eocene calc-alkaline rocks from Kastamonu area, Northern Turkey. *Contrib. Mineral. Petrol.* 58, 63-81.

Pupin, J. P. 1980. Zircon and granite petrology. *Contrib. Min. Petrol.* 73, 207–220.

Reis, N.J., Faria, M.S.G. de, Fraga, L.M.B., Haddad, R.C. 2000. Orosirian Calc-Alkaline Volcanism and the Orocaima Event in the Northern Amazonian Craton, Eastern Roraima State, Brazil. *Rev. Bras. Geoc.* **30** (3), 380-383.

Reis, N.J., Fraga, L.M.B., Faria, M.S.G. de, Almeida, M.E. 2003. Geologia do Estado de Roraima. *Géologie de la France* **2-3-4**, 71-84 (in Portuguese).

Rickwood, P. 1989. Boundary lines within petrologic diagrams which use oxides of major and minor elements. *Lithos* **22**, 247-263.

Roberts, M.P., Clemens, J.D. 1993. The origin of high-K, calc-alkaline, I-type granitoid magmas. *Geology* **21**, 825-828.

Rosa-Costa L.T., Ricci P.S.F., Lafon J.M., Vasquez M.L., Carvalho J.M.A., Klein E.L., Macambira E.M.B. 2003. Geology and geochronology of Archean and Paleoproterozoic domains of the southwestern Amapá and Northwestern Pará, Brazil, southeastern Guiana Shield. *Géologie de la France* **2-3-4**, 101-120.

Santos, J.O.S. dos. 2002. Field Workshop: Manaus (AM)-Pacaraima (RR) Transect. GIS Brasil Program. CPRM, Manaus, Internal Report (in Portuguese).

Santos, J.O.S. dos, Olszewski, W. 1988. Idade dos granulitos tipo Kanuku em Roraima. In: SBG/DNPM, Congresso Latino-Americano de Geologia, 7, Belém, Anais, p. 378-388 (in Portuguese).

Santos, J.O.S. dos, Silva, L.C., Faria, M.S.G. de, Macambira, M.J.B. 1997. Pb-Pb single crystal, evaporation isotopic study on the post-tectonic, sub-alkalic, A-type Moderna granite, Mapuera intrusive suite, State of Roraima, northern Brazil. In: SBG, Symposium of Granites and Associated Mineralizations, 2, Extended Abstract and Program. p. 273-275.

Santos, J.O.S. dos, Hartmann, L.A., Gaudette, H.E., Groves, D.I., McNaughton, N.J., Fletcher, I.R. 2000. A new understanding of the provinces of the Amazon Craton based on integration of field mapping and U-Pb and Sm-Nd geochronology. *Gond. Res.* **3** (4), 453-488.

Santos, J.O.S. dos, Groves, D.I., Hartmann, L.A., McNaughton, N.J., Moura, M.B., 2001. Gold deposits of the Tapajós and Alta Floresta domains, Tapajós–Parima orogenic belt, Amazon Craton, Brazil. *Mineralium Deposita* **36**, 278–299.

Santos, J.O.S dos, Hartmann, L.A., Bossi, J., McNaughton, N.J., Fletcher, I.R. 2003a. Duration of the Trans-Amazon Cycle and its correlation within South America based on U–Pb SHRIMP geochronology of the La Plata Craton, Uruguay. *Intern. Geol. Rev.* **45** (1), 27–48.

Santos, J.O.S. dos, Potter, P.E., Reis, N.J., Hartmann, L.A, Fletcher, I.R., McNaughton, N.J. 2003b. Age, source and Regional Stratigraphy of the Roraima Supergroup and Roraima-like Sequences in Northern South America, based on U-Pb Geochronology. *Geol. Soc. Am. Bull.* **115** (3), 331-348.

Santos, J.O.S. dos, Reis, N.J., Chemale, F., Hartmann, L.A., Pinheiro, S. da S., McNaughton, N.J. 2003c. Paleoproterozoic Evolution of Northwestern Roraima State – Absence of Archean Crust, Based on U-Pb and Sm-Nd Isotopic Evidence. In: of South American Simposyum on Isotope Geology, 4, Pucon, Chile.

Santos, J.O.S. dos, Van Breemen, O.B., Groves, D.I., Hartmann, L. A., Almeida, M.E., McNaughton, N.J., Fletcher, I.R. 2004. Timing and evolution of multiple Paleoproterozoic

magmatic arcs in the Tapajós Domain, Amazon Craton: constraints from SHRIMP and TIMS zircon, baddeleyite and titanite U–Pb geochronology. *Precamb. Res.* vol. 131, 1-2, **10**, 73-109.

Santos, J.O.S. dos, Hartmann, L.A., Faria, M.S.G. de, Riker, S.R.L., Souza, M.M. de, Almeida, M.E., McNaughton, N.J. 2006. A Compartimentação do Cráton Amazonas em Províncias: Avanços ocorridos no período 2000-2006. In: SBG, Simpósio de Geologia da Amazônia, 9, Belém, CD-ROM. (in Portuguese)

Sardinha, A.S. 1999. Petrografia do Granito Igarapé Azul, Sudeste do Estado de Roraima. Trabalho de Conclusão de Curso, UFPA, Belém, 32p. (in Portuguese).

Scheller, T. 1998. *Zircon*. DOS Shareware, UFPA, Belém, Pará-Iso.

Schobbenhaus, C., Hoppe, A., Lork, A., Baumann, A. 1994. Idade U/Pb do Magmatismo Uatumã no Norte do Cráton Amazônico, Escudo das Guianas (Brasil): Primeiros Resultados. In: SBG, Congresso Brasileiro de Geologia, 38, Camboriú, Anais, 2, 395-397 (in Portuguese).

Shand, S.J., 1927. Eruptive Rocks, D. Van Nostrand Company, New York, pp. 360.

Sheppard, S., Occhipinti, S.A., Tyler, I.M. 2004. A 2005–1970 Ma Andean-type batholith in the southern Gascoyne Complex, Western Australia. *Precamb. Res.* **128**, 257–277.

Söderlund, U. 1996. Convetional U-Pb dating *vs.* single-zircon Pb evaporation dating of complex zircons from a pegmatite in the high-grade gneisses of southwestern Sweden. *Lithos* **38**, 93-105.

Stacey, J.S., Kramers, J.D. 1975. Approximation of terrestrial lead isotope evolution by a two-stage model. *Earth Plan. Sci. Letters* **26**, 207-221.

Steiger, R.H., Jager, J. 1977. Convention of the use of decay constants in geo- and cosmochronology. *Earth Plan. Sci. Letters,* **36**:359-362.

Tassinari, C.C.G., Macambira M.J.B. 1999. Geochronological Provinces of the Amazonian Craton. *Episodes* **22** (3), 174-182.

Tassinari, C.C.G., Macambira M.J.B. 2004. A Evolução Tectônica do Cráton Amazônico. In: Mantesso-Neto, Virginio, Bartoreli, Andrea, Carneiro, Celso Dal Ré, Brito-Neves, Benjamin Bley de (eds), Geologia do Continente Sul-Americano - Evolução da Obra de Fernando Flávio Marques de Almeida, São Paulo, Ed. Beca, p. 471-485 (in Portuguese).

Teixeira, W., Tassinari, C.C.G., Cordani, U.G., Kawashita, K. 1989. A review of the Geochronology of the Amazonian Craton tectonic implications. *Precamb. Res.* **42**, 213-227.

Thompson, A.B., 1996. Fertility of crustal rocks during anatexis. Trans. Royal Society of Edinburgh. Earth Sci. 87, 1–10.

Thuy Nguyen, T.B., Satir, M., Siebel, W., Venneman, T., van Long, T. 2004. Geochemical and isotopic constraints on the petrogenesis of granitoids from Dalat zone, southern Vietnam. *Journal of Asian Earth Sciences* 23, 467-482.

Vanderhaeghe, O., Ledru, D., Thiéblemont, D., Egal, E., Cocherie, A., Tegyey, M. and Milési, J.P. (1998) Contrasting mechanisms of crustal growth. Geodynamic evolution of the Paleoproterozoic granite-greenstone belts of French Guiana. *Precamb. Res.* **92**, 165-193.

Van Staal, C.S., Dewey, J.F., MacNiocaill, C., McKerrow, W.S. 1998. The Cambrian-Silurian tectonic evolution of the northern Appalachians and British Caledonides: History of a complex, west and southwest Pacific-type segment of Iapetus. In Blundell, D., and Scott, A.C. (Eds.) Lyell: The past is the key to the present: *Geol. Soc. London, Special Publication* **143**, 199–242.

Vasquez, M.L., Macambira, M.J.B., Galarza, M.A. 2003. Granitóides Transamazônicos da Região Iriri-Xingu – Estado do Pará. In: SBG, Simpósio de Geologia da Amazônia, 8, Manaus, Resumos Expandidos (CD-ROM) (in Portuguese).

Watson, E.B., Harrison, T.M. 1983. Zircon saturation revisited: temperature and composition effects in a variety of crustal magma types. *Earth Plan. Sci. Letters* **64**, 295-304.

Whalen, J.B., Currie, K.L., Chappell, B.W. 1987. A-type granites: geochemical characteristics, discrimination and petrogenesis. *Contrib. Mineral. Petrol.* **95**, 407-419.

Wilson, M., 1991. *Igneous Petrogenesis: a global tectonic approach*. Harper Collins Acad., 2nd ed., London. 466p.

Wolf, M.B., Wyllie, J.P., 1994. Dehydration-melting of amphibolite at 10 kbar: the effects of temperature and time. *Contrib. Mineral. Petrol.* **115**, 369–383.

Wood, D.A., 1979. A variably veined suboceanic upper mantle*/genetic significance for mid-ocean ridge basalts from geochemical evidence. *Geology* **7**, 499-503.

Table 1. Chemical compositions of main plutonic associations of Northern Uatumã-Anauá Domain (NUAD), such as Martins Pereira granitoids, lenses and pods of leucogranites, Serra Dourada Granite and Anauá Complex. The geochemical data were obtained from this study[1] and CPRM (2000a)[2].

	MPG																		**PLL**		**SDG**		**AC**				
	Tonalites				Granodiorites and Monzogranites														Leucogranites		Granites		Enclave	TTG-like			
Sample	MA-009B[1]	MA-176B[1]	MA-007C[1]	MA-246C1[1]	MF-011B[2]	MF-011A[2]	MA-172A[1]	MA-261B[1]	MA-119[1]	MA-061A[1]	PT-010[2]	MF-132A[2]	MA-007A[1]	RL-050[2]	RL-046[2]	MJ-213A[2]	RL-013[2]	PT-006A[2]	MA-246C2[1]	MA-007B[1]	MF-157[2]	MF-151[2]	MF-131B[2]	MF-129C[2]	MF-051B[2]	RL-116[2]	RL-119A[2]
Rock Type	bTnGn	bTn	ebTnGn	mbTnGn	bMgr	bGd	bMgrP	bMtGd	bMtMgr	BMtMgrP	bGd	mbMtMgr	bMtMgrP	bGd	bGd	bMgr	Mgr	bMgr	LcSgr	LcSgr	bMgr	msSgr	aGbN	AMP	MtD	MtTn	MtTn
Major elements (wt %)																											
SiO_2	49.33	55.91	60.04	64.55	62.85	63.52	65.16	66.91	68.03	68.23	68.24	68.72	68.87	70.95	71.14	73.96	74.33	74.60	72.92	73.92	70.30	71.70	41.30	50.20	52.50	59.40	59.80
TiO_2	2.71	1.11	1.15	0.88	0.86	0.80	0.86	0.72	0.40	0.78	0.56	0.39	0.78	0.28	0.28	0.22	0.22	0.19	0.08	0.06	0.41	0.31	2.00	2.60	0.90	0.77	0.61
Al_2O_3	12.44	17.09	16.05	15.96	15.61	15.27	14.71	14.13	15.25	13.38	15.06	15.66	13.55	15.42	15.46	13.70	14.66	13.89	14.42	14.15	14.30	14.50	14.00	12.00	22.00	17.00	18.90
$Fe_2O_3^*$	20.96	8.61	7.01	5.76	7.50	7.96	5.70	5.27	2.96	4.87	5.73	3.78	4.23	2.66	2.68	2.26	1.92	2.20	0.49	0.50	3.87	2.99	19.87	18.74	7.90	6.26	3.27
MnO	0.22	0.15	0.13	0.15	0.16	0.15	0.10	0.10	0.07	0.09	0.14	0.08	0.08	0.10	0.10	0.06	0.06	0.10	0.02	0.01	0.07	0.07	0.29	0.36	0.11	0.13	0.12
MgO	2.42	2.77	2.78	1.84	3.14	2.22	1.48	1.30	1.05	1.36	1.62	1.01	1.03	0.60	0.52	0.44	0.36	0.36	0.15	0.07	0.94	0.66	8.60	4.50	2.60	3.10	2.00
CaO	5.66	6.07	5.54	2.39	3.65	3.74	3.00	2.56	3.12	2.55	2.73	2.22	2.59	2.42	2.22	1.21	1.53	1.51	0.85	1.17	1.50	0.77	10.10	8.70	7.20	5.30	5.50
Na_2O	2.54	3.91	3.47	2.70	2.94	3.24	2.70	2.80	3.05	2.79	2.73	3.44	2.81	3.73	3.84	2.82	3.46	3.12	2.07	2.37	2.90	2.50	1.50	2.20	5.20	3.20	4.40
K_2O	2.10	3.19	2.31	4.17	3.14	2.63	4.46	4.49	4.31	4.50	3.44	4.75	4.89	3.93	3.84	5.44	3.46	4.13	8.31	7.31	5.00	5.30	1.20	0.42	0.87	2.20	1.60
P_2O_5	1.31	1.19	0.39	0.30	0.14	0.26	0.47	0.37	0.20	0.38	0.13	0.22	0.38	0.10	0.11	0.03	0.07	0.05	0.06	0.01	0.10	0.17	0.33	0.22	0.32	0.21	0.32
LOI	0.10	0.90	0.70	1.10	0.95	0.87	1.10	0.90	0.90	0.90	0.58	0.64	0.60	0.42	0.47	0.28	0.21	0.38	0.80	0.60	0.33	0.67	0.65	0.01	0.33	0.45	0.23
TOTAL	99.79	100.90	99.57	99.80	100.95	100.67	99.74	99.55	99.34	99.83	100.95	100.92	99.81	100.60	100.67	100.42	100.29	100.54	100.17	100.17	99.72	99.64	99.84	99.95	99.93	98.02	96.75
Trace element (ppm)																											
Ni	21	16	26	26	-	-	14	12	7	20	-	-	20	-	-	-	-	-	2	3	-	-	-	31	5	14	5
Cr	821	-	753	547	-	-	274	342	68	274	-	-	342	-	-	-	-	-	205	68	-	-	-	138	34	90	48
Rb	184	97	183	228	296	280	307	282	157	233	186	191	187	140	149	216	153	169	193	229	204	414	32	11	53	83	36
Cs	5.72	0.91	8.50	4.98	-	-	14.60	13.68	6.40	8.10	9.10	2.53	6.10	2.52	2.53	2.52	7.13	10.07	1.01	2.01	9.0	9.0	2.5	-	36.0	2.5	2.5
Ba	563	1374	536	749	292	465	865	967	710	853	695	841	1025	952	1372	1217	959	961	1577	1808	684	373	460	75	908	679	757
Sr	456	683	494	284	176	327	200	199	298	180	225	291	217	544	517	290	448	277	314	246	203	103	272	123	1887	601	1221
Ga	31.30	25.86	25.59	26.72	13.18	12.14	22.81	23.42	17.57	20.40	17.19	16.17	18.70	11.09	5.05	5.04	5.09	5.03	12.28	13.46	12	20	16	-	31	19	19
Ta	2.51	0.71	1.82	1.12	2.50	2.50	1.52	1.72	0.81	1.60	2.50	2.50	1.70	2.50	2.50	2.50	2.50	2.50	0.20	0.20	2.50	2.50	5.00	-	12.00	2.50	2.50
Nb	32.50	17.95	26.90	21.74	14.19	16.18	25.14	19.56	9.24	23.20	13.14	12.13	23.40	11.09	12.13	8.06	7.13	10.07	2.21	2.21	9.0	28.0	12.0	17.0	5.0	2.5	10.0
Hf	33.70	19.98	9.20	11.48	20.00	20.00	16.32	10.75	9.24	11.30	20.00	20.00	10.90	20.00	20.00	20.00	20.00	20.00	2.31	2.91	-	-	-	-	-	-	-
Zr	1239	956	320	379	155	284	626	383	286	434	167	169	383	182	200	180	177	158	49	81	166	174	206	126	392	190	177
Y	120	44	48	50	25	22	69	52	28	47	30	19	60	13	6	12	14	4	83	6	47	56	31	33	22	19	19
Th	42	12	26	53	25	25	49	53	47	27	25	25	39	25	25	25	25	25	17	26	-	-	-	-	-	5	9
U	9	2	5	4	5	5	8	8	6	6	5	5	12	5	5	5	5	5	2	4	-	-	-	-	-	5	12
La	94.19	128.19	48.55	86.56	37.24	52.83	111.72	86.47	48.05	63.50	33.18	32.59	82.60	30.29	48.05	107.61	48.12	23.04	24.66	22.50	40.62	40.89	21.57	17.32	28.22	27.64	32.40
Ce	260.21	251.93	114.39	211.72	90.40	113.18	309.61	196.35	101.18	130.20	75.72	73.21	160.20	71.87	95.07	229.33	101.90	50.05	49.11	46.60	98.52	107.80	71.35	44.01	65.33	67.84	72.09
Pr	33.00	24.63	13.96	22.52	-	-	28.64	21.18	9.66	15.79	-	-	18.84	-	-	-	-	-	5.53	5.05	-	-	-	-	-	-	-
Eu	3.28	2.52	1.89	1.68	0.79	0.96	2.19	1.71	1.11	1.52	0.95	0.80	1.95	0.63	0.77	1.87	0.75	0.54	1.46	1.20	1.02	0.70	2.49	1.79	1.60	1.28	1.42
Gd	22.44	9.77	10.59	11.67	4.86	3.78	14.67	10.69	4.48	9.16	3.49	4.16	10.76	2.76	2.65	9.55	4.68	1.80	5.27	1.61	4.60	5.18	7.07	5.27	3.11	3.59	2.75
Tb	3.65	1.29	1.49	1.64	-	-	2.35	1.69	0.65	1.27	-	-	1.58	-	-	-	-	-	1.27	0.24	-	-	-	-	-	-	-
Dy	19.84	7.26	8.31	8.81	4.86	2.52	11.73	8.79	3.60	7.61	3.38	4.14	8.50	2.11	2.05	6.04	3.10	1.10	9.49	1.03	3.89	4.16	5.35	6.89	2.13	3.16	2.25
Ho	3.88	1.41	1.53	1.68	0.97	0.38	2.27	1.63	0.82	1.32	0.67	0.71	1.59	0.38	0.40	1.09	0.61	0.22	2.71	0.18	0.72	0.77	1.07	1.41	0.35	0.59	0.42
Er	11.75	4.15	4.66	4.86	2.63	0.94	6.69	4.39	2.23	4.29	1.77	1.79	4.89	0.85	0.99	2.37	1.58	0.55	10.71	0.65	1.61	1.76	2.90	3.94	0.80	1.37	0.96
Tm	1.86	0.59	0.69	0.72	-	-	0.99	0.64	0.42	0.58	-	-	0.72	-	-	-	-	-	2.04	0.09	-	-	-	-	-	-	-
Yb	12.28	4.08	4.23	4.65	1.83	0.80	6.10	3.70	2.38	4.16	1.07	1.08	4.94	0.63	0.85	1.37	1.72	0.41	14.13	0.62	0.97	1.18	1.82	3.20	0.60	1.04	0.79
Lu	1.85	0.70	0.65	0.79	0.22	0.14	0.99	0.58	0.43	0.58	0.16	0.12	0.71	0.09	0.11	0.18	0.23	0.08	2.48	0.10	0.14	0.16	0.27	0.35	0.09	0.12	0.09
ETR total	633.94	534.38	278.29	455.85	194.69	217.16	623.67	430.78	212.38	312.28	156.55	153.05	380.08	146.18	193.66	483.34	219.13	97.18	153.10	100.36	205.24	222.64	171.79	117.95	137.72	146.96	148.14

Table 1 (Continued)

	MPG																		PLL		SDG		AC				
	Tonalites				Granodiorites and Monzogranites														Leucogranites		Granites		Enclave	TTG-like			
Sample	MA-009B[1]	MA-176B[1]	MA-007C[1]	MA-246C1[1]	MF-011B[2]	MF-011A[2]	MA-172A[1]	MA-261B[1]	MA-119[1]	MA-061A[1]	PT-010[2]	MF-132A[2]	MA-007A[1]	RL-050[2]	RL-046[2]	MJ-213A[2]	RL-013[2]	PT-006A[2]	MA-246C2[1]	MA-007B[1]	MF-157[2]	MF-151[2]	MF-131B[2]	MF-129C[2]	MF-051B[2]	RL-116[2]	RL-119A[2]
Rock Type	bTnGn	bTn	ebTnGn	mbTnGn	bMgr	bGd	bMgrP	bMtGd	bMtMgr	BMtMgrP	bGd	mbMtMgr	bMtMgrP	bGd	bGd	bMgr	Mgr	bMgr	LcSgr	LcSgr	bMgr	msSgr	aGbN	AMP	MtD	MtTn	MtTn
Mg#	18.61	38.91	43.99	38.75	45.34	35.64	33.96	32.82	41.26	35.61	35.85	34.64	32.53	30.71	27.96	27.95	26.82	24.58	37.74	21.71	32.50	30.41	46.16	32.23	43.73	38.77	36.54
Rb/Sr	0.40	0.14	0.37	0.80	1.68	0.86	1.54	1.42	0.53	1.29	0.83	0.66	0.86	0.26	0.29	0.74	0.34	0.61	0.62	0.93	1.00	4.02	0.12	0.09	0.03	0.14	0.03
Rb/Ba	0.33	0.07	0.34	0.30	1.01	0.60	0.36	0.29	0.22	0.27	0.27	0.23	0.18	0.15	0.11	0.18	0.16	0.18	0.12	0.13	3.35	0.90	14.38	6.82	17.13	8.18	21.03
Eu(n)/Eu*	0.39	0.69	0.52	0.38	0.45	0.58	0.4	0.42	0.68	0.44	0.74	0.53	0.5	0.58	0.71	0.41	0.44	0.68	0.93	1.66	0.47	0.29	0.85	0.98	1.07	0.78	1.15
$(La/Sm)_n$	2.16	6.74	2.67	3.70	4.15	5.61	3.89	4.03	5.72	3.53	5.00	4.24	4.09	5.12	7.98	3.93	5.41	5.10	3.58	5.42	3.15	2.83	1.33	1.89	3.19	2.89	4.55
$(Gd/Yb)_n$	1.47	1.93	2.02	2.02	2.14	3.83	1.94	2.33	8.31	1.78	2.62	3.11	1.76	3.51	2.52	5.62	2.20	3.56	0.3	2.08	3.82	3.55	3.13	1.33	4.18	2.79	2.82
$(La/Yb)_n$	5.17	21.2	7.74	12.54	13.69	44.69	12.34	15.76	4.58	10.29	20.87	20.32	11.27	32.17	38.17	52.90	18.85	38.01	1.18	24.36	28.20	23.40	7.99	3.65	31.71	17.94	27.72

Abbreviations: MPG. Martins Pereira Granite; PLL. Pods and lenses of leucogranite; SDG. Serra Dourada Granite; AC. Anauá Complex. a. amphibole; b. biotite; e. epidote; m. muscovite; D. diorite; Gb. gabbro; Gd. granodiorite; Mgr. monzogranite; N. norite; Sgr. syenogranite; Tn. tonalite; Gn. gneiss; Lc. leuco; Mt. meta; P. porphyritic.

Table 2. Petrography summary and geographic coordinates of analyzed samples by the single-zircon Pb-evaporation and U-Pb ID-TIMS methods.

Sample code	Stratigraphic unit	Geog. coord. N	Geog. coord. W	Sample description	U-Pb ID TIMS	MSWD	Sinlge Zi Pb-evap	USD
MA-172A	Martins Pereira Granite	01° 02' 49"	59° 55' 51"	Biotite porphyritic monzogranite with abundant tabular and ovoid alkalifeldspar megacrystals. The matrix is isotropic, coarse grained with local cataclastic texture.	-	-	1975 ± 6 (6)	2.9
MA-61A	Martins Pereira Granite	01° 01' 43"	60° 01' 29"	Biotite mylonitic granodiorite, fine- to medium grained matrix with protomylonitic to mylonitic textures and NE-SW foliation (granolepidoblstic). Titanite and epidote are the main accessory minerals.	-	-	1973 ± 2 (8)	1.4
MA-007A	Martins Pereira Granite	00° 59' 39"	60° 24' 21"	Biotite porphyritic metamonzogranite, medium to coarse grained matrix and accessory minerals such as epidote, magnetite and minor apatite, titanite, allanite and zircon. ENE-WSW foliation locally filled by subconcordant pods and lenses of leucogranite.	-	-	1971 ± 2 (4)	1.1
MF-156	Serra Dourada Granite	01° 18' 03"	54° 00' 20"	Equigranular monzogranite coarse to medium-grained showing aluminous minerals such as biotite, muscovite and locally cordierite (pinitized) and sillimanite. Dynamic recrystallization and planar fabrics are subordinated.	1962 ± 6 (upper)	1.7	1948 ± 11 (2)	2.0
					156 ± 30 (lower)	-	2138 ± 3 (2)	0.1
MA-246C2	Pods and lenses of leucogranites	01° 11' 11"	60° 17' 38"	White graysh, equigranular, leucogranite in lenses and pods with isotropic fabrics, locally showing dynamic recrystalization and cataclasis. The mineral assemblage is composed by alkalifedspar, quartz, plagioclase, biotite, muscovite, epidote, and rare opaque minerals, allanite, titanite, apatite and zircon.	-	-	2354 ± 6 (1)	2.2
					-	-	2134 ± 15 (3)	5.3
					-	-	1997 ± 8 (2)	0.1
					-	-	1959 ± 5 (4)	2.1
					-	-	1909 ± 6 (5)	4.1

Notes: In parenthesis the number of zircon analyses used to calculate the age. Key: U-Pb ID TIMS. Conventional U-Pb results, Pb-evap. Pb-evaporation results.

Table 3. Zircon single-crystal Pb-evaporation isotopic data from Martins Pereira Granite (MA-172A, 061A and 007A), Serra Dourada Granite (MF-156), and lenses of leucogranite (MA-246C2) samples.

sample/zircon number	Temp. (^{0}C)	ratios	^{204}Pb/^{206}Pb	2σ	^{208}Pb/^{206}Pb	2σ	^{207}Pb/^{206}Pb	2σ	(^{207}Pb/^{206}Pb)c	2σ	age	2σ	Th/U
Martins Pereira Granite - Porphyritic (ovoids) biotite monzogranite													
MA-172A/1	1550	8/8	0.000110	14	0.17363	181	0.12186	15	0.12186	15	1984	2	0.49
MA-172A/2	1500	34/34	0.000019	2	0.12364	21	0.12141	26	0.12119	29	1974	4	0.35
MA-172A/3	1450	30/38	0.000402	3	0.12353	30	0.12674	60	0.12094	40	1971	6	0.35
MA-172A/4	1450	20/20	0.000155	16	0.11822	39	0.12336	39	0.12089	20	1970	3	0.33
	1500	34/34	0.000068	5	0.15392	19	0.12260	15	0.12169	12	1981	2	0.44
MA-172A/5	1500	36/36	0.000120	2	0.12514	28	0.12290	14	0.12131	14	1976	2	0.35
	1550	16/16	0.000000	0	0.11807	95	0.12070	19	0.12070	19	1967	3	0.33
MA-172A/6	1500	30/30	0.000116	4	0.17099	111	0.12372	16	0.12216	21	1988	3	0.48
		208 (216)								**mean age**	**1975**	**6**	**usd: 2.9**
Martins Pereira Granite - Mylonitic biotite monzogranite													
MA-061A/02	1550	40/40	0.000251	3	0.10772	23	0.12506	17	0.12117	36	1974	11	0.30
MA-061A/03	1450	8/8	0.000000	1	0.09694	97	0.12028	73	0.12028	73	1961	22	0.27
MA-061A/04	*#1450*	*0/24*	*0.000456*	*44*	*0.10745*	*26*	*0.12590*	*11*	*0.12590*	*11*	*2042*	*2*	*0.30*
	**1500*	*0/6*	*0.000000*	*1*	*0.10825*	*112*	*0.12591*	*72*	*0,12590*	*72*	*2042*	*10*	*0.31*
MA-061A/05	*#1450*	*0/30*	*0.000647*	*15*	*0.22820*	*963*	*0.12116*	*23*	*0.12116*	*23*	*1848*	*21*	*0.65*
MA-061A/06	1450	8/8	0.000052	6	0.16154	101	0.12162	15	0.12162	15	1970	6	0.46
MA-061A/07	1450	32/32	0.000085	3	0.14130	56	0.12211	15	0.12119	9	1974	3	0.40
MA-061A/09	1450	26/26	0.000267	8	0.11054	20	0.12485	17	0.12123	25	1975	7	0.31
	**1500*	*0/8*	*0.000115*	*4*	*0.13236*	*32*	*0.12406*	*26*	*0.12253*	*27*	*1994*	*4*	*0.37*
MA-061A/10	1450	28/28	0.000191	5	0.13814	32	0.12331	26	0.12117	33	1978	5	0.39
MA-061A/11	**1450*	*0/28*	*0.000168*	*6*	*0.11267*	*89*	*0.12126*	*31*	*0.12126*	*31*	*1941*	*9*	*0.32*
MA-061A/12	1450	8/8	0.000361	26	0.21707	24	0.12526	15	0.12526	15	1963	11	0.61
	1500	8/8	0.000075	1	0.19636	48	0.12124	43	0.12124	43	1960	13	0.56
MA-061A/13	1450	36/36	0.000129	1	0.16711	105	0.12264	14	0.12088	15	1969	5	0.47
	1500	40/40	0.000121	2	0.23122	489	0.12259	10	0.12109	12	1973	3	0.67
	1550	30/30	0.000170	13	0.15605	181	0.12312	21	0.12094	13	1970	4	0.44
		264 (360)								**mean age**	**1973**	**2**	**usd: 2.9**
Martins Pereira Granite - Porphyritic biotite metamonzogranite													
MA-007A/01	1540	38/38	0.000071	5	0.14894	18	0.12198	34	0.12107	34	1972	5	0.42
	1550	36/36	0.000082	10	0.15636	141	0.12195	66	0.12074	57	1967	8	0.43
MA-007A/02	**1450*	*0/34*	*0.000102*	*27*	*0.16074*	*447*	*0.12040*	*54*	*0.11883*	*89*	*1939*	*13*	*0.46*
MA-007A/04	1500	36/36	0.000081	4	0.24268	34	0.12158	43	0.12076	30	1968	4	0.69
MA-007A/05	**1450*	*0/28*	*0.000098*	*13*	*0.13021*	*20*	*0.11918*	*27*	*0.11773*	*32*	*1922*	*5*	*0.37*
	1500	32/32	0.000045	7	0.16279	18	0.12159	39	0.12099	48	1971	7	0.46
MA-007A/06	1500	38/38	0.000030	6	0.14321	283	0.12146	22	0.12110	22	1973	3	0.41
		180 (242)								**mean age**	**1971**	**2**	**usd: 0.1**
Serra Dourada Granite - Muscovite-biotite monzogranite with cordierite and sillimanite													
MF156/12	1450	26/34	0.000000	0	0.12405	18	0.13301	23	0.13301	23	2138	3	0.35
MF156/15	1450	36/36	0.000037	2	0.08816	21	0.13360	13	0.13299	11	2138	1	0.25
		62 (70)								**mean age**	**2138**	**3**	**usd: 0.1**
MF156/06	1550	4/8	0.000078	7	0.47918	1656	0.12012	17	0.11907	19	1943	3	0.14
MF156/11	1550	6/6	0.000073	28	0.54277	132	0.12102	24	0.12004	44	1957	7	0.15
		10 (14)								**mean age**	**1948**	**11**	**usd: 2.0**
Pods and lenses - Leucogranite													
MA-246C2/01	1500	24/24	0.000038	2	0.04358	104	0.15111	46	0.15066	52	2354	6	0.12
	**1550*	*0/8*	*0.000044*	*2*	*0.04139*	*58*	*0.14857*	*78*	*0.14800*	*78*	*2323*	*9*	*0.11*
		24 (32)								**mean age (Group I)**	**2354**	**6**	**usd: 2.2**
MA-246C2/10	1500	36/36	0.000233	13	0.06005	30	0.13863	40	0.13533	56	2169	7	0.17
	1550	8/8	0.000246	106	0.05694	47	0.13545	143	0.13254	47	2132	6	0.16
MA-246C2/14	1450	8/8	0.000423	26	0.10097	44	0.13804	694	0.13248	699	2131	92	0.28
MA-246C2/16	1500	38/38	0.000464	12	0.06177	32	0.13868	42	0.13209	31	2126	4	0.17
	1550	24/32	0.000515	28	0.06177	26	0.13899	29	0.13207	60	2126	8	0.17
		114 (122)								**mean age (Group II)**	**2134**	**15**	**usd: 5.3**
MA-246C2/17	1500	20/20	0.000116	102	0.05330	396	0.12487	87	0.12280	93	1998	13	0.15
MA-246C2/21	1500	34/34	0.000119	28	0.03507	14	0.12453	31	0.12273	68	1997	10	0.10
	**1550*	*0/6*	*0.000000*	*0*	*0.03531*	*29*	*0.12630*	*148*	*0.12630*	*148*	*2047*	*21*	*0.10*
		54 (60)								**mean age (Group III)**	**1997**	**8**	**usd: 0.1**
MA-246C2/07	1500	20/20	0.000270	15	0.05075	55	0.12369	53	0.12004	56	1957	8	0.14
MA-246C2/09	1500	22/22	0.000236	9	0.10952	280	0.12285	87	0.11972	57	1952	9	0.31

Table 3 (Continued)

sample/zircon number	Temp. (^{0}C)	ratios	^{204}Pb/^{206}Pb	2σ	^{208}Pb/^{206}Pb	2σ	^{207}Pb/^{206}Pb	2σ	(^{207}Pb/^{206}Pb)c	2σ	age	2σ	Th/U
MA-246C2/13	1450	8/8	0.000099	4	0.04017	313	0.12051	117	0.11918	118	1944	18	0.11
MA-246C2/23	*1450	0/14	0.000551	22	0.04188	34	0.12441	74	0.11713	57	1913	9	0.12
	1500	34/34	0.000408	4	0.11232	105	0.12535	27	0.12009	21	1958	3	0.32
	1550	6/6	0.000392	18	0.10542	57	0.12604	30	0.12080	39	1968	6	0.30
		90 (104)							**mean age (Group IV)**		**1959**	**5**	**usd: 2.1**
MA-246C2/05	1500	36/36	0.000340	28	0.06289	153	0.12044	21	0.11578	29	1892	4	0.18
	1550	36/36	0.000111	45	0.04114	280	0.11986	30	0.11842	49	1933	7	0.12
	1580	8/8	0.000430	20	0.06177	158	0.12252	67	0.11674	72	1907	11	0.18
MA-246C2/06	#1450	0/16	0.001815	73	0.09369	108	0.13676	209	0.10994	108	1799	18	0.27
	1500	38/38	0.000413	39	0.06081	62	0.12311	27	0.11721	45	1914	7	0.17
	1550	36/36	0.000398	17	0.07336	570	0.12357	31	0.11822	33	1930	5	0.21
	1580	32/32	0.000455	8	0.06004	19	0.12307	41	0.11703	50	1912	8	0.17
MA-246C2/08	1450	8/8	0.000579	40	0.04980	93	0.12373	66	0.11594	86	1895	13	0.14
	1480	30/30	0.000147	4	0.05632	54	0.11870	22	0.11668	16	1906	3	0.17
	1500	38/38	0.000164	11	0.06134	160	0.11910	24	0.11694	19	1910	3	0.19
	1550	12/12	0.000179	2	0.05614	162	0.11889	100	0.11623	61	1899	9	0.17
MA-246C2/18	#1450	0/8	0.001175	176	0.07656	957	0.12798	513	0.11209	576	1834	93	0.24
	1500	16/16	0.000368	148	0.05822	30	0.12204	143	0.11686	75	1909	12	0.18
MA-246C2/19	1500	8/8	0.000590	574	0.19248	833	0.12400	688	0.11607	1043	1897	162	0.60
		298 (322)							**mean age (Group V)**		**1909**	**6**	**usd: 4.1**

Notes: Crystal numbers are indicated. The column number of ratios shows the total of isotopic ratios used to the age calculation and, in parenthesis, the total isotopic ratios measured. Evaporation steps in italics were not included in the age calculation of each grain due to: * too much higher or lower values of the ^{207}Pb/^{206}Pb ratio in relation to the average of the zircon, and # ^{204}Pb/^{206}Pb > 0.0004 (and ^{204}Pb/^{206}Pb > 0.0006 for the leucogranite sample). Th/U ratios are calculated by: Th = [(^{208}Pb/^{206}Pb)/(lTh * T)-1] + (^{208}Pb/^{206}Pb); U = [(^{208}Pb/^{206}Pb)/(lU * T)-1] + (^{208}Pb/^{206}Pb); lTh = 4.94750 * 10^{-12} ; lU = 1.55125 * 10^{-11} (in Klotzli, 1999).

Table 4. U-Pb isotopic zircon data (ID-TIMS) from Serra Dourada granitoid (sample MF-156).

Sample		Concentrations				Atomic ratios						Ages (Ma)			
Zircon Number	Weight (mg)	ppm U	ppm Pb	^{206}Pb/^{204}Pb^{c1}	%err	^{207}Pb*/^{235}U^{c2}	%err	^{206}Pb*/^{238}U ^{c2}	%err	^{207}Pb*/^{206}Pb*^{c2}	%err	^{206}Pb*/^{238}U	^{207}Pb*/^{235}U	^{207}Pb*/^{06}Pb*	^{d} (%)
MF-156-1	0.144	35.20	12.33	129.714	1.040	543.181	0.225	0.328881	0.079	0.119786	0.204	1833	1890	1953	94
MF-156-2	0.304	12.16	4.42	818.679	0.459	547.834	0.152	0.331237	0.118	0.119952	0.088	1844	1897	1956	94
MF-156-4	0.213	18.01	5.29	683.428	0.366	436.517	0.324	0.266823	0.223	0.118652	0.234	1525	1706	1936	79
MF-156-5	0.166	34.19	12.01	233.930	0.793	553.956	0.354	0.334560	0.347	0.120088	0.068	1860	1907	1958	95
MF-156-6	0.770	5.51	1.90	816.957	0.700	536.251	0.457	0.326122	0.394	0.119258	0.231	1820	1879	1945	94

Notes: Maximum total blanks for zircon analyses are 10 pg for Pb and 2 pg for U. Stacey and Kramers (1975) values were used.
^{c1} Measure ratios corrected for mass fractionation; ^{c2} Ratios corrected for spike, fractionation, blank and initial common Pb following Stacey and Kramers (1975) model. Erros are at 2 s; ^{d} Concordance in relation to Concordia curve: 100t(^{206}Pb/^{238}U)/t(^{207}Pb/^{206}Pb).

Table 5. Summary of new and previous Pb-Pb and U-Pb (ID-TIMS and SHRIMP) ages yielded by zircon from volcano-plutonic rocks older than 1900 Ma of the Ventuari-Tapajós (or Tapajós-Parima) Province.

Symbol	Reference Number	Rock Type	Lithostratigraphic Unit	Age (Ma)	Reference	Method
Guiana Central Domain						
GC1	1	Hornblende-biotite gneiss with titanite (Miracélia Gneiss)	Rio Urubu "A-type" gneisses	1935 ± 5	Fraga (2002)	B
	2	Hornblende-biotite gneiss with allanite (Igarapé Branco Gneiss)	Rio Urubu "A-type" gneisses	1937 ± 5	Fraga (2002)	B
GC2	3	Quartz jotunite	Serra da Prata C-type	1933 ± 2	Fraga *et al.* (2003)	B
	4	Clinopyroxene porphyrytic charnockite	Serra da Prata C-type	1934 ± 1	Fraga *et al.* (2003)	B
	5	Hypersthene quartz syenite	Serra da Prata C-type	1934 ± 3	Fraga *et al.* (2003)	B
	6	Clinopyroxene porphyrytic charnockite	Serra da Prata C-type	1936 ± 4	Fraga *et al.* (2003)	B
	7	Charnockite hydrothermalized	Serra da Prata C-type	1943 ± 5	Fraga *et al.* (2003)	B
	8	Quartz jotunite gneiss	Serra da Prata C-type	1966 ± 37	Fraga *et al.* (2003)	A
GC3	9	Vilhena Mylonite	Rio Urubu "I-type" gneisses	1932 ± 10	CPRM (2003)	D
	10	Mucajaí Metagranite	Rio Urubu "I-type" gneisses	1938 ± 9	CPRM (2003)	D
	11	Granitic gneiss	Rio Urubu "I-type" gneisses	1943 ± 7	Gaudette et al. (1996)	C
	12	Granitic gneiss	Rio Urubu "I-type" gneisses	1944 ± 10	Santos & Olszewski (1988)	C
	13	Tonalite orthogneiss	Rio Urubu "I-type" gneisses	1951 ± 24	Fraga *et al.* (1997)	A
GC4	14	S-type leucogranite	Taiano S-type	1969 ± 4	CPRM (2003)	D
Surumu Domain						
S1	15	Tabaco Mountain Dacite	Surumu Group	1966 ± 9	Schobbenhaus *et al.* (1994)	C
	16	Tabaco Mountain Dacite	Surumu Group	1977 ± 8	Schobbenhaus *et al.* (1994) mod. by CPRM (2003)	C
	17	Uraricáa Rhyodacite	Surumu Group	1984 ± 7	Santos *et al.* (2003b)	D
	18	Cavalo Mountain Rhyodacite	Surumu Group	2006 ± 4	Costa *et al.* (2001)	B
S2	19	Orocaima Granodiorite	Pedra Pintada Suite	1956 ± 5	CPRM (2003)	D
	20	Pedra Pintada Monzogranite	Pedra Pintada Suite	2005 ± 45	Almeida *et al.* (1997)	A
Parima Domain						
P1	21	Prainha meta-andesite	Parima Group	1948 ± 6	Santos *et al.* (2003c)	D
Uatumã-Anauá Domain						
UA1	22	Leucosyenogranite (ma246c2)	Pods of leucogranite	1909 ± 6	This paper	B
UA2	23	Monzogranite (mf156)	S-type Serra Dourada	1948 ± 11	This paper	B
	24	Monzogranite (mf156)	S-type Serra Dourada	1962 ± 6	This paper	C
	25	Metamonzogranite	Martins Pereira Granite	1938 ± 17	Almeida et al. (1997)	A
UA3	26	Metamonzogranite	Martins Pereira Granite	1960 ± 21	Almeida *et al.* (1997)	A
	27	Metamonzogranite	Martins Pereira Granite	1972 ± 7	CPRM (2003)	C
	28	Metamonzogranite (ma007a)	Martins Pereira Granite	1971 ± 2	This paper	B
	29	Mylonitic monzogranite (ma061a)	Martins Pereira Granite	1973 ± 2	This paper	B
	30	Monzogranite (ma172a)	Martins Pereira Granite	1975 ± 6	This paper	B
UA4	31	Metatonalite	Anauá Complex	2028 ± 9	Faria *et al.* (2002)	D
Tapajós Domain						
T1	32	Granite	Creporizão Suite	1957 ± 6	Santos *et al.* (2000)	C
	33	Creporizão Monzogranite	Creporizão Suite	1963 ± 6	Santos *et al.* (2001)	D
	34	JL Monzogranite	Creporizão Suite	1966 ± 5	Santos *et al.* (2001)	D
	35	Joel Monzogranite	Creporizão Suite	1968 ± 7	Santos *et al.* (2004)	D
	36	km130 Monzogranite	Creporizão Suite	1968 ± 16	CPRM (2000b)	B
	37	Ouro Roxo Metandesite II	Creporizão Suite	1974 ± 6	Santos *et al.* (2001)	D
T2	38	Biotite leucomonzogranite	Old São Jorge Granite	1981 ± 2	Lamarão *et al.* (2002)	B
	39	Hornblende-biotite monzogranite	Old São Jorge Granite	1983 ± 8	Lamarão *et al.* (2002)	B
	40	Granite	Old São Jorge Granite	1984 ± 1	CPRM (2000b)	B
T3	41	Trachyte	Vila Riozinho Volcanics	1998 ± 3	Lamarão *et al.* (2002)	B
	42	Trachyte	Vila Riozinho Volcanics	2000 ± 4	Lamarão *et al.* (2002)	B
T4	43	Rio Claro Monzogranite	-	1997 ± 3	CPRM (2000b)	B
	44	Jamanxim Rapakivi Monzogranite	-	1997 ± 5	Santos *et al.* (1997)	C
T5	45	Cabruá Tonalite	Cuiu-Cuiu Complex	2005 ± 7	Santos *et al.* (2001)	D
	46	Conceição Tonalite	Cuiu-Cuiu Complex	2006 ± 3	Santos *et al.* (1997, 2004)	C
	47	Ouro Roxo Andesite	Cuiu-Cuiu Complex	2012 ± 8	Santos *et al.* (2001)	D
	48	JL Tonalite	Cuiu-Cuiu Complex	2015 ± 9	Santos *et al.* (2001)	D
	49	Amana Monzogranite	Cuiu-Cuiu Complex	2020 ± 12	Santos *et al.* (2001)	D
	50	Cuiú-Cuiú Meta-tonalite	Cuiu-Cuiu Complex	2033 ± 7	Santos *et al.* (2001)	D

Notes: A. Pb-evaporation on single filament; B. Pb-evaporation on double filament; C. U-Pb ID-TIMS; D. U-Pb SHRIMP. Reference Number 1 to 50 and symbols GC1-T5 are the same as in Fig. 12.

Table 6. Summary of ages and possible sources of the inherited zircons from volcano-plutonic and (meta)sedimetary rocks older than 1900 Ma of the Ventuari-Tapajós (or Tapajós-Parima) Province.

Domain	Reference Number	Rock Type	Lithostratigraphic Unit	Age (Ma)	Interpretation	Reference	Method
Guiana Central Domain							
GC4	14	Leucogranite	S-type Taiano Granite	2047 ± 7	Late Transamazonian	CPRM (2003)	D
				2072 ± 3			
	-	Taiano Paragneiss	Cauarane Group	2038 ± 17	Late Transamazonian	CPRM (2003)	D
				2093 ± 62			
				2223 ± 19	Early Transamanzonian	Gaudette *et al.* (1996)	C
GC3	9	Vilhena Mylonite	Rio Urubu "I-type" gneisses	2145 ± 5	Early Transamanzonian	CPRM (2003)	D
Surumu Domain							
	-	Uiramutã Quartz sandstone	Arai Formation (Roraima Supergroup)	1958 ± 19	Pedra Pintada/Surumu	Santos *et al.* (2003b)	D
				2123 ± 14	Early Transamanzonian		
				2718 ± 18	Archean		
S1	17	Uraricáa Rhyodacite	Surumu Group	2027 ± 32	Late Transamazonian	Santos (2002)	D
	16	Surumu Rhyodacite	Surumu Group	2163 ± 10	Early Transamanzonian		
Parima Domain							
P	-	Uatatás Quartzite	Parima Group	1971 ± 9	Pedra Pintada/Surumu	Santos *et al.* (2003c)	D
				2098 ± 16	Late Transamazonian		
				2201 ± 10	Early Transamanzonian		
				2781 ± 6	Archean		
				2872 ± 6	Archean		
Uatumã-Anauá Domain							
UA2	23	S-type monzogranite (mf156)	S-type Serra Dourada Granite	2138 ± 11	Early Transamanzonian	This paper	B
UA1	22	Leucogranite (ma246c2)	Pods and lenses of leucogranite	1959 ± 5	Martins Pereira	This paper	B
				1997 ± 8	Anauá?		
				2128 ± 3	Early Transamanzonian		
				2354 ± 6	Siderian		
Tapajós Domain							
T1	34	JL Monzogranite	Creporizão Suite	2003 ± 5	Cuiu-Cuiu	Santos *et al.* (2001)	D
T3	41	Trachyte	Vila Riozinho Volcanic Rocks	2852 ± 4	Archean	Lamarão *et al.* (2002)	B
				2591 ± 3	Late Archean		
T5	47	Ouro Roxo Andesite	Cuiu-Cuiu Complex	2040 ± 5	Late Transamazonian	Santos *et al.* (2001)	D
	50	Cuiú-Cuiú Meta-tonalite	Cuiu-Cuiu Complex	2056 ± 7	Late Transamazonian		
	48	JL Tonalite	Cuiu-Cuiu Complex	2046 ± 5	Late Transamazonian		
				2100 ± 7	Early Transamanzonian		
				2380 ± 8	Siderian		
				2483 ± 19	Siderian		

Notes: A. Pb-evaporation on single filament; B. Pb-evaporation on double filament; C. U-Pb ID-TIMS; D. U-Pb SHRIMP. Reference Number 1 to 50 and symbols GC1-T5 are the same as in fig. 12.

4.4 - Evidence of the widespread 1.90-1.89 Ga I-type, high-K calc-alkaline magmatism in Southeastern Roraima, Brazil (center-southern region of Guyana Shield) based on geochemistry and zircon geochronology

M.E. Almeida[1,2*], M.J.B. Macambira[2], M.A.G. Toro[2], L.S. dos Santos[2]

[1]CPRM – Geological Survey of Brazil, Av. André Araújo 2160, Aleixo, CEP 69060-001 – Manaus, Amazonas, Brazil

[2] Isotope Geology Laboratory, Center of Geosciences, Federal University of Pará, Rua Augusto Corrêa s/n, Guamá, CEP 66075-110 - Belém, Pará, Brazil

Corresponding author; ph.: +55-92-2126-0357, fax: +55-92-2126-0319, e-mail address: marcelo_almeida@ma.cprm.gov.br

ARTIGO A SER SUBMETIDO

Words: summary (90), abstract (387), body text (11693), table (411) and figure (971) captions.

Total: 15 tables and 6 figures.

ABSTRACT

The southern Uatumã-Anauá Domain (SUAD) in the SE Roraima State (Brazil), center-southern portion of the Guyana Shield, is characterized by a widespread ca. 1.90 Ga calc-alkaline magmatism, represented by the Água Branca (1901 ± 5 Ma), Caroebe (1898 ± 2 Ma and 1891 ± 2 Ma) and Igarapé Azul (1891 ± 6 Ma and 1889 ± 2 Ma) granitoid rocks (Água Branca Suite), Jatapu volcanic rocks (1893 ± 4 Ma) and most rarely by the Santa Maria hypersthene-bearing Tonalite (1890 ± 2 Ma). A-type granitoid rocks are represented by the Murauauú Granite (1871 ± 5 Ma), probably related to 1.88-1.87 Ga Mapuera and Abonari magmatism. Beyond of crystallization ages, some zircons also yielded three main inherited interval ages: a) 1972 ± 3 Ma to 1963 ± 4 Ma (Martins Pereira Granite) and subordinated b) 2142 ± 10 Ma (Transamazonian) and 2359 ± 7 Ma (Siderian). The zircon geochronology results of SUAD show that crystallization age range (and inheritances) is very similar to the calc-alkaline Parauari-(Tropas)-Iriri magmatism (1898-1879 Ma) in the Tapajós domain (Brazil Central Shield). In general sense, these two domains record an important period of Orosirian crustal growth in Amazonian craton, but their origin is still a matter of debate. The Caroebe and Igarapé Azul granites (and coeval Jatapu volcanics) have I-type, high-K calc-alkaline affinities, chondrite-normalized REE patterns moderately fractionated and small negative Eu anomalies. For the hornblende-bearing facies of Caroebe granitoid rocks, the low Al_2O_3 (or $Na_2O + K_2O$) / ($FeO + MgO + TiO_2$) ratios and relatively high Mg# values suggest an origin through dehydration melting of amphibolites to metabasaltic-metatonalitic source rocks. The biotite-bearing facies shows local chemical overlap composition with the Igarapé Azul granitoid rocks. These last exhibit normally restricted rich-SiO_2 range and moderate to very low contents of Al_2O_3 [or (Na_2O+K_2O) or (CaO)]+FeO+MgO+TiO_2, suggesting that additional input of metagreywacke source play a role in their genesis. The magmatic evolution picture is maybe compatible with volcanic arc setting, but the trace element compositions are strongly dependent of protholith composition and, therefore, not necessarily indicative of the tectonic setting of magma formation. The inherited zircons also suggest an older basement involvement during the emplacement these granitoid rocks, however, isotopic data (*e.g.* Nd-Pb) are not available, making difficult a better evaluation of the evolutionary models.

Keywords: Geochemistry, Geochronology, Paleoproterozoic, Granitoids, Guyana Shield

INTRODUCTION

The Guyana Shield corresponds to the northern segment of the Amazonian Craton in South America **(Fig. 1a-b)** and was partially formed during periods of intense granitic magmatism in the Proterozoic times at 2.1 to 1.5 Ga interval. However, scarce geological mapping and only few petrographical, geochemical and geophysical studies are available (*e.g.* CPRM, 1999, 2000a; Delor *et al.*, 2003).

The studied area in this paper is located in the southeastern Roraima (Brazil), center-southern portion of Guyana Shield, and shows expressive ca. 1.90 Ga calc-alkaline magmatism (up to 64000 m^2, **Fig. 2**), but its characteristic and significance are not fully understood (Oliveira *et al.*, 1996; Almeida *et al.*, 2002; CPRM, 2003). Although only recently discovered in this region, magmatism with 1.90-1.80 Ga ages is commonly recorded in the southern segment of Amazonian Craton (Tapajós domain, Brazil Central Shield) and has been interpreted of different ways for explain its tectonic evolution. The first hypothesis argues that this magmatism is generated in subduction-related setting (Santos *et al.*, 2000, 2004) but, in contrast, Almeida *et al.*

(2001), Vasquez *et al.* (2002) and Lamarão *et al.* (2002) pointed out an alternative post-collisional and intracontinental evolution.

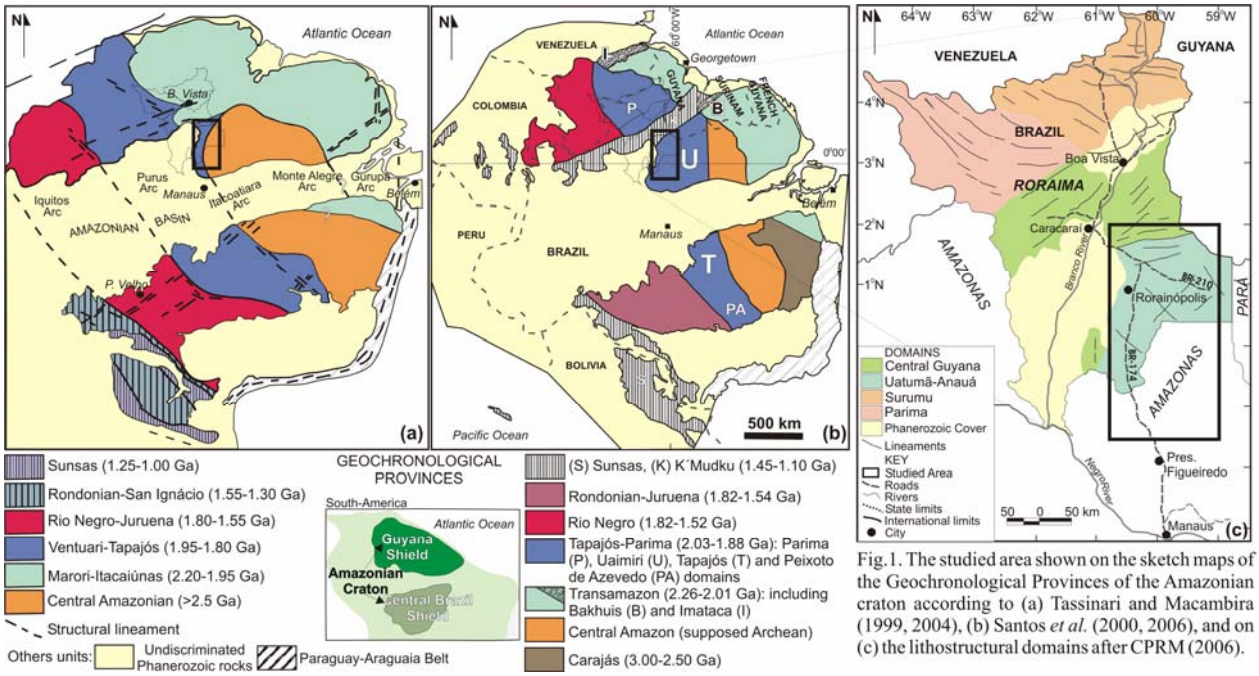

Fig.1. The studied area shown on the sketch maps of the Geochronological Provinces of the Amazonian craton according to (a) Tassinari and Macambira (1999, 2004), (b) Santos *et al.* (2000, 2006), and on (c) the lithostructural domains after CPRM (2006).

Magmatism with 1.90-1.80 Ga is described also in many other parts of the world, such as northern Australia (*e.g.* Page, 1988, Griffin *et al.*, 2000), northern America (Dunphy and Ludden, 1998; St-Onge *et al.*, 1999) and Sweden (*e.g.* Billström and Weihed, 1996; Lahtinen and Huhma, 1996). This time interval is recognized as an important period of episodic crustal growth and supercontinent formation (Condie, 1998).

This paper focuses the discussion on the origin of this widespread calc-alkaline magmatism younger than 1.90 Ga in the center-southern portion of Guyana Shield (**Fig. 1**), using geochemical and zircon geochronology results to further constraint its petrogenesis and tectonostratigraphic history. The possible tectonic setting of these rocks is also discussed.

GEOLOGICAL SETTING

In the last years, regional geological mapping (CPRM 2000a, 2005, Almeida *et al.*, 2002, Almeida and Macambira, in press) and few zircon geochronological data (Almeida *et al.,* 1997, Santos *et al.,* 1997a, Macambira *et al.,* 2002, CPRM, 2003) have showed that Paleoproterozoic granitoids and volcanic rocks (1.97-1.81 Ga) are widespread in southeastern Roraima, intruding subordinated basement rocks with maximum ages around 2.03 Ga (Faria *et al.,* 2002).

According to recent evolutionary models proposed for the Amazonian craton, the study area can be divided into different provinces. According to Tassinari and Macambira (1999, 2004), the study area is largely enclosed by Ventuari-Tapajós and Central Amazonian provinces, with a subordinate northeastern section falling within the Maroni-Itacaiúnas province. Santos *et al.* (2000, 2006) argue that all provinces were collectively affected by the K´Mudku Shear Belt in this same region **(Fig. 1 a-b)**. These models point out that Paleoproterozoic orogenic belts or magmatic arcs (*e.g.* Ventuari-Tapajós or Tapajós-Parima and Maroni-Itacaiúnas or Transamazon provinces) accreted to the Archean craton with time and/or represent a set of rocks produced from melting of Archean crust (**Fig**. **1a-b**; Cordani *et al.,* 1979, Teixeira *et al.,* 1989, Tassinari and Macambira, 1999, 2004; Santos *et al.,* 2000, 2004, 2006).

The Ventuari-Tapajós (or Tapajós-Parima) Province is a Paleoproterozoic orogenic belt showing north-northwest trends and includes geological units which range from ~2.10 to 1.87 Ga in age (Santos *et al.,* 2000, 2006; Tassinari and Macambira 1999, 2004). The Central Amazonian Province **(Fig. 1a-b)** has granitoids and volcanic rocks (1.88 to 1.70 Ga) with no regional metamorphism and compressional folding (Santos *et al.,* 2000, Tassinari and Macambira 1999), and its basement rarely crops out. The age for this basement has been estimated by some Nd-model ages at around 2.3-2.5 Ga (Tassinari and Macambira, 1999, 2004). According to these authors, the recorded Archean rocks in the Amazonian craton are only exposed in Imataca (Venezuela), Carajás and southern Amapá-northwestern Pará (Brazil) regions.

The Maroni-Itacaiúnas (or Transamazon) Province is also characterized by an orogenic belt with Rhyacian ages (2.25 to 2.00 Ga, **Fig. 1a-b**) and is correlated to Birimian belt in West Africa (Tassinari and Macambira, 1999, 2004; Santos *et al.,* 2000; Delor *et al.,* 2003). The K´Mudku Shear Belt is represented by wide mylonitic zones with ca. 1.20 Ga (low grade) and cross-cut at least three provinces (Rio Negro, Tapajós-Parima and Transamazon, Santos *et al.,* 2000).

Reis *et al.* (2003) and CPRM (2006) has been subdivided the center-southern Guyana Shield into four major lithostructural domains: Surumu, Parima, Central Guyana and Uatumã-Anauá **(Fig. 1c)**. The southeastern Roraima is composed of the Central Guyana and Uatumã-Anauá domains only.

The Central Guyana Domain (CGD) primarily consists of granulites, orthogneiss, mylonites and metagranitoids (Rio Urubu Metamorphic Suite) associated with low to high metamorphic

grade metavolcanosedimentary covers (Cauarane Group) and S-type granite (Curuxuim Granite). The lineaments are strongly NE-SW trends **(Figs. 1c and 2)**.

The Uatumã-Anauá Domain (UAD) is characterized by E-W to NE-SW lineaments and the northern part of the domain (NUAD) shows an older metamorphic basement inlier **(Figs. 1 and 2)** formed in a presumed island arc environment (Faria *et al.*, 2002). This basement is composed by TTG-like metaigneous rocks (Anauá Complex), enclosing meta-mafic to meta-ultramafic xenoliths, and is associated with some inliers of metavolcano-sedimentary rocks (Uai-Uai Group) and intruded by S-type (Serra Dourada Granite) and high-K, I-type calc-alkaline (Martins Pereira) granitic magmatism of around 1.98-1.96 Ga (Almeida *et al.* 2002). In the southern area of Uatumã-Anauá domain (SUAD), intrusive younger granites (with no regional deformation and metamorphism) are most common. The most prominent magmatism is related to the calc-alkaline Caroebe and Igarapé Azul granitoid rocks (Água Branca Suite) with coeval Jatapu volcanic rocks. Locally igneous charnockitic (Igarapé Tamandaré) and enderbitic (Santa Maria) plutons were also recorded. Several A-type granitic bodies are widespread in the Uatumã-Anauá Domain **(Fig. 2)** represented by Moderna-Água Boa (1.81 Ga) and Mapuera-Abonari (1.87 Ga) granites.

Some geochemical and geochronological data for the magmatism from SUAD will be showed below, including a petrogenesis and evolution models discussion. The data was obtained from Caroebe, Água Branca and Igarapé Azul granites, including coeval Jatapu volcanics, and Murauauú (Mapuera type) and Santa Maria hypersthene granites.

ANALYTICAL PROCEDURES

Whole-rock Geochemistry Analyses

Whole-rock chemical analyses of 18 samples (milled under 200 mesh) were done at the Acme Analytical Laboratories Ltd, Vancouver, British Columbia, Canada. The analytical package include inductively coupled plasma - atomic emission spectrometer (ICP-AES) analyses after LiO_2 fusion for all major oxides (SiO_2, TiO_2, Al_2O_3, MnO, MgO, CaO, K_2O, Na_2O, P_2O_5) and LOI. Total iron concentration is expressed as Fe_2O_3. The trace elements were analyzed by inductively coupled plasma-mass spectrometer (ICP-MS), with rare-earth and incompatible elements determined from a $LiBO_2$ fusion and precious and base metals determined from an aqua regia digestion. Additional 16 analyses were compiled (and partially reinterpreted) from CPRM (2000a). These last whole-rock chemical analyses were done at the Geosol Laboratories S.A., Belo Horizonte, Minas Gerais, Brazil.

Zircon Geochronology Analyses

Samples of two to ten kg were crushed, powered and milled under 60 to 80 mesh, washed and dried out. After that, heavy mineral fractions were obtained by water mechanical concentration. These samples were then processed by means of a hand-magnet and a Frantz Isodynamic Separator followed by mineral separation in dense liquid. The lowest magnetic zircon concentrates (from five magnetic fractions) were then selected for hand-picking and photomicrographed via a convensional optical microscope. As much as possible, only alteration-free zircon grains with no metamictization features, inclusions and fractures were selected for analysis (see zircon descriptions below).

The zircon single-grain dating by U-Pb isotopic dilution in thermal ionization mass spectrometer (1 sample) - ID-TIMS - and step-wise Pb-evaporation (9 samples) analyses were performed at the Finnigan MAT262 multicollector mass spectrometer (Laboratory of Isotope Geology - Pará-Iso - Federal University of Pará, Brazil) in dynamic mode using the ion counting detector at the. The used U decay constants are those recommended by IUGS (Steiger and Jäger, 1977) and errors are given at the 95% confidence level. In the Pb-evaporation method on single zircon (Kober, 1986; 1987), the selected grains were tied in Re-filaments and analysed into mass spectrometer for isotope analyses.

The ages were calculated with 2σ error and initial common Pb corrected according to the Stacey and Kramers (1975) model for those blocks of isotopic ratios (maximum of 18 ratios in 10 mass scans) in which the $^{204}Pb/^{206}Pb$ ratios were lower than 0.0004. Those blocks which presented values higher than 0.0004 were discarded. The quality statistics is express for USD or Unified Standard Deviation (square root of the MSWD - Mean Standard Weigth Deviation). The data were processed using the DOS-based *Zircon* shareware (Scheller, 1998). The Pb-evaporation technique, including the complete procedures, is available in Klein and Moura (2001).

The U-Pb ID-TIMS procedures developed at the Pará-Iso are described by Krymsky (2002). All zircon fractions selected for analysis were air abraded in 1.2-1.8 psi pressure for 30-40 minutes. These grains were abraded together with pyrite crystals (20 mg and 0.1-0.5 mm diameter). After the abrasion, the zircon crystals were washed in HNO_3 and HCl (100^0C, 30 minutes) and after rinsed with H_2O-Millipore (3 times). The crystals were washed with metanol, weighted, spiked with ^{235}U-^{205}Pb tracer solution (10 μL) and dissolved with a mixture of HF and HCl which were carried out in Teflon bombs at 245^o C.

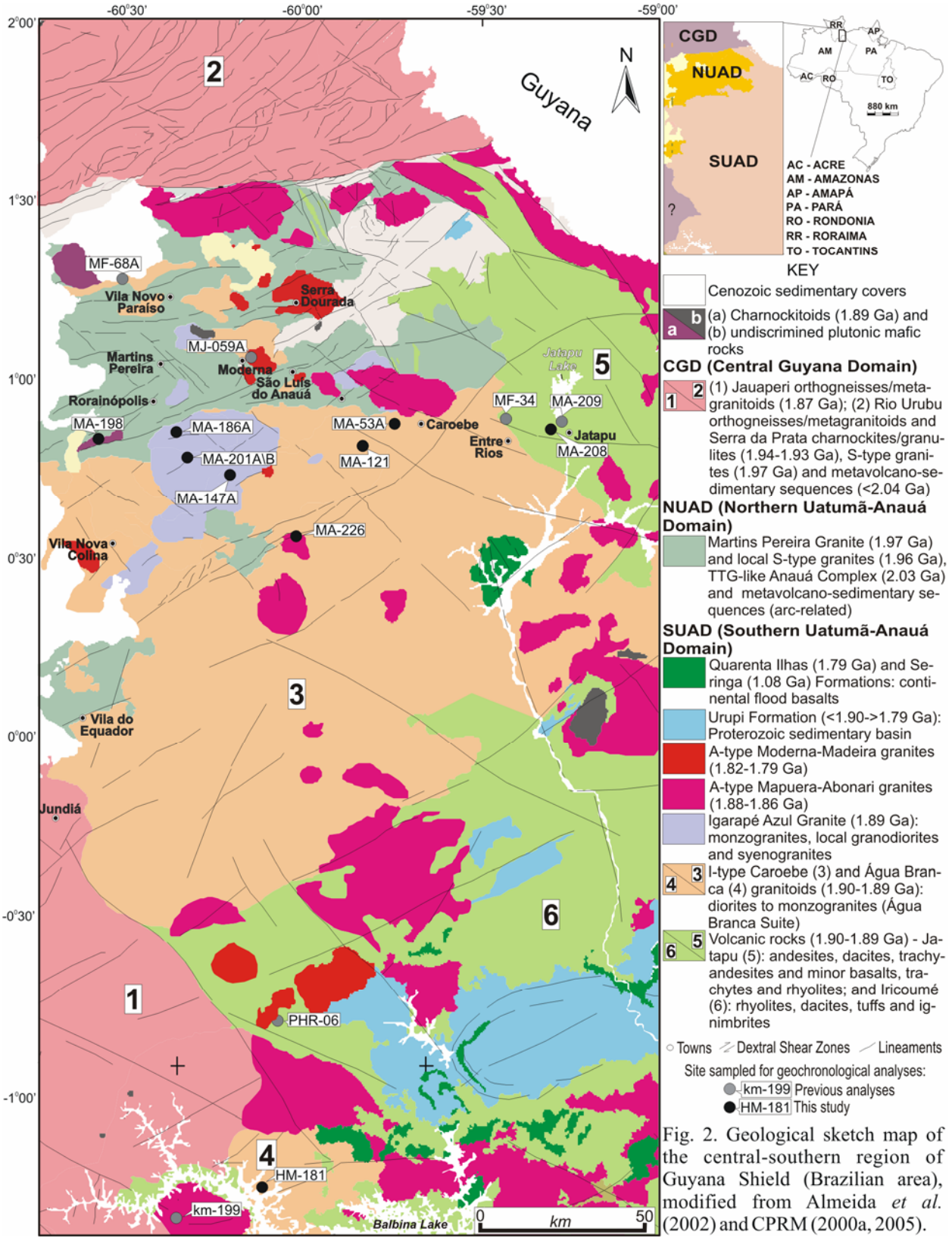

Fig. 2. Geological sketch map of the central-southern region of Guyana Shield (Brazilian area), modified from Almeida *et al.* (2002) and CPRM (2000a, 2005).

U and Pb were isolated from zircon solution with anion-exchange resin (Dowex® 1x8 200-400 mesh Cl-form) in HCl medium in 50-70 µl columns and collected in different beakers. U and

Pb from zircon were loaded onto the same outgassed Re-filament with SiO_2-gel and 1N H_3PO_4 and analyzed at 1400-1600^o C. For zircon analyses, blanks are <30 pg Pb and <1 pg U. The obtained data are processed in ISOPLOT/Excel program version 2 (Ludwig, 1999). The $^{208}Pb/^{206}Pb$ ratios were corrected for common Pb using also the Stacey and Kramers (1975) model.

WHOLE-ROCK GEOCHEMICAL RESULTS

Major oxides and trace elements

Representative chemical analyses of samples of Caroebe-Igarapé Azul granites (this study, CPRM, 2000a) and Jatapu volcanics (CPRM, 2000a) are listed in **Table 1**. The bulk-rock concentrations of Caroebe and Igarapé Azul granitoid rocks are characterized by the higher and smaller range of SiO_2% contents, respectively. The Jaburuzinho facies (hornblende-bearing) of Caroebe granite shows the lowest contents of SiO_2 (49.50%-61.85%), whereas the Alto Alegre facies (biotite-bearing) shows 65.95%-69.14% of SiO_2 and there is a compositional gap of 4% of SiO_2 between them, while the highest SiO_2 contents are observed in the Igarapé Azul granites (67.87%-72.25%). In Harker diagrams, the regression lines show the same mean trend for these granitoid rocks, which exhibit TiO_2, Al_2O_3, F_2O_3, MgO, CaO and P_2O_5 abundances decrease **(Fig. 3a-f)** and K_2O increase **(Fig 4a)** with SiO_2 increasing. In the Na_2O *vs.* SiO_2 diagram, the samples remain nearly constant but, in general, the data are scattered **(Fig. 3g)**.

All samples are of subalkaline affinity **(Fig. 4b)** and belong to the calc-alkaline series (**Fig. 4c**; *e.g.* Irvine and Baragar, 1971), showing high-K affiliation (*e.g.* Peccerillo and Taylor, 1976), locally plotting in the shoshonitic field, near to the high-K boundary **(Fig. 4a)**. These rocks also show similar patterns to the normal calc-alkaline andesites (*e.g.* Brown *et al.*, 1984) of continental margin in the log[CaO/(Na_2O+K_2O)] *vs.* SiO_2 plot **(Fig. 4d)**.

The Jaburuzinho facies of Caroebe Granite confirm its I-type character on the Na_2O *vs.* K_2O diagram **(Fig. 5b)**, plotting in the field outlined for typical I-type granite of the Lachlan Fold Belt (White and Chappell, 1983), however, several samples plot out of the fields. Compared to typical S-types (White and Chappell, 1983), the Alto Alegre facies shows also higher Na_2O in the same K_2O contents (Na_2O/K_2O<1), and the Igarapé Azul Granite presents types more enriched in K_2O **(Fig. 5b)**. The Na_2O *vs.* K_2O diagram suggests a transitional increasing of K_2O contents (with Na_2O nearly constant) from Caroebe Granite (Jaburuzinho facies) to Igarapé Azul types.

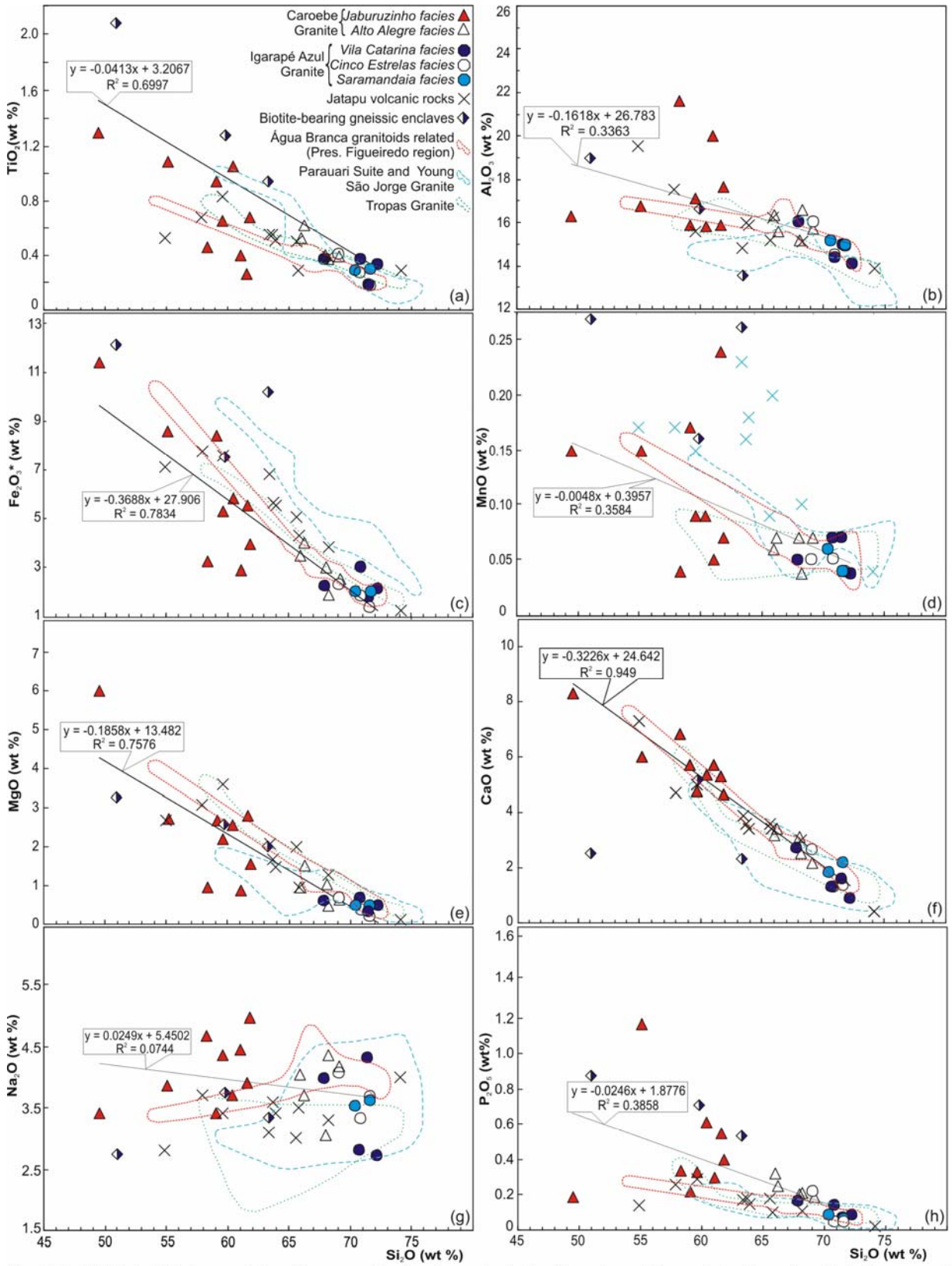

Fig. 3. (a-h) Selected Harker variation diagrams of major elements for the Caroebe and Igarapé Azul granites, including coeval Jatapu volcanics. For references see table 1. For the linear regression are used only the Caroebe and Igarapé Azul granite samples. Compositional fields of Tropas (Santos *et al.* 2004), Parauari (Vasquez *et al.*, 2002; Santos *et al.*, 2004), Young São Jorge (Lamarão *et al.*, 2002) granites from Tapajós Domain and Água Branca related granitoids (Valério, 2006) are also plotted for comparison.

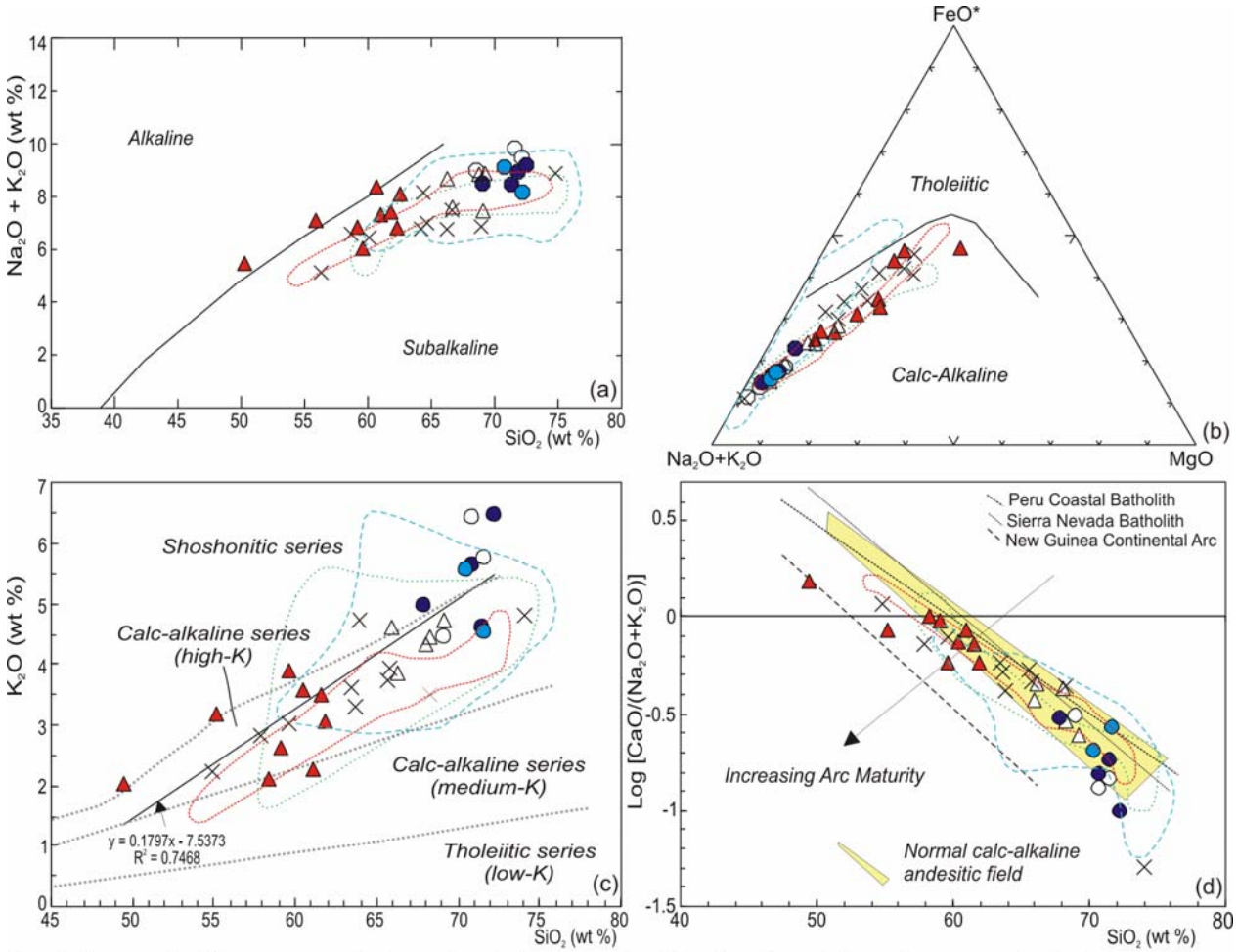

Fig. 4. Geochemical diagrams showing the calc-alkaline character of the Caroebe and Igarapé Azul granites (and coeval Jatapu volcanic rocks): (a) Na_2O+K_2O *vs.* SiO_2 (for the linear regression are used only the Caroebe and Igarapé Azul granite samples) and (b) AFM diagrams (Irvine and Baragar, 1971); (c) K_2O *vs.* SiO_2 plot displaying the shoshonite, high-K, medium-K and low-K fields (from Peccerilo and Taylor, 1976 mod. by Rickwood, 1989); and (d) log[CaO/(Na_2O+K_2O)] *vs.* SiO_2 (from Brown *et al.,* 1984). Compositional fields of Tropas, Parauari, Young São Jorge (Tapajós Domain) and and Água Branca related granitoids are also plotted for comparison. References and symbols as in Fig. 3.

There is also a compositional overlap between the Alto Alegre facies and Igarapé Azul granite in this diagram, as well as in other diagrams based on major elements (see **Fig. 3a-h, 4a-d and 5a**). The geochemical affinity among coeval volcanic rocks of Jatapu region and Caroebe granites **(Fig. 3a-h, 4a-d and 5a-b)**, except for the lowest Na_2O and highest MnO contents in the ast, has been also discussed by Reis *et al.* (2000). The calc-alkaline granitoid rocks from Tapajós Domain (*e.g.* Tropas granite), demonstrate also similarities with Caroebe granites, mainly the Fe_2O_3t, MgO and CaO contents **(Figs 3 c, e and f)**, but Na_2O is normally lower **(Fig. 3g)** in the same SiO_2 content. On the other hand, the Parauari Granite shows higher SiO_2 (59%-76%) and Fe_2O_3t **(Fig. 3c)**, and lower Al_2O_3 **(Fig. 3b)** and MgO **(Fig. 3e and 4c)**.

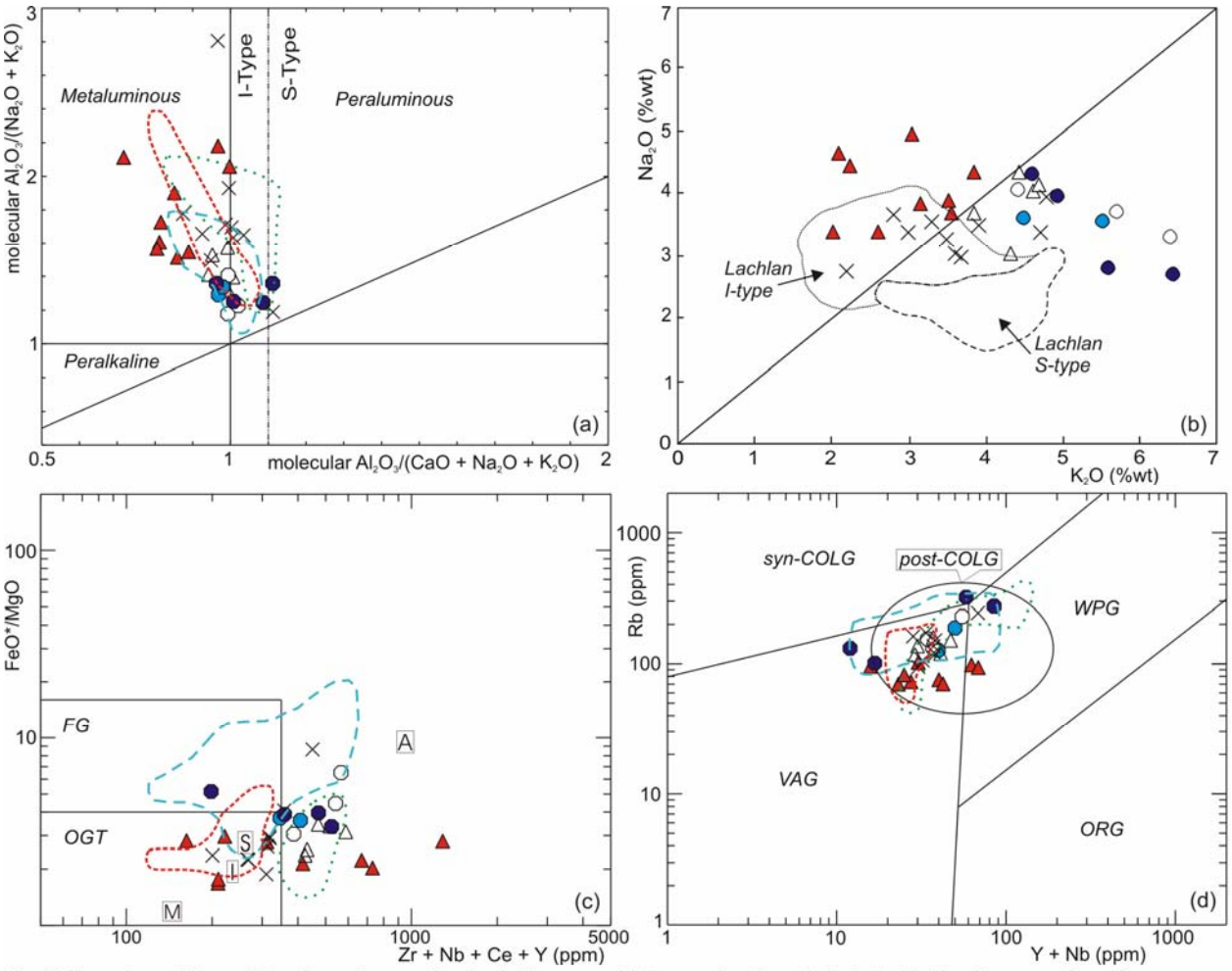

Fig. 5. Caroebe and Igarapé Azul granite samples (including coeval Jatapu volcanic rocks) plotted in the diagrams (for references see table 1): (a) Molecular $Al_2O_3/(Na_2O+K_2O)$ *vs.* molecular $Al_2O_3/(CaO+Na_2O+K_2O)$ (Maniar and Piccoli, 1989; mod. Shand, 1927) and (b) Na_2O *vs.* K_2O plots showing S-type and I-type granites compositional data from Lachlan Folded Belt (LFB); (c) Rb *vs.* (Y+Nb) and (d) $(K_2O+Na_2O)/CaO$ *vs.* (Zr+Nb+Ce+Y). Fields representing Tropas, Parauari-Young São Jorge (Tapajós Domain) and Água Branca related granitoids are plotted for comparison. In (c), VAG (Volcanic Arc Granites), ORG (Ocean Ridge Granites), syn-COLG (Syn-collisional Granites) and WPG (Within-Plate Granites) fields are from Pearce *et al.* (1984) and post-COLG (post-collisional granites) from Pearce (1996); In (d), OGT (Orogenic granite types: unfractionated I- and S-type granites) and FG (Fractionated felsic I- and S-type granites) fields are taken from Whalen *et al.* (1987). Compositional average of A-, M-, I-, S- and I-type are also represented. References and symbols as in Fig. 3.

In the FeO*/MgO *vs.* Zr+Nb+Ce+Y diagram (**Fig. 5c**, Whalen *et al.*, 1987), the Caroebe Granite samples plot partially on the OGT field, showing types with higher Zr+Nb+Ce+Y (*e.g.* MA-178B, diorite). The Igarapé Azul granites plot out of OGT and FG fields (except the MA-88, muscovite-bearing syenogranite), exhibiting subtle higher FeO*/MgO ratios and enrichment in Zr+Nb+Ce+Y. On the Rb *vs.* Y+Nb diagram (**Fig. 5d**, Pearce *et al.*, 1984) almost all Caroebe, Igarapé Azul and Jatapu samples plot in the VAG field, suggesting chemical affinity with volcanic arc magmatism. However, local magmatic differentiation and hydrothermal processes (Pearce *et al.*, 1984) could explain the crossing of VAG and syn-COLG (MF-10B) and WPG (MA-88) boundaries by some samples of Igarapé Azul Granite. The same is not true for the

samples of Caroebe Granite. This one cross over the VAG and WPG boundary, because the more Y-rich samples are not the most differentiated types (*e.g.* MA-178B, diorite). The probable explanation in this case could be related to the source composition and/or anomalous enrichment in accessory minerals (*e.g.* allanite).

In this sense, the trace elements in the Caroebe and Igarapé Azul granites are considerably more scattered than major elements, particularly for Ba, Sr, Zr and Nb Harker diagrams **(Fig. 6b-e)**. However, Rb plots a positive correlation with increasing SiO_2 contents **(Fig. 6a)**. Contrasting with this scattered pattern, the Jatapu volcanic rocks exhibit a linear trend in almost all these diagrams. The volcanic rocks show Sr in negative linear trend and Nb, Zr, Ba and Rb in positive correlation with increasing SiO_2 contents **(Fig. 6a-e)**. The Mg# deeply decreases with the SiO_2 increasing **(Fig. 6f)**, with the Jaburuzinho facies exhibiting highest values (37.5-51.5) comparatively to the Alto Alegre facies (34.1-43.0) and Igarapé Azul (21.5-37.8) granitoid rocks.

The primitive mantle-normalized multi-element diagrams or "spider diagrams" of the Caroebe and Igarapé Azul granites show discrete differences **(Fig. 7a-d)**. The Jaburuzinho facies exhibits wider range contents and moderate enrichment in some large-ion lithophile elements (LILE), such as Ba (50-400x), Th (50-150x) and U (25-120x), contrasting with low Rb (70-100x), K (60-100x) **(Fig. 7a)** and high field strength elements (HFSE: *e.g.* Nb, Ta and Ti) contents. The Alto Alegre facies shows "spider diagrams" with narrow range **(Fig. 7b)** and generally exhibits similar patterns of Jaburuzinho facies, except for a more enrichment in Rb (100-200x), K (110-120x), and for the moderately negative anomaly of P (7-15x) and Ti (0.4-3x).

The Saramadaia and Cinco Estelas facies of Igarapé Azul Granite **(Fig. 7c)** show stronger Sr (3-30x), P (3-10x), Ti (1.5-2x) negative anomalies in the "spider diagrams". In contrast, they are more enriched in Rb (150-300x) and Th (150-550x) and exhibit less pronounced Nb (20-35x) and Ta (20-45x) negative anomalies. The Vila Catarina facies **(Fig. 7d)** presents the most heterogeneous "spider diagrams", ranging from low to high Nb, La, P, Sm and Tb contents.

Similarly to the Caroebe granites, the Jatapu volcanic rocks present "spider diagrams" **(Fig. 7e)** with low to moderate enrichment in Rb, Ba, K, Zr and Y and less pronounced Nb, Sr and P negative anomalies, except for the MF-144B sample. The "spider diagrams" of Caroebe types and Jatapu volcanics **(Fig. 7a-b, e)** are also chemical compatible with the granitoid rocks from primitive to normal continental arcs (Brown *et al.,* 1984), showing locally HFSE enrichment (*e.g.* Nd, P, Hf, Zr and Sm). The more heterogeneous patterns make the Igarapé Azul "spider

diagrams" have a transitional behavior from normal (*e.g.* Rb, K, Th, U, Nb and Ta) to mature (*e.g.* Ba, Sr, P, Hf) arc granitoid rocks **(Fig. 7c-d)**.

Contemporaneous calc-alkaline granitoid rocks from other areas of SUAD (*e.g.* northeastern Amazonas, Presidente Figueiredo region) and from Tapajós Domain (Tropas and Parauari granitoid rocks) has showed chemical similarities mainly with the Caroebe Granite. The granitoid rocks of Presidente Figueiredo (Valério, 2006) and Tropas (Santos *et al.,* 2004) regions yielded Ti, Al, Fe, Mg, Ca (**Fig. 3a-e**) and "spider diagrams" (**Fig. 7f**) similar to the Caroebe Granite, including locally lower values of P (**Fig. 3h**) and Na_2O+K_2O (**Fig. 4a**).

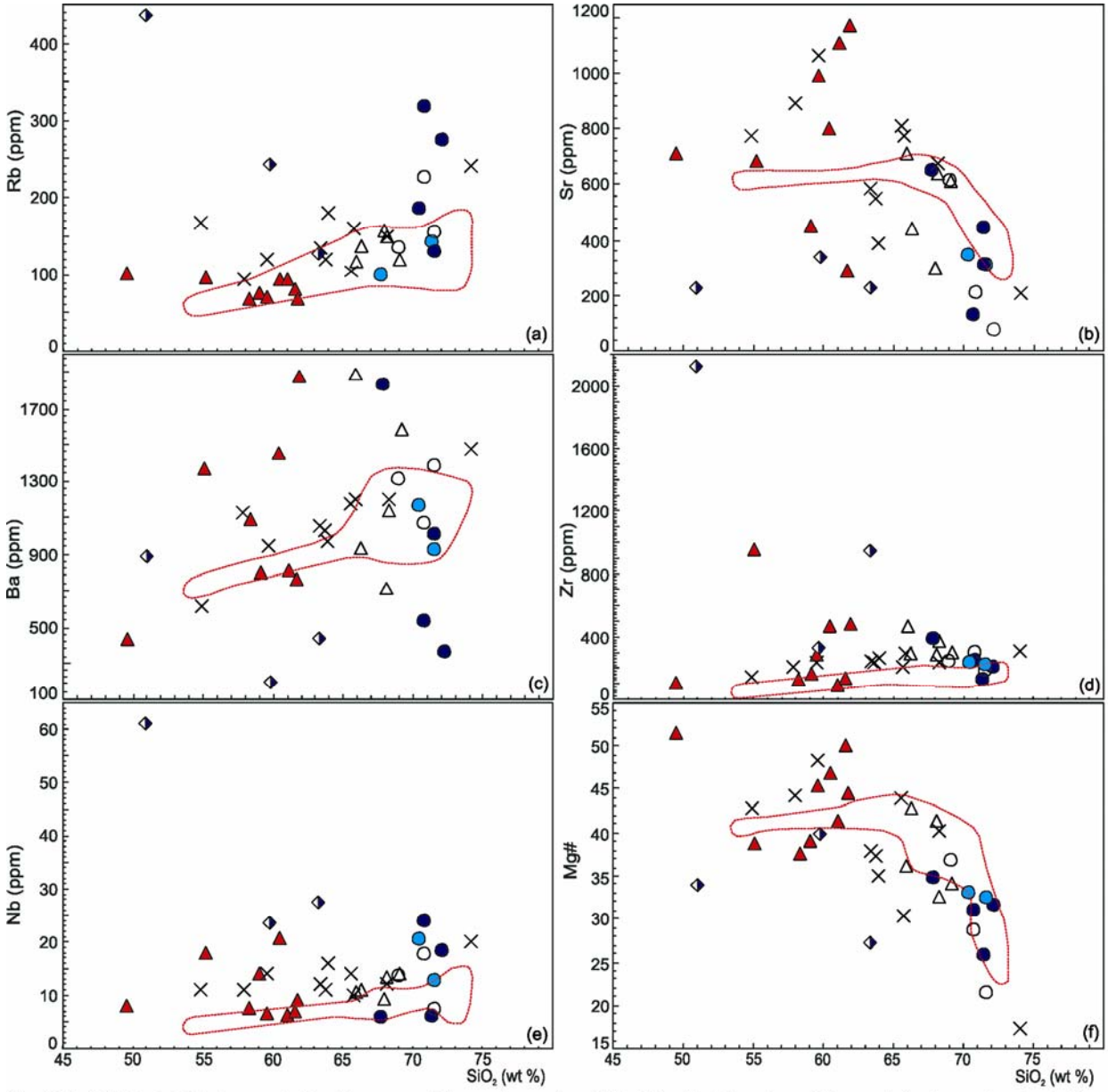

Fig. 6. (a-f) Selected Harker variation diagrams of trace elements and Mg# for the Caroebe and Igarapé Azul granites, including coeval Jatapu volcanics. Obs: Mg# = [100 x molar MgO/(MgO+0.9FeO_{tot}). Symbols as in Fig. 3.

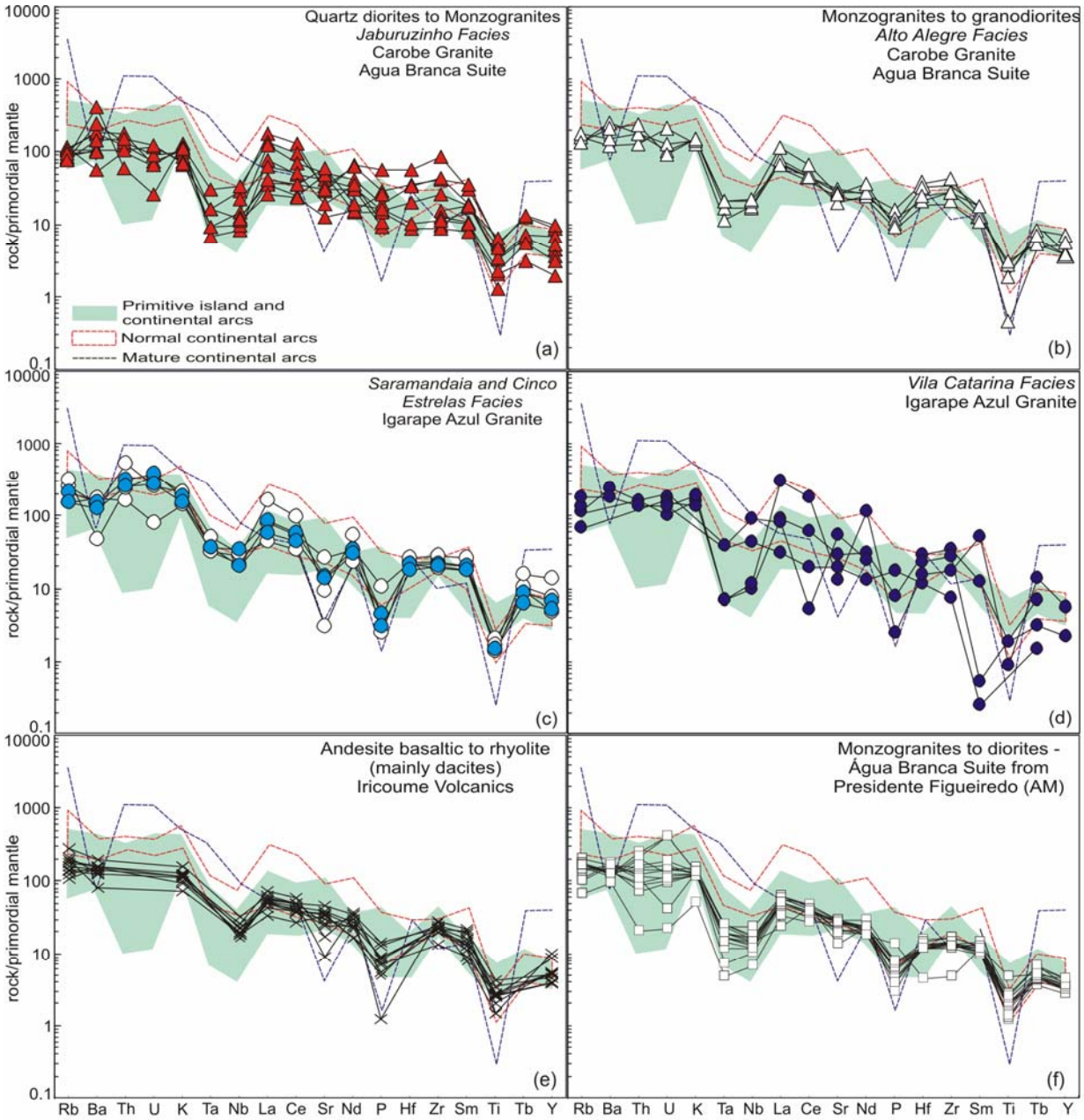

Fig. 7. Primitive mantle-normalized multi-element diagrams (Wood *et al.*, 1979) from *Caroebe Granite*: (a) Jaburuzinho and (b) Alto Alegre facies, *Igarapé Azul Granite*: (c) Saramandaia and Cinco Estrelas facies; (d) Vila Catarina facies; and (e) coeval Jatapu volcanic rocks. References and symbols as in Fig. 3.

Rare-earth element (REE) geochemistry

All analyzed samples show fractionation between the light (LREE) and heavy (HREE) rare-earth elements (REE) on the chondrite-normalized diagrams (**Fig. 8**). Similarly to the "spider diagrams", the Jaburuzinho facies of Caroebe Granite is characterized by wide range of REE contents, reflecting its broad compositional spectrum, but the REE fractionation is the same of Alto Alegre facies (**Fig. 8a-b**). Both facies demonstrate strong to moderate REE fractionation

[(La/Yb)n = 11.26-29.32], nearly flattened HREE pattern [(Gd/Yb)n = 1.52-2.26] and low to moderate Eu negative anomalies (Eu/Eu* = 0.60-0.78). Sometimes, the middle REE (MREE) are depleted relative to HREE, inducing a mildly concave-upwards in HREE patterns (**Fig. 8a-b**), mainly in the Jaburuzinho facies (MA-103, MF-068A and MJ-061B samples). Furthermore, the Jaburuzinho facies also exhibit REE patterns (**Fig. 8a**) with no anomalies (MA-053C) to positive Eu anomalies (MA-053B).

All petrographic facies of Igarapé Azul also exhibit moderate to weak negative Eu anomalies (Eu/Eu* = 0.48-0.86), locally strong (Eu/Eu* = 0.36-0.39). Mildly concave-upward HREE pattern [(Gd/Yb)n = 1.27-1.81] and moderate fractionated patterns [(La/Yb)n = 8.69-21.94] are observed in the Saramandaia and Cinco Estrelas facies (**Fig. 8c**). Only one sample (MA-88) exhibit flatted HREE and wing-bird pattern (strong LREE depleted), but no amphibole occurrence is described for these granites. In contrast, the REE patterns of Vila Catarina facies (**Fig. 8d**) are highly fractionated [(La/Yb)n = 27.05-40.65], although the sample MA-02 also shows concave-upward HREE pattern. In general sense, chemical changes caused by post-magmatic processes (hydrothermal alteration) could be at least partially affected the REE system, generating heterogeneous patterns in the Igarapé Azul Granite.

The Jatapu volcanic rocks (**Fig. 8e**) are characterized by REE patterns similar to those for Caroebe granitoid rocks, such as negative Eu anomaly (Eu/Eu* = 0.62-0.83) and REE total contents, but the formers are slightly most REE fractionated [(La/Yb)n = 22.63-60.09], mainly in HREE [(Gd/Yb)n = 2.45-4.20]. The contemporaneous calc-alkaline granitoid rocks from Tapajós Domain and northeastern Amazonas taken for comparison exhibit wide range of REE total contents, moderate REE fractionation, weak (Parauari) to strong (Tropas) negative Eu anomalies and flat (Tropas) to fractionated (Parauari) HREE patterns (**Fig. 8f**).

Further the major and trace elements geochemistry similarities, the Tropas and mainly the Água Branca granitoid rocks (Presidente Figueiredo region) shows REE patterns similarities with the Caroebe granites (**Fig. 8a-b, f**). Such as the Jaburuzinho facies (Caroebe Granite), the hornblende-bearing Presidente Figueiredo granite sample show similar total range of ETR and local positive Eu anomaly. The hornblende-free granite samples show lower total contents of REE, but the REE-pattern is compatible with the Alto Alegre facies (Caroebe Granite).

The Younger São Jorge Granite (Lamarão *et al.,* 2002) shows contrasting REE patterns (**Fig. 8f**) to those showed by Caroebe and Igarapé Azul granites (**Fig. 8a-d**). The former exhibits

low REE contents, strong fractionated REE patterns, low HREE abundances, very weak negative Eu anomaly, locally with no Eu anomaly (**Fig. 8f**). In addition to highly fractionated REE patterns, the Younger São Jorge Granite also shows low Y (10 to 11 ppm) and moderate to high Sr/Y ratios (25.5 to 122.7).

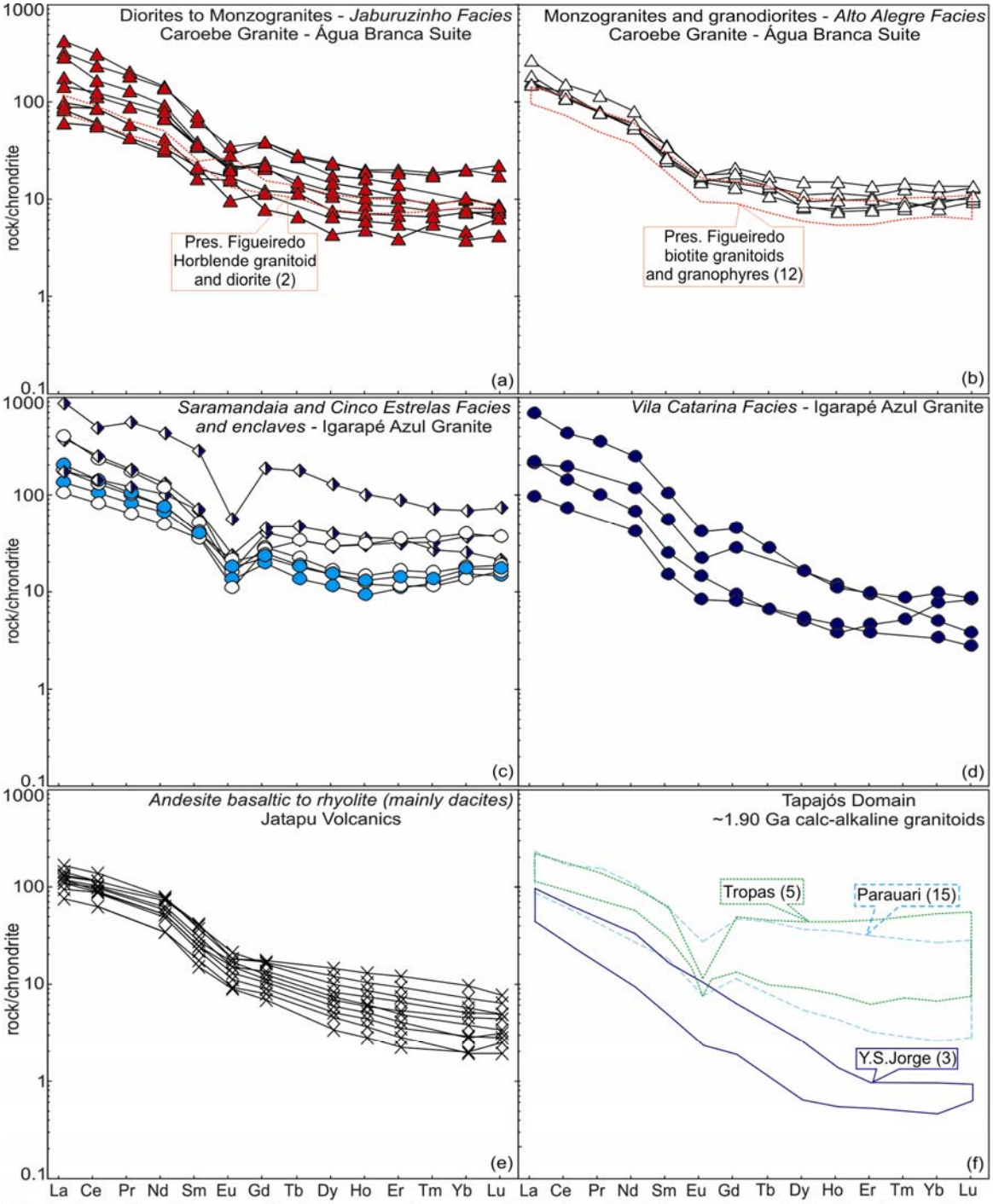

Fig. 8. REE chondrite-normalized diagrams (Boynton, 1984) from (a) Jaburuzinho and (b) Alto Alegre facies (*Caroebe Granite*); (c) Saramandaia and Cinco Estrelas facies and (d) Vila Catarina facies (*Igarapé Azul Granite*); (e) *Jatapu volcanic rocks* and (f) REE-pattern envelope of *Tropas*, *Parauari* and *Younger São Jorge granites* References and symbols as in Fig. 3.

PETROGENETIC CONSIDERATIONS

Two broad petrogenetic concepts are extensively evoked in the geological literature for explain the origin of calc-alkaline felsic magmas: 1) Derivation from basaltic parent magmas by fractional crystallization or AFC processes (*e.g.* Grove and Donnelly-Nolan, 1986; Bacon and Druitt, 1988); 2) Derivation from crustal rocks by partial melting (*e.g.* Bullen and Clynne, 1990; Roberts and Clemens, 1993; Tepper *et al.,* 1993; Guffanti *et al.*, 1996).

The first concept requires high volumes of mafic mantle-derived magmas for generate, by fractional crystallization, the extensive volume of rocks observed in southeastern Roraima and northeastern Amazonas (**Fig. 2**). In this region, rocks with basaltic composition are also scarce, identified locally in the Jatapu region (CPRM 2000a). Plutonic mafic counterparts are represented only by some diorites (SiO_2 49.5%-55.1%) in the Caroebe Granite, which is dominated by granodiorites and monzogranites. More than 85% of Caroebe granitoid rocks samples have up to 58% SiO_2 content (**Fig. 5, Table 1**). Furthermore, the fractional crystallization concept is normally associated to curvilinear trends in the Harker diagrams (*e.g.* El-Sayed *et al.*, 2002, 2004, Bakhit *et al.*, 2005) but, in contrast, all studied calc-alkaline granitoid rocks exhibit well-defined linear trends (**Fig. 3a-h**).

The restite unmixing model (White and Chappell, 1977) has been widely used to explain linear trends on variation diagrams for granite suites by variable separation of residuum from melt (*e.g.* Scambos *et al.*, 1986; Wyborn and Chappell, 1986; Chappell *et al.*, 1987; Barbero and Villaseca, 1992; Burnham, 1992; Barton and Sidle, 1994). On the other hand, how widely the restite unmixing model can be applied, however, is controversial. Wall *et al.* (1987), Clemens (1989) and Bateman (1988) argue that, in many granite suites, linear variations are better explained by fractionation, accumulation and magma mixing, and restite unmixing will usually result in linear trends only if the restites are chemically homogeneous, which is improbable given the large volumes of most granites and the likelihood of disequilibrium partial melting in the source (Barbero *et al.*, 1995).

The subtle compositional gap (4.10%) in SiO_2 observed in the Harker diagrams among Jaburuzinho (more mafic end-member) and Alto Alegre (more felsic end-member) facies of Caroebe Granite, associated to local field evidence, could suggest only subordinated participation of magma mixing/mingling process in the granites genesis. Thus, the fractional crystallization and mixing processes probably do not play important role in the Caroebe and Igarapé Azul genesis and, partial melting could be dominantly process. In the most of chemical diagrams, the

Igarapé Azul samples show good agreement with the Caroebe Granite, concerning linear trends. Furthermore, in several plots, the Alto Alegre facies and Igarapé Azul Granite samples exhibit commonly compositional overlap. Except for the Vila Catarina facies, there are similarities in the "spider diagrams" and REE patterns. These features and the close spatial and temporal association (see zircon ages discussion below), suggest that Caroebe (and Jatapu volcanics) and Igarapé Azul granites can be linked to the same magmatic source by partial melting.

For the Caroebe Granite and Jatapu volcanics some chemical features suggest that amphibole (local MREE depletion in relation to HREE) and titanite (*e.g.* negative Ti anomalies) played a dominant role during the magma segregation. In contrast, the relative higher abundances of Sr and local positive Eu anomaly point out for a smaller amount of plagioclase in their residues. The petrographic facies of Igarapé Azul shows negative Eu anomalies that support the plagioclase restrict presence in the residue of melting. Concave-upward HREE pattern is observed in the Saramandaia and Cinco Estrelas facies, with only one sample exhibiting flattened HREE and wing-bird pattern (strong LREE depleted), but no amphibole occurrence is described in these granites. In contrast, the REE patterns of Vila Catarina facies are highly fractionated; suggesting participation of residual garnet (?) during the role of magma segregation, but also no garnet is described in these rocks. The sample MA-02 shows concave-upward HREE pattern, suggesting possibly titanite and/or amphibole (Hoskin *et al.,* 2000) as residual phases, however titanite is very scarce and amphibole is not present in this facies.

In the Igarapé Azul Granite, chemical exchanges caused by post-magmatic processes (hydrothermal alteration) could be at least partially disturbed the REE system, generating heterogeneous patterns. The local high K/Ba (310-413) and low K/Rb (23-35) ratios observed in the Igarapé Azul types also suggest that this granite was affected by hydrothermal alteration, supporting the observed field and petrographic relationships.

However, the magmatic evolution of these granites (mainly Igarapé Azul type) seems more complex, suggesting that other parameters, such as a source of different composition, variable melting conditions and crustal contamination (*e.g.*, Zorpi *et al.*, 1989, 1991; Patiño-Douce, 1996, 1999; Petford *et al.*, 1996; Poli *et al.*, 1996), could be involved in their genesis. For example, the three different petrographic facies of Igarapé Azul Granite provided two main REE patterns and, in general, their chemical patterns are not so homogeneous in comparison with the Caroebe types.

Roberts and Clemens (1993), Tepper *et al.* (1993) and Jonasson (1994) show that a variety of granitoid rocks (including I-type calc-alkaline types) can be generated by partial melting under different H_2O contents of lower crustal metabasalts or another mafic to intermediate sources. Several others experimental constrains are available (*e.g.* Patiño-Douce, 1996, 1999, and references therein), yielding compositional differences of magmas produced by partial melting of common crustal rocks, such as amphibolites, tonalitic gneisses, metagreywackes and metapelites under variable melting conditions. This compositional variation can be visualized in terms of major oxides ratios and molar oxide ratios in figures **9a-c** and **9d**, respectively, revealing melts obtained from partial melting of three important crustal sources: felsic pelites, metagreywackes and amphibolites, including metabasalts and metatonalites. For example, in these plots, partial melts derived from mafic-intermediate rocks have lower $Al_2O_3/(FeO+MgO+TiO_2)$, $(Na_2O+K_2O)/(FeO+MgO+TiO_2)$ and molar $Al_2O_3/(MgO+FeO_t)$ ratios than those originated from metapelites-metagreywackes (**Fig 9a-d**).

The Caroebe Granite and Jatapu volcanic samples plot generally on the amphibolite and metabasalt-metatonalite fields, showing low $Al_2O_3/(FeO+MgO+TiO_2)$, $(Na_2O+K_2O)/(FeO+MgO+TiO_2)$ and molar $Al_2O_3/(MgO+FeO_t)$ ratios, but exhibit higher $CaO/(FeO+MgO+TiO_2)$ ratios. This feature, associated with relatively high Mg# values (37.5-51.4), precludes a derivation by felsic pelite or metagreywacke, mainly for the Jaburuzinho types (Caroebe granitoid rocks). Only two samples of Jaburuzinho facies have higher $Al_2O_3/(FeO+MgO+TiO_2)$ ratios (MA-053B,C) and few mafic members of Caroebe Granite present low-silica (<58%) and dioritic composition. Regardless of the degree of partial melting, dioritic melts derived by dehydration melting of metabasaltic sources in excess of ca. 1100^oC are generally characterized by Mg# <44 and Na_2O >4.3% (Wolf and Wyllie, 1994, Rapp, 1995, Rapp and Watson, 1995, and references therein). However, the unfractionated HREE patterns and moderate to high Sr/Y showed by Caroebe diorites preclude the involvement of substantial amounts of residual garnet and point out the melting temperatures could have been lower.

The Alto Alegre facies (Caroebe Granite) show some samples plotting out of amphibolite and metabasalt-metatonalite fields, overlapping locally the Igarapé Azul Granite compositions. The Igarapé Azul Granite plots preferentially on the metagraywacke field (**Fig. 9a-d**), however, the samples distribution is sometimes scattered, implying a local heterogeneous geochemical pattern (**Fig. 9d**) and higher $CaO/(FeO+MgO+TiO_2)$ ratios. These granitoid rocks exhibit also

normally restricted range and moderate to very low contents of Al_2O_3+FeO+MgO+TiO_2, Na_2O+K_2O+FeO+MgO+TiO_2 and CaO+FeO+MgO+TiO_2 (**Fig. 9a-c**). This geochemical pattern suggests that the input of metagreywacke source play important role in the Igarapé Azul Granite genesis, reflecting probably the compositional heterogeneity in the metasedimentary source and metabasalt-metatonalite source mixing?, including post-magmatic alterations. The Cauarane metavolcano-sedimentary sequence, represent the most suitable sources. Further, metagraywackes with igneous parentage are also reported by CPRM (2000a), suggesting an original heterogeneity in these sources. Records of probable restites (surmicaceous enclaves?) in the Igarapé Azul granitoids are represented by (muscovite)-biotite-rich gneissic enclaves.

In these sense, combining these features with REE patterns, at least two origins can be pointed out for the Igarapé Azul granitoids: a) similar REE patterns to those of Caroebe granitoids (*e.g.* low to moderate fractionated REE, flat HREE and low negative Eu anomalies), could be linked with metabasalt-metatonalite sources, and further variable input of metagreywacke sources (Saramandaia and Cinco Estrelas facies); b) most fractionated total REE and HREE (local higher negative Eu anomaly), suggesting retention of residual garnet in the source indicate higher input of melts from metagreywacke sources (Vila Catarina facies), although no garnet was observed in the petrographic studies.

Thus, the original melt of Igarapé Azul granitoids was probably generated by partial melting of metabasalt-metatonalite and metasedimentary sources in different and unknown proportions. This hypothesis is in agreement with the hybrid origin proposed by Sardinha (1999, 2001). The Igarapé Azul melt was also affected by important hydrothermal activity in the final stages of crystallization, according with the field (pegmatite abundance), petrographic (epidote, sericite, minor carbonate secondary minerals) and chemical (K/Rb and Ba/Rb ratios) relationships. In addition, assimilation of host metagranitoids of Martins Pereira at least locally is suggested for the Igarapé Azul genesis: a) evidence of host-rock xenoliths and b) 1.97-1.96 Ga inherited zircon age records (see zircon ages discussion below).

The plots with experimental melts data suggest that the origin of Caroebe granitoids (and Jatapu volcanics) involves partial melting of amphibolite source under water-rich conditions, with low input of melt from metagreywacke source. As well as the Igarapé Azul granitoids, the 1.96-1.97 Ga inherited zircon yielded by Alto Alegre facies also implies local possibly of assimilation of host Martins Pereira metagranitoids. The origin of high-K, calc-alkaline I-type

granites generated also by partial melting of metagreywacke sources (reflecting sometimes largely your igneous parentage) are supported by Barker *et al.* (1992), Altherr *et al.* (2000) and Thuy Nguyen *et al.* (2004) in the Alaska, Germany and Vietnam granitoids, respectively.

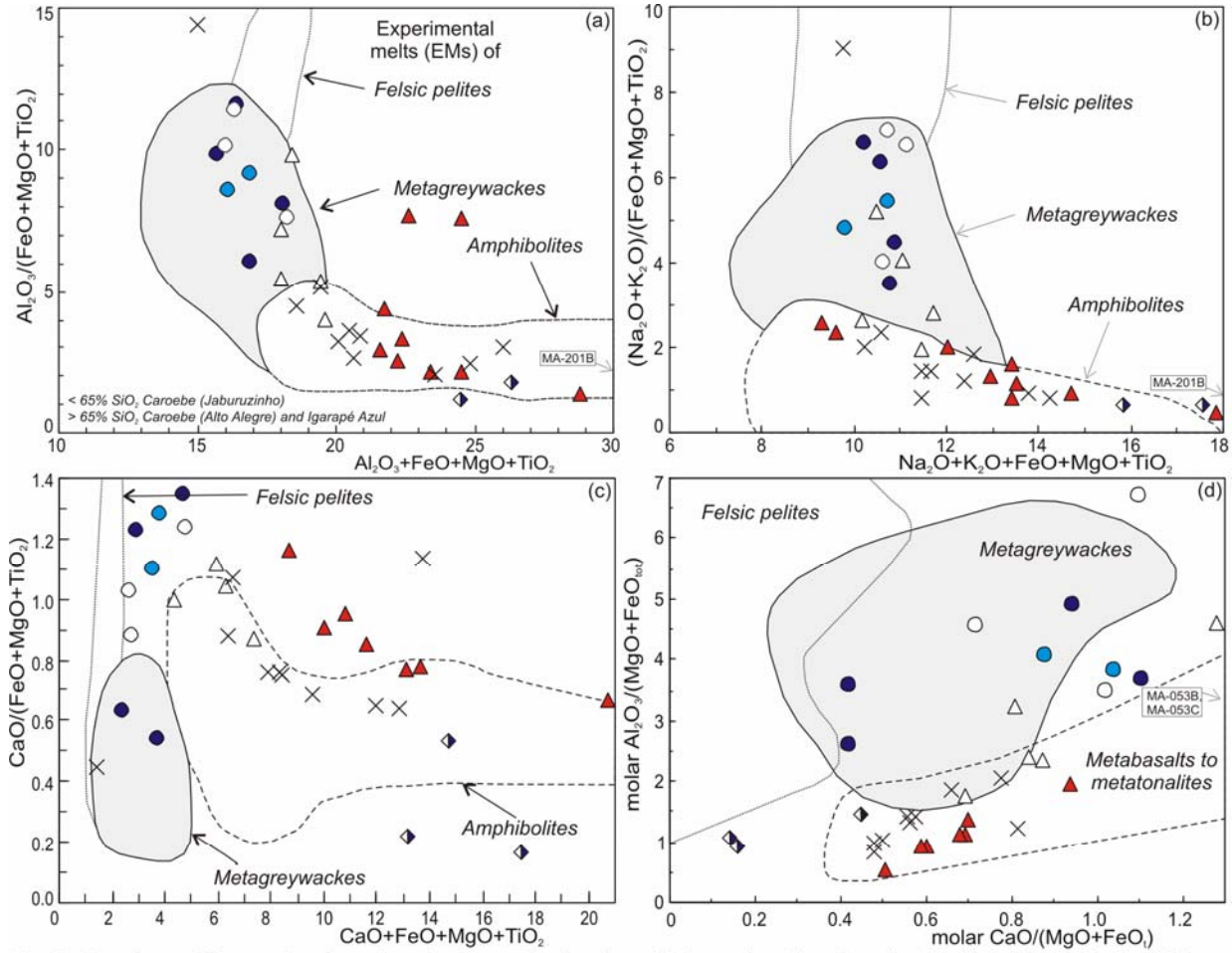

Fig. 9. Caroebe and Igarape Azul granites (and coeval volcanic rocks) samples plotted on the (a) $Al_2O_3/(FeO+MgO+TiO_2)$ *vs.* $Al_2O_3+FeO+MgO+TiO_2$, (b) $(Na_2O+K_2O)/(FeO+MgO+TiO_2)$ *vs.* $Na_2O+K_2O+FeO+MgO+TiO_2$, (c) $CaO/(FeO+MgO+TiO_2)$ *vs.* $CaO+FeO+MgO+TiO_2$ and (d) molar $Al_2O_3/(MgO+FeO_{tot})$ *vs.* molar $CaO/(MgO+FeO_t)$ diagrams. Outlined fields denote compositions of partial melts obtained in experimental studies by dehydration melting of felsic pelites, metagreywackes, amphibolites-metabasalts and metatonalites sources (Wolf and Wyllie, 1994; Patino-Douce, 1996, 1999; Patiño-Douce and Beard, 1996, Singh and Johannes, 1996; Thompson, 1996, and references therein). Symbols as in fig. 03. See text for discussion.

ZIRCON GEOCHRONOLOGY RESULTS (Pb-EVAPORATION AND U-Pb ID-TIMS)

A total of 4 samples of Caroebe and Igarapé Azul granitoids were selected for dating, including a biotite-rich enclave. Thus, Jatapu andesite, Água Branca Granite (type area), Murauaú Granite and Santa Maria hypersthene tonalite samples were analyzed.

Caroebe (MA-121 and 053A samples) and Água Branca Granitoids (HM-181 sample)

Two samples of Caroebe Granite (MA-121: Jaburuzinho facies; MA-053A: Alto Alegre facies), correlated to the Água Branca granitic magmatism, were analyzed by the single-zircon

Pb-evaporation technique. One sample from Agua Branca granitoid (HM-181) of type-area was also dated for comparison. The samples location and summary of petrographic description are available, respectively, in the **Fig. 2** and **Table 2**. The Pb isotopic data are showed in **Table 3**.

The zircon crystals of HM-181 sample are brown, with well-defined faces, locally with rounded vertices, showing some inclusions in the cores and cracks on the borders. They are transparent to translucent, exhibiting 120-310 μm in long and length/width 3.1:1 to 1.6:1 ratios. Four crystals yielded individual ages varying from 1905 Ma to 1885 Ma (Th/U: 0.50-0.80), resulting a mean age of 1901 ± 5 Ma and USD: 1.2 (**Table 3; Fig. 10a**). Another one revealed to be an inherited zircon with an age of 2142 ± 10 Ma yielded for just one isotopic block of 8 isotopic ratios (Th/U: 0.65).

The crystallization age obtained in hornblende-biotite granodiorite sample (HM-181) from Água Branca Suite (**Table 2**) was similar to that of Jaburuzinho facies of the Caroebe Granite (sample MA-121). Zircon crystals from hornblende-biotite quartz monzodiorite sample (MA-121) of Jaburuzinho facies (Caroebe Granite, **Table 2**) has typical magmatic origin (Th/U: 0.49-0.64, see **Table 3**), showing euhedral elongated prismatic shapes and parallel oscillatory zoning. The crystals are pale yellow to pale brown, transparent, but locally few crystals are turbid and have inclusions (apatite and Fe-Ti oxide minerals) in the core domains. Fractures are scarce. They are 140-290 μm in long and length/width ratios are between 3.3:1 and 2.1:1. A total of 6 crystals were analyzed yielding individual ages varying from 1905 Ma to 1888 Ma, and a mean age of 1895 ± 3 Ma and USD: 2.1 (**Table 3; Fig. 10b**).

The crystals from the biotite granodiorite sample (MA-053A) of Alto Alegre facies (Caroebe Granite, **Table 2**) are brown to pale brown, with well-defined faces and slightly rounded vertices, with few inclusions and scarce cracks. They are transparent to translucent, showing 100-320 μm in long and length/width ratios between 3.2:1 and 1.3:1. The individual ages from 3 zircon crystals are between 1905 Ma and 1885 Ma (Th/U: 0.51-0.85), defining a mean age of 1891 ± 2 Ma and USD: 1.4 (**Table 3; Fig. 10c**), which is slightly lower than the ages of two samples previously presented. Inherited zircon age is recorded in 2 crystals, yielding a mean age of 1963 ± 4 Ma (**Table 3, Fig. 10c**). Despite of different ages and locally lower Th/U (0.16-0.17) in the inherited zircon crystals, they show similar optical features in comparison with the other analyzed ones.

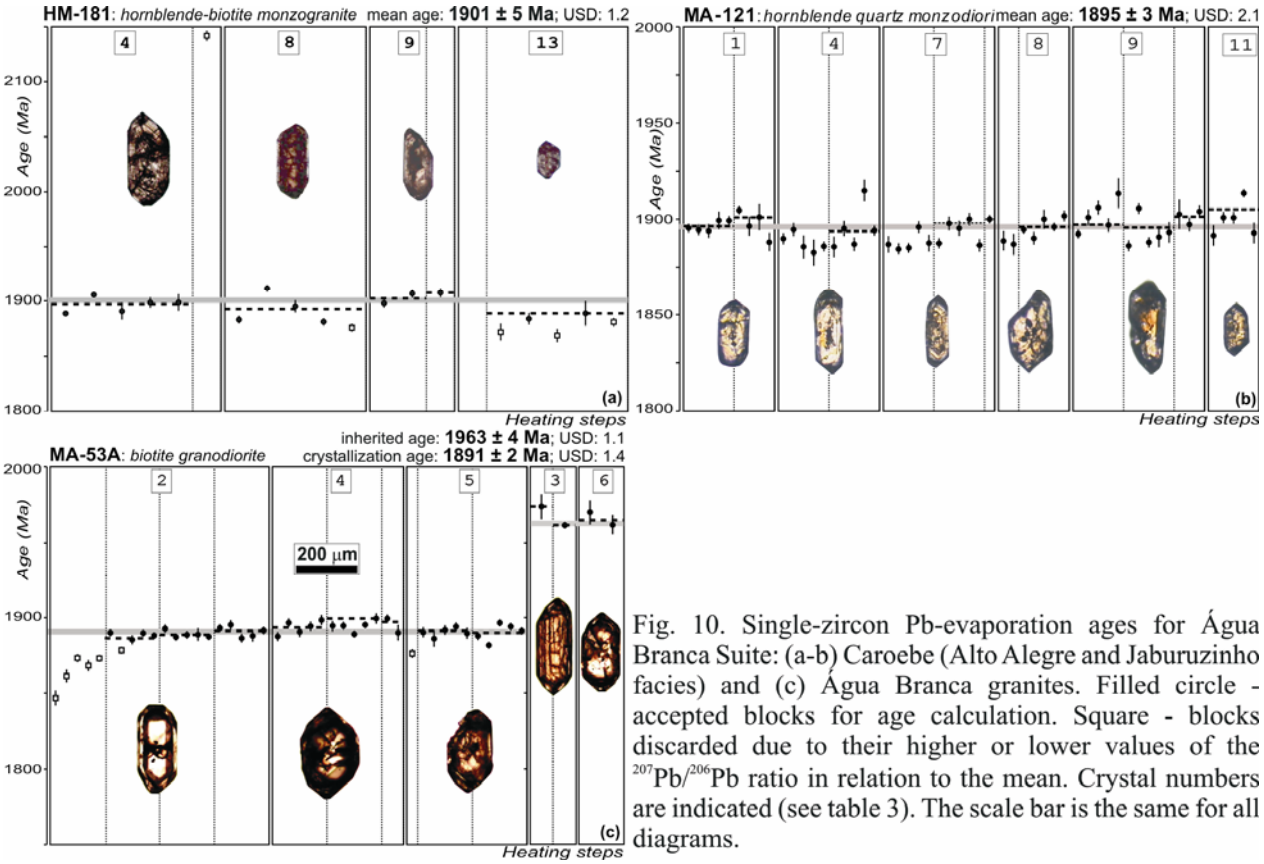

Fig. 10. Single-zircon Pb-evaporation ages for Água Branca Suite: (a-b) Caroebe (Alto Alegre and Jaburuzinho facies) and (c) Água Branca granites. Filled circle - accepted blocks for age calculation. Square - blocks discarded due to their higher or lower values of the $^{207}Pb/^{206}Pb$ ratio in relation to the mean. Crystal numbers are indicated (see table 3). The scale bar is the same for all diagrams.

Igarapé Azul granitoids (MA-147A and 186A samples) and biotite-bearing enclave (MA-201b sample)

Two samples of Igarapé Azul Granite (MA-147A: Cinco Estrelas facies; MA-186A: Saramandaia facies) and one biotite-bearing quartz diorite (MA-210B: enclave) were analyzed by the single-zircon Pb-evaporation technique. One sample of Igarapé Azul Granite was also selected for U-Pb TIMS analysis. (See **Fig.2** and **tables 2** and **3**).

Zircon crystals from fine-grained leucocratic monzogranite sample (MA-147A) of Cinco Estrelas facies (**Fig. 2, Table 2**) show euhedral prismatic shapes, locally with bypiramidal edges, exhibiting 270-360 µm in long and length/width ratios between 2.8:1 and 1.3:1. Some crystals display oscillatory zoning, parallel to external faces. They are pale brown to brown, transparent but, locally in few crystals, cracks and inclusions are common (apatite and Fe-Ti oxide minerals). A total of 6 crystals were analyzed yielding individual ages varying from 1902 Ma to 1882 Ma (Th/U: 0.43-1.08), and a mean age of 1889 ± 5 Ma and USD: 3.0 (**Table 3; Fig. 11a**). Only one zircon recorded higher age (1 isotopic block of 4 isotopic ratios) of 1964 ± 4 Ma (Th/U: 0.40).

The zircon crystals from the porphyritic monzogranite sample (MA-186A) of Saramandaia facies are brown, with well-defined faces, in general with rounded vertices, containing some inclusions in the cores and scarce cracks. They are transparent to translucent, prismatic to stubby, showing 90-350 μm in long and length/width ratios between 4.1:1 and 1.2:1. Three crystals from this sample (**Fig. 2, Table 2**) showed individual ages varying from 1897 Ma to 1887 Ma (Th/U: 0.55-0.68), resulting a mean age of 1889 ± 2 Ma and USD: 1.4 (**Table 3; Fig. 11b**) which is in good agreement with the age yielded by the Cinco Estrelas facies sample. The Samandaia facies sample shows more evident inheritance record, exhibiting 2 inherited crystals that yielded a mean age of 1972 ± 3 Ma (Th/U:0.38-0.48).

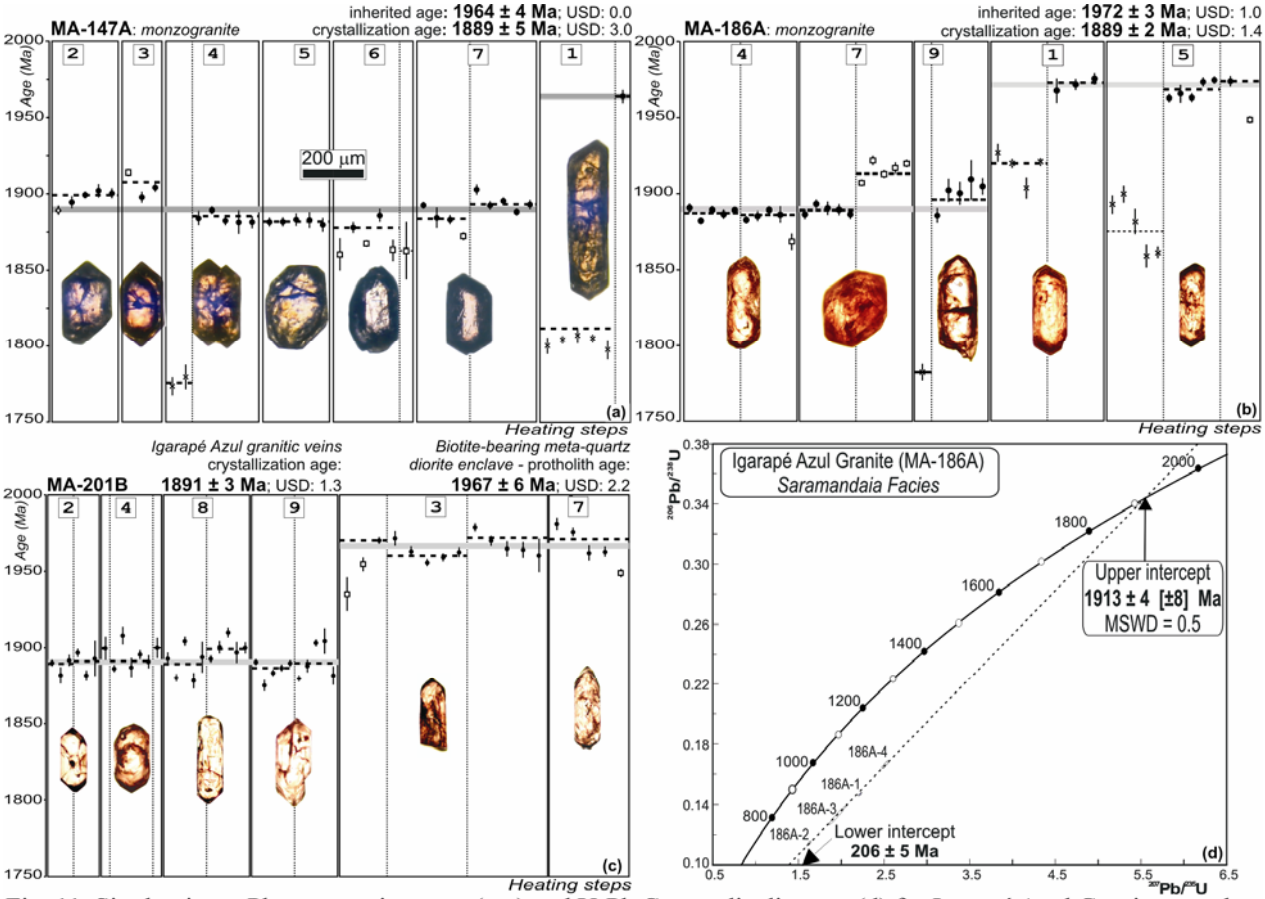

Fig. 11. Single-zircon Pb-evaporation ages (a-c) and U-Pb Concordia diagram (d) for Igarapé Azul Granite samples. Filled circle - accepted blocks for age calculation. Square - blocks discarded due to their higher or lower values of the $^{207}Pb/^{206}Pb$ ratio in relation to the mean. X - rejected blocks due to show $^{204}Pb/^{206}Pb > 0.0004$. Crystal numbers are indicated (see table 3). The scale bar is the same for all diagrams.

One enclave sample (MA-201B, foliated biotite-bearing quartz diorite) was also selected for single zircon Pb-evaporation analysis (**Fig. 2, Table 2**). The zircon crystals of MA-201B are transparent to translucent and prismatic, showing 80-330 μm in long and length/width ratios between 4.1:1 and 1.9:1. They are also pale yellow to brown, showing locally inclusions in the

cores and scarce cracks. This sample yielded 2 different mean ages. The first one was yielded for four crystals which individual ages varying from 1890 Ma to 1900 Ma (Th/U: 0.43-0.70), resulting in a mean age of 1891 ± 3 Ma and USD: 1.3 (**Table 3; Fig. 11c**). This age is identical to those obtained in the host granitoid rocks, yielded by zircon from the fine granitic veins that cross-cut the enclave. The second mean age was obtained from 2 crystals and is 1967 ± 6 Ma (Th/U: 0.27-0.61). It probably represents the protolith age of foliated enclave (**Table 3; Fig. 11c**).

In function of the ambiguous results obtained in the sample MA-186A, four more zircon crystals were analyzed by the U-Pb ID-TIMS method. In spite of the grains had been abraded, the analytical points are very discordant and the discordia line yielded a superior intercept at 1913 ± 4 Ma (**Fig. 11d, Table 4**). This comparatively higher U-Pb age (ca. 20 Ma) could be related to the interference of common Pb or due to the small amounts of the inherited isotopic component (observed in the Pb-evaporation analysis), resulting in a local mixing age.

Jatapu Volcanics (MA-208 sample)

Zircon from andesite (MA-208) sampled in the Jatapu river region (**Table 2**) shows euhedral bypiramidal crystals, locally with broken edges and/or rounded vertices. They are colorless, transparent and some crystals have inclusions, such as apatite and Fe-Ti oxide minerals, exhibiting 70-390 μm in long and length/width ratios between 3.7:1 and 2:1. The inherited crystals show also corroded and rounded borders and lower $^{208}Pb/^{206}Pb$ (< 0.15) and Th/U (0.15-0.57) ratios in comparison with the younger crystals ($^{208}Pb/^{206}Pb$ >0.15, Th/U: 0.43-0.98).

The zircon from the andesite was analyzed by the single-crystal Pb-evaporation technique, yielding a mean age of 1893 ± 5 Ma and USD: 2.2 (**Table 3; Fig. 12**) from 4 crystals with individual ages ranging from 1898 to 1886 Ma. This age is in good agreement with the results obtained in dacite porphyry of this same region also by single-zircon Pb-evaporation (1893 ± 2 Ma; Macambira *et al.*, 2002). But, in contrast, some zircons analyzed in the andesite sample have showed strong evidences of inherited age. For instance, others 4 crystals analyzed yielded individual ages varying from 1970 Ma to 1960 Ma, and a mean age of 1966 ± 3 Ma with a USD: 1.3 (**Table 3; Fig. 12**).

Santa Maria Enderbite (MA-198 sample)

The undeformed hypersthene tonalite sample (MA-198) from ENE-WSW elongated Santa Maria body (**Fig. 2, Table 2**) was analyzed by the single-zircon Pb-evaporation technique. The sample exhibit prismatic to stubby crystals with 120-480 μm in long and length/width ratios between 2:1 and 1.3:1, generally showing brown colors (colorless and pale yellow crystal are rare), transparent to translucent and well-defined faces and vertices. They have also commonly apatite and Fe-Ti oxide mineral inclusions, and scarce fractures.

A mean age of 1891 ± 1 Ma and USD: 1.2 (**Table 3; Fig. 13**) was obtained from 6 individual crystals with homogeneous age range from 1894 to 1889 Ma (Th/U: 0.48-0.68, see **Table 3**). This crystallization age falls down in the same age range of the others studied granitoid rocks of SUAD (*e.g.* Caroebe and Igarapé Azul granites).

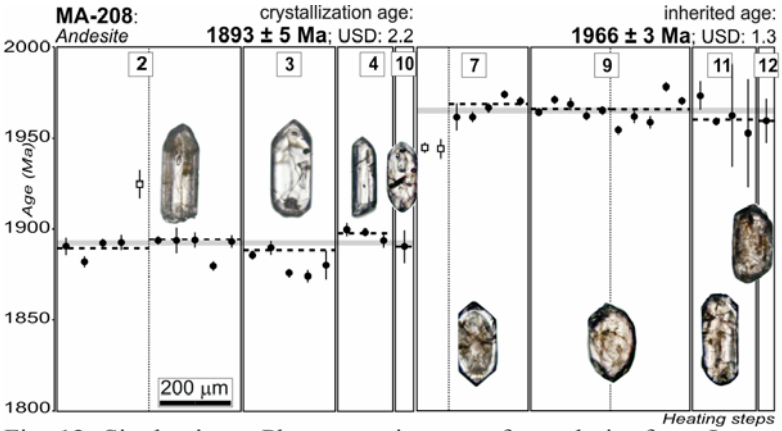

Fig. 12. Single-zircon Pb-evaporation ages for andesite from Jatapu region. Filled circle - accepted blocks for age calculation. Square - blocks discarded due to their higher or lower values of the $^{207}Pb/^{206}Pb$ ratio in relation to the mean. Crystal numbers are indicated (see table 3).

Murauaú Granite (Mapuera Suite, MA-226 sample)

A circular-like body of pale pink porphyry granite intrudes the Caroebe Granite in the Murauaú river region (**Table 2**), but the northern area of this granite was strongly deformed by dextral NE-trending brittle-ductile shear zones related to the Jauaperi Fault System (**Fig. 2**), obliterating the intrusion field relationships. The granite from deformed area was sampled (MA-226) for analysis with the objective of determines the crystallization age and the maximum age of the shear zone.

Seven zircon crystals analyzed by single-zircon Pb-evaporation technique, yielding three main age patterns showing individual crystals ages ranging from 2366 to 1866 Ma (Th/U: 0.35-0.37, **Table 3**). The younger population (two zircon crystals) resulted in a mean age of 1871 ± 5 Ma and USD: 2.6 (**Table 3; Fig. 14**), interpreted as the crystallization age of Murauaú Granite

(Th/U:0.35-0.44). This crystallization age is ~20 Ma lower in relation to the Caroebe and Água Branca granites (1901-1892 Ma), but fall down in the Mapuera granitoids interval age (1880-1860 Ma, see **Table 5**), reinforcing the initial petrographic and field correlations (CPRM, 2000a).

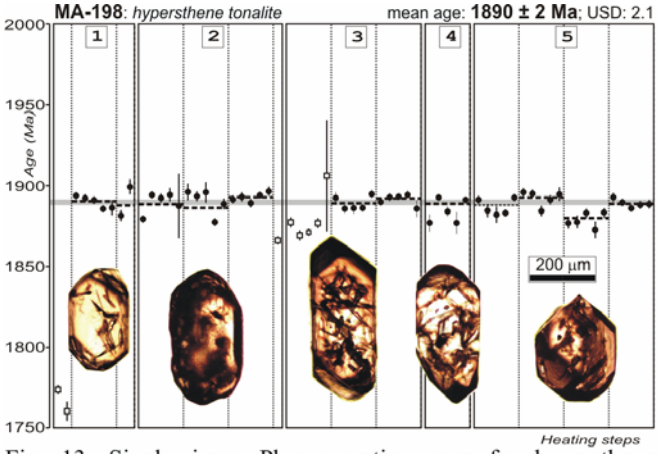

Fig. 13. Single-zircon Pb-evaporation ages for hypersthene tonalite (Santa Maria Enderbite). Filled circle - accepted blocks for age calculation. Square - blocks discarded due to their higher or lower values of the $^{207}Pb/^{206}Pb$ ratio in relation to the mean. Crystal numbers are indicated (see table 3).

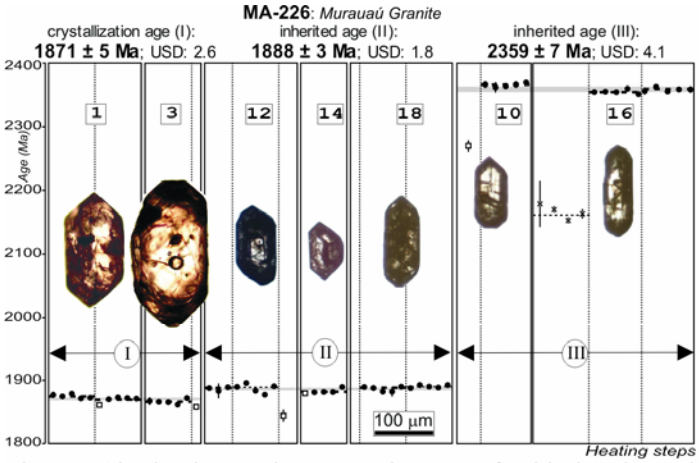

Fig. 14. Single-zircon Pb-evaporation ages for biotite sheared monzogranite (Murauaú Granite, Mapuera Suite?). Filled circle - accepted blocks for age calculation. Square - blocks discarded due to their higher or lower values of the $^{207}Pb/^{206}Pb$ ratio in relation to the mean. X - rejected blocks due to show $^{204}Pb/^{206}Pb >$ 0.0004. Crystal numbers are indicated (see table 3).

In addition, two other crystal populations yielded a higher mean age of 1888 ± 3 Ma with USD: 1.8 (Th/U:0.35-0.42) and 2359 ± 7 Ma with USD: 4.1 (Th/U:0.31-0.37), interpreted as inherited origin (**Table 3**). No optical difference among these 3 populations of zircon was detected in the binocular microscope. These crystals are prismatic, showing 110-250 µm (in long) and length/width ratios between 3.1:1 and 1.7:1. Generally, they are pale brown to colorless,

transparent to translucent, with well-defined faces and vertices. Apatite and Fe-Ti oxide mineral inclusions and fractures are scarce.

ZIRCON AGES AND GEOLOGICAL IMPLICATIONS

Zircon Geochronology constraints

Several authors have used field, petrographic and geochemical criteria (*e.g.* Costi *et al.*, 1984; Jorge-João *et al.*, 1985; Oliveira *et al.*, 1996; CPRM, 2000a; Almeida and Macambira, 2003) for to correlate the undeformed hornblende-bearing granitoid rocks of southeastern Roraima (and northwestern of Pará State) to the Água Branca Granite (Araújo Neto and Moreira, 1976; Veiga Jr. *et al.,* 1979) in the northeastern Amazonas (nearly 400 km far away to south). Furthermore, the 1972 ± 7 Ma (U-Pb SHRIMP) to 1960 ± 21 Ma (Pb-evaporation) zircon ages obtained by CPRM (2003) and Almeida *et al.* (1997) in the southeastern Roraima, were respectively misleadingly interpreted as "Igarapé Azul" and "Agua Branca" ages. New geological mapping and preliminary geochronological data (Almeida *et al.*, 2002) pointed out that these ages were obtained from samples of Martins Pereira granitoids and not from the Água Branca and Igarapé Azul types. At that time, only two whole-rock Rb-Sr isochronic ages were available for the Água Branca granitoids (and correlated rocks). These isochronic ages were taken by Santos and Reis Neto (1982) and Jorge-João *et al.* (1985), yielding respectively 1942 Ma ± 32 Ma and 1910 ± 23 Ma (Sr_i: 0.70225 ± 0.00031, MSWD: 1.26). The last one was obtained in hornblende granitoid rocks of northwestern of Pará (**Table 5, Fig. 15**).

More recently in the southeastern Roraima, the undeformed and ENE-trending elongated hornblende-bearing granitoid body, with 105 km^2 (Igarapé Dias quartz monzodiorite) was dated by U-Pb SHRIMP on zircon (CPRM, 2003), yielding concordant analytical points with mean age of 1891 ± 6 Ma (**Table 5, Fig. 15**). The zircon ages (1898-1890 Ma) obtained by Valério (2006) in the northeastern Amazonas (hornblende-biotite granitoid rocks) are also very similar those of Caroebe-Água Branca granites (**Table 5**) and in general sense, all zircon ages are in good agreement (within error limits) with the WR Rb-Sr isochronic age of 1910 ± 23 Ma.

In the present study, the Igarapé Dias quartz monzodiorite age (1891 Ma) and northeastern Amazonas (1898-1890 Ma) are included in same interval age (1901-1889 Ma) of the Caroebe, Água Branca and Igarapé Azul granites, suggesting that all these granitoid rocks could be correlated to the Água Branca magmatic event.

The same is true for the volcanic rocks. The zircon ages of the andesite (1893 ± 5 Ma, this paper) and dacite (1893 ± 2 Ma, Macambira *et al.*, 2002) from the Jatapu region are in agreement (within error limits) with the ages of volcanic samples of Iricoumé Group from the other regions (*e.g.* 1896 ± 7 Ma, CPRM, 2003). However, in northeastern Amazonas some authors (Costi *et al.,* 2000; Valério *et al.*, 2005, Valério, 2006) pointed out that the Iricoumé volcanics with more acid compostion (rhyolites) and alkaline chemical affinities are coeval and cogenetic with Mapuera-Abonari granitoids, showing 1888 ± 3 Ma and 1883 ± 4 Ma ages (**Table 5, Fig. 15**). These data suggest at least two main younger volcano-plutonic events in the SUAD: a) I-type, calc-alkaline magmatism with 1901-1889 Ma interval age, enclosing Água Branca, Caroebe, Igarapé Azul granites and Jatapu volcanic rocks, and b) A-type, alkaline magmatism showing 1888-1871 Ma interval age, represented by Mapuera granitoids and Iricoumé volcanic rocks.

Locally, charnockitic rocks also belong to this important calc-alkaline volcano-plutonic event. Hypersthene tonalites (Santa Maria Enderbite) exhibit similar age (1891 ± 1 Ma), suggesting more dry conditions and highest temperatures on the granites formation in the SUAD. The Santa Maria type (**Table 5, Fig. 15**) shows higher age in comparison with the charnockitoids from the Jaburu river (1873 ± 6 Ma, zircon U-Pb ID-TIMS, Santos *et al.*, 2001a). In the Central Guyana Domain, two generation events of charnockites are also described: a) charnockites of Mucajai Suite (AMG association revisited by Fraga 2002) with 1564 ± 21 Ma (single-zircon Pb evaporation, Fraga *et al.,* 1997); and b) older and locally deformed charnockites of Serra da Prata Suite (1934-1943 Ma, single-zircon Pb evaporation, Fraga, 2002). All these data pointed out for at least three charnockite generation events in the center-southern Roraima State: 1.94-1.93 Ga, 1.89-1.87 Ga (**Table 5, Fig. 15**) and 1.54 Ga.

The Murauaú Granite (1871 ± 5 Ma) is correlated to younger granites from Mapuera Suite, which belongs to the 1.87 Ga A-type magmatism event recognized in the southeastern Roraima, northeastern Amazonas and northwestern of Pará (**Fig. 15, Table 5**). This A-type event is related to the final stage of magmatic activity of the Agua Branca-Iricoumé magmatism and delimits the start of the more crustal stability period of the UAD. However, the Murauaú and Mapuera types correlation must be regarded with care because key data to identifying the type and the origin these granites (*e.g.* isotopic-geochemical data) were not sufficiently available. The younger A-type ~1.81 Ga Moderna (Santos *et al.*, 1997a) and Madeira (*e.g.* Costi *et al.*, 2000) granitoid rocks are also showed at the **Fig. 15**.

All these geochronological data support that the granitoids and volcanic rocks of SUAD belongs to the same magmatic event, responsible for a widespread calc-alkaline 1.90 Ga volcano-plutonism (**Fig. 15**), showing a high magma volume generated on the relative little interval time (1901-1873 Ma). The same is observed in the southern region of Tapajós-Parima belt or Ventuari-Tapajós Province (**Table 5**; *e.g.* Santos *et al.*, 1997b, 2000, 2004; CPRM, 2000b,c; Lamarão *et al.*, 2002), located on the Tapajós domain (see discussion below).

The older and inherited ages (1972-1962 Ma) observed in all granitoids and volcanics dated (except for Jaburuzinho facies and hypersthene granite), are very similar to the crystallization interval ages (1975-1962 Ma) of Martins Pereira and Serra Dourada granitoids from NUAD (Almeida *et al.,* 2002). These abundant inherited records in the SUAD granitoid rocks (**Table 6, Fig. 15**) pointed out a participation of the metagranitoids of NUAD in their genesis. Minor evidences of Transamazonian (2142 ± 10 Ma) and Siderian (2359 ± 7 Ma) zircons are also identified, respectively, in the Água Branca and Murauaú granites (**Table 6, Fig. 15**), suggesting, at least locally, the presence of the Transamazonian and Central Amazonian crusts.

The magmatic rocks of Tapajós domain (TD) also present several inheritances from several sources. The Iriri volcanics show 2.66-2.46 Ga, 2.01 Ga and 1.96 Ga inherited zircons, suggesting, respectively, Central Amazonian crust, Cuiú-Cuiú and Creporizão provenances (**Table 6, Fig. 15**). The Younger São Jorge granite also exhibit Archean (2.73 Ga) and Creporizão (1.96 Ga) inheritance ages and coeval Ingarana mafic rocks show Cuiú-Cuiú inherited zircons ages (2.00 Ga). The Maloquinha granites show 4 generations of the inherited zircon (**Table 6**): 2.84-2.46 Ga (Central Amazonian crust), 2.21 Ga (Transamazon or Maroni-Itacaiúnas crust), 2.00 Ga (Cuiú-Cuiú arc) and 1.98 Ga (Creporizão granitoids).

Tapajós and Uatumã-Anauá domains: Lithostratigraphy and Tectonic Evolution

The SUAD granitoid rocks and volcanics (1901-1873 Ma) show important chronological similarities with the TD ones in the southern Tapajós-Parima orogenic belt or Ventuari-Tapajós Province. However, the charnockites and high-K calc-alkaline Igarapé Azul granitoids-like are not described in the TD. In the Tapajós region, the 1898-1870 Ma granitoid rocks (see **Table 5, Fig. 15**) crop out in the post-orogenic domain (*e.g.* CPRM, 2000b, c), represented by Tropas, Parauari, Younger São Jorge and Maloquinha granitoids, Ingarana mafic rocks and coeval volcanics. The origin of this magmatism has been attributed to large-scale taphrogenesis that

marked the break up of a large Paleoproterozoic continent (Vasquez *et al.*, 2002, Lamarão *et al.*, 2002, 2005), contrasting with a arc-related orogenic origin (Tropas Orogeny, Santos *et al.*, 2000).

For instance, in the SUAD, some chemical discriminant diagrams (**Fig. 4, 5 and 7**) pointed out that Caroebe and Igarapé Azul granitoids belong to the "active continental margin" setting with variable crustal contributions. In the special case of Caroebe granitoids, they contain hornblende and biotite, are metaluminous to weakly peraluminous, and have the characteristics of I-type granites and high-K calc-alkaline series. This picture is compatible with volcanic arc setting, but the trace element compositions are strongly dependent of protolith composition and, therefore, can not necessarily be indicative of the tectonic setting of magma formation (*e.g.* Roberts and Clemens, 1993).

This point of view is also corroborated by Barbarin (1999). According Barbarin (1999), high-K calc-alkaline granitoid rocks (KCG) are present in various geodynamic settings and they indicate much more a variation of the tectonic regimes than a specific geodynamic environment. These granitoid rocks generally are good indicators of major changes in the geodynamic environment, being normally abundant in the orogenic belts related to continental collision, mostly when the collision is ending, either during periods of relaxation (separating periods of culmination of collisional events) or transition from a compressional regime to a tensional regime (*e.g.* Lameyre, 1988; Bonin, 1990).

Thus, the younger 1.90-1.89 Ga high-K calc-alkaline granitoid rocks (Caroebe, Água Branca and Igarapé Azul, as well as Tropas and Parauari types) could be associated with the latest subduction related processes(?) or, alternatively, represent a intracontinental tectonic evolution (*e.g.* Vasquez *et al.*, 2002; Lamarão *et al.*, 2002, 2005), suggesting a transition for more stable tectonic crustal conditions, characterized by the 1.88-1.87 Ga A-type Mapuera and Abonari granitoids.

CONCLUSIONS

The geochemical data support that Caroebe and Igarapé Azul granitoids origin can be linked to partial melting of crustal protoliths with different compositions (amphibolite or metatonalites and minor metagraywacke sources), leaving restites with variable proportions of amphibole, titanite and plagioclase as result of melting under variable H_2O contents. This H_2O variation can locally generate coeval hypersthene granitoid rocks (*e.g.* Igarapé Tamandaré and Santa Maria), suggesting dry conditions and high temperatures on the granite formation.

The geochronological constraints, based on the ages of inherited zircons (1.97-1.96 Ga), show that the Martins Pereira granites from NUAD are locally related to the Caroebe (Alto Alegre facies) and mainly of Igarapé Azul origin. Local evidence of inherited zircon with Transamazonian and Siderian ages, suggest, at least partially, the involvement of Maroni-Itacaiúnas (or Transamazon) and Central Amazonian (or Amazon) Provinces in the generation of some granites (*e.g.* Água Branca and Murauauá granites).

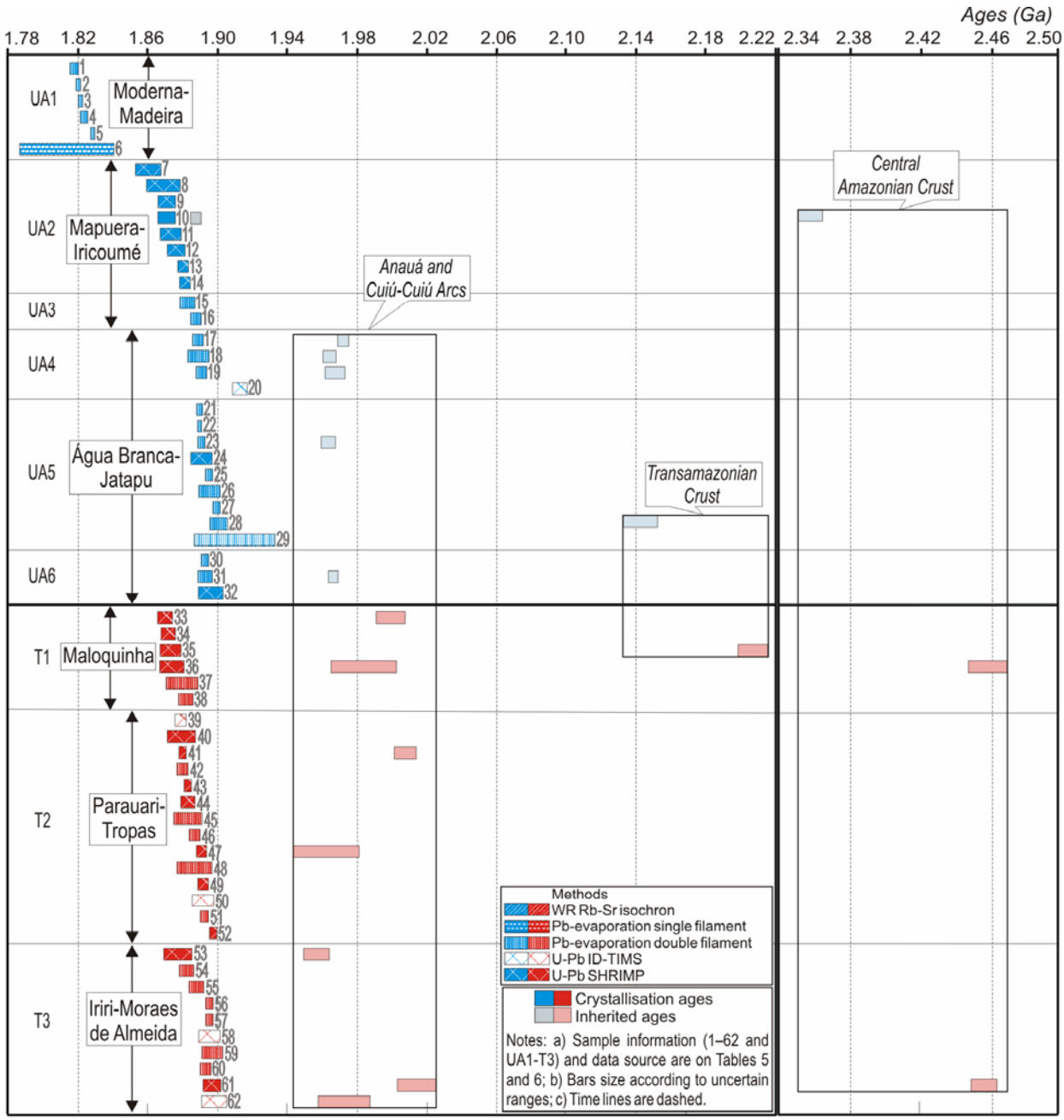

Fig. 15. Temporal distribution of main magmatic rocks younger than 1900 Ma (and respectives inheritances) of the Tapajós-Parima or Ventuari-Tapajós Province, grouped by Uatumã-Anauá (UAD) and Tapajós (TD) geological domains. For references see tables 5 and 6.

In the SUAD, the zircon geochronology results point out that several granitoids (Água Branca, Caroebe, Igarapé Azul and Santa Maria) and the Jatapu volcanic rocks belong to the same magmatic event (1901-1889 Ma). This age range is very similar to that of the calc-alkaline Parauari-(Tropas)-Iriri magmatism (1898-1879 Ma) in the TD, despite in this last one the high-K calc-alkaline granitoid rocks with metasedimentary source contributions (*e.g.* Igarapé Azul Granite) and charnockitic rocks are absent. In general sense, The Água Branca-(Caroebe-Igarapé Azul)-Iricoumé (SUAD) and Parauari-Iriri (TD) magmatism represent an important period of Orosirian crustal growth in the Ventuari-Tapajós (or Tapajós-Parima) Province and their origin is still a matter of debate.

The magmatic evolution picture is maybe compatible with volcanic arc setting, but metaturbitidic and ophiolite sequences are not observed in association with the calc-alkaline granitoid rocks (and coeval volcanism) in the SUAD. Furthermore, the trace element compositions are strongly dependent of source composition and, therefore, not necessarily indicative of the tectonic setting of magma formation. The several inherited ages yielded by the SUAD granitoid rocks also suggest an important crustal involvement during the emplacement these granitoid rocks and a juvenile origin on the magmatic arc setting is unlike for this portion of Guyana Shield. However isotopic data (*e.g.* Nd-Pb) are not available for these rocks, making difficult a better evaluation of the evolutionary models.

Acknowledgements

Special thanks to the colleagues of Geological Survey of Brazil and Para-Iso (UFPA) respectively for discussions and helpful during isotopic analyses,. The authors are also grateful to Geological Survey of Brazil for the research grants and FINEP (CT-Mineral 01/2001 Project) and Isotope Geology Laboratory of Federal University of Pará for support of laboratorial works.

References

Almeida, M.E., Brito, M.F.L., Ferreira, A.L., Monteiro, M.A.S. 2001. Evolução Tectono-estrutural da região do médio-alto curso do rio Tapajós. In: N.J. Reis and M.A.S. Monteiro (Orgs), Contribuições à Geologia da Amazônia, 2, , Belém, SBG, p.57-112. (in Portuguese).

Almeida, M.E., Fraga, L.M.B., Macambira, M.J.B. 1997. New geochronological data of calc-alkaline granitoids of Roraima State, Brazil. In: IG/USP, South-American Symp. on Isotope Geology, 1, Extend Abst., p.34-37.

Almeida, M.E., Macambira, M.J.B. 2003. Aspectos geológicos e litoquímicos dos granitóides cálcio-alcalinos Paleoproterozóicos do sudeste de Roraima. In: SBGq, Congresso Brasileiro de Geoquímica, 9, Anais, p. 775-778 (in Portuguese).

Almeida, M.E., Macambira, M.J.B. Geology and Petrography of Paleoproterozoic Granitoids from Uatumã-Anauá Domain (Guyana Shield), Southeast of Roraima State, Brazil. Revista Brasileira de Geociências. In press.

Almeida, M.E., Macambira, M.J.B., Faria, M.S.G. de. 2002. A Granitogênese Paleoproterozóica do Sul de Roraima. In: SBG, Congresso Brasileiro de Geologia, 41, Anais, p 434 (in Portuguese).

Altherr, R., Holl, A., Hegner, E., Langer, C., Kreuzer, H. 2000. High-potassium, calc-alkaline I-type plutonism in the European Variscides: northern Vosges (France) and northern Schwarzwald (Germany). *Lithos* **50**, 51–73.

Araújo Neto, H., Moreira, H.L. 1976. Projeto Estanho de Abonari: Relatório Final. BRASIL. Departamento Nacional da Produção Mineral, Manaus, Convênio DNPM/CPRM, relat. inédito. 2v (in Portuguese).

Bacon, C.R., Druitt, T.H. 1988. Compositional evolution of the zoned calcalkaline magma chamber of mount Mazama, crater Lake, Oregon. *Contrib. Miner. Petrol.* **98**, 224–256.

Bakhit, F., El-Nisr,S., Saleh, G., El-Afandy, A. 2005. Geochemistry and Petrogenesis of Neoproterozoic Granitoids in Kilkbob Area, Southeastern Desert, Egypt. *Mineralogical Society Of Poland – Special Papers* **26**, 121-125.

Barbarin, B. 1999. A review of the relationships between granitoid types, their origins and their geodynamic environments. *Lithos* **46**, 605–626.

Barbero, L., Villaseca, C. 1992. The Layos Granite. Hercynian complex of Toledo (Spain): An example of parautochthonous restite-rich granite in a granulitic area. *Trans. R. Soc. Edinburgh Earth Sci.* **83**, 127-138.

Barbero, L., Villaseca, C., Rogers, G., Brown, P.E. 1995. Geochemical and isotopic disequilibrium in crustal melting: An insight from the anatectic granitoids from Toledo, Spain. *J. Geophys. Res. Solid Earth* **100**, 15745- 15765.

Barker, F., Farmer, G.L., Ayuso, R.A., Plafker, G., Lull, J.S. 1992. The 50 Ma granodiorites of the eastern Gulf of Alaska: melting in an accretionary prism in the forearc. *J. Geophys. Res.* **97**, 6757–6778.

Barton, M., Sidle, W.C. 1994. Petrological and geochemical evidence for granitoid formation: The Waldoboro pluton complex, Maine. *J. Petrol.* **35**, 1241-1274.

Bateman, R. 1988. The Center Pond pluton: The restite of the story (phase separation and melt evolution in granitoid genesis). Comment. *Am. J. Sci.* **288**, 282-287.

Billström, K., Weihed, P. 1996. Age and provenance of host rocks and ores in the Palaeoproterozoic Skellefte district, northern Sweden. *Econ. Geol.* **91**, 1054–1072.

Bonin, B. 1990. From orogenic to anorogenic settings: evolution of granitoid suites after a major orogenesis. *Geol. J.* **25**, 261–270.

Boynton, W.V. 1984. Cosmochemistry of the rare earth elements: meteorite studies. *In*: Henderson, P.(ed), *Rare earth element geochemistry*, Elsevier Publ. p. 63-114.

Brito, M.F.L., Almeida, M.E., Macambira, M.J.B. 1999. $^{207}Pb/^{206}Pb$ age of calc-alkaline rapakivi granite in Tapajós Gold Province, Amazon craton – Brazil. In: South-American Symposium on Isotope Geology, 2, Extend Abstracts. Córdoba, Argentina CD-ROM.

Brown, G.C., Thorpe, R.S., Webb, P.C. 1984. The geochemical characteristics of granitoids in contrasting arcs and comments on magma sources. *Journ. Geol. Soc. London* **141**, 413-426.

Bullen, T.D., Clynne, M.A. 1990. Trace element and isotopic constraints on magmatic evolution at Lassen volcanic center. *J. Geophys. Res.* **95**, 19671–19691.

Burnham, C.W. 1992. Calculated melt and restite compositions of some Australian granites. *Trans. R. Sot. Edinburgh Earth Sci.* **83**, 387-397.

Chappell, B.W., White, A.J.R.. Wyborn, D. 1987. The importance of residual source material (restite) in granite petrogenesis. *J. Petrol.* **28**, 111-138.

Clemens, J.D. 1989. The importance of residual source material (restite) in granite petrogenesis: A comment. *J. Petrol.* **30**, 1313-1316.

Condie, K.C. 1998. Episodic continental growth and super-continents: a mantle avalanche connection? *Earth Planet. Sci. Lett.* **163**, 97–108.

Cordani, U.G., Tassinari, C.C.G., Teixeira, W., Basei, M.A.S., Kawashita, K. 1979. Evolução tectônica da Amazônia com base nos dados geocronológicos. In: Congresso Geológico Chileno, 2, 1979, Arica, Anais, v.4, p.177-148 (in Portuguese).

Costi, H.T., Dall'Agnol, R., Moura, C.A.V. 2000. Geology and Pb-Pb geochronology of Paleoproterozoic volcanic and granitic rocks of the Pitinga Province, Amazonian craton, northern Brazil. *Intern. Geol. Rev.* **42**, 832-849.

Costi, H.T.; Santiago, A.F., Pinheiro, S. da S. 1984. Projeto Uatumã – Jatapu; Relatório Final. Manaus: CPRM, SUREG-MA. 133p (in Portuguese).

CPRM. 1999. Programa Levantamentos Geológicos Básicos do Brasil. Roraima Central, Folhas NA.20-X-B e NA.20-X-D (integrais), NA.20-X-A, NA.20-X-C, NA.21-V-A e NA.21-V-C (parciais). Escala 1:500.000. Estado de Roraima. CPRM/Serviço Geológico do Brasil [CD-ROM]. (abstract in English)

CPRM. 2000a. Programa Levantamentos Geológicos Básicos do Brasil. Caracaraí, Folhas NA.20-Z-B e NA.20-Z-D (integrais), NA.20-Z-A, NA.21-Y-A, NA.20-Z-C e NA.21-Y-C (parciais). Escala 1:500.000. Estado de Roraima. CPRM/Serviço Geológico do Brasil [CD-ROM]. (abstract in English)

CPRM. 2000b. Programa Levantamentos Geológicos Básicos do Brasil. Projeto Especial Província Mineral do Tapajós. Geologia e recursos minerais da folha Vila Riozinho, Folha SB.21-Z-A. Escala 1:250.000. Estado do Pará. Nota Explicativa. CPRM/Serviço Geológico do Brasil [CD-ROM]. (abstract in English).

CPRM. 2000c. Programa Levantamentos Geológicos Básicos do Brasil. Projeto Especial Província Mineral do Tapajós. Geologia e recursos minerais da folha Rio Novo, Folha SB.21-Z-C. Escala 1:250.000. Estado do Pará. Nota Explicativa. CPRM/Serviço Geológico do Brasil [CD-ROM]. (abstract in English)

CPRM. 2003. Programa Levantamentos Geológicos Básicos do Brasil. Geologia, Tectônica e Recursos Minerais do Brasil: Sistema de Informações Geográficas - SIG. Rio de Janeiro : CPRM, 2003. Mapas Escala 1:2.500.000. 4 CDs ROM. (abstract in English)

CPRM. 2005. Programa Levantamentos Geológicos Básicos do Brasil. Escala 1:1000.000. Mapa Geologico do Brasil. 41 mapas Brasilia, MME. CD-ROM. (in Portuguese)

CPRM. 2006. Programa Levantamentos Geológicos Básicos do Brasil. Escala 1:1000.000. Mapa Geológico do Estado do Amazonas. Manaus, MME. Text and CD-ROM. (in Portuguese)

Dall'Agnol, R., Silva, C.M.G., Scheller, T. 1999. Fayallite-Hedembergite rhyolites of the Iriri Formation, Tapajós Gold Province, Amazonian craton: Implications for the Uatumã volcanism. In: SBG, Simpósio sobre Vulcanismo e Ambientes Associados, 1, Gramado. Boletim de Resumos.... p.31.

Delor, C., Lahondère, Egal, E., Lafon, J.-M., Cocherie, A., Guerrot, C., Ross, P., Truffert, C., Théveniaut, H., Phillips, D., Avelar, W.G. de. 2003. Transamazonian crustal growth and

reworking as revealed by the 1:500,000-scale geological map of French Guiana (2nd edition). *Géologie de la France* **2-3-4**, 5-57.

Dunphy, J.M., Ludden, J.N. 1998. Petrological and geochemical characteristics of a Paleoproterozoic magmatic arc (Narsajuaq Terrane, Ungawa Orogen, Canada) and comparisons to Superior Province granitoids. *Precamb. Res.* **91**, 109-142.

El-Sayed, M.M., Mohamed, F.H., Furnes, H., Kanisawa, S. 2002. Geochemistry and Petrogenesis of the Neoproterozoic Granitoids in the Central Eastern Desert, Egypt. *Chemie der Erde/Geochemistry* **62** (4), 317-346.

El-Sayed, M.M., Obeid, M.A., Furnes, H., Moghazi, A.M. 2004. Late Neoproterozoic volcanism in the southern Eastern Desert, Egypt: petrological, structural and geochemical constraints on the tectonic-magmatic evolution of the Allaqi Dokhan volcanic suite. *Neues Jahrbuch für Mineralogie - Abhandlungen* **180** (3), 261-286.

Faria, M.S.G. de, Santos, J.O.S. dos, Luzardo, R., Hartmann, L.A., McNaughton, N.J. 2002. The oldest island arc of Roraima State, Brazil – 2.03 Ga: zircon SHRIMP U-Pb geochronology of Anauá Complex. *In*: SBG, Congresso Brasileiro de Geologia, 41, Anais, p. 306.

Fraga, L.M.B. 2002. A Associação Anortosito–Mangerito–Granito Rapakivi (AMG) do Cinturão Guiana Central, Roraima e Suas Encaixantes Paleoproterozóicas: Evolução Estrutural, Geocronologia e Petrologia. Doctoral thesis, CPGG, UFPA. 386p.(in Portuguese).

Fraga, L.M.B., Almeida, M.E., Macambira, J.B. 1997. First lead-lead zircon ages of charnockitic rocks from Central Guiana Belt (CGB) in the state of Roraima, Brazil. In: South-American Symp. on Isotope Geology, 1997, Campos do Jordão. Resumo, Campos do Jordão [s.n.], 1997. p. 115- 117.

Griffin, T.J., Page, R.W., Sheppard, S., Tyler, I.M. 2000. Palaeoproterozoic post-collisional, high-K felsic igneous rocks from the Kimberley region of northwestern Australia. *Precamb. Res.* **101**, 1–23.

Grove, T.L., Donnelly-Nolan, J.M. 1986. The evolution of young silicic lavas at Medicine lake Volcano, California: implications for the origin of compositional gaps in calc-alkaline series lavas. *Contrib. Min. Petrol.* **92**, 281–302.

Guffanti, M., Clynne, M.A., Muffler, L.J.P. 1996. Thermal and mass implications of magmatic evolution in the Lassen volcanic region, California, and constraints on basalt influx to the lower crust. *J. Geophys. Res.* **101**, 3001–3013.

Hoskin, P.W.O., Kinny, P.D., Wyborn, D., Chappell, B.W. 2000. Identifying accessory mineral saturation during differentiation in granitoid magmas: An integrated approach. *J. Petrol.* **41**, 1365–1395.

Irvine, T.N., Baragar, W.R.A. 1971. A guide to the chemical classification of the common volcanic rocks. *Can. J. Earth Sci.* **8**, 523-548.

Jonasson, K. 1994. Rhyolite volcanism in the Krafla central volcano, northeast Iceland. *Bulletin of Volcanology* **56**, 516–528.

Jorge-João, X.S.; Santos, C.A., Provost, A. 1985. Magmatismo adamelítico Água Branca (Folha Rio Mapuera, NW do Estado do Pará). Simp. de Geol. da Amaz., 2, Belém. *Anais*... Belém, Pará, SBG, v.2, p. 93-109 (in Portuguese).

Klein, E.L., Moura, C.A.V. 2001. Age constraints on granitoids and metavolcanic rocks of the São Luis Craton and Gurupi Belt, northern Brazil: implications for lithostratigraphy and geological evolution. *Int. Geol. Rev.* **43**, 237–253.

Kober, B. 1986. Whole grain evaporation for $^{207}Pb/^{206}Pb$ age investigations on single zircons using a double filament source. *Cont. Min. Petrol.* **93**, 482-490.

Kober, B. 1987. Single grain evaporation combined with Pb+ emitter bedding for $^{207}Pb/^{206}Pb$ investigations using thermal ion mass spectrometry, and implications for zirconology. *Cont. Min. Petrol.* **96**, 63-71.

Krymsky, R. 2002. Metodologia de análise de U-Pb em mono zircão como traçador ^{235}U-^{205}Pb. Universidade Federal do Pará, Laboratório de Geologia Isotópica. 7p. (in Portuguese).

Lahtinen, R., Huhma, H. 1996. Isotopic and geochemical constrains on the evolution of the 1.93-1.79 Ga Svecofennian crust and mantle in Finland. *Precamb. Res.* **82**, 13-34.

Lamarão, C.N., Dall'Agnol, R., Lafon, J.-M., Lima, E.F. 2002. Geology, geochemistry and Pb–Pb zircon geochronology of the Paleoproterozoic magmatism of Vila Riozinho, Tapajós gold province, Amazonian craton, Brazil. *Precamb. Res.* **119** (1-4), 189–223.

Lamarão, C.N., Dall'Agnol, R., Pimentel, M.M. 2005. Nd isotopic composition of Paleoproterozoic volcanic and granitoid rocks of Vila Riozinho: implications for the crustal evolution of the Tapajós gold province, Amazon craton. *J. South Am. Earth Sci.* **18**, 277–292.

Lameyre, J. 1988. Granite settings and tectonics. *Rend. Soc. It. Mineral. Petrol.* **43**, 215–236.

Ludwig, K.R. 1999. Using ISOPLOT/Ex, version 2: a geochronological toolkit for Microsoft Excel. Berkeley Geochronological Center Special Publication Ia, 47 pp.

Macambira, M.J.B., Almeida, M.E., Santos, L.S. 2002. Idade de Zircão das Vulcânicas Iricoumé do Sudeste de Roraima: contribuição para a redefinição do Supergrupo Uatumã. In: Simpósio Sobre Vulcanismo Ambientes Associados, 2, 2002, Belém. Anais... p.22 (in Portuguese).

Maniar, P.D., Piccoli, P.M. 1989. Tectonic discrimination of granitoids. *Geol Soc.Am.Bull.* **101**, 635-643.

Moura, C.A.V., Gorayeb, P.S.S., Matsuda, N.S. 1999. Geocronologia Pb-Pb em zircão do Riolito Vila Raiol, Formação Iriri-Sudoeste do Pará. In: Simpósio de Geologia da Amazôniam 6, SBG/NO, Manaus, Brazil, Boletim de resumos expandidos, pp. 475-477 (in Portuguese).

Oliveira, M.J.R., Almeida, M.E., Luzardo, R., Faria, M.S.G. de. 1996. Litogeoquímica da Suíte Intrusiva Água Branca - SE de Roraima. Congr. Brasil. de Geol., 39, Salvador, 1996. *Anais*... Salvador, Bahia, SBG, v.2, p. 213-216 (in Portuguese).

Page, R.W. 1988. Geochronology of early to middle Proterozoic fold belts in northern Australia: a review. *Precamb. Res.* **40/41**, 1–20.

Patiño-Douce, A.E. 1996. Effects of pressure and H_2O content on the composition of primary crustal melts. *Trans. R. Soc. Edinburgh: Earth Sci.* **87**, 11–21.

Patiño-Douce, A.E. 1999. What do experiments tell us about the relative contributions of crust and mantle to the origin of granitic magmas? In: Castro, A., Fernandez, C., Vigneressese, J.L. (Eds.), Understanding Granites: Integrating New and Classical Techniques, 168. *Geological Society of London*, Special Publication **168**, 55–75.

Patiño-Douce, A.E., Beard, J.S. 1996. Effects of P, fO_2 and Mg/Fe ratio on dehydration melting of model metagreywackes. *J. Petrol.* **37**, 999–1024.

Pearce, J.A. 1996. Sources and settings of granitic rocks. *Episodes* **19**, 120-125.

Pearce, J.A., Harris, N.B., Tindle, A.G. 1984. Trace element discrimination diagrams for the tectonic interpretation of granitic rocks. *J. Petrol.* **25**, 956–983.

Peccerillo A., Taylor S.R. 1976. Geochemistry of Eocene calc-alkaline rocks from Kastamonu area, Northern Turkey. *Contrib. Miner. Petrol.* **58**, 63-81.

Petford, N., Atherton, M. 1996. Na-rich partial melts from newly underplated basaltic crust: the Cordillera Blanca Batholith, Peru. *J. Petrol.* **37**, 1491–1521.

Petford, N., Paterson, B., McCaffrey, K., Pugliese, S. 1996. Melt infiltration and advection in microdioritic enclaves. *Eur. J. Mineral.* **8**, 405–412.

Poli, G., Tommasini, S., Halliday, A.N. 1996. Trace element isotopic exchange during acid–basic magma interaction processes. *Trans. R. Soc. Edinburgh: Earth Sci.* **87**, 225–232.

Rapp, R.P. 1995. Amphibole-out phase boundary in partially melted metabasalt, its control over liquid fraction and composition, and source permeability. *J. Geophys.* Res. **100**, 15601 15610.

Rapp, R.P., Watson, E.B. 1995. Dehydration melting of metabasalt at 8–32 kbar: implications for continental growth and crust mantle recycling. *J. Petrol.* **36**, 891–931.

Reis, N.R., Faria, M.S.G. de, Fraga, L.M.B., Haddad, R.C. 2000. Orosirian calc-alkaline volcanism from eastern portion of Roraima State – Amazon Craton. *Rev. Bras. Geoc.* **30** (3), 380-383.

Reis, N.J., Fraga, L.M.B., Faria, M.S.G. de, Almeida, M.E. 2003. Geologia do Estado de Roraima. *Géologie de la France* **2-3-4**, 71-84. Abstract in English (in Portuguese)

Rickwood, P. 1989. Boundary lines within petrologic diagrams which use oxides of major and minor elements. *Lithos* **22**, 247-263.

Roberts, M.P., Clemens, J.D. 1993. Origin of high-potassium, calc-alkaline, I-type granitoids. *Geology* **21**, 825–828.

Santos J.O.S., Faria M.S.G. de, Hartmann L.A., McNaughton N.J. 2002. Significant Presence of the Tapajós–Parima Orogenic Belt in the Roraima Region, Amazon Craton based on SHRIMP U-Pb zircon Geochronology. In: SBG, Cong. Bras. Geol., 41, João Pessoa, Anais: 336.

Santos J.O.S., Faria M.S.G de, Hartmann L.A., McNaughton N., Fletcher I.R. 2001a. Oldest charnockitic magmatism in the Amazon Craton: zircon U-Pb SHRIMP geochronology of the Jaburu Charnockite, southern Roraima, Brazil. In: SBG/Norte, Simp. de Geol. da Amaz., 7, Belém. Anais..., p.70-72.

Santos, J.O.S. dos, Groves, D.I., Hartmann, L.A., McNaughton, N.J., Moura, M.B., 2001b. Gold deposits of the Tapajós and Alta Floresta domains, Tapajós–Parima orogenic belt, Amazon Craton, Brazil. Mineralium Deposita **36**, 278–299.

Santos, J.O.S. dos, Hartmann, L.A., Faria, M.S.G. de, Riker, S.R.L., Souza, M.M. de, Almeida, M.E., McNaughton, N.J. 2006. A Compartimentação do Cráton Amazonas em Províncias: Avanços ocorridos no período 2000-2006. In: SBG, Simpósio de Geologia da Amazônia, 9, Belém, CD-ROM. (in Portuguese).

Santos J.O.S., dos, Hartmann L.A., Gaudette H.E. 1997b. Reconaissance U-Pb in Zircon, Pb-Pb in Sulphides and Review of Rb-Sr Geochronology in the Tapajós Gold Province, Pará-Amazonas States, Brazil. In: South American Symp. on Isotope Geol., 1, Campos do Jordão-SP, Extended Abstracts: 280-282.

Santos J.O.S, dos, Hartmann L.A., Gaudette H.E., Groves D.I., McNaughton N.J., Fletcher I.R. 2000. A new understanding of the provinces of the Amazon Craton based on integration of field mapping and U-Pb and Sm-Nd geochronology: Gondwana Research, **3** (4): 453-488.

Santos, J.O.S., dos, Reis Neto, J.M. 1982. Algumas idades de rochas graníticas do Cráton Amazônico. Congr. Brasil. de Geol., 32, Salvador, 1982. Anais... Salvador, BA, SBG, v.1, 339-348. (in Portuguese)

Santos J.O.S., dos, Silva L.C., Faria M.S.G. de, Macambira, M.J.B. 1997a. Pb-Pb single crystal, evaporation isotopic study on the post-tectonic, sub-alkalic, A-type Moderna granite, Mapuera intrusive suite, State of Roraima, northern Brazil. In: Symposium of Granites and Associated Mineralizations, 2. Extended Abstract and Program. Salvador, Brasil: p. 273-275.

Santos, J.O.S., dos, Van Breemen, O.B., Groves, D.I., Hartmann, L. A., Almeida, M.E., McNaughton, N.J., Fletcher, I.R. 2004. Timing and evolution of multiple Paleoproterozoic magmatic arcs in the Tapajós Domain, Amazon Craton: constraints from SHRIMP and TIMS zircon, baddeleyite and titanite U–Pb geochronology. *Precamb. Res.*, vol. 131, 1-2, **10** : 73-109.

Sardinha, A.S. 1999. Petrografia do Granito Igarapé Azul, Sudeste do Estado de Roraima. Trabalho de Conclusão de Curso, UFPA, Belém, 32p. (in Portuguese)

Sardinha, A.S. 2001. Estudo dos minerais opacos do Granito Igarapé Azul, sudeste de Roraima. Relatório de Pesquisa Orientada. UFPA, Centro de Geociências, CPGG, Belém, 37p. (in Portuguese)

Scambos, T.A., Loiselle, M.C., Wones, D.R. 1986. The Center Pond pluton: The restite of the story (phase separation and melt evolution in granitoid genesis). *Am. J. Sci.* **116**, 77-103.

Scheller, T. 1998. *Zircon*. DOS Shareware, UFPA, Pará-Iso.

Shand, S.J. 1927. Eruptive Rocks, D. Van Nostrand Company, New York, pp. 360.

Singh, J., Johannes, W. 1996. Dehydration melting of tonalites: Part II. Composition of melts and solids. *Contrib. Mineral. Petrol.* **125**, 26–44.

Stacey, J.S., Kramers, J.D. 1975. Approximation of terrestrial lead isotope evolution by a two-stage model. *Earth Planetary Science Letters* **26**, 207-221.

Steiger, R.H., Jager, J. 1977. Convention of the use of decay constants in geo- and cosmochronology. *Earth Planetary Science Letters* **36**, 359- 362.

St-Onge, M.R., Lucas, S.B., Scott, D.J., Wodicka, N. 1999. Upper and lower plate juxtaposition, deformation and metamorphism during crustal convergence, Trans-Hudson Orogen (Quebec-Baffin segment), Canada. *Precambrian Res.* **93**, 27–49.

Tassinari, C.C.G., Macambira, M.J.B. 1999. Geochronological Provinces of the Amazonian Craton. *Episodes*, **22** (3), 174-182.

Tassinari, C.C.G., Macambira, M.J.B. 2004. A Evolução Tectônica do Cráton Amazônico. In: Mantesso-Neto, V., Bartoreli, A., Carneiro, C.D.R., Brito-Neves, B.B. de (eds), Geologia do Continente Sul-Americano - Evolução da Obra de Fernando Flávio Marques de Almeida, São Paulo, Ed. Beca, p. 471-485. Abstract in English (in Portuguese).

Teixeira, W., Tassinari, C.C.G., Cordani, U.G., Kawashita, K. 1989. A review of the Geochronology of the Amazonian Craton tectonic implications. *Precamb. Res.* **42**, 213-227.

Tepper, J.H., Nelson, B.K., Bergantz, G.W., Irving, A.J. 1993. Petrology of the Chilliwack batholith, North Cascades, Washington: generation of calc-alkaline granitoids by melting of mafic lower crust with variable water fugacity. *Contrib. Miner. Petrol.* **113**, 333–351.

Thompson, A.B. 1996. Fertility of crustal rocks during anatexis. *Transactions of the Royal Society of Edinburgh. Earth Sciences* **87**, 1–10.

Thuy Nguyen, T.B., Satir, M., Siebel, W., Venneman, T., van Long, T. 2004. Geochemical and isotopic constraints on the petrogenesis of granitoids from Dalat zone, southern Vietnam. *Journal of Asian Earth Sciences* **23**, 467-482.

Valério, C.S. 2006. Magmatismo Paleoproterozóico do extremo sul do Escudo das Guianas, município de Presidente Figueiredo (AM): geologia, geoquímica e geocronologia Pb-Pb em zircão. MSc thesis, Universidade Federal do Amazonas, Manaus. (in Portuguese)

Valério, C.S., Souza, V.S., Macambira, M.J.B., Milliotti, C.A., Carvalho, A.S. 2005. Geoquímica e Idade Pb-Pb de zircão no Grupo Iricoumé na região da borda norte da bacia do Amazonas, município de Presidente Figueiredo (AM). In: SBG-Núcleo Norte, Simp. Vulc. Amb. Relac., 3, Belém, *Anais*: 47-52. (in Portuguese)

Vasquez, M.V., Ricci, P.S.F., Klein, E.L. 2002. Granitóides pós-colisionais da porção leste da Província Tapajós. In: Klein, E.L., Vasquez, M.L., Rosa-Costa, L.T. (orgs), Contribuições à Geologia da Amazônia, 3, Belém, SBG, p. 63-83. Abstract in English (in Portuguese).

Veiga Jr., J.P.; Nunes, A.C.B.; Souza, E.C. de; Santos, J.O.S.; Amaral, J.E., Pessoa, M.R., Souza, S.A. de S. 1979. Projeto Sulfetos do Uatumã; Relat. Final. Manaus, DNPM/CPRM, 6v (in Portuguese).

Wall, V.J., Clemens, J.D., Clarke, D.B. 1987. Models for granitoid evolution and source compositions. *J. Geol.* **95**, 731-749.

Whalen, J.B., Currie, K.L., Chappell, B.W. 1987. A-type granites: Geochemical characteristics and discrimination. *Contrib.Miner. Petrol.* **95**, 420–436.

White, A.J.R., Chappell, B.W. 1977. Ultrametamorphism and granitoid genesis. *Tectonophysics* **43**, 7-22.

White, A.J.R., Chappell, B.W. 1983. Granitoid types and their distribution in the Lachlan Fold Belt, southeastern Australia. *Geol. Soc. Am. Memoir* **159**, 21–34.

Wolf, M.B., Wyllie, J.P., 1994. Dehydration-melting of amphibolite at 10 kbar: the effects of temperature and time. *Contrib. Mineral. Petrol.* **115**, 369–383.

Wood, D.A., Tarney, J., Varet, J., Saunders, A.D., Bougault, H., Joron, J.L., Treuil, M., Cann, J.R. 1979. Geochemistry of basalts drilled in the North America by IPOD leg 49: implications for mantle heterogeneity. *Earth Planet. Sci. Lett.* **42**, 77-97.

Wyborn, D., Chappell, B.W. 1986. The petrogenetic significance of chemically related plutonic and volcanic rock units. *Geol. Mag.* **123**, 619-628.

Zorpi, M.J., Coulon, C., Orisini, J.B. 1991. Hybridization between felsic and mafic magmas in calc-alkaline granitoids — a case study in northern Sardinia, Italy. *Chem. Geol.* **92**, 45–86.

Zorpi, M.J., Coulon, C., Orisini, J.B., Cocirta, C. 1989. Magma mingling, zoning and emplacement in calc-alkaline granitoid plutons. *Tectonophysics* **157**, 315–329.

Table 1. Chemical compositions of main calc-alkaline associations of Southern Uatumã-Anauá Domain, such as Caroebe and Igarapé Azul granitoids and volcanic rocks of Jatapu region. The geochemical data were obtained from this study[1] and CPRM (2000a)[2].

	Caroebe Granite													
	Jaburuzinho Facies									Alto Alegre Facies				
Sample	MF-073C[2]	MA-178B[1]	MA-053C[1]	MF-068A[2]	MA-103[1]	MA-112[1]	MA-053B[1]	MJ-061B[2]	MA-121[1]	MA-144A[1]	MA-053A[1]	MA-119A[1]	MA-150[1]	MA-276[1]
Rock Type	QD	QMzD	Tn	QMzD	Gd	Mgr	QMz	QMz	QMzD	Gd	Gd	Mgr	Gd	Gd
Major elements (wt %)														
SiO_2	49.50	55.13	58.31	59.09	59.60	60.44	61.04	61.60	61.85	65.95	66.24	68.03	68.22	69.14
TiO_2	1.29	1.09	0.46	0.93	0.65	1.05	0.40	0.26	0.68	0.53	0.62	0.40	0.37	0.39
Al_2O_3	16.39	16.85	21.66	16.00	17.19	15.94	20.06	16.00	17.74	16.42	15.70	15.25	16.70	15.81
Fe_2O_3*	11.38	8.61	3.21	8.40	5.29	5.84	2.88	5.53	3.93	3.45	4.00	3.01	1.85	2.53
MnO	0.15	0.15	0.04	0.17	0.09	0.09	0.05	0.24	0.07	0.06	0.07	0.07	0.05	0.07
MgO	6.00	2.73	0.96	2.70	2.19	2.57	0.90	2.80	1.57	0.98	1.51	1.05	0.49	0.66
CaO	8.30	5.98	6.85	5.70	4.75	5.33	5.69	5.30	4.66	3.19	3.42	3.12	2.54	2.18
Na_2O	3.40	3.86	4.66	3.40	4.36	3.70	4.44	3.90	4.95	4.04	3.71	3.05	4.35	4.17
K_2O	2.00	3.15	2.09	2.60	3.86	3.55	2.25	3.50	3.06	4.60	3.84	4.31	4.43	4.70
P_2O_5	0.18	1.17	0.34	0.22	0.33	0.61	0.30	0.55	0.40	0.32	0.25	0.20	0.21	0.19
LOI	1.38	0.90	0.80	0.76	1.20	0.50	1.80	0.54	0.60	0.80	0.50	0.90	0.80	0.60
TOTAL	100.02	99.62	99.38	99.97	99.51	99.62	99.81	100.22	99.51	100.34	99.86	99.39	100.01	100.44
Trace elements (ppm)														
Ni	-	16	8	-	20	25	8.2	-	20	5	23	7	3	4
Cr	-	26	17	-	22	22	17	-	13	4	22	4	4	4
Rb	101	97	69	75	72	93	93.7	82	69	117	136	157	150	120
Cs	-	0.91	2.13	-	1.20	1.00	3.90	-	1.20	1.31	5.50	6.40	1.71	1.60
Ba	433	1374	1088	803	3220	1457	813	764	1881	1893	937	710	1140	1582
Sr	714	683	1394	447	987	800	1105.6	288	1172	713	444	298	638	612
Ga	12	26	25	13	23	21	22.4	5	21	19	22	18	21	19
Ta	-	0.71	0.71	-	0.30	1.30	0.40	-	0.40	0.70	0.50	0.81	0.91	0.90
Nb	8.0	18.0	7.5	14.0	5.2	20.8	6.2	7.0	9.0	10.6	11.1	9.2	13.3	13.9
Hf		19.98	3.65	-	7.00	12.80	3.10	-	11.70	12.66	7.30	9.24	11.19	8.61
Zr	109	956	128	169	290	470	95.3	139	486	470	300	286	379	305
Y	22	44	15	26	22	47	9	18	33	18	19	28	33	27
Th	-	12.17	14.82	-	5.70	17.10	10.40	-	13.20	17.68	12.10	47.24	17.04	22.34
U	-	2.03	3.35	-	0.70	1.80	3.20	-	2.50	2.81	5.70	6.40	3.43	2.50
La	27.55	128.19	30.44	44.59	54.70	99.10	25.40	18.58	88.90	50.44	57.10	48.05	47.48	83.63
Ce	67.78	251.93	67.59	100.08	91.20	186.20	48.50	45.55	132.50	87.52	91.10	101.18	87.60	124.40
Pr	0.00	24.63	6.97	0.00	10.79	21.97	5.10	0.00	15.54	9.58	9.71	9.66	9.52	14.03
Nd	40.50	85.90	24.56	47.50	41.60	82.30	18.90	20.31	54.50	33.26	32.40	32.10	35.89	48.08
Sm	6.81	11.97	4.06	7.06	6.90	13.80	3.10	4.13	7.50	5.33	4.90	5.28	6.96	6.91
Eu	1.51	2.52	1.22	1.48	1.56	2.08	1.15	0.71	1.64	1.18	1.10	1.11	1.28	1.30
Gd	6.08	9.77	3.16	5.74	5.53	10.05	2.00	2.90	5.26	3.81	3.46	4.48	5.52	4.82
Tb	0.00	1.29	0.54	0.00	0.65	1.35	0.31	0.00	0.72	0.62	0.51	0.65	0.83	0.69
Dy	5.58	7.26	2.44	4.71	3.37	7.55	1.39	2.13	3.84	2.70	2.75	3.60	4.80	2.99
Ho	1.14	1.41	0.50	0.91	0.61	1.36	0.34	0.43	0.73	0.58	0.53	0.82	1.07	0.70
Er	2.91	4.15	1.40	2.24	1.74	3.92	0.80	1.14	2.13	1.74	1.65	2.23	2.90	2.12
Tm	0.00	0.59	0.21	0.00	0.24	0.55	0.18	0.00	0.28	0.31	0.26	0.42	0.47	0.28
Yb	2.17	4.08	1.53	1.54	1.66	4.08	0.96	0.77	2.09	1.65	2.02	2.38	2.84	1.92
Lu	0.27	0.70	0.23	0.20	0.25	0.56	0.20	0.13	0.28	0.30	0.33	0.43	0.43	0.35
ETR total	162.30	534.38	144.84	216.05	220.80	434.87	108.33	96.79	315.91	199.02	207.82	212.38	207.59	292.24
Mg#	51.45	38.91	37.48	39.08	45.48	46.78	41.26	50.15	44.42	36.14	42.96	41.27	34.53	34.06
Rb/Sr	0.14	0.14	0.05	0.17	0.07	0.12	0.08	0.28	0.06	0.16	0.31	0.53	0.24	0.20
Ba/Rb	4.29	14.19	15.76	10.71	45.03	15.70	8.68	9.32	27.14	16.19	6.89	4.53	7.60	13.18
$Eu_{(n)}/Eu$*	0.70	0.69	1.00	0.69	0.75	0.52	1.32	0.60	0.76	0.76	0.78	0.68	0.61	0.66
$(La/Sm)_n$	2.54	6.74	4.72	3.97	4.99	4.52	5.15	2.83	7.46	5.96	7.33	5.72	4.29	7.61
$(Gd/Yb)_n$	2.26	1.93	1.66	3.01	2.69	1.99	1.68	3.03	2.03	1.86	1.38	1.52	1.57	2.02
$(La/Yb)_n$	8.56	21.20	13.39	19.52	22.22	16.38	17.84	16.18	28.68	20.64	19.06	13.63	11.26	29.32

Table1 (Continued)

Igarapé Azul Granite

	Vila Catarina Facies				Cinco Estrelas Facies			Saramandaia Facies		Biotite-bearing gneiss (enclaves)		
Sample	MA-002[1]	MF-010B[2]	MF-006A[2]	MA-102A[1]	MA-079[1]	MA-147A[1]	MA-088[1]	MA-186A[1]	MA-201A[1]	MA-201B	MA-213B	MA-085B
RockType	LcMgr	Mgr	LcGd	LcMgr	QMz	Mgr	Sgr	MgrP	MgrP	QD	QMzD	Gd
Major elements (wt %)												
SiO_2	67.87	70.80	71.50	71.63	69.09	70.86	72.25	70.44	71.64	50.94	59.77	63.33
TiO_2	0.37	0.37	0.19	0.18	0.41	0.27	0.33	0.29	0.30	2.11	1.28	0.95
Al_2O_3	16.13	14.50	15.10	15.04	16.16	14.61	14.24	15.27	14.45	18.97	16.63	13.56
Fe_2O_3*	2.25	3.02	1.79	1.38	2.31	1.80	2.12	1.98	2.01	12.20	7.56	10.28
MnO	0.05	0.07	0.07	0.04	0.05	0.05	0.05	0.06	0.04	0.27	0.16	0.26
MgO	0.60	0.68	0.31	0.19	0.68	0.36	0.49	0.49	0.48	3.28	2.54	1.98
CaO	2.68	1.30	1.60	1.36	2.62	1.27	0.91	1.83	2.16	2.52	5.16	2.33
Na_2O	3.97	2.80	4.30	3.68	4.06	3.31	2.71	3.53	3.61	2.75	3.76	3.34
K_2O	4.93	5.60	4.60	5.73	4.44	6.42	6.45	5.55	4.50	5.70	2.40	3.36
P_2O_5	0.16	0.14	0.07	0.05	0.22	0.05	0.09	0.09	0.06	0.87	0.69	0.52
LOI	0.70	0.51	0.31	0.60	0.70	0.70	0.80	0.30	0.50	2.20	0.90	1.10
TOTAL	99.72	99.79	99.84	99.88	100.74	99.70	100.44	99.83	99.75	101.80	93.28	90.73
Trace elements (ppm)												
Ni	19	-	-	20	3	20	5	20	20	17	26	9
Cr	4	-	-	4	4	9	4	9	9	4	9	4
Rb	100	318	143	154	133	226	274	186	130	437	244	127
Cs	1.00	2.50	2.50	2.42	2.00	1.60	10.14	2.80	2.00	8.26	10.48	2.32
Ba	1834	526	1009	1377	1303	1064	363	1166	921	897	196	436
Sr	649	122	444	307	612	211	69	340	307	218	329	221
Ga	19	12	5	17	19	19	17	19	17	38	22	26
Ta	0.30	-	-	0.30	1.40	1.40	2.11	1.60	1.60	1.45	1.31	1.61
Nb	5.9	24.0	6.00	7.4	13.5	17.6	18.3	20.5	12.7	61.8	24.0	27.7
Hf	10.30	-	-	5.34	7.90	9.30	7.33	7.50	6.30	50.79	8.46	25.02
Zr	389	256	131	186	247	304	209	242	224	2127	326	949
Y	11	34	7	27	24	37	67	33	25	193	73	69
Th	15.60	-	-	12.99	15.69	50.60	23.28	29.20	23.90	108.70	11.89	31.88
U	2.70	-	-	3.73	2.20	6.90	9.53	10.40	7.60	9.60	2.82	9.58
La	65.80	63.31	29.90	213.36	54.88	117.80	31.11	61.00	40.20	277.80	54.79	116.53
Ce	114.20	155.04	59.32	342.20	102.56	178.40	63.53	111.40	81.70	400.12	116.04	204.50
Pr	12.09	-	-	42.29	11.77	20.78	7.52	12.36	9.81	67.19	14.86	22.39
Nd	40.10	68.50	25.20	147.88	44.28	68.90	29.00	44.10	38.50	254.57	60.74	79.90
Sm	4.80	10.50	2.88	19.64	7.80	9.70	6.72	7.70	6.90	56.05	13.40	13.72
Eu	1.07	1.74	0.61	3.02	1.51	1.13	0.80	1.32	0.96	4.16	1.79	1.21
Gd	2.43	7.38	2.08	11.44	6.23	7.29	6.98	5.85	4.90	48.50	12.18	10.72
Tb	0.31	-	-	1.34	0.88	1.04	1.56	0.83	0.62	8.37	2.25	1.64
Dy	1.62	5.26	1.71	5.20	4.83	5.19	9.47	4.79	3.66	41.03	13.16	9.63
Ho	0.27	0.84	0.33	0.80	0.86	1.02	2.17	0.91	0.65	7.24	2.61	2.16
Er	0.96	1.95	0.81	2.02	2.39	3.36	7.15	2.91	2.29	18.45	7.48	6.78
Tm	0.17	-	-	0.28	0.36	0.51	1.14	0.43	0.39	2.31	0.89	1.04
Yb	1.64	1.05	0.69	2.06	2.78	3.62	8.23	3.50	3.12	14.57	5.34	7.78
Lu	0.27	0.12	0.09	0.28	0.51	0.59	1.15	0.54	0.47	2.35	0.69	1.23
ETRtotal	245.73	315.69	123.63	791.81	241.62	419.33	176.54	257.64	194.17	1202.72	306.21	479.24
Mg#	34.76	30.98	25.70	31.41	36.84	28.60	21.51	33.00	32.33	34.05	39.76	27.41
Rb/Sr	0.15	2.61	0.32	0.50	0.22	1.07	3.95	0.55	0.42	2.00	0.74	0.58
Ba/Rb	18.34	1.65	7.06	8.92	9.77	4.71	1.33	6.27	7.07	2.05	0.81	3.42
$Eu_{(n)}/Eu$*	0.86	0.58	0.73	0.57	0.64	0.39	0.36	0.58	0.48	1.08	1.91	1.35
$(La/Sm)_n$	8.62	3.79	6.53	6.83	4.43	7.64	2.91	3.66	4.28	3.12	2.57	5.34
$(Gd/Yb)_n$	1.20	5.67	2.42	4.49	1.81	1.63	0.68	1.35	1.27	2.69	1.84	1.11
$(La/Yb)_n$	27.05	40.65	29.13	70.00	13.31	21.94	2.55	11.75	8.69	12.86	6.92	10.10

Table1 (Continued)

	Jatapu Volcanics									
	Andesite Basaltic to Rhyolite									
Sample	MF-135A[2]	MJ-164A[2]	SR-13C[2]	MJ-134A[2]	MF-142A[2]	SR-13D[2]	MF-129B[2]	MJ-133A[2]	MF-144A[2]	MF-144B[2]
RockType	And Bas	Tch And	And	Dac	Dac	Tch	Dac Ph	Dac	Dac Ph	Rhy
Major elements (wt %)										
SiO_2	54.90	57.90	59.60	63.40	63.70	63.90	65.60	65.80	68.20	74.10
TiO_2	0.53	0.68	0.83	0.55	0.55	0.51	0.50	0.29	0.39	0.29
Al_2O_3	19.60	17.60	15.70	14.90	16.10	16.00	15.30	16.30	15.20	14.00
Fe_2O_3*	7.13	7.76	7.59	6.80	5.62	5.50	5.04	4.29	3.82	1.23
MnO	0.17	0.17	0.15	0.23	0.16	0.18	0.09	0.20	0.10	0.04
MgO	2.70	3.10	3.60	2.10	1.70	1.50	2.00	0.95	1.30	0.13
CaO	7.30	4.70	5.00	3.90	3.60	3.40	3.60	3.40	3.00	0.44
Na_2O	2.80	3.70	3.40	3.10	3.60	3.40	3.00	3.50	3.30	4.00
K_2O	2.20	2.80	3.00	3.60	3.30	4.70	3.70	3.90	3.50	4.80
P_2O_5	0.14	0.26	0.29	0.17	0.18	0.15	0.18	0.10	0.11	0.03
LOI	2.17	0.97	0.40	0.91	1.14	0.46	0.57	0.85	0.64	0.65
TOTAL	99.64	99.64	99.56	99.66	99.65	99.70	99.58	99.58	99.56	99.70
Trace elements (ppm)										
Ni	40	26	59	47	24	21	16	22	18	5
Cr	80	59	103	120	63	57	36	70	34	5
Rb	168	93	118	135	120	180	105	160	150	241
Cs	-	-	-	-	-	-	-	-	-	-
Ba	611	1129	939	1052	1029	973	1179	1195	1199	1476
Sr	770	886	1058	585	547	384	810	775	672	206
Ga	-	-	-	-	-	-	-	-	-	-
Ta	-	-	-	-	-	-	-	-	-	-
Nb	11.0	11.0	14.0	12.0	11.0	16.0	14.0	10.0	12.0	20.0
Hf	-	-	-	-	-	-	-	-	-	-
Zr	142	212	238	244	242	267	210	296	238	308
Y	22	19	24	25	26	42	18	18	26	48
Th	-	-	-	-	-	-	-	-	-	-
U	-	-	-	-	-	-	-	-	-	-
La	23.05	36.83	39.02	41.43	34.30	50.88	29.67	36.99	34.55	44.59
Ce	51.37	83.16	91.92	93.58	78.52	111.60	71.06	72.30	69.60	91.30
Pr	-	-	-	-	-	-	-	-	-	-
Nd	20.60	34.26	44.23	37.68	31.11	46.41	30.65	20.61	28.89	44.60
Sm	3.39	5.46	7.77	6.02	4.84	7.20	4.83	2.94	4.25	8.14
Eu	0.69	1.26	1.57	1.11	0.95	1.32	1.09	0.67	0.83	1.34
Gd	2.06	3.19	4.23	3.52	2.69	4.60	2.85	1.81	2.30	4.46
Tb	-	-	-	-	-	-	-	-	-	-
Dy	1.46	2.35	3.19	2.71	1.93	3.88	2.20	1.08	1.66	4.60
Ho	0.26	0.44	0.61	0.53	0.36	0.76	0.43	0.20	0.31	0.92
Er	0.58	1.01	1.53	1.37	0.84	1.96	1.09	0.46	0.73	2.49
Tm	-	-	-	-	-	-	-	-	-	-
Yb	0.40	0.78	1.18	1.07	0.60	1.52	0.94	0.41	0.58	1.99
Lu	0.06	0.11	0.16	0.16	0.09	0.21	0.14	0.08	0.10	0.25
ETRtotal	103.92	168.85	195.41	189.18	156.23	230.34	144.95	137.55	143.80	204.66
Mg#	42.84	44.18	48.44	37.95	37.45	35.07	44.02	30.49	40.24	17.35
Rb/Sr	0.22	0.10	0.11	0.23	0.22	0.47	0.13	0.21	0.22	1.17
Ba/Rb	3.64	12.14	7.96	7.79	8.58	5.41	11.23	7.47	7.99	6.12
$Eu_{(n)}/Eu$*	0.74	0.75	0.76	0.68	0.73	0.66	0.83	0.82	0.73	0.62
$(La/Sm)_n$	4.28	4.24	3.16	4.33	4.45	4.44	3.86	7.92	5.11	3.45
$(Gd/Yb)_n$	4.20	3.32	2.90	2.66	3.62	2.45	2.46	3.52	3.20	1.81
$(La/Yb)_n$	34.39	31.96	22.31	26.15	38.67	22.63	21.39	60.09	40.16	15.11

Abbreviations: Lc. leuco; P. porphyrytic; Ph. porphyry; And. andesite; AndBas.andesite basaltic; Dac. dacite; Gd. granodiorite; Mgr. monzogranite; QD. Quartz diorite; QzM. Quartz monzonite; QMzD. Quartz monzodiorite; Sgr. syenogranite; Tn. tonalite; Tch. trachyte; TchAnd. trachyandesite; Rhy. rhyolite.

Table 2. Petrography summary and geographic coordinates of analyzed samples by the single-zircon Pb-evaporation and U-Pb ID-TIMS methods.

sample	stratigraphic unit	Geog. coord.	sample description	zi U-Pb ID TIMS (Ma)	MSWD	Single zi Pb-evap (Ma)	USD
HM-181	Água Branca Suite (Água Branca Granite; type-area)	01° 09' 10" S 60° 20' 35" W	Hornblende-biotite granodiorite mildly porphyritic (feldspar megacrystals) with medium grained matrix and mafic-rich clots. Accessory minerals: titanite, epidote, magnetite, apatite, allanite and zircon.	-	-	2142 ± 10 (1zi)	-
				-	-	1901 ± 5 (4zi)	1.2
MA-121	Água Branca Suite (Caroebe Granite; Jaburuzinho facies)	00° 48' 48" N 59° 50' 58" W	Hornblende-biotite quartz monzodiorite showing equigranular, medium grained texture and mafic-rich clots. Accessory minerals: titanite, epidote, magnetite, apatite and minor allanite and zircon.	-	-	1895 ± 2 (6zi)	2.1
MA-053A	Água Branca Intrusive Suite (Caroebe Granite; Alto Alegre facies)	00° 51' 55" N 59° 45' 56" W	Biotite monzogranite showing equigranular, medium grained texture and mafic-rich clots. Accessory minerals: titanite, magnetite, apatite and minor epidote, allanite and zircon.	-	-	1963 ± 4 (2zi)	1.1
				-	-	1891 ± 2 (3zi)	1.4
MA-147A	Igarapé Azul Granite (Estrela Guia facies)	00° 43' 59" N 60° 13' 12" W	Leucomonzogranite with biotite (1.3%) and muscovite (1.9%) showing equigranular and fine to medium-grained texture. Enriched in secondary minerals such as epidote (4.6%), chlorite (3.4%) and saussurite (6.1%). Acessory minerals: ilmenite, magnetite, epidote, allanite, zircon and apatite.	-	-	1964 ± 4 (1zi)	-
					-	1889 ± 5 (6zi)	3.0
MA-186A	Igarapé Azul Granite (Saramandaia facies)	00° 51' 03" N 60° 21' 45" W	Monzogranite with biotite (4.6%) and muscovite (1.0%) showing porphyrytic and medium-grained texture. Enriched in secondary minerals such as epidote (1.1%), saussurite (7.9%) and minor chlorite (0.2%). Acessory minerals: ilmenite, magnetite, epidote, zircon and apatite.	lower 206 ± 5	-	1972 ± 3 (2zi)	1.0
				upper 1913 ± 4 (4zi)	0.5	1889 ± 2 (3zi)	1.4
MA-201B	Enclave in Igarapé Azul Granite host (Vila Catarina facies)	00° 46' 21" N 60° 20' 03" W	Biotite-bearing quartz diorite with muscovite (1.0%), showing equigranular, medium- to coarse-grained texture. Acessory minerals: magnetite (6.7%), apatite (1.5%) and minor zircon, epidote and titanite. Secondary minerals: saussurite (2.1%) and chlorite (0.4%).	-	-	1967 ± 6 (2zi)	2.2
				-	-	1891 ± 3 (4zi)	1.3
MA-208	Jatapu Volcanic	00° 50' 02" N 59° 18' 14" W	Andesite with aphanitic texture enclosing some plagioclase (<50% An), amphibole and pyroxene phenocrystals. The plagioclase and amphibole could be replaced respectively by fined-grained and xenomorphic crystals of saussurite and epidote, chlorite and opaque minerals.	-	-	1966 ± 3 (4zi)	1.3
				-	-	1893 ± 5 (4zi)	2.2
MA-198	Santa Maria Enderbite	00° 50' 05" N 60° 34' 36" W	Pyroxene-bearing tonalite showing equigranular, coarse grained texture and caramelish dark green coulour. Corona texture is also commom (pyroxenes surrounded by overgrowth of reddish brown biotite). Accessory minerals: magnetite, titanite, zircon and apatite.	-	-	1890 ± 2 (6zi)	2.1
MA-226	Murauauú Granite (Mapuera Suite?)	00° 33' 39" N 60° 02' 49" W	Biotite monzogranite with equigranular and fine to medium-grained texture, deeply sheared (dynamic recrystalization, quartz ribbon) and local banding. Relicts of zoned plagioclase grains are founded. Acessory minerals: titanite, epidote, local magnetite and minor allanite, zircon and apatite.	-	-	2359 ± 7 (2zi)	4.1
				-	-	1888 ± 3 (3zi)	1.8
				-	-	1871 ± 5 (2zi)	2.6

Notes: In parenthesis the number of zircon analyses used to calculate the age. Key: U-Pb ID TIMS - Conventional U-Pb results. Pb-evap - Pb-evaporation results.

Table 3. Zircon single-crystal Pb-evaporation isotopic data for Água Branca (HM-181), Caroebe (MA-121, 053A), Igarapé Azul (MA-186A, 147A), Murauauá (MA-226) and Santa Maria (MA-198) granitoids, biotite-bearing quartz diorite enclave (MA-210B) and Jatapu volcanic rock (MA-209) samples.

sample/zircon number	Temp.(^{0}C)	ratios	$^{204}Pb/^{206}Pb$	2σ	$^{208}Pb/^{206}Pb$	2σ	$^{207}Pb/^{206}Pb$	2σ	$(^{207}Pb/^{206}Pb)_c$	2σ	age	2σ
Hornblende-biotite granodiorite (Água Branca Intrusive Suite, Água Branca Granite, type-area)												
HM181/04	1540	8/8	0.000000	2	0.22991	2885	0.13326	73	0.13326	73	2142	10
		8 (8)					**USD: 0.0**			**mean age**	**2142**	**10**
HM181/04	1500	32/32	0.000039	4	0.22878	213	0.11669	47	0.11609	51	1897	8
HM181/08	1500	28/32	0.000170	5	0.20347	104	0.11822	75	0.11581	101	1893	16
HM181/09	1500	16/16	0.000059	10	0.22804	113	0.11683	36	0.11643	59	1902	9
	1550	6/6	0.000000	2	0.28207	147	0.11677	56	0.11677	56	1908	9
HM181/13	*#1450*	*0/8*	*0.000834*	*648*	*0.16652*	*216*	*0.11759*	*247*	*0.10625*	*927*	*1736*	*160*
	1500	8/40	0.000059	2	0.17693	88	0.11635	144	0.11555	144	1889	22
		90 (144)					**USD: 1.2**			**mean age**	**1901**	**5**
Biotite-hornblende quartz diorite (Água Branca Intrusive Suite, Caroebe Granite, Jaburuzinho facies)												
MA121/01	1500	34/34	0.000046	7	0.20714	210	0.11666	11	0.11604	8	1896	1
	1550	28/28	0.000057	2	0.17310	96	0.11725	16	0.11647	14	1901	7
MA121/04	1450	36/36	0.000008	4	0.18134	48	0.11604	22	0.11593	22	1889	4
	1500	32/32	0.000011	1	0.22198	72	0.11592	23	0.11587	24	1894	4
MA121/07	1500	36/36	0.000054	10	0.22016	64	0.11673	15	0.11601	20	1896	3
	1550	36/36	0.000030	2	0.22078	49	0.11646	12	0.11614	14	1893	4
	1560	8/8	0.000000	0	0.21366	75	0.11629	14	0.11629	14	1900	2
MA121/08	1450	14/14	0.000125	9	0.20966	67	0.11717	31	0.11549	34	1888	6
	1500	36/36	0.000037	1	0.22480	31	0.11648	10	0.11602	11	1896	2
MA121/09	1450	36/36	0.000071	4	0.18868	62	0.11707	21	0.11614	20	1898	3
	1500	34/34	0.000053	2	0.23310	52	0.11668	31	0.11599	30	1896	5
	1550	22/22	0.000031	6	0.22544	114	0.11671	13	0.11636	15	1901	2
MA121/10	**1450*	*0/34*	*0.000251*	*18*	*0.17284*	*223*	*0.11851*	*27*	*0.11504*	*15*	*1881*	*2*
	**1500*	*0/4*	*0.000000*	*1*	*0.16259*	*314*	*0.11871*	*35*	*0.11871*	*35*	*1937*	*5*
MA121/11	1500	34/34	0.000038	3	0.21466	59	0.11690	15	0.11660	26	1905	4
		434 (470)					**USD: 2.1**			**mean age**	**1895**	**3**
Biotite monzogranite (Água Branca Intrusive Suite, Caroebe Granite, Alto Alegre facies)												
MA53A/03	1450	8/8	0.000067	1	0.05674	16	0.12207	56	0.12118	56	1974	8
	1500	4/4	0.000000	1	0.06020	43	0.12034	15	0.12034	15	1962	2
MA53A/06	1550	14/14	0.000000	0	0.21336	99	0.12057	33	0.12057	34	1965	5
		26 (26)					**USD: 1.1**			**mean age**	**1963**	**4**
MA53A/02	**1430*	*0/30*	*0.000236*	*7*	*0.16696*	*20*	*0.11731*	*8*	*0.11429*	*25*	*1869*	*4*
	1500	26/32	0.000042	2	0.18518	43	0.11615	8	0.11555	8	1889	1
	1550	32/32	0.000021	1	0.18057	38	0.11584	7	0.11555	7	1889	1
	1580	38/38	0.000021	1	0.17945	24	0.11599	9	0.11571	10	1891	1
MA53A/04	1450	36/36	0.000296	4	0.19825	56	0.11989	8	0.11586	13	1893	2
	1500	36/36	0.000404	8	0.26129	107	0.1214	8	0.11587	10	1894	2
	1550	16/16	0.000345	3	0.2999	78	0.12078	11	0.11609	25	1897	4
MA53A/05	*#1430*	*0/8*	*0.000257*	*1*	*0.17002*	*46*	*0.11822*	*17*	*0.11476*	*17*	*1876*	*3*
	1500	38/38	0.000045	1	0.20056	23	0.11632	10	0.11571	10	1891	2
	1550	30/30	0.000053	5	0.20114	24	0.11632	17	0.11563	18	1890	3
		252 (296)					**USD: 1.4**			**mean age**	**1891**	**2**
Epidote leucogranite with biotite and muscovite (Igarapé Azul Granite, Estrela Guia facies)												
MA147/01	*#1450*	*0/36*	*0.000675*	*8*	*0.17537*	*35*	*0.11932*	*14*	*0.11027*	*10*	*1804*	*2*
	1500	4/4	0.000080	8	0.14060	43	0.12155	27	0.12048	29	1964	4
		4 (40)					**USD: 0.0**			**mean age**	**1964**	**4**
MA147/02	*#1450*	*0/10*	*0.001202*	*158*	*0.18253*	*433*	*0.12223*	*25*	*0.10487*	*246*	*1712*	*43*
	1500	28/36	0.000041	4	0.23647	76	0.11677	10	0.11622	11	1899	2
MA147/03	1500	12/18	0.000000	0	0.15104	156	0.11639	21	0.11639	21	1902	3
MA147/04	*#1450*	*0/12*	*0.001020*	*19*	*0.20180*	*40*	*0.12254*	*30*	*0.10855*	*29*	*1776*	*5*
	1500	36/36	0.000043	4	0.20913	26	0.11601	12	0.11534	11	1885	2
MA147/05	*#1450*	*0/36*	*0.002973*	*9*	*0.34956*	*147*	*0.13919*	*25*	*0.09836*	*40*	*1594*	*8*
	1500	90/90	0.000188	5	0.37980	43	0.11783	10	0.11511	11	1882	2
MA147/06	1450	12/32	0.000154	7	0.21765	146	0.11657	22	0.11448	24	1882	4
	**1500*	*0/8*	*0.000084*	*17*	*0.26827*	*89*	*0.11505*	*117*	*0.11391*	*120*	*1863*	*19*
MA147/07	1450	26/30	0.000085	5	0.23781	173	0.11666	12	0.11555	20	1889	3

Table 3 (Continued)

sample/zircon number	Temp.(^{0}C)	ratios	$^{204}Pb/^{206}Pb$	2σ	$^{208}Pb/^{206}Pb$	2σ	$^{207}Pb/^{206}Pb$	2σ	$(^{207}Pb/^{206}Pb)_c$	2σ	age	2σ
	1500	32/32	0.000055	4	0.29694	36	0.11666	20	0.11583	14	1893	2
		240 (380)					**USD: 3.0**			**mean age**	**1891**	**6**
Biotite monzogranite with muscovite and epidote (Igarapé Azul Granite, Saramandaia facies)												
MA186/1	*#1450*	*0/28*	*0.001232*	*7*	*0.14034*	*23*	*0.13406*	*11*	*0.11765*	*18*	*1921*	*3*
	1500	24/24	0.000169	8	0.13142	37	0.12330	16	0.12111	17	1973	3
MA186/5	*#1450*	*0/36*	*0.000873*	*26*	*0.16921*	*23*	*0.12502*	*22*	*0.11472*	*53*	*1876*	*8*
	1500	38/38	0.000180	10	0.16757	19	0.12337	9	0.12081	19	1969	3
	1550	6/10	0.000177	7	0.16723	75	0.12354	22	0.12117	24	1974	3
		68 (136)					**USD: 1.0**			**mean age**	**1972**	**3**
MA186/4	1450	30/36	0.000091	2	0.21450	224	0.11673	8	0.11557	8	1889	1
	1500	30/38	0.000094	1	0.20894	78	0.11665	10	0.11539	11	1886	2
MA186/7	1450	40/40	0.000435	7	0.23793	94	0.12132	8	0.11558	10	1889	2
	**1500*	*0/40*	*0.000195*	*10*	*0.21916*	*115*	*0.11976*	*9*	*0.11714*	*19*	*1913*	*3*
MA186/9	*#1450*	*0/8*	*0.001829*	*11*	*0.20094*	*48*	*0.13380*	*29*	*0.10896*	*34*	*1782*	*6*
	1500	40/40	0.000288	12	0.19396	79	0.11973	18	0.11606	29	1897	4
		140 (286)					**USD: 1.4**			**mean age**	**1889**	**2**
Muscovite-biotite quartz diorite (biotite-bearing enclave in Igarapé Azul Granite host, Vila Catarina facies)												
MA201B/3	1450	6/20	0.000000	0	0.13700	85	0.12092	32	0.12092	32	1970	5
	1500	40/40	0.000023	3	0.09448	27	0.12053	27	0.12026	29	1960	4
	1550	36/36	0.000024	7	0.09473	36	0.12134	38	0.12104	43	1972	6
MA201B/7	1450	26/34	0.000065	15	0.13976	143	0.12184	52	0.12098	60	1971	9
		108 (130)					**USD: 2.2**			**mean age**	**1967**	**6**
MA201B/2	1500	16/16	0.000012	8	0.17761	99	0.11576	28	0.11560	25	1890	4
	1550	24/24	0.000034	7	0.18071	71	0.11614	67	0.11570	66	1891	10
MA201B/4	1450	8/8	0.000000	0	0.15066	128	0.11625	100	0.11625	100	1900	15
	1500	34/34	0.000010	3	0.16836	146	0.11583	34	0.11571	40	1891	6
	1550	8/8	0.000000	0	0.16394	81	0.11629	88	0.11629	88	1900	14
MA201B/8	1450	32/32	0.000072	4	0.19673	85	0.11661	69	0.11559	70	1889	11
	1500	34/34	0.000039	5	0.19779	87	0.11668	39	0.11622	43	1899	7
MA201B/9	1500	36/36	0.000035	15	0.22993	53	0.11587	29	0.11542	28	1887	4
	1550	28/28	0.000043	11	0.24776	167	0.11620	61	0.11563	70	1890	11
		220 (220)					**USD: 1.3**			**mean age**	**1891**	**3**
Andesite (Jatapu Volcanic rock)												
MA208/7	**1450*	*0/14*	*0.000081*	*7*	*0.15664*	*12*	*0.12037*	*35*	*0.1192*	*35*	*1945*	*5*
	1500	34/34	0.00005	35	0.11339	10	0.12123	32	0.12082	31	1969	5
MA208/9	1450	28/28	0.000022	2	0.02024	19	0.12095	24	0.12063	21	1966	3
	1480	28/36	0.000082	11	0.05157	139	0.12193	55	0.12089	56	1970	8
MA208/11	1450	16/22	0.000118	8	0.05429	216	0.12181	35	0.12025	37	1960	5
MA208/12	1450	8/8	0.00007	24	0.12551	61	0.12114	161	0.1202	164	1960	24
		114 (142)					**USD: 1.3**			**mean age**	1966	3
MA208/2	1450	32/36	0.000178	17	0.33144	982	0.11784	62	0.11558	34	1889	5
	1500	38/38	0.000035	6	0.34356	378	0.11642	22	0.11587	22	1894	3
MA208/3	1500	30/36	0.000059	47	0.24595	483	0.1161	45	0.1154	25	1886	4
MA208/4	1500	22/22	0.000031	3	0.27797	88	0.11663	33	0.11612	22	1898	3
MA208/5	**1500*	*0/8*	*0,000000*	*2*	*0.34995*	*724*	*0.11357*	*179*	*0.11357*	*179*	*1858*	*28*
MA208/6	**1450*	*0/4*	*0,000000*	*2*	*0.22383*	*372*	*0.11465*	*29*	*0.11465*	*29*	*1875*	*5*
MA208/10	1450	8/8	0.000032	38	0.15001	72	0.11608	106	0.11565	118	1890	18
		130 (152)					**USD: 2.2**			**mean age**	1893	5
Pyroxene-bearing tonalite (Santa Maria Enderbite)												
MA198/1	**1450*	*0/16*	*0.000239*	*11*	*0.15289*	*215*	*0.11188*	*42*	*0.1083*	*31*	*1830*	*7*
	1500	36/36	0.000042	3	0.21636	110	0.11624	13	0.11564	10	1890	2
	1550	14/14	0.000067	8	0.21481	46	0.1163	37	0.11549	55	1888	9
MA198/2	1450	36/36	0.000036	5	0.17197	75	0.11597	24	0.11554	22	1889	3
	1500	32/32	0.000012	1	0.19441	154	0.11545	27	0.11539	25	1886	4
	1550	32/32	0.000024	2	0.20493	41	0.11609	8	0.11581	8	1893	1
	**1600*	*0/4*	*0.000038*	*6*	*0.21786*	*88*	*0.11462*	*14*	*0.1141*	*16*	*1874*	*2*
MA198/3	**1450*	*0/36*	*0.000047*	*2*	*0.13994*	*50*	*0.11539*	*18*	*0.11456*	*11*	*1886*	*3*
	1500	40/40	0.000027	1	0.16674	64	0.11592	11	0.11557	13	1889	2
	1550	32/32	0.000027	4	0.17937	84	0.11608	8	0.11577	8	1892	*1*

Table 3 (Continued)

sample/zircon number	Temp.(^{0}C)	ratios	$^{204}Pb/^{206}Pb$	2σ	$^{208}Pb/^{206}Pb$	2σ	$^{207}Pb/^{206}Pb$	2σ	$(^{207}Pb/^{206}Pb)_c$	2σ	age	2σ
MA198/4	1450	28/28	0.000058	5	0.19464	275	0.11627	16	0.11556	16	1889	*3*
MA198/5	1450	36/36	0.000041	2	0.23494	36	0.11609	12	0.1155	14	1888	*2*
	1500	32/32	0.000088	2	0.23966	43	0.11701	11	0.1159	9	1894	1
	1550	34/34	0.000115	6	0.23739	85	0.11647	13	0.11498	11	1880	2
	1600	34/34	0.000072	2	0.23677	29	0.11657	8	0.11555	7	1889	1
		266 (392)					**USD: 2.1**			**mean age**	**1890**	**2**
Mylonitic monzogranite (Murauaú Granite)												
MA226/10	**1450*	*0/6*	*0.000123*	*49*	*0.08105*	*57*	*0.14506*	*22*	*0.14347*	*67*	*2270*	*8*
	1500	32/32	0.000022	9	0.11179	77	0.15176	14	0.15176	14	2366	2
MA226/16	*#1450*	*0/32*	*0.004657*	*51*	*0.27911*	*164*	*0.19585*	*49*	*0.13479*	*34*	*2161*	*4*
	1480	36/36	0.000029	1	0.11560	36	0.15111	10	0.15073	11	2355	1
	1510	38/38	0.000009	1	0.13326	18	0.15129	14	0.15118	14	2360	2
		106 (144)					**USD: 4.1**			**mean age**	**2359**	**7**
MA226/12	1450	20/20	0.000221	1	0.13016	37	0.11840	11	0.11552	13	1888	2
	1500	28/28	0.000080	3	0.12844	88	0.11667	14	0.11558	17	1889	3
	#1550	*0/12*	*0.000349*	*37*	*0.14478*	*68*	*0.11744*	*19*	*0.11272*	*54*	*1844*	*9*
MA226/14	1500	22/28	0.000086	2	0.12237	53	0.11623	8	0.11510	9	1882	1
MA226/17	**1450*	*0/40*	*0.000280*	*2*	*0.14414*	*72*	*0.11794*	*11*	*0.11420*	*12*	*1868*	*2*
	**1500*	*0/28*	*0.000038*	*2*	*0.14879*	*40*	*0.11782*	*27*	*0.11734*	*27*	*1916*	*4*
MA226/18	1500	38/38	0.000039	2	0.12377	14	0.11606	10	0.11552	10	1888	2
	1550	38/38	0.000048	2	0.12261	14	0.11626	8	0.11563	8	1890	1
		146 (232)					**USD: 1.8**			**mean age**	**1888**	**3**
MA226/01	1500	36/36	0.000145	3	0.12202	14	0.11660	7	0.11463	9	1874	1
	1550	32/32	0.000165	3	0.12276	46	0.11660	7	0.11430	13	1869	2
MA226/02	*#1450*	*0/34*	*0.000365*	*7*	*0.11253*	*17*	*0.11742*	*15*	*0.11238*	*11*	*1839*	*2*
	**1500*	*0/36*	*0.000261*	*11*	*0.10639*	*48*	*0.11677*	*11*	*0.11341*	*11*	*1855*	*2*
MA226/03	1500	38/38	0.000216	3	0.15026	63	0.11688	11	0.11410	12	1866	2
	**1550*	*0/4*	*0.000251*	*2*	*0.15427*	*148*	*0.11697*	*30*	*0.11359*	*30*	*1858*	*5*
		106 (180)					**USD: 2.6**			**mean age**	**1871**	**5**

Notes: Crystal numbers are indicated. The column number of ratios shows the total of isotopic ratios used to the age calculation and, in parenthesis, the total isotopic ratios measured. Evaporation steps in italics were not included in the age calculation of each grain due to: * too much higher or lower values of the $^{207}Pb/^{206}Pb$ ratio in relation to the average of the zircon, and # $^{204}Pb/^{206}Pb > 0.0004$.

Table 4. U-Pb isotopic data (ID-TIMS) for zircon from Igarapé Azul granite sample (MA-186A).

Sample		Concentrations		Atomic ratios								Ages (Ma)			
Zircon Number	Weight (mg)	ppm U	ppm Pb	$^{206}Pb/^{204}Pb^{c1}$	%err	$^{207}Pb^*/^{235}U^{c2}$	%err	$^{206}Pb^*/^{238}U^{c2}$	%err	$^{207}Pb^*/^{206}Pb^{*c2}$	%err	$^{206}Pb^*/^{238}U$	$^{207}Pb^*/^{235}U$	$^{207}Pb^*/^{206}Pb^*$	(%)
MA-186A-1	0.56	13.90	2.49	418.134	0.263	2.19649	0.272	0.146600	0.241	0.899070	0.108666	882	1180	1777	50
MA-186A-2	0.465	59.51	8.76	300.536	0.099	1.62097	0.402	0.114056	0.377	0.938852	0.103076	696	978	1680	41
MA-186A-3	0.92	9.33	1.49	344.142	1.610	1.93824	2.970	0.132913	2.870	0.974348	0.105764	804	1094	1728	47
MA-186A-4	0.273	92.60	18.53	488.003	0.210	2.51441	0.422	0.166274	0.417	0.988353	0.109676	992	1276	1794	55

Notes: Maximum total blanks for zircon analyses are 10 pg for Pb and 2 pg for U. Stacey and Kramers (1975) values were used.
[c1] Measure ratios corrected for mass fractionation; [c2] Ratios corrected for spike, fractionation, blank and initial common Pb following Stacey and Kramers (1975) model. Erros are at 2 σ; [d] Concordance in relation to Concordia curve: $100t(^{206}Pb/^{238}U)/t(^{207}Pb/^{206}Pb)$.

Table 5. Summary of new and previous zircon Pb-evaporation and U-Pb (ID-TIMS and SHRIMP), and local WR Rb-Sr isochron ages, yielded from volcano-plutonic rocks younger than 1900 Ma of the Ventuari-Tapajós (or Tapajós-Parima) Province.

Symbol	Reference Number	Rock type (sample code)	Stratigraphic unit	Age (Ma)	Reference	Method
Uatumã-Anauá Domain (Southern Area)						
UA1	1	Madeira Granite (PHR-178)	Madeira Suite	1817 ± 2	Costi *et al.* (2000)	C
	2	Madeira Granite (PHR-191)	Madeira Suite	1820 ± 1	Costi *et al.* (2000)	C
	3	Madeira Granite (PHR-193)	Madeira Suite	1822 ± 2	Costi *et al.* (2000)	C
	5	Madeira Granite (PHR-125)	Madeira Suite	1824 ± 2	Costi *et al.* (2000)	C
	5	Europa Granite (PHR-192)	Madeira Suite	1829 ± 1	Costi *et al.* (2000)	C
	6	Moderna Granite (MJ-59A)	Madeira Suite	1814 ± 27	Santos *et al.* (1997b)	B
UA2	7	Weathered gneiss (JO-05)	Mapuera Suite?	1868 ± 8	Santos *et al.* (2002)	E
	8	Mylonitic granite (MF-17)	Meretxa Granite (Mapuera Suite?)	1869 ± 10	CPRM (2003)	E
	9	Hastingsite syenogranite (km 199)	Abonari Granite (Mapuera Suite)	1871 ± 5	Santos *et al.* (2002)	E
	10	Mylonitic monzogranite (MA-226)	Murauauú Granite (Mapuera Suite?)	1871 ± 5	This paper	C
	11	Charnockite (MF-99)	Jaburu Charnockite	1873 ± 6	Santos *et al.* (2001a)	E
	12	Mylonite (JO-08)	Alalaú Granite (Mapuera Suite?)	1876 ± 4	Santos *et al.* (2002)	E
	13	Weathered granitoid (JO-07)	Mapuera Suite?	1879 ± 3	Santos *et al.* (2002)	E
	14	Weathered granitoid (JO-06)	Mapuera Suite?	1880 ± 3	Santos *et al.* (2002)	E
UA3	15	Epizonal rhyolite	Iricoumé Volcanics (Presidente Figueiredo region)	1883 ± 4	Valério *et al.* (2005)	C
	16	Rhyolite (PHR-06)	Iricoumé Volcanics (Pitinga region)	1888 ± 3	Costi *et al.* (2000)	C
UA4	17	Monzogranite (MA-186A)	Igarapé Azul Granite (Saramandaia Facies)	1889 ± 2	This paper	C
	18	Monzogranite (MA-147A)	Igarapé Azul Granite (Cinco Estrelas Facies)	1889 ± 5	This paper	C
	19	Granitic veins in biotite-bearing enclave (MA-201B)	Igarapé Azul Granite (Vila Catarina facies)	1891 ± 3	This paper	C
	20	Monzogranite (MA-186A)	Igarapé Azul Granite (Saramandaia Facies)	1913 ± 4	This paper	D
UA5	21	Mylonitic biotite granite	Água Branca Suite (Presidente Figueiredo region)	1890 ± 2	Valério (2006)	C
	22	Enderbite (MA-198)	Santa Maria Enderbite	1890 ± 2	This paper	C
	23	Monzogranite (MA-53A)	Água Branca Suite (Caroebe Granite, Alto Alegre Facies)	1892 ± 2	This paper	C
	24	Quartz Monzodiorite (MF-68A)	Água Branca Suite (Igarapé Dias Quartz Monzodiorite)	1891 ± 6	CPRM (2003)	E
	25	Quartz Monzodiorite (MA-121)	Água Branca Suite (Caroebe Granite, Jaburuzinho Facies)	1895 ± 3	This paper	C
	26	Porphyrytic biotite granite	Água Branca Suite (Presidente Figueiredo region)	1895 ± 6	Valério (2006)	C
	27	Mylonitic hornblende-biotite granite	Água Branca Suite (Presidente Figueiredo region)	1898 ± 3	Valério (2006)	C
	28	Granodiorite (HM-181)	Água Branca Suite (Água Branca Granite, type-area)	1901 ± 5	This paper	C
	29	-	Água Branca Suite (Northwestern of Pará)	1910 ± 23	Jorge-João *et al.* (1985)	A
UA6	30	Porphyry Dacite (MA-209)	Jatapu Volcanics (Jatapu River)	1893 ± 2	Macambira *et al.* (2002)	C
	31	Andesite (MA-208)	Jatapu Volcanics (Jatapu River)	1893 ± 4	This paper	C
	32	Canoas Rhyodacite (MF-34)	Jatapu Volcanics (BR-174, km 164)	1896 ± 7	Santos *et al.* (2002)	E
Tapajós Domain						
T1	33	Caroçal Granite	Maloquinha Suite	1870 ± 4	Santos *et al.* (2001b)	E
	34	Pepita Alaskitic Granite	Maloquinha Suite	1872 ± 2	Santos *et al.* (2001b)	E
	35	Barro Vermelho Granite	Maloquinha Suite	1873 ± 6	Santos *et al.* (2001b)	E
	36	Santa Rita Granite	Maloquinha Suite	1874 ± 7	Santos *et al.* (2001b)	E
	37	Leucomonzogranite	Maloquinha Suite	1880 ± 9	Lamarão *et al.* (2002)	C
	38	Syenogranite	Maloquinha Suite	1882 ± 4	CPRM (2000b)	C
T2	39	Rosa de Maio Granite	Parauari Suite	1879 ± 3	Santos *et al.* (1997a)	D
	40	Anortosite	Ingarana Gabbro	1879 ± 3	Santos *et al.* (2001b)	E
	41	Gabbro	Ingarana Gabbro	1880 ± 2	Santos *et al.* (2004)	E
	42	Monzogranite	Jardim do Ouro Granite	1880 ± 3	Lamarão *et al.* (2002)	C
	43	Crepori River Granite	Parauari Suite	1883 ± 2	CPRM (2000b)	E
	44	Penedo Granite	Parauari Suite	1883 ± 4	Santos *et al.* (2001b)	E
	45	Cumaru Rapakivi Granite	Parauari Suite	1883 ± 8	Brito *et al.* (1999)	C
	46	Gabbro	Ingarana Gabbro	1887 ± 3	CPRM (2000b)	C
	47	Sao Jorge Monzogranite	Younger São Jorge Granite?	1887 ± 10	Santos *et al.* (2004)	E
	48	Monzogranite	Younger São Jorge Granite	1891 ± 3	Lamarão *et al.* (2002)	C
	49	Ouro Roxo Tonalite	Tropas Granite	1892 ± 3	Santos *et al.* (2004)	E

Table 5 (continued)

Symbol	Reference Number	Rock type (sample code)	Stratigraphic unit	Age (Ma)	Reference	Method
T2	50	Abacaxis Monzogranite	Tropas Granite	1892 ± 6	Santos *et al.* (1997a)	D
	51	Granite	Parauari Suite	1893 ± 2	CPRM (2000b)	C
	52	Tropas Tonalite	Tropas Granite	1898 ± 2	Santos *et al.* (2000)	E
T3	53	Pacu Rhyodacite Tuff	Iriri Volcanics	1870 ± 8	Santos *et al.* (2001b)	E
	54	Ignimbrite	Moraes de Almeida Volcanics	1875 ± 4	Lamarão *et al.* (2002)	C
	55	Trachyte	Moraes de Almeida Volcanics	1881 ± 4	Lamarão *et al.* (2002)	C
	56	Rhyolite	Iriri Volcanics	1888 ± 2	CPRM (2000b)	C
	57	Alkali-rhyolite	Iriri Volcanics	1888 ± 2	Dall'Agnol *et al.* (1999)	C
	58	Rhyolite	Iriri Volcanics	1888 ± 6	Moura *et al.* (1999)	D
	59	Rhyolite	Moraes de Almeida Volcanics	1890 ± 6	Lamarão *et al.* (2002)	C
	60	Dacite	Iriri Volcanics	1893 ± 3	CPRM (2000c)	C
	61	Uruá Tuff	Iriri Volcanics	1897 ± 5	Santos *et al.* (2004)	E
	62	Basalt	Iriri Volcanics	1898 ± 7	Santos *et al.* (1997a)	D

Notes: A. WR Rb-Sr isochron; B. Pb-Pb evaporation on single filament; C. Pb-Pb evaporation on double filament; D. U-Pb ID TIMS; E. U-Pb SHRIMP. Numbers 1-62 are the same of fig. 15.

Table 6. Summary of ages and possible sources of the inherited zircon crystals from volcano-plutonic rocks younger than 1900 Ma of the Ventuari-Tapajós (or Tapajós-Parima) Province.

Domain	Reference Number	Rock type	Stratigraphic unit	Age (Ma)	Inheritance Interpretation	Reference	Method
Uatumã-Anauá Domain (Southern Area)							
UA6	31	Andesite (Jatapu river)	Jatapu Volcanic	1966 ± 3	Martins Pereira Granite	This paper	C
UA4	18	Monzogranite (Cinco Estrelas Facies)	Igarapé Azul Granite	1964 ± 4	Martins Pereira Granite	This paper	C
	19	Biotite-bearing meta-quartz diorite enclave	Igarapé Azul Granite	1967 ± 6	Martins Pereira Granite	This paper	C
	17	Monzogranite (Saramandaia Facies)	Igarapé Azul Granite	1972 ± 3	Martins Pereira Granite	This paper	C
UA5	23	Monzogranite (Alto Alegre Facies)	Água Branca Suite (Caroebe Granite)	1963 ± 4	Martins Pereira Granite	This paper	C
	28	Granodiorite	Água Branca Suite (Água Branca Granite)	2142 ± 10	Early Transamanzonian	This paper	C
UA2	10	Murauauá Granite	Mapuera Suite	1888 ± 3	Água Branca Suite?	This paper	C
				2359 ± 7	Siderian (Central Amazonian)	This paper	C
Tapajós Domain							
T3	53	Pacu Rhyodacite Tuff	Iriri Volcanic	1956 ± 7	Creporizão Suite	Santos *et al.* (2001b)	E
T2	47	Monzogranite	Younger São Jorge Granite?	1962 ± 19	Creporizão Suite	Santos *et al.* (2004)	E
				2733 ± 9	Archean		E
	41	Gabbro	Ingarana Gabbro	2007± 6	Cuiú-Cuiú Complex	Santos *et al.* (2004)	E
T3	62	Basalt	Iriri Volcanic	1972 ± 15	Creporizão Suite	Santos *et al.* (1997a)	D
	61	Uruá Tuff	Iriri Volcanics	2014 ± 11	Cuiú-Cuiú Complex	Santos *et al.* (2004)	E
				2457 ± 7	Siderian		E
				2662 ± 18	Archean		E
T1	36	Santa Rita Granite	Maloquinha Suite	1983 ± 19	Creporizão Suite	Santos *et al.* (2001b)	E
				2459 ± 11	Siderian		E
				2849 ± 10	Archean		E
	33	Caroçal Granite	Maloquinha Suite	1999 ± 8	Cuiú-Cuiú Complex	Santos *et al.* (2001b)	E
				2634 ± 9	Archean		E
				2679 ± 10	Archean		E
				2714 ± 8	Archean		E
	35	Barro Vermelho Granite	Maloquinha Suite	2207 ± 8	Early Transamanzonian	Santos *et al.* (2001b)	E

Notes: Method references as in table 5. Reference Number 1 to 62 and symbols UA1-T3 are as in Fig. 15.

4.5 - Nd-Pb isotopic constraints on the Paleoproterozoic geodynamic evolution of the central region of the Guyana Shield, Brazil

Marcelo E. Almeida[1,2*], Moacir J. B. Macambira[2], Franck Poitrasson[3], Cândido A.V. Moura[2], Elma C. Oliveira[2]

[1] CPRM – Geological Survey of Brazil, Av. André Araújo 2160, Aleixo, CEP 69060-001, Manaus, Amazonas, Brazil

[2] Isotope Geology Laboratory, Center of Geosciences, Federal University of Pará, Rua Augusto Corrêa s/n, Guamá, CEP 66075-110, Belém, Pará, Brazil

[3] Laboratoire des Mécanismes et Transferts en Géologie, CNRS, Université Paul Sabatier, Av. Edouard Belin 14, 31000 - Toulouse, France

* Corresponding author; ph.: +55-92-2126-0357, fax: +55-92-2126-0319, e-mail adress: marcelo_almeida@ma.cprm.gov.br

ARTIGO A SER SUBMETIDO

Words: summary (85), abstract (300 words), body text (9397 words, including references), figure captions (698 words) and table caption (292 words)

Total: 4 tables and 8 figures

ABSTRACT

Previous zircon geochronology from southeastern Roraima, central part of the Guyana Shield, show that the granitoids from Uatumã-Anauá domain exhibits different magmatic events with distinct interval ages. New Nd-Pb isotopic data yield convencing evidence of crustal origin. In the Northern Uatumã-Anauá domain, the 1.97 Ga Martins Pereira Granite shows NdT_{DM} model ages with 2.67-2.33 Ga range, including negative $\varepsilon Nd_{1.97}$ (-0.92 to -4.74) and high $^{207}Pb/^{204}Pb$ (15.58-15.70) ratios. This renders the Martins Pereira granitoids a good example of high-K calc-alkaline magmatism generated by reworking and recycling of a pre-existing, older crust (*e.g.* Archean Central Amazonian province sources), related probably to the final stages of Anauá Arc evolution (collisional event). The S-type Serra Dourada Granite is related to the early collisional stage (1962 Ma) and their NdT_{DM} model ages (2.53-2.39 Ga) and $\varepsilon Nd_{1.96}$ (-1.08 to -4.34) imply also older crustal-derived sources. The most suitable sources is the 1.96 Ga metavolcano-sedimentary sequence (Cauarane Group-related) that shows similar NdT_{DM} model ages (2.46-2.27 Ga, local 2.64 Ga) and $\varepsilon Nd_{1.97}$ +1.23 to -4.16. In the southern Uatumã-Anauá domain, the 1.90-1.89 Ga Caroebe Granite presents very homogeneous $^{207}Pb/^{204}Pb$ ratios (ca. 15.54). The $\varepsilon Nd_{1.89}$ (+0.46 to –2.05, locally -2.60 to -4.27) and NdT_{DM} model ages (2.29-2.16 Ga, locally 2.47-2.37 Ga) are similar to the 1.89 Ga Igarapé Azul granitoids ($\varepsilon Nd_{1.89}$ -0.02 to -1.61 and NdT_{DM} 2.28-2.14 Ga), however this last shows more scattered $^{207}Pb/^{204}Pb$ ratios (15.42-15.65). Thus, no conspicuous juvenile pattern is identified and mantle-derived origin is not probably a viable model for these granitoids. Their origin involves probably Transamazonian TTG metaigneous rocks (juvenile crust?) and Orosirian metavolcano-sedimentary sources by partial melting in association with older sialic crustal sources (*e.g.* Central Amazonian and Archean provinces) in the extensional setting driven by underplating mechanism. This geological picture is similar to other domains of the Ventuari-Tapajós (or Tapajós-Parima) geochronological province.
Keywords: Nd-Pb isotopes, high-K calc-alkaline granites, Guyana Shield, geodynamic evolution

INTRODUCTION

The Guyana Shield represents the northern segment of the Amazonian Craton in South America, partially formed during periods of intense granitic magmatism between 2.1 and 1.5 Ga (**Fig. 1a-b**). Geochronological and isotopic studies are scarce, which make hard to establish a refined timing of the lithostructural, magmatic and metamorphic events up until the last decade. The main crustal evolution models for this region (**Fig. 1a-b**; Cordani *et al.,* 1979, Teixeira *et al.,* 1989, Tassinari 1996, Tassinari and Macambira, 1999, 2004; Santos *et al.,* 2000, 2004) pointed out that several Paleoproterozoic orogenic belts (*e.g.* Ventuari-Tapajós or Tapajós-Parima and Maroni-Itacaiúnas or Transamazon) provinces are accreted through time to an older Archean craton (Central Amazonian Province).

The study area is located in the southeastern Roraima (Brazil), central portion of the Guyana Shield and, despite of recent geological, geochemical and geochronological data (*e.g.* Oliveira *et al.,* 1996, Santos *et al.,* 2000, Almeida *et al.,* 2002, Almeida and Macambira, 2003, CPRM 2000, 2003), its characteristic and geological significance are not fully understood. This paper focuses on the crustal formation of the central portion of the Guyana Shield (**Fig. 1**), using previous zircon geochronological data and new Nd-Pb isotopic signatures of granitoids to further

constraints their lithostratigraphy, sources (mainly unexposed basement terranes) and geodynamic evolution. Thus, the studied granitoids could allow the construction of tectonic models, using isotope tracers in order to more clearly define the nature of the crust and relative contributions of crustal-derived and/or mantle-derived melts.

REGIONAL GEOLOGY AND PREVIOUS GEOCHRONOLOGICAL DATA

Regional geological maps (CPRM, 2000, Almeida *et al.*, 2002) and some few zircon geochronological data (Almeida *et al.,* 1997, Santos *et al.,* 1997, Macambira *et al.,* 2002, CPRM, 2003) have showed that Paleoproterozoic granitoids and volcanic rocks (1.97-1.81 Ga) are widespread in southeastern Roraima, intruding inliers of basement rocks with maximum ages around 2.03 Ga (Faria *et al.,* 2002). According to the geochronological provinces models (*e.g.* Tassinari and Macambira 1999, 2004, Santos *et al.,* 2000, 2004, 2006) the study area is part of the Ventuari-Tapajós (western part) or Tapajós-Parima and Central Amazonian (eastern part) province, and probably of the Maroni-Itacaiúnas Province and K´Mudku Shear Belt (northeasternmost portion) (**Fig. 1a-b**).

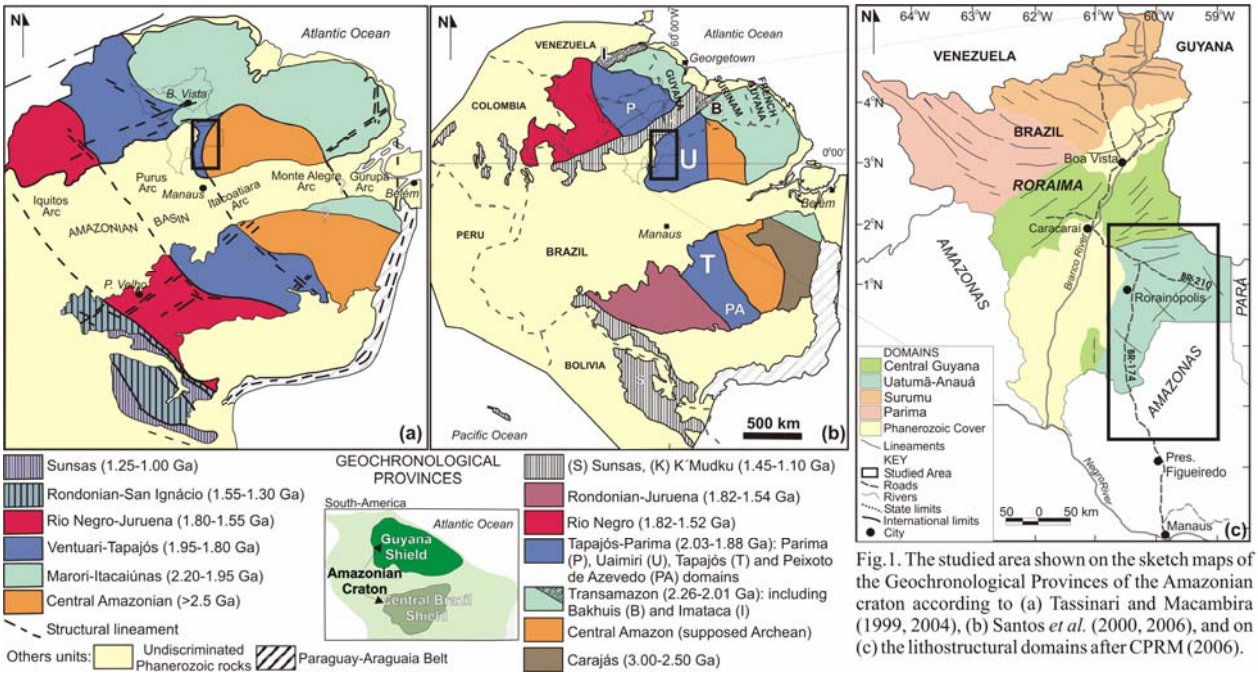

Fig.1. The studied area shown on the sketch maps of the Geochronological Provinces of the Amazonian craton according to (a) Tassinari and Macambira (1999, 2004), (b) Santos *et al.* (2000, 2006), and on (c) the lithostructural domains after CPRM (2006).

The Ventuari-Tapajós (or Tapajós-Parima) province is a paleoproterozoic orogenic belt with north-northwest trend and include geological units which range from ca. 2.10 to 1.87 Ga in age (Santos *et al.,* 2000; Tassinari and Macambira 1999, 2004). The Central Amazonian Province (**Fig. 1a-b**) includes granitoids and volcanic rocks with no regional metamorphism and

compressional folding (Tassinari and Macambira, 1999, Santos *et al.,* 2000). Tthe basement rarely crops out and is poorly studied. Estimates of its formation age are yielded by some Nd model ages at ca. 2.3-2.5 Ga and older (Tassinari and Macambira, 1999, 2004), but the Archean rocks are only exposed in the Carajás region (southeastern Pará, Brazil). The Maroni-Itacaiúnas (or Transamazon) Province is characterized as an orogenic belt with Rhyacian ages (2.25-2.00 Ga, **Fig. 1a-b**) and is correlated to Birimian belt in West Africa (Tassinari and Macambira, 1999, 2004; Santos *et al.,* 2000; Delor *et al.,* 2003). The K´Mudku Shear Belt (low grade) is characterized by mylonitic zones with ca. 1.20 Ga and cross-cut at least three provinces including Tapajós-Parima and Transamazon provinces.

The model of Reis *et al.* (2003) modified by CPRM (2006) is based only on lithostructural features, taking into account the different lithological associations and geochronological data for the Roraima and northeastern Amazonas. These authors subdivided this region into four major domains with roughly estimated limits, each one containing a wide range of rock types and stratigraphic units: Surumu, Parima, Central Guyana and Uatumã-Anauá domains (**Fig. 1c**).

According to Reis *et al.* (2003), the Central Guyana Domain (**Figs 1c and 2**) shows essentially granulites, orthogneiss, mylonites and metagranitoids (Rio Urubu Metamorphic Suite) associated with low (Cauarane Group) to high (Murupu Metamorphic Suite) metamorphic grade metavolcano-sedimentary sequences, S-type granite (Curuxuim Granite) and a strong NE-SW trend. The Uatumã-Anauá Domain in the northern area (**Fig. 2**) is characterized by E-W to NE-SW lineaments and old metamorphic basement formed in an inferred island arc setting (Faria *et al.,* 2002). This basement is composed by metagranitoids to orthogneisses TTG-like (2028 Ma; Anauá Complex), enclosing metamafic to metaultramafic xenoliths, in association with inliers of metavolcano-sedimentary rocks (Cauarane Group), and is intruded by S-type (Serra Dourada Granite) and high-K, I-type calc-alkaline (Martins Pereira) granites (1975-1962 Ma, **Table 1**).

In the southern area of Uatumã-Anauá domain (**Fig. 2**), younger intrusive granites with no regional deformation and metamorphism are the most common. The most expressive magmatism is related to the calc-alkalines Caroebe, Água Branca and Igarapé Azul granitoids (**Table 1**) associated with coeval Iricoumé volcanic rocks (1901-1889 Ma), but locally it was also observed igneous charnockitic (Igarapé Tamandaré) and enderbitic (Santa Maria) plutons (1890 Ma). Several A-type granitic bodies are widespread in the Uatumã-Anauá Domain represented by

Moderna-Água Boa (1.81 Ga) and Mapuera-Abonari (1.87 Ga) granitic events (*e.g.* Costi *et al.,* 2000, Santos *et al.,* 1997, CPRM, 2003).

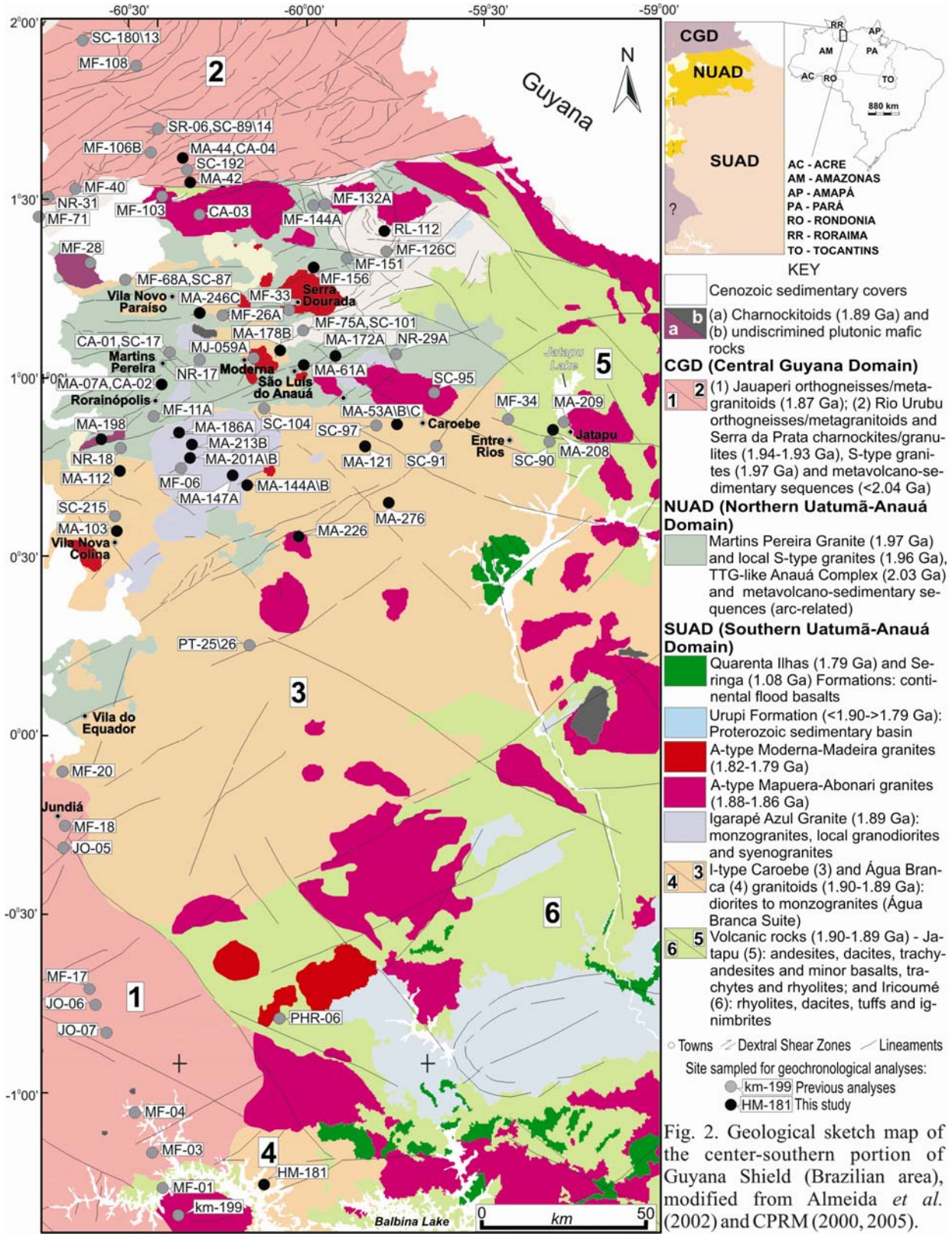

Fig. 2. Geological sketch map of the center-southern portion of Guyana Shield (Brazilian area), modified from Almeida *et al.* (2002) and CPRM (2000, 2005).

ANALYTICAL PROCEDURES

The isotopic ratios of Nd from whole-rock and Pb from feldspar were measured respectively in a Finnigan Mat 262 and VG Sector 54 mass spectrometers at the Isotope Geology Laboratory (Pará-Iso) of the Federal University of Pará (Belém, Brazil). For the Sm-Nd analysis, rock powders (ca. 100mg milled under 200 mesh) were dissolved in high pressure teflon vials at 220°C for one week under $HF+HNO_3$, further with HCl 6N and finally under HCl 2N at 145°C. After evaporation, the REE were separated from matrix elements by cation exchange chromatography (Dowex 50WX-8 resin).

Samarium and Nedimium were separated from the others REE by anion exchange chromatography (Dowex AG1-X4 resin). A mixed ^{150}Nd –^{149}Sm spike was used and the Nd data were normalized to a $^{146}Nd/^{144}Nd$ ratio of 0.7219. Procedural blanks were 0.160 ng for Sm and 0.587 ng for Nd. The La Jolla Nd standard yielded a $^{143}Nd/^{144}Nd$ ratio of 0.5118339 ± 9 and the Sm and Nd concentrations for BCR-01 standard were 6.56 ppm and 28.58 ppm, respectively. The crustal residence ages were calculated using the model of De Paolo (1981) for the depleted mantle (T_{DM}).

Other isotopes systems, such as Pb, are also useful to study granite petrogenesis. Lead is a common trace element in feldspars (Heier *et al.*, 1967; Patterson and M. Tatsumoto, 1964), and it is well known that the U/Pb and Th/Pb ratios of feldspar (especially K-feldspar) are low (*e.g.* Doe, 1970). These attributes allow feldspar to record the isotopic composition of Pb that was incorporated at the time of its formation and although multiple intracrustal processes produce scatter in the initial Pb isotopic compositions of rocks, the variations can be studied. So, in order to assess the initial Pb isotope composition of a rock, the feldspars are currently selected (see references above), because they normally contain Pb but very minor U. In this case, for initial Pb isotope composition analyses, low U is essential because any U present will have decayed to an 'excess' Pb radiogenic component.

Progressive leaching of feldspar grains shows a decrease in the amount of radiogenic Pb that may indicate the preferential leaching of the more radiogenic reservoirs (Housh and Bowring, 1991, McCulloch and Woodhead, 1993). Indigenous Pb *vs.* Pb introduced after crystallization may be assessed using leach/residue pairs (Hemming *et al.,* 1996). Sinha (1969) found a general agreement between the least radiogenic isotope composition of feldspars and the

Pb isotope composition of associated sulfides, suggesting that this method of severe leaching could yield a good estimate of initial Pb isotopic composition.

For the Pb isotopic system, the evolution of lead in the Earth's crust has been modeled on the basis of the U/Th/Pb ratios in the different bulk reservoirs (Doe and Zartman, 1979, Zartman and Doe, 1981; Zartman and Haines, 1988) and stages of isotopic homogenization (Stacey and Kramers, 1975; Cumming and Richards, 1975). Despite these models have limited application at the local and district scale, they are powerful tools for global and regional-scale studies, helping to identify the main geochemical reservoirs.

The feldspar grains were picked under a stereomicroscope and a qualitative selection was made taking into account the grain clarity, lack of inclusions, and absence of cracks. An initial mass between 30 to 50 mg of pure feldspar grains was weighed for each sample. According to Tomascak (1995), a single analysis by thermal ionization mass spectrometry (TIMS) requires 50–100ng of Pb. Based on the expected concentration of Pb in the feldspars, only 10 to 20mg of feldspar should be needed.

The method used for Pb feldspar leaching is based on Housh and Bowring (1991) and Ludwig and Silver (1977), but with partial modifications. In the first stage of chemical preparation, the grains are transferred into clean Teflon vials and a cleaning solution of HNO_3** 7.5N (20 drops) is added. Vials are capped and transferred to a hot plate (100°C) for at least 20 minutes to remove surface contaminants and labile lead. This step is to help ensure that any lead introduced after crystallization, either from the environment or through the actions of fluids moving through the pluton, is removed before leaching. The grains are then rinsed with Milli-Q water two times. The same process is repeated, now with HCl** 6N. In the second step, HF** 1N is added to the grains and the vial is left in an ultrasonic bath for 5 minutes. After, the solution is heated for 30 minutes (100ºC) on a hot plate, and an aliquot of 0.5 ml is collected and HBr*** 0.5 N is added (50 drops). This procedure is repetead until the grains are totally dissolved. In general, 10 to 15 aliquots are collected by sample. Each sample solution was processed through anion exchange column chemistry to isolate lead, that was loaded onto a Re-filament for TIMS analysis.

Procedural blanks are processed using the same chemical preparation techniques as were used for the grains to assess the ambient amount of lead introduced during sample processing (0.27 ng for 37 mg). In order to obtain the isotope composition of the grain part not contaminated

by external lead, a total of 50 analyses were performed on 14 selected samples (2 to 6 analyses per sample). After a preliminary analysis for all samples, the choice of a new leached solution of each sample was made given the previous isotopic results obtained on the same sample. The results shown in **Table 2** are those considered from the least contaminated parts of the grains from external lead.

Nd AND Pb ISOTOPE RESULTS

The initial Nd and Pb ratios are used for granitoid rocks as the main indicator of the source material. It is used together with some other geological criteria (geochronological, petrogenetic, structural) in order to estimate the relative amount of continental crust accreted or recycled during each interval of geological time, for the area studied in the Guyana Shield. The association of the Sm-Nd and Pb isotopic measurements with the available geochronological data obtained by other methods permitted an improved interpretation for the origin of the granitoid rocks under examination.

Table 2 shows new (22) and previous (36) Sm-Nd isotopic results on whole-rock for Uatumã-Anauá Domain (mainly granitoids), further new Pb isotope results from leached feldspars (14) of Martins Pereira, Caroebe and Igarapé Azul granitoids. In **Table 3** are shown Sm-Nd isotopic data (96 results were compiled or modified) from several other geochonological provinces (Ventuari-Tapajós or Tapajós-Parima, Maroni-Itacaiúnas or Transamazon and Central Amazonian) and respective domains (Carajás, Imataca, Central Amapá, French Guyana, Tapajós, Surumu and Central Guyana). The summary of main geological features of Uatumã-Anauá Domain granitoids rocks is also available in the **Table 4**.

Sm-Nd on whole-rock

Northern Uatumã-Anauá Domain: Martins Pereira and Serra Dourada granitoids

The main granitoids studied in the Northern Uatumã-Anauá Domain belongs to the Martins Pereira (1.97 Ga) and the Serra Dourada (1.96 Ga) granites, including small bodies of younger leucogranites with 1.90 Ga (lenses and pods with meter to centimeter-scale) filling the Martins Pereira NNE-SSW trending foliation. The oldest rocks in this region are represented by the Anauá Complex (2.03 Ga TTG-like association).

The Anauá Complex and the metavolcano-sedimentary rocks correlated to the Cauarane Group (low to medium metamorphism grade) and the Murupu Metamorphic Suite (high

metamorphism grade) are the oldest basement units known in the southeastern Roraima. For the Anauá Complex only two samples has been analyzed (see **tables 2 and 4**), yielding coherent T_{DM} model ages (2.37-2.33 Ga) and low to moderate negative $\varepsilon Nd_{2.03\ Ga}$ (-0.19 and -2.21).

In the Northern Uatumã-Anauá Domain, no Nd data are available for the metavolcano-sedimentary sequence, but the related rocks of Cauarane Group (see **Table 3**) in other areas (*e.g.* Guyana Central Domain) exhibits two main isotopic patterns. The first is related to paragneiss samples (*e.g.* garnet gneiss) with results showing moderate negative $\varepsilon Nd_{2.07\ Ga}$ (-1.12 to -4.16) values and higher NdT_{DM} model ages (2.46-2.41 Ga) including a Neoarchean NdT_{DM} age (2.64 Ga). The second gneissic type shows $\varepsilon Nd_{2.07\ Ga}$ near to zero to positive (+0.35 to +1.23) and lower NdT_{DM} ages (2.32-2.27 Ga), probably related to the volcanic protholith signatures (juvenile sources).

The Serra Dourada and Martins Pereira granitoids (1.98-1.96 Ga event) intrude this older basement in the Northern Uatumã-Anauá Domain. The S-type Serra Dourada granitoids confirms its wide crustal origin from partial melting of metavolcano-sedimentary sequence, showing negative $\varepsilon Nd_{1.96\ Ga}$ values (-1.08 and -4.34) and NdT_{DM} of 2.53-2.39 Ga for its sources, which are 420 to 560 Ma older than the crystallization age of these granites (**tables 1, 2 and 4, Fig. 3**).

The same is true for the I-type, high-K Martins Pereira granitoids (**tables 2 and 4, Fig. 3**), whose results show T_{DM} ages of 2.43-2.38 Ga and slightly negative $\varepsilon Nd_{1.97\ Ga}$ (-1.42 to -2.17), including samples with higher T_{DM} ages (2.67-2.64 Ga) and $\varepsilon Nd_{1.97\ Ga}$ negative values (-4.74 and -3.89). The 1.90 Ga intrusive lenses of leucogranite (one sample) yielded negative εNd (-3.48) and NdT_{DM} model age (2.38 Ga). These data are in agreement with Martins Pereira host results and reflect the zircon inheritance origin recorded (at least 3 older populations) in the single-zircon Pb evaporation for the leucogranite sample (**Table 1**). CPRM (unpubl.) Sm-Nd data present a similar isotope pattern for the Martins Pereira granitoids (**Table 2**). The Nd data pointed out moderate negative $\varepsilon Nd_{1.97\ Ga}$ values (-0.92 to -3.20) and NdT_{DM} ages with 2.36-2.33 Ga range (locally 2.57 Ga).

In summary, all of early Orosirian rocks of Northern Uatumã-Anauá Domain (2.03 to 1.96 Ga) show similar behaviour in the Sm-Nd isotopic system. The εNd is negative (-0.92 to -4.74) and the dominantly Siderian NdT_{DM} model ages (2.47-2.33 Ga), with subordinated Neoarchean ages (2.67-2.57 Ga). This suggests an input from mainly older crustal sources for the Serra Dourada-Martins Pereira genesis.

Southern Uatumã-Anauá Domain: Caroebe and Igarapé Azul granitoids

The granitoids of the Southern Uatumã-Anauá Domain are intrusive in the older Northern Uatumã-Anauá Domain rocks. They are represented mainly by the I-type Caroebe, Igarapé Azul, Água Branca granitoids and coeval Jatapu volcanism (1.90-189 Ga), including locally minor A-type plutonic bodies of Mapuera (1.88-1.86 Ga) and Moderna (1.82-1.79 Ga) granitoids related (**Table 1**). The Caroebe Granite and related plutons show two main facies named as Alto Alegre (with biotite and no hornblende) and Jaburuzinho (with biotite and hornblende) and both facies exhibit two different Nd isotopic patterns. The first pattern is characterized by moderate to high negative $\varepsilon Nd_{1.89\ Ga}$ values (-2.05 to -4.27) and NdT_{DM} model ages of 2.29 to 2.47 Ga. This pattern is most common in the Alto Alegre facies, although it is also observed in the Jaburuzinho facies. The Água Branca Granite in the type-area, far 300 km to the south of Caroebe Granite, also shows moderate to high negative $\varepsilon Nd_{1.\ 90\ Ga}$ values (-3.00) and Siderian NdT_{DM} model age (2.39 Ga). Although petrographically similar to the Jaburuzinho facies, the Água Branca Granite Nd results are in agreement with those of the Alto Alegre facies (**tables 2 and 4, Fig. 3**).

The second pattern is dominant in the Jaburuzinho types (**tables 2 and 4, Fig. 3**) showing $\varepsilon Nd_{1.89\ Ga}$ values close to zero (+0.46 to -1.18) and relatively lower NdT_{DM} model ages (2.16 to 2.26 Ga). The Igarapé Azul granitoids have a felsic character and only biotite (locally muscovite), but their Nd signature (**tables 2 and 4, Fig. 3**) is similar to the Jaburuzinho types (hornblende-bearing), exhibiting $\varepsilon Nd_{1.89\ Ga}$ close to zero (-0.02 to -1.61) and Rhyacian NdT_{DM} model ages (2.14-2.28 Ga). Such as the Igarapé Azul and Caroebe granitoids (mainly the Jaburuzinho facies), the coeval Iricoumé volcanic rocks (**Table 2, Fig. 3**) show slight negative εNd values (-0.27 to -1.76) and Rhyacian NdT_{DM} model ages (2.19-2.28 Ga).

Despite differences in the crystallization ages, the A-type Mapuera (1.88-1.86 Ga), Moderna and Madeira (1.82-1.79 Ga) granitoids and related rocks show Nd signatures based on the Rhyacian NdT_{DM} model ages and low negative εNd values (**Table 3**). The Mapuera samples yielded $\varepsilon Nd_{1.87\ Ga}$ between -0.56 and -1.22 and NdT_{DM} model ages of 2.17-2.28 Ga, whereas the Moderna types show similar values of $\varepsilon Nd_{1.81\ Ga}$ (-0.44 to -1.47) and NdT_{DM} model ages (2.17-2.28 Ga) (**Table 2, Fig. 3**).

In general, all granitoids of Southern Uatumã-Anauá Domain have dominantly Rhyacian NdT_{DM} model ages and low to moderate negative and, local positive εNd values, including subordinated Siderian NdT_{DM} model ages associated to the much more negative εNd values. This

picture contrasts with the Martins Pereira and Serra Dourada isotopic Nd patterns in the Northern Uatumã-Anauá Domain, characterized by Siderian (locally Neoarchean) NdT_{DM} model ages and highest negative εNd values.

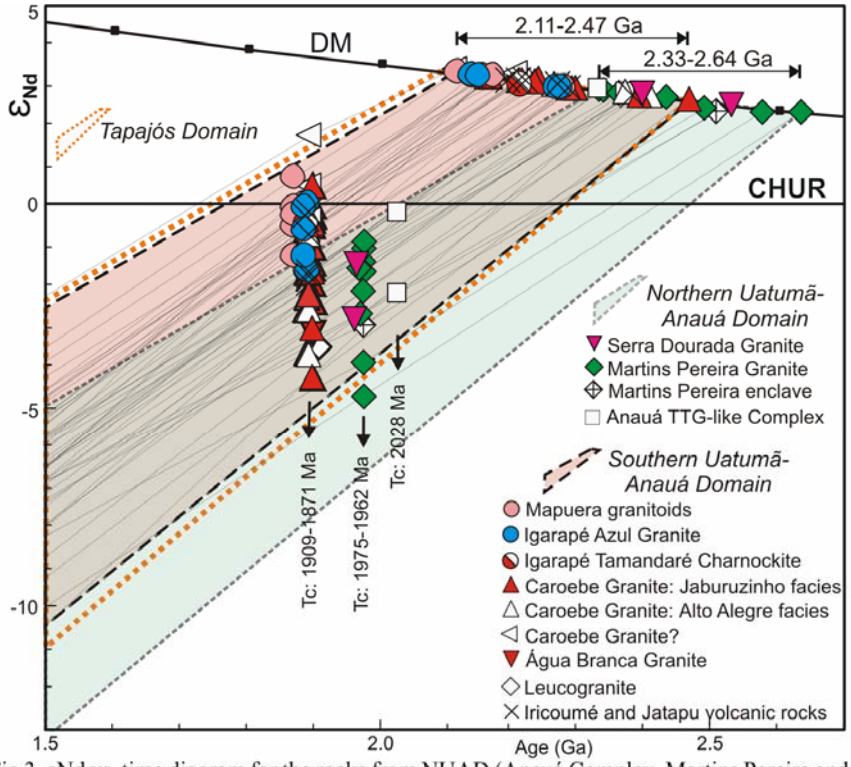

Fig 3. εNd vs. time diagram for the rocks from NUAD (Anauá Complex, Martins Pereira and Serra Dourada granitoids) and SUAD (Caroebe, Água Branca, Igarapé Azul, Mapuera granitoids, Igarapé Tamandaré charnockite, Iricoumé and Jatapu volcanic rocks). The Nd evolution field of Tapajós domain is also plotted for comparison. For details, see text and tables. Tc: crystallization ages range.

Pb on leached feldspars

In this Pb isotope study, the Northern Uatumã-Anauá Domain is represented by the 1.97 Ga Martins Pereira granitoid rocks and 1.90 Ga lenses of leucogranites, which yielded high Pb initial ratios, mainly the $^{207}Pb/^{204}Pb$ (15.70 to 15.57), which overlap those of the Southern Uatumã-Anauá Domain granitoids Pb composition (**Table 2**). In the Southern Uatumã-Anauá Domain, the Caroebe and Igarapé Azul granitoids show different behavior, although both exhibit $^{207}Pb/^{206}Pb$ ratios above of the upper crust evolution curve in the Plumbotectonic model (**Fig. 4**; Doe and Zartman, 1979, Zartman and Doe, 1981). Contrasting with the relatively more scattered pattern of the Igarapé Azul granites ($^{206}Pb/^{204}Pb$: 16.62 to 15.87; $^{207}Pb/^{204}Pb$: 15.65 to 15.42; $^{208}Pb/^{204}Pb$: 36.18 to 35.59), the Caroebe Granite shows the less radiogenic types and more homogeneous Pb initial ratios range ($^{206}Pb/^{204}Pb$: 16.41 to 15.90; $^{207}Pb/^{204}Pb$: 15.54; $^{208}Pb/^{204}Pb$: 36.09 to 35.49).

In summary, all studied granitoids show Pb radiogenic patterns, exhibiting $^{207}Pb/^{204}Pb$ (15.70-15.42), $^{206}Pb/^{204}Pb$ (16.87-15.87) and $^{208}Pb/^{204}Pb$ (36.18-35.49) initial ratios and they plots generally above of the upper crust evolution curve in the Zartman and Doe (1981) model. This behavior contrast with the Pb initial ratios of DM (Rehkamper and Hofmann, 1997), lower crust average (Rudnick and Goldstein 1990) and EM II present-day reservoirs and points to dominant crustal-derived reservoir contributions for the Martins Pereira, Caroebe and Igarapé Azul granitoids with no mantle-derived lead. Only one sample (MA-101) shows $^{207}Pb/^{206}Pb$ isotope ratios near to the orogen global growth curve and the EMII and lower crust fields (**Fig. 4**; Doe and Zartman, 1979, Zartman and Doe, 1981). In this same diagram, the granitoids samples also show much more low Pb ratios than southwestern of United States of America basalts (SWUSAB), these last considered as a paleopreoteroic mantle reservoir (~1.8 Ga) similar to actual EMII reservoir (Kempton *et al.*, 1991, Greenough and Kyser, 2003).

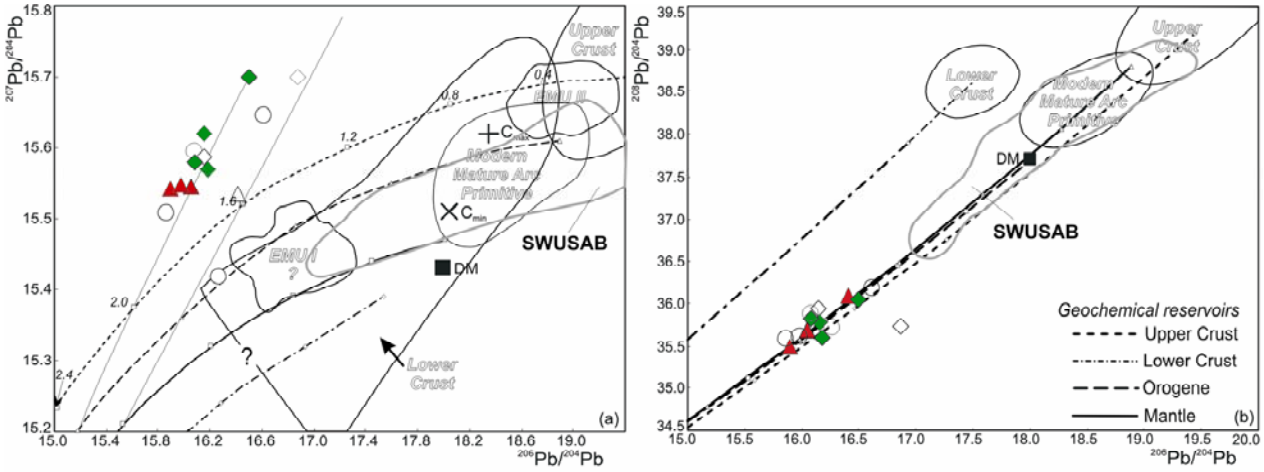

Fig 4. Plots of Pb isotopic compositions of leached feldspars from Martins Pereira, Caroebe and Igarapé Azul granitoids: (a) $^{207}Pb/^{204}Pb$ *vs.* $^{206}Pb/^{204}Pb$; (b) $^{208}Pb/^{204}Pb$ *vs.* $^{206}Pb/^{204}Pb$. The lead-isotope evolution curves are from Plumbotectonic model (version II) of Zartman and Doe (1981) and represent the isotopic composition of mantle, orogen, upper and lower crust reservoirs along the time. Other reservoirs fields are plotted for comparison, such as DM (Rehkamper and Hofmann, 1997), EMI and EMII (Zindler and Hart, 1986), mature arc primitive (Zartman and Doe, 1981) and continental crust (maximum and minimum average; Rudnick and Goldstein, 1990). Proterozoic enriched mantle reservoir of the southwestern United States of America basalts (SWUSAB, Kempton *et al.*, 1991 in Greenough and Kyser, 2003) are also plotted. Tick marks in the each curve indicate progressively older time in 0.4 b.y increments. Symbols as in fig.3.

DISCUSSION

Nd isotope signatures of the Geochronological Provinces older than 1.8 Ga and their boundaries in the southeastern Roraima

In the Nd isotope system, the Sm-Nd model ages (T_{DM}) are currently used in crustal evolution analysis of a given terrain. Normally, these ages are related to the evolution of the mantle during geologic time, admitting episodes of fractioning due to the extraction of basaltic

magmas. This implies that the residual mantle sources become enriched gradually in Sm (higher Sm/Nd ratio) and depleted in incompatible elements.

However, the T_{DM} ages must be interpreted very carefully (*e.g.* Arndt and Goldstein, 1987). Chemical and isotopic variations in mantle material are attested by the existence of geochemically distinct present-day reservoirs (DMM, HIMU, EMI, EMII, etc.), including also the possibilities of mixtures between such different reservoirs and crustal sources (Zindler and Hart, 1986). In this sense, the depleted mantle model is employed as a reasonable first approximation.

Thus, the T_{DM} ages have been considered to be "crust-formation ages", since they are obtained calculating the time when a given sample had an isotopic composition identical to the depleted mantle, presumed to be its "ultimate source". But this is true when only a short time elapsed between the formation of the mantle-derived magma and the final emplacement of the differentiated material in the continental crust, including the not modification Sm/Nd ratio of the sample by subsequent geological events. According to Arndt and Goldstein (1987), such assumptions may be valid only in a limited number of cases, with the Sm-Nd systematic generally providing an estimate of the average time that the material in the sample has been resident in the continental crust.

In the Archean Central Amazonian (or Amazon) Province (**Fig. 1**), only in the Carajás Block Nd data is available, contrasting with other areas, such as Iricoumé-Mapuera-Trombetas (Guyana Shield) and Iriri-Xingu (Central Brazil Shield) regions, for which the isotope data are very scarce. This province is interpreted in two different ways. The first model (Tassinari and Macambira 1999, 2004) argue that this region is characterized by a "hidden" basement (>2.5 Ga), inferred by the NdT_{DM} model ages (3.0-2.5 Ga) and negative εNd values from widespread younger intrusive granites and volcanics (1.88-1.81 Ga). Archean rocks crop out in the southeastern portion (Carajás Block), showing 3.04-2.73 Ga NdT_{DM} model ages range (Sato and Tassinari 1997, Dall´Agnol *et al.*, 1999) and εNd with +4.55 to –0.54 (**Table 3**; **Fig. 5**). The second model (Santos *et al.,* 2000, 2004) does not recognize an older basement in the Iricoumé-Mapuera and Iriri-Xingu regions and pointed out a domain of 1.88-1.70 Ga rocks based on the U-Pb ages of the younger granites and volcanic rocks (underplating setting), although the range of the NdT_{DM} model ages (2.85-2.41 Ga) and εNd (+1.52 to -14.39) also indicate older sialic crustal sources (Santos *et al.,* 2000).

Archean terranes are also observed in the central Amapá (Brazil) and Imataca (Venezuela) regions, considered as dominantly Rhyacian domains (**Table 3** and **Fig. 1**). For the granitic-granulitic association in the central Amapá, the crystallization (2.90-2.58 Ga) and NdT_{DM} model (3.42-2.92 Ga) ages reinforce an Archean origin **(Fig. 5**). In the Imataca region, the rocks are Transamazonian in age (ca. 2.0 Ga), but keep several records about their Archean origin (NdT_{DM} model ages: 3.91-2.71 Ga) (Tassinari *et al.,* 2004). In the Maroni-Itacaiúnas (or Transamazon) Province, Rhyacian crust occurs mainly in the easternmost region of the Guyana Shield, such as French Guyana (*e.g.* Avelar *et al.,* 2003; Delor *et al.,* 2003). Based on the available Nd data (**Table 3; Fig. 5**) this region is roughly subdivided in the northern and southern areas. The southeastern of French Guyana (near to the Amapá boundary) is dominated by 2.16-2.10 Ga granitic-migmatitic rocks with 2.58-2.24 Ga NdT_{DM} model ages range and εNd varying from +1.74 to –2.24. The northern area is characterized by 2.16-2.13 Ga granite-greenstone terrain with juvenile signature (NdT_{DM} model age: 2.29-2.19 Ga and εNd: +3.60 to +1.63).

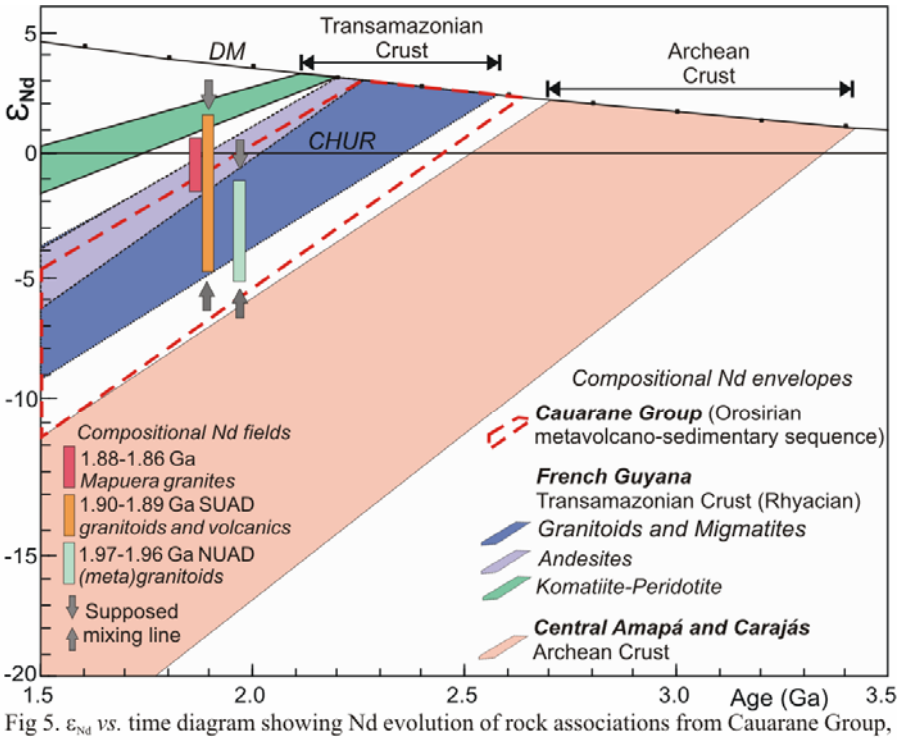

Fig 5. ε_{Nd} *vs.* time diagram showing Nd evolution of rock associations from Cauarane Group, Archean (Carajás and Central Amapá) and Transamazonian (French Guyana) terranes. The SUAD and NUAD sample fields are also plotted. For discussions and references see text and tables. Symbols as in fig.3.

In the Central Brazil Shield, a juvenile origin is also proposed for the Ventuari-Tapajós (or Tapajós-Parima) Province based manly in Sm-Nd data from the Tapajós domain (**Table 3, Fig. 5**). This domain is represented by two main magmatic events (2.05-1.96 Ga and 1.90-1.87 Ga)

showing 2.44-2.09 Ga NdT_{DM} model ages and εNd yielding +2.22 to –4.16 range (Sato and Tassinari, 1997; Santos *et al.*, 2000). On the other hand, in the region near to the boundary of Central Amazonian Province, Lamarão *et al.* (2005) argue that the Nd signature of the granitoids and volcanic rocks are not compatible with a mantle-derived origin. As shown in **Table 3**, they obtained similar NdT_{DM} model ages (2.46-2.28 Ga) to the other authors, but the εNd are variously negatives (-1.01 to –5.19). This different Nd pattern could be related to geographical differences, whith the juvenile rocks being dominant in the westernmost areas of Tapajós Domain (Orogenic Domain, 2.05-1.96 Ga) and the crustal sources being most common in the easternmost areas (Post-orogenic Domain; 1.90-1.89 Ga), close to the Central Amazonian Province boundary.

The scenario pointed out by Lamarão et al. (2005) for the Tapajós domain is similar to the Uatumã-Anauá domain in southeastern Roraima and except for two samples tentatively correlated to the Água Branca Suite ("post orogenic" domain), which yielded positive $\varepsilon Nd_{1.89\ Ga}$ (**Table 3**, Sato and Tassinari, 1997), all southeastern Roraima region does not show data suggestive of mantle-derived magmas, including the correspondent "orogenic" domain. Santos et al. (2006) revisited the Tapajós-Parima and Central Amazonian boundary in the Guyana Shield, and proposed that it would be located to the east of study area, in the NW Pará State (**Fig. 1b)**. Probably, all southeastern Roraima is included in the Ventuari-Tapajós (or Tapajós-Parima) Province, with older provinces such Maroni-Itacaiúnas (or Transamazon) and Central Amazonian as sources of magmatism in the Uatumã-Anauá Domain.

Crustal formation and constraints on sources based on integrated use of the Nd-Pb isotopes: Martins Pereira, Igarapé Azul and Caroebe granitoids examples

In general, Nd and Pb data are seen separately; however, these two systems combined on one diagram (using εNd and $^{207}Pb/^{204}Pb$) permit a more comprehensive assessment of possible sources of the plutonic rocks, especially granitoids. The Martins Pereira, Igarapé Azul and Caroebe granitoids have been taken as example, we try to estimate the most suitable source(s) based on the Nd and Pb integrated analysis. In contrast with Nd data, the Pb isotopic data from potential sources are not available, such as rocks of Cauarane Group, Anauá Complex (exposed basement) and Central Amazonian and Transamazonian crusts (unexposed basement).

In this sense, the use of U-Pb system isotope system (initial Pb ratios) associated with Sm-Nd system, and supported by previous geochronological data, allows a more comprehensive evaluation about of origin of the granitoids under investigation. Therefore, these isotope tool

yield important constraints about the discussion of "juvenile" derivation, formed by mantle extraction-crust differentiation, "reworked" origin by melting of crustal protoliths, or reflecting mixing of material derived from the mantle at different times (Arndt and Goldstein, 1987).

Tomascak *et al.* (2005) argued that $^{207}Pb/^{204}Pb$ ratio is a more powerful tracer for petrogenetic studies than $^{206}Pb/^{204}Pb$, especially in areas where magmatic source components have significant time-integrated differences in U/Pb, such as for the Martins Pereira granitoids. The $^{206}Pb/^{204}Pb$ could vary considerably in mantle and crustal materials in response to small changes in U/Pb, which changes may be unrelated to the nature of source materials.

However, in southeastern Roraima, this is only since recently that a reasonable number of Nd isotopes data have become available (Costa, 2005; CPRM unpubl.) and Pb isotopic data do not exist, making it difficult to determinate potential magamtic sources and crustal signatures. Despite of this scarcity of data, Serra Dourada and Martins Pereira granitoids show Nd and Pb signatures that confirm a crustal origin based on the Orosirian to Rhyacian metavolcano-sedimentary sequence and Archean mixing sources (see **Fig. 5, tables 2 and 3**).

For the Martins Pereira granitoids, the continental sources are older than those of the Caroebe and Igarapé Azul ones. The restricted 1980-1967 Ma crystallization ages of Martins Pereira granitoids and the low to moderate negative $\varepsilon Nd_{1.97\ Ga}$ values (-0.92 to -4.74), high $^{207}Pb/^{204}Pb$ and relatively high NdT_{DM} model ages (2.33-2.67 Ga), suggest dominantly remelting of Neoarchean sources. The same is true for the S-type Serra Dourada granites that pointed out older metasedimentary sources, as recorded in the Cauarane sequence. In the Caroebe and Igarapé Azul granitoids these isotope results give important constraints for the Arndt and Goldstein (1987) discussion, involving a "juvenile" derivation (mantle extraction-continental crust differentiation), "reworked" origin (remelting of previously crustal protoliths) or mixing of material derived from the mantle at different times.

For the studied granitoids of southeastern Roraima, the crystallization ages and NdT_{DM} model ages are not concordant. Furthermore, positive (or slightly negative) εNd values and low $^{207}Pb/^{204}Pb$ initial ratios are absent and also preclude a derivation only from mantle sources. Hence, three hypothesis are provided to explain the origin of the parental magmas: (1) mixture of mantle-derived magmas or juvenile crust (Transamazonian) with subordinate liquids derived from radiogenic crust (Archean); (2) derivation from an enriched mantle; (3) derivation from

remelting of slightly older radiogenic crust (Transamazonian), which implies a dominantly crustal source for the parental magmas.

A mixing origin from Transamazonian komatiites-peridotites of greenstone belt sequence (depleted source) and Archean sialic basement (enriched source) could explain the Nd isotope signatures. However, the elemental contents of these rocks, in particular the compatible elements, are not consistent with a significant input of mantle material. The mantle-crust mixing scenario is also less likely than derivation from a single (or multi) crustal source (*e.g.* lower crust and juvenile crust). This picture is corroborated by data dispersion in samples from Martins Pereira, Caroebe and Igarapé Azul granitoids in a εNd and SiO_2 plot (**Fig. 6a**), including the absence of trends between compatible element contents and Nd isotopes (**Fig. 6b**) and their non-primary nature (**Fig. 6c**).

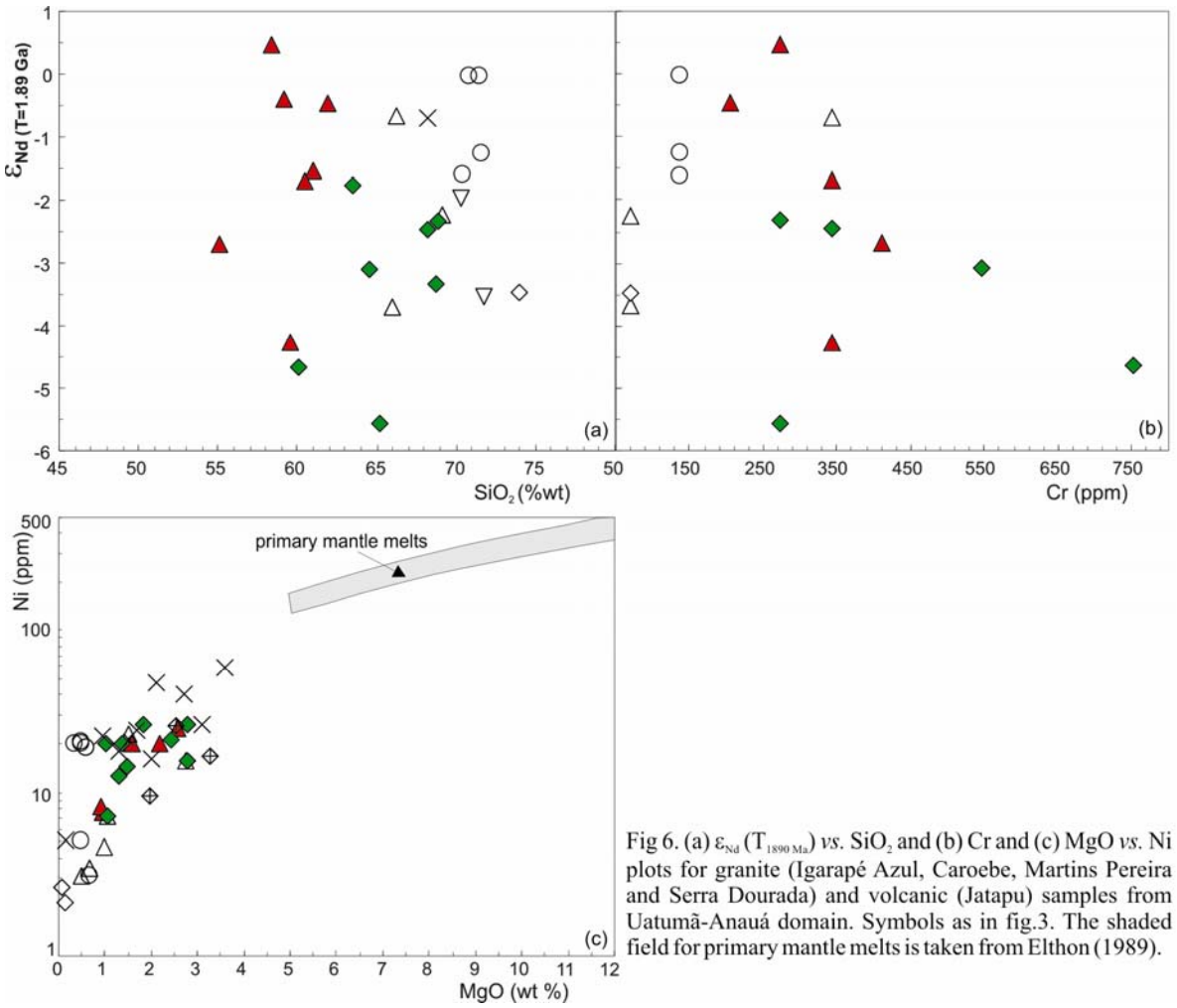

Fig 6. (a) ε_{Nd} ($T_{1890\,Ma}$) *vs.* SiO_2 and (b) Cr and (c) MgO *vs.* Ni plots for granite (Igarapé Azul, Caroebe, Martins Pereira and Serra Dourada) and volcanic (Jatapu) samples from Uatumã-Anauá domain. Symbols as in fig.3. The shaded field for primary mantle melts is taken from Elthon (1989).

A derivation from an enriched (paleo)mantle based on the Nd signatures is suggested by some authors for the high-K (slightly shoshonitic) calc-alkaline rocks in the Tapajós domain (*e.g.*

Vasquez *et al.,* 2002) and could be a suitable model for the Caroebe and Água Branca granites in southeastern Roraima. The slightly negative εNd values and NdT_{DM} model ages of ca. 2.25 Ga for the 1.90 Ga andesites and gabros of the Tapajós domain are interpreted as crustal enrichment or contamination of the subcontinental litospheric mantle. The mantle contamination by crustal material is also a possible hypothesis for the petrogenesis of Caroebe and Igarapé Azul granites, perhaps indirectly related to the subduction process of the Anauá Arc through the time. Several mantle geochemical reservoirs are plotted in the **Fig. 7**, including present-day (EMI and EMII) and Proterozoic (SWUSAB) enriched mantle examples, however all analyzed granitoid samples show lower $^{143}Nd/^{144}Nd$ and $^{206}Pb/^{204}Pb$ ratios. Only two samples (Igarapé Azul and Caroebe granites) plot close to the field of EMI reservoir boundary (**Fig. 4a**).

In contrast, Nd and Pb data indicate that the parental magmas of these granites were produced mainly by reworking/remelting of Paleoproterozoic crust and very locally by Archean sialic sources. Two potential crustal sources, with different isotopic contents, are selected for comparison: (i) Cauarane Group rocks of Northern Uatumã-Anauá Domain (back-arc basin related to the Anauá arc?), and (ii) Transamazonian andesites and granite-migmatitic rocks from French Guyana.

The metavolcano-sedimentary (Cauarane Group) rock samples present similar NdT_{DM} model ages (2.27-2.64 Ga) and εNd values (+0.21 to -5.40, at 1.97 Ga) of Caroebe and Igarapé Azul granites at 1.89 Ga. The protholiths of the Cauarane Group also can be subdivided into 2 types in relation to Nd isotopic data: (a) sedimentary and (b) volcanic origin (**Table 3**). The first exhibits radiogenic Nd signatures ($\varepsilon Nd_{2.07\ Ga}$ -1.12 to -4.16) and much higher NdT_{DM} model ages (2.41-2.64 Ga), contrasting with the less radiogenic Nd contents ($\varepsilon Nd_{2.07\ Ga}$ +0.35 to +1.23) and lower NdT_{DM} model ages (2.27-2.32 Ga) of the second ones (**Table 2**).

The Caroebe and Igarapé Azul granitoids show dominantly negative (-1.31 to -4.37) $\varepsilon Nd_{1.89\ Ga}$, with only locally slightly positive and negative values (+0.37 to –0.59). These least radiogenic Nd types exhibit also the youngest NdT_{DM} model ages (2.16-2.24 Ga), showing the same Nd isotope composition of the Transamazonian andesites and granite-migmatitic terrane of French Guyana in the 1.89 Ga times (**Fig. 3**). This feature suggests that these rocks (*e.g.* andesites or metatonalites) could be suitable sources for the Caroebe and Igarapé Azul granites, in agreement with the petrogenetic models for the high-K calc-alkaline granites (Roberts and Clements, 1989).

The most Nd radiogenic values yielded by Caroebe and Igarapé Azul granitoids show the oldest NdT_{DM} model ages (2.23-2.47 Ga). This characteristic could indicate progressive input of older "enriched" material, such as Cauarane metasedimentary rocks, Martins Pereira granitoids and/or Archean basement sources to the original melt produced by partial melting of Transamazonian "depleted" source (**Fig. 3**). This hypothesis is reinforced by the geochemical data and by the several 1.97-1.96 Ga inherited ages found in the Caroebe (Alto Alegre facies) and mainly in the Igarapé Azul granites (**Table 1**). In this last type are also observed biotite-rich gneissic enclaves with 1.96 Ga, negative $\varepsilon Nd_{1.89\ Ga}$ (-1.95 and -3.52) and higher T_{DM} model age (2.51-2.72 Ga).

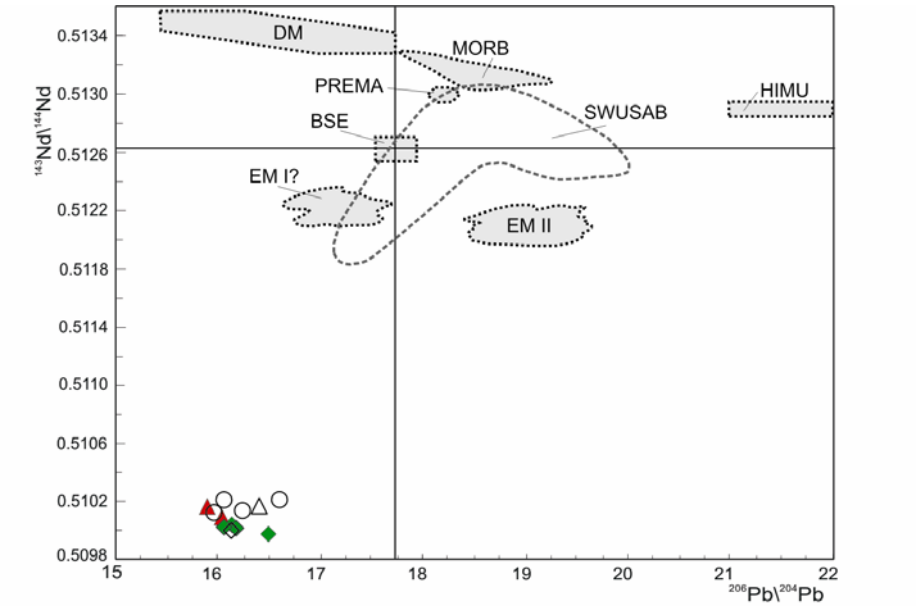

Fig 7. $^{143}Nd/^{144}Nd_{(i)}$ *vs.* $^{206}Pb/^{204}Pb_{(i)}$ isotope correlation diagram for Martins Pereira (1.97 Ga), Caroebe and Igarapé Azul (1.89 Ga) granitoids samples. The mantle geochemical reservoirs are extracted from Zindler and Hart (1986) and the $^{206}Pb/^{204}Pb$ of BSE was taken from Allegre *et al.* (1988). Proterozoic enriched mantle reservoir of the Southwestern United States of America basalts (SWUSAB, Kempton *et al.*, 1991 in Greenough and Kyser, 2003) are also plotted for comparison. Symbols and captions as in figs 3 and 4.

Thus the lowest $^{207}Pb/^{204}Pb$ and locally high-εNd source component of Caroebe and Igarapé Azul magmas, including local Pb and Nd isotopic heterogeneity, are interpreted as having a dominantly crustal derivation. The granitoids origin is probably related to the remelting of the Transamazonian more depleted source (andesites, metatonalites and amphibolites?) and addition of crustal material (*e.g.* Cauarane Group and Martins Pereira granitoids). According to Tomascak *et al.* (2005), it is likely that mantle heat was required to produce large-scale melting of the mafic to intermediate, metaigneous lower crust, even if compelling evidence for mantle material involvement is lacking.

An outline of geodynamic evolution of the central Guyana Shield at the Orosirian times

The whole-rock Nd isotope and previous geochronological data (Costa, 2005, Lamarão *et al.,* 2005, CPRM unpubl., this study), pointed out for the similarities between the Uatumã-Anauá (Guyana Shield) and Tapajós (Brazil Central Shield) domains and both belong probably to the same province (Ventuari-Tapajós or Tapajós-Parima) and has been experienced the same tectonic evolution. According to Lamarão *et al.* (2002), the Tapajós domain records global scale accretionary processes related to the formation of the Atlantica supercontinent in the early Orosirian times times (2.04-1.96 Ga, Lamarão *et al.,* 2002, Santos *et al.,* 2000, 2004), followed by a 1.90-1.87 Ga intracontinental taphrogenetic event. The tectonic setting of the Tapajós domain is considered thus transitional, in time and space, between a subduction-related setting, involving the generation of a magmatic arc, and a stable continental block affected dominantly by vertical and extensional tectonics. The main examples of calc-alkaline granitoids generated in post-collisional (or post-orogenic) and extensional setting are related to Basin-and-Range province in the SW of USA (*e.g.* Hawkesworth *et al.,* 1995, Coleman and Walker 1992) and to Caledonian orogenic belt (*e.g.* Atherton and Ghani, 2002).

In contrast, Santos *et al.* (2000, 2004) included these 1.90-1.87 Ga granitoids (except Maloquinha Granite) and coeval volcanic rocks in the arc-related orogenic setting (Tropas Orogeny). These authors pointed out that the Tropas Orogeny has started with the arc island Tropas magmatism (1898-1893 Ma), followed by formation of the Parauari continental arc magmatism (1893-1879 Ma). The A-type Maloquinha granitoids are younger (1882-1870 Ma) and correspond to the post orogenic setting. Others Paleoproterozoic terranes in the world also comprise 1.9-1.8 Ga calc-alkaline granitoids, sometimes with associated coeval volcanics, such as in northern Australia (Hooper and Lamboo Complexes, *e.g.* Page, 1988, Griffin *et al.,* 2000), northern United States (Trans-Hudson orogenic belt, *e.g.* Dumphy and Ludden, 1998; St-Onge *et al.,* 1999), Sweden and Finland (Svecofennian Orogen, *e.g.* Billström and Weihed, 1996; Lahtinen and Huhma, 1997). All these orogens have their geological history reasonably well understood, including several isotopic, geochemical data and petrotectonic assemblage compatible with the arc-island or arc-continental tectonic setting (*e.g.* turbidite and ophiolites sequences), contrasting with the majority of Amazonian Craton provinces, including the Tapajós domain.

The Nd and Pb isotope data presented here show that the addition of mantle-derived magmas, if really it occurred, was probably very limited in the Uatumã-Anauá Domain, although over a wide orogenetic area, most granites may be accounted for a binary mixture between a recycled crustal component and a depleted mantle-like component. But the isotope pattern showed by Uatumã-Anauá Domain granitoids is better explained by the melting of older crust (recycling) than by a mantle-crust mixing or a juvenile and arc-related origin. Thus, the regional crustal melting was the dominant magmatic process in this region and this older crust could be heterogeneous isotopically (*e.g.* Transamazonian granite-greenstone terranes, metavolcano-sedimentary sequences, and local Archean TTG terranes), resulting in variable NdT_{DM} and εNd values.

For the Northern Uatumã-Anauá Domain **(Fig. 8a)**, a primitive arc is admitted (Faria *et al.*, 2002; Anauá Complex, 2.03 Ga), although it crops out as inliers in the northeastern area and only few isotopic analyses are available. The granitic rocks studied in the Northern Uatumã-Anauá Domain probably correspond to the late continental arc (Martins Pereira, 1.97 Ga) to early collisional (Serra Dourada, 1.96 Ga) transitional setting **(Fig. 8b)**, generated from anatexis of older continental sources (Transamazonian to locally Archean in age). This accretionary model is in agreement with those of Lamarão *et al.* (2002) and Santos *et al.* (2000, 2004) for the Tapajós domain. However Lamarão *et al.* (2005) discard a juvenile origin and pointed out an Andean-type magmatic arc setting where the magmas could be modified by interaction with crust. Alternatively, these authors consider that the 2.0 Ga high-K calc-alkaline magma types are resulted of remelting of an older Paleoproterozoic juvenile arc with a small contribution from Archean sialic sources in the post- to late-orogenic setting, thus questionning the existence of a subduction zone.

In the Southern Uatumã-Anauá Domain, the 1.90-1.89 Ga granitoids and volcanic rocks show isotopic data a little more heterogeneous, but in general sense also exhibit an isotopic continental crust pattern (multicrustal sources). This feature, associated to the dominantly Rhyacian NdT_{DM} ages, is in agreement with the petrogenetic model based on the melting of tonalites, andesites and/or amphibolites sources, such as those observed in the Transamazonian granite-greenstone terranes (juvenile sources). These magmas could be locally contaminated by the metavolcano-sedimentary sequences or minor Archean sources. In contrast to Northern Uatumã-Anauá Domain evolution, no ophiolites sequences (or ocean crust) remnants and arc-

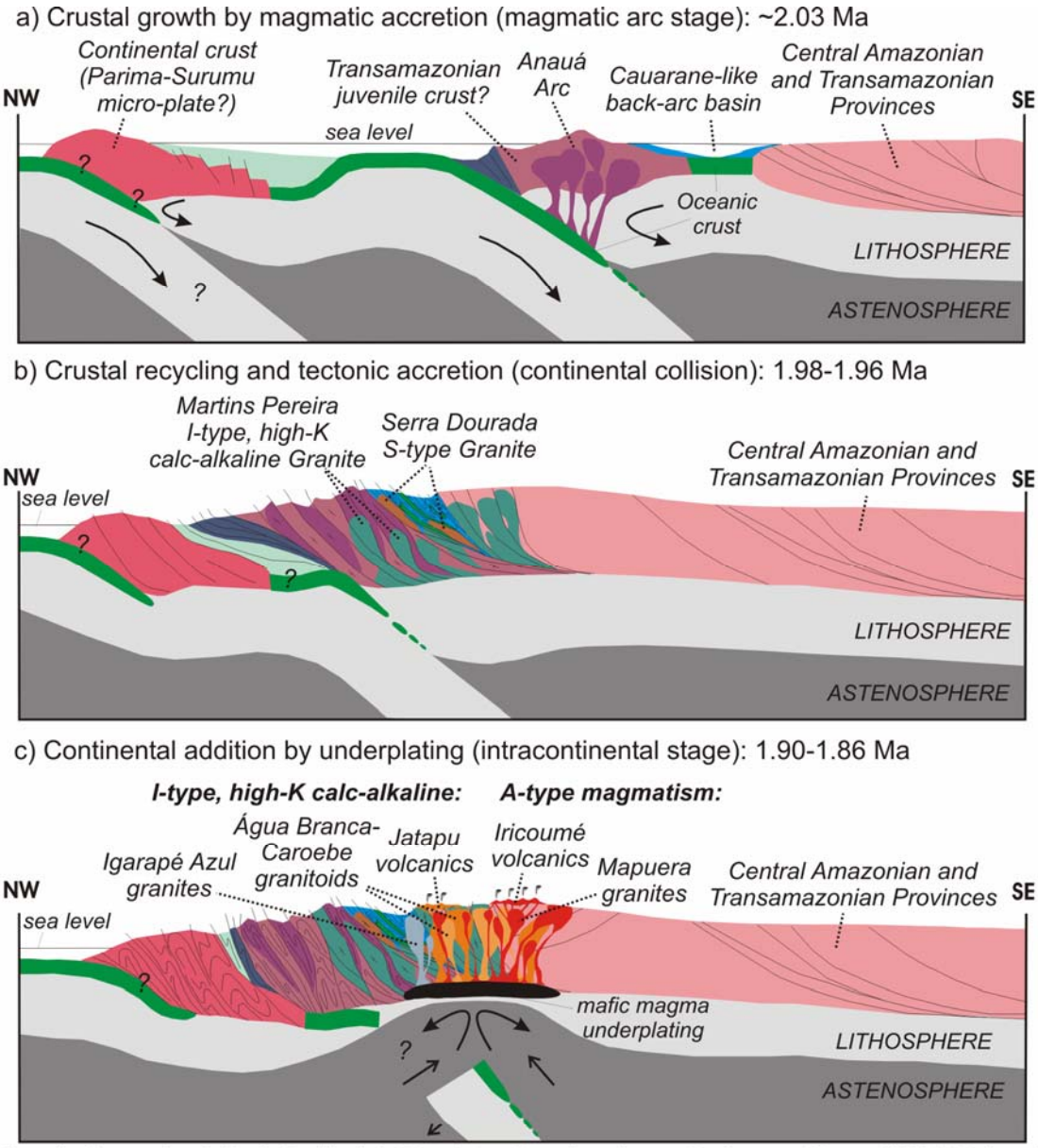

Fig. 8. Schematic paleotectonic model for the Orosirian in the Uatumã-Anauá Domain, southeastern Roraima, central Guyana Shield. (a) In the northern area (NUAD), at ~2030 Ma oceanic crust subducts at the western margin of the continental or oceanic plate. Melting of the subducted oceanic crust generate TTG magmas and fluids that ascent to the overlying mantle wedge and lower crust (Anauá Complex), enclosing ultamafic to mafic xenoliths. Back-arc basin are associated to this environment and produce graywackes, arkoses and locally MORB basalts (Cauarane-like sequences); (b) At 1980-1960 Ma the Anauá arc collides with Central Amazonian and Transamazon (or Maroni-Itacaiúnas) Provinces in the westside. This collision produce by partial melting crustal S-type granites (Serra Dourada) and several magma pulses of high-K calc-alkaline granitoids (Martins Pereira). In more advanced collisional stage (1.94-1.92 Ga?) blocks located to east could be collided with the Anauá Arc. In the boundaries (suture zone?) thrust sheets of granulites are locally exposed at middle-upper crust levels; (c) After convergent dominant process (arc and collisional stages) in early Orosirian times, a major distensional event is dominant in the southern area (SUAD) at 1900-1860 Ma interval. Similarly some Caledonian post-orogenic models (*e.g.* Atherton and Ghani, 2002), in this stage happen the slab rupture and breakoff, or alternatively delamination and mantle plumes (?) processes, including upward astenosphere migration and magma mafic underplating at the mantle-crust boundary. The lower crustal rocks melt yielding felsic magmas. Different degrees of interaction these magmas with others pre-existing crustal rocks will result in the Água Branca, Caroebe, Igarapé Azul and Mapuera granitoids with coeval volcanism (Jatapu and Iricoumé) and minor charnockitoids.

related sedimentation, including no metamorphism and deformation, are recorded in the Southern Uatumã-Anauá Domain. Thus, following the Lamarão *et al.* (2005) hypothesis for the Tapajós domain, the 1.90-1.89 Ga granitoids studied in Southern Uatumã-Anauá Domain have been to large scale taphrogenesis marking the break up of a large Paleoproterozoic continent driven by

underplating mechanism **(Fig. 8c)**. Derivation of the original magmas from remelting of crustal sources older than ca. 1.9 Ga and their association with a continental-scale extensional event are consistent with the geological, geochemical and Pb-Nd isotopic data.

CONCLUSIONS

The relatively high NdT_{DM} model ages and the negative $\varepsilon_{Nd(T)}$ values observed in the southeast of Roraima preclude an exclusive derivation from mantle sources. The isotopic data discussed herein, indicate that the magma sources for the granitoids can be better explained as dominantly Paleoproterozoic (Rhyacian) with limited Archean crustal contributions (*e.g.* Igarapé Azul and Caroebe granitoids) or by Siderian to Archean sialic sources and negligible crustal Paleoproterozoic contributions (*e.g.* Serra Dourada and Martins Pereira granitoids).

In the Northern Uatumã-Anauá Domain, the S-type (1.96 Ga, Serra Dourada) and older high-K calc-alkaline (1.97 Ga, Martins Pereira) granitoids could be related to the early stages of collisional phase after the Anauá arc amalgamation with older crustal sialic basement (Central Amazonian and Maroni-Itacaiúnas provinces) with Rhyacian to Archean age.

The absence of remnants of oceanic crust and arc-basin related sequences in the Southern Uatumã-Anauá Domain suggests that Igarapé Azul and Caroebe high-K calc-alkaline granitoids (1.90-1.89 Ga) and Mapuera A-type granites (ca.1.87 Ga) were produced in the post-orogenic setting related to an extensional tectonic driven by underplating mafic magma process from dominant depleted (*e.g.* andesites, tonalites, amphibolites) and/or enriched (*e.g.* paraderived rocks) crustal sources, both Rhyacian in age (Maroni-Itacaiúnas or Transamazon province). This model contrasts with arc-related hypothesis of Santos *et al.* (2000), however, field detailed mapping, structural and metamorphic analyses, including much more laboratory data, are necessary for a construction of a more realistic model in the central segment of Guyana Shield.

The geochronological and isotope similarities between the Uatumã-Anauá and Tapajós domains suggest that both belong to the same province (Ventuari-Tapajós or Tapajós-Parima) and these constraints show that not all the province necessarily possess a juvenile origin, instead (at least in the southeast of Roraima) rocks of crustal origin dominate. The similarities are related especially to the crystallization age range of the main granitic events: (i) 2.03-1.96 Ga (Orogenic Domain) and (ii) 1.90-1.86 Ga (Post-orogenic Domain). However, the absence of granulitic-charnockitic rocks and the paucity of S-type granites in the Tapajós domain point out that the collisional setting was less important in the Tapajós region compared to the Uatumã-Anauá

domain. Furthermore, isotopic data suggesting Archean crust sources (Lamarão *et al.,* 2005) are more limited in Tapajós domain.

ACKNOWLEDGEMENTS

Special thanks to the colleagues of CPRM (Geological Survey of Brazil) and Pará-Iso (UFPA) for discussions and helpful during the isotopic analyses. The authors are also grateful to CPRM-Geological Survey of Brazil for the research grants and FINEP (CT-Mineral 01/2001 Project), CAPES (BEX 1041-05-3) and Pará-Iso for support of laboratorial works.

REFERENCES

Allègre, C.J., Lewin, E., Dupré, B. 1988. A Coherent Crust Mantle Model for the Uranium Thorium Lead Isotopic System. *Chemical Geology* 70 (3), 211-234.

Almeida M.E., Fraga L.M.B., Macambira M.J.B. 1997. New geochronological data of calc-alkaline granitoids of Roraima State, Brazil. In: IG/USP, South-American Symp. on Isotope Geology, 1, Ext. Abst., p.34-37.

Almeida M.E., Macambira M.J.B. 2003. Aspectos geológicos e litoquímicos dos granitóides cálcio-alcalinos Paleoproterozóicos do sudeste de Roraima. In: SBGq, Cong. Brasil. Geoq., 9, Anais, p. 775-778 (in Portuguese).

Almeida, M.E., Macambira, M.J.B., Faria, M.S.G. de. 2002. A Granitogênese Paleoproterozóica do Sul de Roraima. In: SBG, Congresso Brasileiro de Geologia., 41, Anais, p 434 (in Portuguese).

Almeida, M.E., Macambira, M.J.B., Galarza, M.A., Santos, L.S. Evidence of the Widespread 1.90-1.89 Ga I-type, high-K calc-alkaline magmatism in Southeast of Roraima State, Brazil (central portion of Guyana Shield) based on Geochemistry and Zircon Geochronology. *In preparation*.

Almeida, M.E., Macambira, M.J.B., Oliveira, E.C. Geochemistry and Zircon Geochronology of the I-type High-K Calc-alkaline and S-Type Granitoids from Southeast of Roraima State, Brazil: Orosirian Magmatism Evidence (1.98-1.96 Ga) in central portion of Guyana Shield. *Precambrian Research* submitted.

Arndt, N.T., Goldstein, S.L. 1987. Use and abuse of crust-formation ages. *Geology* 15 : 893–895.

Atherton, M.P., Ghanni, A.A. 2002. Slab breakoff: a model for Caledonian, Late Granite syn-collisional magmatism in the orthotectonic (metamorphic) zone of Scotland and Donegal, Ireland. *Lithos* 62 : 65–85.

Avelar, V.G., Lafon, J.M., Correia, F.C., Jr., Macambira, E.M.B. 1999. O magmatismo Arqueano da região de Tucumã-Província Mineral de Carajás: novos resultados geocronológicos. *Rev. Bras. Geoc*. 29, 453-460 (abstract in English).

Avelar, V.G., Lafon, J.M., Delor, C., Guerrot, C., Lahondère, D. 2003. Archean crustal remnants in the easternmost part of the Guiana Shield: Pb-Pb and Sm-Nd geochronological evidence for Mesoarchean versus Neoarchean signatures. *Géologie de la France* 2-3-4, 83-99.

Billström, K., Weihed, P. 1996. Age and provenance of host rocks and ores in the Palaeoproterozoic Skellefte district, northern Sweden. *Econ. Geol.* 91, 1054–1072.

Coleman, D.S., Walker, J.D. 1992. Generation of juvenile granitic crust during continental extension: *Journal of Geophysical Research* 92, 11011-11024.

Cordani, U.G., Tassinari, C.C.G., Teixeira, W., Basei, M.A.S., Kawashita, K. 1979. Evolução tectônica da Amazônia com base nos dados geocronológicos. In: Congresso Geológico Chileno, 2, 1979, Arica, Anais, v.4, p.177-148 (in Portuguese).

Costa, S. dos S. 2005. Análise integrada dos dados geofísicos, geológicos e de sensoriamento remoto do Cinturão Guiana Central e áreas adjacentes do estado de Roraima. Doctoral thesis, Unicamp, São Paulo. 157 p. Unpublished. (abstract in English)

Costi, H.T. 2000. Petrologia de Granitos Alcalinos com Alto Flúor Mineralizados em Metais Raros: o Exemplo do Albita granito da Mina Pitinga, Amazonas, Brasil. Doctoral thesis Universidade Federal do Pará, Belém, 345p. Unpublished. (abstract in English)

Costi, H.T., Dall'Agnol, R., Moura, C.A.V. 2000. Geology and Pb-Pb geochronology of Paleoproterozoic volcanic and granitic rocks of the Pitinga Province, Amazonian craton, northern Brazil. *Intern. Geol. Rev.* 42, 832-849.

CPRM. Sm-Nd isotope databank. Brasilia, MME. Unpublished.

CPRM. 2000. Programa Levantamentos Geológicos Básicos do Brasil. Caracaraí, Folhas NA.20-Z-B e NA.20-Z-D (integrais), NA.20-Z-A, NA.21-Y-A, NA.20-Z-C e NA.21-Y-C (parciais). Escala 1:500.000. Estado de Roraima. CPRM, 157 p. CD-ROM. (abstract in English)

CPRM. 2003. Programa Levantamentos Geológicos Básicos do Brasil. Geologia, Tectônica e Recursos Minerais do Brasil: Sistema de Informações Geográficas - SIG. Rio de Janeiro : CPRM , 2003. Mapas Escala 1:2.500.000. 4 CDs ROM. (abstract in English)

CPRM. 2005. Programa Levantamentos Geológicos Básicos do Brasil. Escala 1:1000.000. Mapa Geológico do Brasil. 41 mapas Brasilia, MME. CD-ROM. (in Portuguese)

CPRM. 2006. Programa Levantamentos Geológicos Básicos do Brasil. Escala 1:1000.000. Mapa Geológico do Estado do Amazonas. Manaus, MME. Text and CD-ROM. (in Portuguese)

Cumming, G.L., Richards, J.R. 1975. Ore Pb-isotope ratios in a continuously changing Earth. *Earth Planet. Sci. Lett.* 28, 155-171.

Dall'Agnol, R., Rämo, O.T., Magalhães, M.S. de, Macambira, M.J.B. 1999. Petrology of the anorogenic, oxidised Jamon and Musa granites, Amazonian Craton: implications for the genesis of Proterozoic A-type granites. *Lithos* 46, 431–462

De Paolo, D. 1981. Neodymiun isotopes in the Colorado Front Range and crust-mantle evolution in the Proterozoic. *Nature* 291,193-196.

Delor, C., Lahondère, D., Egal, E., Lafon, J.-M., Cocherie, A., Guerrot, C., Rossi, P., Truffert, C., Théveniaut, H., Phillips, D., Avelar, V.G. de. 2003. Transamazonian crustal growth and reworking as revealed by the 1:500,000-scale geological map of French Guiana (2nd edition). *Géologie de la France* 2-3-4, 5-57.

Doe, B.R. 1970. Pb Isotopes. Springer, Berlim.

Doe, B.R., Zartman, R.E. 1979. Plumbotectonics: the Deposits, H.L. Bames, Editor, Second Edition, pages Phanerozoic; in Geochemistry of Hydrothermal Ore 22-70; John Wiley and Sons, New York.

Dunphy, J.M., Ludden, J.N. 1998. Petrological and geochemical characteristics of a Paleoproterozoic magmatic arc (Narsajuaq Terrane, Ungawa Orogen, Canada) and comparisons to Superior Province granitoids. *Precamb. Res.* 91, 109-142.

Elthon, D. 1989. Pressure origin of primary mid-ocean ridge basalts. In: Saunders, A.D., Norry, M.J. (Eds.), Magmatism in the Ocean Basins. Geological Society Special Publication no. 42. Geological Society, London, pp. 125-136.

Faria, M.S.G. de, Santos, J.O.S. dos, Luzardo, R., Hartmann, L.A., McNaughton, N.J. 2002. The oldest island arc of Roraima State, Brazil – 2.03 Ga: zircon SHRIMP U-Pb geochronology of Anauá Complex. In: SBG, Congresso Brasileiro de Geologia, 41, Anais, p. 306.

Fraga, L.M.B. 2002. A Associação Anortosito–Mangerito–Granito Rapakivi (AMG) do Cinturão Guiana Central, Roraima e Suas Encaixantes Paleoproterozóicas: Evolução Estrutural, Geocronologia e Petrologia. Doctoral thesis, CPGG, UFPA, 386p. Unpublished. (abstract in English).

Fuck, R.A., Pimentel, M.M., Machado, N., Daoud, W.K. 1993. Idade U-Pb do Granito Madeira, Pitinga (AM). In: Congresso Brasileiro de Geoquímica, 4., Brasilia, 1993. Volume de Resumos Expandidos. Brasilia, SBGq, p.246-249. (in Portuguese).

Greenough, J.D., Kyser, T.K. 2003. Contrasting Archean and Proterozoic lithospheric mantle: isotopic evidence from the Shonkin Sag sill (Montana). *Contrib. Mineral. Petrol.* **145**, 169-181

Griffin, T.J., Page, R.W., Sheppard, S., Tyler, I.M. 2000. Palaeoproterozoic post-collisional, high-K felsic igneous rocks from the Kimberley region of northwestern Australia. *Precamb. Res*. 101, 1–23.

Gruau, G., Martin, H., Lévêque, B., Capdevilla, R. 1985. Rb-Sr and Sm-Nd geochronology of Lower Proterozoic granite-greenstone terrains in French Guyane, South America. *Precamb. Res.* 30, 63-80.

Hawkesworth, C. J., Turner, S., Gallagher, Hunter, A., Bradshaw, T., Rogers, N. 1995. Calc-alkaline magmatism, lithospheric thinning and extension in the Basin and Range. *J. Geophys. Res.* 100 (B7), 10271-10286

Heier, KS., Palmer, P.D., Taylor, S.R. 1967. Comment on the Pb distribution in southern Norwegian Precambrian alkali feldspars. *Nor. Geol. Tidskr.* 47, 189.

Hemming, S.R., McDaniel, D.K., McLennan, S.M., Hanson, G.N. 1996. Pb isotope constraints on the provenance and diagenesis of detrital feldspars from the Sudbury Basin, Canada. *Earth Planet. Sci. Lett.*142, 501-512.

Hogan, J. P., Sinha, A. K. 1991. The effect of accessory on the redistribution of lead isotopes during crustal model. *Geochim. Cosmochim. Acta* 55, 335-348.

Housh, T., Bowring, S.A. 1991. Lead isotopic heterogeneities within alkali feldspars: implications for the determination of initial lead isotopic compositions. *Geochim. Cosmochim. Acta* 55, 2309-2316.

Jorge-João, X.S., Santos, C.A., Provost, A. 1985. Magmatismo adamelítico Água Branca (Folha Rio Mapuera, NW do Estado do Pará). In: SBG, Simpósio de Geologia da Amazônia, 2, Belém. *Anais*... v.2, p. 93-109 (in Portuguese).

Huhma, H., 1986. Sm–Nd, U-Pb and Pb–Pb isotopic evidence for the origin of the early Proterozoic Svecokarelian crust in Finland. *Geol. Surv. Finland Bull.* 337, 48p.

Kempton, P.D., Fitton, J.G., Hawkesworth, C.J., Ormerod, D.S. 1991. Isotopic and trace element constraints on the composition and evolution of the lithosphere beneath southwestern United States. *J. Geophys. Res.* 96,13713–13735.

Lahtinen, R., Huhma, H. 1997. Isotopic and geochemical constraints on the evolution of the 1.93-1.79 Ga Svecofennian crust and mantle in Finland. *Precamb. Res.* 82, 13-34.

Lamarão, C.N., Dall'Agnol, R., Lafon, J.M., Lima, E.F. 2002. Geology, geochemistry and Pb–Pb zircon geochronology of the Paleoproterozoic magmatism of Vila Riozinho, Tapajós gold province, Amazonian craton, Brazil. *Precamb. Res.* 119 (1-4), 189–223.

Lamarão, C.N., Dall'Agnol, R., Pimentel, M.M. 2005. Nd isotopic composition of Paleoproterozoic volcanic and granitoid rocks of Vila Riozinho: implications for the crustal evolution of the Tapajós gold province, Amazon craton. *J. South Am. Earth Sci.* 18, 277–292.

Leite, A. da S.S., Dall´Agnol, R., Macambira, M.J.B., Althoff, F.J. 2004. Geologia e geocronologia dos granitóides arqueanos da região de Xinguara-PA e suas implicações na evolução do terreno granito-greenstone de Rio Maria, Cráton Amazônico. *Rev. Bras. Geoc.* 34(4), 447-458. (abstract in English)

Lenharo S.L.R. 1998. Evolução magmatica e modelo metalogenetico dos granitos mineralizados da regiao de Pitinga, Amazonas, Brasil. Doctoral thesis, Universidade de São Paulo, São Paulo, 290 p. Unpublished. (abstract in English)

Ludwig, K.R., Silver, L.T., 1977. Lead-isotope inhomogeneity in Precambrian igneous K-feldspars. *Geochim. Cosmochim. Acta* 41(10), 1457-1471.

Macambira, M.J.B., Teixeira, J.T., Daoud, W.K., Costi, H.T. 1987. Geochemistry, mineralization and age of tin-bearing granites from Pitinga, northwestern Brazil. *Revista Brasileira de Geociências*, 17 (4), 562-570.

Macambira, M.J.B., Almeida, M.E., Santos, L.S. 2002. Idade de Zircão das Vulcânicas Iricoumé do Sudeste de Roraima: contribuição para a redefinição do Supergrupo Uatumã. In: SBG, Simpósio Sobre Vulcanismo Ambientes Associados, 2, Anais, p.22 (in Portuguese).

Macambira, M.J.B., Lancelot, J.R. 1996. Time constraints for the formation of the Archean Rio Maria crust, southeastern Amazonian craton, Brazil. *Intern. Geol. Rev.* 38, 1134–1142.

McCulloch, M.T., Woodhead, J.D. 1993. Lead isotopic evidence for deep crustal-scale fluid transport during granite petrogenesis. *Geochim. Cosmochim. Acta* 57, 659-674.

Nironen, M. 1997. The Svecofennian Orogen: a tectonic model. *Precamb. Res*. 86, 21–44.

Oliveira, M.J.R.; Almeida, M.E.; Luzardo, R., Faria, M.S.G. de. 1996. Litogeoquímica da Suíte Intrusiva Água Branca - SE de Roraima. Congr. Brasil. de Geol., 39, Salvador, 1996. Anais... Salvador, Bahia, SBG, v.2, p. 213-216 (in Portuguese).

Page, R.W., 1988. Geochronology of early to middle Proterozoic fold belts in northern Australia: a review. *Precamb. Res.* 40/41, 1–20.

Patterson, C.;Tatsumoto, M. 1964. The significance of lead isotopes in detrital feldspar with respect to chemical differentiation within the earth's mantle, *Geochim. Cosmochim. Acta* 28, 1-22.

Pimentel, M.M., Machado, N. 1994. Geocronologia U–Pb dos terrenos granito–greenstone de Rio Maria, Pará. In: SBG, Congr. Bras. Geol., 38, São Paulo, *Anais*...pp. 390–391.

Pimentel, M.M., Spier, C.A., Ferreira Filho, C.F. 2002. Estudo Sm-Nd do Complexo máfico-ultramáfico Bacuri, Amapá: idade da intrusão, metamorfismo e natureza do magma original. *Rev. Bras. Geoc.* 32, 371-376. (abstract in English)

Rehkamper, M., Hofmann, A.W. 1997. Recycled ocean crust and sediment in Indian Ocean MORB. *Earth Planet. Sci. Lett.* 147 (1-4), 93-106.

Reis, N.J., Fraga, L.M.B., Faria, M.S.G. de, Almeida, M.E. 2003. Geologia do Estado de Roraima. Géologie de la France, 2-3-4, 71-84. (abstract in English).

Rudnick, R.L., Goldstein, S.L. 1990. The Pb isotopic composition of lower crustal xenoliths and the evolution of lower crustal Pb. *Earth Planet. Sci. Lett.* 98, 192-207.

Santos, J.O.S. dos, Faria, M.S.G. de, Hartmann, L.A., McNaughton, N.J. 2002. Significant presence of the Tapajós-Parima Orogenic Belt in the Roraima region, Amazon Craton based on SHRIMP U-Pb zircon geochronology. In: SBG, Congresso Brasileiro de Geologia, 51, João Pessoa, Anais... p. 336.

Santos J.O.S. dos; Faria M.S.G.; Hartmann L.H.; McNaughton N.J.; Fletcher I.R. 2001a. Oldest charnockitic magmatism in the Amazon craton: zircon U-Pb SHRIMP geochronology of the Jaburu charnockite, southern Roraima, Brazil. In: SBG\Norte, Simp. Geol. Amaz, 7, CD-ROM (in Portuguese).

Santos, J.O.S. dos, Groves, D.I., Hartmann, L.A., McNaughton, N.J., Moura, M.B. 2001b. Gold deposits of the Tapajós and Alta Floresta domains, Tapajós–Parima orogenic belt, Amazon Craton, Brazil. *Mineralium Deposita* 36, 278–299.

Santos, J.O.S. dos, Hartmann, L.A., Faria, M.S.G. de, Riker, S.R.L., Souza, M.M. de, Almeida, M.E., McNaughton, N.J. 2006. A Compartimentação do Cráton Amazonas em Províncias: Avanços ocorridos no período 2000-2006. In: SBG, Simpósio de Geologia da Amazônia, 9, Belém, CD-ROM.

Santos J.O.S. dos, Hartmann L.A., Gaudette H.E., Groves D.I., McNaughton N.J., Fletcher I.R. 2000. A new understanding of the provinces of the Amazon Craton based on integration of field mapping and U-Pb and Sm-Nd geochronology: *Gondwana Research* 3 (4), 453-488.

Santos, J.O.S. dos, Reis, N.J., Chemale, F., Hartmann, L.A., Pinheiro, S. da S., McNaughton, N.J. 2003. Paleoproterozoic Evolution of Northwestern Roraima State – Absence of Archean Crust, Based on U-Pb and Sm-Nd Isotopic Evidence. In: Simposyum of South-American on Isotope Geology, 4, Pucon, Chile.

Santos J.O.S. dos, Silva L.C., Faria M.S.G. de, Macambira, M.J.B. 1997. Pb-Pb single crystal, evaporation isotopic study on the post-tectonic, sub-alkalic, A-type Moderna granite, Mapuera intrusive suite, State of Roraima, northern Brazil. In: Symposium of Granites and Associated Mineralizations, 2. Extended Abstract and Program. Salvador, Brasil: p. 273-275.

Santos, J.O.S. dos, Van Breemen, O.B., Groves, D.I., Hartmann, L. A., Almeida, M.E., McNaughton, N.J., Fletcher, I.R. 2004. Timing and evolution of multiple Paleoproterozoic magmatic arcs in the Tapajós Domain, Amazon Craton: constraints from SHRIMP and TIMS zircon, baddeleyite and titanite U–Pb geochronology. *Precamb. Res.* 131 (10), 73-109.

Sato, K., Siga Jr., O. 2002. Rapid growth of continental crust between 2.2 to 1.8 Ga in the South American Platform: integrated Australian, European, North American and SW USA crustal evolution study. *Gondwana Research* 5, 165–173.

Sato, K., Tassinari, C.C.G. 1997. Principais eventos de acreção continental no Cráton Amazônico baseados em idade-modelo Sm–Nd, calculada em evoluções de estágio único e estágio duplo, in: Costa, M.L.C., Angélica, R.S. (Eds.), Contribuições à Geologia da Amazônia. Sociedade Brasileira de Geologia, Belém, Brazil, 1, pp. 91–142. (abstract in English)

Sinha, A.K. 1969. Removal of radiogenic lead from potassium feldspars by volatilization. *Earth Planet. Sci. Lett.* 7, 109-115.

Stacey, J.S., Kramers, J.D. 1975. Approximation of terrestrial lead isotope evolution by a two-stage model. *Earth Planet. Sci. Lett.*, 26, 207-221.

St-Onge, M.R., Lucas, S.B., Scott, D.J., Wodicka, N., 1999. Upper and lower plate juxtaposition, deformation and metamorphism during crustal convergence, Trans-Hudson Orogen (Quebec-Baffin segment), Canada. Precambrian Res. 93, 27–49.

Tassinari, C.C.G. 1996. O Mapa Geocronológico do Cráton Amazônico no Brasil: revisão dos dados isotópicos. Tese de Livre docência, Instituto de Geociências da Universidade de São Paulo. 139p. (abstract in English).

Tassinari, C.C.G., Macambira, M.J.B. 1999. Geochronological Provinces of the Amazonian Craton. *Episodes* 22 (3),: 174-182.

Tassinari, C.C.G., Macambira, M.J.B. 2004. A Evolução Tectônica do Cráton Amazônico. In: Mantesso-Neto, V., Bartoreli, A., Carneiro, C.D.R., Brito-Neves, B.B. de (eds), Geologia do Continente Sul-Americano - Evolução da Obra de Fernando Flávio Marques de Almeida, São Paulo, Ed. Beca, p. 471-485. (abstract in English)

Tassinari, C.G.C., Munhá, J.M.U., Teixeira, W., Palácios, T., Nutman, A.P., Sosa, C.S., Santos, A.P., Calado, B.O. 2004. The Imataca Complex, NW Amazonian Craton, Venezuela: Crustal evolution and integration of geochronological and petrological cooling histories. *Episodes* 27 (1), 1-12.

Teixeira, W., Tassinari, C.C.G., Cordani, U.G., Kawashita, K. 1989. A review of the Geochronology of the Amazonian Craton tectonic implications. *Precamb. Res.* 42, 213-227.

Tomascak, P.B. 1995. The petrogenesis of granitic rocks in southwestern Maine. PhD Thesis, University of Maryland, College Park, MD.

Tomascak, P.B.; Brown, M.; Solar, G.S., Beckera, H.J.; Centorbi, H.J., Tian, J. 2005. Source contributions to Devonian granite magmatism near the Laurentian border, New Hampshire and Western Maine, USA. *Lithos* 80, 75– 99.

Väisänen, M., Mänttäri, I. Hölttä, P. 2002. Svecofennian magmatic and metamorphic evolution in southwestern Finland as revealed by U-Pb zircon SIMS geochronology. *Precamb. Res.* 116, 111-127.

Valério, C.S. 2006. Magmatismo Paleoproterozóico do extremo sul do Escudo das Guianas, município de Presidente Figueiredo (AM): geologia, geoquímica e geocronologia Pb-Pb em zircão. MSc thesis, Universidade Federal do Amazonas, Manaus, ?p. (abstract in English).

Valério, C.S., Souza, V.S., Macambira, M.J.B., Milliotti, C.A., Carvalho, A.S. 2005. Geoquímica e idade Pb-Pb de zircão do Grupo Iricoumé na região da borda norte da bacia do Amazonas, município de Presidente Figueiredo (AM). In: SBG, Simp. Vulc. Amaz. Amb. Assoc., 3, Anais, p.47-52.

Vasquez, M.V., Ricci, P.S.F., Klein, E.L. 2002. Granitóides pós-colisionais da porção leste da Província Tapajós. In: Klein, E.L., Vasquez, M.L., Rosa-Costa, L.T. (orgs), Contribuições à Geologia da Amazônia, 3, Belém, SBG, p. 63-83. (abstract in English)

Wyborn, L.A. 1988. Petrology, geochemistry and origin of a major Australian 1880–1840 Ma felsic volcano-plutonic suite, a model for intracontinental felsic magma generation. *Precamb. Res.* 4041, 37–60.

Zartman, R.E., Doe, B.R. 1981. Plumbotectonics - the model. *Tectonophysics* 75, 135-162.

Zartman, R.E., Haines, S. 1988. The plumbotectonic model for Pb isotopic systematics among major terrestrial reservoirs – a case for bi-directional transport. *Geochim. Cosmochim. Acta* 52, 1327–1339.

Zindler, A, Hart, S. 1986. Chemical geodynamics. *Am. Rev. Earth Planet. Sci.* 5(14), 493-571.

Table 1. Summary of previous geochronological data from Uatumã-Anauá domain.

Sample code	Rock Type	Lithostratigraphic Unit	Crystallization age (Ma)	Reference	Method	Inherited age (Ma)	Reference	Method	obs
Northern Uatumã-Anauá Domain									
MA-246C2	Leucogranite	Pods and lenses of leucogranite	1906 ± 5 zi	Almeida *et al.* (subm.)	C	1959 ± 5 zi	Almeida *et al.* (subm.)	C	Martins Pereira
						1997 ± 8 zi	Almeida *et al.* (subm.)	C	Anauá Arc?
						2128 ± 3 zi	Almeida *et al.* (subm.)	C	Early Transamanzonian
						2354 ± 6 zi	Almeida *et al.* (subm.)	C	Siderian
MF-156	Monzogranite	S-type Serra Dourada Granite	1948 ± 11 zi	Almeida *et al.* (subm.)	C	2138 ± 11 zi	Almeida *et al.* (subm.)	C	Early Transamanzonian
			1962 ± 6 zi	Almeida *et al.* (subm.)	D				
MF-132A	Metamonzogranite	Martins Pereira Granite	1938 ± 17 zi	Almeida *et al.* (1997)	B				
NR-017	Metamonzogranite	Martins Pereira Granite	1960 ± 21 zi	Almeida *et al.* (1997)	B				
MA-007A	Metamonzogranite	Martins Pereira Granite	1971 ± 2 zi	Almeida *et al.* (subm.)	C				
MF-132A	Metamonzogranite	Martins Pereira Granite	1972 ± 7 zi	CPRM (2003)	F				
MA-061A	Mylonitic granodiorite	Martins Pereira Granite	1973 ± 2 zi	Almeida *et al.* (subm.)	C				
MA-172A	Monzogranite	Martins Pereira Granite	1975 ± 5 zi	Almeida *et al.* (subm.)	C				
MF-075	Metatonalite	Anauá Complex	2028 ± 9 zi	Faria *et al.* (2002)	F				
Southern Uatumã-Anauá Domain									
-	Água Boa Granite	Madeira Suite	1679 ± 60 wr	Macambira *et al.* (1987)	A				$^{87}Sr/^{86}Sr_o$ = 0.7113
-	Madeira Granite	Madeira Suite	1691 ± 64 wr	Macambira *et al.* (1987)	A				$^{87}Sr/^{86}Sr_o$ = 0.7062
-	Água Boa Granite	Madeira Suite	1794 ± 19 zi	Lenharo (1998)	D				
MJ-59A	Moderna Granite	Madeira Suite	1814 ± 27 zi	Santos *et al.* (1997)	B				
-	Madeira Granite	Madeira Suite	1815 ± 5 zi	Lenharo (1998)	D				
-	Madeira Granite	Madeira Suite	1817 ± 2 zi	Costi *et al.* (2000)	C				
-	Madeira Granite	Madeira Suite	1822 ± 1 zi	Costi *et al.* (2000)	C				
-	Madeira Granite	Madeira Suite	1824 ± 2 zi	Costi *et al.* (2000)	C				
-	Europa Granite	Madeira Suite	1829 ± 1 zi	Costi *et al.* (2000)	C				
-	Madeira Granite	Madeira Suite	1834 ± 6 zi	Fuck *et al.* (1993)	D				
-	Pitinga Mine Granite	Mapuera Suite	1861 ± 20 zi	Lenharo (1998)	F				
-	Pitinga Mine Granite	Mapuera Suite	1864 ± 13 zi	Lenharo (1998)	F				
-	Pitinga Mine Granite	Mapuera Suite	1865 ± 15 zi	CPRM (2003)	F				
MF-17	Meretxa Mylonitic Granite	Mapuera Suite?	1869 ± 10 zi	CPRM (2003)	F				
JO-05	Weathered gneiss	Mapuera Suite?	1871 ± 11 zi	CPRM (2003)	F				
km 199	Abonari Syenogranite	Mapuera Suite	1871 ± 5 zi	CPRM (2003)	F				
JO-07	Weathered granitoid	Mapuera Suite?	1879 ± 2 zi	Santos (2002)	F				
JO-06	Weathered granitoid	Mapuera Suite?	1880 ± 3 zi	Santos (2002)	F				
MA-226	Murauaú Granite	Mapuera Suite	1871 ± 5 zi	Almeida *et al.* (in prep.)	C	1888 ± 3 zi	Almeida *et al.* (in prep.)	C	Caroebe?

Table 1 (continued)

Sample code	Rock Type	Lithostratigraphic Unit	Crystallization age (Ma)	Reference	Method	Inherited age (Ma)	Reference	Method	obs
						2359 ± 7 zi	Almeida *et al.* (in prep.)	C	Siderian
-	São Gabriel Granite	Mapuera Suite?	1889 ± 2 zi	Valério (2006)	C				
MA-186A	Monzogranite	Igarapé Azul Granite. Saramandaia Facies	1889 ± 3 zi	Almeida *et al.* (in prep.)	C	1972 ± 3 zi	Almeida *et al.* (in prep.)	C	Martins Pereira
MA-201B	Granitic veins in biotite-bearing enclave	Igarapé Azul Granite. Vila Catarina Facies	1891 ± 3 zi	Almeida *et al.* (in prep.)	C	1967 ± 6 zi	Almeida *et al.* (in prep.)	C	Martins Pereira
MA-147A	Monzogranite	Igarapé Azul Granite. Cinco Estrelas Facies	1891 ± 6 zi	Almeida *et al.* (in prep.)	C	1964 ± 4 zi	Almeida *et al.* (in prep.)	C	Martins Pereira
MA-186A	Monzogranite	Igarapé Azul Granite. Saramandaia Facies	1913 ± 4 zi	Almeida *et al.* (in prep.)	C				
MA-198	Enderbite	Santa Maria Enderbite	1891 ± 1 zi	Almeida *et al.* (in prep.)	C				
-	Biotite mylonitized granite	Água Branca Suite	1890 ± 2 zi	Valério (2006)	C				
MA-53A	Monzogranite	Caroebe Granite. Alto Alegre Facies (Água Branca Suite)	1891 ± 2 zi	Almeida *et al.* (in prep.)	C	1963 ± 4 zi	Almeida *et al.* (in prep.)	C	Martins Pereira
MF-68A	Quartz Monzodiorite	Igarapé Dias Quartz Monzodiorite (Água Branca Suite)	1891 ± 6 zi	CPRM (2003)	F				
-	Biotite porphyrytic granite	Água Branca Suite	1895 ± 6 zi	Valério (2006)	C				
MA-121	Quartz Monzodiorite	Caroebe Granite. Jaburuzinho Facies (Água Branca Suite)	1898 ± 2 zi	Almeida *et al.* (in prep.)	C				
-	Biotite-hornblende mylonitized granite	Água Branca Suite	1898 ± 3 zi	Valério (2006)	C				
HM-181	Monzogranite (type-area)	Água Branca Granite (Água Branca Suite)	1901 ± 5 zi	Almeida *et al.* (in prep.)	C	2142 ± 10 zi	Almeida *et al.* (in prep.)	C	Early Transamanzonian
-	-	Northwestern of Pará (Água Branca Suite)	1910 ± 23 wr	Jorge-João *et al.* (1985)	A				$^{87}Sr/^{86}Sr_o$ = 0.70225
-	Epizonal Rhyolite	Iricoumé Volcanics	1883 ± 4 zi	Valério *et al.* (2005)	C				
PHR-06	Rhyolite (Pitinga region)	Iricoumé Volcanics	1888 ± 3 zi	Costi *et al.* (2000)	C				
MA-209	Porphyry Dacite (Jatapu River)	Jatapu Volcanics	1893 ± 2 zi	Macambira *et al.* (2002)	C				
MA-208	Andesite (Jatapu River)	Jatapu Volcanics	1893 ± 4 zi	Almeida *et al.* (in prep.)	C	1966 ± 3 zi	Almeida *et al.* (in prep.)	C	Martins Pereira
MF-34	Canoas Rhyodacite	Iricoumé Volcanics	1896 ± 7 zi	CPRM (2003)	F				

Notes: A. Rb-Sr iscohron. B. Pb-evaporation on single filament; C. Pb-evaporation on double filament; D. U-Pb ID-TIMS; E. U-Pb LA-MC-ICP-MS; F. U-Pb SHRIMP. Abbreviations: wr. whole-rock. zi. zircon.

Table 2. Sm-Nd (whole rock) and Pb (leached feldspars) isotopic data of Uatumã-Anauá Domain in south central Guyana Shield.

Province		Tectonic Domain	Sample	Rock type	T_{crist} (Ma)	Ref.	Sm (ppm)	Nd (ppm)	Sm/Nd	$^{147}Sm/^{144}Nd$	1σ (10^{-7})	$^{143}Nd/^{144}Nd$	1σ (10^{-6})	$eNd_{(0)}$	$eNd_{(t)}$	$T_{(DM)}$	Ref.	Pb^{206}/Pb^{204}	1σ (10^{-2})	Pb^{207}/Pb^{204}	1σ (10^{-2})	Pb^{208}/Pb^{204}	1σ (10^{-2})	Ref.
1	2		*Moderna Granitoids*																					
VT	KSB	UA	MF-103	Alaskite	1810	G, e.a.	7.02	39.61	0.18	0.10713	-	0.511549	-	-21.24	-0.44	2.14	CPRM unpubl.	-	-	-	-	-	-	-
VT	KSB	UA	CA-03	Syenogranite	1810	G, e.a.	12.15	68.53	0.18	0.10718	-	0.511497	9	-22.26	-1.47	2.22	CPRM unpubl.	-	-	-	-	-	-	-
VT	TP	UA	MF-33B	Monzogranite protomylonite	1810	G, e.a.	4.69	30.53	0.15	0.09289	-	0.511280	-	-26.49	-2.39	2.23	CPRM unpubl.	-	-	-	-	-	-	-
			Mapuera Granitoids																					
VT	TP	SUA	MF-04	Granophyre	1871	D, e.a.	9.28	51.30	0.18	0.10931	-	0.511596	15	-20.33	0.66	2.12	CPRM unpubl.	-	-	-	-	-	-	-
VT	TP	SUA	MF-03	Granite	1871	D, e.a.	8.83	51.87	0.17	0.10290	-	0.511481	11	-22.57	-0.04	2.15	CPRM unpubl.	-	-	-	-	-	-	-
VT	TP	SUA	KM 199	Hornblende granite	1871	D, e.a.	15.97	93.45	0.17	0.10332	-	0.511474	20	-22.71	-0.28	2.17	CPRM unpubl.	-	-	-	-	-	-	-
MI	TP	UA	SC-19	Granite	1871	D, e.a.	15.25	97.30	0.16	0.09470	-	0.511353	5	-25.07	-0.56	2.17	Costa (2005)	-	-	-	-	-	-	-
TP	TP	UA	SC-95	Hornblende-biotite granite	1871	D, e.a.	8.55	45.35	0.19	0.11390	-	0.511556	6	-21.11	-1.22	2.28	Costa (2005)	-	-	-	-	-	-	-
			Igarapé Azul Granite																					
VT	TP	SUA	MA-147A	Monzogranite	1889	B	10.53	71.95	0.15	0.08850	10	0.511292	4	-26.30	-0.02	2.14	This study	16.08	2	15.59	2	35.88	6	This study
VT	TP	SUA	MF-6A	Leucogranodiorite	1890	B, e.a.	4.76	30.72	0.15	0.09362	-	0.511354	13	-25.00	-0.04	2.15	CPRM unpubl.	16.62	4	15.65	4	36.18	12	This study
VT	TP	SUA	MA-201A	Monzogranite	1890	B	6.95	39.27	0.18	0.10705	4	0.511458	4	-23.00	-1.27	2.27	This study	16.27	5	15.42	4	35.71	12	This study
TP	TP	SUA	SC-91*	Granite	1889	B, e.a.	3.23	24.85	0.13	0.07860	-	0.511136	9	-29.30	-0.67	2.28	mod.Costa (2005)	-	-	-	-	-	-	-
VT	TP	SUA	MA-186A	Monzogranite	1890	B	7.60	44.45	0.17	0.10329	5	0.511394	7	-24.30	-1.61	2.28	This study	15.98	1	15.54	1	35.61	4	This study
VT	TP	SUA	MA-187	Monzogranite	-	-	-	-	-	-	-	-	-	-	-	-	-	15.87	1	15.51	2	35.59	5	This study
			Caroebe Granite (Alto Alegre facies)																					
TP	TP	SUA	MA-53A	Granodiorite	1891	B	3.94	29.16	0.14	0.08176	3	0.511173	5	-28.60	-0.68	2.17	This study	16.41	7	15.54	7	36.09	18	This study
TP	TP	SUA	SC-97	Monzogranite	1891	B, e.a.	2.88	19.48	0.15	0.08930	-	0.511233	6	-27.41	-1.34	2.22	Costa (2005)	-	-	-	-	-	-	-
TP	TP	SUA	MA-276	Granodiorite	1891	B, e.a.	6.25	45.50	0.14	0.08310	6	0.511110	6	-29.80	-2.24	2.26	This study	-	-	-	-	-	-	-
VT	TP	SUA	SC-104	Granodiorite	1891	B, e.a.	6.03	34.21	0.18	0.10660	-	0.511384	7	-24.46	-2.60	2.37	Costa (2005)	-	-	-	-	-	-	-
VT	TP	SUA	MA-144A	Granodiorite	1891	B, e.a.	4.84	30.10	0.16	0.09715	6	0.511211	19	-27.80	-3.69	2.41	This study	-	-	-	-	-	-	-
			Caroebe Granite (Jaburuzinho facies)																					
CA	TP	SUA	MA-53C	Tonalite	1898	B, e.a.	5.95	32.10	0.19	0.11211	7	0.511605	10	-20.20	0.46	2.16	This study	-	-	-	-	-	-	-
CA	TP	SUA	MA-121	Quartz monzodiorite	1898	B	8.02	55.82	0.14	0.08685	12	0.511243	3	-27.20	-0.45	2.17	This study	15.90	1	15.54	2	35.49	5	This study
VT	TP	SUA	MA-144B	Diorite	1898	B, e.a.	11.43	65.95	0.17	0.10476	10	0.511466	5	-22.90	-0.46	2.21	This study	-	-	-	-	-	-	-
VT	TP	SUA	SC-215	Monzogranite	1898	B, e.a.	6.54	38.61	0.17	0.10240	-	0.511436	6	-23.45	-0.47	2.21	Costa (2005)	-	-	-	-	-	-	-
VT	KSB	SUA	MF-68A	Quartz monzodiorite	1891	D	9.95	52.35	0.19	0.11492	-	0.511600	11	-20.25	-0.40	2.23	CPRM unpubl.	-	-	-	-	-	-	-
CA	TP	SUA	MA-53B	Quartz monzonite	1898	B, e.a.	3.96	22.81	0.17	0.10502	4	0.511415	5	-23.90	-1.53	2.29	This study	-	-	-	-	-	-	-
VT	TP	SUA	MA-112	Monzogranite	1898	B, e.a.	9.04	53.40	0.17	0.10231	9	0.511373	7	-24.70	-1.69	2.29	This study	-	-	-	-	-	-	-
VT	TP	SUA	MF-26A	Monzogranite protomylonite	1900	B, e.a.	7.62	50.02	0.15	0.09205	-	0.511225	-	-27.56	-2.05	2.29	CPRM unpubl.	-	-	-	-	-	-	-
VT	TP	SUA	MA-178B	Quartz monzodiorite	1898	B, e.a.	10.32	69.66	0.15	0.08953	11	0.511162	25	-28.79	-2.69	2.32	This study	16.05	1	15.54	2	35.69	5	This study
VT	TP	SUA	MA-103	Granodiorite	1898	B, e.a.	6.65	40.29	0.17	0.09975	5	0.511209	17	-27.90	-4.27	2.47	This study	-	-	-	-	-	-	-
			Caroebe Granite?																					
VT	TP	SUA	PT 25*	Granite	1891	B, e.a.	6.29	31.87	0.20	0.11932	104	0.511758	27	-17.17	1.62	2.11	mod. Sato and Tassinari (1997)	-	-	-	-	-	-	-
VT	TP	SUA	PT 26*	Granodiorite	1891	B, e.a.	4.44	38.28	0.12	0.07016	72	0.511081	33	-30.37	0.33	2.21	mod. Sato and Tassinari (1997)	-	-	-	-	-	-	-

Table 2 (Continued)

Province		Tectonic Domain	Sample	Rock type	T_{crist} (Ma)	Ref.	Sm (ppm)	Nd (ppm)	Sm/ Nd	$^{147}Sm/^{144}Nd$	1σ (10^{-7})	$^{143}Nd/^{144}Nd$	1σ (10^{-6})	$eNd_{(0)}$	$eNd_{(t)}$	$T_{(DM)}$	Ref.	Pb^{206}/Pb^{204}	1σ (10^{-2})	Pb^{207}/Pb^{204}	1σ (10^{-2})	Pb^{208}/Pb^{204}	1σ (10^{-2})	Ref.
			Água Branca Granite																					
VT	TP	SUA	HM-181	Granodiorite	1901	B	6.45	38.28	0.17	0.10183	5	0.511298	8	-26.10	-3.00	2.39	This study	-	-	-	-	-	-	-
			Igarapé Tamandaré Charnockite																					
VT	KSB	SUA	MF-28	Charnockite	1890	B, e.a.	7.88	43.89	0.18	0.10861	-	0.511526	8	-21.69	-0.32	2.21	CPRM unpubl.	-	-	-	-	-	-	-
			Iricoumé and Jatapu Volcanic rocks																					
CA	TP	SUA	PHR-06	Rhyolite	1888	C	9.77	55.65	0.18	0.10620	-	0.511500	-	-22.20	-0.27	2.19	Costi (2000)	-	-	-	-	-	-	-
VT	TP	SUA	MF-144A	Dacite porphyry	1893	F, e.a.	5.46	33.52	0.16	0.09850	-	0.511379	-	-24.56	-0.70	2.21	CPRM unpubl.	-	-	-	-	-	-	-
VT	TP	SUA	MF-01	?	1896	D, e.a.	8.78	45.80	0.19	0.11595		0.511625	9	-19.76	-0.14	2.22	CPRM unpubl.	-	-	-	-	-	-	-
CA	TP	SUA	MF-34	Hornblende-biotite andesite	1893	F, e.a.	8.27	50.93	0.16	0.09817		0.511337	19	-25.38	-1.44	2.26	CPRM unpubl.	-	-	-	-	-	-	-
TP	TP	SUA	SC-90	Rhyodacite	1893	F, e.a.	4.33	27.85	0.16	0.09400	-	0.511269	6	-26.71	-1.76	2.27	Costa (2005)	-	-	-	-	-	-	-
TP	TP	SUA	NR-29A	?	1893	F, e.a.	26.55	158.43	0.17	0.10132	-	0.511365	-	-24.83	-1.66	2.28	CPRM unpubl.	-	-	-	-	-	-	-
			Leucogranites (pods and lenses)																					
VT	TP	NUA	MA-07B	Leucosyenogranite	1906	B	2.68	17.88	0.15	0.09066	4	0.511127	11	-29.50	-3.48	2.38	This study	16.15	2	15.59	2	35.95	6	This study
VT	TP	NUA	MA-46B	Leucomonzogranite	-	-	-	-	-	-	-	-	-	-	-	-	-	16.87	1	15.70	2	35.74	5	This study
			Enclaves (biotite-bearing gneisses)																					
VT	TP	SUA	MA-213B*	Quartz monzodiorite	1973	B, e.a.	12.26	55.73	0.22	0.13307	5	0.51166	6	-19.10	-2.92	2.51	This study	-	-	-	-	-	-	-
VT	TP	SUA	MA-201B*	Quartz diorite	1967	B	41.72	159.79	0.26	0.15719	128	0.51183	7	-15.70	-5.93	2.72	This study	-	-	-	-	-	-	-
			Serra Dourada Granite																					
VT	TP	NUA	MF-156	Syenogranite with cordierite	1962	A	4.84	24.50	0.20	0.11990	-	0.51158	18	-20.70	-3.19	2.38	CPRM unpubl.	-	-	-	-	-	-	-
VT	TP	NUA	MF-151	Monzogranite with muscovite	1962	A, e.a.	9.14	45.45	0.20	0.12124	-	0.51152	16	-21.81	-4.34	2.53	CPRM unpubl.	-	-	-	-	-	-	-
			Martins Pereira Granite																					
VT	TP	NUA	NR-18	Metamonzogranite	1973	A, e.a.	6.69	43.08	0.16	0.09385	-	0.51122	9	-27.74	-1.74	2.33	CPRM unpubl.	-	-	-	-	-	-	-
VT	KSB	NUA	TP-01	Monzogranite	1973	A, e.a.	10.17	56.21	0.18	0.10939	-	0.51145	11	-23.19	-3.20	2.34	CPRM unpubl.	-	-	-	-	-	-	-
VT	TP	NUA	MF-11A	Granodiorite	1973	A, e.a.	6.92	35.21	0.20	0.11884	-	0.51158	14	-20.64	-0.92	2.36	CPRM unpubl.	16.50	1	15.70	2	36.04	5	This study
VT	TP	NUA	MA-61A	Mylonite granodioritic	1973	A	10.91	58.19	0.19	0.11335	5	0.51148	9	-22.50	-1.42	2.38	This study	16.18	3	15.57	3	35.59	8	This study
VT	TP	NUA	MA-07A	Metamonzogranite	1971	A	12.55	68.74	0.18	0.11037	10	0.51144	6	-23.40	-1.55	2.38	This study	16.09	2	15.58	2	35.82	7	This study
VT	KSB	NUA	MA-246C1	Metatonalite	1973	A, e.a.	9.81	53.44	0.18	0.11098	8	0.51141	6	-23.90	-2.17	2.43	This study	16.15	1	15.62	1	35.77	4	This study
VT	TP	NUA	MF-132A*	Metamonzogranite	1972	D	6.68	31.57	0.21	0.12793	-	0.51161	-	-20.05	-2.67	2.49	CPRM unpubl.	-	-	-	-	-	-	-
VT	TP	NUA	MA-07C*	Epidote-biotite Metatonalite	1973	A, e.a.	11.69	55.99	0.21	0.12622	10	0.51152	5	-21.70	-3.89	2.58	This study	-	-	-	-	-	-	-
VT	TP	NUA	MA-172A	Monzogranite	1975	A	17.87	97.09	0.18	0.11130	8	0.51129	3	-26.40	-4.74	2.64	This study	-	-	-	-	-	-	-
			Anauá Complex																					
VT	TP	NUA	MF-126C	Metatonalite	2028	E, e.a.	6.91	36.46	0.19	0.11465	-	0.51153	-	-21.56	-0.19	2.33	Faria *et al.* (2002)	-	-	-	-	-	-	-
VT	TP	NUA	SC-101*	Orthogneiss	2028	E, e.a.	6.08	48.33	0.13	0.07600	-	0.51091	12	-33.63	-2.21	2.50	mod. Costa (2005)	-	-	-	-	-	-	-

Nd T_{DM} ages are calculated using the model of De Paolo (1981) for Nd evolution of the depleted mantle. Obs: e.a. estimated age; *highly fractionated samples. showing $0.125<^{147}Sm/^{144}Nd<0.08$. has been recalculated based on Nd evolution by double-stage. Geochronological Provinces: 1. Tassinari and Macambira (2004); 2. Santos *et al.* (2006); KSB. K' Mudku Shear Belt; VT-TP. Ventuari-Tapajós (or Tapajós-Parima); MI. Maroni-ItaTPiúnas; TP. Central Amazonian. Domain: UA – Uatumã-Anauá (SUA - Southern; NUA - Northern). Crystalization ages (References): A. Almeida *et al.* (subm.); B. Almeida *et al.* (in prep.); C. Costi *et al.* (2000); D. CPRM (2003); E. Faria *et al.* (2002); F. Macambira *et al.* (2002); G. Santos *et al.* (1997).

Table 3. Some Sm-Nd (whole rock) isotopic data of Ventuari-Tapajós (or Tapajós-Parima), Maroni-Itacaiúnas (or Transamazon) and Central Amazonian Provinces.

Provinces		Tectonic Domain	Sample	Rock type	T_{crist} (Ma)	Ref.	Sm (ppm)	Nd (ppm)	Sm/ Nd	f(Sm/Nd)	$^{147}Sm/^{144}Nd$	$^{143}Nd/^{144}Nd$	1σ (10^{-6})	$\varepsilon Nd_{(0)}$	$\varepsilon Nd_{(t)}$	$T_{(DM)}$	Ref.
1	2		*Basement rocks (Carajás Archean TTG terrane)*														
TP	CI	C	246	Mogno Trondhjemite?	2871	I, e.a.	1.99	13.70	0.15	-0.55	0.08804	0.510810	-	-35.66	+4.55	2.73	mod. Sato and Tassinari (1997)
TP	CI	C	245	Granodiorite (Mogno Trondhjemite)	2871	I, e.a.	3.61	22.63	0.16	-0.51	0.09646	0.510862	-	-34.64	+2.43	2.86	mod. Sato and Tassinari (1997)
TP	CI	C	MJ 08	Arco Verde Tonalite	2957	H	2.55	18.60	0.14	-0.58	0.08272	0.510515	12	-41.41	+2.02	2.97	Dall´Agnol *et al.* (1999)
TP	CI	C	HRM 284	Rio Maria Granodiorite	2874	C	3.06	18.60	0.16	-0.50	0.09932	0.510834	9	-35.19	+0.86	2.98	Dall´Agnol *et al.* (1999)
TP	CI	C	161	Tonalite (Xingu Complex)	2974	A, e.a.	1.18	7.92	0.15	-0.54	0.08972	0.510641	-	-38.96	+0.32	2.98	mod. Sato and Tassinari (1997)
TP	CI	C	243	Granodiorite (Xinguara Granite)	2865	G, e.a.	3.81	23.81	0.16	-0.60	0.07838	0.510393	-	-43.79	-0.14	3.02	mod. Sato and Tassinari (1997)
TP	CI	C	160	Gneiss (Mogno Trondhjemite)	2871	I, e.a.	5.55	50.24	0.11	-0.66	0.06684	0.510149	-	-48.55	-0.54	3.03	mod. Sato and Tassinari (1997)
TP	CI	C	Z 509B	Rio Maria Granodiorite	2874	C	5.89	29.26	0.20	-0.39	0.12160	0.511235	15	-27.37	+0.43	3.03	Dall´Agnol *et al.* (1999)
TP	CI	C	244	Granodiorite (Mogno Trondhjemite)	2871	I, e.a.	3.18	17.85	0.18	-0.45	0.10763	0.510956	-	-32.81	+0.12	3.04	mod. Sato and Tassinari (1997)
			Imataca terrane														
MI	CI	I	V4	?	2000	e.a.	19.60	107.53	0.18	-0.44	0.11020	0.511218	13	-27.70	-5.51	2.71	Tassinari *et al.* (2004)
MI	CI	I	V2	?	2000	e.a.	13.30	101.65	0.13	-0.60	0.07910	0.510654	11	-38.70	-8.54	2.73	Tassinari *et al.* (2004)
MI	CI	I	V8	?	2000	e.a.	1.74	8.91	0.20	-0.40	0.11830	0.511345	18	-25.22	-5.11	2.74	Tassinari *et al.* (2004)
MI	CI	I	V6	?	2000	e.a.	5.52	17.73	0.31	-0.04	0.18810	0.512041	10	-11.65	-9.48	2.98	Tassinari *et al.* (2004)
MI	CI	I	V5	?	2000	e.a.	4.71	18.80	0.25	-0.23	0.15130	0.511778	11	-16.78	-5.14	3.16	Tassinari *et al.* (2004)
MI	CI	I	V3	?	2000	e.a.	2.66	10.66	0.25	-0.23	0.15080	0.511705	30	-18.20	-6.44	3.33	Tassinari *et al.* (2004)
MI	CI	I	V1	?	2000	e.a.	4.95	20.29	0.24	-0.25	0.14740	0.511575	12	-20.74	-8.12	3.47	Tassinari *et al.* (2004)
MI	CI	I	V7	?	2000	e.a.	5.18	19.29	0.27	-0.17	0.16230	0.511789	18	-16.56	-7.77	3.91	Tassinari *et al.* (2004)
			Granitic-Granulitic rocks (Central Amapá Archean terrane)														
MI	T	A	TP13B	Felsic Granulite	2580	e.a.	3.33	24.60	0.14	-0.58	0.08190	0.510544	8	-40.85	-2.76	2.92	Avelar *et al.* (2003)
MI	T	A	TP17A	Tonalitic orthogneiss	2850	e.a.	1.72	11.16	0.15	-0.53	0.09340	0.510747	16	-36.89	+1.03	2.94	Avelar *et al.* (2003)
MI	T	A	TP19B	Tonalitic orthogneiss	2850	e.a.	3.10	17.12	0.18	-0.45	0.10850	0.511026	6	-31.45	+0.93	2.96	Avelar *et al.* (2003)
MI	T	A	BA14A	Felsic Granulite	2600	e.a.	1.93	14.40	0.13	-0.58	0.08100	0.510420	5	-43.27	-5.20	3.09	Avelar *et al.* (2003)
MI	T	A	Sm03\80.4	Gneiss	-	-	4.54	27.76	0.16	-0.50	0.09890	0.510737	8	-37.08	-	3.10	Pimentel *et al.* (2002)
MI	T	A	EG18	Granite	2900	e.a.	7.14	52.17	0.14	-0.56	0.08280	0.510443	18	-42.82	-2.01	3.18	Sato and Tassinari (1997)
MI	T	A	Sm03\72.5	Gneiss	-	-	4.95	24.63	0.20	-0.38	0.12160	0.511128	7	-29.46	-	3.22	Pimentel *et al.* (2002)
MI	T	A	Sm03\52.0	Gneiss	-	-	2.37	13.77	0.17	-0.47	0.10410	0.510752	5	-36.79	-	3.23	Pimentel *et al.* (2002)
MI	T	A	TP13A	Garnet-bearing granulite	2580	e.a.	4.11	22.00	0.19	-0.43	0.11300	0.510909	6	-33.73	-5.98	3.28	Avelar *et al.* (2003)
MI	T	A	Sm03\87.2	Gneiss	-	-	3.61	17.67	0.20	-0.37	0.12350	0.511071	10	-30.57	-	3.40	Pimentel *et al.* (2002)
MI	T	A	EG02	Tonalite	2900	e.a.	7.18	46.68	0.15	-0.50	0.08740	0.510508	32	-41.55	-5.06	3.42	Sato and Tassinari (1997)
			Granitic-Migmatitic rocks (Southeastern French Guyana)														
MI	T	FG	B85	Migmatitic granodiorite	2100	e.a.	11.40	61.80	0.18	-0.44	0.11110	0.511543	5	-21.36	+1.74	2.24	Avelar *et al.* (2003)
MI	T	FG	B25A	Granite	2100	e.a.	5.84	34.40	0.17	-0.48	0.10260	0.511417	4	-23.82	+1.57	2.24	Avelar *et al.* (2003)
MI	T	FG	B107	Tonalite	2130	e.a.	4.72	21.90	0.22	-0.34	0.13030	0.511777	6	-16.80	+1.38	2.32	Avelar *et al.* (2003)
MI	T	FG	B64A	Granodiorite	2160	e.a.	6.57	32.20	0.20	-0.37	0.12320	0.511653	6	-19.21	+1.19	2.35	Avelar *et al.* (2003)
MI	T	FG	B34	Granite	2100	e.a.	0.96	5.98	0.16	-0.51	0.09690	0.511241	3	-27.25	-0.33	2.36	Avelar *et al.* (2003)
MI	T	FG	B20	Migmatitic paragneiss	2100	e.a.	12.30	83.40	0.15	-0.55	0.08920	0.511084	4	-30.31	-1.32	2.41	Avelar *et al.* (2003)
MI	T	FG	B68A	Garnet-bearing granulite	2100	e.a.	3.23	17.53	0.18	-0.43	0.11130	0.511405	6	-24.05	-1.02	2.45	Avelar *et al.* (2003)
MI	T	FG	B99B	Granite	2100	e.a.	3.06	17.30	0.18	-0.45	0.10730	0.511256	3	-26.96	-2.86	2.58	Avelar *et al.* (2003)
			Greenstone Belt Sequence (Northern French Guyana)														
MI	T	FG	T160*	Komatiite Peridotitic	2155	D, e.a.	1.81	6.84	0.26	-0.19	0.16010	0.512302	28	-6.55	+3.60	2.19	mod. Gruau *et al.* (1985)
MI	T	FG	T100*	Komatiite Peridotitic	2155	D. e.a.	1.66	6.54	0.25	-0.22	0.15310	0.512182	38	-8.90	+3.19	2.22	mod. Gruau *et al.* (1985)

Table 3 (Continued)

Provinces		Tectonic Domain	Sample	Rock type	T_{crist} (Ma)	Ref.	Sm (ppm)	Nd (ppm)	Sm/ Nd	f(Sm/Nd)	$^{147}Sm/^{144}Nd$	$^{143}Nd/^{144}Nd$	1σ (10^{-6})	$\varepsilon Nd_{(0)}$	$\varepsilon Nd_{(t)}$	$T_{(DM)}$	Ref.
MI	T	FG	T188*	Komatiite Peridotitic	2155	D. e.a.	2.54	10.54	0.24	-0.26	0.14570	0.512070	30	-11.08	+3.06	2.22	mod. Gruau *et al.* (1985)
MI	T	FG	T111*	Komatiite Peridotitic	2155	D. e.a.	1.88	7.45	0.25	-0.23	0.15240	0.512162	19	-9.29	+3.00	2.23	mod. Gruau *et al.* (1985)
MI	T	FG	L200	Andesite	2131	D. e.a.	4.69	27.65	0.17	-0.48	0.10260	0.511440	16	-23.37	+2.41	2.21	mod. Gruau *et al.* (1985)
MI	T	FG	L365	Andesite	2131	D. e.a.	4.16	20.04	0.21	-0.36	0.12550	0.511722	55	-17.87	+1.63	2.29	mod. Gruau *et al.* (1985)
			Mafic and intermediate rocks														
VT	TP	T	JO-69	Ingarana Gabbro	1900	J	2.26	12.61	0.18	-0.58	0.10830	0.511500	-	-22.20	-0.64	2.24	Santos *et al.* (2000)
VT	TP	T	JO-66	Mamoal Metandesite	1900	J	22.59	164.34	0.14	-0.45	0.08310	0.511100	-	-30.00	-2.31	2.28	Santos *et al.* (2000)
			Young S.Jorge Granite														
VT	TP	T	RCR 72	Quartz monzonite	1891	F, e.a.	2.64	18.99	0.14	-0.57	0.08400	0.511063	-	-30.72	-3.38	2.34	Lamarão *et al.* (2005)
VT	TP	T	F 09/10	Monzogranite	1891	F	7.07	49.83	0.14	-0.56	0.08580	0.510993	-	-32.09	-5.19	2.46	Lamarão *et al.* (2005)
			Older S.Jorge Granite														
VT	TP	T	CMM 103	Quartz monzonite	1981	F, e.a.	6.00	41.67	0.14	-0.56	0.08700	0.511156	-	-28.91	-1.01	2.28	Lamarão *et al.* (2005)
VT	TP	T	RCR 59	Granite porphyry	1981	F, e.a.	7.48	50.96	0.15	-0.55	0.08880	0.511145	-	-29.12	-1.69	2.33	Lamarão *et al.* (2005)
VT	TP	T	RCR 27A	Monzogranite	1981	F	13.94	89.96	0.15	-0.52	0.09370	0.511206	-	-27.93	-1.74	2.34	Lamarão *et al.* (2005)
VT	TP	T	RCR 35	Monzogranite	1983	F	7.67	49.08	0.16	-0.52	0.09450	0.511168	-	-28.68	-2.67	2.41	Lamarão *et al.* (2005)
VT	TP	T	RCR 58	Quartz monzodiorite	1981	F, e.a.	5.89	33.05	0.18	-0.45	0.10770	0.511360	-	-24.93	-2.30	2.43	Lamarão *et al.* (2005)
			Granites and Volcanic rocks														
VT	TP	T	MA 5	Creporizão Tonalite?	1960	e.a.	9.02	45.12	0.20	-0.39	0.12088	0.511773	33	-16.87	+2.22	2.09	mod. Sato and Tassinari (1997)
VT	TP	T	MA 13	Creporizão Tonalite?	1960	e.a.	9.37	46.34	0.20	-0.38	0.12217	0.511749	26	-17.34	+1.42	2.16	mod. Sato and Tassinari (1997)
VT	TP	T	CR 9	?	-	-	10.41	67.36	0.15	-0.52	0.09346	0.511281	18	-26.47	-	2.24	mod. Sato and Tassinari (1997)
VT	TP	T	PT 29 3	Iriri Rhyolite?	1890	e.a.	6.31	39.10	0.16	-0.50	0.09751	0.511192	23	-28.21	-4.16	2.44	mod. Sato and Tassinari (1997)
			Pedra Pintada Suite														
MI	TP	S	SC-51	Granite porphyry	1958	B, e.a.	6.91	38.24	0.18	-0.44	0.10920	0.511511	6	-21.98	+0.01	2.24	mod. Costa (2005)
MI	TP	S	SC-222	Granite porphyry	1958	B, e.a.	7.38	42.06	0.18	-0.46	0.10610	0.511455	10	-23.08	-0.30	2.26	mod. Costa (2005)
MI	TP	S	SC-67	Biotite granite	1958	B, e.a.	2.91	20.07	0.14	-0.56	0.08750	0.511172	6	-28.60	-1.15	2.27	mod. Costa (2005)
			Surumu Group														
MI	TP	S	SC-83b	Rhyodacite	1984	L, e.a.	6.76	32.13	0.21	-0.35	0.12720	0.511818	11	-16.00	+1.72	2.16	mod. Costa (2005)
MI	TP	S	SC-50	Dacite	1984	L, e.a.	7.64	39.79	0.19	-0.41	0.11620	0.511646	13	-19.35	+1.16	2.19	mod. Costa (2005)
MI	TP	S	SC-166	Rhyodacite	1984	L, e.a.	8.39	46.91	0.18	-0.45	0.10810	0.511505	5	-22.10	+0.47	2.23	mod. Costa (2005)
MI	TP	S	SC-46	Rhyodacite	1984	L, e.a.	5.86	34.55	0.17	-0.48	0.10260	0.511396	8	-24.23	-0.26	2.27	mod. Costa (2005)
MI	TP	S	SC-53b	Rhyodacite	1984	L, e.a.	9.61	52.88	0.18	-0.44	0.10990	0.511369	15	-24.75	-2.65	2.47	mod. Costa (2005)
			Jauaperi Complex														
VT	TP	CG?	MF-20	Granitic Gneiss	1869	K, e.a.	2.64	20.63	0.13	-0.61	0.07741	0.511244	19	-27.19	+1.54	2.02	CPRM unpubl.
VT	TP	CG?	MF-18	Hornblende augen gneiss	1869	K, e.a.	16.54	90.23	0.18	-0.44	0.11085	0.511617	7	-19.92	+0.76	2.12	CPRM unpubl.
VT	TP	CG?	MF-17	Hornblende gneiss	1869	K, e.a.	9.72	53.51	0.18	-0.44	0.10977	0.511567	7	-20.89	+0.04	2.17	CPRM unpubl.
			Serra da Prata Suite														
MI	KSB	CG	LF-63A	Hypersthene-quartz syenite	1934	E	6.58	35.59	0.18	-0.43	0.11180	0.511657	-	-19.14	+1.95	2.08	Fraga (2002)
MI	KSB	CG	LF-26	Charnockitoid	1934	E, e.a.	9.00	41.17	0.22	-0.41	0.11535	0.511630	-	-19.02	+1.19	2.14	Fraga (2002)
MI	KSB	CG	SC-33	Deformed granite	1934	E, e.a.	8.47	45.72	0.19	-0.44	0.11100	0.511599	6	-20.27	+1.02	2.15	mod. Costa (2005)
MI	KSB	CG	LF-10E	Charnockitoid	1934	E, e.a.	7.25	36.76	0.20	-0.39	0.11923	0.511686	-	-18.57	+0.67	2.19	Fraga (2002)
MI	KSB	CG	SC-210*	Mafic granulite	1934	E, e.a.	8.16	31.72	0.26	-0.21	0.15560	0.512160	5	-9.32	+0.89	2.20	mod. Costa (2005)
MI	KSB	CG	SC-212*	Clinopyroxene granodiorite	1934	E, e.a.	3.54	16.73	0.21	-0.35	0.12780	0.511754	22	-17.24	-0.14	2.28	mod. Costa (2005)
			Barauana Granulite														
VT	KSB	CG	MF-40A	Granulite charnockitic	1938	B, e.a.	6.63	36.81	0.18	-0.45	0.10883	0.511590	-	-20.44	+1.43	2.12	CPRM unpubl.
VT	KSB	CG	SR-LF-6A	Granulite	1938	B,	9.71	51.82	0.19	-0.42	0.11329	0.511622	-	-19.82	+0.94	2.16	CPRM unpubl.
VT	KSB	CG	NR-31	Granulite	1938	B, e.a.	4.65	32.27	0.14	-0.56	0.08714	0.511245	-	-27.17	+0.09	2.17	CPRM unpubl.
VT	KSB	CG	MF-106B	Granulite charnockitic	1938	B, e.a.	9.05	52.40	0.17	-0.47	0.10442	0.511483	-	-22.53	+0.43	2.18	CPRM unpubl.

Table 3 (Continued)

Provinces		Tectonic Domain	Sample	Rock type	T_{crist} (Ma)	Ref.	Sm (ppm)	Nd (ppm)	Sm/ Nd	f(Sm/Nd)	$^{147}Sm/^{144}Nd$	$^{143}Nd/^{144}Nd$	1σ (10^{-6})	$\varepsilon Nd_{(0)}$	$\varepsilon Nd_{(t)}$	$T_{(DM)}$	Ref.
			Rio Urubu Complex														
MI	KSB	CG	LF-06A	Igarapé Branco hornblende-biotite gneiss	1937	E	14.00	68.09	0.21	-0.37	0.12431	0.511841	-	-15.55	+2.47	2.05	Fraga (2002)
MI	KSB	CG	LF-08	Miracelia biotite-hornblende metagranite	1935	E	8.04	45.83	0.18	-0.46	0.10604	0.511585	-	-20.54	+1.99	2.07	Fraga (2002)
MI	KSB	CG	SC-14a*	Biotite granite	1937	E, e.a.	2.44	9.38	0.26	-0.20	0.15740	0.512252	24	-7.53	+2.26	2.11	mod. Costa (2005)
MI	KSB	CG	SC-09	Granite porphyry	1937	E, e.a.	9.28	55.04	0.17	-0.48	0.10190	0.511465	5	-22.88	+0.71	2.16	mod. Costa (2005)
MI	KSB	CG	MF-71	Biotite gneiss	1937	E, e.a.	10.52	65.80	0.16	-0.51	0.09669	0.511391	11	-24.33	+0.55	2.16	CPRM unpubl.
MI	KSB	CG	SC-01	Leucogranite	1937	E, e.a.	8.44	58.30	0.14	-0.56	0.08750	0.511253	10	-27.02	+0.15	2.17	mod. Costa (2005)
MI	KSB	CG	MF-108	Biotite gneiss	1937	E, e.a.	13.36	76.16	0.18	-0.46	0.10602	0.511513	21	-21.95	+0.61	2.17	CPRM unpubl.
MI	KSB	CG	SC-180b	Amphibolite	1937	E, e.a.	10.62	63.04	0.17	-0.48	0.10190	0.511451	6	-23.15	+0.44	2.18	mod. Costa (2005)
MI	KSB	CG	SC-14c*	Hornblende gabbronorite	1937	E, e.a.	2.52	9.60	0.26	-0.19	0.15880	0.512219	11	-8.17	+1.26	2.18	mod. Costa (2005)
MI	KSB	CG	SC-157	Leucogranite	1937	E, e.a.	10.99	56.49	0.19	-0.40	0.11760	0.511642	9	-19.43	+0.25	2.23	mod. Costa (2005)
MI	KSB	CG	SC-40b	Biotite granite	1937	E, e.a.	3.86	20.14	0.19	-0.41	0.11580	0.511562	48	-20.99	-0.86	2.31	mod. Costa (2005)
MI	KSB	CG	SC-89	Gneiss	1937	E, e.a.	6.28	40.67	0.15	-0.53	0.09340	0.511229	9	-27.49	-1.79	2.31	mod. Costa (2005)
			Cauarane Group and rocks related														
MI	TP	CG	SC-04	Gneiss	2074	B, e.a.	4.24	23.00	0.18	-0.43	0.11140	0.511523	9	-21.75	+0.98	2.27	mod. Costa (2005)
MI	KSB	CG	SC-170a	Biotite gneiss	2074	B, e.a.	2.86	14.23	0.20	-0.38	0.12150	0.511674	9	-18.80	+1.23	2.27	mod. Costa (2005)
MI	KSB	CG	SC-37	Gneiss	2074	B, e.a.	8.53	47.39	0.18	-0.45	0.10890	0.511457	6	-23.04	+0.35	2.32	mod. Costa (2005)
MI	TP	CG	SC-58	Garnet gneiss	2074	B, e.a.	4.69	27.87	0.17	-0.48	0.10180	0.511285	7	-26.39	-1.12	2.41	mod. Costa (2005)
MI	TP	CG	SC-49	Paragneiss	2074	B, e.a.	6.07	34.83	0.17	-0.46	0.10530	0.511305	6	-26.00	-1.66	2.46	mod. Costa (2005)
MI	KSB	CG	SC-61a	Garnet gneiss	2074	B, e.a.	6.66	38.07	0.17	-0.46	0.10570	0.511183	10	-28.38	-4.16	2.64	mod. Costa (2005)

Nd T_{DM} ages are calculated using the model of De Paolo (1981) for Nd evolution of the depleted mantle. Obs: mod. = modified of

*highly fractionated sample showing $0.125<^{147}Sm/^{144}Nd<0.09$ and $-0.60<f(Sm/Nd)<-0.35$ (Sato and Siga Jr. 2002) has been recalculated based on Nd evolution by double-stage (Sato and Tassinari, 1997).

Geochronological Provinces: 1. Tassinari and Macambira (2004); 2. Santos *et al.* (2000); KSB. K' Mudku Shear Belt; VT-TP. Ventuari-Tapajós (or Tapajós-Parima); MI-T - Maroni-Itacaiúnas (or Transamazonic); CA. Central Amazonian. *Domains*: CG. Central Guyana; S. Surumu; T. Tapajós; C. Carajás; FG. French Guyana

Crystalization ages (References): e.a. estimated age; A. Avelar *et al.* (1999); B. CPRM (2003); C. Dall´Agnol *et al.* (1999). D. Delor *et al.* (2003); E Fraga (2002); F. Lamarão *et al.* (2002); G. Leite *et al.* (2004); H. Macambira and Lancelot (1996). I. Pimentel and Machado (1994); J. Santos *et al.* (2000); K. Santos *et al.* (2002); L. Santos *et al.* (2003)

Table 4. Summary of geological characteristics of the UAD granitoids

Units	Anauá Complex	Martins Pereira Granite	Serra Dourada Granite	Caroebe and Água Branca Granites	Igarapé Azul Granite
Age	2028 Ma	1975-1971 Ma	1962 Ma	1901-1891 Ma	1891-1889 Ma
Inheritances	-	2042 Ma?	2138 Ma	1963 Ma; 2142 Ma	1972-1964 Ma
Composition	Metatonalites, minor metagranites and metadiorites	Granodiorites to mozogranites, locally tonalites	Monzogranites to syenogranites, rarelly granodiorites	Diorites to monzogranites	(Leuco)granodiorites to (leuco)monzogranites, rarelly quartz monzonites and syenogranites
Main varietal minerals	Hornblende, biotite	Biotite, local muscovite	Biotite, muscovite	Hornblende, biotite	Biotite, muscovite
Main accessory minerals	Titanite, epidote, allanite, Fe-Ti oxides and sulphides	Epidote, allanite, apatite	Cordierite, sillimanite	Titanite, epidote, allanite, Fe-Ti oxides	Epidote
Trends	Calc-alkaline Tonalitic-Trondjemitic?	Calc-alkaline Granodioritc (Chilean-type)	Granites of crustal origin field	Calc-alkaline Granodioritic (Peru to Sierra Nevada-types)	Granites of crustal origin field
Outcrop style	Basement inliers	Large batholith intruding Anauá Complex rocks	Discrete batholith in association with meta-volcanosedimentary rocks	Large batholith intruding older units	Discrete batholith and small bodies intruding older units
Deformation	Well-folaited to weakly foliated, locally with compositional layering	Range in deformational style from well-foliated to massive	Massive to weakly foliated	Massive to foliated (local shear zones)	Massive to foliated (local shear zones)
Enclaves	Metamafic to metaultramafic	Metadiorites to metatonalites (predominate) and paragneiss (scarce)	Not observed	Mafic microgranular	Biotite-bearing tonalite to quartz diorite (surmicaceous); metagranodiorite; paragneisses; and biotite porphyrytic diorite-tonalite microgranular
Geochemical signature	Metaluminous, TTG-like, I-type, calc-alkaline, medium-K, moderate negative Nb and negative to positive Sr-Ti anomalies; low LILE and LREE fractionated (La_n/Yb_n = 3.6-8.0); discrete positive Eu anomaly ($Eu_{(n)}/Eu^*$ = 0.78-1.15) and low HREE (< 5x chrondrite)	Metaluminous to peraluminous, I-type, calc-alkaline, high-K, variable but high LILE and REE contents, moderate to pronounced negative P-Ti anomalies and fractionated LREE patterns (La_n/Yb_n = 4.6-52.9); negative Eu anomalies ($Eu_{(n)}/Eu^*$ = 0.38-0.74)	Peraluminous, normal S-type, high-SiO_2, low-CaO, moderate to high negative Sr, Ti, Ba and Nb anomalies, moderate fractionated LREE pattern (La_n/Yb_n = 23.4-28.2) and moderate to pronounced negative Eu anomalies ($Eu_{(n)}/Eu*$ = 0.29-0.47)	Metaluminous, I-type, calc-alkaline, high-K, moderate to high CaO, negative Ti and Ta-Nb anomalies; moderate fractionated LREE pattern (La_n/Yb_n =8.6-29.3); negative to low positive Eu anomalies ($Eu_{(n)}/Eu^*$ = 0.52-1.32)	Metaluminous to peraluminous, I-type, calc-alkaline, high-K, high-SiO_2, moderate to low CaO, negative Sr, Ti, P and Ta-Nb anomalies, moderate to high fractionated LREE pattern (La_n/Yb_n =8.7-70.0) and low to pronounced negative Eu anomalies ($Eu_{(n)}/Eu^*$ = 0.36-0.86)
ε_{Nd}	-2.21 to -0.19	-4.74 to –0.92	-4.34 to -3.19	-2.05 to +0.46 (local –4.27 to -2.60)	-1.61 to –0.02
Nd T_{DM}	2.50-2.33 Ga	2.64-2.33 Ga	2.53-2.38 Ga	2.29-2.17 Ga (local 2.47-2.32 Ga)	2.28-2.14 Ga
Pb initial	-	15.70-15.57	-	15.54	15.65-15.42
Magma sources	Mantle-derived: generation of (depleted) mantle magma melts under high pressure in the garnet stability field (?) and pre-existing older crustal fragment as basement	Crustally-derived: generation of crustal melts by partial melting of amphibolitic, andesitic and/or tonalitic sources and local input of metavolcano-sedimentary older basement	Crustally-derived: generation of crustal melts by partial melting of metavolcano-sedimentary older basement under moderate pressures (cordierite stability field)	Crustally-derived: generation of crustal melts by partial melting of amphibolitic, andesitic and/or tonalitic (juvenile) sources	Multiple crustal sources: generation of crustal melts by partial melting of amphibolitic, andesitic and/or tonalitic (juvenile) sources; metavolcano-sedimentary basement and Martins Pereira older granitic intrusion (sialic)
Tapajós Domain correlations	Cuiú-Cuiú Complex	Creporizão Granite	Small S-type eucogranite bodies in the Cuiú-Cuiú Complex?	Tropas and Parauari granitoids	?

5 - CONCLUSÕES GERAIS

Os novos dados geológicos, petrográficos, geoquímicos, isotópicos e geocronológicos apresentados no decorrer deste trabalho, rediscutidos e integrados com os dados disponíveis na literatura, permitiram avanços do ponto de vista litoestratigráfico e petrológico acerca dos granitóides do setor centro-sul do Escudo das Guianas, particularmente do sudeste de Roraima. Apesar disso, este significativo acervo de dados é ainda insuficiente para delinear hipóteses por demais conclusivas. Mesmo porque algumas regiões vizinhas, entre elas estão, por exemplo, as áreas estaduais limítrofes entre Amazonas-Roraima e Roraima-Pará e a divisa Brasil-Guiana as quais constituem importantes peças neste quebra-cabeça geológico, carecem enormemente de informações geológicas básicas. A seguir serão listadas as principais conclusões a partir dos resultados obtidos nos granitóides dos domínios tectono-estratigráficos Guiana Central e Uatumã-Anauá, com ênfase neste último.

5.1 - DOMÍNIO GUIANA CENTRAL (DGC)

a) O Domínio Guiana Central, junto ao limite (materializado pelo sistema de falha do Itã) do Domínio Uatumã-Anauá, apresenta dois grupos distintos de rochas ortometamórficas. O primeiro é constituído por ortognaisses granulíticos (1942 ± 7 Ma) polideformados e metamorfizados em alto grau, sendo correlacionáveis aos charnoquitóides sintectônicos da Suíte Serra da Prata (1943-1933 Ma). Estes destoam dos milonitos (1889 ± 4 Ma) e granitos foliados (1724 ± 14 Ma) os quais, além de serem mais jovens, exibem apenas uma fase de deformação normalmente associada a amplas zonas de cisalhamento NE-SW, em baixo a médio grau (preservando muitas vezes suas características ígneas como por exemplo fluxo magmático). Milonitos e meta-granitóides mais antigos (1938-1932 Ma) também são descritos em outros setores do Domínio Guiana Central, sendo agrupados na Suíte Metamórfica (ou Complexo) Rio Urubu;

b) A idade de 1724 ± 14 Ma obtida em granitóide sintectônico (associada a idades Ar-Ar de outros autores) confirma ainda a possibilidade da existência de um episódio tectonicamente ativo entre 1,94-1,93 Ga e 1,20 Ga. Além disso, granitóides com características petrográficas e idade (1889 ± 4 Ma) similares ao do Granito Caroebe, indica que estes intrudem o embasamento do Domínio Guiana Central;

c) Estes dados materializam uma ampla variedade de protólitos ígneos que, aliada às diferentes e complexas relações metamórfico-estruturais, dificultam o empilhamento estratigráfico das unidades do Domínio Guiana Central. Sugere-se a redenominação da Suíte Metamórfica Rio Urubu para Complexo, de modo a agrupar numa mesma unidade tal diversidade de litótipos (ígneos e metamórficos), de padrões estruturais (polifásico *vs*. monofásico) e de grau metamórfico (baixo a alto grau).

5.2 - DOMÍNIO UATUMÃ-ANAUÁ (DUA)

5.2.1 - Setor Norte

a) Além do conjunto representado pela associação TTG Anauá e pelas seqüências metavulcanossedimentares do tipo Cauarane, pouco investigado neste trabalho e que materializa muito provavelmente um sistema de arco, o setor norte do Domínio Uatumã-Anauá apresenta os (meta)granitos Martins Pereira e Serra Dourada como as unidades ígneas de maior abrangência territorial. A única mineralização de ouro explorada comercialmente está hospedada nestes granitóides (garimpo Anauá);

b) O Granito Martins Pereira constitui uma massa batolítica composta por monzogranitos, granodioritos e raramente por tonalitos (*trend* cálcio-alcalino granodiorítico, similar aos tipos chilenos), com textura em geral porfirítica e normalmente afetados por deformação heterogênea penetrativa de escala regional, associada às zonas de cisalhamento destrais de direção ENE-WSW. Quimicamente são rochas cálcio-alcalinas, metaluminosas a peraluminosas e de alto-K, exibindo enriquecimento em LILE (K, U e Th, por exemplo) e ETR;

c) A utilização de diagramas de variação (lineares), de petrologia experimental, aliado aos dados isotópicos do Nd e Pb, sugerem para o Granito Martins Pereira uma origem a partir da fusão parcial de fontes crustais anfibolíticas e\ou tonalíticas (ε_{Nd} -0,92 a –1,55, T_{DM} 2,38-2,33 Ga) com localizada contribuição de metagrauvacas (ε_{Nd} –2,37 a –4,74, T_{DM} 2,64-2,43 Ga) e idades supostamente arqueanas (e/ou siderianas?) a riacianas (transamazônicas), gerando idades-modelo T_{DM} mistas. Xenólitos de rochas anfibolíticas e paragnáissicas, apesar de raros, podem ser encontrados no Granito Martins Pereira. Datações em zircão (evaporação de Pb) indicam também um intervalo de cristalização curto e restrito entre 1975 e 1971 Ma para este magmatismo;

d) O Granito Serra Dourada constitui um batólito de menor expressão e é composto essencialmente por monzogranitos e sienogranitos à muscovita, cordierita e sillimanita. Ocupam o campo dos granitos de fusão crustal no diagrama QAP e apresentam quimismo peraluminoso similar aos granitos tipo S normais. Embora em menor grau, também se mostram afetados por deformação heterogênea penetrativa de escala regional;

e) Dados petrográficos (mineralogia aluminosa), geoquímicos (caráter peraluminoso) e isotópicos (ε_{Nd} –3,19 a –4,34, T_{DM} 2,53-2,38 Ga) obtidos no Granito Serra Dourada sugerem fortemente uma origem a partir da fusão parcial de metagrauvacas, também indicando proveniência de fontes com idades supostamente arqueanas (e/ou siderianas?). Muito embora as idades ao redor de 2,38 Ga possam ser provocadas por local contribuição de fontes riacianas (transamazônica), produzindo ao menos localmente idades-modelo T_{DM} mistas (vide Granito Martins Pereira). Datações em zircão (evaporação de Pb) do Serra Dourada indicam cristalização ao redor de 1962 ± 6 Ma, em acordo com dados obtidos em zircão por U-Pb SHRIMP (1969 ± 4 Ma) em outro granito tipo S existente no Domínio Guiana Central, sendo, portanto, ligeiramente mais jovens que os granitóides tipo I, cálcio-alcalinos de alto-K Martins Pereira;

f) Lentes e bolsões de leucogranitos ocorrem subconcordantes aos planos de foliação dos metagranitóides Martins Pereira, podendo ser resultado da fusão parcial deste último durante evento gerador dos granitóides da porção sul em torno de 1900 Ma (vide discussão abaixo). A idade de cristalização obtida em zircão pelo método de evaporação de Pb é de 1909 ± 6 Ma e pelo menos quatro conjuntos de idades herdadas foram também detectadas: i) 1959 ± 5 Ma (Granito Martins Pereira?); ii) 1997 ± 8 Ma (Arco Anauá?); iii) 2134 ± 15 Ma (crosta Transamazônica) e iv) 2354 ± 6 Ma (Crosta Amazônia Central);

g) Os dados disponíveis para o conjunto petrotectônico do setor norte do Domínio Uatumã-Anauá permite a elaboração preliminar de uma proposta evolutiva baseada inicialmente num modelo acrescionário em 2,03 Ga (sistema de arco magmático Anauá e bacias associadas) com subseqüente colisão entre blocos crustais (orógeno colisional). Esta colisão teve início entre 1,97-1,96 (granitóides Martins Pereira e Serra Dourada) e evoluiu ao longo tempo, culminando mais a norte com a geração dos granulitos e ortognaisses do cinturão Guiana Central entre 1,94-1,93 Ga. Eventos tectono-metamórficos recorrentes podem ter afetado este bloco (agora amalgamado) ao longo do Proterozóico (p.ex. ~1,72 Ga e ~1,20 Ga) ;

h) Modelo evolutivo similar envolvendo a geração de um arco primitivo em torno de 2,00 Ga (arco Cuiú-Cuiú) é adotado igualmente no domínio Tapajós (parte sul do Cráton Amazônico, Escudo Brasil Central), embora alguns autores (e.g. Santos *et al.*, 2004) admitam ainda um segundo arco (continental) ao redor de 1,96 Ga (arco Creporizão). Apesar disso, o estágio acrescionário parece não ter evoluído para um estágio colisional de modo significativo na região supracitada, em função da ocorrência restrita de granitos tipo S e ausência de rochas granulíticas.

5.2.2 - Setor Sul

a) A porção sul, ao contrário da porção norte, não registra efeitos deformacionais significativos, exceto por zonas de cisalhamento destrais muito localizadas (p.ex. Sistema de Falhas do Jauaperi). As principais anisotropias dizem respeito às estruturas de fluxo magmático representadas por enclaves e megacristais preferencialmente alinhados, observados na maioria dos corpos graníticos. Dominam neste setor os granitos Caroebe e Igarapé Azul, além de rochas vulcânicas co-genéticas (Jatapu), charnoquitóides (Santa Maria e Igarapé Tamandaré) e granitos tipo A (Moderna e Mapuera). As duas ocorrências minerais mais importantes deste setor estão assentadas (columbita-tantalita em aluvião) ou hospedadas (pegmatitos com ametista), respectivamente, nos granitóides Igarapé Azul e Moderna;
b) O Granito Igarapé Azul está dividido em três fácies principais (Vila Catarina, Saramandaia e Cinco Estrelas) e é composto essencialmente por monzogranitos com baixo conteúdo de minerais máficos que se encontram em geral hidrotermalizados. Estes granitóides ocupam no diagrama QAP o campo dos granitos crustais e quimicamente são rochas cálcio-alcalinas com alto-K, ricas em SiO_2 e ligeiramente peraluminosas, exibindo enriquecimento em LILE e padrões variados de ETR. São caracterizados ainda por uma ampla gama de enclaves: 1) ricos em biotita (surmicáceos); 2) metagranítico (Martins Pereira); 3) paragnáissico (tipo Cauarane); 4) microgranulares tonalitico-granodioríticos.;
c) O Granito Caroebe apresenta volume de máficos superior (8-48%) e aspecto mosqueado que o distingue do Granito Igarapé Azul. Além disso, duas fácies distintas foram cartografadas tendo como base a presença de biotita acompanhada (fácies Jaburuzinho) ou não (fácies Alto Alegre) por hornblenda. A primeira fácies é caracterizada por um aspecto mosqueado mais acentuado, em geral com textura equigranular, e tipos que variam de quartzo dioritos a monzogranitos. A segunda apresenta tipos monzograníticos a granodioríticos em geral

porfiríticos, com caráter geoquímico similar ao dos granitóides Igarapé Azul, muito embora não apresentem efeitos hidrotermais significativos. Em termos geoquímicos o Granito Caroebe apresenta envelope composicional mais amplo de ETR e elementos traços, mostrando conteúdos mais baixos de Rb e K e localmente elevados de Ba, Th, U (LILE) e Nd, P, Hf, Zr e Sm (HSFE);

d) As idades de zircão pelo método de evaporação de Pb apontam idade de cristalização entre 1891-1889 Ma para os granitóides Igarapé Azul e heranças entre 1972-1964 Ma, estas últimas muito próximas das idades de cristalização obtidas nos granitóides Martins Pereira. Idade de cristalização (1891 ± 2 Ma) e heranças (1963 ± 4 Ma) similares são observadas também na fácies Alto Alegre do Granito Caroebe. O Enderbito Santo Maria (1891 ± 1 Ma) e as vulcânicas dacíticas e andesíticas Jatapu (1893 ± 5 Ma, herança de 1966 ± 3 Ma) demonstram fazer parte desse mesmo evento magmático. A fácies Jaburuzinho (1895 ± 2 Ma) e o Granito Água Branca (1901 ± 5 Ma) em sua área tipo apontam idades de cristalização ligeiramente mais antigas e, apesar de heranças em torno de 1,97 Ga não terem sido observadas, resquícios transamazônicos foram registrados localmente (2142 ± 10 Ma). O Granito Murauauá, provável representante do magmatismo Mapuera (tipo A) na região, apresenta idade mais jovens (1871 ± 5 Ma) e duas populações herdadas (1888 ± 3 Ma e 2359 ± 7 Ma);

e) Os diagramas geoquímicos de variação e de petrologia experimental, em conjunto com o conteúdo isotópico do Nd e Pb, indicam que os granitos Igarapé Azul, Caroebe e Água Branca podem ter uma origem comum a partir da fusão parcial de fontes crustais anfibolíticas e\ou tonalíticas-andesíticas com progressiva e variável contribuição de fontes metassedimentares (grauvacas) e talvez das próprias rochas encaixantes (Martins Pereira). A contribuição de fontes crustais dominantemente transamazônicas são mais evidentes no Granito Igarapé Azul (ε_{Nd} -0,02 a -1,61, T_{DM} 2,28-2,14 Ga), nas fácies Alto Alegre (ε_{Nd} -0,68 a -2,24, T_{DM} 2,26-2,17 Ga) e Jaburuzinho (ε_{Nd} +0,46 a -2,69, T_{DM} 2,32-2,16 Ga), além das rochas vulcânicas Jatapu (ε_{Nd} -0,70 a -1,76, T_{DM} 2,28-2,21 Ga), embora localmente, incluindo a área-tipo do Granito Água Branca, ocorram idades siderianas (ε_{Nd} -2,60 a -4,27, T_{DM} 2,47-2,37 Ga), indicando a presença subordinada de fontes mais antigas;

f) Associação granítica cálcio-alcalina similar e contemporânea existente no domínio Tapajós tem sido interpretada por alguns autores como originada em ambiente de margem ativa, controlado por subducção, muitas vezes desenvolvidos em vários estágios, representados

pelos arcos Tropas (1,90 Ga) e Parauari (1,88 Ga). Entretanto, no setor sul do DUA, além da ausência de sucessões meta-vulcanossedimentares e/ou remanescentes de crosta oceânica (sequência ofiolítica?) contemporâneas à geração de um provável arco magmático em 1,90 Ga e a falta de indícios de metamorfismo e deformação, dificulta a vinculação dos granitóides cálcio-alcalinos do sul do DUA a um ambiente de subducção clássica (tipo-B). Nesse sentido, a assinatura geoquímica dos granitóides estaria muita mais vinculada às características das fontes do que propriamente ao ambiente geotectônico;

g) Portanto a proposta evolutiva aqui apresentada tem como base a ascensão local da astenosfera (*slab break-off* e delaminação ou atuação de plumas mantélicas?) produzindo magmas basálticos que estacionariam na base da crosta inferior, provocando a fusão desta e gerando um amplo volume de magmas. Estes últimos ao interagir com o restante da crosta dariam origem a uma diversidade de tipos graníticos (em diferentes condições de pressão de H_2O) entre 1,90 (granitos tipo I) e 1,87 Ga (granitos tipo A). Este modelo pós-colisional, baseado num mecanismo controlado por *underplating*, também é proposto no domínio Tapajós como alternativa a origem acrescionária descrita anteriormente.

Apesar dos dados apresentados contribuírem com o aumento do acervo referente à porção central do Escudo das Guianas, evidentemente as conclusões expostas aqui não têm a pretensão do caráter definitivo. Muito pelo contrário, reconhece-se a necessidade de investigação mais aprofundada, sobretudo do ponto de vista geoquímico-isotópico visando apoiar estudos petrológicos e evolutivos, associados a estudos metamórfico-estruturais.

Além disso, a ausência de mapeamento geológico sistemático nas áreas vizinhas (p.ex. fronteira Brasil-Guiana, limites estaduais Amazonas-Pará-Roraima) dificulta enormemente uma correlação em escala regional, impedindo um melhor entendimento e extrapolação do modelo proposto (p.ex. dinâmica e geometria) e sua conexão com o modelo de Províncias Geocronológicas (Província Ventuari-Tapajós ou Tapajós-Parima).

REFERÊNCIAS

ALMEIDA, M.E. & MACAMBIRA, M.J.B. 2003. Aspectos geológicos e litoquímicos dos granitóides cálcio-alcalinos Paleoproterozóicos do sudeste de Roraima. *In*: CONGRESSO BRASILEIRO DE GEOQUÍMICA, 9, *Anais...,* SBGq, p. 775-778.

ALMEIDA, M.E.; FRAGA, L.M.B.; MACAMBIRA, M.J.B. 1997. New geochronological data of calc-alkaline granitoids of Roraima State, Brazil. In: SOUTH-AMERICAN SYMPOSIUM ON ISOTOPE GEOLOGY, 1, *Extended Abstract*, IG/USP, p.34-37.

ALMEIDA, M.E.; MACAMBIRA M.J.B., FARIA M.S.G. de. 2002. A Granitogênese Paleoproterozóica do Sul de Roraima. *In*: CONGRESSO BRASILEIRO DE GEOLOGIA, 41, *Anais...*, SBG, p 434.

ARANTES, J.L.; MANDETTA. P. 1970. *Relatório preliminar de viagem de reconhecimento geológico dos rios Auaris, Parima, Aracaçá e Urariquera*. Rio de Janeiro, DNPM, Relatório 55. 34p.

ARAÚJO NETO, H.; MOREIRA, H.L. 1976. *Projeto Estanho do Abonari*. Manaus, Convênio DNPM/CPRM, Relatório Final. 2v.

BARTLETT, J.M.; DOUGHERTY-PAGE, J.S.; HARRIS, N.B.W.; HAWKESWORTH, C.J.; SANTOSH, M. 1998. The application of single zircon evaporation and model Nd ages to the interpretation of polymetamorphyc terrains: an example from the Proterozoic mobile belt of south India. *Contributions to Mineralogy and Petrology*, **131**: 181-195.

BONFIM, L.F.C.; RAMGRAB, G.E.; UCHÔA, I.B.; MEDEIROS, J.B. DE; VIÉGAS FILHO, J. DE R.; MANDETTA, P.; KUYUMJIAN, R.M., PINHEIRO, S. DA S. 1974. *Projeto Roraima*. Manaus, DNPM/CPRM, Relatório Final, vol. IA-D e II.

BRAUN, O.P.G. 1973. *Projeto Roraima, 2ª Fase; Levantamento geológico integrado: Relatório de mapeamento preliminar ao milionésimo, correspondente à "Fotointerpretação Preliminar"*. Manaus, DNPM/CPRM, 218p., il.

BROWN, M., 2001. From microscope to mountain belt: 150 years of petrology and its contribution to understanding geodynamics, particularly the tectonics of orogens: *Journal of Geodynamics,* **32** : 115–164.

BROWN, M. & DALLMEYER, R.D. 1996. Rapid Variscan exhumation and role of magma in core complex formation: Southern Brittany metamorphic belt, France. *Journal of Metamorphic Geology*, **14** : 361–379.

CORDANI, U.G. & BRITO NEVES, B.B. 1982. The Geologic Evolution of South America During the Archean and Early Proterozoic. *Revista Brasileira de Geociências*, **12** (1-3) : 78-88.

COSTA, J.B. & HASUI, Y. 1997. Evolução Geológica da Amazônia. In: COSTA, M.L.C. & ANGÉLICA, R.S. (Coord.), C*ontribuições à Geologia da Amazônia*. Belém, FINEP/SBGNO, p. 15-90.

COSTI, H.T., DALL'AGNOL, R., MOURA, C.A.V. 2000. Geology and Pb-Pb geochronology of Paleoproterozoic volcanic and granitic rocks of the Pitinga Province, Amazonian craton, northern Brazil. *International Geology Review,* **42** : 832-849.

COSTI, H.T., SANTIAGO, A.F., PINHEIRO, S. DA S. 1984. *Projeto Uatumã–Jatapu*. Manaus, CPRM, Relatório Final. 133p.

CPRM. 1999. *Programa Levantamentos Geológicos Básicos do Brasil. Roraima Central, Folhas NA.20-X-B e NA.20-X-D (integrais), NA.20-X-A, NA.20-X-C, NA.21-V-A e NA.21-V-C (parciais). Escala 1:500.000. Estado de Roraima*. Manaus, CPRM, 166 p. (em CD-ROM).

CPRM. 2000a. *Programa Levantamentos Geológicos Básicos do Brasil. Caracaraí, Folhas NA.20-Z-B e NA.20-Z-D (integrais), NA.20-Z-A, NA.21-Y-A, NA.20-Z-C e NA.21-Y-C (parciais). Escala 1:500.000. Estado de Roraima*. Manaus, CPRM, 157 p. (em CD-ROM).

CPRM. 2000b. *Programa Levantamentos Geológicos Básicos do Brasil. Província Mineral do Tapajós, Folha SB.21-V-D (Vila Mamãe Anã). Escala 1:250.000. Estados do Amazonas e Pará*. Manaus, CPRM, 157 p. (em CD-ROM).

CPRM. 2003. Programa Levantamentos Geológicos Básicos do Brasil. *Geologia, Tectônica e Recursos Minerais do Brasil: sistema de informações geográficas - SIG*. Rio de Janeiro, CPRM, Mapas. Escala 1:2.500.000. (em 4 CDs-ROM)

CPRM. 2004. *Programa Levantamentos Geológicos Básicos do Brasil. Escala 1:1000.000. Mapa Geológico do Brasil - 41 mapas.* Brasília, CPRM-MME. (em CD-ROM).

CPRM. 2006. *Programa Integração, Atualização e Difusão de Dados da Geologia do Brasil: Subprograma Mapas Geológicos Estaduais. Geologia e Recursos Minerais do Estado do Amazonas.* Manaus, CPRM/CIAM-AM, 2006. Escala 1:1.000.000. Texto explicativo, 148p. (em CD-ROM).

ELLIS, D.J. 1987. Origin and evolution of granulites in normal and thickened crusts: *Geology*, **15** : 167–170.

FARIA M.S.G.DE, LUZARDO R., PINHEIRO S. DA S. 1999. Litoquímica e petrogênese do Granito Igarapé Azul. *In*: SIMPÓSIO DE GEOLOGIA DA AMAZÔNIA, 6, *Anais...*, SBG, p. 577-580.

FRAGA, L.M.B. 2002. *A Associação Anortosito–Mangerito–Granito Rapakivi (AMG) do Cinturão Guiana Central, Roraima e Suas Encaixantes Paleoproterozóicas: Evolução Estrutural, Geocronologia e Petrologia*. Belém, Universidade Federal do Pará, Centro de Geociências, Pós-Graduação em Geoquímica e Petrologia, Tese de Doutorado. 386p.

FRAGA, L.M.B. & REIS, N.J. 1996. A Reativação do Cinturão de Cisalhamento Guiana Central durante o Episódio K'Mudku. In: CONGRESSO BRASILEIRO DE GEOLOGIA, 39, Salvador, *Anais...*, SBG, v.1, p. 424-426.

GAUDETTE, H.E.; LAFON, J.M.; MACAMBIRA, M.J.B.; MOURA, C.A.V; SCHELLER, T. 1998. Comparison of single-filament Pb evaporation/ionization zircon ages with conventional U-Pb results: examples from the Precambrian of Brazil. *Journal of South American Earth Scences*, **11**: 351-363.

GAUDETTE, H.E.; OLSZEWSKI, W.J. JR.; SANTOS, J.O.S. DOS. 1996. Geochronology of Precambriam rocks from the northern part of Guiana Shield, State of Roraima, Brazil. *Journal of South American Earth Scences*, **9**: 183-195.

GIBBS, A.K. & BARRON, C.N. 1993. *The geology of the Guyana Shield*. Oxford University Press, Oxford, N. York, 245 p.

HASUI, Y.; HARALYI., N.L.E.; SCHOBBENHAUS Fº, C. 1984. Elementos geofísicos e geológicos da região amazônica: subsídios para o modelo geotectônico. *In*: SYMPOSIUM AMAZONICO, 2, Manaus. *Anais*..., SBG, v. 1, pp. 129-148.

HOUSH, T. & BOWRING, S.A. 1991. Lead isotopic heterogeneities within alkali feldspars: implications for the determination of initial lead isotopic compositions. *Geochimica et Cosmochimica Acta,* **55** : 2309-2316.

KOBER, B. 1986. Whole grain evaporation for $^{207}Pb/^{206}Pb$ age investigations on single zircons using a double filament source. *Contributions to Mineralogy and Petrology,* **93** : 82-490.

KOBER, B. 1987. Single-grain evaporation combined with Pb+ emitter bedding for $^{207}Pb/^{206}Pb$ investigations using thermal ion mass spectrometry, and implications for zirconology. *Contributions to Mineralogy and Petrology*, **96** : 63-71.

KROGH, T.E. 1973. A low contamination method for hydrothermal decomposition of zircons and extraction of U and Pb for isotopic age determinations. *Geochimica et Cosmochimica Acta*, **37**: 485-494.

KRYMSKY, R. 2002. *Metodologia de análise de U-Pb em mono zircão com traçador ^{235}U-^{205}Pb*. Belém, Universidade Federal do Pará, Laboratório de Geologia Isotópica. 7p.

LAMARÃO, C.N.; DALL'AGNOL, R.; LAFON, J.-M.; LIMA, E.F. 2002. Geology, geochemistry and Pb–Pb zircon geochronology of the Paleoproterozoic magmatism of Vila Riozinho, Tapajós gold province, Amazonian craton, Brazil. *Precambrian Research,* **119** (1-4) : 189–223.

LUDWIG, K.R. 1993. PBDAT. *A computer program for processing Pb-U-Th isotope data*. Version 1.24. USGS Open File Report, 88-542. 34 p.

LUDWIG, K.R. 2001. *User's manual for Isoplot / Ex Version 2.49. A geochronological toolkit for Microsoft Excel*. Berkeley Geochronology Center, Berkeley, CA, USA, 59 p. (Spec. Pub., 1a).

LUDWIG, K.R. & SILVER, L.T. 1977. Lead-isotope inhomogeneity in Precambrian igneous K-feldspars. *Geochimica et Cosmochimica Acta,* **41**(10) : 1457-1471.

MACAMBIRA, M.J.B. & SCHELLER, T. 1994. Estudo comparativo entre métodos geocronológicos aplicados em zircões: o caso do Granodiorito Rio Maria. In: SIMPÓSIO DE GEOLOGIA DA AMAZÔNIA, 4, Belém, *Boletim de Resumos Expandido.*, SBG, p.343-346.

MACAMBIRA, M.J.B.; ALMEIDA, M.E.; SANTOS, L.S. 2002. Idade de Zircão das Vulcânicas Iricoumé do Sudeste de Roraima: contribuição para a redefinição do Supergrupo Uatumã. *In*: SIMPÓSIO SOBRE VULCANISMO E AMBIENTES ASSOCIADOS, 2, *Anais..*, SBG, p.22.

MELO, A.F.F. DE; SANTOS, A.J.; CUNHA, M.T.P.; CAMPOS, M.J., D'ANTONA, R.J. DE G. 1978. *Projeto Molibdênio em Roraima*. Relatório Final. Manaus. DNPM/CPRM, v. 1A-B.

MONTALVÃO, R.G.M.; MUNIZ, C.M.; ISSLER, R.S.; DALL´AGNOL, R.; LIMA, M.I.C.; FERNANDES, P.E.C.A.; SILVA, G.G. 1975. *Folha NA.20-Boa Vista e parte das folhas NA.21-Tumucumaque, NB.20-Roraima e NB.21; Geologia*. Projeto RADAMBRASIL, Rio de Janeiro, MME, DNPM. (Levantamento de Recursos Minerais, 8).

MUNIZ, C.M. & DALL´AGNOL, R. 1974. Geologia do território brasileiro nas folhas Boa Vista (NA.200, Roraima (NB.20/21) e parte da folha Tumucumaque (NA.21). In: CONGRESSO BRASILEIRO DE GEOLOGIA, 28, Porto Alegre, *Anais....*, SBG, v.4. p.247-267.

OLIVEIRA, E.C. 2002. I*mplantação do método sm-nd em minerais metamórficos e sua aplicação em rochas da região central do Amapá, sudeste do Escudo das Guianas*. Belém, Universidade Federal do Pará, Centro de Geociências, Pós-Graduação em Geoquímica e Petrologia. 100p. (Dissertação de Mestrado)

OLIVEIRA, M.J.R.; ALMEIDA, M.E.; LUZARDO, R.; FARIA, M.S.G. DE. 1996. Litogeoquímica da Suíte Intrusiva Água Branca - SE de Roraima. *In*: CONGRESSO BRASILEIRO DE GEOLOGIA, 39, Salvador, *Anais...*, SBG, v.2, p. 213-216.

PAIVA, G. 1929. *Valle do Rio Negro: physiografia e geologia*. Rio de Janeiro, SGM, 40, 62p.

PARRISH, R.R. 1987. An improved micro-capsule for zircon dissolution in U–Pb geochronology. *Chemical Geology*, **66**: 99–102.

PINHEIRO, S. DA S.; NUNES, A.C.B.; COSTI, H.; YAMAGUTY, H.S.; FARACO, M.T.L.; REIS, N.J.; MENEZES, R.G. DE; RIKER, S.R.L.; WILDNER, W. 1981. *Projeto Catrimâni-Uraricoera*. Relatório de Progresso. Manaus, DNPM/CPRM,Vol.II-B.

PINHEIRO, S. DA S.; REIS, N.J.; COSTI, H.T. 1990. *Projeto Caburai*. Relatório Final. Manaus, DNPM/CPRM, 91p.

RAMGRAB, G.E. & DAMIÃO, R.N. 1970. *Reconhecimento geológico dos rios Anauá e Barauana*, Relatório Inédito. Boa Vista, DNPM, 40 p.

RAMGRAB, G.E.; BOMFIM, L.F.C., MANDETTA, P. 1972. *Projeto Roraima. 2a. Fase*. Relatório Final. Manaus, DNPM/CPRM, 38 p.

REIS, N.R. & FRAGA, L.M.B. 1996. Vulcanismo Surumu - Estado de Roraima: Caracterização de seu comportamento químico à luz de novos dados. *In*: CONGRESSO BRASILEIRO DE GEOLOGIA, 39, Salvador, *Anais...*, SBG, v. 2, p. 88- 90.

REIS, N.J.; FRAGA, L.M.; FARIA, M.S.G. DE; ALMEIDA, M.E. 2003. Geologia do Estado de Roraima. *Géologie de la France*, **2-3**: 71-84.

SANTOS, J.O.S. DOS; FARIA, M.S.G. DE; RIKER, S.R.L.; SOUZA, M.M. DE; HARTMANN, L.A.; ALMEIDA, M.E., MCNAUGHTON, N.J.; FLETCHER, I.R. 2006b. A faixa colisional K'Mudku (idade Grenvilliana) no norte do Cráton Amazonas: reflexo intracontinental do Orógeno Sunsás na margem ocidental do cráton. In: SIMPÓSIO DE GEOLOGIA DA AMAZÔNIA, 9, Belém, *Anais...*, SBG. (CD-ROM).

SANTOS, J.O.S. DOS; HARTMANN, L.A.; FARIA, M.S.G. DE; RIKER, S.R.L.; SOUZA, M.M. DE; ALMEIDA, M.E.; MCNAUGHTON, N.J. 2006a. A Compartimentação do Cráton Amazonas em Províncias: Avanços ocorridos no período 2000-2006. In: SIMPÓSIO DE GEOLOGIA DA AMAZÔNIA, 9, Belém, *Anais...*, SBG. (CD-ROM).

SANTOS, J.O.S. DOS; HARTMANN, L.A.; GAUDETTE, H.E.; GROVES, D.I.; MCNAUGHTON, N.J.; FLETCHER, I.R. 2000. A new understanding of the provinces of the Amazon Craton based on integration of field mapping and U-Pb and Sm-Nd geochronology. *Gondwana Research,* **3** (4) **:** 453-488.

SANTOS, J.O.S. DOS; MOREIRA, A.S.; PESSOA, M.R.; OLIVEIRA, J.R. DE; MALOUF, R.F.; VEIGA JR., J.P.; NASCIMENTO, J.O. DO. 1974. *Projeto Norte da Amazônia, Domínio Baixo Rio Negro*; *Geologia da Folha NA.20-Z.* Relatório Final, Manaus, DNPM/CPRM, v.III A.

SANTOS J.O.S. DOS, SILVA L.C., FARIA M.S.G. DE, MACAMBIRA, M.J.B. 1997. Pb-Pb single crystal, evaporation isotopic study on the post-tectonic, sub-alkalic, A-type Moderna granite, Mapuera intrusive suite, State of Roraima, northern Brazil. *In*: SYMPOSIUM OF GRANITES AND ASSOCIATED MINERALIZATIONS, 2, Salvador, *Extended Abstract*..., SBG, p.273-275.

SANTOS, J.O.S. DOS, VAN BREEMEN, O.B., GROVES, D.I., HARTMANN, L. A., ALMEIDA, M.E., MCNAUGHTON, N.J., FLETCHER, I.R. 2004. Timing and evolution of multiple Paleoproterozoic magmatic arcs in the Tapajós Domain, Amazon Craton: constraints from SHRIMP and TIMS zircon, baddeleyite and titanite U–Pb geochronology. *Precamb. Res.,* **131** (10) : 73-109.

SARDINHA, A.S. 1999. *Petrografia do Granito Igarapé Azul, Sudeste do Estado de Roraima*. Belém, Centro de Geociências, Universidade Federal do Pará, 32p. (Trabalho de Conclusão de Curso)

SATO, K. & TASSINARI, C.C.G. 1997. Principais eventos de acreção continental no Cráton Amazônico baseados em idade-modelo Sm–Nd, calculada em evoluções de estágio único e estágio duplo. In: COSTA, M.L.C. & ANGÉLICA, R.S. (Coord.), C*ontribuições à Geologia da Amazônia*. Belém, FINEP/SBGNO, p. 91–142.

SÖDERLUND, U. 1996. Conventional U-Pb dating *vs.* single-zircon Pb evaporation dating of complex zircons from a pegmatite in the high-grade gneisses of southwestern Sweden. *Lithos,* **38** : 93-105.

STACEY, J.S. & KRAMERS, J.D. 1975. Approximation of terrestrial lead isotope evolution by a two-stage model. *Earth and Planetary Science Letters,* **26 :** 207-221.

STEIGER, R.H. & JAGER, J. 1977. Convention of the use of decay constants in geo- and cosmochronology. *Earth and Planetary Science Letters,* **36** : 359-362.

TASSINARI, C.C.G. & MACAMBIRA M.J.B. 1999. Geochronological Provinces of the Amazonian Craton. *Episodes,* **22** (3) : 174-182.

TASSINARI, C.C.G. & MACAMBIRA M.J.B. 2004. A Evolução Tectônica do Cráton Amazônico. In: MANTESSO-NETO, V., BARTORELI, A., CARNEIRO, C.D.R. BRITO-NEVES, B.B. de (Coord.), *Geologia do Continente Sul-Americano - Evolução da Obra de Fernando Flávio Marques de Almeida*, São Paulo, Ed. Beca, p. 471-485.

VALÉRIO, C.S. 2006. *Magmatismo Paleoproterozóico do extremo sul do Escudo das Guianas, município de Presidente Figueiredo (AM): geologia, geoquímica e geocronologia Pb-Pb em zircão*. Manaus, Universidade Federal do Amazonas, Programa de Pós-Graduação em Geociências. (Dissertação de Mestrado)

VANDERHAEGHE, O.; LEDRU, D.; THIÉBLEMONT, D.; EGAL, E.; COCHERIE, A.; TEGYEY, M.; MILÉSI, J.P. 1998. Contrasting mechanisms of crustal growth. Geodynamic evolution of the Paleoproterozoic granite-greenstone belts of French Guiana. *Precambrian Research,* **92**, 165-193.

VASQUEZ, M.V.; RICCI, P.S.F.; KLEIN, E.L. 2002. Granitóides pós-colisionais da porção leste da Província Tapajós. In: KLEIN, E.L., VASQUEZ, M.L., ROSA-COSTA, L.T. (Coord.), *Contribuições à Geologia da Amazônia*, vol. 3, Belém, SBG-NO, p. 63-83.

VEIGA JR., J.P.; NUNES, A.C.B.; SOUZA, E.C. DE; SANTOS, J.O.S. DOS; AMARAL, J.E.; PESSOA, M.R.; SOUZA, S.A. DE S. 1979. *Projeto Sulfetos do Uatumã*. Relatório Final, Manaus, DNPM/CPRM, 6 v.

ANEXO 1
Mapa de Estações Geológicas

MAPA DE ESTAÇÕES

LEGENDA

Costi *et al.*(1984)
- Estação Geológica
- Análise Petrográfica

Santos *et al.* (1974)
- Estação Geológica
- Análise Petrográfica

CPRM (2000)
- Estação Geológica
- Análise Petrográfica
- Análise Geoquímica

Este estudo
- Estação Geológica
- Análise Petrográfica
- Análise Geoquímica

Convenções Cartográficas
- Sede do Município
- Cidade ou Vila (de 5000 a 24999 habitantes)
- Cidade ou Vila (abaixo de 5000 habitantes)
- drenagem
- Estrada federal pavimentada
- Estrada federal não pavimentada
- Estrada vicinais não pavimentada
- Terreno sujeito a inudação
- TI - Terra Indígena
- Localidades
- Campo de Pouso
- BEC (Batalão de Engenharia e Construção)
- Aldeia Indígena
- Área do Projeto

MAPA DE LOCALIZAÇÃO

LOCALIZAÇÃO DA ÁREA

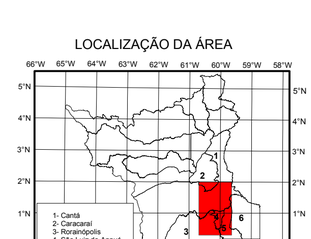

Articulação das Folhas

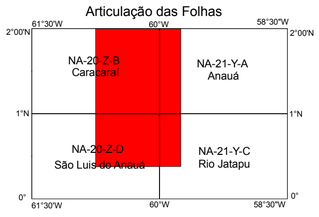

Universidade Federal do Pará
Pós-graduação em Geologia e Geoquímica
Sub-área Petrologia e Geologia Isotópica

Autor: Marcelo Estevs Almeda

Orientador: Moacir José Buenano Macambira

NOVEMBRO DE 2006

Dados digitalizados a partir da base cartográfica digital do IBGE na escala 1:250 000. Folhas: NA-20-ZB, NA-.21-YA , NA- 20-ZD, e NA-20-YC. Os dados foram comple mentados com informações de campo.

Escala 1:250 000

0 5 10 15 20 km

Dados em coordenadas geográficas, não projetadas
Datum: SAD-69
ANO 2006

N

Tratamento cartográfico dos elementos da base sob a responsabilidade da supervisão de geoprocessamento da CPRM - Manaus, realizado pelo técnico especializado da CPRM Aldenir Justino de Oliveira

ANEXO 2
Mapa Geológico

MAPA GEOLÓGICO

MAPA AEROGAMAESPECTROMÉTRICO CONTAGEM TOTAL (U,Th,k)

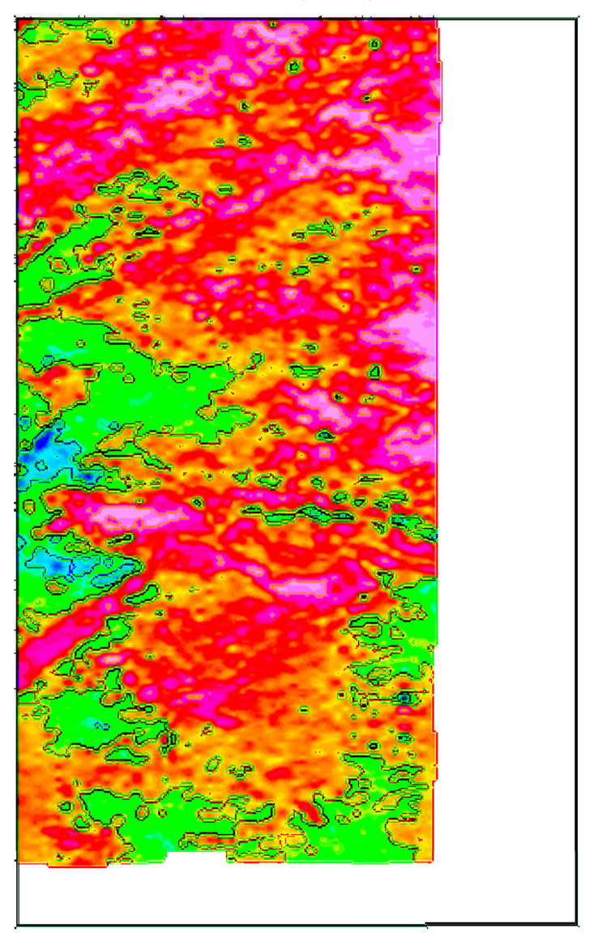

MAPA AEROMAGNETOMÉTRICO - SINAL ANALÍTICO

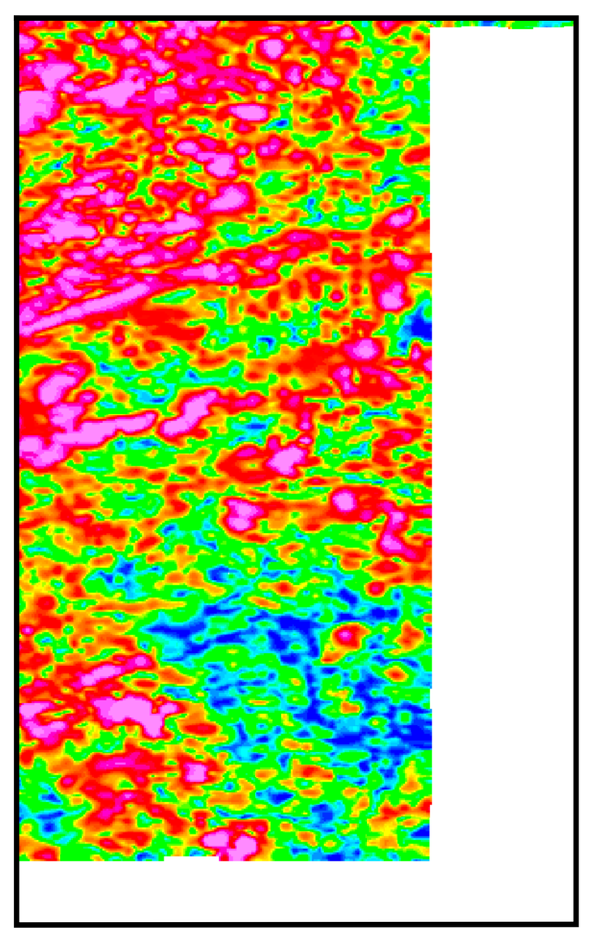

FUSÃO DA IMAGEM SRTM COM A LANDSAT

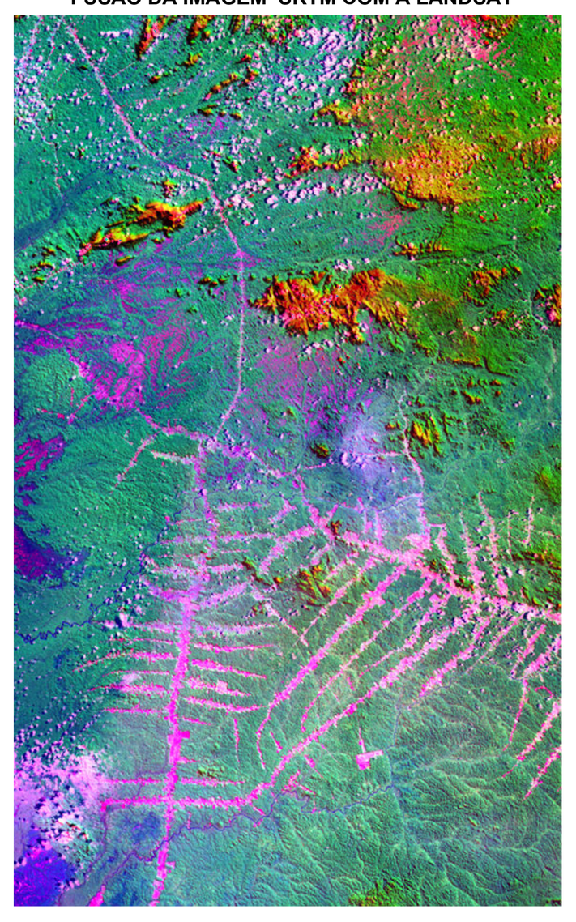

MODELO DIGITAL DO TERRENO

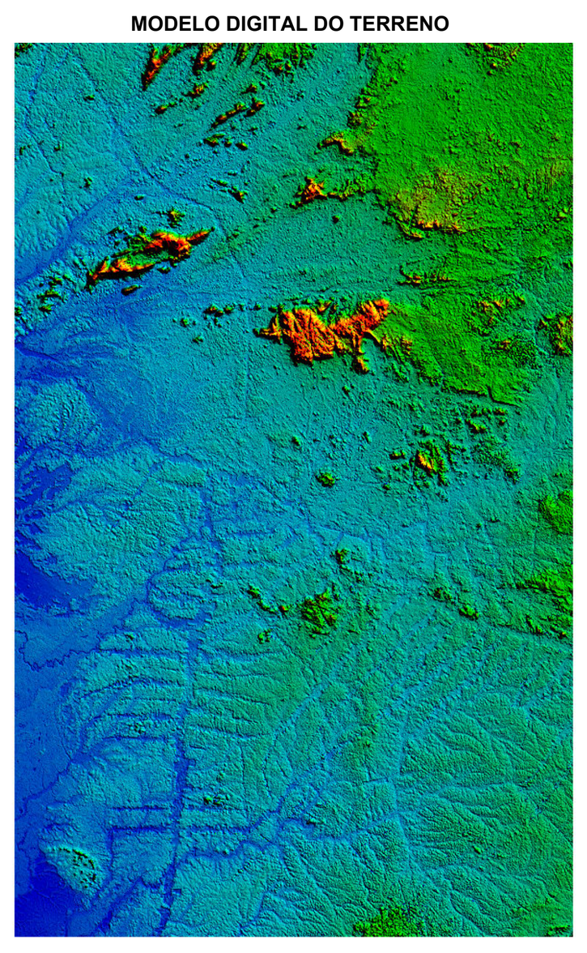

MAPA GEOLÓGICO SIMPLIFICADO

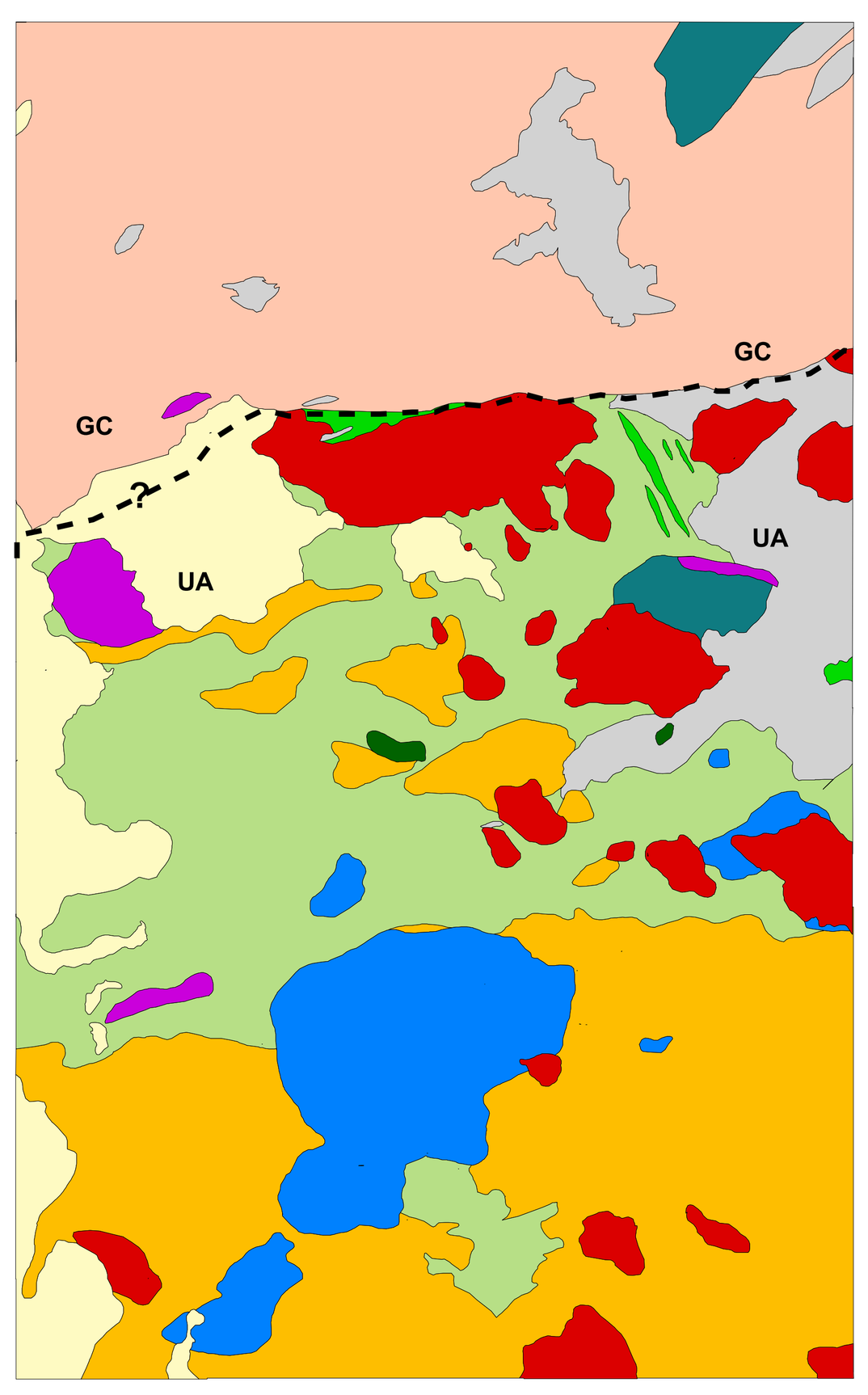

LEGENDA

- Coberturas sedimentares Cenozóicas
- Gabros Indiferenciados
- Granitos tipo A
- Charnoquitóides
- Granitóides félsicos tipo I cálcio-alcalinos de alto-K
- Granitóides tipo I cálcio-alcalinos de alto-K
- Vulcanismo intermediário a ácido
- Ortognaisses, metagranitóides, milonitos e granulitos
- Granitos tipo S
- Granito gnáissico tipo I cálcio-alcalino de alto-K
- Associação TTG e sucessões meta-vulcanossedimentares
- Limite entre os dominios Guiana Central (GC) e Uatumã-Anauá (UA)

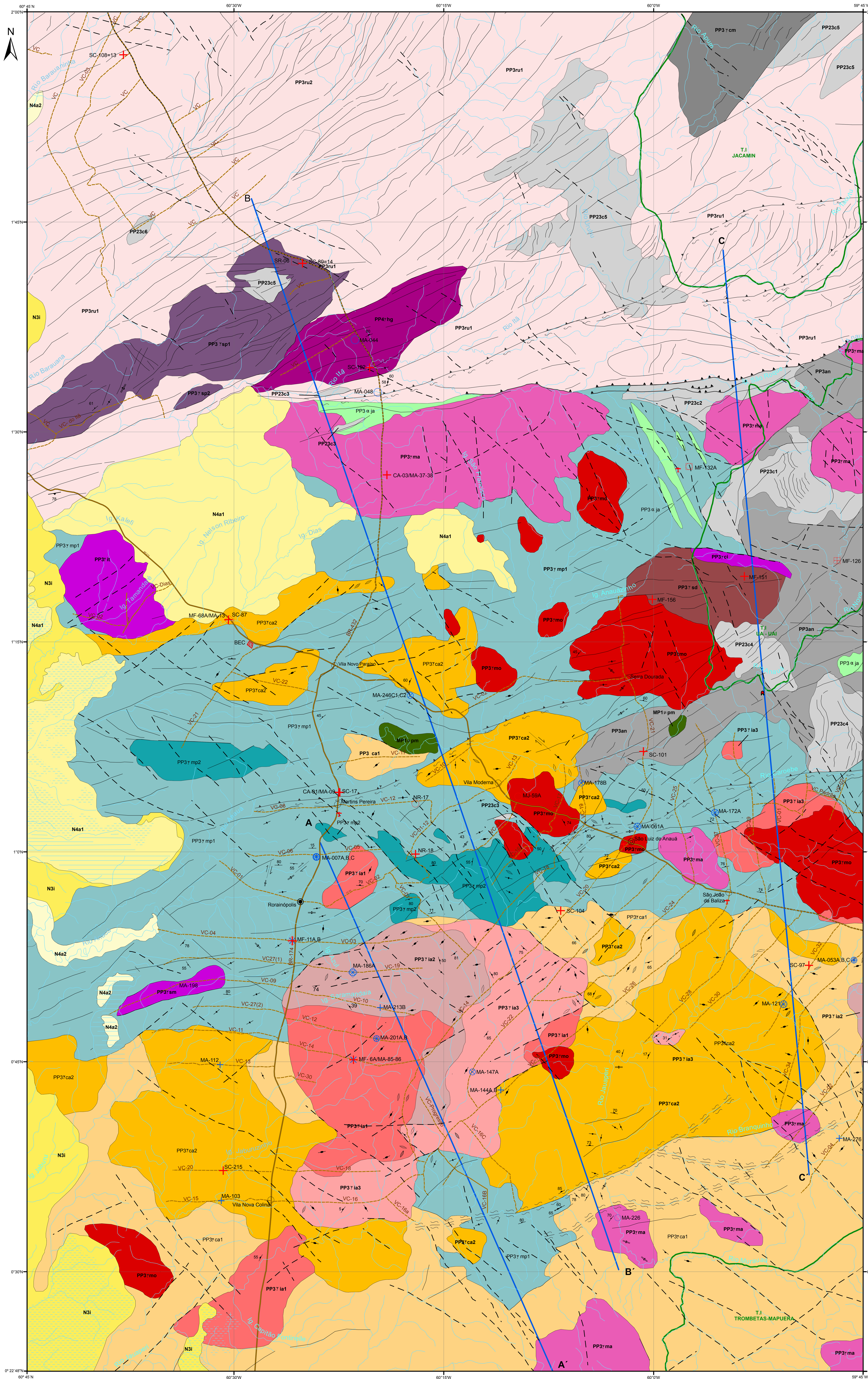

Dados digitalizados a partir da base cartográfica digital do IBGE na escala 1:250 000. Folhas: NA.20-Z-B, NA.21-Y-A , NA.20-Z-D, e NA.20-Y-C. Os dados foram complementados com informações de campo.

Escala 1:250 000

0 5 10 15 20 km

Dados em coordenadas geográficas, não projetadas
Datum: SAD-69

ANO 2006

Tratamento cartográfico dos elementos da base sob a responsabilidade da supervisão de geoprocessamento da CPRM - Manaus, realizado pelo técnico especializado da CPRM Aldenir Justino de Olivera

COLUNA ESTRATIGRÁFICA

EON	ERA	PERÍODO	ÉPOCA	DOMÍNIO UATUMÃ- ANAUÁ (DUA)	DOMÍNIO GUIANA CENTRAL (DGC)
FANEROZÓICO	Cenozóico	Neógeno	Holoceno	N4a2 *Depósitos Aluvionares:* Areia, silte, argila cascalho inconsolidados N4a1 *Depósitos Arenosos em áreas de embasamento:* Areia, silte, argila cascalho inconsolidados	
			Pleistoceno	N3i *Formação Içá:* Arenito, argilito,siltito e turfa	
	Mesoproterozóico	Calimiano		MP1μpm *Rochas plutônicas:* máficas indiscriminadas	
PROTEROZÓICO	Paleoproterozóico	Estateriano		SUL (DUAS)	PP4γhg Hornblenda-biotita granitóides : sienogranitos e monzogranitos fortemente foliados (fluxo magmático),com subordinados granodioritos e quartzo dioritos localmente deformados (1,72 Ga)
		Orosiriano		PP3γmo *Granito Moderna e rochas associadas:* sienogranitos, ortoclásio granitos e monzogranitos a hastingsita (tipo A,~1.81 Ga) PP3γma *Granito Moderna e rochas associadas:* monzogranitos e sienogranitos a biotita (tipo A, ~1.87 Ga) PP3γsm *Enderbito Santa Maria:* hiperstênio-biotita tonalitos (1,89 Ga) PP3γit *Charnoquito Igarapé Tamandaré:* hiperstênio-hornblenda-biotita charnoquitos com termos subvulcânicos associados PP3γci *Charnoquitóides indiscriminados* **Suíte Intrusiva Água Branca (PP3γab)** **Granito Igarapé Azul (PP3γia)** PP3γia1 *Fácies Vila Catarina:* (leuco)monzogranitos e raros (leuco)granodioritos; PP3γia2 *Fácies Saramandaia: monzogranitos e raros leucomonzogranitos e leucogranodioritos* PP3γia3 *Fácies Cinco Estrelas:* (leuco)monzongranitos e (leuco)granodioritos, com raros quartzo monzonitos e sienogranitos (tipo I, 1,89 Ga) **Granito Caroebe (PP3γca)** PP3γca1 *Fácies Alto Alegre:* biotita monzogranitos e granodioritos (tipo I, 1,89) PP3γca2 *Fácies Jaburuzinho:* hornblenda-biotita quartzo dioritos, quartzo monzodioritos, quartzo monzonitos, tonalitos, granodioritos e monzonitos (tipo I, 1,90 Ga) PP3 α ja *Vulcânicas Jatapu :* dacitos, traquidacitos, andesitos basálticos e granodioritos pórfiros (1,89 Ga) **NORTE (DUAN)** **Granito Martins Pereira (PP3γmp):** PP3γmp1 *(meta)monzogranitos a (meta)granodioritos:* associados a escassos biotita tonalitos e bolsões leucograníticos (tipo I,1,97Ga) PP3γmp2 *(meta)monzogranitos a (meta)granodioritos:* com enriquecimento em U-Th-K (tipo I, 1,97 Ga) PP3γsd *Granito Serra Dourada:* monzogranitos e sienogranitos à biotita, muscovita, cordierita e sillimanita (tipo S, 1,96 Ga) PP3an *Complexo Anauá:* metatonalitos, meta-dioritos, metagranitos, metaquartzo dioritos e enclaves de rochas máficas e ultramáficas (tipo TTG, 2,03 Ga) **Grupo Cauarane (PP23c, <2,04 Ga?):** PP23c1 Biotita-clorita-muscovita xistos, andaluzita-biotita-clorita-muscovita xistos, muscovita-clorita xistos, granada-biotita-clorita-muscovita xistos e sillimanita-granada-biotita-muscovita xistos PP23c2 filitos PP23c3 grunerita quartzitos e granada quartzitos PP23c4 hornblenda xistos	**Suíte Intrusiva Serra da Prata (PP3γsp):** PP3γsp1 *Granulito Barauana:* granulitos de composição charnoquítica e enderbítica polideformados (1,94 Ga); PP3γsp2 Charnoquitóides indiscriminados (1,94-1,93 Ga) **Suíte metamórfica Rio Urubu (PP3ru):** PP3ru1 Ortognaisses, (meta) granitóides e leucognaisses PP3ru2 Ortognaisses, (meta) granitóides e milonitos PP3γcm *Granito Curuxuim:* (muscovita)-biotita granitóides à granada (tipo S, ~1,97 Ga?) **Grupo Cauarane (PP23c, < 2,04 Ga?):** PP23c5 Paragnaisses pelíticos PP23c6 Calcissilicáticas

LEGENDA

- Falhas reversas
- Juntas ou falhas rúpteis-dúcteis
- Lineamentos dúcteis
- Contato geológico
- Zonas de cisalhamento transcorrentes
- Zonas de cisalhamento transpressionais
- Veio pegmatítico
- Veio aplítico
- Veio de quartzo
- 72 Foliação principal com mergulho medido
- Foliação principal com mergulho subvertical
- 86 Foliação milonítica com mergulho medido
- Foliação milonítica com mergulho subvertical
- 80 Falha ou fratura com mergulho medido
- Falha ou fratura com mergulho subvertical
- 56 Foliação magmática com mergulho medido
- Foliação magmática com mergulho subvertical

DADOS ISOTÓPICOS PROVENIENTES DE OUTROS ESTUDOS (ver referências e tabela no texto)

- Sm-Nd em rocha total
- Pb evaporação de zircão
- U- Pb convencional em zircão
- Sm-Nd em rocha total e U-Pb convencional em zircão
- U-Pb SHRIMP em zircão
- Sm-Nd em rocha total e U-Pb SHRIMP em zircão
- Pb evaporação de zircão e U-Pb SHRIMP em zircão

DADOS ISOTÓPICOS PROVENIENTES DESTE ESTUDO

- Sm-Nd em rocha total
- Pb-Pb em feldspato
- Pb evaporação de zircão
- Pb evaporação de zircão e Sm-Nd em rocha total
- Pb evaporação de zircão e U-Pb convencional em zircão
- Sm-Nd em rocha total e Pb-Pb em feldspato
- Sm-Nd em rocha total, Pb-Pb em feldspato e Pb evaporação de zircão
- Sm-Nd em rocha total, Pb-Pb em feldspato, Pb evaporação de zircão e U-Pb convencional em zircão

Convenções Cartográficas

- Cidade ou Vila (de 5000 a 24999 habitantes)
- Cidade ou Vila (abaixo de 5000 habitantes)
- Outras localidades
- Campo de Pouso
- Aldeia Indígena
- Drenagem
- Estrada federal pavimentada
- Estrada federal não pavimentada
- Estradas vicinais não pavimentadas
- Terreno sujeito a inudação ou permanentemente inudado
- T.I - Terra Indígena
- BEC (Batalhão de Engenharia e Construção)

Mapa de Localização

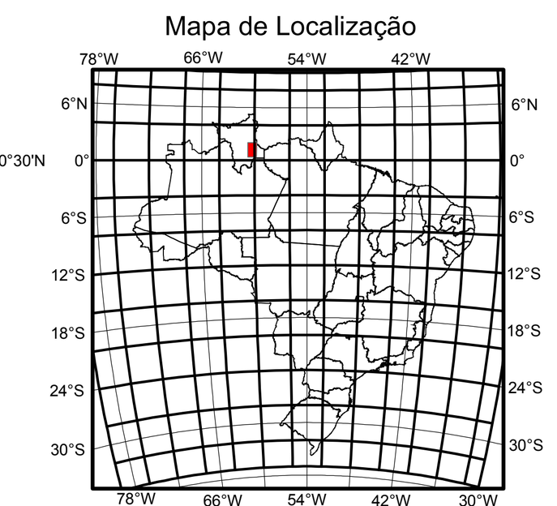

Localização da Área

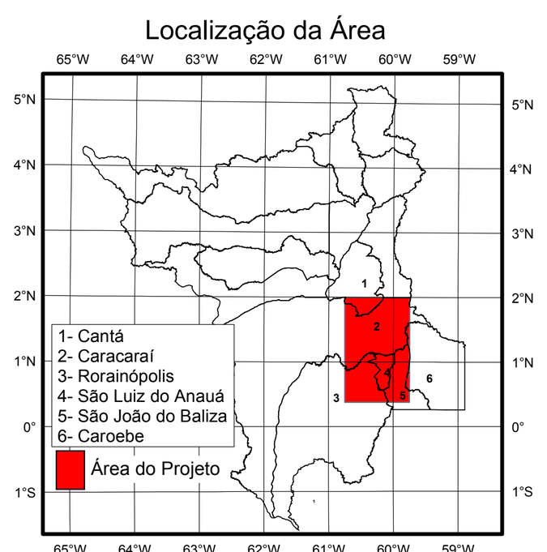

Articulação das folhas

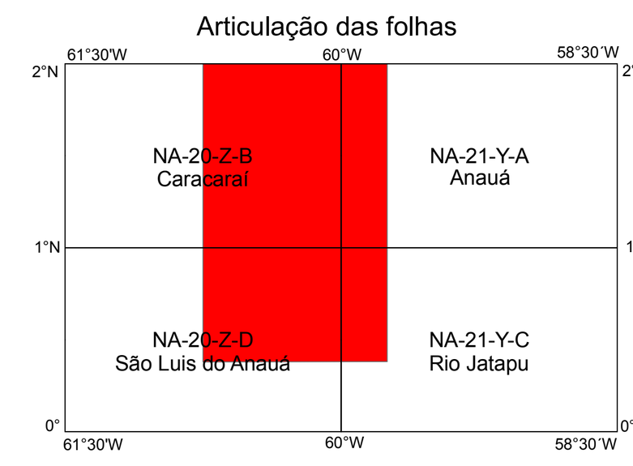

SEÇÕES ESQUEMÁTICAS (com exagero vertical)

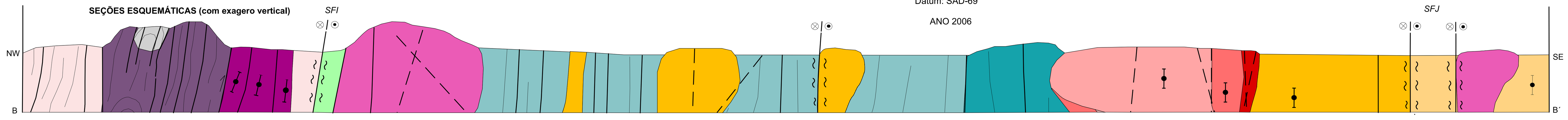

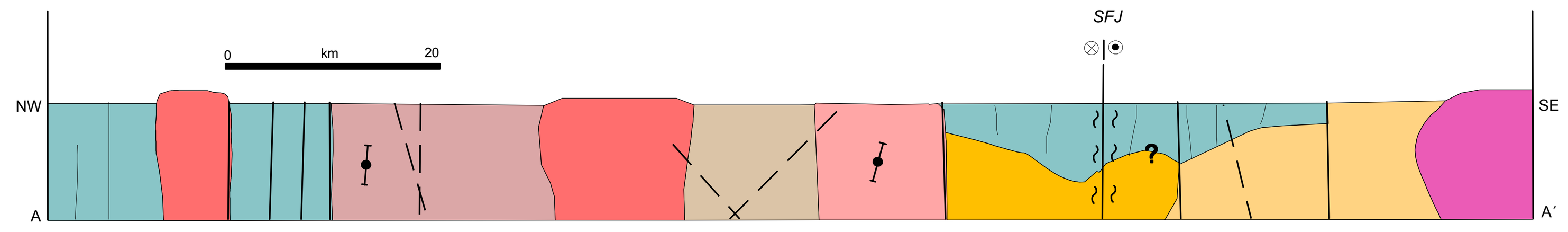

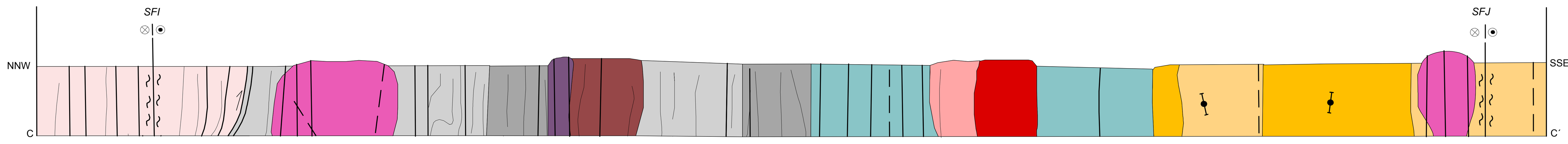

- foliação de fluxo magmático
- foliação milonítica
- foliação principal
- zona de cisalhamento destral
- falha reversa (empurrão)
- falhas rúpteis-dúcteis
- juntas ou falhas rúpteis
- SFJ Sistema de Falhas do Jauaperi
- SFI Sistema de Falhas do Itã

Universidade Federal do Pará
Pós-graduação em Geologia e Geoquímica
Sub-área Petrologia e Geologia Isotópica

Autor: Marcelo Esteves Almeida
Orientador: Moacir José Buenano Macambira

NOVEMBRO DE 2006